NOVEL BIOTHERAPEUTIC DEVICES: STUDIES WITH STEM CELLS, NANOHYBRID VIRAL VECTORS AND MICROCAPSULES FOR CARDIOVASCULAR APPLICATIONS

ARGHYA PAUL

BIOMEDICAL TECHNOLOGY AND CELL THERAPY RESEARCH LABORATORY

DEPARTMENT OF BIOMEDICAL ENGINEERING

FACULTY OF MEDICINE

MCGILL UNIVERSITY

MONTREAL, QUEBEC, CANADA

A THESIS SUBMITTED TO MCGILL UNIVERSITY IN PARTIAL FULFILLMENT OF THE REQUIREMENTS OF THE DEGREE OF

DOCTOR OF PHILOSOPHY

JANUARY, 2012

To my father

And his eternal quest for knowledge

Novel Biotherapeutic Devices: Studies with Stem Cells, Nanohybrid Viral Vectors and Microcapsules for Cardiovascular Applications

ABSTRACT

Cardiovascular diseases are one of the major causes of death, particularly in the Western world. The main cause of this mortality is myocardial infarction (MI) followed by congestive heart failure. Most of these patients undergo bypass surgery or angioplasty followed by stenting to improve blood supply and oxygenation. Although stents are excellent in providing clinical benefits, they have serious disadvantages resulting in limited biocompatibility, thrombosis, and in-stent restenosis (ISR). On the other side, despite the promising early results with stem cell based myocardial therapy, harvesting and delivering autologous cells from elderly patients still poses logistic, economic, and timing constraints resulting in sub-optimal effects.

This thesis aims to: 1) formulate superior cardiac implants for effective myocardial therapy using microencapsulated genetically modified xenogeneic adipose tissue derived mesenchymal stem cells and 2) develop a new bioactive intravascular stent using baculovirus vector-containing polymeric microspheres impregnated on a polymeric stent surface to inhibit ISR.

First, the thesis aims to develop suitable polymeric microcapsules for efficient myocardial transplantation of adipose stem cells. The preparation procedure, the structural and physical characteristics of the microcapsules were investigated and compared with earlier established microcapsule systems. Studies were performed in animal models with acute MI to evaluate the *in vivo* potential. Results show the feasibility of this system as a new class of therapeutic tool for cardiovascular applications which can enhance viable cell retention at transplant site, promote myocardial vasculogenesis, reduce scar area and attenuate progression of cardiac dysfunction. To further enhance the therapeutic efficacy, stem cells were genetically modified before microencapsulation with two newly developed nanohybrid gene delivery systems using angiogenic gene carrying insect cell-specific recombinant baculoviruses (Bac) and nanoparticles (NP).

Taken together, the thesis highlights the advantages of using microencapsulated genetically modified stem cells and identifies Bac nanocomplexes as novel gene delivery systems with potential applications in direct gene therapy and combined stem cell-gene therapy.

To achieve the second objective, the thesis attempts to enhance re-endothelialization of deployed stents while simultaneously inhibiting intimal hyperplasia by overexpression of angiogenic genes in the vasculature using novel baculovirus based stent. The prepared stents were characterized and optimized *in vitro* for favorable gene delivery procedure. Four months *in vivo* data from balloon denuded canine femoral artery confirmed the pre-clinical efficacy of the developed stent.

Overall, this thesis highlights the immense potential of these therapeutic implants as the next generation of biomedical devices with wider applications in cardiovascular and related fields. Further studies will investigate their full potential for clinical trials.

Nouveaux Dispositifs Biotherapeutiques: Etudes sur les Cellules Souches, les Vecteurs Viraux Nanohybrides et les Microcapsules pour des Applications Cardiovasculaires

RÉSUMÉ

Les maladies cardiovasculaires sont la première cause de mortalité, particulièrement dans le monde occidental. L'infarctus du myocarde (IM) suivie par l'insuffisance cardiaque congestive représente les majeures causes de cette mortalité. La plupart de ces patients subissent une chirurgie de pontage ou une angioplastie, suivie par la mise en place d'un stent, afin d'améliorer l'oxygénation du sang et sa circulation. Bien que les stents fournissent des bénéfices cliniques excellents, ils sont associés à de nombreux inconvénients tels que, une moindre biocompatibilité, une thrombose, un blocage du stent et une resténose intrastent (ISR). D'un autre côté, malgré les premiers résultats prometteurs de la thérapie cellulaire du myocarde par mobilisation de cellules souches, le prélèvement de cellules autologues chez les patients âgés pose encore des contraintes logistiques, économiques et de temps. Un des obstacles majeurs au progrès de ces technologies est le manque de systèmes de délivrance adéquats qui engendre une efficacité insuffisante. Cette thèse à pour objectifs de: 1) formuler des implants cardiaques supérieurs pour une thérapie myocardique efficace en utilisant des cellules souches mésenchymateuses - dérivées de tissus adipeux xénogéniques génétiquement modifiés - micro-encapsulées et 2) développer de nouveaux stents bioactifs intra-vasculaires en utilisant des stents polymériques dont la surface soit imprégnée de microsphères polymériques contenant un vecteur baculovirus afin d'inhiber l'ISR.

En ce qui concerne la thérapie du myocarde, cette thèse a pour objectif de développer des systèmes de délivrance de microcapsules adaptés pour une délivrance de cellules souches efficace. La procédure de préparation, les caractéristiques structurelles et physiques des capsules, y compris la stabilité mécanique, la libération contrôlée, le stockage à long terme, la nature immuno-protectrice ont été étudiés et comparés aux systèmes de microcapsules établis antérieurement. Des études ont été réalisées sur des modèles animaux atteints d'IM aigu pour évaluer le potentiel *in vivo*. Les résultats ont montré la faisabilité

de ce système en tant que nouvel outil thérapeutique pour des applications cardiovasculaires. Ce système permet d'améliorer la rétention de cellules viables au niveau du site de transplantation, de promouvoir la vasculogénèse myocardique, de réduire la surface des cicatrices et d'atténuer la progression de la dysfonction cardiaque.

De plus, deux nouveaux nano-complexes pour la délivrance de gènes ont été développés en utilisant des baculovirus recombinants issus de cellules d'invertébrés spécifiques (Bac) hybridés à des nanoparticules (NP) et NPs de dendrimères polycationiques. Ceci a permis d'améliorer la délivrance de gène angiogénique [Angiopoïétine 1 (Ang1) et facteur de croissance vasculaire endothéliale (VEGF)] aux cellules souches et cardiomyocytes. Ainsi, cette thèse souligne les avantages de l'utilisation de cellules souches micro-encapsulées qui expriment des protéines angiogéniques fonctionnellement actives. Ceci a des implications dans la réparation du myocarde. De plus, la thèse identifie les nano-complexes Bac comme de nouveaux systèmes de délivrance de gènes avec des applications potentielles en thérapie génique directe et thérapie génique combinée aux cellules souches.

Afin d'atteindre le second objectif, la thèse vise à améliorer la ré-endothélialisation des stents déployés en inhibant simultanément l'hyperpasie intimale par la surexpression du VEGF dans le système vasculaire en utilisant de nouveaux stents à élution du gène Bac. Pour cela, des Bac revêtus de dendrimères ont été formulés dans des microsphères polymériques dégradables pour éviter l'inactivation du sérum et permettre une libération contrôlée. Ils ont été intégrés couche par couche à la surface de stents hydrogels revêtus de fibrine pour une délivrance locale de gènes au site de déploiement. Les stents préparés ont été caractérisés et optimisés *in vitro* pour une procédure de délivrance de gènes appropriée. Quatre mois de données *in vivo* de l'artère fémorale canine dénudée par un ballon ont confirmé l'efficacité préclinique du stent développé.

Pour conclure, cette thèse met en évidence l'immense potentiel de ces implants thérapeutiques comme la prochaine génération de dispositifs biomédicaux avec des applications dans les domaines cardiovasculaires et apparentés. D'autres études seront effectuées pour déterminer leur efficacité clinique.

ACKNOWLEDGEMENTS

This thesis would not have been accomplished without the love, support, guidance and encouragement of multitude of individuals. I would like to begin by thanking my parents, even though I understand that any amount of gratitude shown to them is woefully inadequate. My father's unconditional support is largely the reason that this doctoral degree is completed in Canada. No works are sufficient to describe my mother's contribution to my life. I owe every bit of my existence to her. This thesis is dedicated to both of them.

I am immensely indebted to my supervisor, Prof. Satya Prakash. He has not only influenced my graduate studies and research, but also has given helped me maintain the focus throughout my research period. He has instilled in me by example, a strong sense of discipline, principle and integrity, for which I am eternally grateful to him. Prof. Prakash is a deeply committed researcher, teacher and advisor and has helped me grow with his invaluable advice, guidance, support and criticism. It is because of him that my graduate studies in McGill have been so enjoyable and rewarding. On the other hand, he has given me enough freedom to design projects independently and help me grow as an independent researcher. I feel myself privileged for being able to work under his experienced supervision towards accomplishing this research successfully.

I would like to acknowledge the guidance and advice from Dr. Dominique Shum-Tim and his continuous support all over my research period in performing the intricate surgical procedures in clinically relevant animal models. I extend my gratitude to my PhD committee members Prof. Chiu and Prof. Galiana for valuable feedbacks, advices and guidance throughout the course of my research. I would like to thank all my colleagues in the Biomedical Technology and Cell Therapy Laboratory, particularly Afshan, Sana, Meenakshi, Wei, Laetitia and Zyad for their laboratory support, and assistance as co-authors to the original reaserch articles presented in the thesis. I am especially thankful to my lifelong friend, and now my wife, Arpita for being the supporting pillar in my life, sharing

my happiness & sorrows, tensions & concerns at all times, and above all, bearing with me through all my idiosyncrasies.

This work was supported by the Natural Sciences and Engineering Research Council (NSERC) and Canadian Institutes of Health Research (CIHR). I gratefully acknowledge the national and provincial doctoral research awards: Alexander Graham Bell NSERC Canada Graduate Scholarships (CGS), CGS-Michael Smith Foreign Study Supplement Award, Fonds de recherche du Québec – Santé (FRSQ), McGill International Doctoral Awards (MIDAS) and James O. Maria Meadows Faculty of Medicine Internal Studentship. These scholarships not only encouraged me to work harder, but also helped me immensely to concentrate completely on my research and perform well, without having to worry about my finances. I am lucky and proud to be a graduate student from Biomedical Engineering department in McGill University.

Arghya Paul

PREFACE

In accordance with the McGill University Thesis Preparation and Submission Guidelines, I have taken the option of writing the experimental section in original Manuscript-Based form with either published or appropriate for publication research works. These manuscripts comprise Chapter 4-11 of this thesis, and are each divided into sections consisting of an abstract, materials and methods, results and discussions. In addition, this thesis contains an overall abstract, introduction, overall research outline, literature review, as well as general discussions on results obtained, claims to original contributions, and recommendations.

TABLE OF CONTENTS

LIST OF TABLES

LIST OF FIGURES

LIST OF ABBREVIATIONS AND TERMINOLOGY

AcNPV	*Autographa california* nuclear polyhedrosis
AFM	Atomic force microscope
Ang1	Angiopoietin 1
APA	Alginate-poly-L-lysine-alginate
Bac	Baculovirus
BMS	Bare metal stent
cDNA	complementary DNA
CHF	Congestive heart failure
CLSM	Confocal laser scanning microscope
DAPI	4',6-diamidino-2-phenylindole
DES	Drug-eluting stent(s)
DNA	Deoxyribonucleic acid
FBS	Fetal bovine serum
FITC	Fluorescein isothiocyanate
FP and RP	Forward and Reverse primer
GCAC	Genipin-crosslinked alginate chitosan
GFP	Green Fluorescent Protein
hASC	Human adipose derived stem cell
hBMSC	Human bone marrow derived stem cell
HUVEC	Human umbilical vein endothelial cell
ISR	In-stent restenosis
LacZ	Gene for β-galactosidase
MGFP	Monster Green Fluorescent Protein
MI	Myocardial Infarction
MS	Microsphere
MSC	Mesenchymal stem cell
MWCO	Molecular Weight Cutoff
NMR	Nuclear Magnetic resonance (spectrometry)
NP	Nanoparticle(s)
PBS	Phosphate buffer saline
PCR	Polymerase chain reaction

PEG	Polyethylene glycol
PLGA	Poly (DL-lactide-*co*-glycolide)
RNA	Ribonucleic acid
RITC	Rhodamine isothiocyanate
RT	Reverse Transcription
SD	Standard Deviation
SEM	Scanning electron microscope
Sf	*Spodoptera frugiperda*
SS	Stainless steel
TEM	Transmission electron microscope
VSMC	Vascular smooth muscle cell
Vegf	Vascular endothelial growth factor
X-gal	Bromo-chloro-indolyl-galactopyranoside
d	day
h	hour
hpi	hours post infection
hpt	hours post transduction
mg	milligram
min	minute
mL	milliliter
moi	Multiplicity of infection
mm	millimeter
pfu	plaque forming unit
µg	microgram
µl	microlitre
µm	micrometre

1.1 Cardiovascular diseases

Cardiovascular diseases are still the leading cause of death in the Western world in spite of the advanced medical therapies, sophisticated surgical and coronary interventional techniques, improved heart failure prognosis and clinically proven risk factor management procedures [1]. During the last decade several approaches have been designed for the treatment of myocardial infarction, post-angioplasty restenosis and thrombosis, hypertension, and induction of therapeutic angiogenesis. As evident from the literature, an important therapeutic strategy has been cardiovascular gene therapy due to recent developments in molecular biology, particularly to promote angiogenesis [2, 3]. But, to date, none of these approaches have been successful under clinical settings. Thus, it is likely that technical and pharmacological shortcomings, which include the safety and efficacy of gene delivery vehicles at the target site and mode of delivery, play an important role in the failures of present treatment approaches [4].

Thus there is an urgent need to develop effective therapeutic strategies to treat the broadly occurring cardiovascular diseases. The optimal cardiovascular therapy application would fulfill the following requirements: site specific delivery of the therapeutics, maintenance of biological functionality of the therapeutic molecules at the target site, effective mode of administration (example: intravascular, intramyocardial, catheter or stent based delivery), high retention and viability of therapeutics at the target site (example: stem cell for implantation in heart), highly efficient gene transfer vector with therapeutically relevant gene expression. In the present thesis, we aim to target two of the most frequently occurring cardiovascular diseases – Congestive Heart Failure (CHF) / Myocardial Infarction (MI) and In-stent Restenosis (ISR) associated with post-stent implantation, by developing new therapeutic tools and strategies as mentioned in the thesis research objective sections.

1.1.1 Congestive Heart Failure

Coronary artery disease accounts for 50% of all cardiovascular deaths and remains a major cause of morbidity and mortality [5]. In developed countries, congestive heart diseases such as MI or heart attack is the most common cause of hospitalization in patients more than 65 years of age with an incidence that has remarkably increased over the past two decades years. CHF has become the only cardiovascular disease that is increasing in incidence over time in North America. Approximately 5 million patients were diagnosed to have CHF in United States alone and 550,000 new cases are diagnosed yearly [6]. At least a tenth of this prevalence is expected to exist in Canada.

These patients have frequent hospitalization with high mortality reaching as high as 40% annually [7]. Coronary artery bypass graft and percutaneous transmural coronary angioplasty and stent implantation are commonly used in patients with AMI. Although medical or pharmacological therapy of CHF is available, but is currently limited by low efficacy to reduce the symptoms and mortality of CHF patients. Heart transplantation is the only potential curative treatment for CHF. However, allograft transplantation will require life-long immunosuppression and the half-life of a cardiac allograft is 9.6 years, with acute rejection, non-specific graft failure and accelerated graft coronary artery disease as the main causes of death in this population [8]. Donor scarcity has been and will continue to be a major problem. Ventricular assist devices are used mostly temporarily as a bridge to recovery or transplantation that has the inherent limitation with donor scarcity as mentioned above. Moreover, the risks of bleeding, embolism and infection are potential devastating problems [9].

A promising approach currently under intensive investigation is stem cell transplantation to improve the function of the injured myocardium through several mechanisms, including myogenesis, angiogenesis, and paracrine effects, which may attenuate left ventricular remodeling [10]. In recent years, we have reported that autologous marrow stromal cells (MSCs), when transplanted into infarcted myocardium, can differentiate into cells of various phenotypes and improve ventricular function [11-13]. The observed beneficial effects of cell

transplantation have then led to many human clinical trials [5, 12]. Despite the promising early results, such clinical application remains limited by the logistic, economic, and timing issues when harvesting autologous cells from elderly sick patients. Furthermore, a number of recent studies have documented a significantly reduced capacity for neovascularization, proliferation, and differentiation as well as increased levels of apoptosis *in vitro* and *in vivo* in MSCs obtained from elderly donors and from patients with diabetes or ischemic heart disease [13]. Moreover, the transplanted cells die shortly after implantation as a result of physical stress, myocardial inflammation, and myocardial hypoxia and solving this issue remains a hurdle for stem cell based therapeutic approaches in CHF. These impairments clearly limit the therapeutic potential of autologous MSCs and highlight the need for an alternative approach.

The present study, for the first time, explores the scope of adipose stem cells (ASCs) for myocardial therapy using tissue engineering and biotechnological approaches. Adipose tissue offers promising clinical advantages over other stem cell sources (bone marrow) due to the ease with which adipose tissue can be accessed as well as the ease of isolating stem cells from harvested tissue. As MSCs obtained from bone marrow are immune tolerant, it appears that ASCs can be also be used as "universal donor cells" for both allo- and xeno-transplantion**.** To enhance the therapeutic effect, ASCs are genetically modified to over-express certain growth factors. So far, a major backlog for its effective clinical implementation is a suitable delivery system which can retain an optimal quantity of the cells at the targeted site for maximal clinical benefit [14]; a system that will give a mechanical as well as an immune protection to the foreign cells, while at the same time will enhance the yields of differentiated cells, maintain cell microenvironments and sustain the differentiated cell functions. Towards this goal, Prakash and Chang proposed the concept of artificial cell where live functional cells are confined in semi-permeable membrane for therapeutic purposes [15]. As a step further, here we have developed polymeric microcapsules which can efficiently entrap stem cells while maintaining their natural physiological properties. The microcapsules have strong and thin multi-

layer semi-permeable membrane components with specific mass transport properties [16]. We have used alginate, a naturally occurring polysaccharide which is by far the most commonly used polymer because of its excellent cell-compatibility, its status as an FDA approved material, ease of operation and mild process conditions [17]. In the present work, we investigate the application of this microencapsulation technology as an ideal tool for myocardial transplantation of stem cells.

1.1.2 In-stent Restenosis associated with stent implantation

Apart from CHF, another important cardiovascular disease is ISR. ISR is the outcome of balloon angioplasty and stent deployment; these interventional procedures performed mostly after an acute MI to remove the fatty plaques/ blockages of the artery and widen the diameter of the blood vessels to re-establish sufficient blood flow to the already damaged heart tissues [18]. ISR or recurrent intimal thickening of the blood vessels results in increased morbidity and tremendous costs to the health care system. The rate of ISR within 6 months could be as high as 20-30% of patients in spite of the initial successful procedure [19, 20]. Each recurrent stenosis requires re-intervention in the best scenario or urgent revascularization either in the cath-lab or operating room with much higher morbidity and mortality. The incidence has been somewhat reduced with the development of drug eluting stents (DES) which inhibit the inflammatory response and the resulting proliferation of smooth muscle cells in the surrounding tissue [21-25]. Several of these latest stents show promise in various ongoing clinical trials [26-29] but the long-term benefits from large studies are still controversial and delayed onset of thrombosis and ISR is still a major concern where lifelong anti-platelets therapy has been suggested in patients with DES [30-33]. Even radioactive stents failed to show any significant reduction of restenosis rates compared to other stents [34]. The use of intravascular brachytherapy came as an alternative therapy [35-38]. However, the potential risks with the long-term use of radiation remain a serious concern. Besides, repeat procedures typically carry a high risk of complications, as well as failure rate.

These multiple concerns related to post stent implantation have rekindled an interest in developing an improved, clinically superior stent device. A diverse range of nano-delivery systems are being used to transport drugs, genes and oligonucleotides from the stent surface to remodel the damaged local vascular biology [39]. A multidisciplinary approach of nanotechnology and biotechnology is the next frontier for this. The present study aims at developing a multidisciplinary approach utilizing the biotechnological facets of baculovirus gene delivery system and nano/bio-materials to design a novel vascular stent which can efficiently accelerate re-endothelialization of damaged artery to attenuate the risk of ISR.

2. Research Outline for Cardiovascular Therapy

2.1 Objectives for Congestive Heart Therapy using Stem Cell Transplants

The primary objective of this section of the thesis is to evaluate the preclinical efficacy of hASCs for stem cell based myocardial therapy and formulate new ways to improve their transplantation efficiency and therapeutic potential using polymeric microcapsules and nanohybrid viral gene delivery systems. The specific research objectives are:

- To investigate the potential of hASCs for myocardial therapy in a xenotransplant model as an alternative to widely used hBMSCs
- To design an efficient delivery system for myocardial transplantation of hASCs using polymeric membrane and characterize its properties
- To establish the microcapsule preparation procedure for hASCs, investigate physical properties of the membrane and confirm the maintenance of viability and innate differential potential of the entrapped cells
- To evaluate the angiogenic potential of the microencapsulated hASCs in myocardially infarcted animal model
- To generate recombinant baculoviruses carrying vascular genes and investigate the potential of microencapsulated hASCs genetically modified with the viruses for myocardial therapy in an animal model of acute infarction
- As an alternative to stem cell therapy, we aim to develop a novel vascular gene carrying nanobiohybrid complex of recombinant baculovirus and TAT peptide/DNA nanoparticles for myocardial angiogenesis
- To investigate the therapeutic potential of the new nanobiohybrid gene delivery system for combined hASC-gene therapy *in vitro* and *in vivo*

2.2 Objectives for Anti-Restenosis Therapy using Therapeutic Vascular Stent

The primary research objective of this section of the thesis is to develop a new intravascular stent which can act as a suitable platform to carry and deliver vascular genes in a controlled way at the target artery site effectively. The specific research objectives are:

- To construct vascular gene carrying baculoviruses capable of transducing vascular tissues and efficiently express functional proteins from transgene
- To develop and characterize a method for enhancing the transduction efficiency by hybridizing the baculovirus with polycationic PAMAM dendrimer nanoparticles
- To prepare and characterize a method for protecting and controlling the release behavior of the hybrid baculoviruses using polymeric microspheres
- To develop a multilayered microsphere coated stent for effective local delivery of entrapped baculoviruses to the damaged vascular tissue at the implant site
- To test and optimize the performance of the bioactive stent under *in vitro* conditions
- To test the stent performance in balloon injured artery using clinically relevant animal model.

2.3 Outline of Thesis Chapters

The thesis is divided in 14 chapters. Chapter 1 describes the background and research objectives of this thesis, followed by an extensive literature survey and analysis of the subject matter in Chapter 2 and 3. Chapter 4-11 are 8 original research manuscripts published or submitted. These articles include the main studies performed to achieve the thesis objectives. **Figure 2.1** gives an overall outline of the areas covered to achieve the objectives. Chapter 12 gives an elaborate discussion of the overall thesis, while Chapter 13 summarizes the

findings of the thesis work, and the claims to original contributions to knowledge. Recommendations for future research are included in Chapter 14 of the thesis.

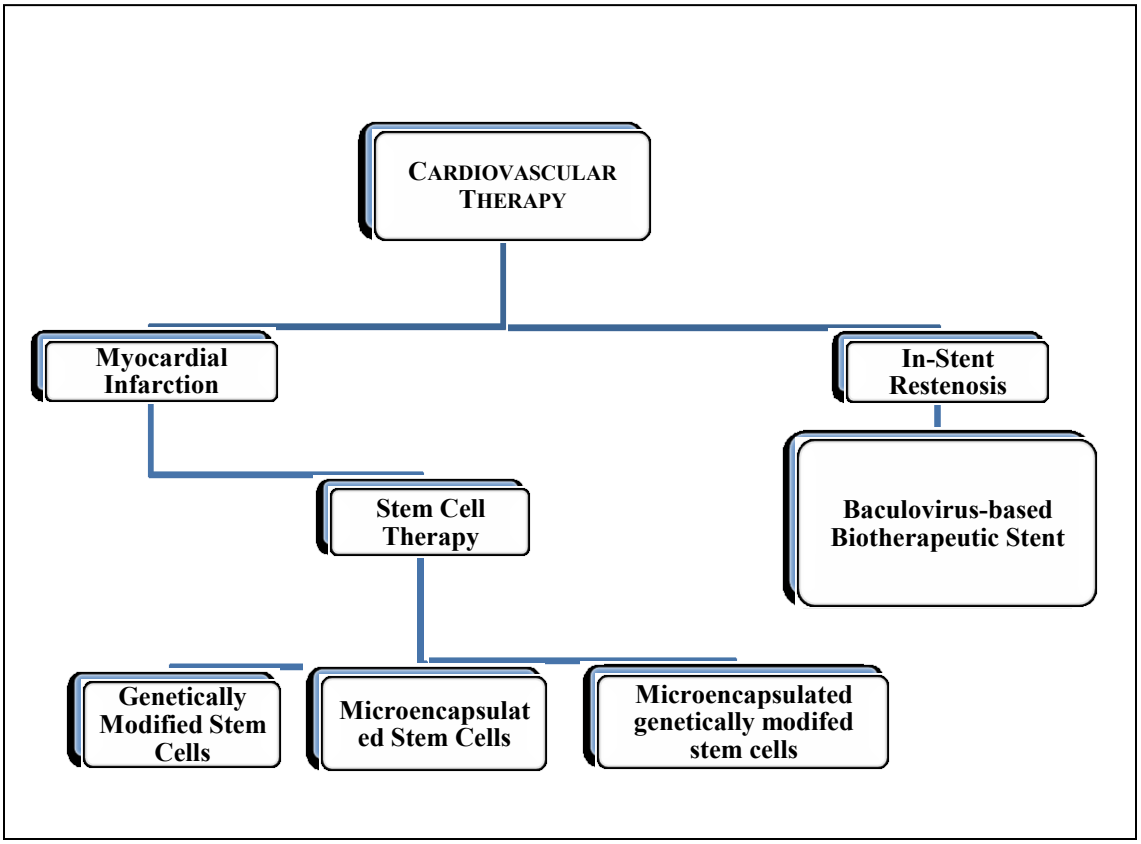

Figure 2.1: Schematic Outline of the Overall Thesis work for Cardiovascular Therapy

Cardiovascular diseases (CVDs) are the leading cause of death worldwide where more people die annually from CVDs than from any other cause [40]. Presently available therapies only delay the progression of the disease. CVDs are mainly caused by disorders of the heart and blood vessels, and include coronary heart disease (congestive heart failure or heart attacks), cerebrovascular disease (stroke), raised blood pressure (hypertension), peripheral artery disease, rheumatic heart disease, congenital heart disease and heart failure.

A major cause of coronary artery disease is accumulation of atheromatous plaques, which is an unstable collection of lipids and white blood cells, within the walls of the coronary arteries that supply oxygen and nutrients to the heart muscle. This eventually leads to myocardial infarction (MI), in other words, heart attack. To get rid of the blockage, the present treatment of choice is balloon angioplasty followed by stenting, as an alternate to highly invasive coronary artery bypass grafting [41]. But stent implantation leads to high incidence rate of in-stent restenosis (ISR) i.e. reoccurrence of stenosis leading to narrowing of artery and restricted blood flow [42]. Thus there is an urgent need to address these complications efficiently. The literature review presented in this chapter, aims to investigate the current status of cardiovascular therapy and explore the following fields:

Section I: Current Status of stem cell therapy as new approach to treat congestive heart diseases.

Section II: Insights into the evolving cardiovascular stent technology for anti-restenosis therapy.

3. 1. Introduction

The pathological findings in ischemic heart diseases are characterized by extensive cardiomyocyte apoptosis, necrosis and replacement of myocardial tissue with non-contractile fibrous cells after myocardial infarction. Since mature cardiomyocytes are terminally differentiated cells, their natural replacement with fibrous tissue results in permanent loss of contractile myocardium and the formation of dilated heart [43].

Embryonic or fetal originated cardiomyocytes have long been the focus for cell based therapy of CHF [44]. Recent studies suggest that stem cells can prevent the progression of heart failure, improve cardiac function and differentiate into vascular cell types to restore blood flow [40]. The implications of such therapy for cardiac regeneration are causing great excitement. Stem cells have the unique properties of self renewal, pluripotency and a high proliferative capability which contributes to a large biomass potential [45]. Hence these cells act as a useful source for acquiring renewable adult cell lines. This, in turn, acts as a potent therapeutic tool to treat various diseases related to heart, liver, kidney as well as neurodegenerative diseases. But a major backlog for its effective clinical implementation till date is a suitable route of administration or delivery system which can help retain an optimal quantity of functionally active stem cells at the targeted site for a maximal clinical benefit. We need a system that will give a mechanical as well as an immune protection to the foreign cells; while at the same time it will enhance the yields of differentiated cells, maintain cell microenvironments and sustain the differentiated cell functions. This is particularly important in case of myocardial transplantation where the transplanted cells tend to die or washout in the blood stream due to the mechanical forces of the continuously beating heart.

Note: Parts of this chapter have been published in the following journals:
1. Paul A, Ge Y, Prakash S, Shum-Tim D (2009) *J. Regenerative Medicine.* 4 (5): 733-745
2. Paul A and Prakash S. (2010). *Future Virology*. 5 (5): 533-537.

3.2 Current modes of stem cell delivery

3.2.1 *Based on routes of stem cell administration*

Several approaches have been made for delivering bone marrow stem cells (BMSCs) to the targeted sites. This includes intrahepatic delivery to reach liver [46], catheter based delivery of therapeutic progenitor cells directly into the ventricular wall [47, 48], delivery through renal artery in sheep model with ischemia reperfusion injury [49]. Examples of various modes of stem cell delivery to target different organs like heart, liver and kidney are summarized in **Table 3.1.**

Table 3.1 Modes of stem cell delivery to target liver, heart and kidney.

Target organs	Stem Cell Delivery Route	Effects		Ref.
		Strengths	**Limitations**	
LIVER	Intravenous	Convenient; less invasive	Immunoreaction; Entrapment of cells in lungs	[50]
	Intrahepatic	Conducive to the cells repopulating in the liver	Invasive method	[46]
	Intraperitoneal	Higher amount of cells can be delivered	Probability of mechanical damage to the cells	[51]
HEART	Transepicardial	Large number of cells can be delivered	Highly invasive	[52]
	Intravenous	Widely used in clinical settings; Convenient way	Lack of specific targeting; Less useful for treating chronic myocardial ischemia	[53]
	Transendocardial	Good for therapies that does not need any target	Meticulous method	[48]
	Trans-coronary-venous	Greater cell retention potential; good safety profile	Lack of site-specificity; technically difficult	[54]
KIDNEY	Intra-arterial	Efficient engraftment into glomerular and tubular structures during the early phase of ischemia reperfusion injury	The optimal time frame for acute renal failure stem cell therapy is unknown.	[49]

3.2.2 *Based on tissue engineering approaches*

Apart from selecting efficient route of administration, the success of cell therapy also relies on the biocompatibility of supporting constructs. A lot of emphasis has been given to transplantation of neonatal cardiomyocytes, skeletal myoblasts, embryonic stem cells, marrow stromal cells and genetically modified cells using biocompatible scaffolds to repair the damaged myocardial tissues [55-58]. The different types of scaffolds include natural matrices, such as collagen tubes, alginate hydrogels and fibrin mesh [59-61]. 3-dimentional constructs using collagen and matrigel are also being proposed for efficient cell transplantation [62, 63]. Another approach is to utilize thermo-sensitive polymers and electrospun nanofibre based scaffolds to prepare biografts that can promote better cell proliferation as well as implant biodegrability [58, 64, 65]. Biodegradable polymers, such as polyurethane, carbonate, polyglycolic acid, polycaprolactone, polylactic acid, are also being used for this purpose. A few of them have produced significant results in preclinical and clinical settings [66]. However, these modes of cell delivery have common drawbacks. Apart from high chances of getting immune rejection, a major portion of the transplanted cells get damaged soon after injection and most of the remaining biologically active cells get washed out by the beating heart [67, 68].

3.3 Introduction to polymeric microcapsules for stem cell delivery

Cell immobilization has long been suggested as an efficient delivery method for cell transplantation but it was recently reported that cell immobilization can lead to modification of cell wall and cell membrane compositions [69]. These physiological alterations may have a profound impact on cell stress resistance. Although not much is known about the physiological effects of microencapsulation technique on the stem cells, the results of cellular physiological alterations due to other immobilization methods provide us the idea on how to study the stem cell behavior and its microenvironment within the microcapsules. There are reports that microencapsulated hybridoma cells have shown better growth pattern, improved viability and antibody production in

comparison to other immobilization techniques [70]. Thus microencapsulation of cells is being studied extensively nowadays to confront the limitations of traditional immobilization technologies. Cell microencapsulation is used to encapsulate biologically active materials in specialized ultrathin semi-permeable polymer membranes [71].

3.4 Basic concept

Since the pioneering discovery by T.M.S Chang, the concept of microcapsules has been extensively developed and used in numerous areas [71]. The principle of mammalian cell microencapsulation is that the permeability of the membrane is engineered to allow the passage of oxygen, important nutrients, and cellular products, but it stops the ingress of immunoglobulins or immune cells responsible for transplant rejection [15, 71]. Thus microencapsulation technology can not only be used to deliver therapeutic products for chronic diseases, but also can be utilized for immunoprotecting healthy xenogeneic and allogeneic cells for transplantation into a recipient. The protected cells then function and secrete an effective supply of the needed hormone, protein, or other bioactive secretory products for the host. **Figure 3.1** illustrates how an encapsulation membrane serves as an immunological barrier, allowing the bi-directional exchange of small molecules including nutrients, wastes, selected substrates and products, and preventing the passage of large substances such as cells, immunocytes and antibodies [16]. Thus, cell encapsulation promises immuno-isolation, which has initiated a flurry of research into bioartificial organs and tissue engineering.

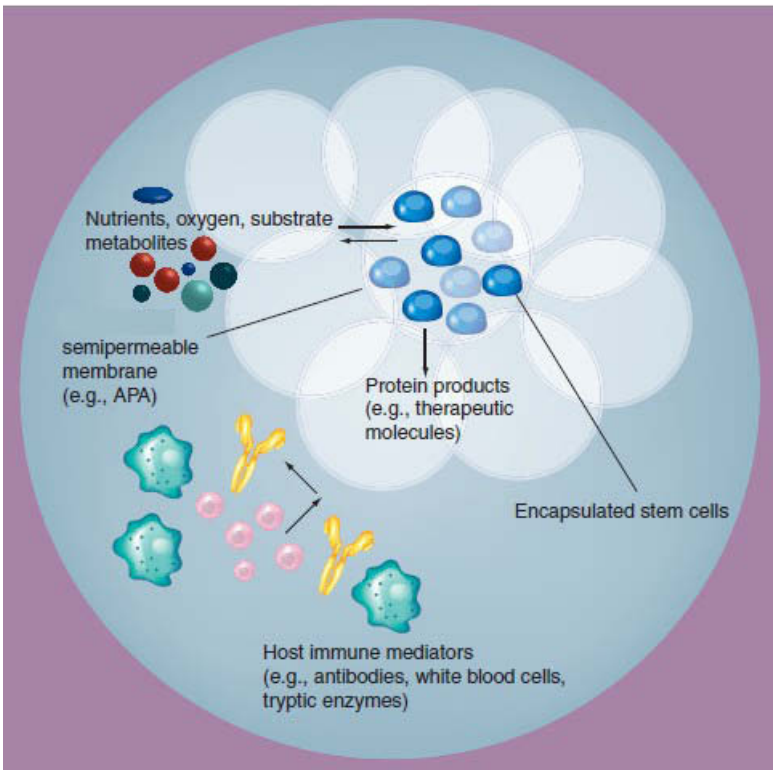

Figure 3.1 Mechanism of action of microcapsule membrane entrapping stem cells

Currently the safety and efficacy study of the encapsulated human islets in a "Monolayer Cellular Device" for allogeneic islets transplantation in type1 diabetic patients is in the Phase1 clinical trial at the University Clinical Hospital Saint-Luc, Brussels [16]. Accompanying these myriad avenues of research there has been the development of a multitude of polymers from which we need to select the suitable polymer when encapsulating a given cell species.

3.5 Microencapsulated Stem Cell Preparation Technology

The polymer matrix and the capsule preparation method are critical parameters in preparing microcapsules. These factors decide the performance of the microcapsules based on their resulting mechanical strengths, pore sizes and uniformity. In order to successfully encapsulate cells while maintaining its function, a polymer with low immunogenicity, good biocompatibility and degradation characteristics has to be selected. Among the various encapsulation techniques which are fundamentally different from each other by the nature of entrapment mechanism, the method employed here is microencapsulation by

polyelectrolyte complexation mechanism. This method utilizes the interaction of the oppositely charged polymers to form a physical barrier around the living cells. As charged polymers are water soluble they constitute an advantageous system that is compatible with cellular microenvironment. While both natural and synthetic polymers can used for the preparation, natural polymers are more cell compatible, react under milder conditions and allow for the encapsulation of fragile cells. The alginate-PLL (poly-L-Lysine) system used here utilizes the natural polymer alginate; but the challenge involving the production of such uniform capsules is to ensure excellent repeatability and reproducibility both within and between batches. The technique used to produce capsules Alginate-Poly-L-Lysine-Alginate (APA) capsules is based on the entrapment of individual cells or tissue in an alginate droplet that is then transformed into a rigid bead by gelation in a Ca^{2+} rich solution [72]. Stepwise, the cells to be encapsulated are first suspended in a solution of alginate that has been purified. The viscous alginate-cell suspension is then passed through a needle using a syringe pump. Before exiting the needle, compressed air is administered to shear the alginate-cell solution into relatively homogenous droplets. The alginate-cell droplets are then extruded through the needle tip and allowed to fall in a gently stirred calcium chloride solution, where they are transformed into rigid beads as described above. After gelation in calcium chloride, the beads are suspended in a polycationic solution like PLL so as to form a membrane that is permselective and immunoprotective. By varying the PLL concentration, alginate concentration or contact time, the porosity of the membrane can be manipulated. Lastly, the capsules are washed and suspended in a solution of alginate to bind all positively charged PLL residues still present at the capsule surface. This step is necessary to improve capsular durability and biocompatibility. Also, if a liquefied core is desired, the final APA capsules can be washed in a sodium citrate solution, which chelates calcium and solubilizes the intracapsular alginate gel. **Figure 3.2** shows a design of the microencapsulation apparatus [16].

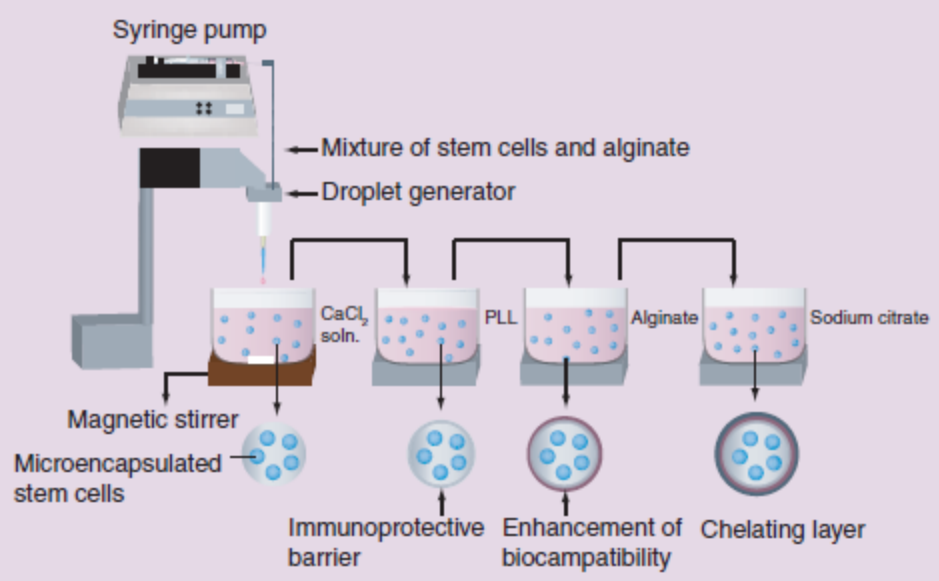

Figure 3.2 Microencapsulation of stem cells by Alginate-Poly-L-Lysine-Alginate polymeric membrane

Large scale microcapsule production has been initiated by a Swiss based company Inotech with the Encapsulator, the first commercially available instrument for the controlled polymer microencapsulation of drugs, animal cells, plant cells, microorganisms and enzymes which combines the faculties of defined bead diameter, sterile working conditions and high productivity. The Encapsulator's technique is based on a harmonically vibrating nozzle. The laminar liquid jet is broken into droplets by vibration. The machine is capable of producing microcapsules of uniform spherical shape, with a selected diameter between 200µm and 2000µm, under sterile conditions, without harm to cells, with a high throughput volume and low dead volume and with high cell viability. It is most suitable for cell encapsulation as it produces monodisperse beads with a small diameter which prevents diffusion limitations; the narrow size distribution prevents cell necrosis. The APA system employing polyelectrolyte complexation has proven advantageous as its aqueous-based, relatively mild encapsulation conditions do not compromise cell viability. Furthermore, modifications have been developed that have improved mechanical stability and biocompatibility. Apart from APA, some other biological membranes that can be used for preparing microcapsules are summarized along with their characteristics in **Table 3.2** [16]**.**

Table 3.2 Microcapsule preparation using different biological membranes

Membrane type/ Technique used	Characteristics
Calcium alginate	• low acid resistance • decreased mechanical strength
Agarose Emulsification/internal gelatinization	• stable up to 12 hours *in vitro* • agarose not sufficiently immunoprotective
Alginate-Chitosan (AC)	• improved bio- and immunocompatibity when coated with Poly-Ethylene-Glycol (PEG) • superior capsule strength, flexibility and biocompatibility with glutaraldehyde coating • mechanical instability in uncoated capsule
Alginate- Poly-l-Lysine- Alginate (APA)	• established synthesis protocols • mild encapsulation conditions, cell compatible core, flexible membrane permeability • strong short/mid-term mechanical stability in implantation studies • low inflammatory response if coated with PEG • high mechanical instability
Alginate-Cellulose Sulfate-Polymethylene co-Guanidine- Alginate	• Flexible membrane permeability, better mechanical stability than APA • Independent adjustment of capsule size, wall thickness and mechanical strength
Hydroxymethyl methacrylate-Methyl Methacrylate	• Improved mechanical stability due to insolubility in aqueous conditions • Easy scale-up, control over desired properties • Diffusion properties of aqueous solutes limited

3.6 Properties of Microencapsulated Stem Cells

Although the usage of microencapsulated cells has extended to the many cell lineages, most applications in the context of stem cells have been, so far, investigational and limited mostly to *in vitro* experiments. The few *in vivo* studies that attempted encapsulation of mesenchymal stem cells (MSCs) have mainly focused on their regenerative application in ostegenesis and chondrogenesis following fractures [73, 74]. The general rationale of microencapsulated stem cells, which are microcapsules encapsulating stem cells, for its application in stem cell delivery can be categorized into the following: 1) to protect the stem cells against native immunological responses, 2) to maintain the stem cell microenvironment and 3) to protect the cells against external mechanical forces and frictions.

3.6.1 *Immunological protection*

Although stem cell transplantation has emerged as a potential therapeutic tool for tissue (cartilage, bone) regeneration, myocardial infarction, renal failure and liver diseases, in general, the donor's (if allogeneic or xenogeneic) stem cells behave with strong immunogenicity when transplanted into a recipient with different major histocompatibility antigens. So it is always considered safer and more desirable to use autologous stem cells for the purpose though the later have some major drawbacks as mentioned by Stolzing *et al* [75]. The group reported that adult stem cells obtained from elderly donors or those with diabetes, renal failure and severe ischemic heart disease differentiate very slowly and show early signs of apoptosis. In such cases, as an alternative to autologous stem cell transplantation, allogeneic and xenogeneic stem cell transplantation with the help of encapsulation technology may be useful, most notable among them being the islet cells [74]. The polymer barrier formed by the microencapsulated cells provides immunological protection to its cargo. In a recent study by Zhang *et al*., the authors used encapsulated VEGF-secreting Chinese hamster ovary (CHO) cells to induce therapeutic effect in a rat model with myocardial infarction [76]. An important point of thought in the field of adult-derived stem cells is whether there is a need for an immunological barrier at all. Our recent work using

allogeneic and xenogeneic stem cell transplant without barrier or suppression in an immunocompetent rat model suggest that marrow stromal cells may act as a "universal donor" [13]. However, this topic is yet controversial, and other cells lines may not be immune privileged. Thus, further work examining both encapsulated and non-encapsulated cells in an *in vivo* environment is needed to characterize these properties.

3.6.2 *Maintenance of stem cell microenvironment*

An important way through which microcapsules affect the encapsulated cells is by regulation of the microenvironment. An essentially semi-permeable barrier, microcapsules selectively filter the passage of macromolecules, limiting the expansion of encapsulated cells both mechanically, and by diffusion, modifying the natural competition for growth factors and nutrients. This control over the microenvironment has resulted in much *in vitro* experimentations optimizing the differentiation of stem cells, such as studies examining adult and embryonic stem cells differentiation into hepatocytes [77]. In studies by Liu and Chang, bone marrow stem cells were co-encapsulated with hepatocytes in microencapsulated stem cells and transplanted in Gunn rats [78]. The report suggested that the co-encapsulated stem cells increase the durability and functioning of hepatocytes within the microcapsules. In fact, it helped the hepatocytes to lower the ammonia level and blood bilirubin level in treated Gunn rats. Steinert *et al*. showed chondrogenic differentiation of murine mesenchymal progenitor cells encapsulated in highly viscous biologically compatible alginate coatings. The cells were prior transfected with cDNA encoding bone morphogenetic protein-4 that helps in cartilage repair by enhancing the production of chondrogenic components and suppressing chondrogenic hypertrophy [79].

3.6.3 *Mechanical barrier for stem cells*

The polymer layers of the microcapsules allow diffusion of small molecules and protein in and out of the membrane. The mechanical role performed by the semi permeable barrier ensures that no direct cell-cell contact occurs between transplanted and host cells, while allowing for paracrine interaction between the biological environment (host) and the transplant graft. An

early application of this concept can be seen in the work by Zilberman *et al.* where genetically engineered microencapsulated mesenchymal stem cells carrying bone morphogenetic protein-2 (BMP-2) were used to treat mechanical bone defects [80]. BMP-2 has been investigated as a potential therapeutic protein to induce osteogenesis. It can also induce bone formation through differentiation of adult MSCs. Thus the effects observed due to such treatment can be attributed to both the autocrine and paracrine mechanism of the adult MSCs which have been engineered to overexpress BMP-2 proteins so as to serve as a platform for cell based gene therapy. Implanted microencapsulated adult MSCs were shown to elicit cartilage and bone formation. These effects were due to paracrine response of the host cells. Further investigations on the stem cell functioning within the microcapsules revealed that the encapsulated adult MSCs were differentiating only into cartilage cells without any evidence of osteoblastic differentiation. This was contrary to what they got in case of freely implanted adult MSCs where the later differentiated to cartilage cells and osteoblasts. A possible explanation for this could be that cell-cell contact, apart from paracrine effects, is necessary for osteoblastic differentiation of adult MSCs.

3.7 Microencapsulated stem cells for CHF

Myocardial infarction has remained a significant cause of morbidity and mortality among adults, accounting for more than 15 million new cases each year worldwide [81]. The loss of cardiomyocytes that initiates the remodeling process eventually leads to progressive heart failure. Cardiomyocytes are terminally differentiated cells that have exited the cell cycle and are unable divide in certain circumstances. But, the cells with stem cell properties have been identified in the heart that may be able to divide and multiply giving rise to new cardiomyocytes with properties similar to native cardiac cells [82]. Although a number of clinical trials have been conducted to test the feasibility of cellular therapy on heart failure but the results, in our view, have so far been humble [83, 84]. This is mainly because of some logistical problems like choosing the best way of cell delivery, optimization of cellular retention and minimizing causes of cellular loss [85, 86].

Thus cell retention following implantation remains a major challenge in such cases. This is because unlike other organs, the heart constantly contracts which contributes to the mechanical loss by squeezing the injected cells out of the myocardium. It has been noticed that following direct intramyocardial injection, labeled cells can be found throughout the body, mostly in organs such as the lung or the liver. Our preliminary studies showed that of all the injected cells, about 5-15% of injected cells were retained within the myocardium [14]. Following this tremendous mechanical loss, cells are subjected to the ischemic cardiac environment, furthering the biological losses, leaving only a fraction for therapeutic benefit. Basically when the size of the injectate is larger than the blood vessel diameter, the contractive forces of the heart become unable to wash out the later into the blood stream **(Figure 3.3A** and **3.3B)**. But this is not the case during free cell delivery where the pressure generated by the injection coupled by with that generated by the beating heart is able to force the cells through the disrupted blood vessels and into the systemic circulation [16].

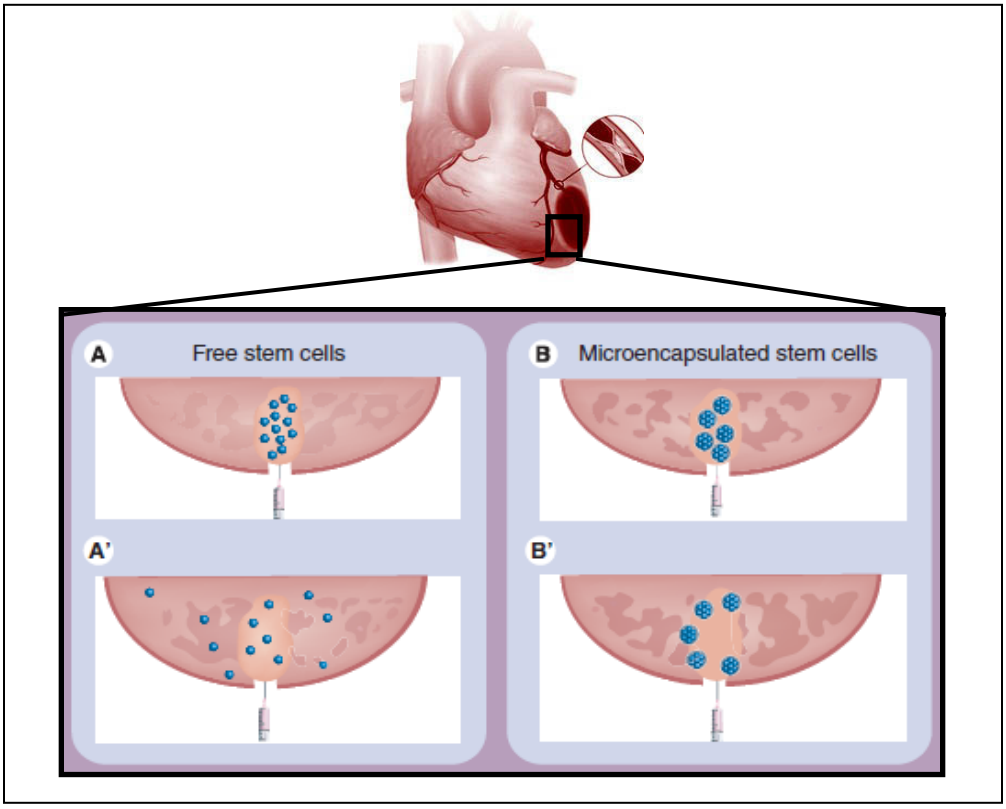

Figure 3.3 Mechanism for retention of microencapsulated stem cells for cellular cardiomyoplasty in myocardially infarcted heart. Stem cell delivery without (A) and with microencapsulation (B) into beating heart through intramyocardial injection. Pictures denote the myocardial cross sections having numerous blood vessels where the needle disrupts the vascular bed once pierced into it. A "complete washout" of the injected free stem cells into the blood vessels is seen in A' while B' depicts a retention of the microcapsules, encapsulating the stem cells.

3.8 Genetically modified Stem Cells for CHF

3.8.1 *Vectors used for stem cell based gene therapy*

Various types of vectors are being used for direct gene therapy and stem cell based gene therapy which includes mammalian viruses and non-viral vectors [87-92]. But both vectors have significant drawbacks; mammalian viral vectors are limited by high risk of immunogenicity, concerns with safety issues and chance of integration to host genome, non-viral vectors are limited by low transfection efficiency.

3.8.2 *Baculovirus as a non-toxic, biologically safe gene delivery vector*

Invertebrate-originated recombinant baculovirus using the BacMam expression system offers a powerful tool to solve the problem. This can be an ideal vector for different gene therapy applications as it combines the advantages of highly efficient transient transgene expression, ease in generation, and a wide cell tropism [93]. Although the transient expression can be termed as a kind of backlog to the system, but it is a much desirable feature, thinking from biosafety perspectives. The transient expression is attributed to the lack of natural mechanism of baculovirus to integrate with the host genome which, on the other hand, is an inherent nature of the commonly used mammalian viruses such as adenovirus, adeno-associated, and lentivirus [94-96]. Where these mammalian viral vectors have the probability to randomly integrate into the host's crucial genomic regions, thereby resulting in unexpected tumerogenesis, baculovirus holds a much better safety profile. Many safety issues are currently under consideration with present mammalian virus-based gene therapy trial [97]. At this point in time, insect cell specific baculovirus can play an important role as a potential biologically safe gene delivery vehicle.

3.8.3 *Mechanism of baculovirus entry and transgene delivery*

Studies performed earlier have shown that AcMNPV enters mammalian cells via clathrin mediated endocytosis via macropinocytosis. This is followed by an acid-induced fusion event, which releases the nucleocapsid into the cytoplasm, which is then taken up by the early endosomes within 30 min and late endosome within 45 min of transduction. These are then transported through the nuclear pore to the nucleus [98, 99]. Another group reported that caveolae of the plasma membrane are involved in baculovirus entry into the cells. Using genistein, a caveolar endocytosis inhibitor, they showed considerable enhancement of baculovirus transduction efficiency [100]. Moreover Bilello *et al* demonstrated that transient depletion of the extracellular calcium resulted in significant increase in delivery of exogenous genes in nondividing hepatocytes [101]. This is indicative that baculovirus entry may require contact with the basolateral surface in some cell types.

3.8.4 *Improved gene delivery by modulating the transduction conditions*

To increase the transduction efficiency of baculoviruses so as to make it comparable to other mammalian viruses, a lot of investigations are being done to optimize the transduction protocol. This includes regulation of the viral dosage, transduction media and temperature conditions, confluency of mammalian cells, treatment with epigenetic factors. Several studies have also used biotechnological tools to modify the baculovirus with a variety of membrane attachment proteins (such as avidin-displaying baculovirus and RGD displaying baculovirus) for improvement in transduction rate towards particular cells [102, 103]. In an interesting study Dong *et al* demonstrated using HepG2 cells that that low pH pathway can double the transduction efficiency (21% in comparison to 10% of the control) which can be further enhanced (to 78.5%) by completely blocking the endocytosis pathway using NH_4Cl [104]. It was reconfirmed, using co-localization studies, similar to the insect cell infection studies, that low pH pathway of baculovirus in transduced mammalian cells is independent of the endocytosis pathway [105].

3.8.5 *Superior features of baculovirus to genetically modify stem cells*

Over the last decade or so, new applications of baculovirus have been developed for transducing mammalian cells by engineering naturally occurring wild type viruses with mammalian promoters, which are also known as BacMam viruses. Moreover, the recombinant viruses are easy to construct and can be generated at high titers simply by infecting insect cells. This advantage, along with the easy baculovirus purification process (ultracentrifuge/chromatography), simplifies the large scale preparation of high titre baculovirus vectors to a great extent. Unlike other commonly used mammalian viruses like retrovirus and adenovirus, baculoviruses are non-pathogenic as they cannot replicate in mammalian cells and non-toxic as they don't invoke any cytopathic effect [106]. Thus baculoviruses have become a promising tool for gene therapy applications because of lack of pre-existing memory immune responses upon first administration and their comparatively safer biological profile in transduced stem cells. BacMam viruses have shown to transduce a wide spectrum of mammalian

cells such as hepatocytes, fibroblast, cardiovascular, pancreatic, and a diverse range of cancer and mesenchymal stem cells [94, 105]. Recently, they are also being used to deliver recombinant toxin genes for targeted toxin or suicide gene expression in cancer cells and siRNA/shRNA delivery for silencing specific genes in primary cell lines [107, 108].

3.8.6 *Emerging interest on baculovirus mediated stem cell therapy*

In order to enhance the therapeutic efficacy, BMSC can be genetically engineered using a suitable gene delivery system prior to cell transplantation in order to allow the engrafted cells to proliferate and integrate with the host cells [109]. This genetic modification can promote angiogenesis, tissue regeneration of the infracted portion and even support differentiation of the stromal cells *in vivo* [110, 111]. But the success of such experimental cell-based gene therapies is mainly based on the cell delivery system, its biosafety profile, efficiency of gene transfer and the subsequent expression profile of the transplanted cells without affecting the host cells' natural biological capabilities.

In summary, building upon the current literatures this thesis, in part, investigates the design and formulation of biologically safe therapeutic tools for effective myocardial therapy using new polymeric microcapsules to deliver stem cells, suitable vehicles for direct gene delivery and stem cell based gene therapy.

Section II: Intravascular Stent based Anti-restenosis Therapy

3.9 Introduction

A major medical complication related with cardiovascular blockage is the in-stent restenosis (ISR) which occurs as a result of treatment of the artery with balloon angioplasty and stent deployment [112]. ISR occurs after stenting when the vessel lumen re-narrows due to excessive neointimal proliferation in response to vascular injury (**Figure 3.4**). The initial explanation for this phenomenon was attributed to the recurrence of disease, specifically coronary artery disease. However, upon further analysis, scientists observed that instead of being a recurrence, restenosis is actually the body's injury control mechanism in response to the angioplasty, which is characterized by a proliferation of smooth muscle cells similar to scarring. As a result, the narrowing of the passageway and the subsequent reduction of blood flow could lead to potentially devastating effects such as myocardial infarction or even death. The inflammatory mechanism modulates and controls this sequence of events by involving several cellular and humoral factors into the complex process. Cellular factors of this immune response include platelets, leukocytes, endothelial cells, smooth muscle cells, and fibroblasts [113].

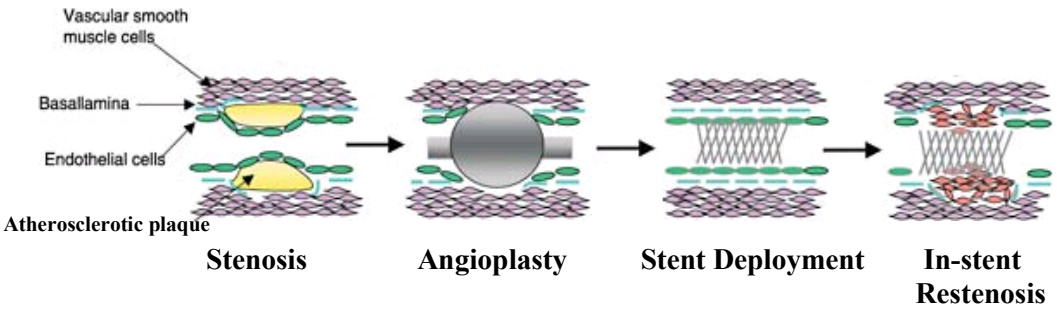

Figure 3.4: Mechanisms contributing to the formation of vascular restenosis

3.10 Currently available cardiovascular stents

Coronary and vascular stents are used to treat coronary heart disease as part of percutaneous coronary intervention and peripheral artery disease, respectively. Coronary stents, which are by far the most popular, are commonly used to treat coronary artery disease caused by atherosclerosis.

Note: Parts of this chapter has been published in the following journals:
1. Paul A, Elhayek E, Shum-Tim D, Prakash S (2010). *Curr Drug Deliv.* 7(3):216-224
2. Paul A, Abbasi S, Shum-Tim D, Prakash S (2010). *Current Nanoscience.* 6(5):469-478

3.10.1 *Bare Metal Stent*

Bare-metal stents (BMSs) or uncoated vascular stents were first introduced two decades ago as more effective means for treating coronary heart disease. Upon introduction, the metal scaffolding device virtually eliminated complications of abrupt artery closure due to vessel recoil and negative remodeling associated with stand-alone balloon angioplasties. For effective stent treatment, the stent material is chosen in such a way so as to make it flexible, supportive, expandable, and biocompatible. But the deployment of stents induces a completely different chronic vascular biological response with more intense inflammatory reaction and thus creates greater neointimal growth [114-116]. Despite ongoing improvements in the stent pattern, deliverability and metallic composition of the devices, there were no significant changes in the onset of chronic ISR in patient. Most stents are made out of 316L stainless steel, but due to the high occurrence of restenosis and thrombosis resulting from this material, researchers are investigating more biocompatible alternative materials such as gold, titanium, tantalum, and nitinol stents [112].

3.10.2 *Drug eluting stent*

To counteract the limitations and complications associated with BMSs, stent technology and design evolved to incorporate local drug delivery through a drug coating on the stent that interferes with inflammatory, migratory, proliferatory, and secretory pathways of the extracellular matrix, thus, inhibiting the thickening of the arterial walls or restenosis [117]. Stents capable of this innovative approach are known as DES. A number of DESs are being developed, each varying with its delivery platform, polymer coating (or absence of coating), and drug selection [118]. In order to find out a suitable drug for the stent coating, a vast number of drugs have been studied which includes the paclitaxel and a range of the Limus family related drugs. Paclitaxel functions by stabilizing the microtubules and inhibiting the cell division [119], whereas the Limus family drugs like sirolimus, zotarolimus, biolimus A9 and everolimus once locally delivered to the cells from the stents inhibit neointimal hyperplasia by binding with the cytoplasmic FKBP 12 protein to stop the smooth muscle cell division in

the G1/S phase [120-124]. The drugs, tacrolimus and pimecrolimus, after eluting from the vascular stent, form complex with FKBP12 and binds to calcineurin to block the activation of the Nuclear Factor of Activated T cells, thus preventing the cell cycle activation and proliferation [125]. A list of developing new generation pharmacological stents with different modes of action, for diverse stent platforms is being summarized in **Table 3.3**.

Table 3.3 Currently available types of stent platforms used to treat restenosis

Stent Type	**Examples**	**Mode of action**
Drug eluting stent	Cypher (J&J/Cordis), Taxus (Boston Scientific), Xience V (Abbott Vascular), Endeavor (Medtronic)	A stent that slowly releases a drug to block cell proliferation and/or restenosis
Bare metal stent, stainless steel	Bx Velocity (J&J/Cordis), Express2 (Medtronic), Millennium Matrix (Sahajanand Medical Technologies)	A vascular thin metal wire or mesh stent without a coating, typically first-generation technology
Bare metal stent, CoCr	Driver (Medtronic), Multi-Link Vision (Abbott Vascular), Corronnium (Sahajanand Medical Technologies)	A vascular thin metal wire or mesh without a coating, typically next-generation technology
Absorbable stent	AMS (Biotronik), ABSORB trial (Abbott Vascular), REVA/RESORB trial (REVA Medical), Arterius (West Yorkshire, UK)	Completely biodegradable, bioabsorbable stent, typically polymer or magnesium, sometimes coated with anti-restenotic agent
Bioactive stent	Genous (OrbusNeich), Titan2 BAS (Hexacath)	A stent that reacts with the body's natural processes to achieve an anti-restenotic effect
Radioactive stent	(MoBeta, Inc.)	Stent with a radiation-emitting coating
Drug-eluting balloon	SeQuent Please (B. Braun Melsungen), DIOR (EuroCor), Elutax (Aachen Resonance)	Angioplasty balloon that, after deflation, leaves behind an anti-restenotic drug

3.11 Rapidly evolving stent technology using gene therapy approaches

There is a growing interest on the nano-delivery systems to promote re-endothelialization and inhibit SMC proliferation. **Figure 3.5** gives a brief summary of the multidisciplinary approach of nano-biotechnology to further develop the stent technology. Below are some illustrative details of different nano-scale delivery systems including recombinant viruses, non-viral biomacromolecular vectors, polymeric nanoparticles to deliver cargos such as drugs, plasmids, oligonucleotides. The main focus of this thesis which is on stent carrying with nano gene delivery systems is discussed in the following section.

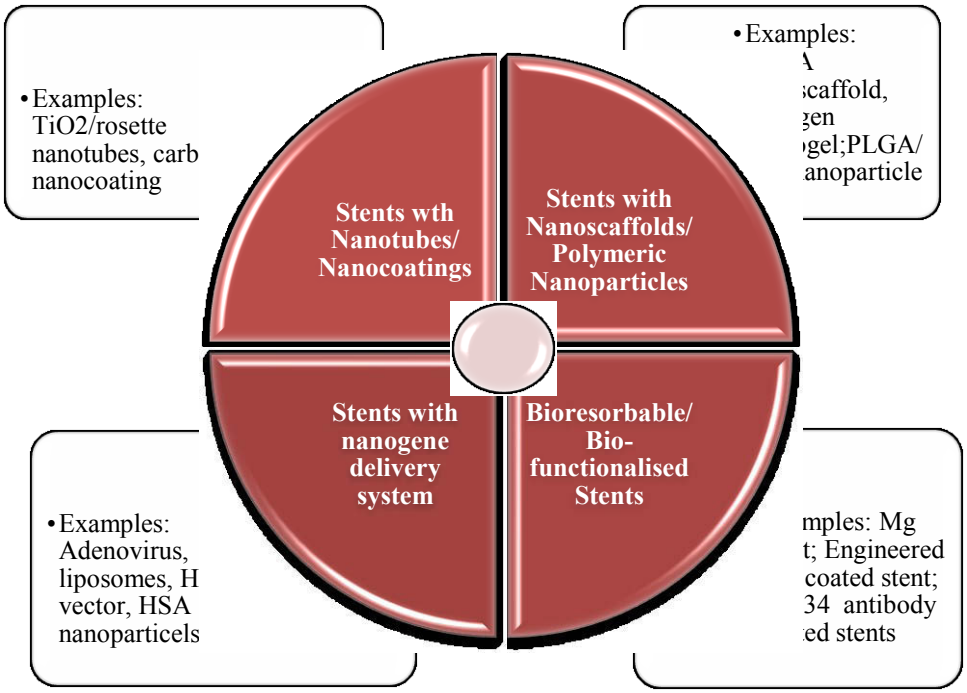

Figure 3.5 Diverse applications of nano- and biotechnological tools for designing next generation stents

3.11.1 *Viral particles for stent based gene delivery*

Gene-eluting stents to carry out gene-based therapy, using recombinant viruses with dimension of around 100nm, have been developed to reduce the occurrence of in-stent restenosis and thrombosis, while promoting re-endothelialization of blood vessel walls. Sharif *et al* have illustrated the delivery of the endothelial nitric oxide synthase (eNOS) gene into the vasculature via

adenoviral gene-eluting stents. This study succeeded in augmenting endothelial regeneration, meanwhile limiting SMC proliferation. The expression of eNOS in the blood vessels leads to an increase in NO production, which acts as a vasodilator and brings about anti-thrombotic and anti-proliferative effects [126]. The therapeutic effects of eNOS in the iliac rabbit arteries after the placement of the adenoviral gene-eluting stent (AdeNOS) were compared with a β-galactosidase gene-eluting stent (AdβGal) as a control; both stents were coated with phosphorylcholine [127]. Positively charged phosphorylcholine coating allows the virus vector to bind the stent through ionic bonds, which are weaker than alternate covalent bonds; thus, causing the release of adenovirus vectors more rapidly [128, 129]. The AdeNOS-stented iliac arteries illustrated significantly higher re-endothelialization than those treated with AdβGal stents after 14 days of stent deployment, which was more pronounced when using high cholesterol-diet animals [127].

To compare the efficiencies of adenoviruses and AAVs as vectors for gene-eluting stents, Sharif et al. have studied the two in vivo. The reporter gene, β-Galactosidase, was delivered either via first-generation adenoviruses (replication-defective) or AAV serotype 2, using Phosphorylcholine-coated stents to rabbit iliac arteries. The study reported that both viral vectors carried out stable and prolonged gene delivery to the local vasculature [130]. The expression levels of the β-Galactosidase gene delivered by adenovirus remained high consistently over the 28-day period, whereas the expression levels illustrated a decreasing trend when the gene delivery was mediated by AAV. Johnson *et al* have explored Phosphorylcholine-coated stent-based gene delivery of the Tissue Inhibitor Metalloproteinase-3 (TIMP-3), mediated by adenovirus, in porcine coronary arteries. The rationale behind using TIMP-3 as the therapeutic gene is that it limits vascular SMC migration, while augmenting their apoptosis. The study illustrates that by the localized over-expression of TIMP-3, the apoptosis of SMC is promoted, which results in a significant decrease in neointimal formation and cell density [128].

Other stent coatings for viral vector elution have also been studied. Ye et al. studied the use of a bioresorbable microporous polymer, namely poly-*L*-lactic acid (PLLA)/poly-ε-caprolactone (PCL) to coat the stent. The adenoviruses are embedded in the polymeric coating by weak hydrophilic bonds. They suggest that PLLA/PCL-coated stents can be incorporated for gene delivery *in vivo*, as they show the successful expression of the β-galactosidase reporter gene in stented rabbit carotid arteries [131]. In an interesting study, a new stent was developed by tethering adenovirus to collagen-coated stents through monoclonal anti-viral antibodies that were covalently bound to the collagen surface [132]. The stent showed efficient and localized gene delivery and expression from the collagen-coated stent to the porcine coronary arteries. In this study, collagen showed no increase in inflammation in the stented vessels, and no thrombotic complications were observed upon the use of anti-platelet therapeutics.

3.11.2 *Non-viral liposomes and nanoparticles particles for gene therapy*

Sharif *et al* have studied the use of liposomal complexes to delivery genes in order to inhibit in-stent restenosis [133]. In order to avoid bio-safety concerns, they inspected the deposition of liposomes onto phospholorylcholine-coated stents. The liposomes were designed to deliver the eNOS gene, to reduce ISR and increase re-endothelialization. Although liposomal delivery caused expression in macrophages, unlike adenoviral delivery which showed gene expression in SMCs at the struts of the stent, a significant increase in re-endothelialization was observed [133]. A new cationic liposome complex has been reported to efficiently deliver DNA to arterial tissue *in vivo* [134]. It will be interesting to exploit this system for stent based gene therapy applications.

Nanoparticles carrying drugs have already been loaded onto stents and delivered to the arterial tissue locally [135]. Due to the minute size, cellular uptake is easy which may allow the genes encapsulated within the nanoparticles to also be transfected. One main advantage of using nanoparticles as gene carriers is the ability to modify their surfaces to allow local targeted delivery via stents, thereby lowering systemic toxicity [136]. Plasmid/polyethylenimine (PEI) complexes were been used in a recent study to deliver gene from stent surface

coated with hyaluronic acid [137]. The preliminary *in vitro* report showed that the modified stent increased stent biocompatibility, as well as gene transfer efficiency. Similarly, the drug-loaded nanoparticles can be substituted with gene-loaded nanoparticles and deposited onto the stent surface for gene delivery [138].

3.12 Conclusion

To conclude, although DESs had been able to circumvent a number of obstacles related to interventional cardiology temporarily, but they showed a lot of long term complications and side effects. This literature review section tried to give an overview of the potential applications of nanodelivery systems, along with polymer coating technology, to develop a safer and effective next generation stent. **Table 3.4** summarizes the essential parameters that are needed to be considered for this.

Table 3.4: Considerations for selecting suitable stent coatings

Material characteristics of the stent coating • availability of clinical grade materials with reproducible characteristics • potential impurities like endotoxin, cross-linker • biocompatibility, non-cytotoxicity to the host system • non-thrombogenity, non-tumorigenity • not trigger host immune response • no interference with cell functions *in vitro* and *in vivo*
Mode of drug delivery from stent surface • Hydrogels or biopolymers or microspheres • Microparticles or nanoparticles or viruses • Polyelectrolyte complexes or polycations • Self assembled micelles
Formulation and processing the stent • Ease of processing • Reproducibility of critical desired features • Devoid of harsh chemicals, temperatures or pH during synthesis • preservation of therapeutic characteristics during processing & storage

Building upon current literatures on stent based anti-restenosis therapy, the last part of the thesis investigates the design, formulation and suitability of a new polymer coated gene eluting stent loaded with microspheres to induce favorable effect in the local vascular biology and attenuate ISR and thrombosis.

Preface for Chapter 4-11

Presented in the following eight chapters are the studies performed in order to achieve the research objectives. Each chapter discusses various important aspects of the thesis research project. **Chapter 4** investigates the potential of adipose stem cells, as an alternative to bone marrow stem cells for xenotransplantation and assesses their therapeutic potential compared to bone marrow cells. The work provides ground for further investigation on adipose stem cells under pre-clinical settings. **Chapter 5** introduces biocompatible polymeric microcapsules as an effective delivery platform for adipose stem cells, which also has the capacity to induce angiogenic effects. **Chapter 6** illustrates the *in vivo* efficacy of the developed microencapsulated stem cell delivery system in myocardially infarcted rat model. **Chapter 7** further extends the implication of this system for successful stem cell based gene therapy. For this, stem cells were genetically modified with advanced baculovirus gene delivery system complexed with dendrimer nanoparticles before microencapsulating them for myocardial transplantation. In addition, **Chapter 8** gives further insights to the potential of recombinant baculoviruses for genetically modifying other types of mesenchymal stem cells, such as the one originated from bone marrow, for rapid and transient transgene expression using polymeric microcapsules. As an alternative to stem cell based gene therapy, **Chapter 9** introduces a novel and efficient way to directly deliver angiogenic genes to the target site using nanobiohybrid complex of recombinant baculoviruses and peptide nanoparticles. After confirming its *in vivo* potential for myocardial angiogenesis, as a next step we investigated and examined its prospect in stem based gene therapy applications in **Chapter 10**. In order to address the complications associated with presently available vascular stents, we have designed and developed a novel gene eluting stent using recombinant vascular gene carrying baculovirus formulated in porous microspheres. **Chapter 11** presents the four month study and analysis of this newly developed stent to attenuate neoinitmal hyperplasia and subsequent restenosis in clinically relevant animal model.

During this thesis research period, I was able to contribute to 33 peer-reviewed articles (published/in press/submitted) with 16 as first author, 22 proceedings/abstracts/ presentations, 5 book chapters and 2 patents. Of these I have selected to use 8 articles pertaining to the thesis research goal, in which I am the first author.

A. Original research articles (published/in press/submitted as first author) presented in this thesis:

1. **Paul A.**, Srivastava S, Chen G, Shum-Tim D, Prakash S (2011). Functional assessment of adipose stem cells as an efficient alternative to marrow stem cell for xenotransplantation in cardiovascular diseases: *in vitro* and *in vivo* studies in myocardially infarcted immunocompetent model. *Cell Biochemistry and Biophysics*. Dec 29. [Epub ahead of print]

2. **Paul A,** Cantor A, Shum-Tim D, Prakash S (2010). Superior Cell Delivery Features of Genipin Crosslinked Polymeric Microcapsules: Preparation, In Vitro Characterization and Pro-Angiogenic Applications Using Human Adipose Stem Cells. *Molecular Biotechnology*. 48(2):116-27.

3. **Paul A,** Guangyong Chen, Afshan Khan, Rao VTS, Shum-Tim D, Prakash S (2012). Genipin-crosslinked microencapsulated human adipose stem cells augment transplant retention resulting in attenuation of chronically infarcted rat heart fibrosis and cardiac dysfunction**.** *Cell Transplantation* (in press)

4. **Paul A,** Shao W, Abbasi S, Shum-Tim D, Prakash S. (2011) PAMAM dendrimer-baculovirus hybridized nanocomplex for adipose stem cell based gene therapy: functional assessment in myocardial therapy using PEG surface functionalized microcapsule formulation (under consideration in *Molecular Pharmaceutics*)

5. **Paul A**, Shum-Tim D and Prakash S. Investigation on PEG Integrated Alginate–Chitosan Microcapsules for Myocardial Therapy Using Marrow Stem Cells Genetically Modified by Recombinant Baculovirus (2010). *Cardiovascular Engineering and Technology*. 1(2): 154-164.

6. **Paul A**, Binsalamah Z, Khan A, Abbasi S, Elias C, Shum-Tim D, Prakash S (2011). A Nanobiohybrid Complex Of Recombinant Baculovirus And Tat/DNA Nanoparticles For Delivery Of Ang-1 Transgene In Myocardial Infarction Therapy. *Biomaterials*. 32(32):8304-18.

7. **Paul A**, Nayan M, Khan A, Shum-Tim D, Prakash S (2011). Hybrid nanocomplex of baculovirus and TAT/DNA nanoparticles as a novel gene delivery vehicle for adipose stem cell-gene therapy: functional assessment in myocardially infarcted rat model (2011). *International J of Nanomedicine*. 2012; 7:663-82.

8. **Paul A**, Shum-Tim D, Prakash S (2012). Novel biohybrid gene-eluting stent using recombinant baculoviruses: investigation in denuded femoral artery of canine model (McGill ROI # 12048 filed)

B. Original research and review articles as first author not included in the thesis:

9. **Paul A,** Shao W, Shum-Tim D, Prakash S (2012). Carbon Nanotube Nanobiohybrid Stent. *Nature Nanotechnology* (under consideration).

10. **Paul A,** Khan A, Shum-Tim D, Prakash S (2010). BacMam virus transduced cardiomyoblasts can be used for myocardial transplantation using AP-PEG-A microcapsules: molecular cloning, preparation and in vitro analysis. *Journal of Biomedicine and Biotechnology*. doi:10.1155/2010/858094

11. **Paul A**, Jardin BA, Kulamarva A, Malhotra M, Elias CB, Prakash S (2010). Recombinant baculovirus as a highly potent vector for gene therapy of human colorectal carcinoma: molecular cloning, expression, and in vitro characterization. *Molecular Biotechnology.* 45(2):129-39.

12. **Paul A**, Burdon T, Al-Salami H, Shum-Tim D, Prakash S (2012). Dendrimer nanoparticles**:** Current perspectives and future potential in medicine. *Current Molecular Medicine* (under consideration).

13. **Paul A,** Elhayek E, Shum-Tim D, Prakash S (2010). Recent Advancements in Pharmacological Stent Therapy Using Polymeric Materials: Opportunities and Challenges. *Current Drug Delivery* 7(3):216-224.

14. **Paul A** and Prakash S. (2010). Baculovirus reveals a new pH-dependent direct cell-fusion pathway for cell entry and transgene delivery. *Future Virology* 5 (5): 533-537.

15. **Paul A**, Abbasi S, Shum-Tim D, Prakash S (2010). Nano- and Biotechnological Approaches in Current and Future Generation of Cardiovascular Stents. *Current Nanoscience.* 6(5):469-478

16. **Paul A** , Ge Y, Prakash S, Shum-Tim D (2009) Microencapsulated stem cells for tissue repairing: implications in cell-based myocardial therapy. *J. Regenerative Medicine.* 4 (5): 733-745

C. Original research and review articles as co-author not included in the thesis:

17. Shao W, **Paul A**, Rodes L, Prakash S (2012) A novel human serum albumin nanoparticle conjugated carbon nanotubes for intracellular delivery of paclitaxel: preparation and in-vitro analysis. *Cell Biochemistry and Biophysics* (submitted).

18. Khan AA, **Paul A**, Abbasi S, Prakash S (2011). Nanoparticles co-encapsulating hVEGF and hAng-1 can induce mitotic and antiapoptotic effect on vascular endothelial cells. *International Journal of Nanomedicine.* 6:1069-81.

19. Abbasi S, **Paul A,** Prakash S (2011). Investigation of siRNA-loaded polyethyleniminine-coated human serum albumin nanoparticle complexes for the treatment of breast cancer. *Cell Biochemistry And Biophysics* 61(2):277-87.

20. Burdon T, **Paul A**, Noiseux N, Prakash S, Shum-Tim D (2011). Bone Marrow Stem Cell Derived Paracrine Factors for Regenerative Medicine: Current Perspectives and Therapeutic Potential. *Bone Marrow Research.* Article ID 207326, doi:10.1155/2011/207326.

21. Apte S, **Paul A**, Prakash S, Shum-Tim D (2011). Current developments in the tissue engineering of autologous heart valves: moving towards clinical use. *Future Cardiology* 7(1) 77-97.

22. Nayan M, **Paul A**, Chen G, Chiu R, Prakash S, Shum-Tim D (2011). Superior therapeutic potential of young bone marrow mesenchymal stem cells by direct intramyocardial delivery in aged recipients with acute myocardial infarction: in vitro and in vivo investigation. *Journal of Tissue Engineering* 2011:741213.

23. Bhathena J, Kulamarva A, Martoni C, Urbanska A, Malhotra M, **Paul A**, Prakash S (2011). Diet-induced metabolic hamster model of nonalcoholic fatty liver disease. *Diabetes, Metabolic Syndrome and Obesity: Targets and Therapy* (4):195-203.

24. Binsalamah Z, **Paul A**, Khan A, Prakash S, Shum-Tim D (2011). Intramyocardial Sustained Delivery of Placental Growth Factor Using Nanoparticles as a Vehicle for Delivery in the Rat Infarct Model. *International Journal of Nanomedicine* 6:2667-2678.

25. Bhathena J, Martoni C, Kulamarva A, Malhotra M, **Paul A**, Urbanska A, Prakash S (2011). Oral probiotic microcapsule formulation ameliorates non-alcoholic fatty liver disease in Bio F1B Golden Syrian hamsters. *Hepatology* (submitted)

26. Abbasi S, **Paul A**, Shao W and Prakash S (2011). Cationic albumin nanoparticles for enhanced drug delivery to treat breast cancer: preparation and in vitro assessment. *Journal of Drug Delivery* 2012:686108.

27. Rodes L, **Paul A**, Coussa-Charley M, Al-Salami H, Tomaro-Duschesneau C, Fakhoury M, Prakash S (2011). Transit time affects the community stability of Lactobacillus and Bifidobacterium species in an in-vitro model of human colonic microbiota. *Artificial Cells, Blood Substitutes, and Biotechnology: An International Journal* 39(6):351-6.

28. Binsalamah Z, **Paul A**, Prakash S, Shum-Tim D (2012). Nanomedicine in Cardiovascular Therapy: Recent Advancements. *Expert Review of Cardiovascular Therapy* (in press)

29. Shao W, **Paul A**, Abbasi S, Chahal PS et al. (2011) A novel polyethyleneimine coated adeno associate virus-like particle formulation for efficient siRNA delivery using PEI-coated: implications in breast cancer therapy *International Journal of Nanomedicine*. 2012, 1575-1586.

30. Urbanska A, **Paul A**, Bhathena J, and Prakash S (2010). Suppression of Tumorigenesis: Modulation of Inflammatory Cytokines by Oral Administration of Microencapsulated Probiotic Yogurt Formulation (2010). *International Journal of Inflammation*. Vol 2010, Article ID 894972, doi:10.4061/2010/894972.

31. Huu AL, **Paul A**, Shum-Tim D, Prakash S (2012). Recent advancements in tissue engineering for stem cell based cardiac therapies. *Stem Cell International* (submitted).

32. Prakash S, Khan A, **Paul A** (2010). Nanoscaffold based stem cell regeneration therapy: recent advancement and future potential. *Expert Opinion in Biological Therapy* 10(12):1649-61.

33. Malhotra M, Kulamarva A, Sebak S, **Paul A**, Bhathena J, Mirzaei M, Prakash S (2009). Ultrafine chitosan nanoparticles as an efficient nucleic acid delivery system targeting neuronal cells. *Drug Development and Industrial Pharmacy*. Vol 35(6):719 – 726.

D. Book Chapters:

1. **Paul A**, Bhathena J, Prakash S (2011). Stem cell bioengineering and microencapsulation: current perspective and future potentials. Chapter 10, Pg 287-313. Book: Stem Cell Bioengineering and Tissue Engineering Microenvironment**.** *World Scientific Publishing Co. Ltd, US.* Editors: Prof Prakash and Shum-Tim.

2. Shao W, **Paul A**, Prakash S (2012) Nanotubes as an emerging tool for biomedical applications. Book: Selected Topics in Nanomedicine. *Imperial College Press* Editor: Prof TMS Chang.

3. Shao W, **Paul A**, Prakash S (2012). Carbon nanotubes in medicine: potentials and limitations Book: Recent Progress in Carbon Nanotube Research. *Intech Publisher* Editor: Dr. S Suzuki (under consideration)

4. **Paul A**, Shum-Tim D, Prakash S (2012) Nanobiotechnological Tools for Myocardial Therapy. Book: Cellular Cardiomyoplasty: Methods and Protocols. *Springer, New York, USA* Editor: Prof RL Kao (to be submitted)

5. Huu AL, **Paul A**, Prakash S, Shum-Tim D (2012) Route of Delivery, Cell Retention and Efficiency of Polymeric Microcapsules in Cellular Cardiomyoplasty Book: Cellular Cardiomyoplasty: Methods and Protocols. *Springer, New York, USA* Editor: RL Kao (to be submitted)

E. Patents:

1. Prakash S, **Paul A**, Shum-Tim D (2012). Novel baculovirus based stent device. *Report of Invention# 12048 filed to McGill University for provisional patent*

2. Prakash S, Khan AA, **Paul A**, Shum-Tim D, Noiseux N (2011). New delivery system for stem cell derived conditioned media. *Report of Invention# 12033 filed to McGill University for provisional patent*

F. Proceedings, abstracts and presentations:

1. **Paul A**, Shum-Tim, Prakash S (2012). Nanomedicine for Myocardial Gene Therapy. 12th Biomedical Graduate Conference (Montreal, Feb 16) *Awarded Best Cardiovascular Graduate Research Project.*

2. **Paul A,** Khan A, Abbasi S, Shum-Tim D, Prakash S (2011). PEG Incorporated Polymeric Microcapsules for Intramyocardial Delivery of Stem Cells Genetically Modified by Baculovirus. *NSTI Nanotech Conference*, Boston, US.

3. **Paul A,** Khan AA, Shum-Tim D, Prakash S (2010). Microencapsulated genetically modified stem cells for heart tissue regeneration. *2nd World Congress of International Academy of NanoMedicine*, Turkey.

4. **Paul A**, Shum-Tim D, Prakash S (2010). BacMam virus mediated gene transfer to cardiomyocytes and marrow stromal cells: Implications in myocardial therapy. *62nd Indian Pharmaceutical Congress, IPC, India.*

5. **Paul A**, Elias C, Shum-Tim D, Prakash S (2009). Rapid re-endothelisation of injured cardiovascular tissues by recombinant insect cell nucleopolyhedrosis viruses. *Canadian Cardiovascular Conference*, Alberta, Canada.

6. **Paul A**, Jardin B, Shum-Tim D, Elias C, Prakash S (2009)**.** Gene therapy of injured vascular tissues using nuclear polyhedrosis virus. *The 32nd Conference of the Canadian Medical and Biological Engineering Society,* Alberta.

7. **Paul A** and Prakash S (2009) Efficient Gene Delivery to Mouse Brain Neuroblast Cells using Recombinant Viral Particles. *3rd International Congress of Nanobiotechnology and Nanomedicine.* June 22-24, 2009 at the San Francisco.

8. **Paul A**, Malhotra M, Elias C, Shum-Tim D, Prakash S (2009). Viral vector based gene therapy for angiogenesis of damaged cardiac tissues: a novel approach. *McGill University Biomedical Engineering Student Research Day* (Awarded Best Presentation)

9. **Paul A**, Hamoudeh M, Malhotra M, Elias C, Shum-Tim D and Prakash S (2008). Viral vector based gene therapy for angiogenesis of damaged cardiac tissues: a novel approach. *Canadian Cardiovascular Conference* 2008, Toronto. (Published in *The Canadian Journal of Cardiology.*Vol 24 Supplement SE).

10. Binsalamah Z, **Paul A,** Khan A, Prakash S, Shum-Tim D (2011). Intramyocardial Sustained Delivery of Placental Growth Factor Using Nanoparticles as a Vehicle for Delivery in the Rat Infarct Model. *Annual Terrence Donnelly Cardiac Residents' Research Day*. (Best Presentation)

11. Khan AA, **A Paul,** Abbasi S, Prakash S (2011). Nanoparticles co-encapsulating hVEGF and hAng1 can induce mititic and antiapoptotic effect on vascular endothelial cells. *NSTI Nanotech 2011* Vol 3. Chapter 3 pp 183-185.

12. Binsalamah Z, **Paul A,** Khan A, Prakash S, Shum-Tim D (2011). Intramyocardial Delivery of Growth Factor Using Nanoparticles. *McGill Cardiovascular Research Day.* (Sarah Strathmore Best Presentation award)

13. Shum-Tim D, Binsalamah Z, **Paul A**, Cantor A, Khan A, Prakash S. (2011). The Application of Microcapsules and Nanoparticles in Cellular Cardiomyoplasty. *Chongqing International Heart Congress.*

14. Binsalamah Z, **Paul A**, Cantor A, Khan A, Prakash S, Shum-Tim D (2011) Novel Cardiovascular Devices: The Efficacy of Using Microencapsulation and Nanoparticles for Cell-based Therapy in Myocardial Regeneration. *Annual Meeting of the Canadian Society of Clinical Perfusion*, Vancouver.

15. Abbasi S, **Paul A,** Khan AA, Prakash S (2011). siRNA delivery using biodegradable nanoparticles for breast cancer therapy *NSTI Nanotech 2011* Vol 1. Chapter 1 pp 74-76.

16. Binsalamah Z, **Paul A,** Khan A, Prakash S, Shum-Tim D (2011). Delivery of Growth Factor Using Nanoparticles. *Annual Research Day of the Montreal Children`s Hospital*. (Best Presentation)

17. Malhotra M, **Paul A**, Prakash S (2010). Peptide tagged, non-toxic chitosan nanoparticles for enhanced siRNA delivery. *RNAi and miRNA World Congress*. Boston, MA, USA.

18. Kulamarva A, Bhathena J, **Paul A**, Malhotra M and Prakash S (2009). Microcapsule carbon nanotube devices for targeted delivery. *Nanotoday 2009*, August 2-5 2009, Singapore.

19. Malhotra M, **Paul A**, Kulamarva A and Prakash S (2009) Improved tranfection of chitosan nanoparticles, surface coated with cell penetrating peptides. *6th Interdisciplinary Graduate Student Research Symposim (IGSRS)*, McGill University, Montreal, Canada.

20. Malhotra M, Kulamarva A, **Paul A** and Prakash S (2009). Surface functionalized chitosan nanoparticles for gene delivery. *32nd Canadian Medical and Biological Engineering Conference*, Calgary, Alberta.

21. Elias C, **Paul A**, Jardin B, Prakash S and Shum-Tim D. (2009) Baculoviruses: Practical aspects of their use as Gene therapy vectors. *12th International Meeting on Baculovirus and Insect Cell Culture*, USA.

22. Kulamarva A, Bhathena J, Malhotra M, **Paul A** and Prakash S (2008). Targeted carbon nanotube delivery for biomedical applications: preparation and in-vitro analysis. *Nanomaterials Conference*, Playa del Carmen, Mexico.

G. Contributions of authors

In all the original research articles included in this thesis as individual chapters, I am the first author and was responsible for designing studies, conducting experiments, analyzing data, and preparing manuscripts. Prof. Prakash, reported as the last author in all the manuscripts, is the research advisor and also the corresponding author. Other reported co-authors have provided suggestions and assistance in performing experiments, and proofread the manuscripts.

Functional Assessment of Adipose Stem Cells for xenotransplantation using Myocardial Infarction Immunocompetent Models: Comparison with Bone Marrow Stem Cells

Arghya Paul[1], Sapna Srivastava[2], Guangyong Chen[2], Dominique Shum-Tim[2] and Satya Prakash[1*]

[1] Biomedical Technology and Cell Therapy Research Laboratory, Department of Biomedical Engineering, Faculty of Medicine, McGill University, 3775 University Street, Montreal, Québec H3A 2B4, Canada.

[2] Cardiothoracic Surgery and Surgical Research, Royal Victoria Hospital, Room # S8.73B 687 Avenue Des Pins Ouest, Montreal, Quebec H3A 1A1, Canada.

*Correspondence author; Email: satya.prakash@mcgill.ca
Tel: +1-514-398-3676; Fax: +1-514-398-7461

Preface: This paper investigates the potential of adipose derived mesenchymal stem cells for myocardial therapy, as an alternative to widely used bone marrow derived mesenchymal stem cells in xenotransplant model. *In vitro* results confirm that adipose stem cells have several advantages over bone marrow stem cells and *in vivo* data reveals their superior therapeutic potential for myocardial therapy.

Original article published in ***Cell Biochemistry and Biophysics***
[Dec 29, 2011 Epub ahead of print]

4.1 Abstract

Recently, preclinical studies have shown that allogeneic adipose derived stem cells (ASCs), like bone marrow derived mesenchymal stem cell (BMSCs) have significant clinical benefits in treating cardiovascular diseases (CVD), such as ischemic/infarcted heart. In this study, we tested whether ASCs are also immune tolerant, such that they can be used as universal donor cells for myocardial regenerative therapy. The study also focuses on investigating the potential therapeutic effects of human ASCs (hASCs) for myocardial infarction in xenotransplant model, and compares its effects with that of hBMSCs. The *in vitro* study confirms the superior proliferation potential and viability of hASCs under normoxic and stressed hypoxic conditions compared to hBMSCs. hASCs also show higher potential in adopting cardiomyocyte phenotype. The major findings of the *in vivo* study are that (1) both hASCs and hBMSCs implanted into immunocompetent rat hearts with acute myocardial infarction survived the extreme environment of xenogeneic mismatch for 6 weeks; (2) both hASCs and hBMSCs showed significant improvement in myocardial pro/anti inflammatory cytokine levels with no detectable inflammatory reaction, despite the lack of any immunosuppressive therapy; and (3) hASCs contributed to the remarkable improvement in cardiac function and reduced infarction which was significantly better than that of hBMSC and untreated control groups. Thus, our findings suggest the feasibility of using ASCs, instead of BMSCs, as universal donor cells for xenogeneic or allogeneic cell therapy.

Keywords: adipose derived stem cell, regenerative medicine, myocardial infarction, bone marrow, inflammation, cytokines, cell therapy, cardiomyoplasty

4.2 Introduction

CVD is one of the leading causes of death worldwide, mainly caused by ischemic heart disease [139]. Ischemic heart disease refers to the decrease in oxygenated blood flow to the myocardium or heart muscle, which leads to hypoxic condition in the heart muscle due to inadequate supply of oxygen mainly caused by coronary artery disease. This ischemic condition eventually leads to myocardial infarction (MI), which results in a loss of cardiomyocytes [140]. Cardiomyocytes are considered to be terminally differentiated cells and regeneration is limited in adult life. This irreversible damage to the heart can lead to severe complications such as myocardial wall rupture, arrhythmia, aneurysms and eventual heart failure[2]. The lack of oxygen to the myocardium triggers a series of molecular, cellular and physiological changes. These changes, along with the heart's limited repair mechanism, lead to scar tissue formation, ventricular remodeling, loss of heart function and eventually heart failure [141]. Although total heart transplantation can be a viable treatment for this, the shortage of donor organs and the need for lifetime immunosuppressive drugs makes this option suboptimal. Recent experimental findings suggest the therapeutic potential of stem cell therapy in heart disease, including acute MI [142-147]. The observed beneficial effects of cell transplantation have then led to many clinical trials [148-152]. In addition to improvement of cardiac function, BMSC can be useful for xenotransplantation due to its immune tolerance potential, as reported in our earlier works [153-156]. Similar results are also obtained by other researchers too [157-159]. Although the majority of research in stem cell therapy for cardiovascular disease has involved BMSCs, ASCs, which are mesenchymal stem cells within the stromal–vascular fraction of subcutaneous adipose tissue, are an ideal alternative [160]. This is mainly because of their high abundance and greater yield in viable cell mass, easy availability from liposuction materials, and ease of isolation due to less invasive harvesting procedure in comparison to BMSCs. Moreover, comparisons of immunophenotype between these two stem cells have shown that they are >90% identical [161]. ASCs are reported to produce and secrete essential growth factors and have diverse regenerative effects to induce

wound healing. Recent studies have shown the potential of ASCs in allogeneic myocardial transplantation and in other immunosuppressive ischemic models [162-164].

Although there is a substantive body of literature that supports the notion that ASCs have immense potential in cardiovascular diseases, it is not yet clear whether they have the prospective of a 'universal donor' for cellular cardiomyoplasty, in other words, whether they can be immunosuppressive and whether their immunoprivileged properties can be retained universally in animal models. Furthermore, it is not yet proven whether these cells can retain their ability to improve ventricular function after myocardial ischemia within a xenogeneic environment. With the abundance and availability of ASCs, the current study aims to investigate their immune tolerance property and compare the therapeutic potential of hASCs with hBMSCs *in vitro* and *in vivo* under myocardial milieu for xenotransplantation.

4.3 Materials and methods

4.3.1 Cell Culture

Cells procured from Invitrogen (Carlsbad, CA) were cultured in stationary cell culture flasks established according to procedures recommended by the company. Briefly, the cells were grown in Complete MesenPRO RS Medium (Invitrogen) in a 37°C incubator with 5% CO2 and 90% humidity. Regular passages were done when the cell reached 80-85% confluency to prevent the cells from differentiating or slowing their rate of division.

4.3.2 Normoxic and hypoxic cell proliferation assay

The proliferation studies of ASCs and BMSCs under normoxic and hypoxic condition were done using standard Non- Radioactive Cell Proliferation MTS Assay (Promega). MTS is chemically reduced by viable cells into formazan, which is soluble in tissue culture medium. The dehydrogenase enzyme activity found in the metabolically active cells is measured in terms of light absorbance values in this assay. For this, the cells were seeded in a 96-well plate with $2x10^4$

cells per well using normal media. After 96h of culture under normoxic condition, the measurement of the absorbance of the formazan using MTS assay was carried out using the plate reader (Victor3 Multilabel Counter from Perkin Elmer, Woodbridge, Canada) at 490nm. Since the production of formazan is directly related to the number of living cells, the intensity of the produced color is an indicator of the viable cells. To induce the hypoxic condition, the seeded cells were replaced with fresh media with no serum content and incubated for 24h in a hypoxic modular incubator chamber (Billup-Rothenberg Inc.) with less than 1% O_2 at 37^{o}C [162]. After the incubation period, the percentage viability of the cells was analyzed using the above mentioned standard cell proliferation assay. For this, the results were represented as percentage viable with respect to initial number of cells seeded.

4.3.3 Osteogenic and adipogenic differentiation assay

To induce differentiation, hBMSCs and hASCs were first seeded in 24-well plates at a high confluency of $6x10^4$ cells/well using standard media. After 24h of culture, the media was replaced with either StemPro osteogenesis (Invitrogen, Canada) or StemPro adipogenesis differentiation media to induce differentiation. During this period, the induction media were replaced every alternate day with fresh induction media. After an induction period of 3 weeks, the cells were stained with either Oil Red O stain, which stains the lipid molecules, to assess adipogenic differentiation or Alizarin Red stain, which stains mineralized extracellular matrix, to assess osteogenic differentiation [165].

4.3.4 Induction of myogenic differentiation of stem cells treated with 5-azacytidine

After hBMSCs and hASCs were grown to confluency, the cells were washed with phosphate buffered saline (PBS). The cells were then treated with 5-azacytidine (Sigma-Aldrich, St. Louis, MO, USA) at a concentration of 9µmol/L and incubated for 24 hours as reported by Rangappa *et al* [166]. After the incubation period, the cells were washed and replaced with culture medium and

placed in a CO_2 incubator. The cell media were replaces with fresh media every 3 days for a month.

4.3.5 Immunochemistry to identify cardiac specific protein in differentiated cells

To determine whether 5-azacytidine treatment can induce MSCs and ASCs to express cardiac muscle specific or related proteins, an immunocytochemistry examination was performed with mouse monoclonal antibody (Santa Cruz Biotechnology, CA, US) against cardiac-specific human troponin I [167]. For this, the cells were washed three times with PBS, permeabilized and fixed for 10 min with 0.1% Triton X-100 in 4% paraformaldehyde. After being washed in PBS, cells were blocked with 1% BSA for 30 min, incubated with the primary antibodies (1: 100 dilution) at 4°C overnight, followed by a Rhodamine-conjugated anti-mouse IgG secondary antibody (1: 1000 dilution) for 1 h. The cardiac markers were then detected under fluorescence microscope (Nikon Eclipse TE2000-U) at 200x magnification.

4.3.6 Rat myocardial ischemia model and implantation of stem cell

Lewis rats (200-250g, Charles River, Quebec, Canada) were used in this study. All procedures were approved by the Institution Animal Care Committee at the McGill University Health Center and were in compliance with the Guide for the Care and Use of Laboratory Animals (NIH publication No. 85-23, revised 1996) and the Guide to the Care and Use of Experimental Animals of the Canadian Council on Animal Care.

The rats were maintained on standard rat chow diet. Myocardial infarction was induced by occlusion of the left anterior descending coronary artery (LAD) as described previously [155, 156, 168]. Briefly, rats were anesthetized with 5% isofluorane (MTC Pharmaceuticals, Cambridge, Ontario, Canada), intubated with a 18-gauge catheter and ventilated at 85 breaths/min, using a Harvard rodent ventilator (Harvard Apparatus Co. Inc, Boston, MA). Anesthesia was maintained with 3% isofluorane. A 1.5 cm left anterolateral thoracotomy was performed in

the fifth intercostal space under sterile conditions to expose the heart, and the left coronary artery was ligated 1 to 2mm from its origin with a 7-0 polypropylene non-absorbable suture (Ethicon, Inc., Somerville, NJ). Successful performance of coronary occlusion was verified by the development of a pale colour in the ventricle after ligation. After 10 minutes of noticeable ischemia, hBMSC or hASCs ($3x10^6$ cells from passage 5 suspended in 150 µL media; n=14) were injected in the rats at three different sites (apex, right edge and left edge) of the peri-infarcted area of the left ventricle using a 28-gauge syringe. In the untreated control group (n=14), 150 µL of media was injected. A sham-surgery group, in which all surgical procedures were the same, except for the LAD ligation, was studied and did not present any differences when compared to control rats (data not shown). Small blebs under the injected area were confirmed in every case. After achieving hemostasis, the muscle and skin were closed in layers using absorbable suture. After surgery, all rats were individually caged for a 24h period of recovery. After this period, all the infarcted rats recovered to good clinical condition, and exhibited no respiratory distress nor ascites, peripheral oedema, or pleural effusion. In order to detect the presence of the implanted cells in the myocardium, a separate experiment was carried out where the cells (hASC and hBMSC) were stably transduced with LacZ retrovirus, as mentioned elsewhere, before intramyocardial implantation in the infarcted rat hearts (n=4).

4.3.7 Transthoracic echocardiography

Transthoracic echocardiography was performed on all surviving animals in rat groups treated with hBMSCs (n=14), hASCs (n=14) and medium as untreated control (n=14) at week 1, 4 and 6 after ligation. Baseline echocardiography was also performed on rats before coronary artery ligation. Echocardiograms were obtained with a commercially available system (SonoSite, Titan-Washington, Seattle, WA) equipped with a 15-MHz transducer. After sedating the animals with 2% isoflurane, echocardiography was performed as described elsewhere[4]. Briefly, parasternal long- and short-axis views were obtained with both M-mode and two-dimensional images. End-diastolic (LVEDD) and end-systolic (LVESD) diameters were measured with M-mode

tracings between the anterior and posterior walls from the short-axis view just below the level of the papillary muscles of the mitral valve. This was done according to the American Society of Echocardiology leading-edge method [169]. Left ventricular end-diastolic volume (LVEDV) was calculated as 7.0 x LVEDD^3/ (2.4+LVEDD), and left ventricular end-systolic volume (LVESV) as 7.0 x LVESD^3/ (2.4+LVESD). Ejection fraction (EF) was estimated as (LVEDV-LVESV)/LVEDV.

4.3.8 Histological analysis

Animals were sacrificed 6 weeks after the operation and treatment. The hearts of animals were excised (Groups: untreated control, hASC and hBMSC; n=8, out of 14) for histological analysis. The LV was fixed with 10% formalin overnight and dehydrated methanol and was embedded in paraffin. Each sample was transversely cut into 5µm slices. Sections of each sample were stained with collagen-specific dye, Sirius red 3BA, in saturated picric acid solution (0.1% solution in saturated aqueous picric acid, Sigma) to allow a clear discrimination between cardiomyocytes and collagen matrix as shown in previous studies [155]. Under the staining of Sirius red, collagen fibers appear as red structures. The total area of LV myocardium and red stained Infarct scar area were traced manually and measured by means of image analysis tool ImageJ-1.41 (NIH, US).

Scar area and the total area of LV myocardium were traced manually in the digital images and measured automatically by the computer by means of ImageJ-1.41 (NIH, US). The slides were scanned with 2400dpi, and the pictures were RGB split to green color layer for measurement. Infarct size, expressed as percentage of total left ventricular area, and left ventricular wall thickness were calculated for histological analysis. In order to detect the Lac Z labeled transplanted cells in rat heart after 6 weeks, the sectioned heart sample slides (hASC and hBMSC, n=4) were stained with X-gal (bromo-chloro-indolyl-galactopyranoside) and haematoxylin and eosin (H&E).

4.3.9 Myocardial TNF-α and IL-10 cytokine levels using ELISA

Animals weresacrificed 6 weeks after the operation and treatment, were excised (Groups: sham, untreated control, hASC and hBMSC; n=6, out of 14) for cytokine level analysis. The heart samples were washed with PBS and ventricular tissues from infarcted and peri-infarcted areas were flash frozen in liquid nitrogen. Frozen tissues (0.5 g) were homogenized and membrane-bound fractions were collected and analyzed for total protein assay (Invitrogen) as mentioned elsewhere [170]. This was followed by ELISA test to quantify extracted TNF-α and IL-10 proteins using commercially available kits from Qiagen SA Biosciences.

4.3.10 Statistical Evaluation

All data are expressed as mean ± Standard Deviation (SD). Multiple group comparison was performed by one-way analysis of variance (ANOVA) followed by post-hoc analysis using the Bonferroni procedure for multiple comparison of means**.** Differences were considered significant if $p < 0.05$.

4.4 Results

4.4. 1 Growth kinetics and viability of hASCs and hBMSCs depends on the cell passage number

Cell proliferation assays were performed on passages 3, 5 and 9 of both cell types. Cell were seeded with $2x10^4$ cells per well and after 4 days MTS cell proliferation assay was done. Results in **Figure 4.1A** shows that both the cell types have rapid and highest proliferation in passage 5 (hASCs: 7.45 ± 0.55 $x10^4$; hBMSCs: 6.22 ± 0.38 $x10^4$; $p<0.05$) while with higher passages, such as at passage 9, the proliferation potential decreased (hASCs: $6.56\pm0.18x10^4$; hBMSCs: 5.57 ± 0.23 $x10^4$; $p<0.01$). As shown in the data, hASCs have significantly higher proliferation potential in passage 5 and 9, than hBMSCs of same passages.

4.4.2 hASCs and hBMSCs can maintain their viability after 24 h hypoxic conditions depending on cell passage number

As shown in **Figure 4.1B**, 24h hypoxia under serum free condition has no major effect on cell viability of both hASCs and hBMSCs in lower passages

(above 98% in both passage 3 and 5), and there was no significant differences in cell viability in the two cell types. But this is not the case in higher passages, such as in passage 9, where there was a reduction in cell viability in both cell types (hASCs: 95.71±1.6%; hBMSCs: 87.54±1.1; $p<0.01$). As shown in the data, hASCs maintained a significantly higher viability in passage 9 under serum free hypoxic condition as compared to that of hBMSCs. This data shows that both cell types are suitable for myocardial transplantation after an acute myocardial ischemia.

4.4.3 Efficient differentiation of both hASCs and BMSCs to osteogenic and adipogenic lineages

The osteogenic differentiation of hASCs and hBMSCs was examined using the osteogenesis and adipogenesis induction media. The results shown in **Figure 4.2** indicate both cell types were able to differentiate to the induced lineages with no observable difference between them. These results confirm the multipotency of these cells, an important property of stem cells.

4.4.4 Differentiation potential of hASCs and hBMSCs to cardiomyocyte like lineages

Since 5-azacytidine treatment of cells did not show any changes in morphology characteristic of cardiomyocytes (data not shown), it was of interest to investigate if 5-azacytidine treatment could alter the expression of molecular markers. To test this, immunocytochemistry of hASCs and hBMSCs (**Figure 4.3**) treated with and without 5-azacytidine, for cardiac markers Troponin I was performed after 3 weeks. Treatment with 5-azacytidine resulted in increased expression of both cardiac markers, in both cells as compared to control cells. However, the expression was more pronounced in treated hASCs compared to treated hBMSCs.

4.4.5 *In vivo* survival of the implanted cells after xenotransplantation

Since hASCs differentiated at a greater extent into the cardiomyocyte lineage in vitro, it was of interest to examine if these cells could ameliorate cardiac function after myocardial infarction in a rat model. Both X-gal treated hASCs and hBMSCs were introduced into the ischemic border zone and at 6 weeks the hearts were harvested and sections were stained with H&E and X-gal. The engraftment of both these cells in the rat myocardium was depicted by the presence of blue cells, shown in **Figure 4.4**. This proves the retention of the transplanted cells in the heart even after 6 weeks. The blue color after LacZ staining also proves the cells are expressing the Lacz transgene and hence viable.

4.4.6 Improved myocardial inflammatory/ anti-inflammatory cytokine profile in treated groups

Six weeks after coronary artery ligation, levels of LV myocardial TNF-α, measured in terms of pg/ mg of total protein, was significantly increased in the untreated MI group as compared to the sham-operated control (TNF-α: 22.32±1.83 pg/mg vs. 6.54±1.4 pg/mg, $p<0.01$) as reported in **Figure 4.5**. On the other hand, the anti-inflammatory cytokine IL-10 was significantly decreased in the LV myocardial tissues 6 weeks after MI induction as compared to the sham-operated control (IL-10: 8.11±2.1 pg/mg vs. 18.5±1.32 pg/mg, $p<0.01$). Treatment with the cells at a dose of 3 million cells per animal significantly decreased myocardial pro-inflammatory cytokine marker TNF-α compared to the untreated MI group (TNF-α: 12.13 ±1.95 pg/mg for hASCs, 11.88± 2.1 pg/mg for hBMSCs vs. 22.32±1.83 pg/mg for control, $p<0.01$). Moreover, groups treated with cells significantly increased myocardial anti-inflammatory cytokine marker IL-10 compared to the untreated MI group (IL-10: 12.94 ±1.15 pg/mg for hASCs, 12.66± 1.06 pg/mg for hBMSCs vs. 8.11±2.1 pg/mg for control, $p<0.01$). There were no significant differences between hASCs and hBMSCs for myocardial TNF-α and IL-10 expression after 6 weeks of studies in the infarcted hearts ($p>0.05$).

4.4.7 Attenuation of progressive myocardial infarction by hASCs as compared to hBMSCs: evaluation by LV infarct size and wall thickness

Macroscopic views of sirius red stained heart sections are shown in **Figure 4.6A**. In both the control and the cell treated groups, positively stained fibrous infarct areas were clearly observed in the heart 6 weeks after myocardial infarction. Thin infarcts and left ventricular wall with dilated left ventricular cavity were observed in the control hearts. On the other hand, the hearts in the cell-treated groups had significantly lesser infarct areas (**Figure 4.6B**: 27.0 ±1.45% for hASCs, 31.3± 2.1% for hBMSCs vs. 38.45±1.1 % for control, $p<0.01$) and higher left ventricular wall thickness (1.56 ±0.17 mm for hASCs, 1.33± 0.11mm for hBMSCs vs. 0.87±0.09mm for control, $p<0.01$) than the control heart. A total of 24 rats were analyzed for the determination of infarct size (untreated control, 8; ASCs, 8; BMSCs, 8). The infarct size and wall thickness in the left ventricles at the section of the middle point between ligation and apex were measured as previously described [25]. There was also a significant improvement in the group treated with ASCs compared to hBMSC group ($p<0.01$) with respect to the percentage LV infract area and LV infarct wall thickness.

4.4.8 Superior performance of hASCs in reducing cardiac dysfunction of acutely infarcted rats after 6 weeks

To investigate if the reduction of scar area after stem cell therapy results in improved heart function, the EF% in a rat model of myocardial infarction at different time periods (wk1, 4 and 6) were monitored. The sham operated group maintained an EF of 66±3.5% all throughout the period of study. Whereas, EF of the untreated group significantly decreased to 30.4±0.43%, at wk1 post surgery in comparison to sham operated group, as shown in **Figure 4.7**, indicating successful acute myocardial infarction. There were significant improvements in EF% of rat hearts treated with hASCs and hBMSCs in comparison to the untreated control group on week 4 and week 6 (wk4: 37±1.28% and 35.9±1.24% vs 31.0±1.54%; wk6: 39.7±2.03% and 36.2±1.6% vs 31.0±1.24%; $p<0.01$), although this

improvement was not significant at wk1 post infarction ($p>0.05$). In addition, the hASC treated group showed a significantly greater increase in EF% as compared to hBMSC treated groups on week 6 (39.7±2.03% vs 36.8±1.6%, $p<0.01$), although no significant differences were found between them from week 1 and week 4 EF% data. Thus, the analysis using echocardiographic EF% data suggests that ASCs can be a better alternative to hBMSCs to improve cardiac function after acute myocardial damage.

4.5 Discussion

In the present study, our results confirm the *in vivo* immunotolerance property of hASCs, along with hBMSCs, and establish the superior features of ASCs in improving heart function in an extreme model of xenogeneic mismatch. By attenuating the contractile dysfunction and pathologic remodeling, the ASCs contributed significantly, and better than BMSCs, to a remarkable recovery in ventricular performance after myocardial infarction.

Moreover, the *in vitro* studies showed better cell proliferation and cardiomyocyte differential potential of hASCs compared to hBMSCs, which was dependant on the passage number. In this regard, De Ugarte *et al.* have also shown that hASCs required fewer cells to reach initial confluency as compared to hBSMCs [160]. Thus, taken together it may be suggested that higher proliferative activity of ASCs would provide a greater cell number than hBMSCs in a shorter period, which would prove more beneficial in a clinical setting. Furthermore, both hASCs and hBMSCs were resistant to hypoxic condition depending on passage number. The multipotent characteristic of hASCs and hBMSCs were confirmed by their ability to differentiate to the osteogenic and adipogenic lineages, which is in accordance with other studies [171]. There has been conflicting reports with respect to the differentiation of ASCs and BMSCs to the cardiomyocyte lineage after treatment with 5-azacytidine [172, 173]. Here, we have reported that the treatment of hASCs and hBMSCs with 5-azacytidine results in the differentiation of the cells into the cardiomyocyte phenotype. This was demonstrated by the positive staining of cardiac specific marker, tropinin I compared to control. These

observations are consistent with the studies of Rangappa et al., who also observed positive staining of these markers in rabbit ASCs treated with 5-azacytidine [166]. Furthermore, we have demonstrated for the first time that 5-azacytidine treated hASCs exhibited an increased expression of cardiomyocyte marker as compared to treated hBMSCs by using immunocytochemistry. However, the morphology of both treated cells did not significantly change up to 3 weeks (data not shown), which is in contrast with the studies of Rangappa *et al.*, who have reported formation of cytoplasmic processes, multinucleation and spontaneous beating after 3 weeks [166]. The apparent discrepancy may be due to the possibility that this study is strictly qualitative.

Numerous studies have demonstrated activation of cytokine cascades in the infarcted myocardium. In addition, persistent pro-inflammatory cytokine elevation has been associated with poorer clinical outcome in patients suffering recent MI. Induction and release of the proinflammatory cytokines IL-1, TNF-α, IL-6, and IL-8 are consistently found in experimental models and clinical cases of myocardial infarction [174]. Infarct healing is closely intertwined with an inflammatory cascade triggered by hypoxia and cardiomyocyte death. A vast body of evidence showed dramatic reduction in infarct size with the use of specific anti-inflammatory strategies [175]. Emerging evidence suggests that locally delivered MSCs can lead to an improvement in ventricular function, but the cellular and molecular mechanisms involved remain unclear. In order to confirm the immunotolerance property of ASCs and BMSCs in this study, an extreme model of xenogeneic mismatch from human to immunocompetent rat was chosen, as this would be immunologically more challenging. We previously reported the formation of stable cardiac chimera in mice/pig-to-rat models using bone marrow stromal stem cells [156, 157]. In accordance with these previous results, no significant inflammatory reaction was observed in the current human stem cell-transplantation study too. This is in contrast to the human fibroblast-transplanted group studies where a massive monocellular infiltration has been reported [154]. In fact, the myocardial pro/anti inflammatory cytokine analysis

after 6 weeks of implantation reveals that both ASCs and BMSCs have a positive impact on them, compared to the untreated control.

In the present study, hASC and hBMSC engraftment after coronary ligation also elicited an increase in EF% as compared to control, resulting in a significant improvement in ventricular function. These observations are in accordance with the findings of other investigators who have also shown an improvement in cardiac function using animal and human stem cell transplantation in animal models of myocardial infarction [176, 177]. However, the results are also contrary to that of Van der Bogt *et al*, who reported that there was drastic donor cell death after 4-5 weeks of transplantation [178]. In summary, the present study confirms that ASCs have immense potential in xenotransplantation for infarcted myocardium treatment. This notion is further substantiated by *in vitro* studies of hASCs in efficiently adopting cardiomyocyte phenotype and *in vivo* studies on left ventricular infarct size measurement and echocardiographic analysis, illustrating that hASCs are more potent in reducing scar formation and ameliorating cardiac dysfunction compared to hBMSCs, although the exact mechanism of cardiac improvement remains controversial. Furthermore, we have demonstrated that biodegradable polymeric microcapsules can be an efficient way to deliver hASCs for angiogenic applications [41]. This is an important point because recently we have demonstrated the immense potential of angiogenic therapy for myocardial infarction [42]. Previous studies have reported the differentiation of stem cells to cardiomyocytes in the cardiovascular environment, while others attribute the improvement in cardiac function to the paracrine activity of stem cells and/or cell fusion. Inducing a favorable inflammatory cytokine profile in the infarcted myocardium can also be a way by which ASC initiates its therapeutic effects. Further studies have to be done on the *in vivo* potential of hASCs with regard to their paracrine and angiogenic effect as compared with hBMSCs to properly understand the mechanism. Because of the unique immune-tolerance property of hASCs, these cells can be used as universal donor cells with fascinating therapeutic implications. From a clinical perspective, these cells could be harvested and mass-produced well in advance, tested for their

functional capabilities, and stored as a standardized cell population for immediate off-the-shelf use on any patient without delay after an acute myocardial infarction. Such logistic advantages are not available with the use of autologous stem cells as well as with hBMSC that are currently the cell source of choice. More importantly, the allogeneic hASCs can be obtained from young healthy donors, which could be of great value in patients with genetic cardiomyopathies and in elderly patients with advanced diabetes, heart failure, or cachexia whose own MSCs could be dysfunctional.

4.6 Acknowledgements

The authors would like to thank Minh Duong for her technical assistance in this work. This work is supported in part by research grant from Canadian Institute of Health Research (CIHR; MOP #64308) (to Prakash) and Natural Sciences and Engineering Research Council (NSERC) (To DST, SP and CE) Canada. A.P. acknowledges the financial support from NSERC Alexander Graham Bell Canada Graduate Scholarship.

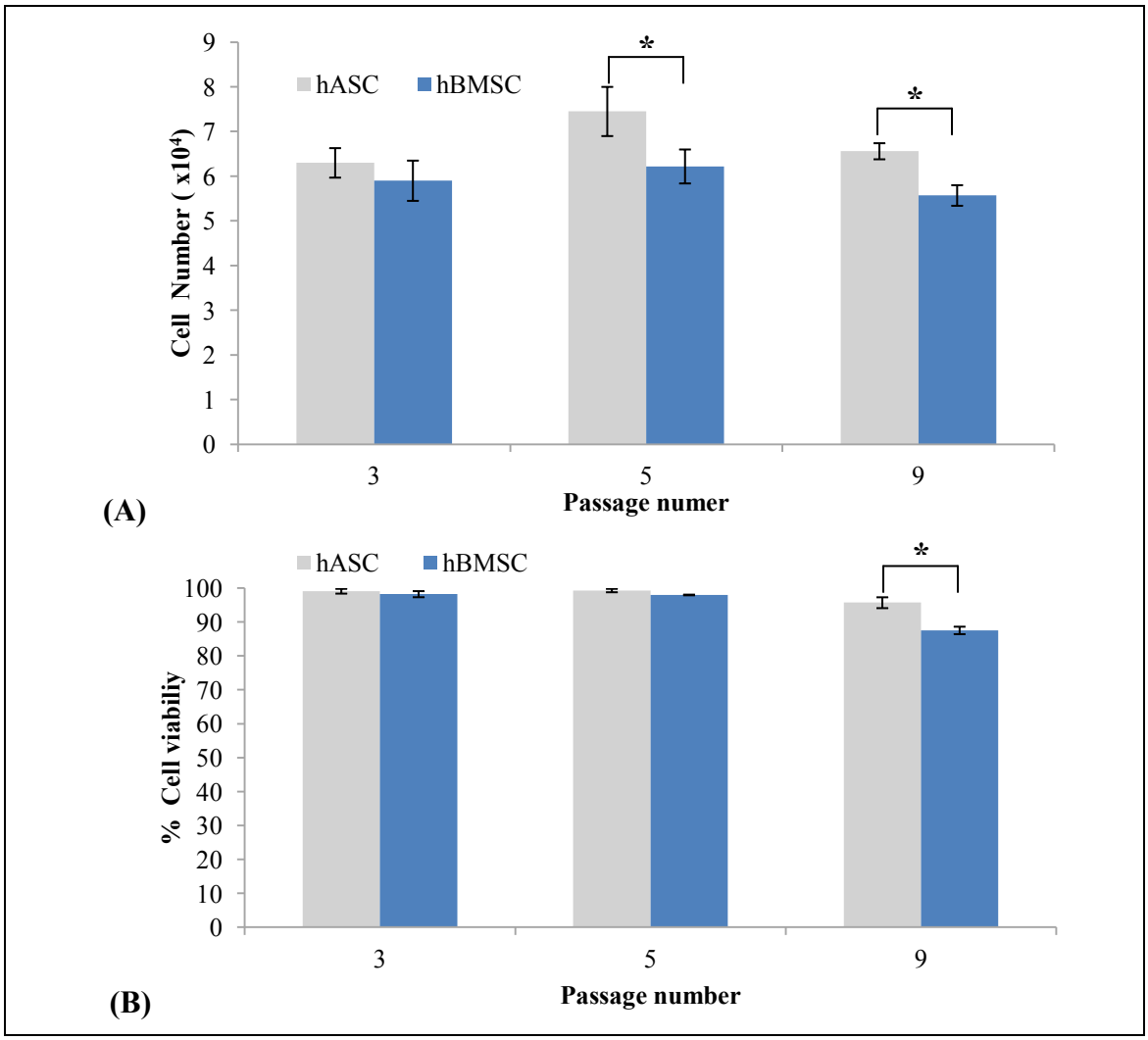

Figure 4.1: (A) Effect of passage number on cell proliferation of hASCs and hBMSCs under normoxic condition. $2x10^4$ cells from different passages were seeded per well in a 96-well plate and grown for 96h with normal MesenPro media (n=3). The data demonstrates highest proliferation in passage 5 in comparison to lower passage3 and higher passage 9. **(B)** Effect of passage number on percentage cell viability of hASCs and hBMSCs under 24h hypoxic condition with serum free media. The data demonstrates that there is no significant effect of hypoxic condition on both cell types in lower passages. Only in passage 9, there was a significant reduction in viability of hBMSCs in comparison to hASCs. Data are expressed as mean ± Standard Deviation (SD). * indicates comparison between groups which are significant ($p<0.05$).

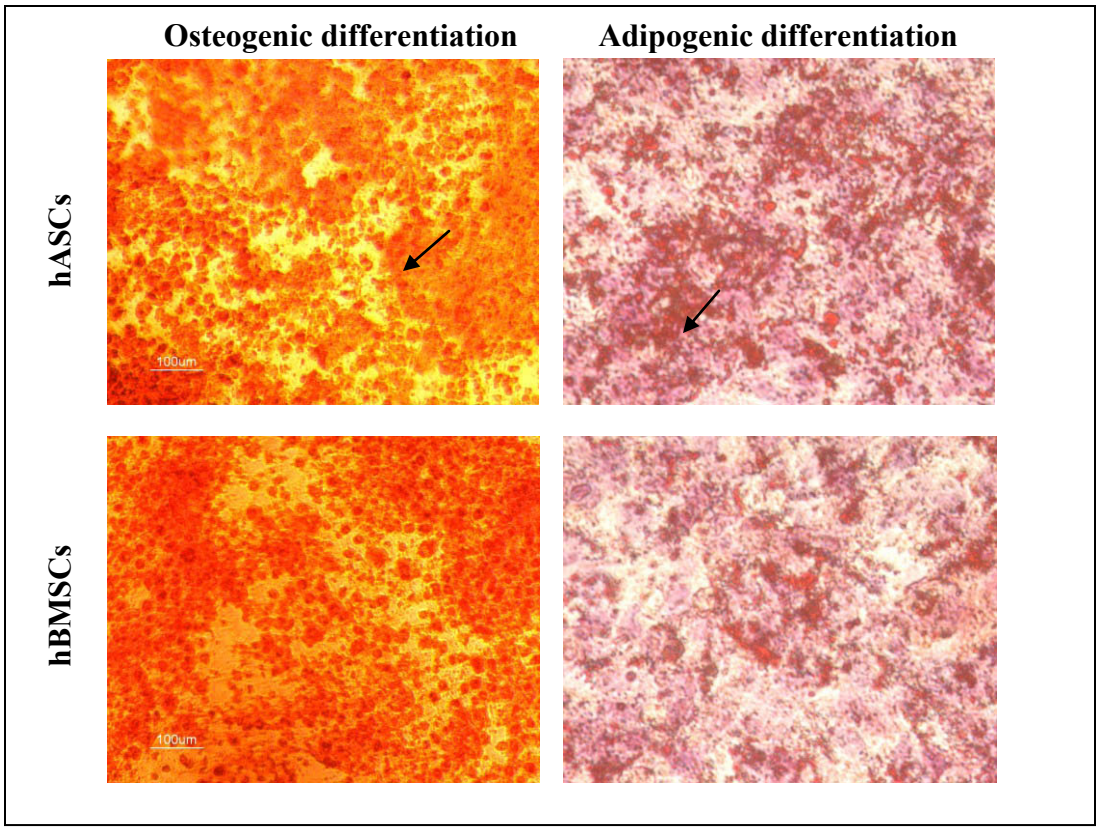

Figure 4.2: Differentiation potential of hASCs and hBMSCs into osteocytes and adipocytes**.** The cells, from passage 5, were seeded at high confluency for osteogenic and adipogenic differentiation using MesenPro media. After overnight culture, the media was replaced with respective induction media. After 21 days of osteogenic induction, the cells were stained with alizarin red to detect the osteogenically differentiated cells. Similarly the cells were stained with oil red O to detect the mature adipocytes. Both hASCs and hBMSCs showed proficient differential potential.

.

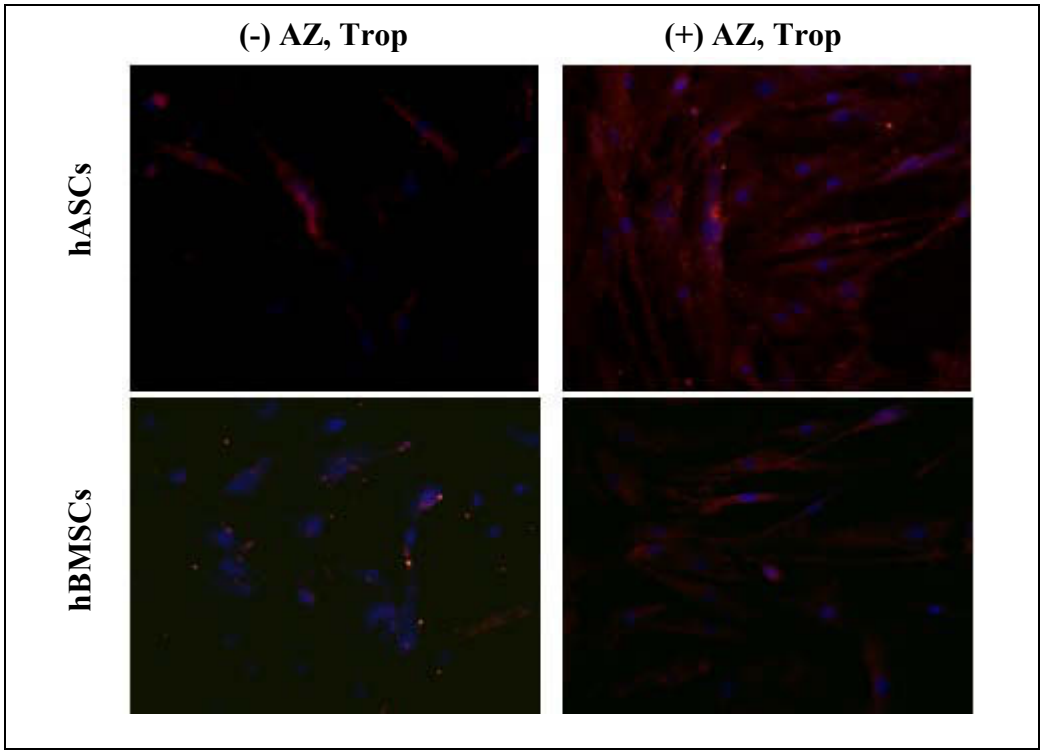

Figure 4.3: Expression of cardiac markers 3 weeks after treatment of hASCs and hBMSCs with 5-azacytidine (AZ). Immunocytochemistry of hASCs and hBMSCs, with and without 5-azacytidine treatment in week 3, for cardiac marker troponin I (Trop). The cells were counterstained with 4', 6-diamidino-2-phenylindole (DAPI) to stain the nucleus. Captured images, using a fluorescence microscope at 200X magnification, demonstrates a marked increase in the Trop staining in the cells treated with AZ compared to the untreated controls. In fact, the staining shows a much higher Trop expression in hASCs compared to hBMSCs.

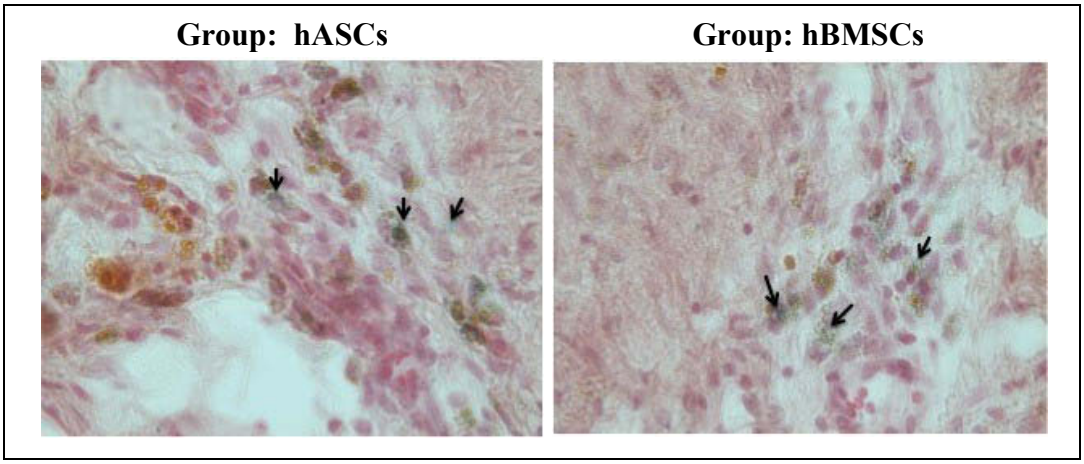

Figure 4.4: Retention of transplanted stem cells in the myocardium illustrated by the histological sections of infarcted rat myocardium stained with H&E and X-gal. The photograph, captured with a BX41 Olympus light microscope at 400X magnification, depicts the successful myocardial engraftment of LacZ expressing blue colored hASCs and hBMSCs (arrows) at the infarcted sites, harvested 6 weeks after coronary ligation. Note the absence of any significant inflammatory responses, such as invasion of neutrophils, despite the lack of any immunosuppression.

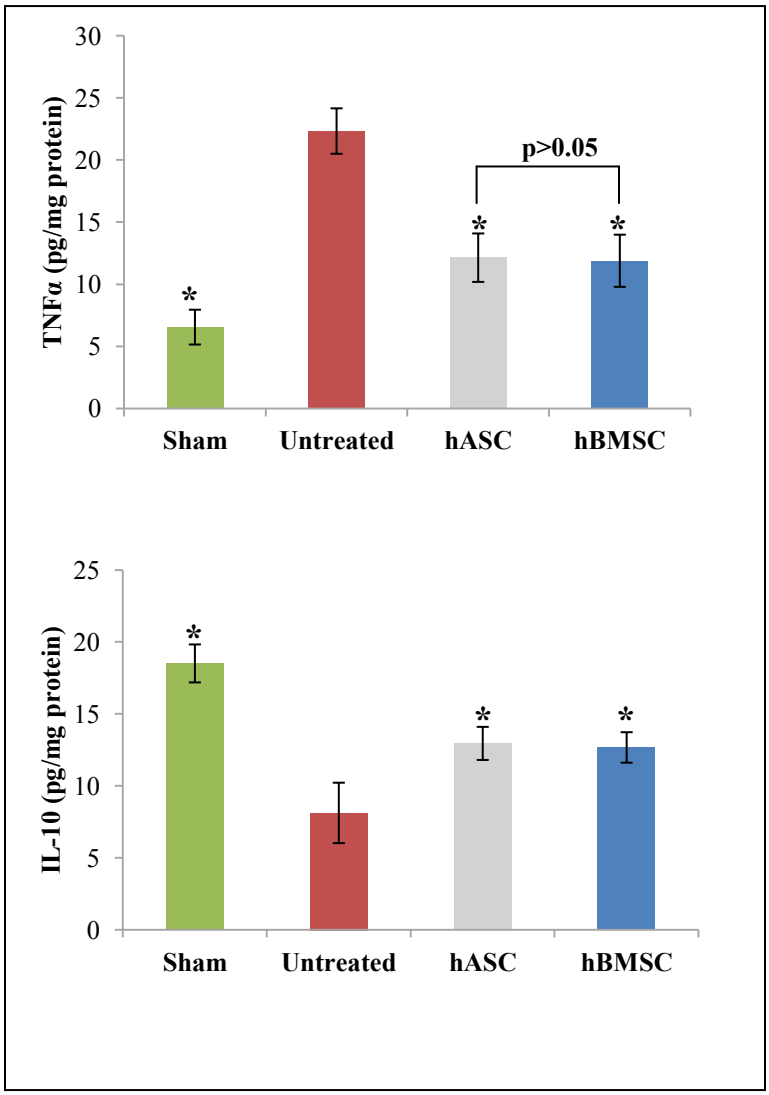

Figure 4.5: Quantification of TNFα and IL-10, measured as pg/ mg total protein, present in the LV infarct and peri-infarct area of untreated rats, hASC and hBMSC treated and sham operated rats, 6 weeks post infarction by ELISA. The data shows a significant decrease of TNF α and increase in IL-10 in the treated group compared to the untreated group. There were no significant differences in myocardial cytokine expressions between the treated hASC and hBMSC groups. Data are expressed as mean ±SD. * indicates $p<0.05$ vs. untreated rats.

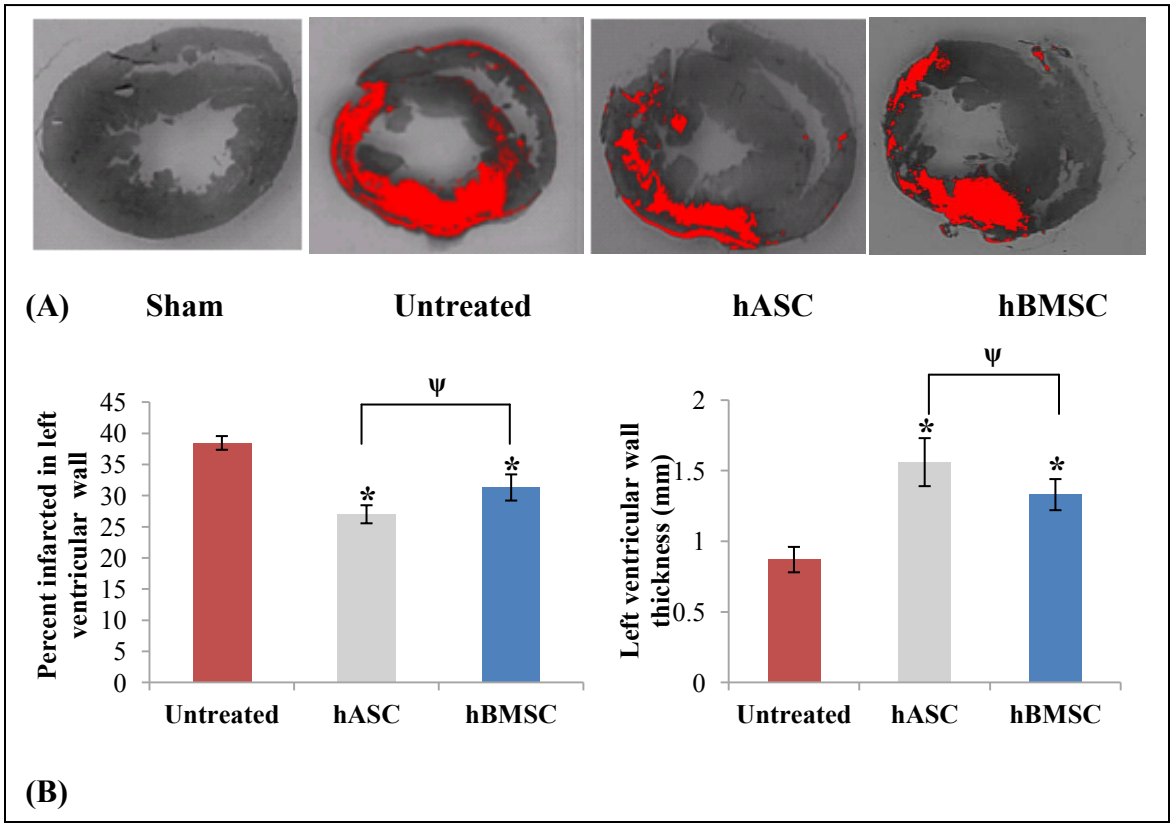

Figure 4.6: (A) Infarct scar area analysis. Representative images of LV myocardial sections stained with sirius red show the markedly decreased cardiac fibrosis after hASC and hBMSC transplantations 6 weeks post infarction compared to the control. The red area represents extracellular matrix deposition in the scar tissue and the fainter orange area represents the myocardium. **(B)** Semi-quantitative analysis of the images of the stained collagen fractions, using ImageJ software, show that hASC and hBMSC transplantations significantly decreased cardiac fibrosis compared to untreated group (n=8) in terms of percent infarction size in LV wall. Moreover, hASC and hBMSC groups have significantly thicker LV walls than untreated group. In both analyses, hASC treatment proved to be significantly better than hBMSC treatment. Data are expressed as mean ±SD. * indicates $p<0.05$ vs. untreated control groups. ψ indicates $p<0.05$ between groups hASC and hBMSC.

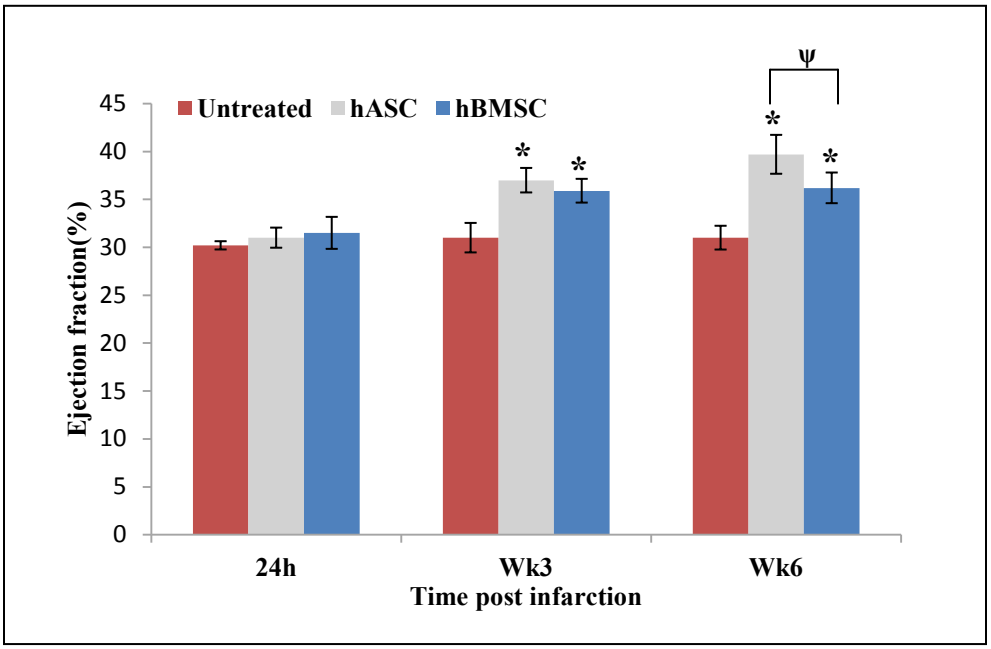

Figure 4.7: Echocardiographic assessment of cardiac function. Effect of stem cell transplantation on cardiac function was analyzed over 6 weeks post infarction. For this, heart EF% was monitored at 24h, week 3 and week 6 after transplantation of medium (n=14), hASCs (n=14) and hBMSCs (n=14) in rat myocardial infarction model using M-mode echocardiograms. The EF% increased significantly after treatment in the hASC and hBMSC groups over the 6 weeks span, but the untreated control group did not show any sign of improvement. The EF% was significantly higher in the treated groups compared to the control at week 3 and 6 after treatment. Furthermore, hASC group showed a significantly better EF% than hBMSC group at wk 6 post transplantation. Data are expressed as mean ±SD. * indicates $p<0.05$ vs. untreated control groups. ψ indicates $p<0.05$ between groups hASC and hBMSC.

Superior cell delivery features of genipin crosslinked polymeric microcapsules: preparation, *in vitro* characterization and pro-angiogenic applications using human adipose stem cells

Arghya Paul[1], Arielle Cantor[1], Dominique Shum-Tim[2], Satya Prakash[1]*

[1] Biomedical Technology and Cell Therapy Research Laboratory, Department of Biomedical Engineering, Faculty of Medicine, McGill University, 3775 University Street, Montreal, Quebec H3A 2B4, Canada.

[2] Cardiothoracic Surgery and Surgical Research, Royal Victoria Hospital, Room # S8.73B 687 Avenue Des Pins Ouest, Montreal, Quebec H3A 1A1, Canada.

*Correspondence author; Email: satya.prakash@mcgill.ca
Tel: +1-514-398-3676; Fax: +1-514-398-7461

Preface: To improve the delivery efficiency of the transplanted adipose stem cells, here we formulated polymeric microcapsules to encapsulate the cells using naturally derived cross-linker genipin, chitosan and alginate. The polymeric membrane not only maintained the cell growth and viability, but also maintained its differentiation potential. Moreover, the entrapped cells also retained their natural ability to secrete biologically active angiogenic factor.

Original article published in ***Molecular Biotechnology.*** **48(2):116-27 (2010).**

5.1 Abstract

The ability of mesenchymal stem cells to self-renew and differentiate into specialized cell lineages makes them promising tools for regenerative medicine. Local injection and use of scaffolds had been employed earlier to deliver these cells; yet, an optimal delivery system remains to be identified. Here, using genipin, which is a non-toxic natural cross linker for proteins, we prepared alginate-chitosan polymeric microcapsules (GCAC) to develop an efficient stem cell delivery system. We investigated the properties of this membrane along with the encapsulated adipose tissue derived stem cells (ASCs) and compared that with the widely used alginate poly-lysine (APA) membranes. The GCAC membrane was able to support cell viability, augment cell growth and showed better results under external rotational and osmotic pressures with about 30% of the ruptured capsules in comparison to 60% ruptured APA capsules. The membrane also provided immune-protection to the entrapped cells as demonstrated by the lymphocyte proliferation assay. The capsule also has potential for long-term storage. The encapsulated four million ASCs also showed steady secretion of approximately 4600pg vascular endothelial growth factor (VEGF) over 15 day time period comparable to that of free cells. Furthermore, the encapsulated ASCs showed around 3.8-fold increase in VEGF secretion after 72 h hypoxic conditions in comparison to normoxic conditions. This increased VEGF expression resulted in improved angiogenic potential of the bioactive capsules as noted by enhanced endothelial cell growth. GCAC encapsulation also did not show any effect on their differentiation ability. Thus, because of these biocompatible and bioactive attributes, genipin cross-linked polymeric microcapsules can emerge as a potentially important tool for improved stem cell-based therapy and cell delivery applications.

Keywords: microcapsules, regenerative medicine, biomaterials, angiogenesis, tissue engineering, stem cell delivery

5.2 Introduction

Mesenchymal stem cells show significant potential in terms of their ability for regenerating various tissues and organ systems due to their capacity for self-renewal, extensive proliferation and multi-lineage differentiation. Most research in the field of stem cell-based therapy has considered bone marrow-derived mesenchymal stem cells (MSCs) as potential donor cells; however, attention has recently shifted to a unique pool of mesenchymal stem cells located within the adipose tissue stroma, namely adipose tissue-derived stem cells [179]. Both MSCs and ASCs have high proliferative rates and can self-renew [180]. They can also differentiate towards specialized cell lineages [181]. Despite these similarities, ASCs do possess several advantages over the traditionally used MSCs. MSCs are of limited clinical use as they are not abundant when harvested from the bone marrow stroma and are difficult to isolate [182]. Conversely, ASCs represent a promising cell source since not only are they pluripotent in nature, but they are readily available and easily isolatable in large numbers from the adipose tissue of patients [180, 181, 183, 184]. In addition, unlike MSCs, ASCs retain their differentiation potential irrespective of donor age [185]. ASCs also have natural ability to secrete vascular endothelial growth factors and induce angiogenesis. Thus they are being used *in vivo* for treating myocardial infarctions [186, 187]. Thus ASCs are of immense importance in the field of tissue-engineering and regenerative medicine [188-190].

In order for ASCs to be introduced into the clinical setting, an ideal means of cell delivery is crucial – one that delivers an optimal number of cells to target sites within the body and ensures maximal cell survival, proliferation and differentiation ability, as well as immune protection and diminished mechanical stress. Local injection and intravenous infusions have been used as methods to deliver cells, but yield unfavorable results as the implanted cells are washed out into their surrounding microenvironment and their retention potential is strongly compromised. The likelihood of immune rejection is also high [168]. Transplantings via three-dimensional scaffolds is an approach that has been introduced to prevent this critical issue. Seedings onto scaffolding systems is a

commonly used method to provide a suitable environment for cell colonization, proliferation and differentiation. A variety of biomaterials have been used to create scaffolds including type I collagen, a biocompatible polymer onto which the cells have a high affinity [191] and poly lactide-co-glycolic acid, a biodegradable polymer supporting cell stability [192]. However, a large proportion of these scaffolds display poor biomechanical properties as they degrade quickly and are highly deformable *in vivo* [192, 193]. Further, cells seeded on scaffolds are exposed and can thus promote inflammatory reactions upon transplantation. To date, the most favorable stem cell delivery system remains unidentified.

Microencapsulation technology could be a potential stem cell delivery system. This system involves trapping cells in a semi-permeable polymer membrane, to allow free bi-directional exchange of oxygen, nutrients and waste between entrapped cells and their environment, while excluding the influx of immune cells [194, 195]. Theoretically, cells can be implanted without immune-suppression since the capsule membrane physically protects them. This is a significant advantage that cell-based microencapsulation has over scaffolding systems since encapsulation protects the cells not only from mechanical stress, but also from the host's immune response [194]. To ensure immune protection of the cells, the microcapsule membrane must exhibit sufficient rigidity so as to withstand the implantation process and environmental conditions *in vivo*. It is vital to design membranes using biomaterials that ensure protection of the cells. Various polymers have been implicated in the encapsulation process, but most research in this field has focused on alginate-poly-L-lysine-alginate (APA) microcapsules. Alginate, a naturally derived poly-anionic polysaccharide extracted from brown seaweed, serves as the capsule core. It is bound to the poly-cation poly-L-lysine (PLL) via electrostatic interactions to form an outer coating [196, 197]. Despite the extensive use of APA microcapsules and their ability to support cell viability, several studies have demonstrated that they lack mechanical strength and stability when applied over the long-term *in vivo*, leading to leakage

of the encapsulated cells [196, 198]. Previous research has also shown that the addition of PLL to alginate may stimulate necrosis of the encapsulated cells [199].

Present study focuses on developing and investigating the potential of a new genipin cross-linked alginate-chitosan (GCAC) microcapsule as an alternative to APA microcapsules and evaluates its prospect for stem cell transplantation using human ASCs. The capsule has an alginate-calcium core, which is later complexed with chitosan, a naturally derived polycation, on the exterior via electrostatic interactions. To further increase the capsular strength, chitosan can be covalently cross-linked to genipin, a naturally derived biocompatible iridoid glucoside from Gardenia fruit [200, 201]. This formulation would allow genipin to diffuse freely through the alginate-chitosan membrane and link to the amino groups in chitosan bound to the alginate core. Using genipin as a cross-linking agent allows for clear visualization of the microcapsule membrane under fluorescence field microscopy [196, 200, 202]. The *in vitro* properties of the encapsulated cells and microcapsules were characterized and compared with that of APA microcapsules for implications in stem cell transplantations. Further studies were also done to explore the angiogenic potential of microencapsulated ASCs under hypoxic and normoxic conditions by investigating their ability to secrete bioactive levels of the angiogenic growth factor such as VEGF [203].

5.3 Materials and methods

5.3.1 Chemicals

Low viscosity alginic acid sodium salt from brown algae (viscosity: ~250 cP, 2 % in water at 25 °C) and poly-L-lysine hydrobromide (PLL; Molecular weight 27,400) were bought from Sigma Chemicals (St. Louis, MO). Chitosan (low viscosity, Mv = 7.2 x 10^4 by viscometry, degree of deacetylation at 73.5% by titration) and genipin were purchased from Wako BioProducts, USA.

5.3.2 Cell culture

Human ASCs (n=1 donor) were obtained from Invitrogen and cultured in DMEM (Invitrogen) supplemented with 10% fetal bovine albumin (FBS). The

cells were routinely maintained as stationary cultures in 75 cm^2 tissue culture flasks and incubated at 37^o C in a controlled environment with an air atmosphere of 5% CO_2. Human umbilical vein endothelial cells (HUVECs) (Sciencell, Carlsbad, California, USA) were cultured and expanded on tissue culture flasks according to the supplier's instructions. They were cultured in endothelial cell medium (ECM) (Sciencell, Carlsbad, California, USA) supplemented with 5% FBS and placed in an incubator containing 5% CO_2 at 37°C.

5.3.3 Preparation of polymeric microcapsules

To prepare the microcapsules, 1.5% sodium alginate solution in de-ionized water was sterile filtered through a 0.22 µm filter. The solution was extruded through an encapsulator (Inotech Corp) using a 300 µm nozzle. The gelation process took place in a 0.1 M $CaCl_2$ solution for 20 minutes. To prepare the GCAC microcapsules, the alginate core beads were then coated with a chitosan layer by immersing them in a chitosan solution (2%) dissolved in dilute acetic acid at a pH of 5.2 for 30 min [200]. Subsequently, the beads were washed twice in normal physiological solution and immersed in genipin solution (5 mg/mL) for 24 hours at 37^o C to promote cross-linking with the chitosan layer. The APA microcapsules were prepared by immersing the alginate capsules in a 0.05% PLL solution dissolved in 0.45% NaCl for 10 minutes. After washing the APA microcapsules twice with physiological solution, they were re-coated with a layer of 0.1% alginate for 5 minutes.

5.3.4 Transduction of ASCs with the LacZ retrovirus

Transductions were performed on the ASCs using the E86 retroviral vector containing the LacZ gene. Viral supernatants were filtered through 0.80 µm filters and infected the cells. 10 mL of viral supernatant and 4 µg/mL polybrene (Sigma) were added to the cells. After 24 hours, the medium containing the viral supernatant was removed and replaced with fresh medium. This procedure was repeated twice. To confirm the efficiency of transduction, an aliquot of transduced ASCs was re-plated in a 6-well plate and stained with the

chromogenic substrate X-gal for detection of β-galactosidase activity. Transduction efficiencies of the cells were 70% - 80%.

5.3.5 Preparation of GCAC & APA microcapsules containing transduced ASCs

Calcium-alginate beads containing s were generated using an encapsulator (Inotech Corp) with a 300 μm nozzle, which dispenses droplets of 1.5% sodium alginate solution containing cells (0.5 x 10^6 cells/mL) into a constantly stirring solution of 0.1 M $CaCl_2$. After 20 minutes of stirring, the newly generated beads were coated with a chitosan layer by immersing them in a chitosan solution for 30 minutes. This was followed by genipin cross-linking to the chitosan layer. To prepare APA microcapsules containing ASCs, the stem cells (0.5 x 10^6 cells/mL) were re-suspended in alginate solution and extruded through the nozzle of the encapsulator. The subsequent coating methods were performed using similar procedures to those involved in the preparation of empty microcapsules as mentioned above. The resulting microcapsules were thoroughly washed, replenished with fresh media to promote cell growth and placed in a 37^o C incubator containing 5% CO_2.

5.3.6. Monitoring cell growth within GCAC and APA microcapsules

Growth within the microcapsules was determined using viability assay kit (Biotium, Inc., Hayward, USA). The live cells were detected by the intracellular esterase mediated conversion of non-fluorescent cell-permeant poly-anionic calcein AM dye to fluorescent green calcein (ex/em ~495 nm/~515 nm). EthD-III enters cells with damaged membranes and upon binding to nucleic acids, produces bright red fluorescence in dead cells (ex/em ~530 nm/~635 nm) [204]. For this, 1000 GCAC and 1000 APA microcapsules encapsulating ASCs were washed with Phosphate Buffered Saline (PBS). The ASCs were recovered from the microcapsules by treating the microcapsules with 27 mM NaCl solution containing 100 mM sodium citrate and 10 mM MOPS (Sigma-Aldrich) for 1 hour at room temperature [204]. The fully broken and semi-dissolved microcapsules

were then centrifuged at 800 rpm for 7 minutes to recover the free cells from the pellet, leaving the sodium citrate solution and capsular parts in the supernatant. The cells were washed three times with PBS to get rid of the excess sodium citrate solution containing dissolved polymeric debris. After staining the recovered cells with calcein AM and EthD-III according to the manufacturer's protocol (PBS containing 2 μM calcein AM and 4 μM EthD-III), the number of viable cells were calculated using hemocytometer and fluorescence microscope. Results were expressed as mean ± standard deviation from triplicate experiments.

5.3.7 Mechanical and osmotic stability of GCAC and APA microcapsules

The mechanical and osmotic stability of the microcapsules was determined using a rotational stress test and an osmotic pressure test [199]. These tests were performed by subjecting 50 ± 5 APA and 50 ± 5 GCAC microcapsules encapsulating ASCs, which were previously stored in a saline solution (0.85% NaCl), to a hypotonic solution of de-ionized water and rotation in a shaker flask at a speed of 150 rpm. The number of un-ruptured microcapsules was observed and counted at various time intervals under a light microscope.

5.3.8 *In vitro* immunoisolation effect of GCAC microcapsules by lymphocyte proliferation assay

Rat peripheral blood lymphocytes were isolated from Sprague-Dawley rats after cardiac puncture by Percoll gradient centrifugation followed by removal of monocytes by plastic adherence as per standard protocol mentioned elsewhere [205]. The isolated lymphocytes were grown in DMEM media supplemented with 10% FBS. Lymphocytes are taken as the responding cell populations while the encapsulated or non-encapsulated ASCs were taken as the stimulating cell populations. The lymphocytes were seeded at 10^4 cells per well in a HTS Transwell-96 well plate (Corning, NY, US) with tissue culture treated receiver wells. As positive control for the co-culture, free ASCs at 10^5 cells per insert in the transwell. As experimental groups, 10^5 encapsulated cells in GCAC capsules,

10^5 encapsulated cells in alginate-chitosan (AC) capsules and 10^5 encapsulated cells in uncoated alginate core capsules were used in the inserts. As negative control, empty GCAC capsules, empty AC capsules and empty alginate core capsules were used in the insert. The experiment was done in triplet per group. After 72h of co-culture, the insert was removed the lymphocyte population was quantified using non-radioactive cell proliferation MTS assay (Promega, Madison, Wisconsin, US) at 490nm absorbance in 1420-040 Victor3 Multilabel Counter (Perkin Elmer, Ontario, Canada) as mentioned elsewhere [206].

5.3.9 Quantification of endothelial growth factor released from encapsulated cells by ELISA

ASCs have angiogenic potential by which they naturally secrete VEGF and induce angiogenesis [186, 187]. To check whether encapsulated s could maintain this angiogenic potential, $4x10^6$ ASCs were encapsulated in GCAC and APA microcapsules and grown under standard conditions for 15 days. Conditioned media were collected from time to time and VEGF release was quantified using a VEGF ELISA kit (R&D Systems). Data are expressed as mean ±SD picogram secreted from the 4 $x10^6$ cells. Non-encapsulated free cells were taken as the standard and empty capsules were taken as the negative control.

5.3.10 Induction of hypoxic condition in encapsulated hASCs

ASCs were encapsulated in microcapsules, as described above, and grown for 3 days so as to allow them to stabilize in the new environment. On the following day, the media from the cultures were replaced with fresh media containing 5% FBS and the flasks were placed in either normoxic (21% O_2) or hypoxic (1% O2) conditions for 72 h [203]. To induce the hypoxic condition, a modular incubator chamber from Billup-Rothenberg Inc. was used. At the end of the incubation period, the conditioned media from culture flasks were collected. Conditioned media from the culture flasks were collected and the VEGF release was quantified using a VEGF ELISA kit according to manufacturer's protocol.

5.3.11 Evaluation of bioactivity of released VEGF by HUVEC proliferation assay

For the cell proliferation assay, $1x10^4$ HUVECs per well were seeded in 96 well plate in triplicate for each sample using standard ECM media. After culturing overnight, the cells were washed twice with PBS and 200µl of the conditioned media from the encapsulated cells under hypoxic/normoxic conditions were added to the cells along with 50µl of normal ECM media. The cells were grown at 37°C in 5% CO_2 for 96h followed by MTS cell proliferation assay according to the manufacturer's protocol.

5.3.12 Cryopreservation study using GCAC and APA microcapsules

The possibility for long-term storage of encapsulated ASCs in both GCAC and APA membranes was tested. For this, the microencapsulated cells were re-suspended in fresh freezing media containing 10% FBS and 10% DMSO. After 30 days of storage, the microcapsules were thawed using a 37°C water bath and re-cultured in fresh medium for 3 days to acclimatize. Then the numbers of viable cells were assessed after capsule depolymerization followed by calcein AM and EthD-III staining as mentioned earlier.

5.3.13 Osteogenic & adipogenic differentiation of ASCs following capsule depolymerization

As mentioned earlier, ASCs were recovered from the microcapsules by treating the microcapsules with NaCl solution containing 100 mM sodium citrate and 10 mM MOPS for 1 hour at room temperature. The PBS washed cells were then re-suspended in culture media. They were then seeded in a 24-well plate at a high confluency of 6x 10^4 cells/well. After 24 hours, the medium was replaced with either adipogenic or osteogenic differentiation medium (Invitrogen) [165]. After the induction period, cells were stained with either LipidTOX Red neutral

stain (Invitrogen) to assess adipogenic differentiation or Alizarin Red stain to assess osteogenic differentiation.

5.3.14 Statistical analysis

One-way analysis of variance (ANOVA) was used to compare means between groups. For all analyses, a level of $p < 0.05$ was used to indicate statistical significance.

5.4 Results

5.4.1 GCAC microcapsules support ASC viability and growth

To test the ability of GCAC microcapsules to support ASC viability and proliferation, the cells were transduced with the LacZ retrovirus and encapsulated in alginate microcapsules coated with chitosan and genipin layers using standard microencapsulation technique depicted in **Figure 5.1**. Cell viability was confirmed from time to time for a period of 15 days using LacZ staining to detect the encapsulated viable blue cells (**Figure 5.2A**). The number of viable cells was quantified using a fluorescence-based method employing calcein AM and EthD-III dyes every alternate day. **Figure 5.2B and 5.2C** confirms the proper cross linking of genipin with chitosan emitting green fluorescence on the outer surface of the capsule under confocal microscope [200, 202]. The green dots inside the capsules confirm the viable calcein stained cells.

Figure 5.3 represents the average number of viable cells number per capsule for APA and GCAC microcapsules at various time intervals. Both APA and GCAC microencapsulated cells showed a rapid increase in average cell number per capsule from 60 to 110 within the first nine days after their encapsulation. Following this period, there was a much slower cell growth and the cell number remained between 115 and 120 till day15 in both type of membranes.

5.4.2 GCAC microcapsules display improved mechanical and osmotic stability

To evaluate the physical integrity and stability of both GCAC and APA microcapsule membranes, 50 ± 5 microcapsules containing ASCs were subjected to rotational stress and osmotic pressure tests. After exposure to both mechanical shaking and osmotic stress for a continuous period of 120 minutes, approximately 30% of the GCAC microcapsules burst, in contrast to an approximate 60% rupture in APA microcapsule membranes (**Figure 5.4**).

5.4.3 GCAC microcapsule membranes have immune-protective potential

In order to assess the immune-protective nature of the microcapsule membrane, GCAC microcapsules containing ASCs were co-cultured with rat lymphocytes for 72h. Non-treated lymphocyte (media only) count was normalized to 1.0 and the cell counts of other groups were calculated as fold increase with respect to it. The result in **Figure 5.5** shows that lymphocytes treated with free cells show highest proliferation (2.7 times) in comparison to GCAC encapsulated cells (1.22 times). The lymphocyte response was higher (1.51 times) when the outer genipin layer was not given to the AC capsules, proving that genipin gives an extra protection to the encased cells. In absence of any polyelectrolyte layer the alginate core was unable to give any protection to the encased cells, which showed 2.41 times lymphocyte proliferation with respect to control. On the other hand, empty capsules of all groups did not show any sign of significant immune stimulation. This is evident from the data of **Figure 5.5** where the lymphocyte proliferation stayed normal and very close to the control.

5.4.4 GCAC and APA microencapsulated ASCs retain natural VEGF release potential

The data in **Figure 5.6** shows that cells encapsulated in both GCAC and APA microcapsules secreted an average of 7360 pg and 7060 pg of VEGF respectively, on Day 1, whereas free ASCs taken as the control expressed an average of 4967 pg VEGF. This temporary increase in VEGF release of the

encapsulated cells is possibly because of the stress conditions, like partial hypoxia and shear stress, induced on the cells during the entire encapsulation procedure [203, 207]. Thus, from day 3 onwards, when the stressed conditions were reduced and the cells were stabilized inside the capsules, the amounts of VEGF released by all the groups were very similar (around 5000pg), except the empty GCAC capsules, and maintained the steady release all throughout the remaining two weeks.

5.4.5 Enhanced angiogenic potential microencapsulated hASCs under hypoxic condition

Under hypoxic condition, $4x10^6$ encapsulated cells secreted around 3.8 times more VEGF than under normoxic condition (18.08ng in comparison to 4.77ng) as seen in **Figure 5.7A**. To check the biological activity of the released VEGF protein from encapsulated hASCs, HUVEC proliferation assay was performed on the hypoxic and normoxic conditioned media from encapsulated cells [203]. Only media was taken as the control. As reported through **Figure 5.7B**, the samples with high VEGF concentrations, i.e. from hypoxic conditioned media, significantly increased the proliferation rate of HUVECs (1.62 times under hypoxic and 1.19 times under normoxic conditions where 1.0 times proliferation was taken as the baseline for normal media). This is an important finding as hASCs are often delivered to places where there is a local hypoxic condition, like ischemic heart or limb. Thus this finding expands the application of the microcapsules for stem cell delivery.

5.4.6 GCAC microcapsules have long-term storage potential

The ability of both GCAC and APA membranes to withstand the effects of freezing was tested at -80^{o} C for a 30-day period. Once thawed and cultured for 3 days, the cell viability within the GCAC microcapsules was only slightly reduced from average 120 cells per capsule to 95 cells per capsule as seen in **Figure 5.8**. On the other hand, APA microencapsulated cells revealed a significantly decreased viable average number (65 cells per capsule) in comparison to that of GCAC capsules.

5.4.7 ASCs maintain their differentiation potential following GCAC microcapsule depolymerization

To determine if ASCs are able to retain their natural differentiation potential following the encapsulation period, GCAC microcapsule membranes were depolymerized. The ASCs were then cultured in either osteogenic or adipogenic differentiation media. Osteogenic differentiation was assessed using Alizarin Red staining after a 21-day period of induction towards this lineage. After a 15-day period, adipogenic differentiation was evaluated by LipidTOX Red neutral lipid staining. The presence of calcium deposits following osteogenic induction, as well as lipid vacuoles following adipogenic induction, are indicative of the ASCs' ability for multi-lineage differentiation after capsular degradation (**Figure 5.9A and B**).

5.5 Discussion

ASCs harbor important properties for cell-based therapies in particular, relating to their inherent pluripotency and large biomass potential, yet an ideal means of delivering these cells to target areas within the human body remains unidentified. In the current study, the potential of GCAC membranes as a method for human ASC microencapsulation was investigated.

The growth kinetics of ASCs was similar in both the commonly used APA microcapsules and the GCAC microcapsules, as assessed by calcein AM fluorescence. This confirms that these naturally derived polymers, namely alginate, chitosan and genipin, are biocompatible and do not negatively impact cell viability. While cell viability within both APA and GCAC microcapsules were comparable, the GCAC membranes did exhibit marked improvements in response to other employed constraints when compared to the standard APA microcapsules. The transduced encapsulated cells stably expressed its LacZ transgene from within the capsules. This suggests that modifying these cells to express therapeutic factors prior to encapsulation can serve to further enhance the regenerative process and induce cell based gene therapy. Fluorogenic analysis of the encased cells established cell survival and proliferation within the microcapsules.

The rotational and osmotic pressure test indicated that incorporating chitosan to the alginate core, followed by genipin cross-linking, can greatly enhance capsular integrity, compared to simply coating the alginate core with a solution of PLL. APA microcapsules were formed via electrostatic interaction between the poly-anionic alginate core and the poly-L-lysine poly-cation coat. GCAC microcapsules were hypothesized to exhibit improved stability since not only were they formed by electrostatic interactions between the carboxyl groups in alginate and the primary amine groups in chitosan, but the ester groups in genipin can then covalently cross-link to the amine groups in chitosan. The observed increased stability of GCAC membranes may be a result of the strong covalent interaction between chitosan and genipin, thereby forming a denser network at the capsular membrane [196]. Preserving microcapsule integrity is of vital importance for *in vivo* maintenance. The durable nature of the GCAC membrane is an important property for the applicability of these microcapsules within the natural, but harsh environment of biological systems. Our *in vitro* results on immune protection of encapsulated ASCs within GCAC membranes demonstrated that GCAC microcapsules confer effective protection against foreign cells (lymphocytes). However, extensive analysis is needed to be done *in vivo* to detect the innate immune response against the encapsulated cells, as recent works have reported that there is ample chance of having incompatibility reactions once the biopolymers come in contact with the vascular system [208]. Moreover, for this work the hASCs used were the one commercially available and donated by one person. In order to have a more significant data, the numbers of donor ASCs have to be increased.

GCAC encapsulated cells also demonstrated a greater ability to withstand the effects of freezing and the re-culturing process as compared to APA encapsulated cells. This is an important quality that can help bring this technology to a large scale. Finally, encapsulated ASCs were able to differentiate into both adipogenic and osteogenic lineages following GCAC microcapsule depolymerization, demonstrating that the encapsulation process does not affect the inherent differentiation potential of these cells. Further studies are needed to

done quantify the levels of differentiation of the encapsulated and free cells using extraction based assays and techniques such as PCR for lineage specific gene expression patterns. The retention of natural angiogenic factor release potential of the ASCs, as seen by the VEGF release over time, also reconfirms that the microenvironment of the encapsulated cells possibly creates a less hostile and more hospitable environment to the cells, which is crucial for efficient cell delivery. The steady release of VEGF from encapsulated cells similar to that of the free cells from day 3 onwards substantiates the fact that there was no hypoxic condition and no external shear stress on both the GCAC and APA encapsulated cells after the third day of encapsulation [203, 207]. The angiogenic potential of the encapsulated cells under hypoxic condition extends the application of the technology. This is because recent works have shown that hypoxic preconditioning of stem cells has immense effect on its therapeutic potential, cell survival and angiogenesis [209-213].

The polymers used to create the microcapsule membrane are biodegradable; therefore it is essential that once the microcapsule disintegrates, the cells maintain their natural stem cell-like properties. The present research focused mainly on the *in vitro* properties of the GCAC microcapsule formulation for ASCs delivery. In order to test the full potential of these microcapsules, additional studies are required to assess the mechanical stability, as well as to confirm the biocompatibility of GCAC microcapsules *in vivo*. Our recent animal study data with APA microcapsules have already shown the effectiveness of microencapsulation technology in myocardial transplantation [214]. Further characterization of the genipin-chitosan cross-linking reaction may help us to further validate the effectiveness of these membranes over APA membranes. Nonetheless, from our *in vitro* results GCAC microcapsules could represent a novel platform for stem cell delivery and transplantation. Merging the fields of microencapsulation and stem cell-based therapy thus has significant applicability for the clinical setting.

5.6 Acknowledgments

This work is supported by research grant to S.P. from Canadian Institute of Health and Research (CIHR MOP 64308) and Natural Sciences and Engineering Research Council (NSERC, Canada) (to D.S. and S.P.). A.P. acknowledges the financial support from NSERC Alexander Graham Bell Canada Graduate Scholarship**.** A.C. acknowledges Faculty of Medicine NSERC Undergraduate Student Research Award.

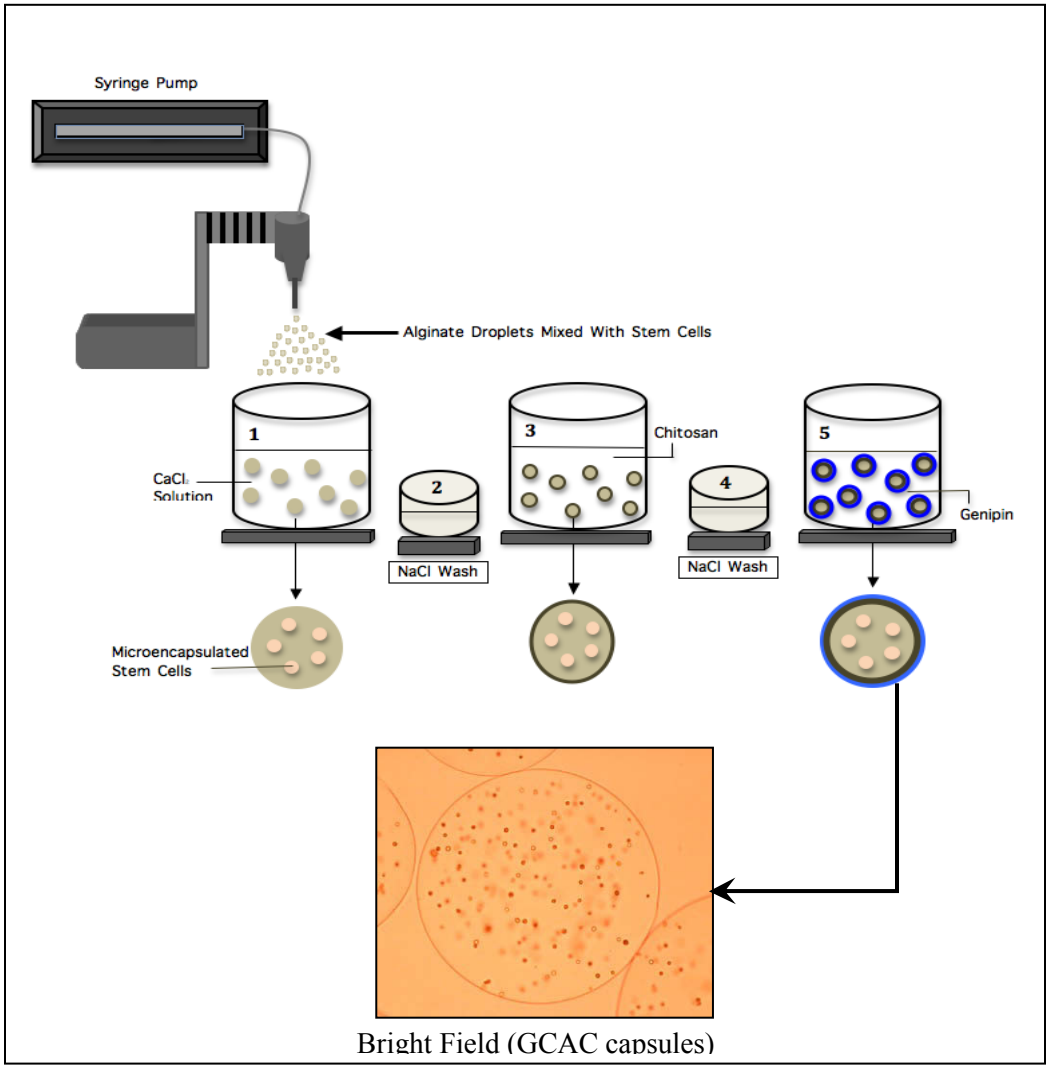

Figure 5.1: Microencapsulation of ADSCs by GCAC microcapsules. A mixture of ASCs (0.5x 10^6 cells/ mL) and alginate (1.5%) was extruded through the nozzle of an encapsulator into a stirred solution of 0.1 M $CaCl_2$ (1) for 20 minutes of mixing. The calcium-alginate beads were then washed (2) with NaCl (0.85%) and coated (3) with a chitosan solution (2%) for 30 minutes, resulting in alginate-chitosan beads. After being washed (4), the beads were cross-linked (5) by a genipin solution (5 mg/mL) for 8 hours at 37°C. The resulting microcapsules were washed, replenished with fresh media and stored in an incubator at 37° C containing 5% CO_2. The bright field picture of the encapsulated cells shows the outer smooth and even surface of the microcapsules (200X).

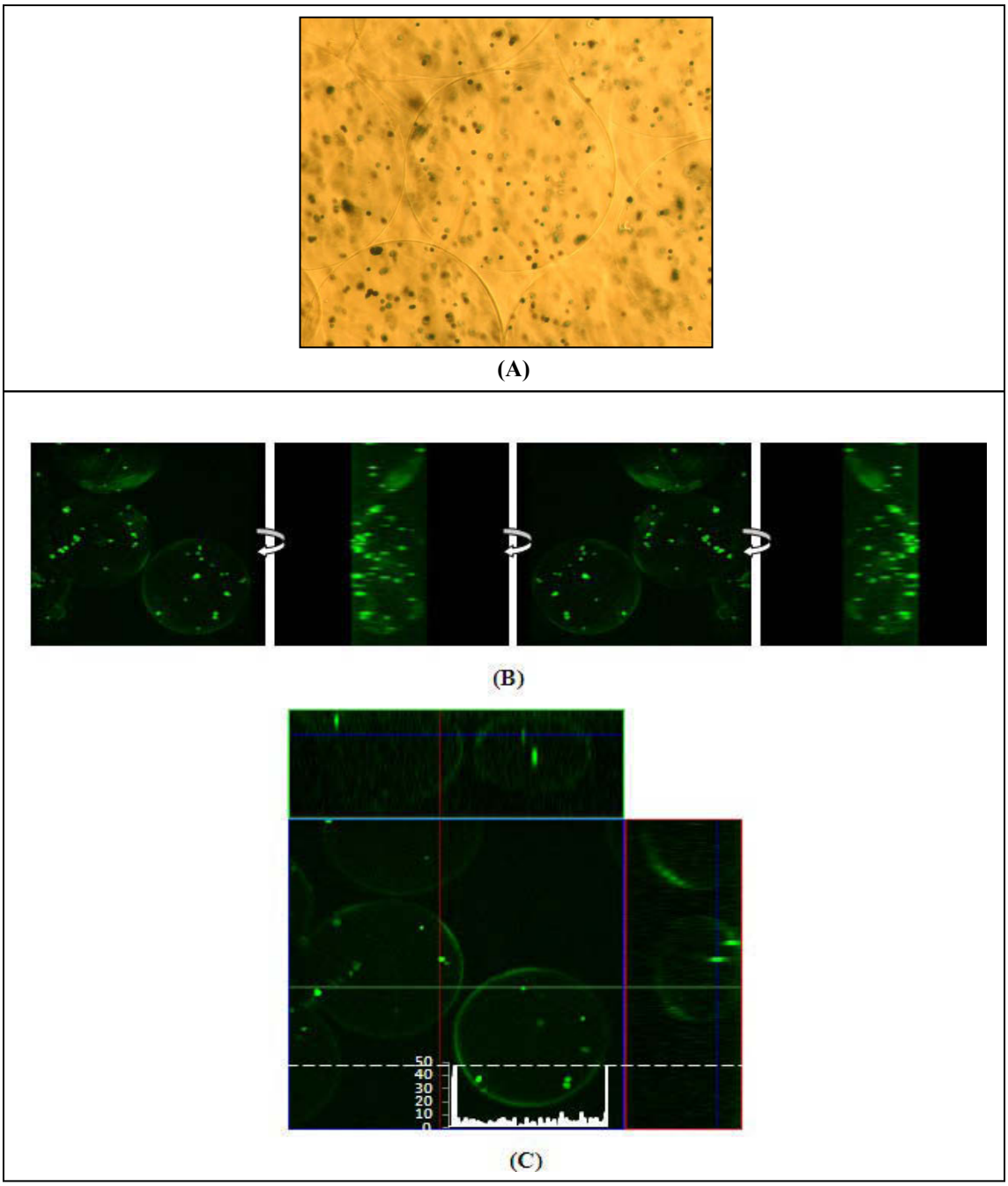

Figure 5.2: GCAC microencapsulation of hASCs. **(A)** LacZ retrovirus transduced cells were encapsulated in GCAC membranes. (A) Photomicrography of microencapsulated transduced ASCs (Magnification of 100X) stained with X-gal for LacZ detection under standard inverted microscope. **(B)** Confocal laser scanning microscopic images of the GCAC microcapsules at an excitation of 488 nm, at different angles (Magnification of 100X). The microcapsular membrane was cross-linked with genipin (5.0 mg/mL) at 37 °C for 24h. The green

fluorescence on the outer surface of the capsules shows the cross-linking between genipin and chitosan. The encapsulated viable cells, stained by calcein AM, are shown as the green dots inside the capsule. **(C)** The picture illustrates the cuts from the three-dimensional data set of the confocal picture of 2B, explicitly showing the structure of the GCAC microcapsules, encapsulating the viable cells. It also shows the fluorescence intensity profile (in white) corresponding to the white dotted line drawn across the plane of the GCAC microcapsules using Image J 1.43m.

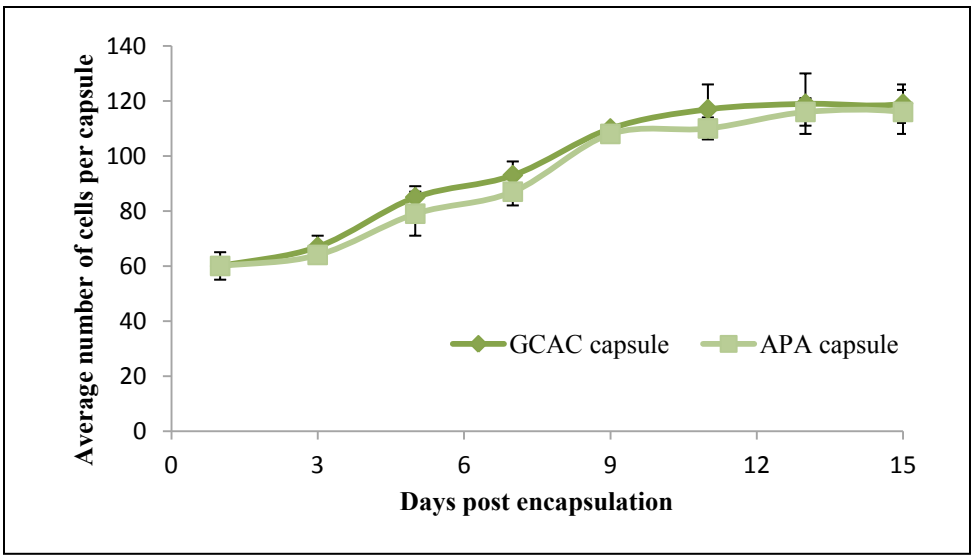

Figure 5.3: Growth kinetics of encapsulated ASCs in APA and GCAC microcapsules. Proliferation of the ASCs within the GCAC (diamond) and APA (squares) microcapsules were measured for a period of 15 days using polyanionic calcein AM dye. Live cells were detected via the intracellular esterase mediated conversion of non-fluorescent calcein AM to green fluorescent calcein. Both GCAC and APA microencapsulated cells displayed an increase in cell number in the first nine days following encapsulation which gradually became steady by day 15. The data represents average number of viable cells per capsule ± SD (n=3). The differences between GCAC and APA capsule groups at all the time intervals were not statistically significant ($p > 0.05$).

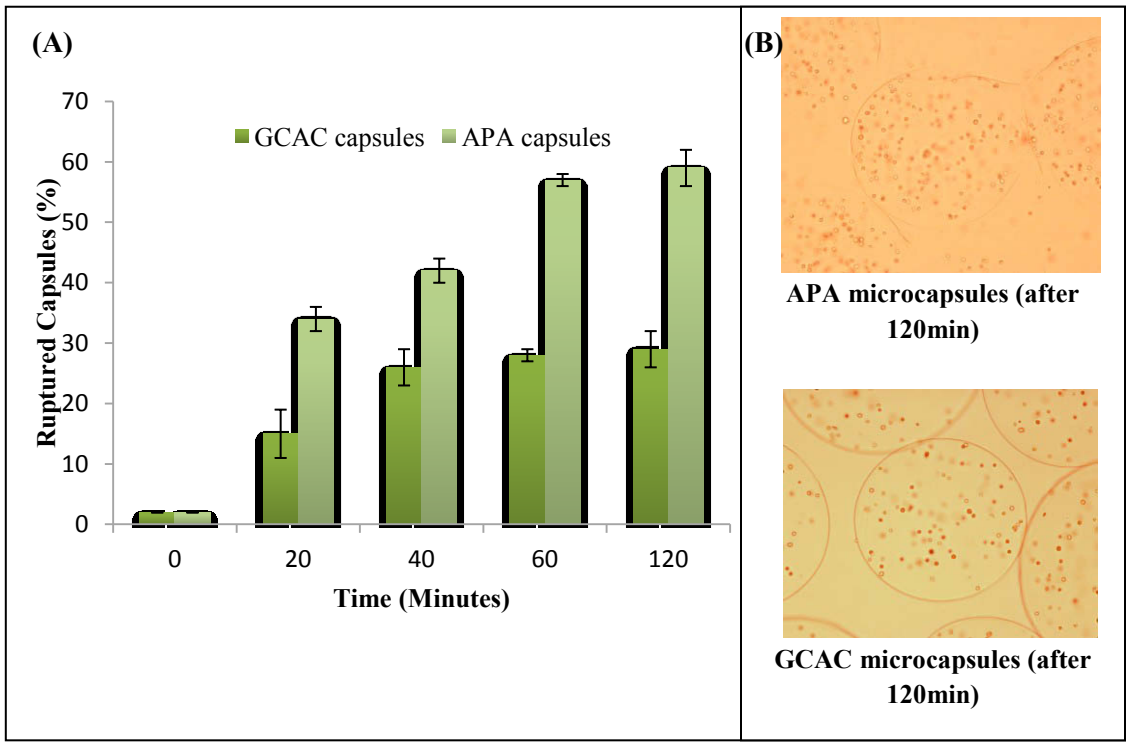

Figure 5.4: Effect of mechanical and osmotic stress on microcapsule integrity. ASC-loaded GCAC and APA microcapsules were subjected to rotational stress (150 rpm) and increased osmotic pressure for a period of 120 minutes. Roughly 60% of APA microcapsules burst **(A)**, while approximately 30% of GCAC microcapsules ruptured **(B)** (Magnification: 100X). The data in the graph represents average percentage of ruptured capsules ± SD (n=3). The differences between GCAC and APA capsule groups at all the time intervals were statistically significant ($p < 0.05$).

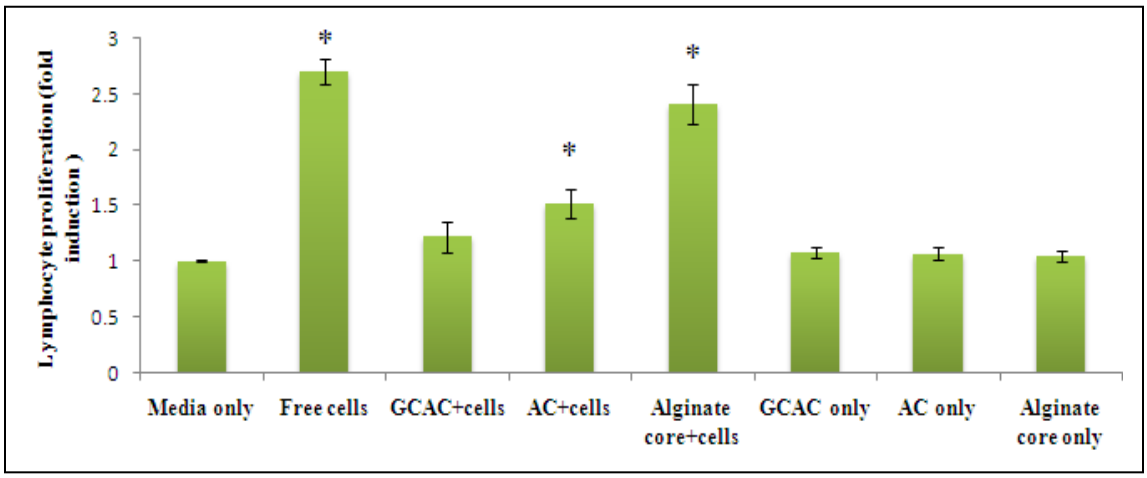

Figure 5.5: Lymphocyte proliferation stimulated by encapsulated and free ASCs. Microcapsules (GCAC, AC, alginate core only) encapsulating ASCs were co-cultured in a transwell 96 well plate along with lymphocytes (present in the reservoir wells) for 72 h. Empty microcapsules were taken as the control groups. MTS cell proliferation assay was done to quantify the number of cells. Non-treated lymphocyte (media only) count was normalized to 1.0 and the cell counts of other groups were represented as fold increase with respect to it. The data represents average number of viable lymphocytes± SD (n=3). *Indicates a significant difference of the groups from the (control) media only group ($p< 0.05$).

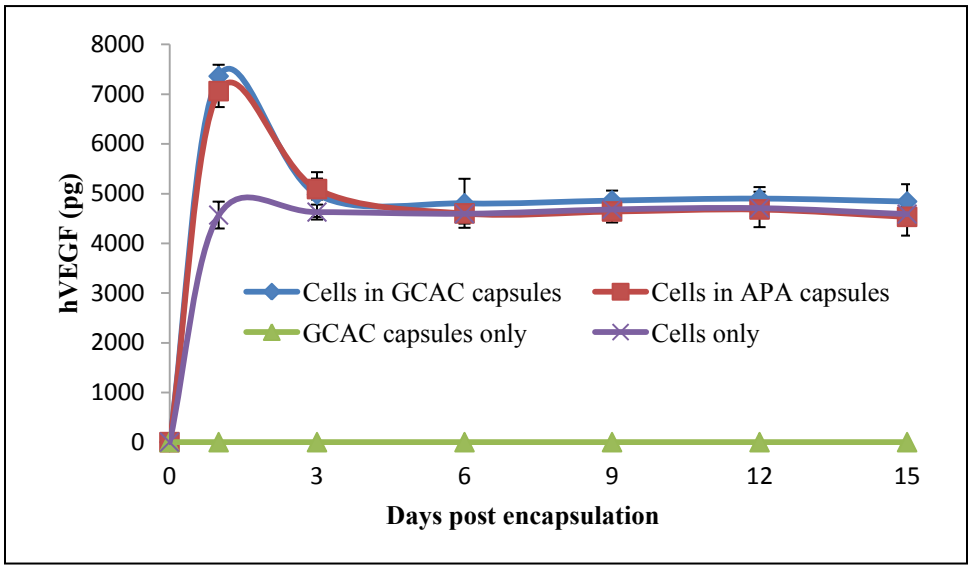

Figure 5.6: Quantification of VEGF present in the conditioned media secreted by encapsulated and free cells using ELISA. 4 million encapsulated and free ASCs were cultured under normal conditions in DMEM+10% FBS over 15 days. The media was changed every alternate day and the conditioned media were collected at regular intervals for performing ELISA. The data represents mean VEGF (in pictograms) ± SD. There was a rapid increase in VEGF secretion on day 1 in both GCAC and APA microcapsules, which dropped by day 3 and became steady for the rest of the time period. Both the encapsulated and free cells had a similar trend of expression over the time period proving that the encapsulation did not alter the angiogenic potential of ASCs.

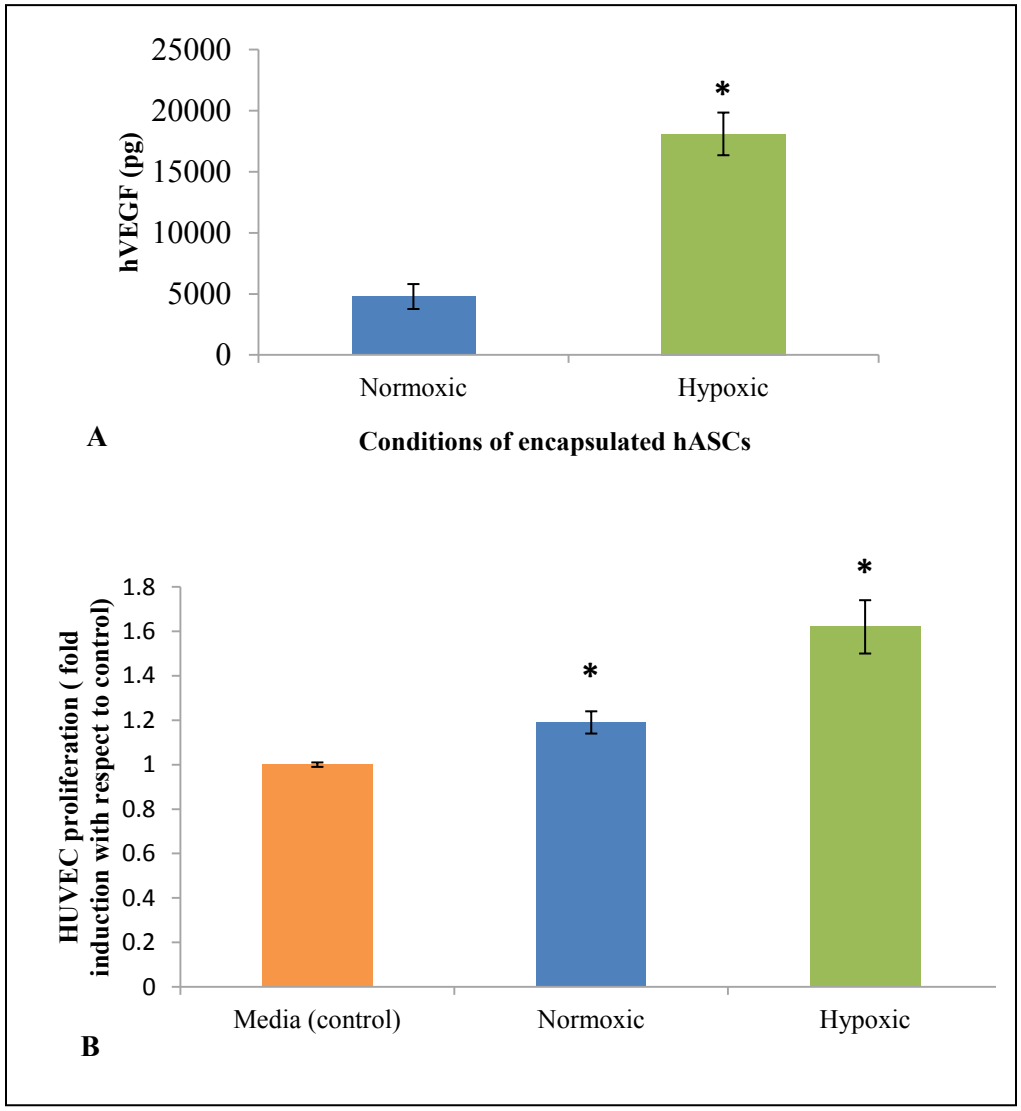

Figure 5.7: Angiogenic potential of GCAC encapsulated hASCs under hypoxic/normoxic condition. $4x10^6$ encapsulated hASCs were cultured under normal conditions in DMEM+10% FBS. 3 days post encapsulation, the cells underwent hypoxic/ normoxic conditions for 72h. The conditioned media containing released VEGF were quantified by ELISA and the average value ±SD (n=3) has been represented in (A). The biological assay of the conditioned media (hypoxic/normoxic/control) was performed on $1x10^4$ HUVECs per well (n=3) (B). The endothelial cells treated with hypoxic media showed an increased cell proliferation in comparison to normoxic /control media after 96h of culture in the 96 well plates. *Indicates a significant difference from control ($p< 0.05$)

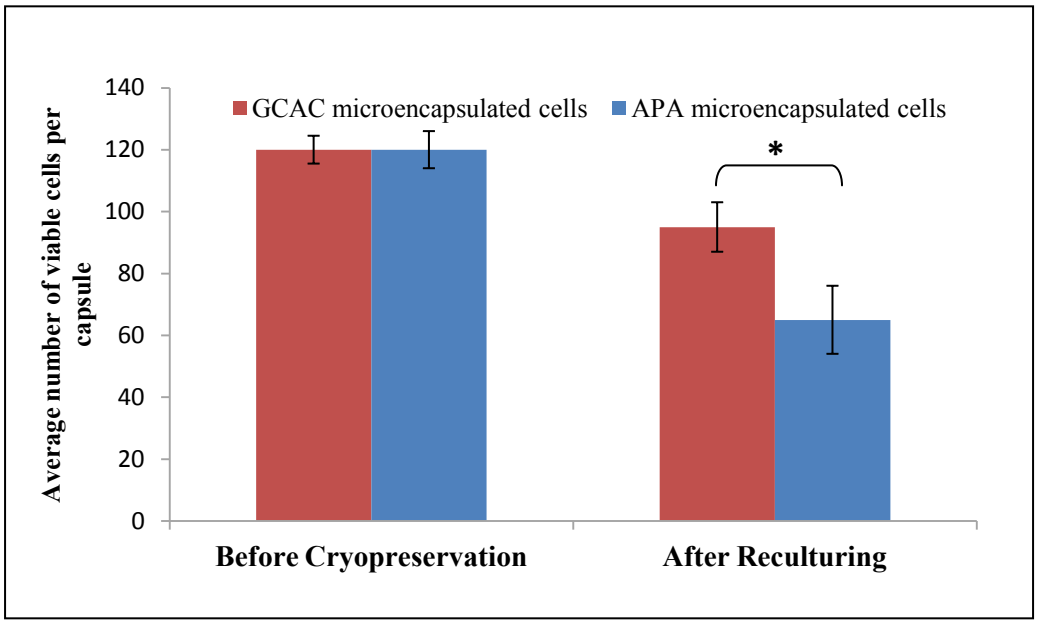

Figure 5.8: Viability of GCAC and APA microencapsulated ASCs before and after cryopreservation. GCAC and APA microcapsules were frozen for a 30-day period at -80^{o}C. Viability within the GCAC microcapsules was slightly reduced after this time, while viability within the APA microcapsules was significantly decreased. The data represents the mean value ± SD (n=3). The average viable cell number difference between APA and GCAC microcapsules was statistically significant (*$p < 0.05$).

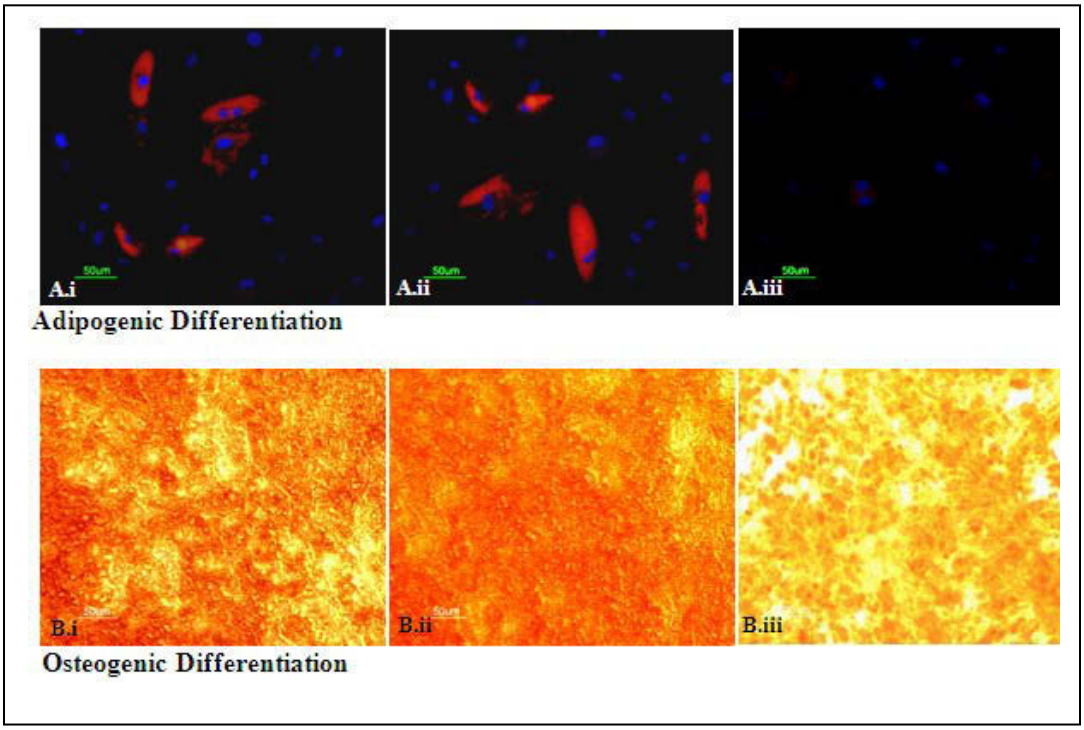

Figure 5.9: Adipogenic and osteogenic differentiation of encapsulated ASCs after depolymerization of microcapsules. After GCAC microcapsule depolymerization, released ASCs were cultured in either adipogenic or osteogenic differentiation media. ASCs maintained their natural potential for differentiation: adipogenic differentiation was assessed via LipidTOX Red neutral lipid staining of lipid vacuoles and DAPI staining of nucleus (A. i: encapsulated differentiated; A. ii: non-encapsulated standard 2 dimensional culture differentiated; A. iii: undifferentiated), while osteogenic differentiation was determined by Alizarin Red staining of calcium deposits (B. i: encapsulated differentiated; B. ii: non-encapsulated differentiated; B. iii: undifferentiated; The arrows show the cell differentiated area.)

Genipin-crosslinked Microencapsulated Human Adipose Stem Cells Augment Transplant Retention Resulting in Attenuation of Chronically Infarcted Rat Heart Fibrosis and Cardiac Dysfunction

Arghya Paul[1], Guangyong Chen[2], Afshan Khan[1], Vijayaraghava T.S. Rao[3], Dominique Shum-Tim[2], Satya Prakash[1]*

[1] Biomedical Technology and Cell Therapy Research Laboratory, Department of Biomedical Engineering, Faculty of Medicine, McGill University, 3775 University Street, Montreal, Quebec H3A 2B4, Canada.

[2]Cardiothoracic Surgery and Surgical Research, Royal Victoria Hospital, Room # S8.73B 687 Avenue Des Pins Ouest, Montreal, Quebec H3A 1A1, Canada.

[3]Institute of Parasitology, McGill University, Macdonald Campus, 2111 Lakeshore Road, Ste. Anne de Bellevue, Quebec, H9X 3V9, Canada.

*Correspondence author; Email: satya.prakash@mcgill.ca
Tel: +1-514-398-3676; Fax: +1-514-398-7461

Preface: After preliminary evaluation of the feasibility of using microcapsules for cell delivery, in this work we evaluated the system's *in vivo* potential in myocardially infarcted rat model. Results demonstrated that microcapsules can significantly enhance the transplant retention at the injected site and thereby induce better therapeutic effect.

Original article accepted (in press) in ***Cell Transplantation (2011)***

6.1 Abstract

Stem cell transplantation has been widely acknowledged for their immense potential in regenerative medicine. In these procedures, the implanted cells need to maintain both their viability and functional properties for effective therapeutic outcomes. This has long been a subject of major concern and intensive studies. Microencapsulation of stem cells within polymeric microcapsules can be an efficient approach to achieve this goal, particularly for heart diseases. This study reports the use of biocompatible, fluorogenic genipin-crosslinked alginate chitosan (GCAC) microcapsules in delivery of human adipose stem cells (hASCs) with an aim to increase the implant retention in the infarcted myocardium for maximum clinical benefits. *In vitro* results show under hypoxic conditions, the microencapsulated cells overexpressed significantly higher amount of biologically active vascular endothelial growth factor (VEGF). We investigated its *in vivo* potential using immunocompetent female rats after induction of myocardial infarction. For this, animal groups (n=8) received empty control microcapsules, $1.5x10^6$ free male hASCs, $1.5x10^6$ microencapsulated male hASCs. Results shows significant retention (3.5 times higher) of microencapsulated hASCs compared to free hASCs after 10 weeks of transplantation. Microencapsulated hASCs showed significantly attenuated infarct size compared to free hASCs and empty microcapsule group (21.6±1.1% vs 27.2±3.1% vs 33.3±3.2%; $p< 0.05$), enhanced vasculogenesis and improved cardiac function (fractional shortening: 24.2±2.1% vs 19.1±0.5% vs 12.0±4.0%; $p< 0.05$). These data suggest that microencapsulated hASCs can contribute significantly to the improvement in cardiac functions. Their greater retentions exhibit reduced fibrosis and cardiac dysfunction in experimental animals. However, further research is needed to fully comprehend the underlying biologic and immunologic effects of microencapsulated hASCs which jointly play important roles in cardiac repair.

Keywords: Cell transplant; adipose stem cell therapy; tissue engineering; myocardial infarction; microencapsulation; regenerative medicine

6.2 Introduction

Cardiovascular diseases, such as cardiomyopathy and ischemic heart diseases are a major cause of concern all over the world [215]. Ischemic heart disease refers to the decrease in oxygenated blood flow to the myocardium or heart muscle, which leads to an inadequate supply of oxygen to the cardiac muscle eventually leading to a permanent damage to the cardiomyocytes followed by myocardial infarction [216]. Stem cell transplantation has been considered as a major breakthrough in treating such diseases. Although the majority of cardiovascular research in stem cell therapy has involved bone marrow derived mesenchymal stem cells (BMSCs), human adipose stem cells (hASCs) are an ideal alternative and as a result have been researched extensively as of late [217-219]. Adipose tissue, like bone marrow, is derived from the mesenchyme. Therefore, ASCs also have the potential to differentiate into mesodermal lineages. ASCs provide the same multipotency as BMSCs and even yield a higher cell number from the same amount of starting material [220]. The safe expendability of this tissue allows for large quantities of stem cells to be harvested without difficulty and at minimal risk [221]. Owing to their potency and relative abundance, ASCs may be the most promising and ideal stem cell studied to date [222-224]. Moreover, ASCs also have natural ability to secrete vascular endothelial growth factors and induce angiogenesis, where the newly formed vessels help in recovery of the blood flow in the damaged tissues, eventually leading to increased oxygen availability [219].

Survival of cells after intramyocardial injection is crucial to the efficacy of therapeutic cell transplantation. Recent studies suggest that a massive mechanical loss of cells takes place in the first minutes after direct intramyocardial injection [225-227]. Similar problems were also noticed by another group where both ASC and MSC could not survive in the harsh cardiac environment, resulting in acute transplanted cell death and subsequent loss of cardiac function [178]. In light of the early time frame in which this cell loss takes place, it is unlikely that it happens only because of instant cell death of the transplanted cells. As the heart differs from other organs in that it is constantly contracting, it is possible that this

may contribute to the mechanical loss by squeezing the injected cells out of the myocardium. As a result, the cells retained in the myocardium immediately after injection represent only a fraction of those initially implanted. It is from this subset that biologic loss can then affect the remaining number of surviving cells.

Extensive research has been dedicated towards the development of efficient cell delivery systems which could promote tissue regeneration. Several cell immobilization techniques have been studied such as 3D scaffolds and gel-based entrapment carriers, but none has actually gained acceptance into the market [228-231]. With these drawbacks and requirements in mind, studies led to the development of better techniques of cell delivery involving cell encapsulation within semi-permeable microcapsules [232-236]. This technique provides the advantage of localized cell retention which in turn facilitates the release of therapeutic agents for prolonged time periods at the target site increasing potential impact in tissue regeneration applications. As shown in our previous studies, the use of polymeric microcapsules can provide an efficient delivery system for the transplantation of mesenchymal stem cells and help in cell based gene therapy for overexpression of the therapeutic proteins [165].

Current study focuses on increasing the retention of the transplanted cells at target site with minimum mechanical and biological loss. Reducing the myocardial loss of cells will increase the retention of higher number of viable cells at the target site which can eventually reduce the cardiac dysfunction. Here, we hypothesized that cell delivery using biodegradable polymeric microcapsules will be a potential tool to achieve this goal (**Figure 6.1**). This is because when the size of the injectate is larger than the blood vessel diameter, like that of microcapsules, the contractive forces of the heart will be unable to wash out the later into the blood stream. On the contrary, with free cell delivery system, the pressure generated by the injection coupled with that generated by the beating heart easily forces the grafted cells through the disrupted blood vessels into the systemic circulation. Moreover, the capsular membrane will also protect the cells against the external harsh microenvironment and foreign bodies in the myocardium.

We have recently demonstrated, using fluorescent microspheres (diameter: 10 µm, impersonating the cells) encapsulated in standard 200 µm alginate poly-l-lysine microcapsules, that microcapsules can reduce the initial mechanical loss of microspheres in the beating heart as detected after 20 min of myocardial transplantation in the left ventricle of infarcted rat heart model [168, 237]. We have also reported the use of genipin, a highly biocompatible and naturally derived iridoid glucoside from Gardenia fruits, for covalent crosslinking outermost coating of the microcapsule membrane for live cell encapsulation and characterized the microcapsule structure and key physical characteristics including mechanical properties, resistance, permeability, and durability [232, 233]. In this article for the first time, we explore the potential of these new GCAC microcapsules *in vivo* for myocardial xenotransplantation in infarcted rat heart using hASCs, and assess their ability to improve the cardiac function and diminish scar formation.

.

6.3 Materials and methods

6.3.1 Chemicals

Low viscosity alginic acid sodium salt from brown algae (viscosity: ~250 cP, 2 % in water at 25 °C) and poly-L-lysine hydrobromide (PLL; Molecular weight 27, 400) were bought from Sigma Chemicals (St. Louis, MO). Chitosan (low viscosity, Mv = 7.2 x 10^4 by viscometry, degree of deacetylation at 73.5% by titration) and genipin were purchased from Wako BioProducts, USA.

6.3.2 Cell culture

Human ASCs (n=1 donor) were obtained from Invitrogen and cultured in DMEM (Invitrogen) supplemented with 10% fetal bovine albumin (FBS). The cells were routinely maintained as stationary cultures in 75 cm^2 tissue culture flasks and incubated at 37^o C in a controlled environment with an air atmosphere of 5% CO_2. Human umbilical vein endothelial cells (HUVECs) (Sciencell, Carlsbad, California, USA) were cultured and expanded on tissue culture flasks according to the supplier's instructions. They were cultured in endothelial cell

medium (ECM) (Sciencell, Carlsbad, California, USA) supplemented with 5% FBS and placed in an incubator containing 5% CO_2 at 37°C.

6.3.3 Preparation of GCAC microcapsules containing hASCs

Calcium-alginate beads containing ASCs were generated using an encapsulator (Inotech Corp) with a 300 µm nozzle, which dispenses droplets of 1.5% sodium alginate solution containing cells ($1x10^6$ cells/mL) into a constantly stirring solution of 0.1 M $CaCl_2$. After 20 minutes of stirring, the newly generated beads were coated with a chitosan layer by immersing them in a chitosan solution (2%) for 30 minutes. Subsequently, the beads were washed twice in 0.9% saline solution and immersed in genipin solution (5 mg/mL) for 12 h at 37^o C to promote cross-linking with the chitosan layer. This was followed by rapid chelation of the inner alginate core of the microcapsules by incubating them in 0.055 mol/L sodium citrate solution for 5 minutes, followed by two washes in saline solution. To confirm the genipin cross-linking to the chitosan layer, the microcapsules were placed in a chambered coverglass system (Lab-Tek) under Laser Scanning Confocal Imaging System (LSM 510, Carl Zeiss, Jena, Germany) equipped with a Zeiss Axiovert 100M microscope. A 488-nm argon laser was used in the single green fluorescence mode and the fluorescence was detected with the emission filter block BP500- 550IR. Genipin reacts with amino terminals of the chitosan layer to emit green fluorescence on the outer surface of the capsule [232]. After reaction confirmation, resulting microcapsules were thoroughly washed, replenished with fresh media to promote cell growth and placed in a 37^o C incubator containing 5% CO_2.

6.3.4 Scanning Electron Microscope: Internal morphology of the hASC containing microcapsule

The internal morphology of the microencapsulated cells was studied by scanning electron microscopy (SEM), using a Hitachi S-4700 FE scanning microscope. The samples for SEM were prepared by rinsing the capsules with water, followed by freeze-drying and fracturing by a razor blade. The obtained

fragmented halves of the microcapsules were mounted on SEM stud with double-sided tape and sputter-coated with gold–palladium for 40s.

6.3.5 Detection of viable encapsulated cells using stably transduced lac Z containing hASCs

In order to assess the viability of the encapsulated cells hASCs were transduced with retroviral vector containing the Lac Z gene before encapsulation. X-gal staining was used from time to time to indicate the viability of the Lac Z-infected cells inside the GCAC microcapsules for 1 month.

6.3.6 Assessment of viability of encapsulated cells using dual cell staining

Viability of the ASCs within the GCAC microcapsules was assessed using poly-anionic calcein AM and ethidium homopolymer EthD-III dyes (Biotium, Inc., Hayward, USA) [165]. The live cells were detected by the intracellular esterase mediated conversion of non-fluorescent cell-permeant calcein AM to fluorescent green calcein. The dead cells were detected by the bright red fluorescence emitted by EthD-III dye, which enters dead cells only through their damaged membranes and binds to nucleic acids. For this, the microcapsules were washed twice with PBS for 10 minutes each and re-suspended in fresh PBS. 2 μM calcein AM and 4 μM EthD-III were then added to the microcapsules and the microcapsules were incubated for 1 hour before being examined under the fluorescent microscope.

6.3.7 Induction of hypoxic and normoxic conditions and quantification of released VEGF from encapsulated hASCs

hASCs were encapsulated in microcapsules, as described above, and grown for 24h so as to allow them to stabilize in the new environment. Similarly, equal number of free cells was cultured in a stationary flask. On the following day, the media from the cultures were replaced with fresh media containing 10% FBS and the flasks were placed in either normoxic (21% O_2) or hypoxic (1% O_2) conditions for 24h, 48h or 96h. To induce hypoxic condition, a modular incubator chamber from Billup-Rothenberg Inc. was used as mentioned elsewhere [162]. At

the end of the incubation period, the conditioned media from culture flasks were collected. Conditioned media from the culture flasks were collected and the VEGF release was quantified using a VEGF ELISA kit (R&D Systems) according to manufacturer's protocol. The data was represented as mean ± Standard Deviation (SD).

6.3.8 Evaluation of bioactivity of conditioned media of encapsulated hASC: endothelial cell proliferation

For the cell proliferation assay, $1x10^4$ cells per well were seeded in 96 well plate in triplicate for each sample. After 24h of culturing with DMEM with 2% FBS the cells were washed twice with PBS. The conditioned media from the encapsulated and free cells under hypoxic/normoxic conditions were added to the cells along with equal amount of fresh DMEM media supplemented with 10% FBS. Wells treated with only DMEM with 10% FBS without any stimulation with conditioned media was taken as the control. The cells were grown at 37^oC in 5% CO_2 for 4 days followed by MTS cell proliferation assay (Promega) according to manufacturer's protocol.

6.3.9 Animal Model

Immunocompetent female Lewis rats (200 to 250 gm, Charles River, QC) were used. All procedures were in compliance with the NIH and Canadian Council on Animal Care guidelines for the use and care of animals.

6.3.10 Intramyocardial microcapsule transplantation

The rats were maintained on standard rat chow diet. Myocardial infarction was induced by occlusion of the left anterior descending coronary artery (LAD) as described previously [237, 238]. Female Lewis rats were anesthetized using 5% isoflurane in an induction chamber. The rats were intubated with an 18-gauge catheter, ventilated at 80 breaths/min under anesthetic condition. A left thoracotomy was performed through the fourth intercostal space to expose the left ventricle. The left coronary artery was ligated 2 mm from its origin with a 7-0

polypropylene suture (Ethicon, Inc, Somerville, NJ). The ischemic myocardial segment rapidly became identifiable through its pallor and akinesia. Fifteen minutes after ligation of the artery, three 50 µl intramyocardial injections in the peri-infarct area of the left ventricle were given group-wise according to **Table 6.1** using a 27-G needle.

6.3.11 Retention of ASCs after 10 weeks: detecting the LacZ labeled cells

Histological assessments of the left ventricular hearts were performed on rats after 10 weeks of myocardial transplantation of LacZ labeled hASCs. Hearts were stained for evidence of cell engraftment using *β-galactosidase*. For *β-galactosidase* activity, hearts were added to a solution containing 1mg/ml 5-bromo-4-chloro-3-indoyl-β-D-galactoside (X-gal), 2% dimethylsulfoxide, 20mM $K_3Fe(CN)_6$, 20mM $K_3Fe(CN)_6.3H_2O$ and 2mM magnesium chloride, 0.02% Nonidet P40 and 0.01% deoxycholate [238]. The specimens were incubated in a 37^oC incubator with a humidified atmosphere of 5% CO_2 for 8h. They were then washed with PBS and fixed in 2% paraformaldehyde overnight. After fixation, the myocardium was embedded in paraffin. Ribbon sections of tissue were cut on microtome, and stained with eosin dye to detect cell cytoplasm.

6.3.12 Retention of ADSCs after 10 weeks: Polymerase Chain Reaction Analysis

Random samples were selected from each group for polymerase chain reaction analysis to confirm the survival of the implanted male hASCs cells in the female rat hearts at week 10. Genomic DNA was purified using DNeasy (Qiagen, Valencia, CA) according to the manufacturer's instructions, and the presence of living human male cells in female rat hearts were confirmed by targeting a specific microsatellite sequence within the human Y chromosome (DYS390). PCR was performed on equal amount of extracted DNA using Taq DNA Polymerase (Invitrogen). To detect specific gene product, the primer pair used was forward primer 5'TATATTTTACACATTTTTGGGCC3' and reverse primer

5'TGACAGTAAAATGAACACATTGC3' with an amplicon size of 250 bp [239, 240]. Amplifications were carried out for 30 cycles at 94^{o}C for 15 s (denaturation), 54^{o}C for 20 s (annealing), and 72^{o}C for 20 s (extension).

6.3.13 Myocardial infarct area analysis

Ten weeks after myocardial infarction, rats were deeply anesthetized and sacrificed by rapid excision of the heart. The excised hearts were immediately soaked in cold saline to remove excess blood from the ventricles and fixed in neutral-buffered 4% formalin. Paraffin embedded samples were sectioned at 5µm, and Masson's trichrome staining (DBS, Pleasanton, CA) was performed to delineate scar tissue (blue color) from the total area of myocardium [241]. Masson's trichrome-stained sections were captured as digital images and analyzed by Image J-1.41 software. Infarct area, epicardial and endocardial length of infarction and ventricular and septal wall thickness were calculated and expressed as a percentage.

6.3.14 Immunohistochemistry for detecting neovascularization

Neovascularization was evaluated by analyzing the capillary and arteriole density in the peri-infarct area. For this, immunohistochemical staining was performed with antibodies against PECAM (Santa Cruz) for identification of endothelial cells and smooth muscle α-actin (Santa Cruz) for tracing the smooth muscle cells. Briefly, for measurement of capillary density, five fields in the peri-infarct area were imaged with 200x magnification and average numbers of capillaries with less than 10µm diameter were counted. The capillary density was quantified as the (mean total PECAM-positive microvessels)/mm^2 using three tissue sections spanning per-infarct tissue region of each animal. Similarly, arteriole densities were quantified as the (mean total smooth muscle α-actin-positive microvessels)/mm^2.

6.3.15 Echocardiography and cardiac performance

Transthoracic echocardiography was performed on all surviving animals in the four groups before operation (baseline), and before sacrifice on week 10. Echocardiograms were obtained with a commercially available system (SonoSite, Titan-Washington, Seattle, WA) equipped with a 15-MHz transducer, according to the American Society of Echocardiology leading-edge method [238]. After sedating the animals, left ventricular end-diastolic (LVEDD) and end-systolic (LVESD) diameters were measured with M-mode tracings between the anterior and posterior walls from the short-axis view just below the level of the papillary muscles of the mitral valve. Two images were obtained in each view and averaged over three consecutive cardiac cycles. Fractional shortening (FS) was determined as [(LVEDD - LVESD) / LVEDD] x 100 (%). All measurements were performed by one experienced observer, who was blinded to the treatment groups.

6.3.16 Statistical analysis

All data are expressed as mean ± Standard Deviation (SD). Multiple group comparison was performed by one-way analysis of variance (ANOVA) followed by post-hoc analysis using the Bonferroni procedure for multiple comparison of means**.** Probability (p) values less than 0.05 were considered to be statistically significant.

6.4 Results

6.4.1 Characteristics of the GCAC microcapsules encapsulating hASCs

The reaction between chitosan and genipin occurred moderately after mixing the two solutions, and could be monitored by detecting the changes in the physical appearance of the mixture from time to time. Results in **Figure 6.2** exemplifies that the chitosan-genipin reaction generated a fluorescent green bright circle circumscribing each microsphere core after 12h of exposure of the AC capsule to genipin, which was not detected in the one which was not exposed to genipin. This is in accordance to our earlier results [232, 233]. The lower panel of **Figure 6.2** shows the fluorescence profile corresponding to the line across the optical section of the microcapsules. It was clear that the intensity of the inner alginate cores was similar to that of the background signals, whereas peaks corresponding to the fluorescence of the microcapsule membrane appeared with the relatively higher intensity at the capsular surface. The cells were also viable in both AC and GCAC capsules, as detected by calcein staining. Bright field picture of the cell containing microcapsules show that they were generally spherical and uniform in shape and size, with an average diameter of about 200 μm. **Figure 6.3** shows that the mesh-like porous internal morphology of blank microcapsule (3A and 3B). The morphology of the cell loaded microcapsules was also similar (3C) to the empty one, confirming that the internal structure of the microcapsules was not influenced by the hASC loading.

Viability of the hASCs was also assessed at regular intervals using poly-anionic calcein AM and ethidium homopolymer EthD-III dyes. **Figure 6.4** is a representative example of the encapsulated cells showing calcein stained encapsulated viable green cells and EthD-III stained dead cells on day 21. The fluorescent outer circles of GCAC microcapsules, due to genipin-chitosan cross-linking, also disappeared after day 21. This indicates that the outer surface has gradually started disintegrating, although the exact time of degradation was not analyzed in this study.

6.4.2 Efficient release of hVEGF molecules from encapsulated hASCs under hypoxic conditions

In order to understand the therapeutic potential of encapsulated cells in infarcted heart, we checked the VEGF release potential of the encapsulated cells under hypoxic condition, which is a very prevalent condition in an ischemic myocardial environment. The data in **Figure 6.5** shows that under hypoxic condition, the encapsulated cells secretes significantly increased amount of VEGF at 24h (6.02 ng/4x10^6 cells vs 3.85 ng/4x10^6 cells; $p<0.05$), 48h (16.21 ng/4x10^6 cells vs 4.63 ng/4x10^6 cells; $p<0.05$) and 96h (20.58 ng/4x10^6 cells vs 6.1 ng/4x10^6 cells; $p<0.05$) in comparison to that under normoxic conditions.

6.4.3 hVEGF released from encapsulated hASCs have mitotic effect on endothelial cells

To check the biological activity of the released protein, a HUVEC proliferation assay was performed on the released conditioned media from 96h hypoxic and normoxic hASC encapsulated samples. The samples with high VEGF concentrations, i.e. from hypoxic conditioned media from free and encapsulated cells, significantly increased the proliferation rate of HUVECs in comparison to that from normoxic conditioned media (163% in hypoxic free and 154.5% in hypoxic encapsulated cells against 31% proliferation in control; 100% proliferation was taken as baseline for normoxic free cells) as illustrated in **Figure 6.6**. Under hypoxic condition, conditioned media from both encapsulated and non-encapsulated cells induced around 5-fold cell proliferation compared to the unstimulated control, while under normoxic condition the proliferation was around 3.3 fold in both cases. Thus, the extent of cell proliferation was directly proportional to the released VEGF amount by the hASCs under different conditions.

6.4.4 Higher retention and survival rate of transplanted cells using GCAC microcapsules

To analyze whether the microcapsules were able to protect the cells against the harsh external beating environment in the heart, harvested heart tissue samples were stained with X-gal in order to trace the transplanted LacZ gene containing cells in the heart. The picture in **Figure 6.7A** gives us a qualitative idea of the amount of encapsulated cells survived in the heart in comparison to free ones. Although the retention of cells were higher in the encapsulated group, there was no trace of the polymeric capsules after 10 weeks, which probably got degraded and bioresorped in the body over time leaving the cells behind. The infarct and peri-infarct portions of the heart tissues were also used for DNA extraction. This was used to detect the presence of Y chromosome of transplanted hASC in the female rat heart using standard PCR. Equal amounts of tissue samples from the peri-infarct region of heart were taken for DNA extraction. The gel electrophoresis of the PCR products shows a clear distinction in band intensities of encapsulated and free cells (**Figure 6.7B**). The encapsulated cells showed 3.54 times more retention of viable transplanted cells in the heart in comparison to non-encapsulated cells (100% vs 28.2%; $p<0.05$) as quantified by relative band intensities using ImageJ software. This semi-quantitative analysis suggests that using microencapsulation technology we need less cell number to achieve desirable cell retention at the target site.

6.4.5 Microencapsulated hASCs efficiently reduce fibrosis in the infarcted tissue

Macroscopic views of Masson's trichrome stained hearts are shown in **Figure 6.8.** In all the groups, positively stained fibrous infarct areas were clearly observed as blue areas in the heart sections 10 weeks after myocardial infarction. We measured the infarct size and other parameters in the left ventricles at the section of the middle point between ligation and apex as previously described elsewhere [241]. As shown in **Table 6.2**, the average percentage infarction size in hearts of MC group (21.6±1.1%) was significantly reduced compared to that in

control hearts (33.3±3.2% in M and 27.2±3.1% in FC). Thin left ventricular wall with dilated left ventricular cavities (average thickness: 0.86mm and 1.41mm) were observed in the M and FC control groups, while the hearts in the MC group had lesser infarcts and thicker left ventricular wall (average thickness: 1.85mm) than the control hearts. There were also significant differences between the control groups and the FC group with respect to the percentage endocardial infarction length and the percentage epicardial infarction length.

6.4.6 Induction of myocardial angiogenesis and arteriogenesis

In this section, we tried to comprehend whether it was the higher angiogenic effect of the microencapsulated hASCs that was responsible for the scar area reduction in treatment groups. We assessed the neovasculature formation in the peri-infarct area by detecting the capillary (**Figure 6.9: A-D**) and artery densities (**Figure 6.9: E-H**). As shown in **Figure 6.9 (I),** we noticed a significant improvement in angiogenesis in the FC and MC groups compared to the M (197 ± 24.1/mm^2 for MC, 144.4 ± 15.45/mm^2 for FC vs. 67.33±17.7/mm^2 for control, $p<0.01$). Moreover, MC group also showed significantly higher capillary density compared to FC. Similar results were obtained with arteriole density in MC group (20.6 ± 4.9/mm^2 for MC, 17.5 ± 3.92/mm^2 for FC vs. 6.9±2.01/mm^2 for control, $p<0.001$) as presented in **Figure 6.10 (J).** Unlike capillary density, MC group showed no significant enhancement in arteriole density compared to FC.

6.4.7 Attenuation of the progression of cardiac dysfunction by microencapsulated hASCs

Here we assessed the cardiac function 10 weeks after myocardial infarction in the all the four groups by echocardiography. The cardiac functional parameters evaluated by M-mode echocardiography, 10 weeks after LAD ligation, are shown in **Figure 6.9**. In the control group (M), significantly decreased fractional shortening was seen, a typical indication of post-infarction cardiac failure. In the group that underwent microencapsulated cell transplantation

(MC), significantly higher FS was observed as compared to groups M (group MC: 24.2±2.1%; group FC: 19.1±0.5%; group M: 12.0±4.0%; $p < 0.05$). FS data indicates a significant cardiac function improvement in group MC compared to group FC. Thus, the analysis using echocardiographic FS% data suggests that encapsulated hASCs can be a better alternative to free hASCs to improve cardiac function after acute myocardial damage.

6.5 Discussions

Cardiomyocytes are considered to be terminally differentiated cells and regeneration is limited in adult life[242]. Thus, the irreversible damage of infarction in the heart increases the risks of having severe complications such as myocardial wall rupture, arrhythmia, aneurysms and eventual heart failure[216]. Application of mesenchymal stem cell therapy in such cases have become one of the most ardently researched and debated subjects in the last ten years [243-246]. The essence of mesenchymal stem cells can be explained through three essential characteristics: firstly, their multilineage differential potential, secondly their immunomodulatory effect and thirdly, their ability to self-regenerate for an unlimited amount of time [247]. In this study, we have used xenogeneic donor mesenchymal stem cells from adipose origin in immunocompetent rats as an alternative to widely used mesenchymal bone marrow stem cells.

Apart from direct free cell delivery, micro and nano-scaffold mediated delivery of stem cells is another widely used approach that has been exploited in the field of regenerative medicine [248]. Seeding cells on these scaffolding systems are used to provide a suitable environment for cell colonization, proliferation and differentiation. Recently, Wei *et al* reported the development of a bioengineered cardiac patch composed of a sliced porous biological scaffold inserted with multilayered mesenchymal stem cells for myocardial regeneration [249]. An array of biomaterials have been used to create scaffolds including type I collagen, a biocompatible polymer onto which the cells have a high affinity and poly lactide-co-glycolic acid, a biodegradable polymer supporting cell stability [192, 193, 217, 250]. In an interesting study, Zhang *et al* reported that

microencapsulated xenogeneic Chinese hamster ovary cells genetically modified to express VEGF can induce significant therapeutic effects in ischemic heart disease [235]. In a similar approach, Goren *et al* also reported microencapsulated mesenchymal stem cells are ideal candidates for hypoimmunogenic long term cell based therapy [251]. Although microcapsules prepared from alginate and poly-l-lysine polymers are being used extensively for such long time study for their ability to support cell viability, several studies have demonstrated that they lack mechanical strength and stability when applied over the long-term *in vivo*, leading to leakage of the encapsulated cells [197, 198, 252]. In addition, addition of PLL to alginate stimulates necrosis of the encapsulated cells [234, 253]. As most synthetic polyelectrolyte materials exhibit a moderate level of cell cytotoxicity, naturally occurring materials constitute ideal polymers for live cell encapsulation. In recent years, genipin has drawn considerable research interests as an alternative cross-linker due to its natural origin and low cytotoxicity, allowing for mild but effective chemical cross-linking. Our earlier studies have showed successful encapsulation of liver cells within genipin crosslinked microcapsules for therapeutic applications [233]. Preliminary studies (data not shown) show that the empty microcapsules can be intact for at least 10 weeks in the culture media. But once they are entrapping the cells, the microcapsules tend to start degrading after 3-4 weeks (**Figure 6.4**). This is because of the proliferation of encapsulated cells under in vitro culture conditions, which is not the case under harsh *in vivo* external environment. But the i*n vivo* data (**Figure 6.7**) confirms that the polymeric microcapsule completely disappeared after 10 weeks leaving the entrapped cells in viable condition. This confirms the bioresorbable and non-toxic nature of the degraded products of the polymeric microcapsule. And this transient nature of the microcapsule is desirable; it disappears from the organ once its job is done. In the present study, our results confirm the higher retention potential of microencapsulated hASCs *in vivo* as shown in **Figure 6.7**, and establish the superior features of biocompatible cell containing GCAC microcapsules in improving heart function in an extreme model of xenogeneic mismatch (**Table 6.1 and Figure 6.10**). An important point while injecting the microcapsules is the

needle size which should not be too small that it breaks the capsules while injecting, at the same time it should not be too big for intramayocardial injection procedure. As it is very difficult to directly quantify the number of transplanted cells in the heart after 10weeks, we relied on the relative comparison between the experimental groups. Although the number of transplanted cells used here was optimal to treat the rat heart infarction, this number will vary based on the animal models used in the respective studies. By attenuating the contractile dysfunction and pathologic remodeling, the microencapsulated hASCs contributed significantly, and better than free hASCs, to a remarkable recovery in ventricular performance after myocardial infarction.

This is the first study to our knowledge, where hASCs are being successfully encapsulated in polymeric microcapsules and delivered as xenotransplant in immunocompetent rats with acute myocardial infarction. This is also the first time where the GCAC microcapsules have been tested *in vivo*. The results supports our hypothesis that the ASCs, encapsulated in GCAC microcapsules, survive longer and sustain their functional properties in the beating heart compared to free cells which, in turn, induce reduction of the infarcted scar area and improve cardiac function significantly. Although the encapsulated microcapsules significantly reduced the myocardial infarction in comparison to free cells and untreated groups, the underlying mechanism is not fully understood. It is true that we were able achieve our goal for better retention of the transplanted viable cells in the infarct area, but we do not know how the encapsulated cells induce its therapeutic effect *in vivo*. Previous studies have reported the transdifferentiation of ASCs to cardiomyocytes in the cardiovascular environment, while others attribute the improvement in cardiac function to the paracrine activity of stem cells or cell fusion [218, 219, 254]. The *in vivo* studies of microencapsulated hASCs presented here suggest that vasculogenesis (**Figure 6.9**) can be a probable mechanism of therapeutic action. The *in vitro* data confirms that microencapsulated cells can effectively induce angiogenesis under hypoxic condition by overexpression of VEGF. VEGF protects the blood vessels from apoptosis, modulates vasomotor response, and supports vessel formation in

the ischemic area, thus reducing the infarct size *in vivo* by improving blood flow [162, 255]. The results from the present study suggest that the improved heart function is a combinatorial effect of at least two major components - the survival of a significantly higher number of grafted cells even after 10 weeks post transplantation and related angiogenic effects of the implanted cells. In terms of future concern, an elaborate *in vivo* work is needed to be done to evaluate whether the genipin crosslinked polymeric microcapsules have any significant effect on the host immune system, and on myocardial and serum cytokine profile. Studies are also needed to be done to accurately determine the degradation rate of the GCAC capsules in the *in vivo* environment. Application of cell based gene therapy using GCAC microencapsulated genetically modified hASCs to modulate inflammatory effects or promote angiogenesis can be the next step for myocardial treatment [170, 241, 255, 256]. Another interesting field of research will be to further enhance the biocompatibility of the GCAC microcapsules by using RGD-conjugated alginate polymers instead of normal alginate, which has shown to help recover cardiac function in infarcted heart [257].

To conclude, the present study demonstrates the first successful step to introduce ASCs for improved xenogeneic myocardial transplantation using novel biocompatible and biodegradable microcapsules. Further interdisciplinary research on developing improved cell-entrapped polymeric microcapsules armed with targeting molecules for site specific delivery, will help us bring this technology much closer to clinical applications.

6.6 Acknowledgments

This work is supported in part by research grant (to D Shum-Tim and S Prakash) from Natural Sciences and Engineering Research Council (NSERC), Canada and Canadian Institutes of Health Research (MOP 64308) to S Prakash. A Paul acknowledges the financial support from NSERC Alexander Graham Bell Canada Graduate Scholarship. VTS Rao acknowledges the doctoral fellowship from Fonds Québécois de la Recherche sur la Nature et les Technologies (Quebec, Canada).

Table 6.1: Animal experimental groups and their abbreviations. The cells used for myocardial transplantation were LacZ labeled male hASCs.

Groups (no. of animals)	Samples	Abbreviations
Group 1 (n=4)	Sham (control)	S
Group 2 (n=8)	Empty Microcapsules (control)	M
Group 3 (n=8)	Free hASCs ($1.5x10^6$)	FC
Group 4 (n=8)	Microcapsulated hASCs ($1.5x10^6$)	MC

Table 6.2: Effect of the groups on infarcted heart: morphometric analysis of the left ventricle after infarction. Values indicate the mean ± SD (n=8; n=4 for sham). All parameters were measured on the mid-line horizontal sections between ligation-point and apex of heart, and calculated according to the following formulae: % infarct size=infarct area/total LV area×100; % endocardial infarct length= endocardial length of infarction/endocardial circumference of LV×100; % epicardial infarct length= epicardial length of infarction/epicardial circumference of LV×100. *: significant compared to control (microcapsules only), †: significant between microencapsulated hASCs and free hASCs.

Group	Average Infarction area/area at risk	Average Left Ventricular wall thickness	Epicardial length of infarction/ epicardial circumference	Endocardial length of infarction/ endocardial circumference	Heart weight/ body weight
	%	mm	%	%	(g/Kg)
S(n=4)	No infarction	2.9±0.4*	No infarction	No infarction	3.7±0.08 *
M (n=8)	33.3±3.2	0.86±0.17	47.4±1.05	61.5±4.32	4.3±0.05
FC (n=8)	27.2±3.1*	1.41±0.1*	38.2±3.88*	53.1±2.02*	4.05±0.2 *
MC (n=8)	21.6±1.1*†	1.85±1.3*†	32.2±2.42*†	44.7±4.12*†	3.98±1.1 *

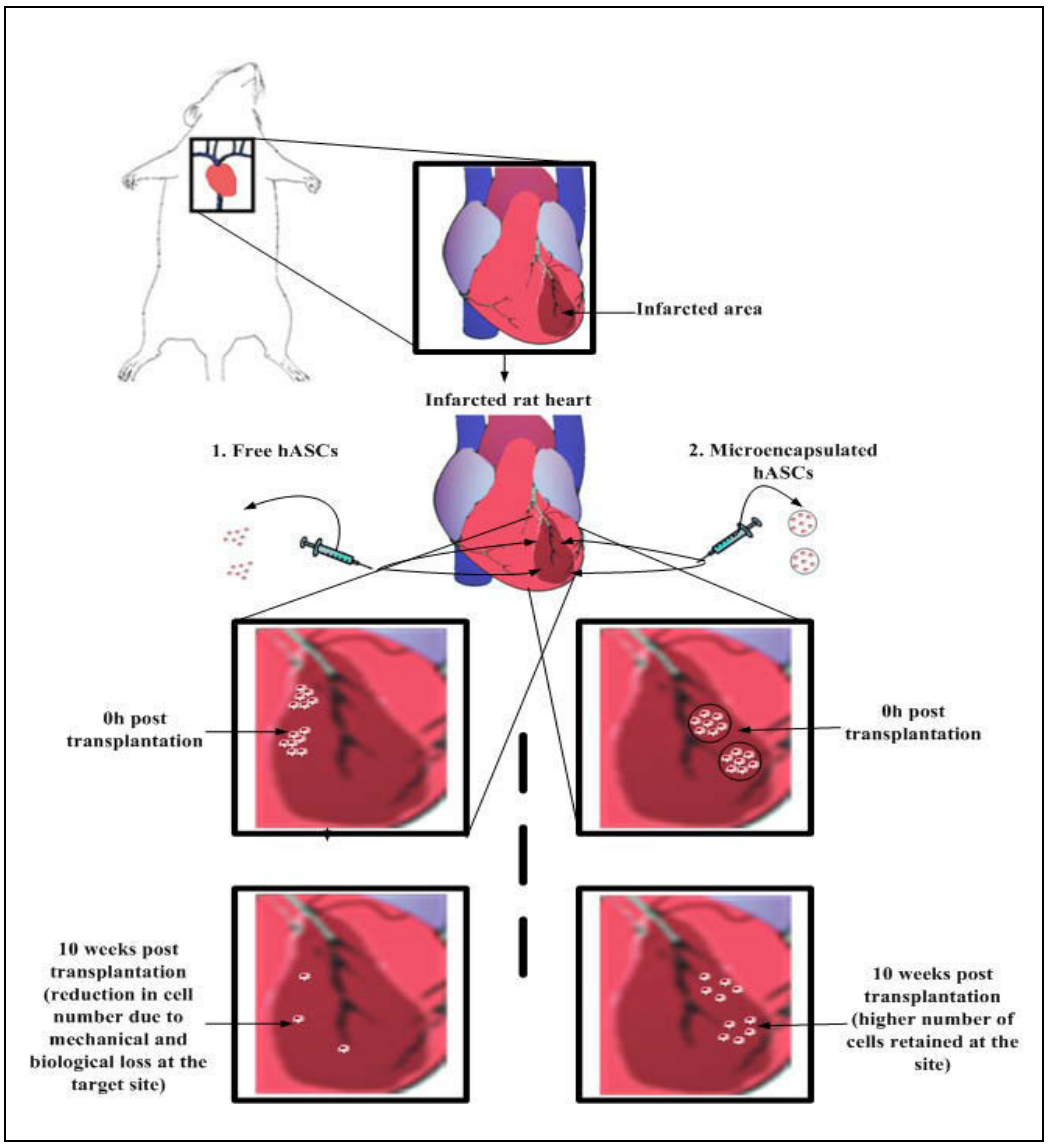

Figure 6.1: Schematic representation of direct intramyocardial delivery of microencapsulated adipose stem cells (hASCs) at the peri-infarct sites in comparison to free hASCs**.** We hypothesized that compared to non-encapsulated free hASCs (Method 1), the microencapsulated hASCs (Method 2) can better retain the transplanted cells at the infarct site, reduce massive mechanical cell washouts into microcirculation and inhibit biological cell losses induced by the beating heart. The higher retention of transplanted viable cells at the infarct site (in this study, 10 weeks post transplantation) can eventually facilitate superior functional improvement of the infarcted heart.

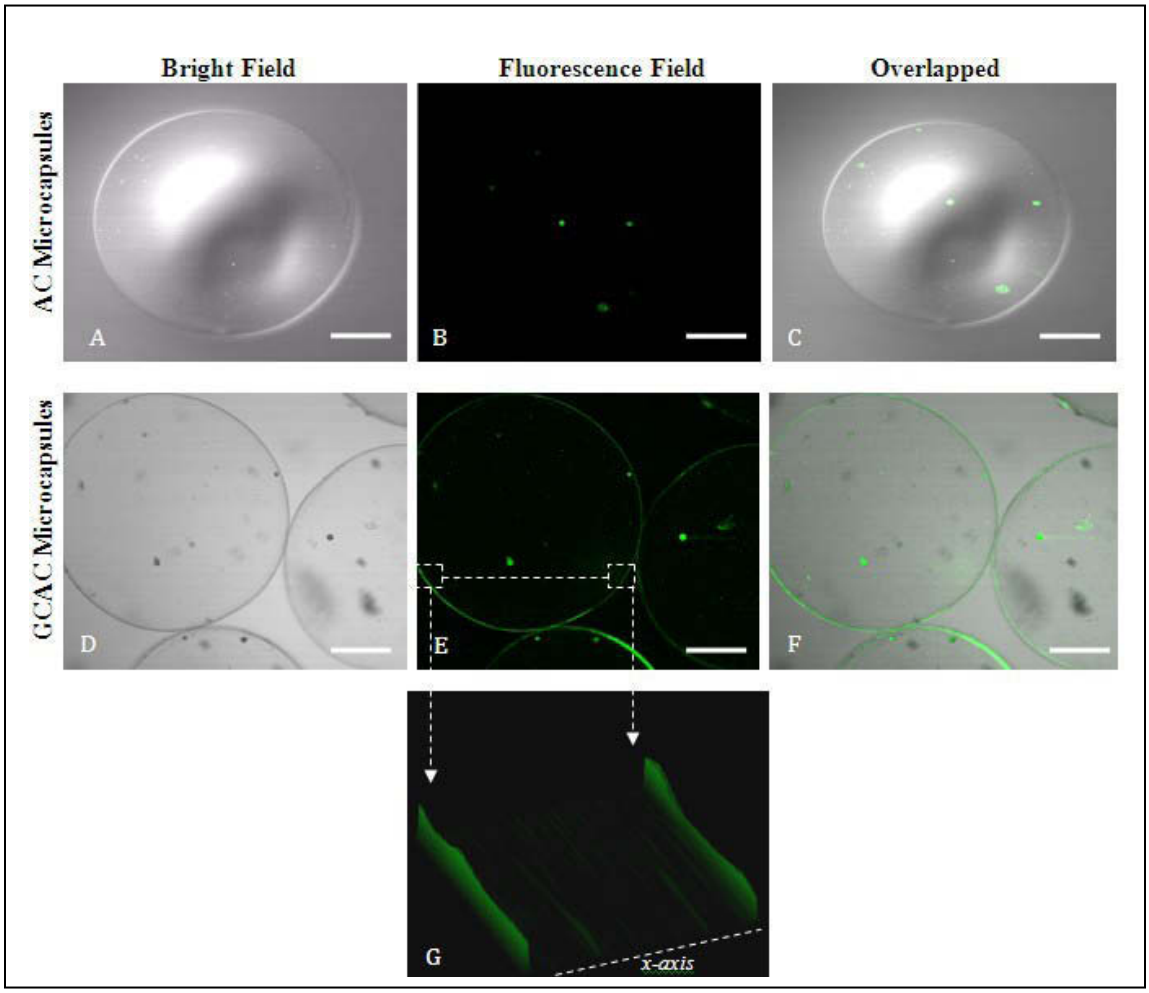

Figure 6.2: Confirmation of reaction between chitosan layer and outer genipin coating in preparing genipin-crosslinked alginate chitosan (GCAC) microcapsules using confocal microscope. The above figure represents the confocal laser scanning microscopic images of the AC (A, B and C) and GCAC microcapsules (D, E and F) at an excitation of 488nm and emission of 530nm. The microcapsular AC membrane was cross-linked with genipin (5.0 mg/mL) for 12h. The green fluorescence on the outer surface of the GCAC capsules indicates the complete cross-linking between genipin and chitosan. This fluorescence was not there in AC capsules which were no treated with genipin. The encapsulated viable cells, stained by calcein AM, are shown as the green dots inside the capsule. The scale bar indicates 50µm. The bottom picture (G) shows the fluorescence intensity profile (in green) corresponding to the white dotted x-axis line drawn across the plane of the GCAC microcapsules using ImageJ 1.43m.

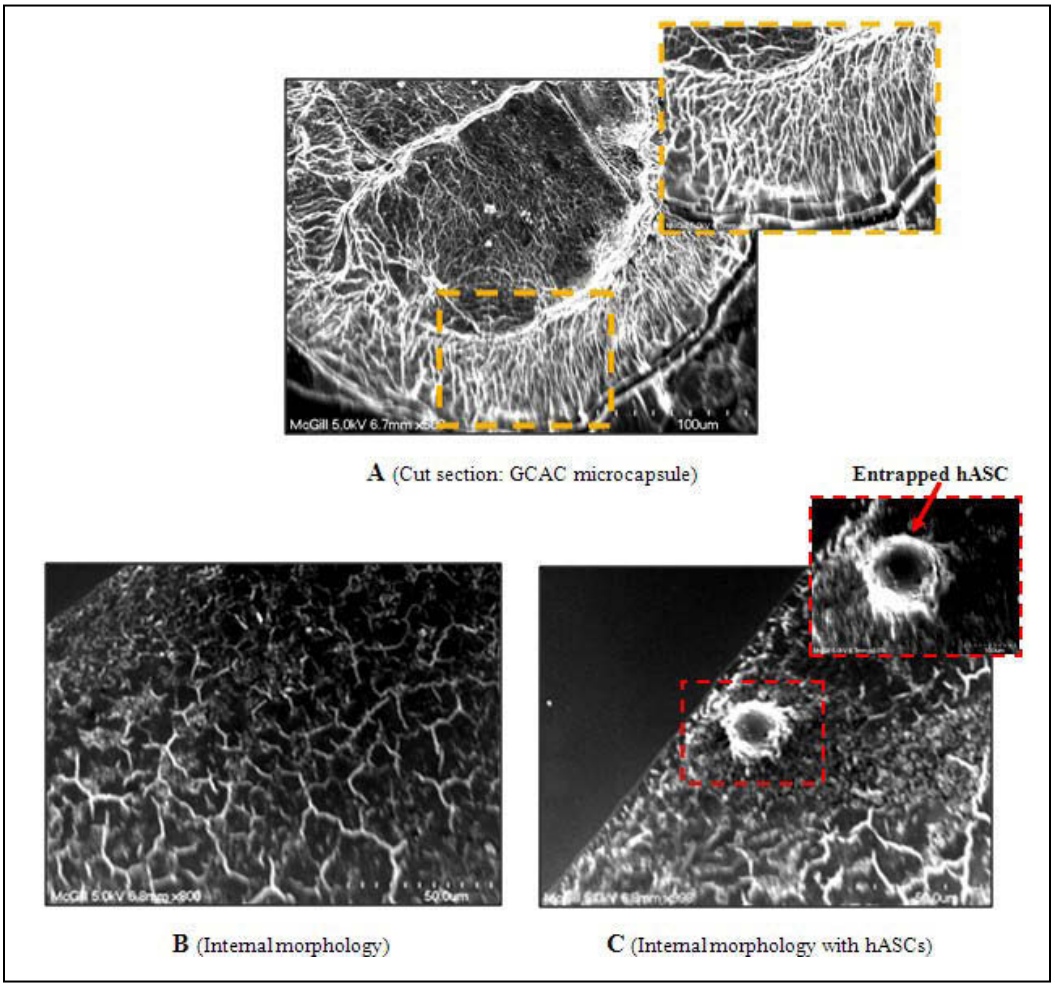

Figure 6.3: Scanning Electron Microscope images of microcapsules with and without stem cells. Images of internal morphology of cell loaded genipin-crosslinked alginate chitosan (GCAC) microcapsules (A; scale bar = 100µm; magnification: 500X) with subset showing a higher magnification (1300X) of the capsular outer membrane (scale bar = 40 µm). The microphotograph in the lower panel represents the internal mesh-like scaffold structure of the empty GCAC microcapsule (B. scale bar = 50µm; magnification: 800X) and hASC loaded GCAC microcapsule (C. scale bar = 50µm; magnification: 800X) with the subset showing the magnified image of the entrapped cell within the capsular scaffold (scale bar = 10µm; magnification: 3013X).

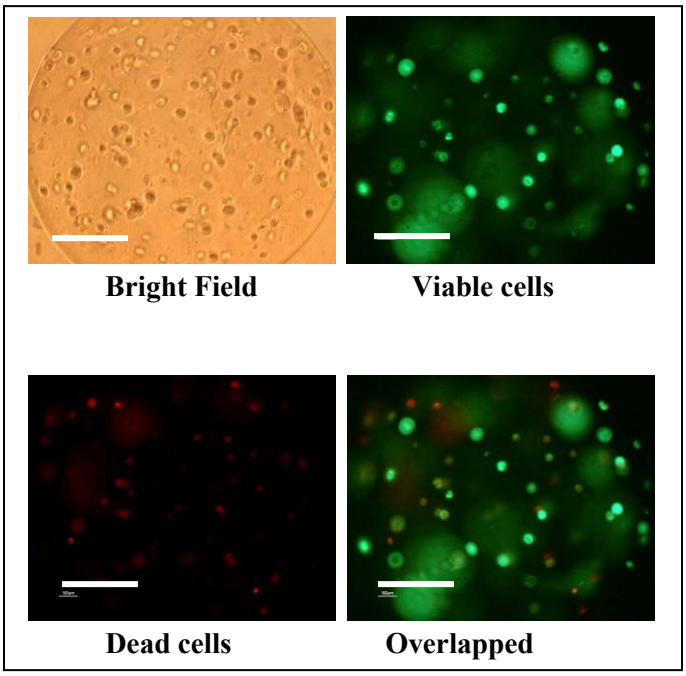

Figure 6.4: Viability of microencapsulated stem cells after 21 days of culture in complete media at 37^{o}C. Viability tests were done by using the calcein AM (showing viable cells in green) and ethidium homopolymer (showing dead cells in red) dye. Representative bright field and fluorescent images of a capsule encapsulating the cells under 400X magnifications in a fluorescence microscope. As the cells are encapsulated in three dimensional microcapsules they are not in the same plane of focus; thus some viable green cells are focused while others are not. Note that the fluorescent outer circles of genipin-crosslinked alginate chitosan microcapsules due to genipin-chitosan cross-linking, also disappeared by day 21. This indicates that the outer surface has gradually started disintegrating by this time. Moreover, after 3 weeks the proliferation ability of the entrapped cells gets gradually reduced mainly because of the microcapsules get completely confluent with the growing cells inside. The scale bar indicates 50µm.

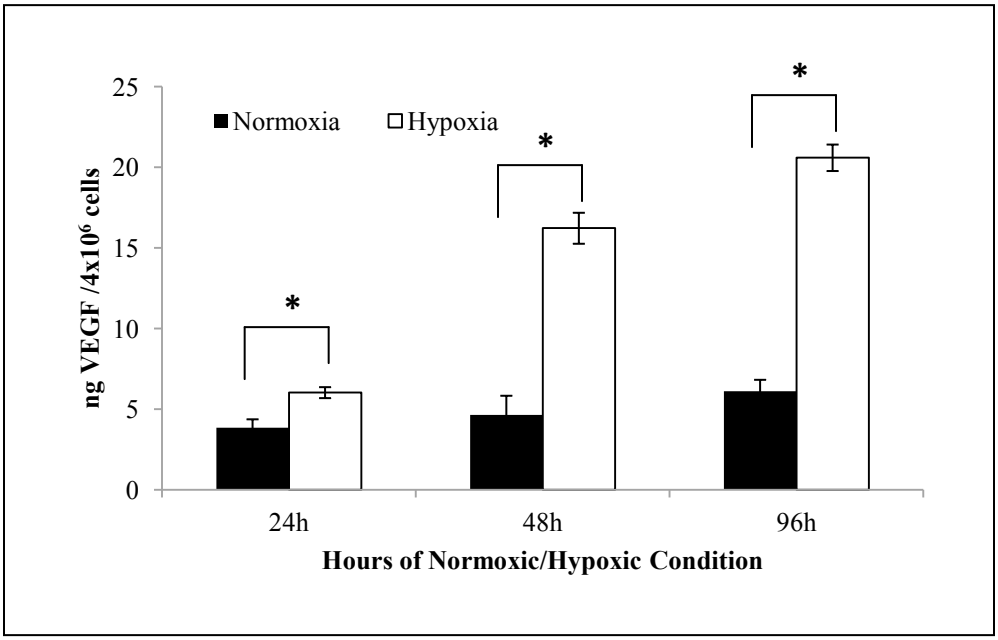

Figure 6.5: Modulation of vascular endothelial growth factor (VEGF) secretion by microencapsulated adipose stem cells under hypoxic and normoxic condition. Secretion of VEGF by GCAC encapsulated hASCs cultured in normoxic or hypoxic conditions over 24h, 48h and 96h was measured by ELISA and is presented as mean ±SD nanogram of secreted factor normalized to $4x10^6$ cells at time of harvest. VEGF production in normoxia and hypoxia was compared with one way ANOVA analysis (n=3;*p<0.05).

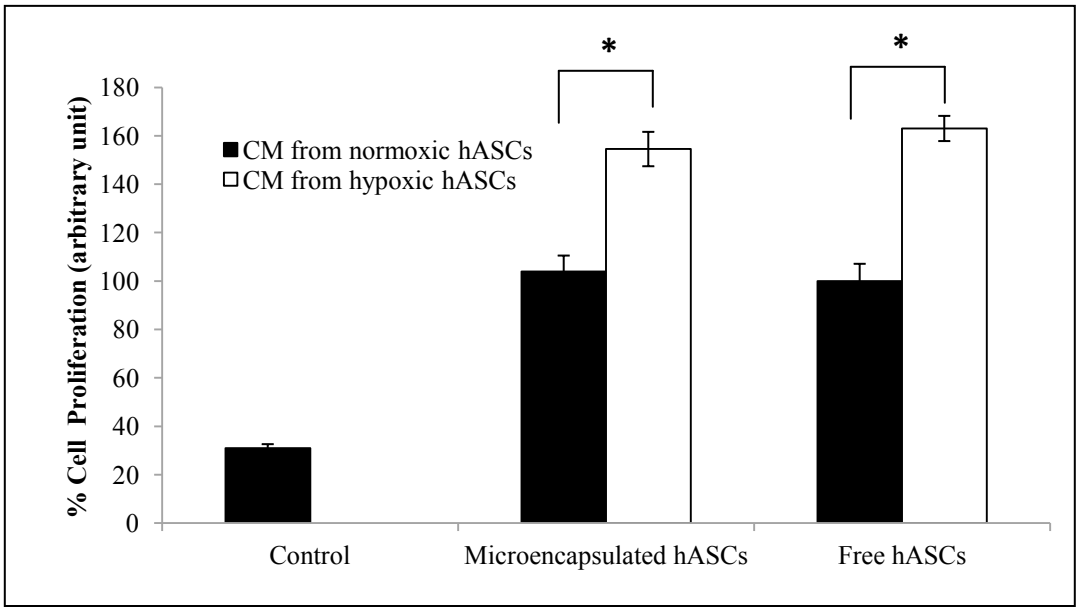

Figure 6.6: Evaluation of bioactivity of released vascular endothelial growth factor (VEGF) from adipose stem cells: endothelial cell proliferation assay. Effects of free and encapsulated hASC supernatants on HUVEC proliferation are represented as percentage of cells on day 4 under hypoxic and normoxic conditions (mean ± SD). For this unstimulated endothelial cells are taken as the control. The average cell number in wells treated with normoxic media from free cells on day 4 of proliferation was taken as 100% and cells from other wells were normalized to it. Numbers of endothelial cells exposed to normoxic media only are significantly lower than those exposed to hypoxic media. This was same for both free and encapsulated cells. VEGF production in normoxia and hypoxia was compared with one way ANOVA analysis (n=3;*p<0.05).

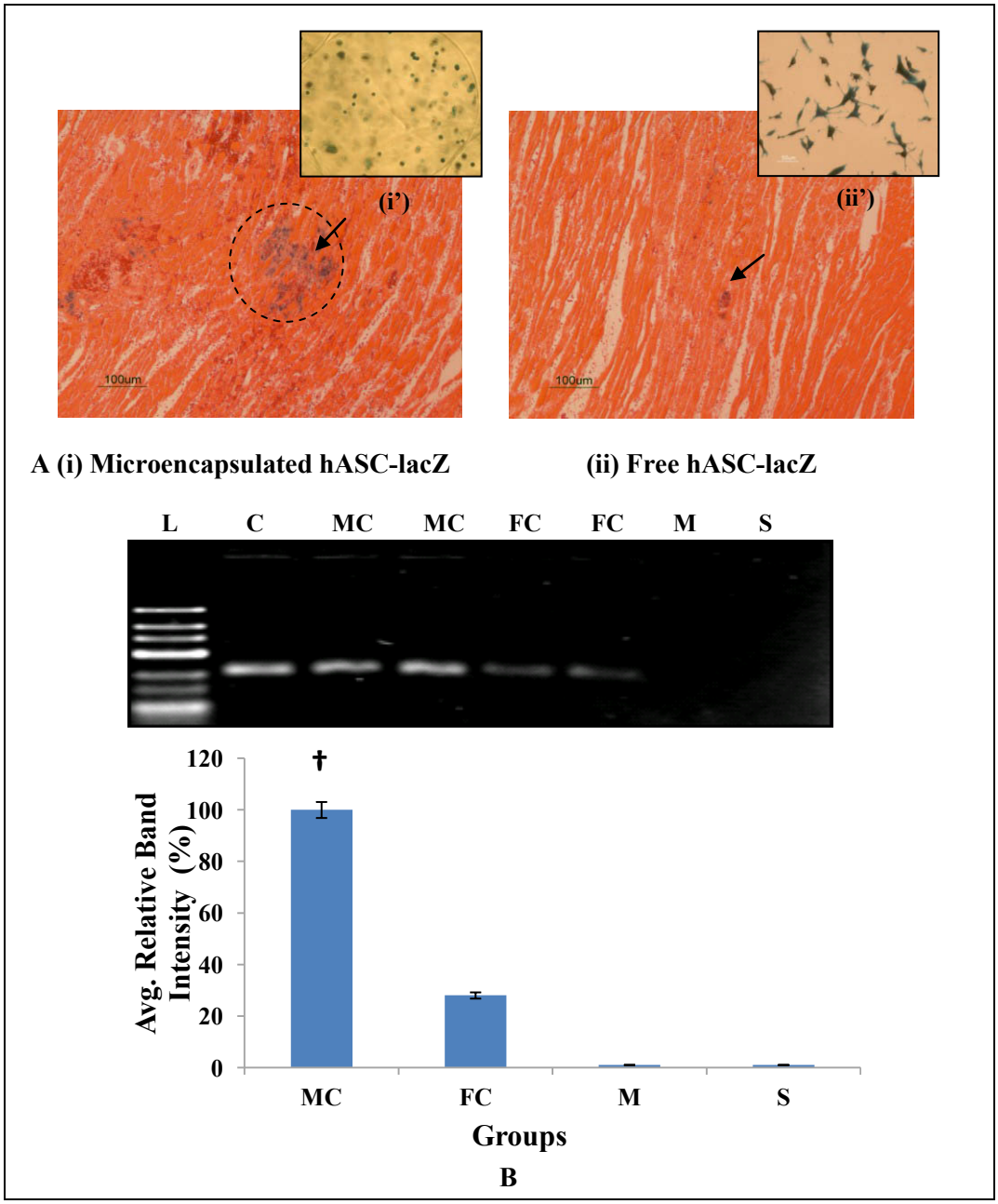

Figure 6.7: Higher retention of adipose stem cells (hASCs) in the left ventricular myocardium using microcapsules 10 weeks post transplantation. Histological sections of the left ventricular heart stained with X-gal in (**Ai**) encapsulated hASCs group and (**Aii**) free hASCs group. The transplanted hASCs are indicated by the arrows. **Ai'** represents the X-gal stained microencapsulated hASCs, with stable LacZ expression, which were used for transplantation in microencapsulated hASC group. This positive X-gal staining illustrates that the encapsulated cells

were viable and express the LacZ transgene from within the microcapsules. **Aii'** represents the X-gal stained monolayer hASC culture, stably transduced with LacZ gene, which were used for transplantation in free hASC group. The scale bars indicate 100µm. **B.** PCR products (250bp) specific for the human Y chromosome (DYS390 sequence) as detected in 2% agarose gel. There were clear and distinct bands in all the female rat hearts with microencapsulated male hASCs at 10 weeks (MC). These band intensities were much lower in free hASC groups (FC). Two PCR products from each group are shown here. The Image J analysis of the band intensities show the FC group with average 28% band intensity taking the band intensity of MC group as 100%. C represents the positive control for the in vitro cultured male hASCs, whereas M represents the negative control for the group M treated with empty microcapsules and S represents the myocardium for the sham group S. †: statistically significant between microencapsulated hASCs and free hASCs.

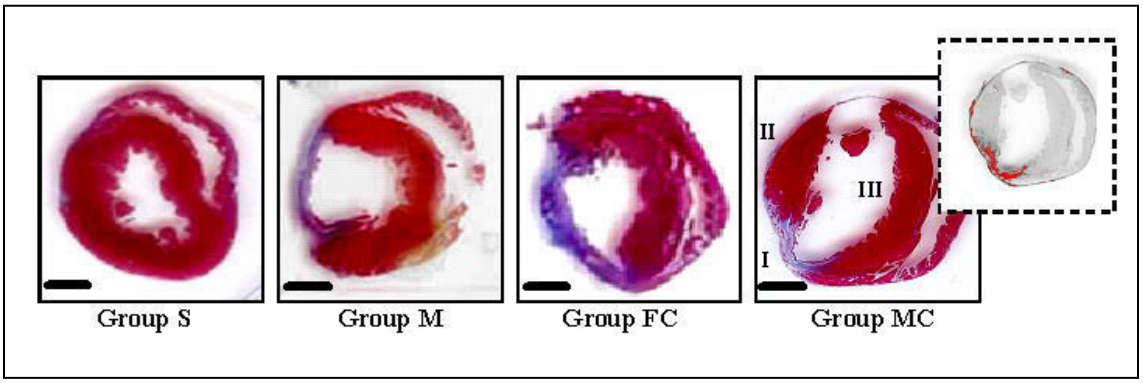

Figure 6.8: Effect of microencapsulated and free human adipose stem cells (hASCs) on infarcted rat heart: Scar area detection. 10 weeks after myocardial infarction, the heart was excised and stained using Masson's trichrome staining method where the blue stained area represents the scar tissues (I: infarcted area in left ventricular wall; II: non-infarcted left ventricular portion III: septum). Infarct scar area and the total area of LV myocardium measured automatically by the means of ImageJ-1.41 (NIH) software, as shown in subset of Group MC. Red area represents ECM deposition in scar tissue and grey area represents myocardium. Compared to groups with microcapsules and free hASCs, encapsulated hASC group had less extracellular matrix deposition area. Scale bars indicate 2mm.

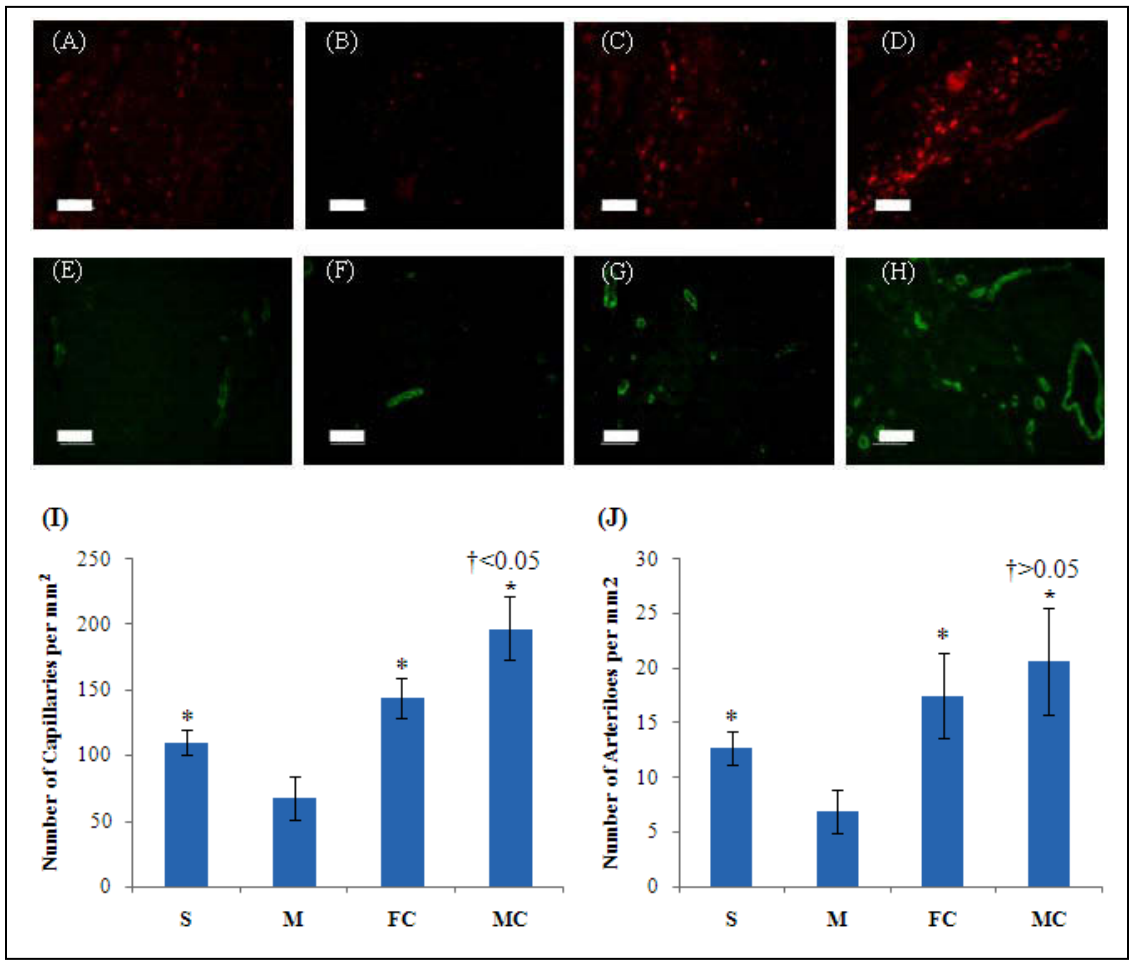

Figure 6.9: Angiogenesis and arteriogenesis in the peri-infarct area of heart. Immunohistological staining of PECAM to detect endothelial cells in (A) Sham, (B) M, (C) FC and (D) MC groups. Immunohistological staining of smooth muscle α-actin for smooth muscle cells in (E) S, (F) M, (G) FC and (H) MC groups. Scale bar indicates 50µm. Quantification of (I) capillary and (J) arteriole density. Data are expressed as mean density ±SD. One-way ANOVA analysis: * represents statistically significant *p* value compared to control (M), † represents the statistically significant *p* value between microencapsulated hASCs and free hASCs.

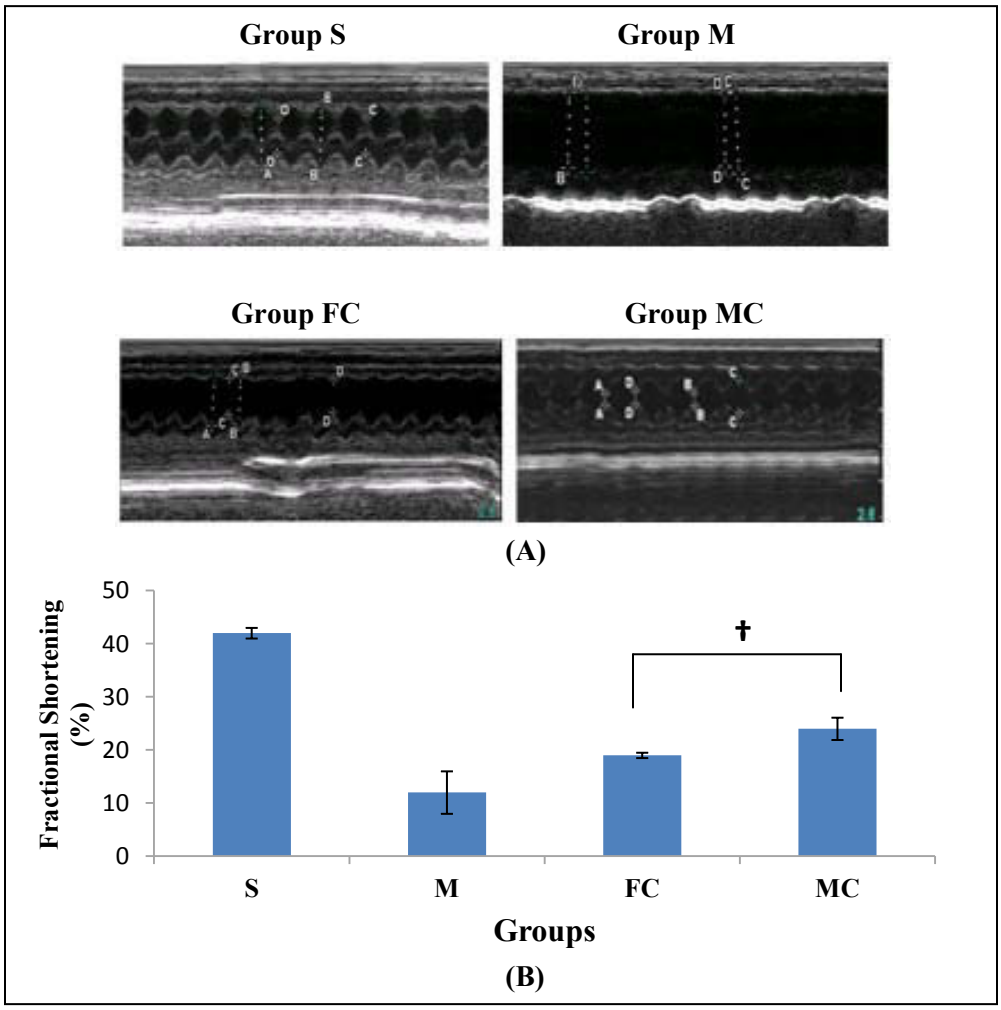

Figure 6.10: Functional effects of microencapsulated and free hASCs on infarcted rat heart: evaluation of cardiac function by echocardiographic analysis (fractional shortening). Ten weeks after myocardial infarction, echocardiography was performed to evaluate cardiac function. Panel **A** shows M-mode echocardiograms from different groups of rats. Effects of microencapsulated hASCs on LV fractional shortening on week 10 are also presented **(B).** Values indicate the mean ± SD (n=8; n=4 for sham) **B:** Left ventricular fractional shortening also improved significantly in group MC compared to group M and group FC. *: statistically significant *p* value compared to control (microcapsules only), †: statistically significant *p* value between microencapsulated hASCs and free hASCs.

PAMAM dendrimer-baculovirus nanocomplex for microencapsulated adipose stem cell-gene therapy in myocardially infarcted rat model

Arghya Paul[1], Wei Shao[1], Sana Abbasi[1], Dominique Shum-Tim[2], Satya Prakash[1*]

[1] Biomedical Technology and Cell Therapy Research Laboratory, Department of Biomedical Engineering, Faculty of Medicine, McGill University, 3775 University Street, Montreal, Quebec H3A 2B4, Canada.

[2] Cardiothoracic Surgery and Surgical Research, Royal Victoria Hospital, Room # S8.73B 687 Avenue Des Pins Ouest, Montreal, Quebec H3A 1A1, Canada.

*Correspondence author; Email: satya.prakash@mcgill.ca
Tel: +1-514-398-3676; Fax: +1-514-398-7461

Preface : After demonstrating the suitability of microcapsules for myocardial cell transplantation, in the present study we aim to enhance the therapeutic potential of the transplanted cells by genetically modifying the cells to overexpress angiogenic proteins. For this we used baculovirus as the vector and showed that surface coating them with dendrimer nanoparticles can enhance their gene delivery efficiency. For improved release of the proteins and enhanced biocompatibility we developed new type of branched PEG surface functionalized microcapsules to deliver the cells. The paper reports encouraging *in vitro* and *in vivo* data which reveal its efficacy as a new class of therapeutic myocardial implant.

Original article submitted in ***Molecular Pharmaceutics*** **(2012)**

7.1 Abstract

The present study aims to develop a new stem cell based gene delivery system consisting of human adipose tissue derived stem cells (hASCs) genetically modified with self assembled nanocomplex of recombinant baculovirus and PAMAM dendrimer (Bac-PAMAM) to over-express vascular endothelial growth factor (VEGF). Cells were enveloped into branched PEG surface functionalized polymeric microcapsules for efficient transplantation. *In vitro* analysis confirmed efficient transduction of hASCs expressing 7.65±0.86 ng functionally active VEGF per 10^6 microencapsulated hASCs (ASC-VEGF). To determine the potential of the developed system, chronically infarcted rat hearts were treated with either empty microcapsules (MC), microencapsulated hASCs expressing MGFP reporter protein (MC+ASC-MGFP) or MC+ASC-VEGF, and analyzed for 10 weeks. Post transplantation data confirmed significantly higher myocardial VEGF expressions with significantly enhanced neovasculature and cardiac performance in MC+ASC-VEGF group (ejection fraction: 48.6±6.1% vs 38.8±5.3% vs 31.5±3.3%, $P < 0.001$). Collectively, this data demonstrates the feasibility of this system for improved therapeutic applications.

7.2 Introduction

Stem cell therapy in cardiovascular diseases, in particular, myocardial infarction has evolved tremendously over the last decade [258-260]. Recently, ASCs and genetically modified ASCs have received particular interests because of these logistic and economic advantages [261, 262]. The human body has abundant subcutaneous and visceral fat deposits and hASCs can be easily aspirated and isolated from these locations with low cost and minimal invasiveness [263]. Furthermore, it has been shown that these cells are able to produce several pro-angiogenic growth factors, in particular VEGF under hypoxic condition, which plays an important role in angiogenesis [264]. In order to explore this angiogenic potential and enhance their therapeutic effects in the damaged myocardium, we aimed to genetically modify the hASCs to over-express VEGF using a non-toxic biologically safe gene delivery vector. Invertebrate cell originated baculovirus is

considered an ideal vector to transduce stem cells [265, 266]. Unlike other commonly used mammalian viruses, such as retrovirus and adenovirus, insect cell originated baculoviruses are non-pathogenic and non-toxic as they cannot replicate in mammalian cells and they do not invoke any cytopathic effects. Thus it is considered a promising tool for cell based gene therapy applications. However, previous reports have also demonstrated that the *in vivo* applications of baculoviruses are impeded by the susceptibility of the viruses to complement-mediated inactivation. Moreover, baculoviruses have lower transduction efficiency, in general, compared to commonly used mammalian viruses which impede its wider applications.

The present study aims to utilize recombinant baculoviruses to genetically modify ASCs. In order to achieve efficient cell transduction, we focused on exploiting the viral membrane characteristics by manipulating its surface charge properties. This is because interactions through electrostatic charges between viral surface and mammalian cell membranes play a critical role during cell entry [267]. It has been reported that noncovalent complexations of adeno- and retroviral vectors with polymers, such as poly-l-lysine and polybrene, can work as superior gene delivery vectors compared to uncoated viruses [268-270]. Polyethyleimine and folate-PEG has also been used as synthetic cationic molecules for viral complexations [271, 272]. Among other widely used polymers, polyamidoamine (PAMAM) dendrimers has been shown to function as highly efficient cationic polymer vectors for gene delivery [273, 274]. PAMAM dendrimers are synthetic nanoparticles with a unique molecular architecture, characterized by their well defined structure, high degree of inter-molecular uniformity, low degree of polydispersity, and multiple terminal functional groups. This makes dendrimer an excellent nanobiotechnological tool for targeted delivery of therapeutic molecules. They have been as efficient as (or more efficient than) both cationic liposomes and other cationic polymers for *in vitro* gene transfer [275]. With this knowledge, we aim to develop an advanced gene delivery system using cationic amino-functional PAMAM dendrimers hybridized to a negatively charged recombinant baculovirus surface by highly reactive, polar amine surface groups of

dendrimers. We postulated that the developed PAMAM dendrimer-baculovirus nanocomplex can efficiently transfer VEGF transgene to hASCs. We also postulated that cationic components of PAMAM dendrimer would charge-associate with negatively baculovirus particles, and would facilitate attachment to the negatively charged cell membrane; and the better the binding to the cell membrane, more virus would be internalized, enhancing gene transfer and expression. To deliver the transduced cell *in vivo* for myocardial therapy we have employed polymeric microcapsules. For this we formulated a new multilayered microcapsule device functionalized with a monolayer of copolymer poly (L-Lysine)-graft-branched poly (ethylene glycol) (PLL-g-brPEG) on the outermost layer. The copolymer structure consists of outer neutrally charged non-immunogenic branched PEG chains grafted with positively charged PLL, which forms the polymer backbone. Surface modification of the delivery systems with such hydrophilic polymers, also imparts resistance against unwanted plasma protein adsorption onto the surface of the microcapsules [276, 277]. As reported in our earlier studies, the microcapsules will also help reduce the high mechanical and biological loss of transplanted hASCs from the site by the contracting myocardium [278-280]. The **graphical abstract** (along with **Figure 7. S1**: **supplementary materials**) illustrates the overall scheme of the entire study.

7.3 Materials and methods

7.3.1 Chemicals

Sodium alginate (viscosity 2%) and poly-L-lysine hydrobromide (PLL; Molecular weight 27,400) were bought from Sigma Chemicals (St. Louis, MO). PAMAM dendrimer (generation 2) with ethylenediamine core (MW: 3256.18) containing 16 surface primary amino groups was procured from Sigma Chemicals and resuspended in phosphate buffered saline (PBS).

7.3.2 Cell culture

Human ASCs were obtained from Invitrogen and cultured in DMEM (Invitrogen) supplemented with 10% Fetal Bovine Serum (FBS). The cells were routinely

maintained as stationary cultures in 75 cm^2 tissue culture flasks and incubated at 37^o C in a controlled environment with an air atmosphere of 5% CO_2. Human umbilical vein endothelial cells (HUVEC) were purchased from Sciencell Research Laboratories (Carslbad, US) and maintained similarly in FBS supplemented Endothelial Cell Medium (ECM) supplied by the company.

7.3.3 Generation of recombinant Bac and formulation of Bac-PAMAM nanocomplex

Recombinant baculovirus carrying Monster Green Fluorescent Protein (Bac_{MGFP}) gene was prepared using protocol described in our recently reported work [281]. Similarly, $VEGF_{165}$ gene carrying recombinant Bac (Bac_{VEGF}) was also generated using human $hVEGF_{165}$ cDNA (Origene Technologies, Rockville, MD), instead of MGFP reporter gene. In order to form the dendrimer-baculovirus nanocomplex, the solutions of the dendrimers (stock solution of 1μmol in PBS) and baculoviruses were first brought to room temperature and adjusted to desired concentrations. PAMAM solution and baculovirus solution were then mixed according to a desired PAMAM/virus ratio (0, 10, 100 and 200 nmol PAMAM molecules per 10^8 viruses). The mixture was incubated at room temperature for 30 min to form complexes, with gentle vortexing from time to time. The mixture was further centrifuged at 24,000rpm for 45min, and the pellet containing the heavier Bac-PAMAM nanocomplex was collected, leaving the unreacted dendrimer in the supernatant. The collected Bac-PAMAM was washed twice using PBS using the same centrifugation process. For every experiment, the preparation was freshly made.

7.3.4 Characterization of Bac-PAMAM nanocomplex

The zeta potential of the Bac-PAMAM nanocomplex under different conditions was measured by the technique of electrophoretic laser Doppler anemometry using a Zeta Potential Analyzer (Brookhaven Instruments Corporation**,** HotsVille, New York, USA). Zeta Potential Analyzer version 3.57 software was used to determine the zeta potential. The zeta potentials were measured for three batches

of nanocomplexes and each measurement was obtained after taking the average of the three runs. Transmission Electron Microscopy (TEM) was used to obtain the size characterization. To perform this, the nanocomplexes were photographed on CM200 FEG-TEM microscope (Philips, Markham, Ontario, Canada).

7.3.5 Bac-PAMAM mediated transduction of hASCs

For the transduction experiments, 5x 10^5 cells were seeded in each well in 6 well plates and incubated overnight. This was followed by washing of the wells with PBS and addition of Bac_{MGFP}, Bac_{MGFP}-PAMAM (10), Bac_{MGFP}-PAMAM (100) and Bac_{MGFP}-PAMAM (200) nanocomplex resuspended in PBS to corresponding wells with a constant MOI[multiplicity of infection=pfu/cell] of 200, where the values within brackets indicate the ratio of PAMAM in nmol per 10^8 viruses. After 4 h of transduction, the cells were replenished with fresh serum supplemented DMEM media. Same protocol was followed for transduction with Bac_{VEGF}-PAMAM.

7.3.6 Preparation of branched PEG functionalized microcapsules encapsulating hASCs

After transduction, the hASCs were encapsulated in alginate microcapsules using previously established procedure [280, 282]. Briefly, transduced or non-transduced cells were suspended in 1.5% sodium alginate (Sigma Chemicals, St. Louis, MO, USA) at a cell concentration of 2x10^6 cells/ mL. The suspension was extruded through an encapsulator (Inotech) fitted with a 300µm nozzle at a voltage of 0.577kV and frequency of 710Hz. The gelation process took place in a 0.1M $CaCl_2$ solution for 15 min. The newly generated alginate microcapsules were immersed in 0.1% (w/v) PLL-g-brPEG (check supplementary data for preparation method) solution for 15min similar to procedure mentioned elsewhere [277]. The formed AP-brPEG microcapsules were then washed twice with physiological solution and then transferred to stationary cell culture flasks resuspended in DMEM medium supplemented with 10% FBS and antibiotic

antimycotic solution (Sigma) for further culture in 37^{o}C incubator with 5% CO_2. Microcapsules were replenished with fresh media every alternate day.

7.3.7 Quantification of VEGF released from encapsulated cells by ELISA

To check whether the Bac_{VEGF}-PAMAM transduced ASCs, encapsulated in microcapsules, can secrete the transgene VEGF, $4x10^6$ ASCs were encapsulated in the microcapsules and grown under standard conditions for 14 days. Conditioned media (CM) were collected at regular intervals and VEGF release was quantified using a VEGF ELISA kit (R&D Systems). Data are expressed as mean ±SD picogram (n=3) secreted from the 4 $x10^6$ cells. Non-encapsulated free cells were taken as the standard and empty capsules were taken as the negative control.

7.3.8 Evaluation of the bioactivities released VEGF from microencapsulated ASCs

Endothelial cell proliferation assay

VEGF are known to stimulate endothelial cell proliferation *in vitro* [283]. For the cell proliferation assay, $1x10^4$ HUVECs per well were seeded in 96 well plate in triplicate for each sample using standard ECM media After culturing overnight, the cells were washed twice with PBS and 200µl of the conditioned media from the encapsulated cells under different conditions were added to the cells along with 50µl of normal ECM media. The cells were grown at 37^{o}C in 5% CO_2 for 96h followed by MTS cell proliferation assay according to the manufacturer's protocol.[24]

Wound healing assay by endothelial cell migration

VEGF can induce endothelial cell migration and wound healing when cultured *in vitro* [283]. To perform this, HUVEC were seeded in six well plates and grown to confluency. After 24 h of serum starvation, the monolayer was carefully mechanically wounded with a 200µl pipette tip. The wells were then washed twice with PBS to remove the cell debris and 1 ml of conditioned media from different groups of encapsulated cells was added along with 200µl of fresh media.

As control groups, conditioned media was treated with antibody against VEGF before addition to the wells. After 12 h, the cells were fixed with 4% paraformaldehyde and stained with crystal violet. The wound healing was visualized with inverted bright field microscope and quantified by calculating the cell migration.

7.3.9 Delivery of microencapsulated hASCs in infarcted rat heart

Immunocompetent female Lewis rats (200 to 250 gm, Charles River, QC) were used to induce myocardial infarction by occlusion of the left anterior descending coronary artery according to our established laboratory procedures [279, 281]. All procedures were in compliance with the Guide for the Care and Use of Laboratory Animals (NIH publication No. 85-23) and the Guide to the Care and Use of Experimental Animals of the Canadian Council on Animal Care. Myocardial infarction was induced by occlusion of the left anterior descending coronary artery as described previously. Fifteen minutes after ligation of the artery, three 50 µl intramyocardial injections in the peri-infarct area of the left ventricle were given using a 27-G needle. Group MC (n=12) received empty micocapsules, group MC+ASC-GFP (n=12) received microcapsules encapsulating Bac_{MGFP}-PAMAM (100) transduced $1.5x10^6$ ASCs, while group MC+ASC-VEGF (n=12) received microcapsules encapsulating Bac_{VEGF}-PAMAM (100) transduced $1.5 x10^6$ ASCs.

7.3.10 Quantification of myocardial VEGF expression post transplantation

4 days post injection, 4 animals from each group were sacrificed and flash frozen in liquid nitrogen before storing at −85°C. The frozen heart samples (peri-infarct and non-infarct region) were weighed, and 3 ml of RIPA buffer (Santa Cruz Biotech, CA) (with PMSF in DMSO, protease inhibitor cocktail, and sodium orthovanadate) was added to per gram of tissue as mentioned elsewhere.[281] The samples were homogenized and centrifuged at 4°C for 10 minutes at 10,000 × g. Thereafter the supernatants were collected and analyzed by ELISA for hVEGF according to the manufacturer's instructions (Quantikine, R&D system,

Minneapolis, MN). The total protein content was determined using Quant-iT protein assay kit (Invitrogen, Burlington, Canada) with bovine serum albumin (BSA) as the standard.

7.3.11 Immunohistochemistry for detecting neovascularization

Neovascularization was evaluated by analyzing the capillary and arteriole density in the peri-infarct area. For this, immunohistochemical staining was performed with antibodies against PECAM (Santa Cruz) for identification of endothelial cells and smooth muscle α-actin (Santa Cruz) for tracing the smooth muscle cells as described elsewhere [284]. Briefly, for measurement of capillary density, five fields in the peri-infarct area were imaged and average numbers of capillaries with less than 10μm diameter were counted. The capillary density was quantified as the (mean total PECAM-positive microvessels)/mm^2 using three tissue sections spanning per-infarct tissue region of each animal. Similarly, arteriole densities were quantified as the (mean total smooth muscle α-actin-positive microvessels)/mm^2.

7.3.12 Echocardiography and cardiac performance

Transthoracic echocardiography was performed on all surviving animals in the four groups before operation (baseline), and before sacrifice on week 10. Echocardiograms were obtained with a commercially available system (SonoSite, Titan-Washington, Seattle, WA) equipped with a 15-MHz transducer. After sedating the animals with 2% isoflurane, echocardiography was performed according to the American Society of Echocardiology leading-edge method as described in earlier studies [279].

7.3.13 Statistical analysis

Quantitative variables are presented as mean ± Standard Deviation (SD) from independent experiments as described in the figure legends. Statistics were performed using two-way and/or one-way ANOVA by Bonferroni's multiple

comparison post-hoc test. All statistical analyses were performed with Prism 5 (GraphPad Software). P value <.05 was considered significant.

7.4 Results

7.4.1 Characterization of electrostatic interaction of baculovirus with PAMAM dendrimer

The overall process for development of a new nanobiohybrid gene delivery system to promote angiogenesis via genetically modifying ASCs, encapsulated in polymeric microcapsules, is schematically illustrated in **graphical abstract and Figure 7. S1 (Supplementary materials).** To confirm the successful formation of hybrid Bac-PAMAM complex, zeta potential of the nanocomplexes were measured as shown in **Figure 7.1A.** At pH 7.4, the zeta potential of the free baculoviruses was negatively charged with a zeta potential of -13.6mV±1.2. The positively charged PAMAM dendrimers, upon conjugation with the negatively charged baculoviruses, formed hybrid nanocomplexes which resulted in an increment of surface charge towards positive. Bac-PAMAM (10) showed a zeta potential of -7.6±2.0mv, while Bac-PAMAM (100) showed 2.36±1.2mv and Bac-PAMAM (200) showed 2.7±3.2mv, where the values within brackets indicate the ratio of PAMAM/virus used in preparing the nanocomplexes. To reconfirm the complex formation, TEM images the products were taken. **Figure 7.1B-C** demonstrates the efficient binding of the rod like baculovirus with PAMAM dendrimers leading to the formation of stable Bac-PAMAM hybrid complex.

7.4.2 Microencapsulated genetically modified hASCs expressing transgene

The transduction protocol for hASCs was first optimized using different formulations of Bac_{MGFP}-PAMAM nanocomplexes in 96 well plates (**Supplementary materials: Figure 7.S2A-E**). This was followed by confirmation of the formation of branched PEG surface functionalization of the microcapsules, entrapping viable ASCs inside, as analyzed by NMR, cell viability assay and confocal microscopy (**Supplementary materials: Figure 7.S3 and Figure 7.S4**). As a next step to demonstrate the gene expression pattern of the

AP-brPEG microencapsulated transduced cells, hASCs were transduced with Bac_{MGFP}, Bac_{MGFP}-PAMAM (10) and Bac_{MGFP}-PAMAM (100) and encapsulated at a concentration of 2 million cells per mL of alginate to prepare the AP-brPEG microcapsules. The microencapsulated cells were cultured for 48h in stationary flasks with standard medium, supplemented with antibiotics. The relative fluorescence units of each well containing 50 capsules resuspended in PBS were then measured using Victor3 Multi Label Plate Counter (Perkin Elmer, USA), as described elsewhere [280, 285]. As shown in **Figure 7.2A and 7.2B-D**, the Bac_{MGFP}-PAMAM (100) group showed significantly high normalized GFP expression compared to Bac_{MGFP} (142.4±16.8% vs 100±7.5%) and Bac_{MGFP}-PAMAM (10) (33.6±10.4%).

The VEGF release kinetics profile (**Figure 7.2E**) of the encapsulated cells, as quantified by ELISA of CM, showed highest protein expression on day 4 in Bac_{VEGF}-PAMAM (100) group (7.65±0.86ng/10^6 cells) compared to Bac_{VEGF}-PAMAM (10) (6.1±0.32ng/10^6 cells) and Bac_{VEGF} (2.7±0.15ng/10^6 cells). This data supports our earlier findings that Bac_{VEGF}-PAMAM (100) system significantly enhances gene delivery efficiency than Bac_{VEGF}-PAMAM (10) and Bac alone. The data also reveals that Bac_{VEGF}-PAMAM (100) group expressed the highest amount of protein than other groups all throughout the 14 days of experiment, whereas Bac_{VEGF} group almost ceased their expression by day 8 and Bac_{VEGF}-PAMAM (10) group by day 14.

7.4. 3 Mitotic and wound healing effect of VEGF secreted from microencapsulated hASCs

The bioactivities of the released hVEGF in media from the Bac_{VEGF}-PAMAM (100) transduced encapsulated hASCs were evaluated *in vitro* by observing the proliferative capacity of the HUVECs. Cell Proliferation MTS Assay kit was used to assess the proliferation capabilities of the HUVECs treated with CM (containing secreted hVEGF) from experimental samples. The results were presented as the percent increase in endothelial cell proliferation relative to that induced by CM from unstimulated control hASCs (taken as 100%). As shown in

Figure 7.3A, CM from group hASC-GFP [hASCs transduced with Bac_{GFP}-PAMAM (100)] showed significant HUVEC proliferation (114.0±2.2%). This is because of the presence of naturally releasing VEGF from hASCs, which once blocked with antibodies did not show any HUVEC proliferation. CM from group hASC-VEGF [hASCs transduced with Bac_{VEGF}-PAMAM (100)] exhibited the highest proliferation (138.6±4.9%). As expected, CM from groups treated with antibodies against hVEGF showed no proliferative effects proving that it was because of the bioactivity of released hVEGF from encapsulated genetically modified hASCs carrying VEGF transgene that contributed to the significant HUVEC proliferations. This proliferation rate was directly dependant on the amount of the VEGF released which explains why hASCs genetically modified with Bac_{VEGF}-PAMAM (100) gene delivery system produce better results than Bac_{VEGF}-PAMAM (100) and untransduced control. Furthermore, we tested the ability of CM (containing secreted hVEGF) to increase HUVEC wound healing in a monolayer. As depicted in **Figure 7.3B and 7.3C**, stimulation of wounded HUVEC monolayer with CM from encapsulated hASC-VEGF induced significant healing of wound area (56.5±5.2%) compared with CM from unstimulated hASC control (7.4±2%) and CM from hASC-MGFP (23.6±3.3%). Pre-incubation of CM with the neutralizing anti-VEGF antibodies completely hindered hASC-VEGF CM induced wound healing, clearly suggesting that chemotactic signals from hVEGF are required for proper wound healing effect.

7.4.4 VEGF expressions at sites of transplantation *in vivo*

In order to confirm whether the microencapsulated stem cells were able to express their VEGF transgene when transplanted *in vivo*, myocardial VEGF expression at the peri-infarct and non-infarct ventricular regions (as shown in **Figure 7.4A&B**) was quantified 4 days post transplantation. **Figure 7.4C** indicates that the MC+hASC-VEGF group, receiving microencapsulated hASCs transduced with Bac_{VEGF}-PAMAM (100), showed significantly higher VEGF expression than MC+hASC-MGFP group, receiving microencapsulated hASCs transduced with Bac_{MGFP}-PAMAM (100), (12.44±2.5ng/mg protein vs 4.6±1.22 ng/mg protein) at

the peri-infarct sites. This suggests that the transplanted microencapsulated cells were viable at the injected site and were able to express their transgene efficiently. This expression was almost negligible at the non-infarct regions in both groups suggesting that the transplanted cells were strongly retained at the locally transplanted areas i.e. at the peri-infarct regions, and did not disperse with time into other places of the beating myocardium.

7.4.5 Angiogenesis and arteriogenesis at the peri-infarct region of rat heart

In this section, we tried to comprehend whether the overexpressed VEGF has any vasculogenic effect in the treatment groups. We assessed the neovasculature formation in the peri-infarct area by detecting the capillary (**Figure 7.5: A-C**) and artery densities **(Figure 7.5: A'-C'**). As shown in **Figure 7.5 (D),** we noticed a significant improvement in angiogenesis in the MC+hASC-MGFP and MC+hASC-VEGF groups compared to the control MC group (164.12 ± 12.9/mm^2 for MC+hASC-VEGF, 104.5 ± 5.2/mm^2 for MC+hASC-MGFP vs. 54.25±8.1/mm^2 for control, $p<0.001$). Moreover, MC+hASC-VEGF also showed significantly higher capillary density compared to MC+hASC-MGFP. Similar results were obtained with arteriole density in MC+hASC-VEGF group (13.75 ± 1.83/mm^2 for MC+hASC-VEGF, 10.25 ± 2.25/mm^2 for MC+hASC-MGFP vs. 5.12±1.95/mm^2 for control, $p<0.001$) as presented in **Figure 7.5 (E).** Similar to angiogenesis data, MC+hASC-VEGF also showed significantly higher arteriole density compared to MC+hASC-MGFP group. These data suggest that the transplanted microencapsulated VEGF expressing ASCs were viable, functional and were able to induce efficient vasculogenesis through their improved paracrine system.

7.4.6 Cardiac function analysis over time

To investigate whether the *in vivo* angiogenic effect of hASC based VEGF expression resulted in improved heart function, the left ventricular EF% of the myocardially infarcted rat models were monitored on day 3 and week 10, post infarction **(Figure 7.6**). The reduced EF% (~30%) observed in all groups 3 days

post infarction confirmed that all the rats received acute myocardial infarction. However, there were significant improvements in EF% of rat hearts on week 10 in MC+hASC-VEGF and MC+hASC-MGFP in comparison to the control MC group (48.6±6.1% and 38.8±5.3% vs 31.5±3.3%; $p<0.01$), although this improvement was not significant on day3 post infarction. Similar results were obtained with left ventricular FS% analysis on week 10 (22.2±1.8% and 19.3±1.8% vs 15.1±0.91%; $p<0.01$). In addition, the VEGF expressing group showed a significantly higher EF% and FS% compared to MGFP expressing group, indicating better cardiac function can be achieved by overexpressing VEGF in transplanted microencapsulated hASCs. In other words, these echocardiographic EF% data suggest that genetically modifying ASCs with Bac_{VEGF}-PAMAM to overexpress VEGF can significantly enhance the therapeutic potential of ASC based therapy.

7.5 Discussion

In order to target the high morbidity and mortality rates due to cardiac failure, a wide range of therapies and technologies are under intense research [286-288]. One of the key areas, currently under intense research, is tissue engineering using various types of biomaterials and nanodelivery systems [289]. Furthermore, previous studies have also demonstrated the beneficial role of alginate in the form of microcapsules, by enhancing the myocardial retention of the transplant [278, 279]. In this study we demonstrated that the newly developed brPEG functionalized microcapsule helps in retention of transplanted cells at the injected sites for enhanced secretion of paracrine factors, particularly at the peri-infarct zone (**Figure 7.4**). Recent *in vivo* studies have shown that brPEG conjugated delivery systems can be a superior alternative to linear PEG conjugates [290, 291]. Here, the covalent coupling of branched PEG chains to the PLL has been employed to mask the surface of the microcapsule which decreases the immune-recognition response (**Supplementary materials: 7.S5A**) and improves biodistribution and biocompatibility of the transplants [165, 292, 293].

Although most studies of stem cell therapy have focused on regenerative functions of ASCs, research on their paracrine effects needs to be explored [294].

Recent work has demonstrated ASCs as an ideal candidate for cell based gene therapies using mammalian viral vectors such as adenovirus, lentivirus and sendai virus [295-297]. Here, we have demonstrated that by overexpressing VEGF in ASCs we can achieve significant therapeutic effect in myocardially infarcted heart. In a similar study, Zhang *et al* demonstrated that microencapsulated VEGF expressing xenogeneic cells can induce substantial therapeutic effects in ischemic heart through angiogenesis [235]. In sync to their report, our present study also demonstrates that the VEGF expressing MC+hASC-VEGF group exhibited enhancement of vascular density (**Figure 7.5**), compared to MC+hASC-MGFP and control MC groups. This resulted in significant attenuation of cardiac dysfunction in rats with acute myocardial infarction (**Figure 7.6**).

The work illustrates the potential application of biologically safe baculovirus for gene delivery to ASCs. In addition, baculovirus has been hybridized with PAMAM dendrimer nanostructures and investigated for enhanced transduction capabilities. Dendrimers have been chosen to coat the baculovirus because of their unique characteristics - their unique chemical and structural make up enhance their binding abilities through statistical and/or cooperative effects, which increase affinity, avidity, and specificity of binding [298]. They have low polydispersity and hyperbranched structure which provides a multivalent periphery. This is ideal for conjugation of functional molecules while maintaining low toxicity *in vitro* and *in vivo* [299, 300]. Thus, dendrimers can make an ideal coating on the baculovirus surface for their better transduction. Numerous amino terminal groups facilitate electrostatic interactions of the positively charged dendrimer enveloped baculovirus with negatively charged cell surface which enhance the cell surface binding, and subsequent viral entry into the cells. Recent research has also shown that dendrimers can have diverse *in vivo* and *ex vivo* applications in therapies relating to cardiac tissue damage and protection [301, 302]. Different methods are currently under investigation for baculovirus mediated enhanced gene delivery using surface modification by chemical coupling and electrostatic interactions [303]. Coating of baculovirus using positively charged polymer PEI are also shown to significantly enhance their *in*

vivo gene therapy potential compared to uncoated viruses [304]. In a similar way, our present study demonstrates that surface modifying the baculovirus with positively charged PAMAM dendrimers can also improve gene transfer efficiency. However, to achieve significant therapeutic effects, specifically with stem cells, maintenance of their natural functionalities is of immense importance. Our present work confirmed this by successfully differentiating the encapsulated Bac_{MGFP}-PAMAM transduced hASCs to adipogenic, chondrogenic and osteogenic lineages as depicted in **Supplementary materials: Figure 7.S5B-D**. In addition, our data revealed that the Bac-PAMAM mediated hVEGF expression from hASCs are biologically active as indicated by their enhanced mitotic and chemotatic activities on HUVEC (**Figure 7.3**). The study presented here has focused mainly on the generation 2 of PAMAM dendrimers to couple with the baculovirus. Further studies on higher and lower generations will be interesting to understand how, if at all, the dendrimer generations affect transduction efficiency. Taken together, the study identifies Bac-PAMAM nano-formulation as a new and improved baculovirus mediated gene delivery system and highlights the advantages of microencapsulated VEGF expressing hASCs for myocardial therapy, corroborated with improved vasculogenesis and cardiac performance.

7.6 Acknowledgement

This work is supported by research grant to Satya Prakash from Canadian Institute of Health Research (MOP 93641) and Natural Sciences and Engineering Research Council (NSERC, Canada) strategic grant to Satya Prakash and Dominique Shum-Tim. Arghya Paul acknowledges the financial support from NSERC - Alexander Graham Bell Canada Graduate Scholarship. Sana Abbasi is supported by the McGill Faculty of Medicine Internal Studentship — G. G. Harris Fellowship. The authors thank Minh, Chen, Zyad, Jan and Patrik for their technical support in animal experiments. We are grateful to Prof. Maryam Tabrizian for providing us with facilities in her laboratory at McGill University, Canada.

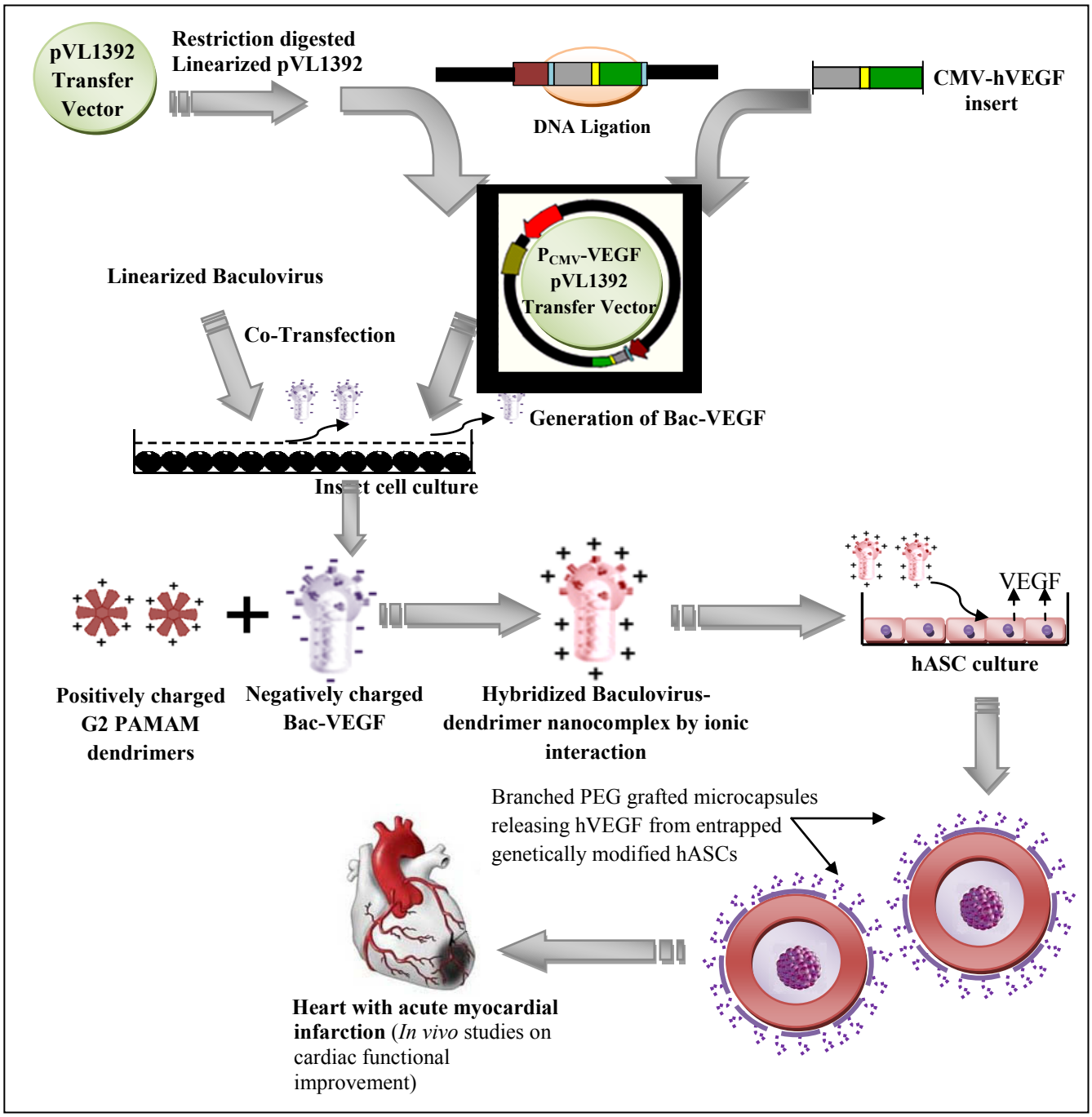

Figure 7.0 Graphical Abstract: Schematic representation of the overall scheme: recombinant baculovirus generation, dendrimer coated positively charged baculovirus preparation, hASC transduction and procedure for myocardial transplantation of hASC using br-PEG coated microcapsules.

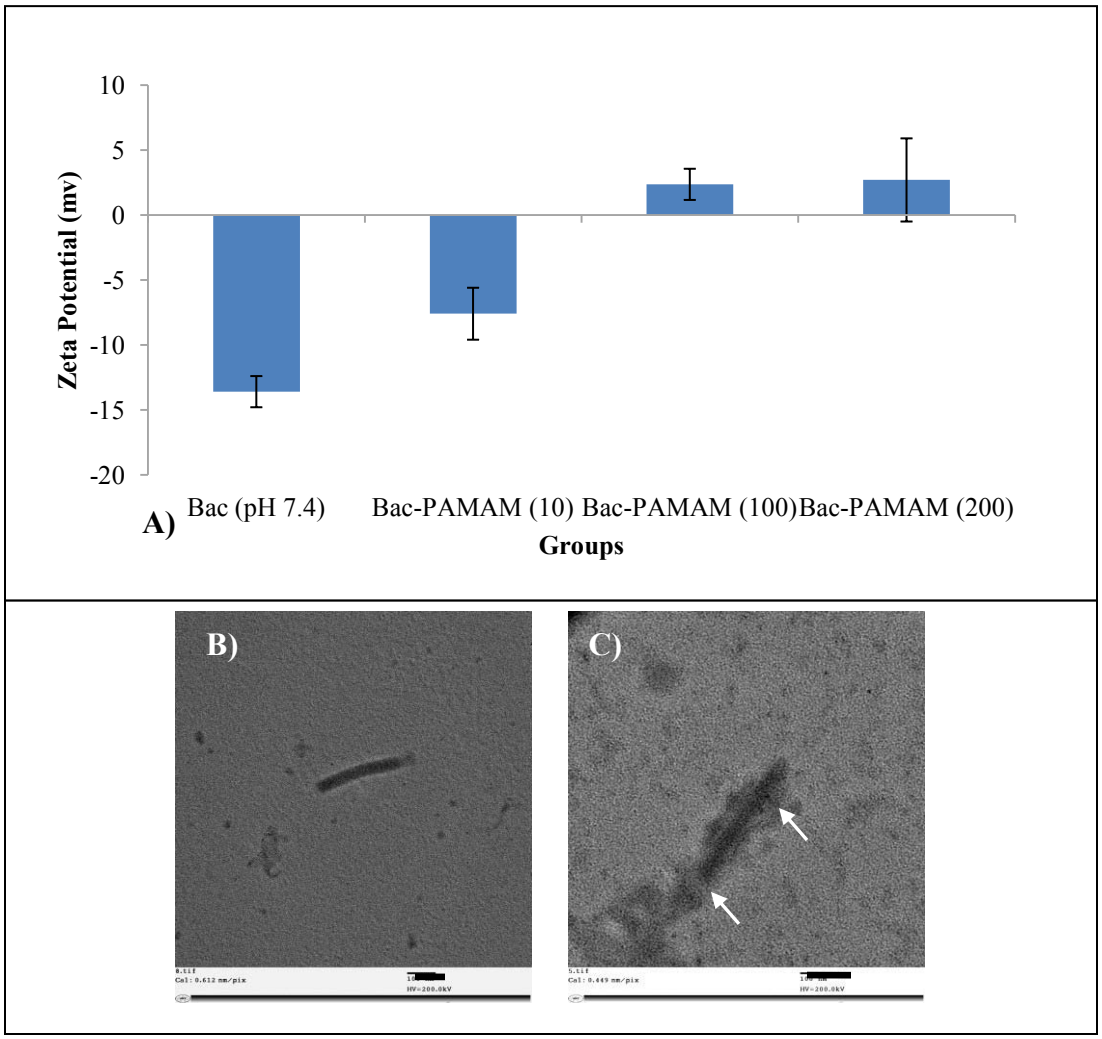

Figure 7.1: Characterization of the Bac-PAMAM nanocomplex. (A): Zeta potential of free Bac, Bac-PAMAM (10), Bac-PAMAM (100), Bac-PAMAM (200), where the values within brackets indicate the ratio of PAMAM molecules in nmol per 10^8 viruses. The data is represented by mean ± standard deviation (SD). (B) TEM images of free Bac (B) and d (100)-Bac (C) suspended in PBS. Arrows indicate the positively charged PAMAM dendrimer coating on the negatively charged baculovirus surfaces to form the hybridized nanostructures. Scale bar indicates 100nm length.

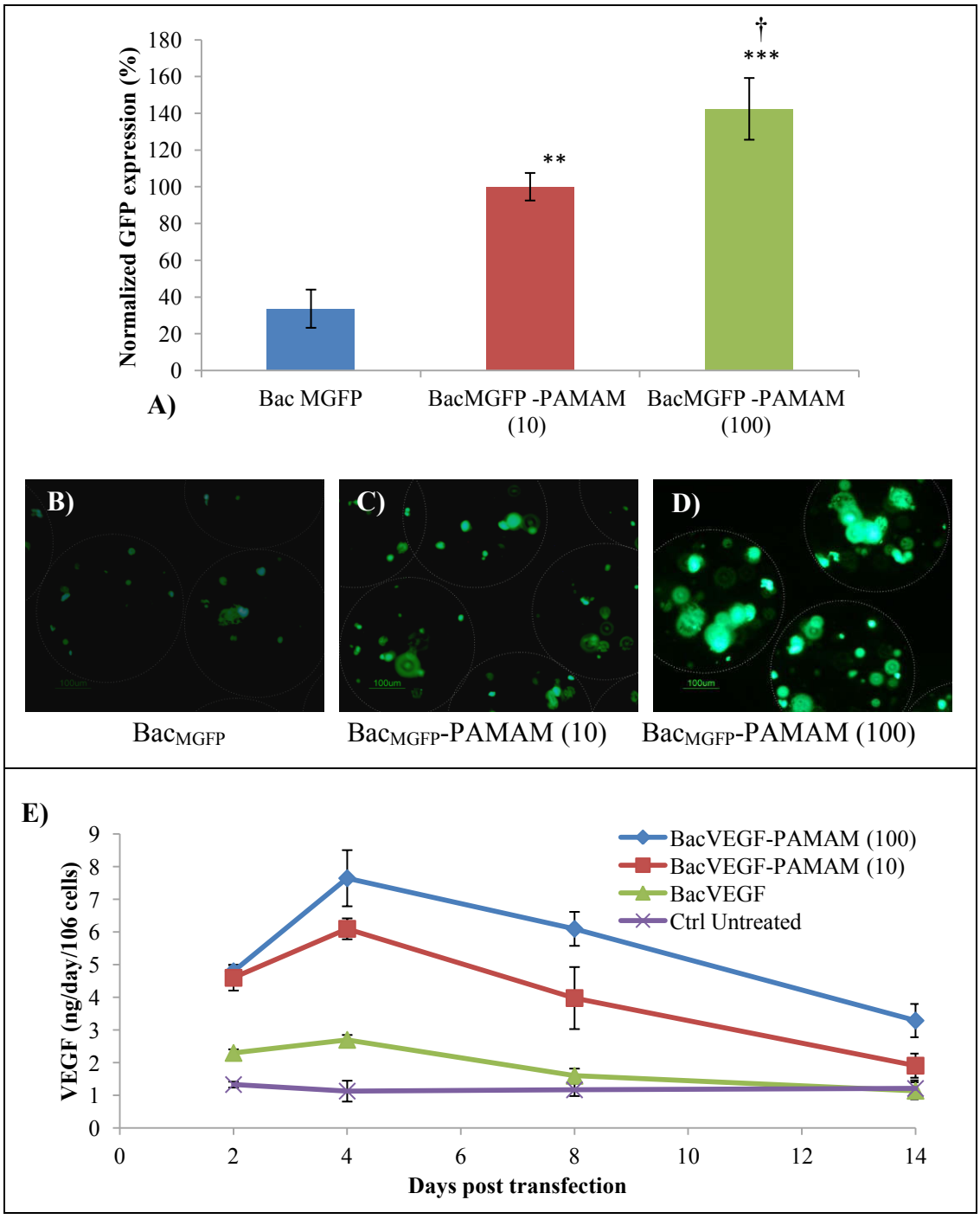

Figure 7.2: A. Transgene expression of AP-brPEG microencapsulated hASCs transduced with d-Bac$_{MGFP}$ under optimal transduction condition with varied ratio of PAMAM/virus (10/100 nmol PAMAM /10^8 virus). The average fluorescein expressed values were normalized to that of cells treated with Bac$_{MGFP}$-PAMAM (10) (taken as 100%), and are represented as normalized mean expression in

percentage value. Background noise reading by non-transduced encapsulated hASCs was subtracted from experimental groups. Results are expressed as mean normalized GFP expression% ± SD. Statistical analysis was performed by one-way ANOVA. *P $\leq$0.05 compared to the Bac_{MGFP} group (n = 3 per group). P<0.01 on comparing Bac_{MGFP}-PAMAM (10) with Bac_{MGFP}-PAMAM (100) are indicated by †. B-D. Representative photomicrographs (Scale bar: 100µm) of corresponding transduced microencapsulated cells were taken using fluorescence microscope on day 2. The white circles show the peripheral surface of the microcapsules. E. Quantification of VEGF present in the conditioned media secreted by encapsulated hASCs transduced with Bac_{VEGF}-PAMAM (10), Bac_{VEGF}-PAMAM (100) and Bac_{VEGF} using ELISA. Non-transduced encapsulated hASCs were taken as control. The conditioned media were collected at regular intervals for performing ELISA. The data represents mean hVEGF (in picograms) ± SD.

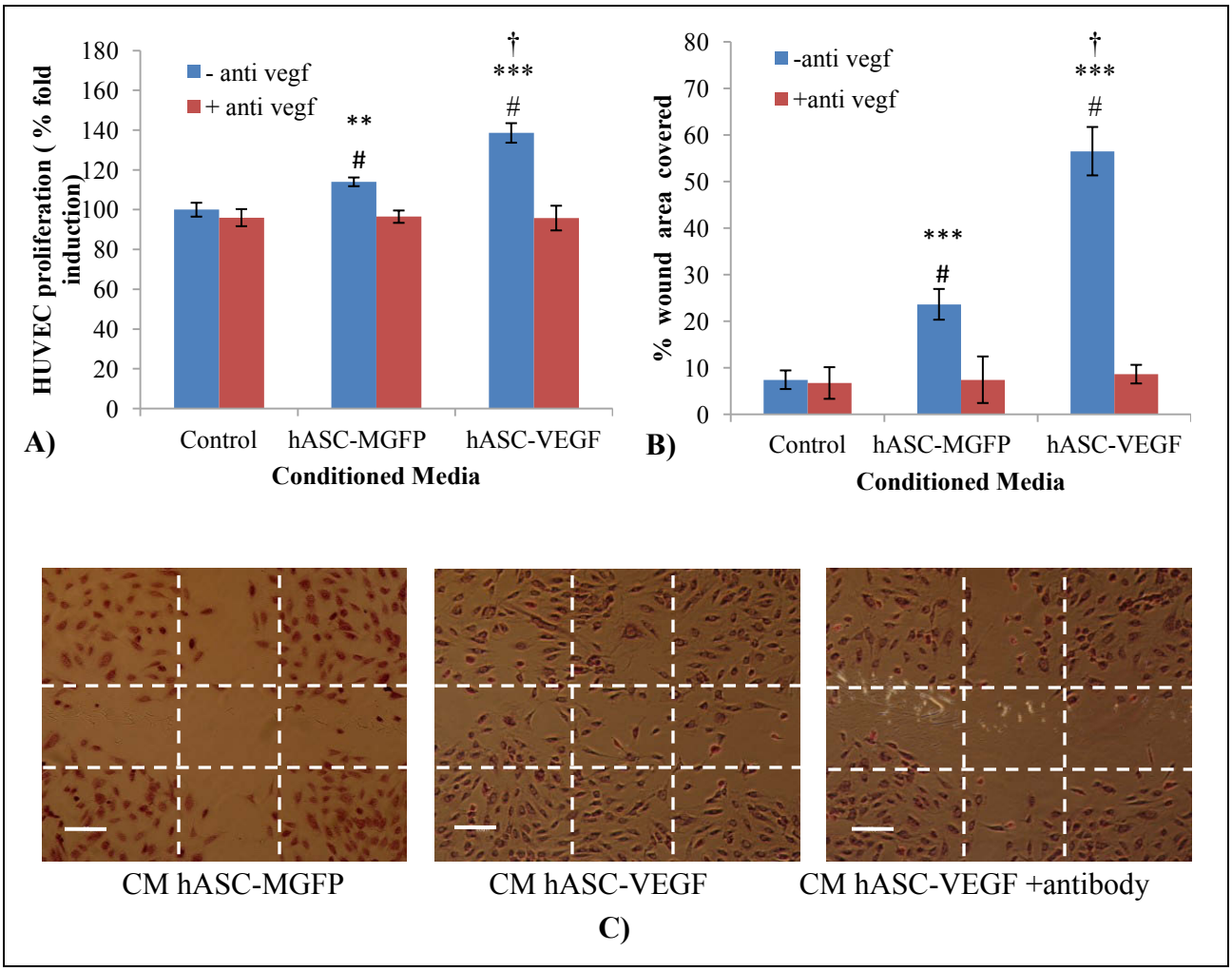

Figure 7.3: Functional assay of released hVEGF. A. Proliferation of HUVEC, grown in the presence of CM from hASCs transduced with Bac_{MGFP}-PAMAM (100) or Bac_{VEGF}-PAMAM (100). As control group, CM from non-transduced cells (Ctrl) was taken. In another set of experiments, CM from individual groups was previously treated with an excess of neutralizing ani-hVEGF antibodies (1µg/ml) before adding to the cells. Proliferation was measured by a colorimetric assay after 4 days of growth and data were normalized to control group (with no antibody). B-C. hVEGF induces migration of endothelial cells in a wound healing assay. HUVEC cell monolayer was wounded with cell scraper and treated with CM from hASCs transduced with Bac_{MGFP}-PAMAM (100) or Bac_{VEGF}-PAMAM (100). HUVEC were photographed (Scale bar: 100µm) after 24 h treatment and

percentage of scratched area (which was initially free of cells, marked by the white dotted border line) covered by the migrated cells were analyzed using Image J software. Mean values ± SD (n=3) are shown in the graphs. ANOVA analysis: Statistically significant differences between group-matched no antibody treated sample data compared with that of antibody treated sample are represented by # denoting $P<0.01$. Statistically significant differences between groups (without antibody treatment) compared to control are indicated as *** = $P<0.001$, ** = $P<0.01$, * = $P<0.05$. $P<0.01$ on comparing hASC-MGFP and hASC-VEGF are indicated by †.

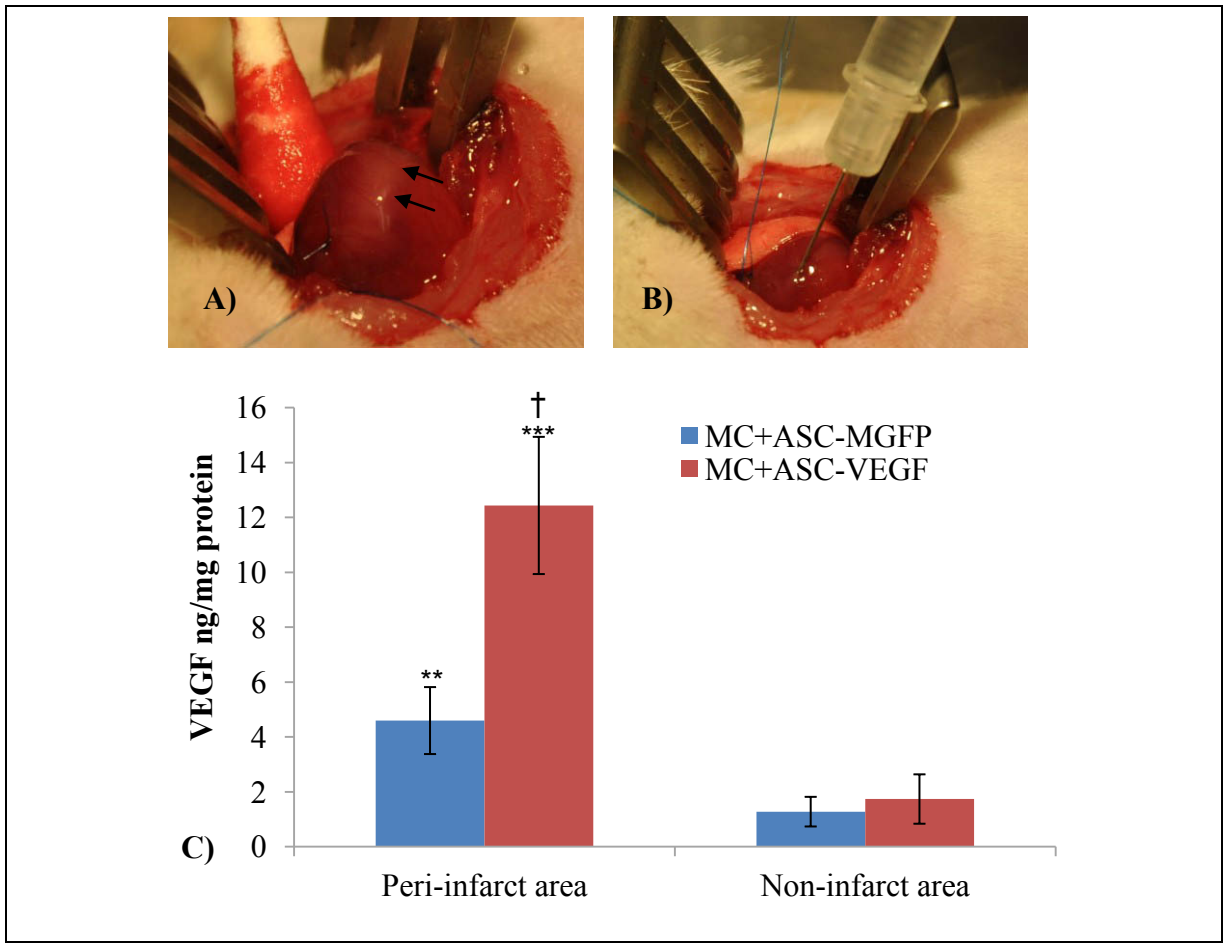

Figure 7.4: Intramyocardial delivery of hASCs using microcapsules. Photograph A represents an infarcted heart caused by left anterior descending artery ligation, with arrows indicating the whitish infarct area in the left ventricular region. Photograph B shows the route of administration i.e. the direct intramyocardial delivery of microencapsulated hASCs to the peri-infarct sites. C. Quantification of hVEGF expression (n=4) at the peri-infarct (site of intramyocardial injection) and non-infarct ventricular region, 4 days post transplantation, as analyzed by hVEGF ELISA. Mean values ± SD are presented in the graph. Statistical analysis by ANOVA: *** = $P<0.001$, when groups were compared between peri-infarct and infarct area. P values comparing area-matched MC+ASC-MGFP group and MC+ASC-VEGF group are indicated by †<0.05.

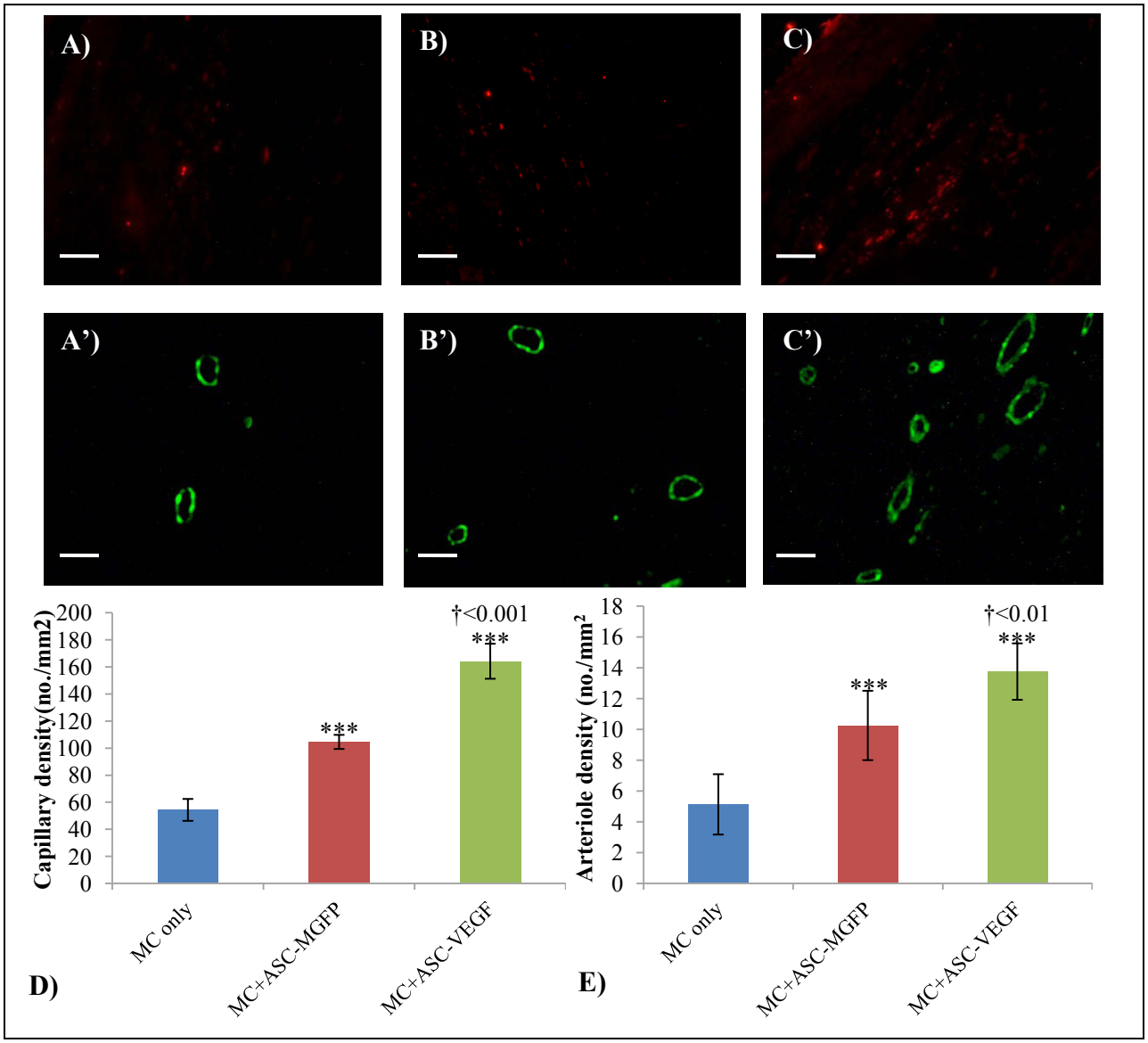

Figure 7.5: Angiogenesis and arteriogenesis in the peri-infarct area. Immunohistological staining of PECAM to detect endothelial cells in (A) Ctrl MC only, (B) MC+ASC-GFP, (C) MC+ASC-VEGF groups. Immunohistological staining of smooth muscle α-actin for smooth muscle cells in (A') Ctrl MC only, (B') MC+ASC-GFP, (C') MC+ASC-VEGF groups. (Photograph Scale Bar: 50µm). Quantification of (D) capillary and (E) arteriole density. Data are expressed as mean density ±SD (n=8). ANOVA analysis: statistically significant differences between groups compared to control are indicated as *** = P<0.001, ** = P<0.01, * = P<0.05. P values comparing MC+ASC-GFP and MC+ASC-VEGF are indicated by †.

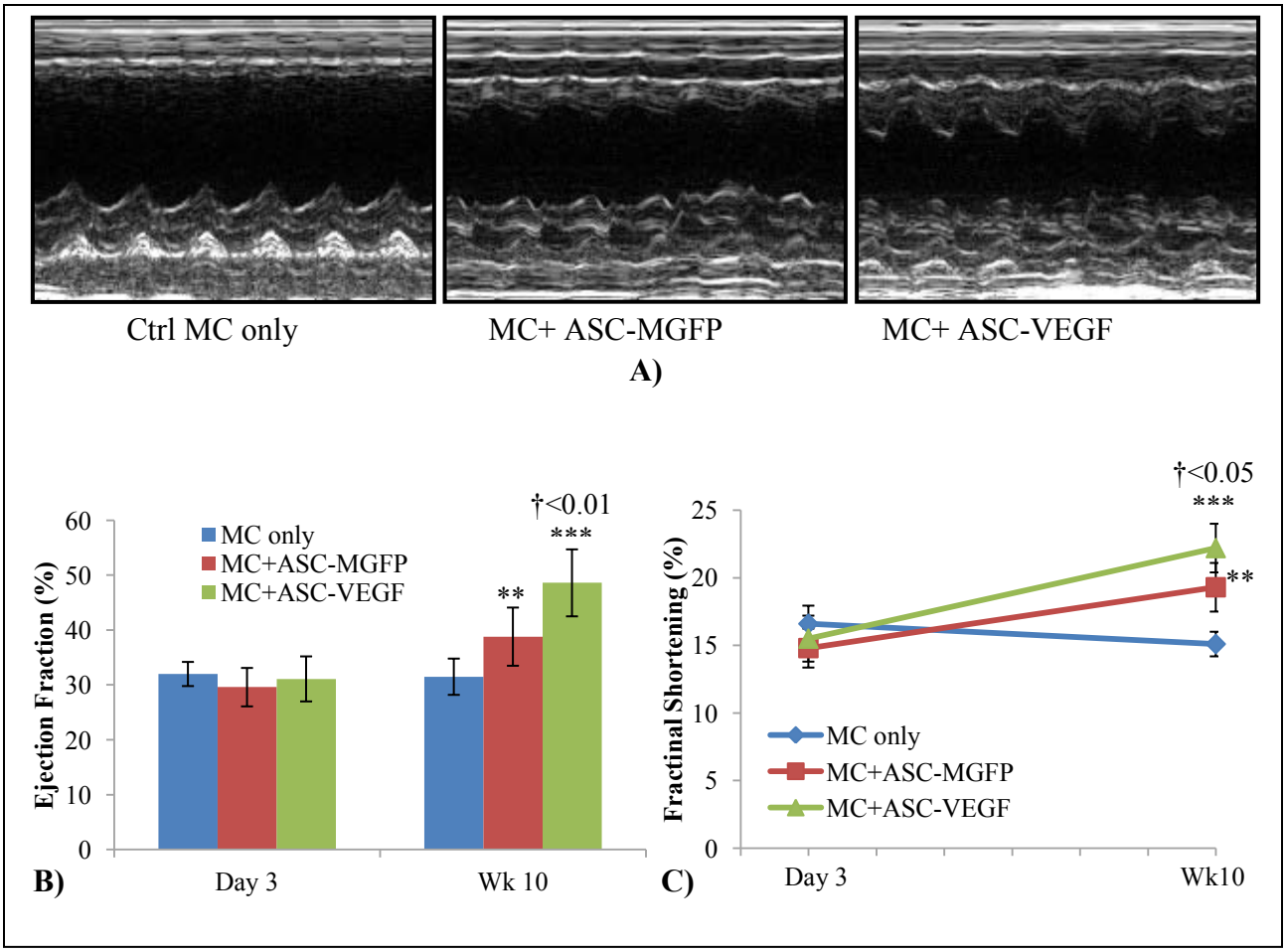

Figure 7.6: Echocardiographic assessment of cardiac function. Effect of microencapsulated ASC-VEGF transplantation on cardiac function was analyzed on day3 and on wk 10 post myocardial infarction in rat model. The heart EF% and FS% were monitored in groups Ctrl MC only (n=8), MC+ASC-GFP (n=8) and MC+ASC-VEGF (n=8). The M-mode echocardiograms of different groups on wk 10 are represented in (A). As demonstrated in the graph (B), the EF% increased significantly after treatment in the MC+ASC-GFP and MC+ASC-VEGF groups over the 10 weeks post infarction compared to control MC group. Furthermore, MC+ASC-VEGF group showed a significantly better improvement in EF% than MC+ASC-GFP. Mean EF% values ± SD are shown in graph. Similarly, the FS% of different groups on day 3 and week 10 post infarction is represented in (C). ANOVA analysis: *** = P<0.001, ** = P<0.01, * = P<0.05 vs. time-matched control. P values comparing time-matched MC+ASC-GFP and MC+ASC-VEGF are indicated by †.

Supplementary Materials

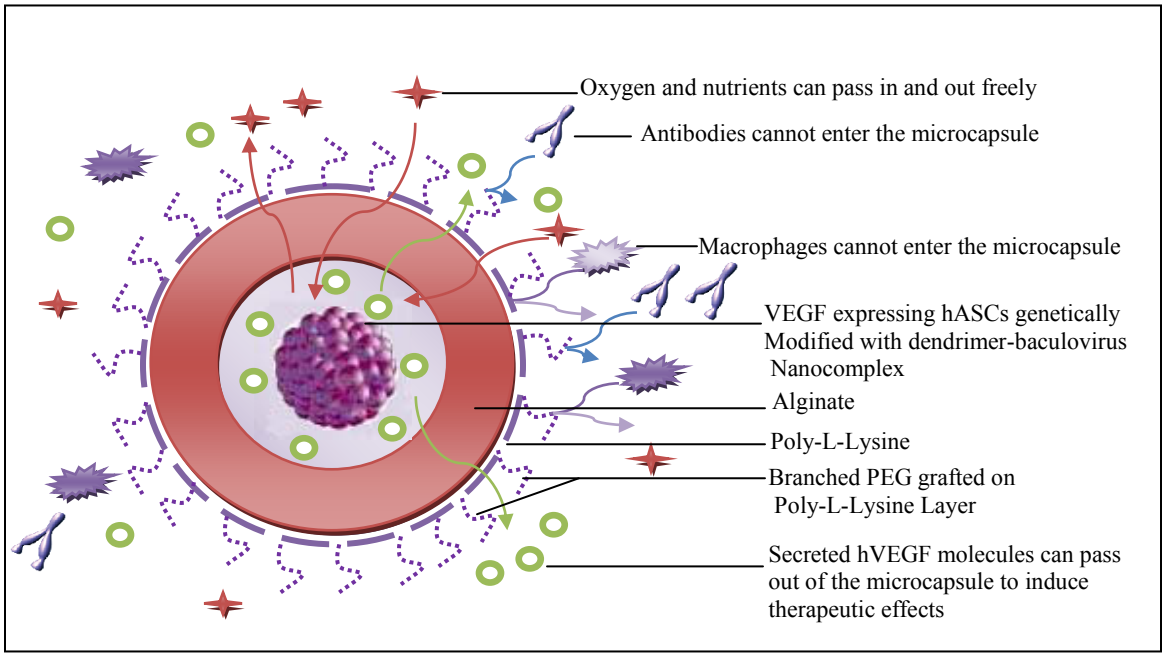

Figure 7. S1: Graphical Abstract for mechanism of action for encapsulated VEGF expressing ASCs. Microencapsulated biologically active cells entrapped in polymeric br-PEG-g-PLL microcapsules. The thin semi-permeable membrane allows bidirectional diffusion of small molecules necessary for cell survival and proliferation (e.g., nutrients, environmental substrates, therapeutic protein products, metabolic waste materials). Larger molecules such as tryptic enzymes and antibodies are blocked from entry by the branched PEG. By varying the PEG type and/or density on the capsular surface, the permeability and surface chemistry can be varied over a large range. This flexibility allows extensive possibilities to fit a desired application.

1. Optimizing the transduction protocol of Bac-PAMAM with hASCs in monolayer

Methods:

Bac-PAMAM mediated transfection of hASCs

For the transfection experiments, 2 x 10^4 cells were seeded in each well in a 96 well plate and incubated overnight. This was followed by washing of the wells with PBS and addition of Bac_{MGFP}, Bac_{MGFP}-PAMAM (10), Bac_{MGFP}-PAMAM (100) and Bac_{MGFP}-PAMAM (200) nanocomplex resuspended in PBS to corresponding wells with a constant MOI[multiplicity of infection=pfu/cell] of 200, where the values within brackets indicate the ratio of PAMAM in nmol per 10^8viruses. After 4 h of transfection, the cells were replenished with fresh serum supplemented DMEM media. The relative fluorescence units of each well were measured 48 h post-transduction using plate reader Victor3 Multi Label Plate Counter (Perkin Elmer, USA). This experiment was done in triplicates, and the mean was calculated. Representative pictures of the wells were taken using fluorescence microscope (Nikon Eclipse TE2000-U). For transfection experiments with Bac_{VEGF}-PAMAM, 5x 10^5 cells per well were seeded in 6 well plates followed by similar transfection protocol.

MTS Cell Proliferation assay

Non-Radioactive Cell Proliferation MTS Assay (Promega, Madison, WI) was used to assess the *in vitro* cytotoxicity of the Bac_{MGFP}, Bac_{MGFP}-PAMAM (10), Bac_{MGFP}-PAMAM (100) and Bac_{MGFP}-PAMAM (200) nanocomplex towards hASCs after incubating the cells with nanocomplexes for 12h in presence of media. To perform the assay, the media from each well were replaced with fresh 100µl media. 20µl of MTS solution was added to each well and incubated for 4 hours at 37°C. The measurement of absorbance of the wells at 490nm was carried out using Victor3 Multilabel Counter (Perkin Elmer, Woodbridge, Ontario, Canada). The assay was also used to determine cell proliferation of HUVEC and lymphocytes.

Results:

Transduction of hASCs with minimum cytotoxicity

In order to use the genetically modified hASCs for therapeutic purposes, we first optimized the transduction conditions. For this Bac_{MGFP}, Bac_{MGFP}-PAMAM (10), Bac_{MGFP}-PAMAM (100), Bac_{MGFP}-PAMAM (200) transduction groups with constant MOI of 200 were used and normalized GFP expression 48h post transduction were evaluated using plate reader. Bac_{MGFP}-PAMAM with all the dendrimer concentrations showed significantly higher GFP expression than Bac_{MGFP} alone as reported in **Figure 7.S2A and 7.S2C-E**. This proves that the nanocomplex can transduce the cells more efficiently than baculovirus alone. A dendrimer concentration of Bac_{MGFP}-PAMAM (100) showed further enhancement in transgene expression, although Bac_{MGFP}-PAMAM (200) showed comparatively lesser transduction ability. Cytotoxicity analysis of the transduction groups demonstrates negligible toxic effects of Bac_{MGFP}, Bac_{MGFP}-PAMAM (10) and Bac_{MGFP}-PAMAM (100) on hASCs with more than 95% cell viability, when exposed for 12h (**Figure 7.S2B**). However, a higher dose of Bac_{MGFP}-PAMAM (200) showed markedly reduced cell viability (75.6±5.1%) compared to untransduced control (100%) and other groups. This also illustrates the reason for reduced GFP expression with Bac_{MGFP}-PAMAM (200) compared to lower doses where there was no significant cytotoxic effects on hASCs.

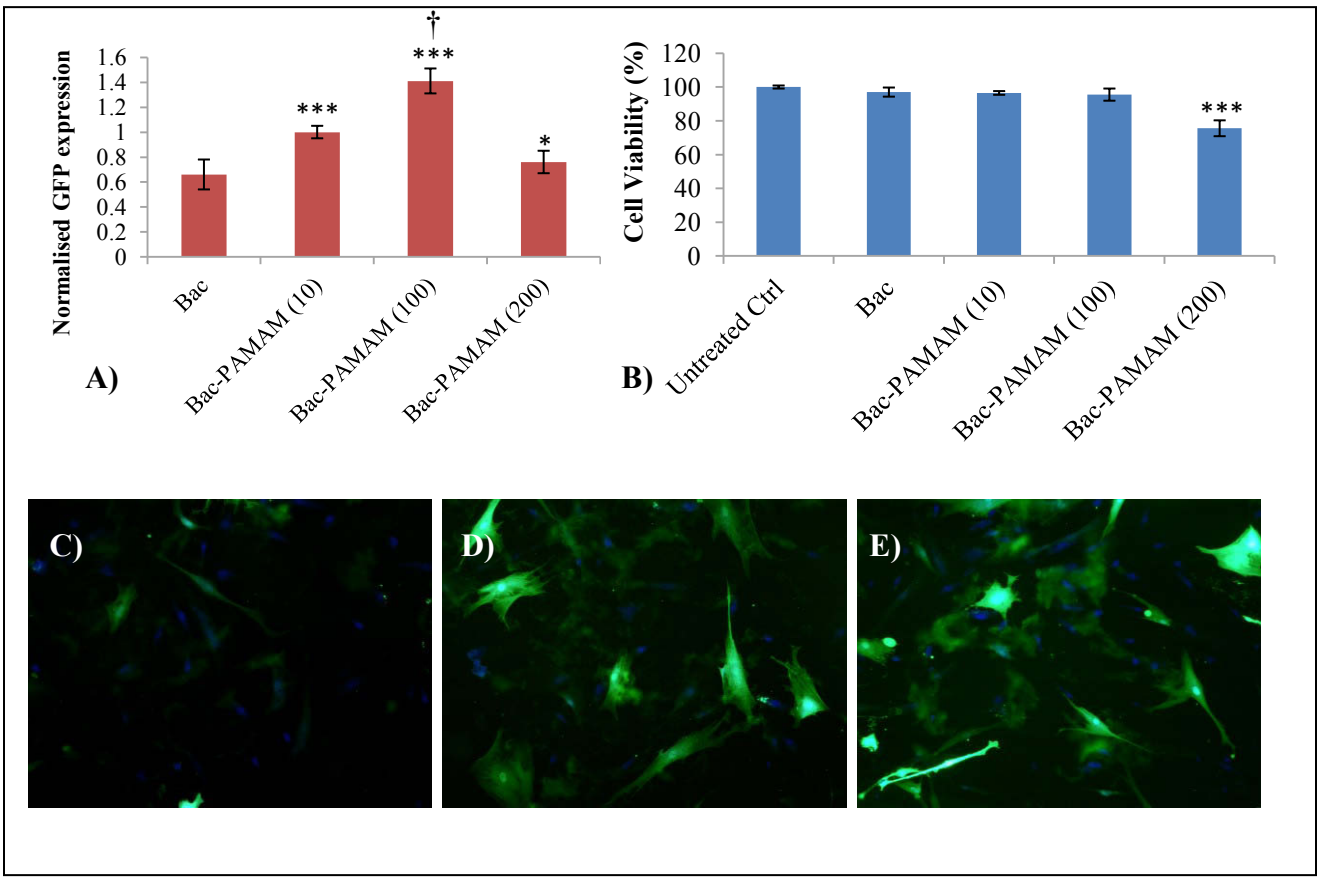

Figure 7.S2: Optimization of transduction condition in hASCs with Bac-PAMAM. $2x10^4$ cells were seeded in each well of 96 well plates and cultured overnight. The nanocomplexes were prepared from different dendrimer concentrations complexed with same number of baculovirus. (A) Effect of dendrimer concentrations on d-Bac mediated cell transduction. Cells were transduced with Bac-PAMAM at constant MOI of 200 with PAMAM/virus ratio of 10, 100 and 200 nmol PAMAM per 10^8 viruses. After 4h transduction, cells were washed with PBS and replenished with complete media. 24h post transduction, cells of each well was analyzed for MGFP expression [percentage normalized taking d (10)-Bac as 100%] in plate reader. Three independent experiments were performed and the mean ± SD are represented in the graphs. (B) Cytotoxic effects of Bac-PAMAM nanocomplexes with different dendrimer concentrations on hASC. $2x10^4$ cells were seeded in each well of 96 well plates and cultured overnight. The cells were incubated with Bac_{MGFP} only, Bac_{MGFP}-PAMAM (10), Bac_{MGFP}-PAMAM (100) and Bac_{MGFP}-PAMAM (200) at a

constant MOI of 200 for 12h followed by cell toxicity analysis. Results are expressed as mean % cell viability ± SD in comparison to untreated control cells. Statistical analysis was performed by one-way ANOVA. *P ≤0.05, ***≤0.001 compared to the Bac_{MGFP} group (n = 3 per group) in (A) and untreated ctrl in (B). P value on comparing Bac_{MGFP}-PAMAM (10) with Bac_{MGFP}-PAMAM (100) are indicated by †<0.01. Representative fluorescence microscopic images (magnification 200X) of transduced cells 24h post transduction: (C) Bac_{MGFP}, (D) Bac_{MGFP}-PAMAM (10), (E) Bac_{MGFP}-PAMAM (100).

2. Conjugation of PLL with NHS-activated **PEG (branched)**

Methods:

Amine reactive branched PEG (brPEG) was used to synthesize the PLL-brPEG. Each methyl-terminated PEG branch contains 12 ethylene glycol units. Three of such branches are attached to a 4-unit PEG stem that contains an amine-reactive *N*-hydroxysuccinimide (NHS) ester at the distal end. These NHS ester can react spontaneously with primary amines ($–NH_2$) of PLL providing efficient PEGylation of PLL. PLL was dissolved in 50 mM sodium borate buffer (pH 8.5) at concentration 80 mg/mL. To this 216 mg brPEG was added and mixed properly to carry out the reaction for 6 h at room temperature. This was followed by extensive dialysis (MW cut-off size 10 kDa) of the reaction mixture with PBS and then with deionized water. The products were freeze dried and finally in dissolved PBS before use. To confirm the reaction ^1H NMR spectra analysis was performed.

Results:

Lyophilized final product PLL-g-brPEG was dissolved in D_2O and proton NMR spectra was analyzed on a 400 MHz Varian Mercury spectrometer (**Figure 7.S3**). The chemical shifts were assigned based on the results from spectra of the individual reagents in addition to the result from the software Mnova 6.2.1from Mestrelab Research.

The grafting ratio of PLL-g-brPEG was calculated from the one-dimensional ^1H NMR spectra of Figure S1 as follows: half the integral of the peak at 2.5 ppm (corresponding to the end-carbon-protons (-O-CH2-C**H_2**-CO-NH-) from the grafted brPEG chain) was divided by the integral of the peak at 4.3 ppm

(corresponding to protons from the poly-lysine backbone (-NH-C**H**R-CO-). The grafting ratio, g, for the PLL-g-brPEG was found to be 1/8, that is one brPEG chain on every eighth lysine residue. From the grafting ratio, g, obtained from the one dimensional ^{1}H NMR spectra of Figure S1, it is possible to estimate the molecular weight, M, of the PLL-g-brPEG copolymer by the formula: $M_{PLL\text{-}brPEG} = M_{brPEG}x(gxM_{PLL}/M_{Lys})+M_{PLL}$. Taking M_{brPEG}=2420.8, M_{PLL}=27400.0, and M_{Lys}=128.0, the equation gives a molecular weight for the copolymer $M_{PLL\text{-}brPEG}$ of 92,175 g/mole.

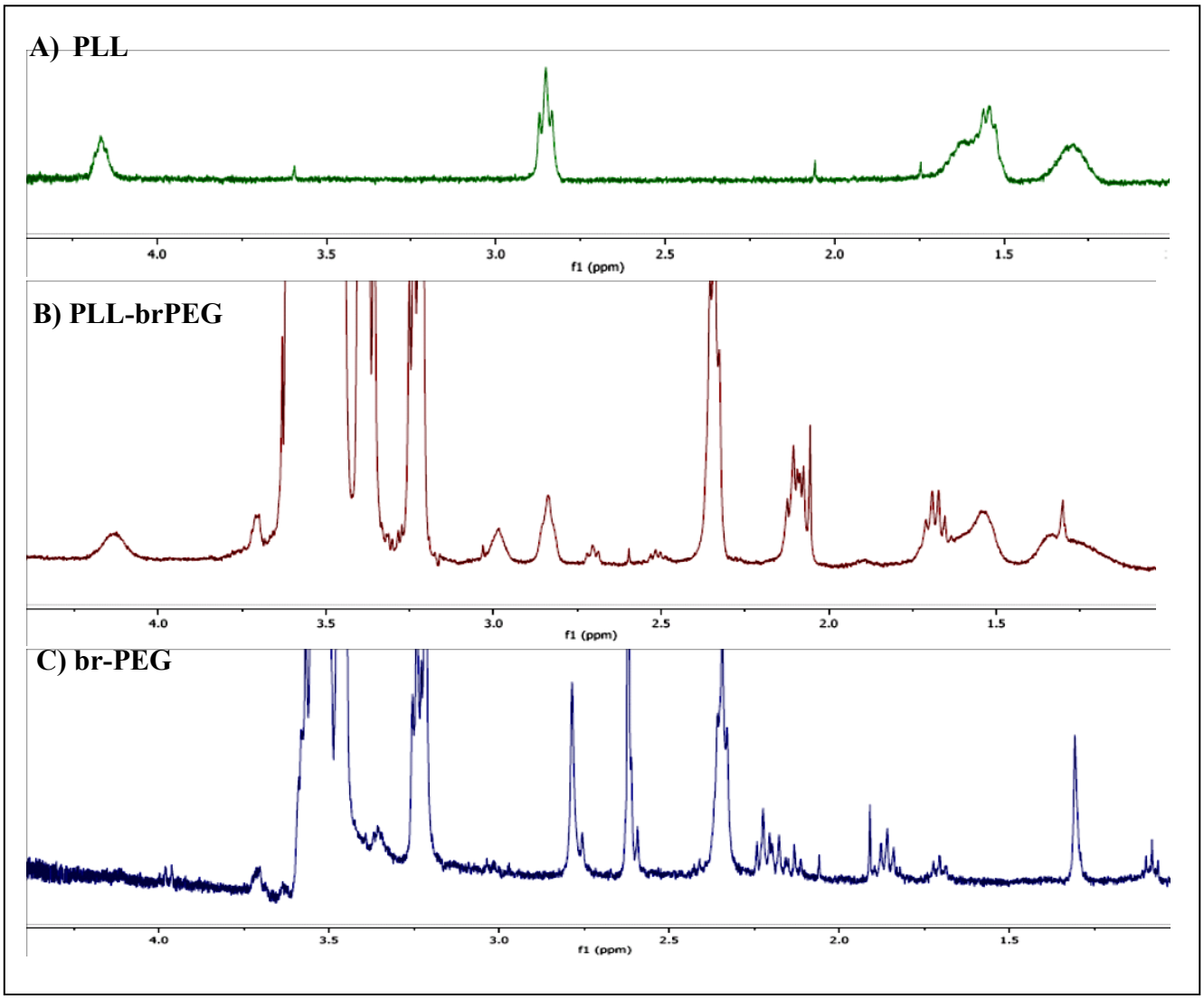

Figure 7.S3: 1H NMR spectra for (A) PLL (0.51% w/w), (B) PLL-brPEG (0.48% w/w), and (C) brPEG (0.54% w/w).

3. Confirmation of PLL-brPEG coated microcapsules entrapping viable ASCs

Methods:

Tracking the PLL-brPEG layer in microcapsules

In order to visualize the coated PLL-g-brPEG layer on the microcapsular surface, PLL-g-PEG derivative with a covalently linked fluorescein label (PLL-g-PEG-*fl*) was also synthesized. Microcapsules coated with this PLL-g-brPEG-*fl* co-polymer were used to confirm the proper coating of the synthesized PLL-brPEG on the capsular surface. To perform this, the microcapsules were placed in a chambered coverglass system (Lab-Tek) under Laser Scanning Confocal Imaging System (LSM 510, Carl Zeiss, Jena, Germany) equipped with a Zeiss Axiovert 100M microscope. A 488-nm argon laser was used in the single green fluorescence mode and the fluorescence was detected with the emission filter block BP500-550IR.

Probing the esterase activity and internal morphology of encapsulated cells

The intracellular esterase activity and plasma membrane integrity of the encapsulated cells were checked from time to time using the polyanionic dye calcein (Biotium Inc, Hayward, CA) which stains only the viable cells producing a green fluorescence under fluorescence microscope. The ethidium homodimers that enter only dead cells with damaged membranes emit red fluorescence upon binding to nucleic acids.

The internal morphology of the microencapsulated cells was studied by scanning electron microscopy (SEM), using a Hitachi S-4700 FE scanning microscope. The samples for SEM were prepared by rinsing the capsules with water, followed by freeze-drying and fracturing by a razor blade. The obtained fragmented halves of the microcapsules were mounted on SEM stud with double-sided tape and sputter-coated with gold–palladium for 40s.

Results:

The resulting positively charged PLL-*g*-PEG polymer bind to the negatively charged surface through electrostatic interaction of the multiple positive charges of the PLL backbone ($-NH3^{+}$) with the negative charges of alginate core of the microcapsules. To confirm this and visualize proper coating of PLL-brPEG on alginate surface, we used fluorescein tagged PLL-g-brPEG-*fl* co-polymer to graft the outer surface layer. Confocal microscope picture in **Figure 7.S4A-C** confirms that the PLL-g-brPEG-*fl* co-polymer coated the alginate core of the microcapsule in a uniform manner, thus making a smooth spherical outer surface.

To test the ability of the microcapsules to support ASC viability, the cells were encapsulated in microcapsules coated with brPEG-PLL using standard microencapsulation protocol. The encapsulated cells were grown in stationary cell culture flasks using complete media, and cell viabilities were confirmed from time to time for a period of 2 weeks using a fluorescence-based method employing calcein AM and EthD-III dyes. As shown in **Figure 7.S4D-F**, the green dots inside the capsules confirm the viable calcein stained cells while red shows the dead cells. **Figure** 7.**S4G and 7.S4H** shows the SEM images of the internal morphology of cut sections of empty and cell loaded AP-brPEG microcapsules grown for 2 weeks. As noted in the figure, the cells stayed entrapped inside the polymeric microcapsules.

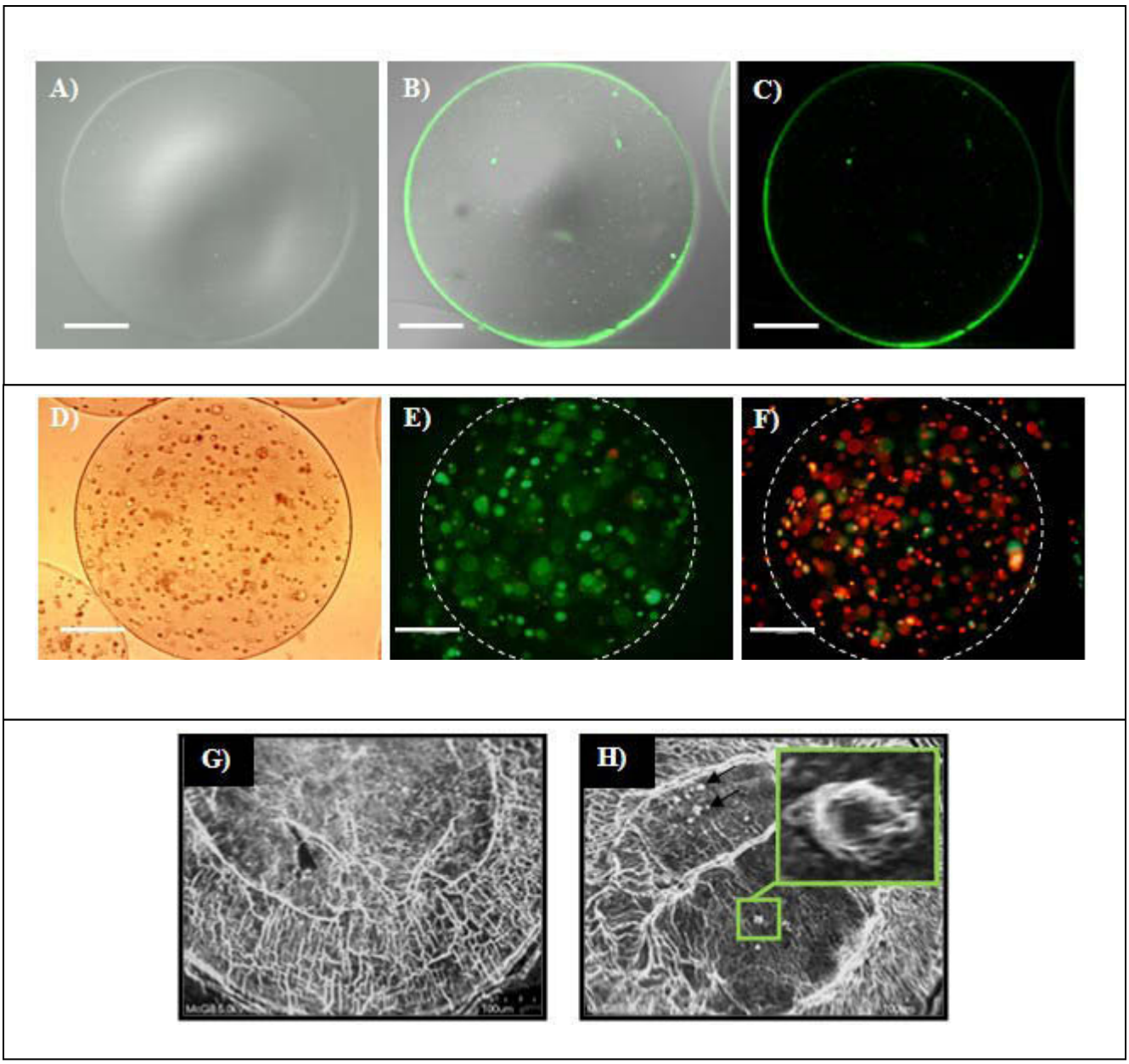

Figure 7.S4: Photomicrographs of empty and hASC loaded AP-brPEG microcapsules. A-C represents the confocal laser scanning microscopic images of the polymeric microcapsules at an excitation of 488 nm and emission of 530nm. The alginate microcapsules were immersed in 0.1% (w/v) PLL-g-PEG-*fl* solution for 15min. (A) Control AP microcapsule with only PLL coating(overlapped: bright/fluorescence field), (B) AP-brPEG-*fl* microcapsule (overlapped: bright/fluorescence field), (C) AP-brPEG-*fl* microcapsule (fluorescence field). The green fluorescence on the outer surface of the AP-brPEG-*fl* capsules indicates

the uniform and complete coating of alginate capsules with PLL-brPEG –*fl* layer. This fluorescence was not there in AP capsules which were no treated with PLL-brPEG-*fl*. The scale bar indicates 50µm. Viability (D-F) of microencapsulated hASCs after two weeks of culture in DMEM media supplemented with 10% FBS at 37^{o}C. Viability tests were done by using the calcein AM (showing viable cells in green) and ethidium homopolymer (showing dead cells in red) dye. Representative bright field (D) and fluorescence field (E) image of microcapsules encapsulating the hASCs under fluorescence microscope confirms that the viability entrapped cells. As negative control, microencapsulated cells were cultured in serum starved media for 48h and checked for viability (F). It shows high number of dead cells due to serum starvation. Scale bar represents 50µm. SEM images (G and H) of AP-brPEG microcapsules: Microphotograph of internal morphology of empty microcapsules (G; magnification: 500X) showing the internal mesh-like scaffold structure of the microcapsule. Figure 6H shows the hASC loaded microcapsules (magnification: 800X) with subset showing a magnified image of the entrapped cell (indicated by arrows) within the capsular scaffold.

4. Confirming the immune-isolation potential of microcapsules along with retention of differentiation potential of entrapped ASCs

Methods:

Lymphocyte proliferation assay to determination immune-isolation potential of microcapsules

Rat peripheral blood lymphocytes were isolated from Sprague-Dawley rats after cardiac puncture by Percoll gradient centrifugation followed by removal of peripheral blood monocytes by plastic adherence. The isolated lymphocytes were grown in DMEM media supplemented with 10% FBS. Lymphocytes are taken as the responding cell populations while the encapsulated Bac_{MGFP}-PAMAM (100) transduced hASCs or non-encapsulated Bac_{MGFP}-PAMAM transduced hASCs were taken as the stimulating cell populations. The lymphocytes were seeded at $1x10^4$ cells per well in a HTS Transwell-96 well plate (Corning, NY, US) with

tissue culture treated receiver wells. As positive control for the co-culture, free hASCs at 10^5 cells per insert in the transwell. As experimental groups, 10^5 encapsulated cells in PLL-g-brPEG coated capsules, 10^5 encapsulated cells in PLL coated capsules and 10^5 encapsulated cells in uncoated alginate core capsules were used in the inserts. As negative control, empty PLL-g-brPEG coated capsules, empty PLL coated capsules and empty alginate core capsules were taken in the insert. After co-culturing for 72h the insert was removed and MTS assay was performed to quantify the cell proliferation.

Depolymerization of microcapsules and inducing differentiation of entrapped cells

The hASCs were recovered from the microcapsules, after 72h of co-culture with lymphocytes, by treating the capsules with 27mM NaCl solution containing 100mM sodium citrate and 10mM MOPS (Sigma-Aldrich) for 1h at room temperature for depolymerization. The completely broken and semi-dissolved alginate capsules were then centrifuged at 800 rpm for 7 min to recover the free cells from the pellet, leaving the sodium citrate solution and capsular parts in the supernatant. The cells were then washed thrice with PBS and resuspended in culture media containing serum and seeded in twenty four-well plate at a high confluency for adipogenic, chondrogenic and osteogenic differentiation. After cell seeding, the medium was replaced with StemPro adipogenesis, chondrogenesis and osteogenesis differentiation medium (Invitrogen). The media were then replaced with fresh differentiation media on every fourth day. On day 7 of adipogenesis induction culture, the cells were washed with PBS and fixed in 4% formaldehyde solution. LipidTOX Red neutral lipid staining solution (Invitrogen) was added to the fixed cells in order to monitor the intracellular accumulation of neutral lipids within the adipogenically differentiated cell population. For detecting the osteogenic cell population, the cells were cultured for 21 days followed Alizarin Red staining. For chondrogenic analysis, after 21 days of culture, 1% Alcian Blue solution prepared from 0.1N HCl was used to stain the cartilage proteoglycans of the differentiated hASCs that turn chondrocytes blue.

Results:

Immune protective potential of brPEG functionalized microcapsules

In order to assess the immune-protective nature of the microcapsule membrane, AP-brPEG microcapsules containing Bac_{MGFP}-PAMAM (100) transduced ASCs were co-cultured with rat lymphocytes for 72h. Non-treated lymphocyte (media only) count was normalized to 1.0 and the cell counts of other groups were calculated as fold increase with respect to it. The result in **Figure 7.S5A** shows that lymphocytes treated with free cells show highest proliferation (2.76 times) in comparison to brPEG-PLL encapsulated cells (1.11 times). The lymphocyte response was higher (1.98 times) when br-PEG was not present in the outer layer of AP capsules, proving that branched PEG gives an extra protection to the encased cells. In absence of any polyelectrolyte layer the alginate core was unable to give any protection to the encased cells, which showed 2.55 times lymphocyte proliferation with respect to control. On the other hand, empty capsules of all groups did not show any sign of significant immune stimulation, which is evident from the graph where the lymphocyte proliferation was similar to that of control. Noticeably, in a separate study, when the number of free/entrapped cells was increased 5 times, there were no significant lymphocyte proliferations between all the groups (data not shown). This was most probably because of the relatively stronger immunosuppressive effect induced by the escalated number ($5x10^5$ instead of 10^5 cells) of hASCs on the lymphocyte population.

Differentiation potential of microencapsulated genetically modified hASCs

To confirm the retention of differentiation potential of the Bac_{MGFP}-PAMAM transduced encapsulated hASCs, the cells were isolated from the capsules by depolymerization, after 72h of co-culture with lymphocytes. They were then seeded at high confluency and induced towards adipogenic, chondrogenic and osteogenic lineages with appropriate differentiation media. Untransduced cells were induced for differentiation as control. LipidTOX Red neutral lipid staining showed that both the transduced encapsulated and control cells have differentiated into adipocytes as evident by the formation of stained lipid vacuoles **(Fig. 7.S5B**

and 7.5B'). The picture also shows the same cell expressing GFP (transduced with Bac_{MGFP}-PAMAM) was differentiated into adipogenic lineage. Osteogenic differentiation of the cells was carried on till day 21. The cells were then stained with Alizarin red which forms complex with calcium deposits of the osteocytes in a chelation process to give a birefringent orange-red color. The staining revealed efficient osteogenic differentiation of the cells, like the control **(Fig. 7.S5C and 7.S5C').** The Alcian blue staining showed similar result, where the chondrocytes formed by the encapsulated and non-encapsulated control cells turned blue in color owing to proteoglycans (acid mucopolysaccharides and glycosaminoglycans) that turns chondrocytes blue **(Fig. 7.S5D and 7.S5D').** From the above results, it can be concluded that neither microencapsulation nor Bac_{MGFP}-PAMAM (100) transduction altered the differentiation potential of the stem cells.

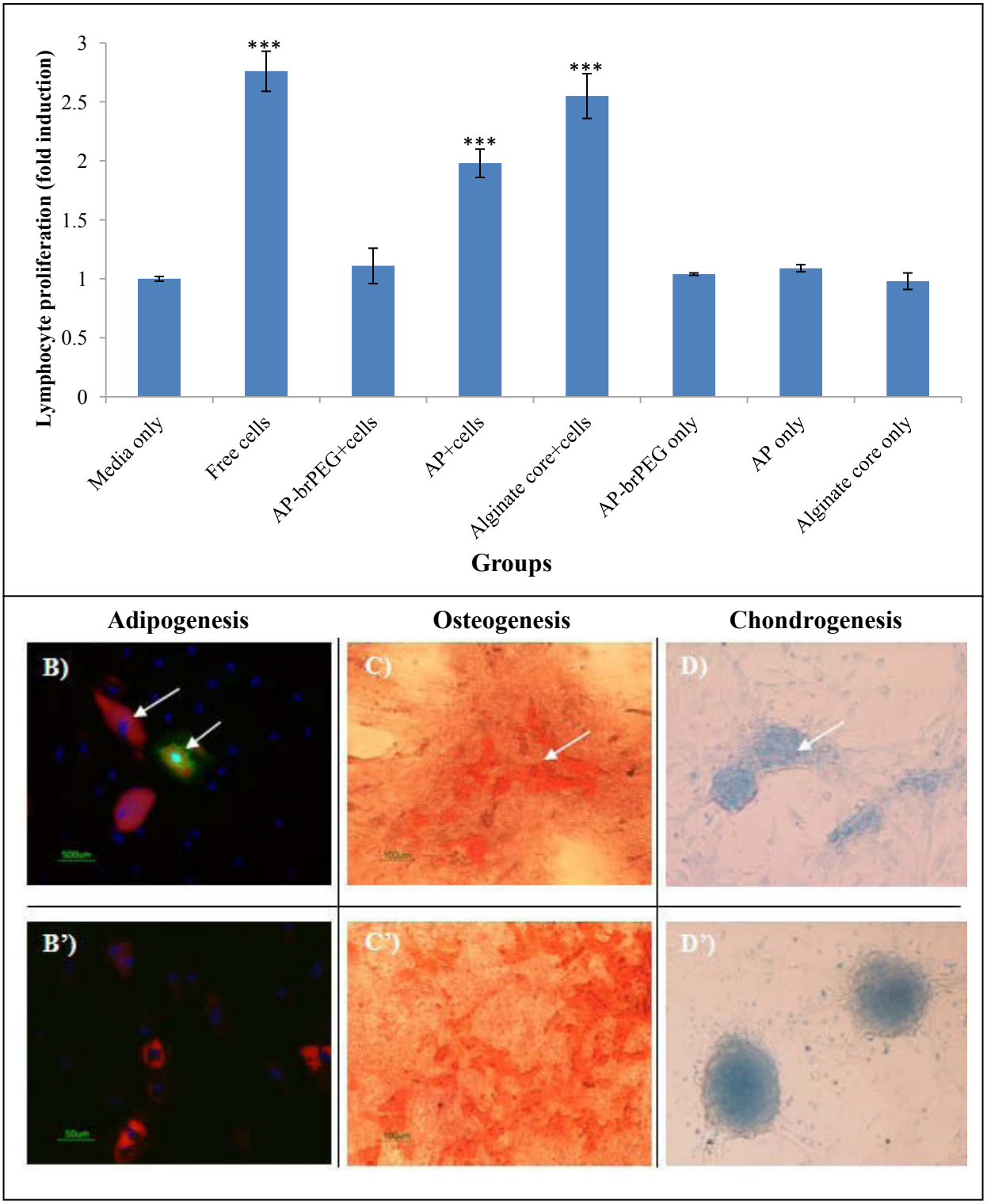

Figure 7.S5: A. Lymphocyte proliferation stimulated by encapsulated and free ASCs genetically modified by Bac_{MGFP}-PAMAM (100) with MOI of 200. Microcapsules (AP-brPEG, AP, alginate core only) encapsulating ASCs were co-cultured in a transwell 96-well plate along with lymphocytes (present in the

reservoir wells) for 72 h. Empty microcapsules were taken as the control groups. MTS cell proliferation assay was done to quantify the number of cells. Non-treated lymphocyte (media only) count was normalized to 1.0 and the cell counts of other groups were represented as fold increase with respect to it. The data represents average number of viable lymphocytes ± SD (n = 3). * indicates the significant difference of the groups from the (control) media only group ($P<0.05$). Figure B to D represents adipogenic, osteogenic and chondrogenic differentiation of encapsulated hASCs transduced by Bac_{MGFP}-PAMAM (100) after capsular depolymerization, following 72 h of co-culture with lymphocytes. hASCs maintained their natural potential for differentiation: adipogenic differentiation was assessed via LipidTOX Red neutral lipid staining of lipid vacuoles and DAPI staining of nucleus (B. encapsulated d-Bac transduced cells, B'. control encapsulated non-transduced cells). Osteogenic differentiation was determined by Alizarin Red staining of calcium deposits (C. encapsulated d-Bac transduced cells, C'. control encapsulated non-transduced cells). Alcian blue staining of the chodrogenically differentiated cells shows the formed chondrocytes (D. encapsulated d-Bac transduced cells, D'. control encapsulated non-transduced cells). The arrows indicate the cell differentiated areas. Note the presence of MGFP expression in the Bac_{MGFP}-PAMAM (100) transduced hASC (B) even after differentiation to adipogenic lineage.

Investigation on PEG integrated alginate-chitosan microcapsules for myocardial therapy using marrow stem cells genetically modified by recombinant baculovirus

Arghya Paul[1], Dominique Shum-Tim[2], Satya Prakash[1, 3*]

[1] Biomedical Technology and Cell Therapy Research Laboratory, Department of Biomedical Engineering, Faculty of Medicine, McGill University, 3775 University Street, Montreal, Quebec H3A 2B4, Canada.

[2] Divisions of Cardiac Surgery and Surgical Research, The Montreal General Hospital, 1650 Cedar Ave, Suite C9-169, Montreal, Quebec H3G 1A4, Canada.

*Correspondence author; Email: satya.prakash@mcgill.ca

Tel: +1-514-398-3676; Fax: +1-514-398-7461

Preface : As an alternative to the genetically modified microencapsulated adipose stem cells for angiogenic therapies described in earlier chapters, this chapter investigates the applicability of bone marrow stem cells genetically modified by recombinant baculovirus for microcapsule mediated cell based gene therapy.

Original article published in ***Cardiovascular Engineering and Technology*** **1(2): 154-164 (2011)**

8.1 Abstract

Bone marrow derived mesenchymal stem cell (BMSCs) therapy can significantly improve cardiac ventricular function following ischemic injury. Their potential can be further enhanced by using genetically modified cells, overexpressing certain therapeutic biomolecules. However, such therapy is limited by low efficiency of transplantation of the cells, secreting inadequate therapeutic proteins. To address these issues, we developed recombinant baculoviruses to genetically modify the BMSCs and investigated the potential of using poly-ethylene-glycol (PEG) integrated alginate-chitosan microcapsules (AC) for efficient myocardial transplantation. The data indicates that the cells encapsulated in AC-PEG microcapsules grew rapidly from 80 cells per capsule to above 100 cells per capsule within a week, reaching a confluency of average 110 cells by day 9 of encapsulation. The microcapsules proved superior to commonly used AC microcapsules in terms of immune protection. After 11 days of co-culture of the encapsulated cells with highly confluent lymphocytes, the viable cell population in AC-PEG microcapsules was reduced by only 20%, whereas in AC microcapsules it was reduced to more than 50%. AC-PEG microcapsules also had significantly higher mechanical (65% vs 10%) and osmotic (92% vs 52%) stability than commonly used AC microcapsules as seen after 2h of external stresses. The entrapped genetically modified cells showed highest transgene expression on day 1, which was gradually reduced to 48% after one week and to 14% after two weeks. This expression pattern was also dependant on initial viral incubation time, with 8h incubation being the optimum. The encapsulated cells, transduced with baculovirus, also retained their inherent potential to differentiate into multiple lineages. Because of the above characteristics, the baculovirus transduced microencapsulated BMSCs have immense potential in myocardial cell-based gene therapy, although preclinical studies are needed to be done to establish their functional benefits on myocardial implantation.

Keywords: Microencapsulation, alginate, poly (ethylene glycol), baculovirus, transduction, transplantation, cell delivery, cell-based gene therapy.

8.2 Introduction

The advancements in pharmacological and biomedical techniques, therapeutic interventions and surgical practices have resulted in a marked improvement in the survival rate of patients with various cardiovascular diseases. Many patients surviving advanced cardiovascular diseases progressed to develop congestive heart failure (CHF), which still remains a major concern in the field of cardiovascular disorders, including ischemic heart disease and cardiomyopathy [43, 305]. Stem cell therapy has been suggested as a novel approach to address myocardial cell loss, particularly using bone marrow-derived mesenchymal stem cells (BMSC) or other progenitor cells [306]. These pluripotent cells have the potential for self-renewal or regeneration of myocardium, bone, and cartilage [307-309]. It has been shown that BMSCs get mobilized in response to ischemia and exhibit tropism in an ischemic heart [310]. In order to enhance the therapeutic efficacy, BMSC can be genetically engineered using a suitable gene delivery system prior to cell transplantation in order to allow the engrafted cells to proliferate and integrate with the host cells [109]. This genetic modification can promote angiogenesis, tissue regeneration of the infracted portion and even support differentiation of the stromal cells *in vivo* [110, 111]. But the success of such experimental cell-based gene therapies is mainly based on the cell delivery system, its biosafety profile, efficiency of gene transfer and the subsequent expression profile of the transplanted cells without affecting the host cells' natural biological capabilities. This is particularly important in direct intramyocardial transplantation where, apart from rapidly losing their viability due to the harsh environment, the beating heart makes the retention of the transplanted cell at the target site very difficult [68]. Other modes of free cell administrations such as transepicardial, intravenous and transendocardinal routes have major drawbacks of frequent organ embolism, mechanical damage to cells, lack of specific targeting and immune rejection. In order to confront these issues, microencapsulation technology is being studied here.

Microencapsulation is the procedure by which materials such as enzymes, genes or even cells are enclosed within microscopic, semipermeable containers

[311]. These synthetic semipermeable microcapsules, sometimes referred to as artificial cells, were designed in our lab to retain the cells inside while allowing permeable molecules to cross the membrane [312-314]. These encapsulated cells are supported by external oxygen and nutrients. Their secreted products are diffused out of the microcapsules in order to carry out their functions [315, 316]. Furthermore, microencapsulated cells are protected from immune rejection because leukocytes and antibodies cannot penetrate the capsule [317-319]. Thus, it becomes an ideal tool for allogeneic and xenogeneic transplantation. The concept of microencapsulation may therefore eliminate the requirement for immune suppressants when used in transplantations.

In this work, recombinant baculoviruses carrying Monster Green Fluorescent Protein transgene under the control of mammalian CMV promoter were generated (Bac-MGFP) to transduce the cells before encapsulation. Baculovirus is a powerful tool for different gene therapy applications as it combines the advantages of viral transient expression, ease of generation, and a wide cell tropism [320]. To deliver the transduced cells, we developed poly-ethylene-glycol (PEG) incorporated alginate-chitosan (AC) microcapsules and investigated their properties and potential as a novel stem cell based gene delivery system for cardiac transplantation. The positively charged chitosan binds with negatively charged alginate through electrostatic interaction, which results in interfacial adsorption of chitosan by the alginate core. An improper coating can make the capsular surface charged. Hydrophilic, non-ionic and inert nature of PEG makes it an ideal candidate to neutralize the surface charge and hence, increase the immunoprotective potential of the capsules by alleviating the chance of having surface protein adhesions [321]. The transduced encapsulated cells were further studied to explore whether they can retain their natural ability for multi-lineage differentiation.

8.3 Materials and Methods

8.3.1 Cell Cultures

Sf9 insect cells (Invitrogen Life Technologies, Carlsbad, CA) were maintained at 27^{o}C in SF900 III serum free medium in stationary flasks. The cells were maintained in the exponential growth phase and sub-cultured twice per week. For larger volumes, cells were prepared in shaker flasks (Erlenmeyer, Corning), being agitated at 120 rpm in 27^{o}C shaker. Human bone marrow derived mesenchymal stem cells (Lonza, MD, USA) were cultured in mesenchymal stem cell basal medium (Lonza), supplemented with MCGS growth factors (Lonza) at 37°C incubator with 5% carbon dioxide. Lymphocyte leukemia cells from mouse origin were purchased from ATCC and routinely subcultured in MEM (minimum Eagle's essential medium) supplemented with 10% FBS.

8.3.2 Construction of BacMam vector and generation of Bac-MGFP virus by co-transfection

The pVL1392 baculoviral transfer vector and phMGFP vector carrying the Monster Green Fluorescent Protein (MGFP) were obtained from BD Biosciences and Promega respectively. The phMGFP and pVL1392 vectors were digested with restriction enzymes BglII and XbaI; the cut out $P_{CMV\text{-}hMGFP}$ gene and digested pVL1392 vector were ligated to form the pVL1392-P_{CMV}-P_{MGFP} transfer vector. To generate the recombinant MGFP baculoviruses, 1x10^{6} Sf9 cells were seeded in six-well plates. A transfection mixture comprising of 1ug of the constructed BacMam transfer vector, linearized baculovirus DNA (BD Baculogold) and 6µL of the Cellfectin transfection reagent diluted in 200µL media (Invitrogen Life Technologies, Carlsbad, CA) was prepared. The mixture was incubated for 45 minutes at room temperature and then was co-transfected to the seeded cells. After 5h of incubation at 27^{o}C the transfection media was replaced with Sf900III media and the cells were further incubated at 27°C. The cell cultures were collected 96h post transfection, centrifuged at 1000g for 10 min and then the supernatant containing the baculovirus was filtered through a 0.22-µM membrane

and stored at 4°C (P0 Virus Stock). The viral stock, measured in terms of plaque forming unit (pfu), was amplified by scale-up in shaker flask cultures [322]. Briefly, Sf9 cells were grown till the mid-exponential phase and diluted to 2×10^6 cells/mL with SF900III medium. The cultures were infected with the P0 virus stock at a multiplicity of infection (MOI= pfu/cell) of 0.1. During the infection process, the total and viable cell densities were measured using trypan blue in a hemocytometer. The infected cell culture containing the amplified recombinant baculoviruses was harvested (P1 stock) by centrifugation when cell viability was between 75-80%. In a similar way, baculovirus containing CMV promoter but no MGFP gene (Bac-null) was also generated. The viral titre, measured as pfu/mL was determined using the Novagen's Baculovirus Fast Plax Titer Kit according to the manufacturer's protocol. Briefly, the Sf9 cells were plated in six-well plates with 1 million cells per well. After serial dilution of the viral stocks in Sf900III media, the 200µL aliquots were added to each well. At the end of 1h incubation, 2mL media was added to each well followed by a 30h incubation period at 27^{o}C in a sealed humid chamber. The cells were then fixed and treated with Fast Plax monoclonal primary antibody specific to the baculovirus glycoprotein64 followed by β-galactosidase conjugated goat anti-mouse antibody. Lastly, X-Gal staining was performed. Bright field pictures were taken, using Nikon Eclipse TE2000-U microscope, to detect the infected cells stained with dark blue color.

8.3.3 Transduction of bone marrow stem cells

In order to transduce, the cells were seeded in six-well plates at $2x10^5$ hBMSCs/ well and were allowed to attach to the bottom of the plate overnight in the incubator. In order to infect the cells, the cell media was replaced by 500µL of PBS containing Bac-MGFP virus at varied MOI. After 8h of viral incubation at 27^{o}C, the viral solution was removed and the cells were washed twice with PBS and then replenished with 2mL of fresh media. To check the fluorescein expression, 2x 10^4cells/well were seeded in ninety six-well plates and transduced with viral vectors under different conditions. After 24h, fluorescein readings (485nm/535nm) of the individual wells were taken with a plate reader (Victor3

Multilabel Counter from Perkin Elmer). Pictures of the transduced cells expressing GFP protein were taken using the Nikon Eclipse TE2000-U fluorescent microscope under fluorescent field. They were counterstained with 4', 6-diamidino-2-phenylindole (DAPI; Invitrogen) to stain the nucleus.

8.3.4 Encapsulation of transduced hBMSCs in PEG incorporated microcapsules

The transduced hBMSCs were encapsulated in alginate microcapsules using previously established procedures. Briefly, right after viral incubation, the cells were trypsinized and suspended in 1.5% sodium alginate (Sigma Chemicals, St. Louis, MO, USA) at a cell concentration of $2x10^6$ cells/ mL. The suspension was extruded through an encapsulator (Inotech) fitted with 300μM nozzle at a voltage of 0.577kV and frequency of 710Hz. The gelation process took place in a 0.1M $CaCl_2$ solution for 15 min. AC microcapsules were prepared by immersing the calcium alginate capsules in 0.5% chitosan solution dissolved in dilute acetic acid at a pH of 5.2 for 30 min. The capsules were washed for 5 min after every coating with physiological solution. To prepare AC-PEG capsules, the AC microcapsules were treated with 0.5% solution of PEG (MW 10000; Sigma Chemicals, St. Louis, MO) dissolved in 0.45% NaCl for 10 min. The capsules were then washed twice with physiological solution. The washed capsules were then transferred to stationary cell culture flasks, and resuspended in medium with antibiotics (Sigma) for further culture in 37^oC incubator with 5% CO_2. These microcapsules were replenished with fresh media every alternate day. To take pictures of the encapsulated transduced cells expressing GFP protein, fluorescent microscope was used.

8.3.5 Monitoring cell growth of microencapsulated cells

The cell growth within microcapsules was assessed using polyanionic calcein AM dye (Biotium Inc, Hayward, USA). Using this dye, the live cells were detected by the intracellular esterase mediated conversion of the non-fluorescent cell-permeant calcein AM to the fluorescent green calcein. 50 microcapsules encapsulating the cells were first washed with PBS and then incubated with

200μL of fresh PBS containing 2 μM calcein AM. After 1h, the wells were checked under the fluorescence microscope and fluorescein measurements (excitation 485nm, emission 535nm) of the wells were taken with a plate reader (Perkin Elmer). The background fluorescence as detected in the wells with microcapsules without any cell was taken as the negative control.

8.3.6 Immunoprotective behavior of the microcapsules against lymphocytes

In order to investigate the potential of the membranes to provide immunoprotection to the encapsulated cells, 50 capsules encapsulating hBMSCs were co-cultured in static condition with $2x10^5$ seeded lymphocytes per well in a twelve-well plate at 37^oC in a standard humidified incubator with 5% CO_2. As these highly confluent lymphocytes secrete a high amount of cytokines, the viability of the encapsulated cells will depend on the immune-isolation properties of the capsular membrane [323, 324]. Capsules were withdrawn from this co-culture from time to time in order to check the viability of the encapsulated cells with calcein AM dye following the method mentioned above.

8.3.7 Stability tests of the microcapsules

The mechanical stability of the microcapsules was determined using osmotic pressure and rotational stress test. These tests were done so as to create an external harsh environment for the capsules which they are going to experience once administered intramyocardially into the beating heart. The osmotic pressure test was performed by directly transferring 500 microcapsules, encapsulating $2x10^6$ cells/mL of alginate, previously stored in 0.85% saline solution to 5mL deionized water in a 25 mL volumetric flask. In order to assess the ability of the microcapsules to withstand this osmotic stress, samples were collected at regular intervals and photomicrographs were taken for morphological analysis under the microscope. Free cells released from the broken capsules were also counted using a hemocytometer in order to obtain the percentage of cells that remained entrapped in the intact microcapsules. To implement the rotational stress test, the capsules were shaken in a horizontal shaker (Environ) at a speed of 150 rpm at

37^{o}C for 120 min. Samples were collected at regular intervals for counting the released cells and checking the morphology (intact/broken) of the microcapsules using bright field microscope.

8.3.8 Depolymerizing and inducing differentiation of entrapped cells

The hBMSCs were recovered from the microcapsules after 15 days of culture by treating the capsules with 27mM NaCl solution containing 100mM sodium citrate and 10mM MOPS (Sigma-Aldrich) for 1h at room temperature [325]. The completely broken and semi-dissolved alginate capsules were then centrifuged at 800 rpm for 7 min to recover the free cells from the pellet, leaving the sodium citrate solution and capsular parts in the supernatant. The cells were then washed thrice with PBS and resuspended in culture media containing serum and seeded in twenty four-well plate at a high confluency for adipogenic, chondrogenic and osteogenic differentiation according to the manufacturer's protocol. After cell seeding, the medium was replaced with StemPro adipogenesis, chondrogenesis and osteogenesis differentiation medium (Invitrogen). The media were then replaced with fresh differentiation media on every fourth day. On day 14, the cells were washed with PBS and fixed in 4% formaldehyde solution. Oil Red O staining solution was added to the fixed cells in order to monitor the intracellular accumulation of neutral lipids within the adipogenically differentiated cell population. For chondrogenic analysis, 1% Alcian Blue solution prepared from 0.1N HCl was used to stain the cartilage proteoglycans that turns chondrocytes blue. For detecting the osteogenic cell population, the cells were cultured for 21 days followed Alizarin Red staining.

8.4 Results

8.4.1 Generation of recombinant baculoviruses by co-transfection in insect cells

The recombinant baculoviruses were generated as depicted in **Figure 8.1** using the BacMam expression system. The titre of the amplified virus stock was 2.4x10^{9}pfu/mL, as determined by an immunological assay method which was

originally developed by Kitts and Green [326]. This method uses immunological techniques to detect the baculoviral external glycoprotein gp64 on the infected sf9 cell surface. The dark blue color plaques in **Figure 8.2** shows the insect cells infected with baculovirus 24h post infection.

8.4.2 Modulation of transgene expression by regulating viral dosage

In order to optimize the in vitro transduction efficiency of baculovirus in hBMSCs, $2x10^4$ cells were seeded in ninety six-well plates and transduced with 200µL PBS containing Bac-MGFP of various doses under transduction temperature of 27^{o}C. After 8h of transduction, the cells were washed twice with PBS and replenished with fresh medium. Viral dosage plays an important role in transduction of the cells which is evident in **Figure 8.3A** where a gradual increase of viral dose from 10^7 pfu to $10x10^7$ pfu per well shows a corresponding increase in transgene expression, while a greater dose of $20x10^7$ pfu per well did not show any increase in expression. The fluorescence image of **Figure 8.3B** illustrates the effect of increasing viral dosage on hBMSCs transgene expression.

8.4.3 Biocompatible and immunoprotective nature of AC-PEG microcapsules

In order to test whether the PEG incorporated capsules supports cell survival and proliferation or not, Bac-null transduced cells were encapsulated in AC-PEG microcapsules. Initially, the average cell population per capsule was approximately 80. Using calcein staining the total number of viable cells per capsule was measured and calculated through the fluorescein plate reader at different time intervals. The ability of the AC-PEG capsules to provide immunogenic protection to the encapsulated human stem cells were studied by co-culturing microencapsulated Bac-null transduced cells with a significantly high population of lymphocytes derived from mouse origin for 11 days. For this, AC microcapsules without PEG treatment, encapsulating same number of cells was taken as the control. It can be concluded from **Figure 8.4A** that growth of the encapsulated cells in presence of lymphocytes started to decrease significantly from day 3 of encapsulation, when no PEG was used; while in AC-PEG capsules

there was slow ceasing of growth from a much later time, from day 7 (average 92 cells in comparison to 102 cells per capsule without lymphocytes). A longer co-culture for 11 days showed 65 viable cells per AC-PEG capsules in comparison to about 40 viable cells per AC capsules.

8.4.4 Strong mechanical properties of AC-PEG capsules

The mechanical and osmotic stability of the PEG modified membrane was compared with unmodified AC microcapsules. In this case, the cell encapsulated capsules were subjected to rotational and osmotic stress as mentioned previously in the method section. The AC capsules were unable to withstand the mechanical forces and nearly 90% of them broke within 2h as evident from **Figure 8.5A** that shows the percentage of cells still encapsulated. In comparison, about 64% of the cells remained encapsulated in AC-PEG microcapsules after 1h, which remained constant even after 2h of rotation. Even under osmotic stress of 2h, around 92% of the cells remained encapsulated in AC-PEG microcapsules while in AC it went down to 54% (**Figure 8.6A**).

8.4.5 Transgene expression of baculovirus transduced cells microencapsulated in AC-PEG capsules

In order to demonstrate the gene expression pattern of the AC-PEG microencapsulated transduced cells, hBMSCs were Bac-MGFP transduced for either 4h or 8h, and right away encapsulated at a concentration of 2 million cells per mL of alginate to prepare the AC-PEG microcapsules. The microcapsules containing cell were then cultured in stationary flasks with standard medium supplemented with antibiotics. The relative fluorescence units of each well containing 50 capsules resuspended in 200µL PBS were then measured at different time intervals using Victor3 Multi Label Plate Counter (Perkin Elmer, USA). **Figure 8.7A** reveals that the transgene expression had a rapid expression pattern with the highest expression observed on day 1 with a viral incubation time of 8h, as is evident by the normalized gene expression data with time. It shows the highest expression (considered as 100%) on day 1 that gradually diminished with

time. Interestingly, this was also the trend with encapsulated cells transduced for 4h. The graph shows that the normalized GFP expression level remained high at around 70% on day 5, but dropped to 27% on day 9 and 15% on day 14. However, normalized GFP expression was consistently higher in 8h plot compared to the 4h plot where the expression almost ceased by day 9. Day 1 and day 7 pictures in **Figure 8.7B** illustrates this gradual decrease of fluorescein expression by the transduced encapsulated cells with time. It is also evident from the pictures that viral incubation time has an impact on the transgene expression profile of the transduced cells, where 8h incubation gave better expression profile than 4h. This decrease in transgene expression is mainly because of the transient nature of cell expression mediated by baculovirus.

8.4.6 Retention of differentiation potential of baculovirus transduced encapsulated cells

To confirm the retention of differentiation potential of the baculovirus transduced encapsulated hBMSCs, the cells were isolated from the capsules after 15 days of culture. They were then seeded at high confluency and induced towards adipogenic, chondrogenic and osteogenic lineages with appropriate differentiation media [327, 328]. Untransduced non-encapsulated cells were induced for differentiation as positive control. After 14 days of culture, the cells were fixed. Oil Red O staining showed that both the encapsulated and non-encapsulated control cells have differentiated into adipocytes as evident by the formation of lipid vacuoles (**Figure 8.8A and 8.8A'**). The Alcian blue staining showed similar result, where, the chondrocytes formed by the encapsulated and non-encapsulated control cells turned blue in color owing to proteoglycans (acid mucopolysaccharides and glycosaminoglycans) that turns chondrocytes blue, even though the percentage of differentiated cells appeared lower in transduced encapsulated cells (**Figure 8.8B and 8.8B'**). Osteogenic differentiation of the cells was carried on till day 21. The cells were then stained with Alizarin red which forms complex with calcium deposits of the osteocytes in a chelation process to give a birefringent orange-red color. The staining revealed efficient

osteogenic differentiation of the cells, like the control (**Figure 8.8C and 8.8C'**). From the above obtained results, it can be concluded that neither encapsulation nor viral transduction altered the differentiation potential of the stem cells. This is an important finding which demonstrates that microcapsules can be a potential delivery system for stem cells which can not only protect the stem cells from external hostile environment but also can retain their therapeutic differential potential.

8.5 Discussion

BMSC based cell and gene therapy have captured considerable attention as a potential platform for systemic and local gene delivery for tissue regeneration. It is considered to be an effective therapeutic approach for treating myocardial infarction that leads to an irreversible loss of cardiomyocytes and progression of heart failure [329]. Furthermore, they can be genetically modified to overexpress growth factors and relevant therapeutic proteins. Hence, genetically modified hBMSCs offer a new approach in tissue engineering and regenerative medicine. In the current study, we have successfully used baculoviruses for transducing the marrow stromal cells and optimized the transduction protocol. These viruses have become an increasingly attractive tool in gene therapy due to its non-pathogenic nature in mammalian cells [328, 330]. In this study, they have been used as the gene delivery vehicle for delivery of exogenous recombinant DNA into the mammalian cells using the BacMam expression system. These recombinant BacMam baculoviruses can express their transgenes under the control of strong mammalian promoters in mammalian cells [331-333]. It can transport more than 38 kilobases of transgene [334]. Moreover, the baculovirus does not express its own genes and cannot replicate in mammalian cells. The above characteristics make this virus a biologically safe and a potent vector for gene therapy applications. Although the cell transgene expression was limited to a week and reduced rapidly afterwards, the expression can be extended or even enhanced, based on the requirements, by modulating the transduction conditions (such as viral dose, temperature, treatment with epigenetic factors and

protein expression enhancers like trichostatin A and sodium butyrate) [327, 335, 336]. The transient expression is however ideal in some cases as it no longer stays there once its job is done, thus alleviating unwanted side effects.

A number of delivery systems are being studied using different biodegradable polymers and tissue engineering techniques to deliver the therapeutic cells to the target site, particularly for myocardial transplantation [337]. Bone marrow or embryonic stem cells seeded on PGA/collagen scaffold has been shown to improve blood pressure and function of infracted heart [338, 339]. Fujita *et al.* showed that poly (glycolic acid) - collagen sponge supplemented with basic fibroblast growth factors can support proliferation and differentiation of bone marrow stem cells [340]. Another group used rat bone marrow stem cells for left ventricular tissue engineering using degradable PLA, polytetrafluroethylene and collagen scaffold [341]. However, the major concern with heart transplantation is not only to deliver the cells to the desired site effectively without damaging them but also to give protection to the transplanted cells against the harsh environment. This is particularly difficult in case of direct intramyocardial delivery, where the myocardium continuously and forcefully contracts in such a way that any injectate containing the stem cells could easily be washed out mechanically into any nearby bloodstream, in addition to being biologically damaged and immunologically rejected [68, 342]. Direct intramyocardial delivery by injecting microencapsulated marrow stromal cells to the peri-infarct region of acutely infarcted heart can be of immense potential as shown by our recent preliminary preclinical data [343]. It shows that the retention of cells can be increased by approximately four times by using microcapsules in comparison to free cells.

Thus, in order to develop a more advanced delivery system for myocardial transplantation, we have designed these smooth, spherical and much more resilient PEG integrated polymeric microcapsules with a diameter of around 400µm encapsulating an average of 80 cells per capsule. Our data showed that the cells within the AC-PEG microcapsules remained viable and even proliferated with time. The encapsulated cells were also able to express its transgene and

retain its natural potential to differentiate into different lineages. The external PEG coating gave the capsule a better mechanical and osmotic stability than our previously designed uncoated AC capsules [323]. This increase in stability can be contributed to the penetration of PEG into the alginate core of the capsule that gives an added firmness to the capsule when exposed to stress conditions [344]. The reason for such significant stability can also be attributed to the strong interpenetrating network formed by PEG on the capsular surface, which is absent in case of AC capsules. Treatment of the capsules with PEG, in addition, gave a much firmer and longer immunoprotection to the cells in presence of highly confluent lymphocytes in comparison to microcapsules without PEG. It is important to have microcapsules with minimum surface charges in order to avoid foreign body reactions when transplanted [345]. Earlier studies have also shown that PEG helps to decrease fibrous overgrowth in vivo and reduce thrombogenecity of foreign material surfaces. Alginate, chitosan and PEG are all biocompatible, biodegradable and bioresorbable polymers which eventually get broken down into non-toxic metabolites or waste by-products according to their varied degradation time in the body. Thus the material residues are also of no potential harm to the body. An important point to mention here is that the PEG coating decreases the permeability of the microcapsules due to its highly dense interpenetrating network. Hence, PEG coated AC capsules are going to release its cell products much slower than the non coated AC capsules. But, by altering the PEG concentration and by using different molecular weights of PEG these membrane characteristics can be altered as desired.

8.6 Conclusion

The current study revealed that AC-PEG microcapsules can be used as an efficient delivery system for stem cell transplantation as well as for cell based gene therapies using baculoviruses for therapeutic protein production. The incorporation of PEG gave the capsules a better mechanical stability as well immunogenic property without interfering with their cell viability, proliferation and differentiation ability. AC-PEG microcapsules may thus become an

innovative and integral part of stem cell based regenerative medicine that can be useful in the growing fields of myocardial tissue engineering. But further studies are needed to be done to characterize the mechanical properties of the capsules extensively, for example, single-capsule compression test to determine the capsule shell wall modulus. In order to attain a better understanding of its future potential and concerns for biomedical applications, much more comprehensive *in vitro* and *in vivo* studies on the biocompatibility and biodegradability of the membrane need to be done.

8.7 Acknowledgments

This work is supported by research grant (to D.S. and S.P.) from Natural Sciences and Engineering Research Council (NSERC), Canada. A.P. acknowledges the financial support from NSERC Alexander Graham Bell Canada Graduate Scholarship.

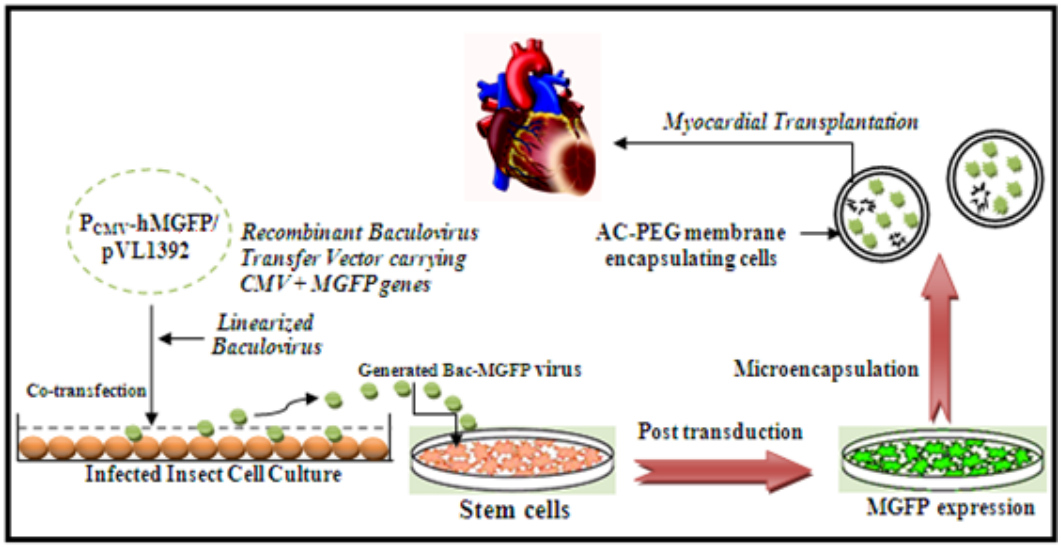

Figure 8.1: Schematic representation for generation of recombinant baculovirus and microencapsulation of transduced hBMSCs for myocardial transplantation. The P_{CMV}-hMGFP/pVL1392 plasmid, prepared by inserting hMGFP and CMV promoter from phMGFP vector into the baculovirus transfer vector pVL1392, was co-transfected with linearized baculovirus into the Sf9 cells. The generated Bac-MGFP virus was used to transduce the hBMSCs, which were then microencapsulated in AC-PEG membrane for transplantation.

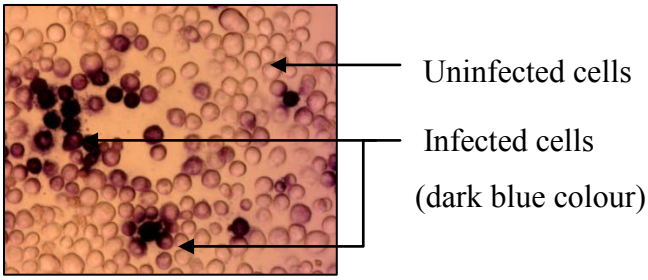

Figure 8.2: Immunological staining of baculovirus infected Sf9 cells using FastPlax Titre kit.Sf9 cells were infected with diluted baculoviral stock and after 24hrs the cells were fixed and gp64 protein was detected on the cell surfaces by using monoclonal anti-gp64 antibody and β-galactosidase conjugated secondary antibody.

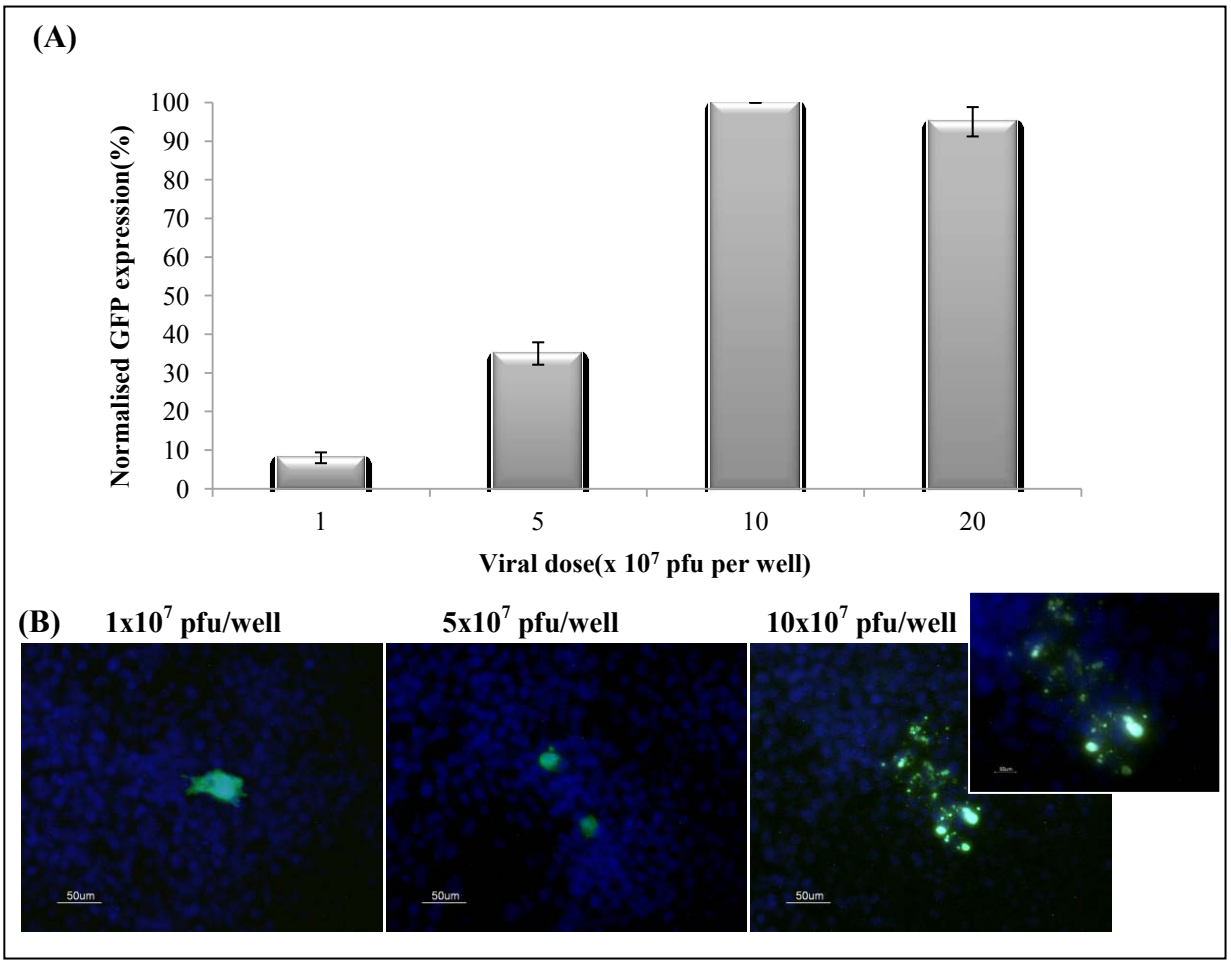

Figure 8.3: Enhancement of transgene expression by increasing viral dose. $2x10^5$ hBMSCs per well were transduced with Bac-MGFP for 8h at 27°C at different viral doses. Quantification (fluorescein expression; 485nm/535nm) of fluorescent hBMSCs was made with relation to viral dosage 24 hpt **(A).** The average fluorescein expressed values were normalized to that of the cells having 8h of viral incubation with a dose of $10x10^7$pfu (taken as 100%), and are represented as normalized mean expression in percentage value. The data represent mean of three independent readings and the error bars represent Standard Deviation (SD) of the mean. Fluorescence images of cells 24 hpt with different viral dosages are shown in **(B)** under 100X mafnification. Photomicrograph for $10x10^7$pfu/ well has been magnified to 200X and shown in the subset.

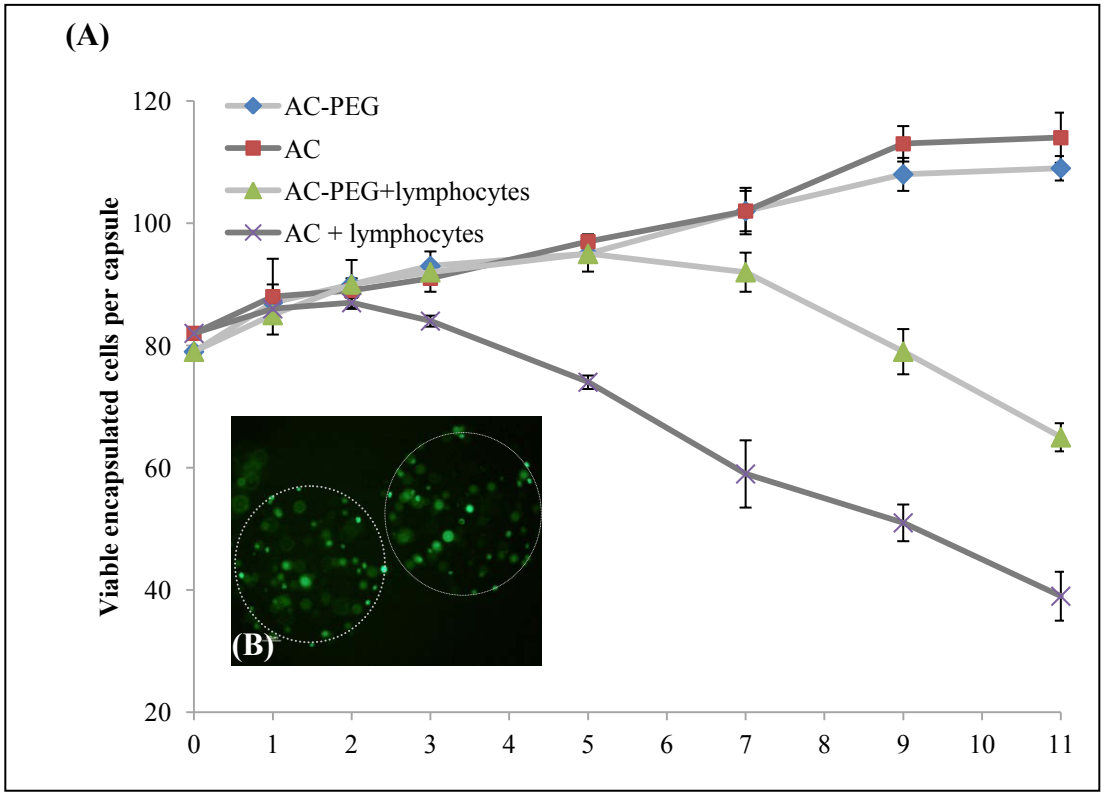

Figure 8.4: Effect of PEG incorporation on immunoprotective potential of the membranes. Microcapsules prepared by microencapsulating of $2x10^6$ Bac-null transduced hBMSCs /ml of alginate were cultured in DMEM+10% FBS in 37^oC incubator for 8days in presence or absence of highly populated murine lymphocytes. Medium was replaced on every alternate day. Samples were collected at regular intervals and subjected to cell growth test using the calcein AM staining. The data represent the mean of three independent studies ± SD **(A).** Representative fluorescent image of capsules encapsulating the cells in a fluorescence microscope (showing viable cells in green) are shown in **(B).** The white circle shows the peripheral surface of the microcapsules.

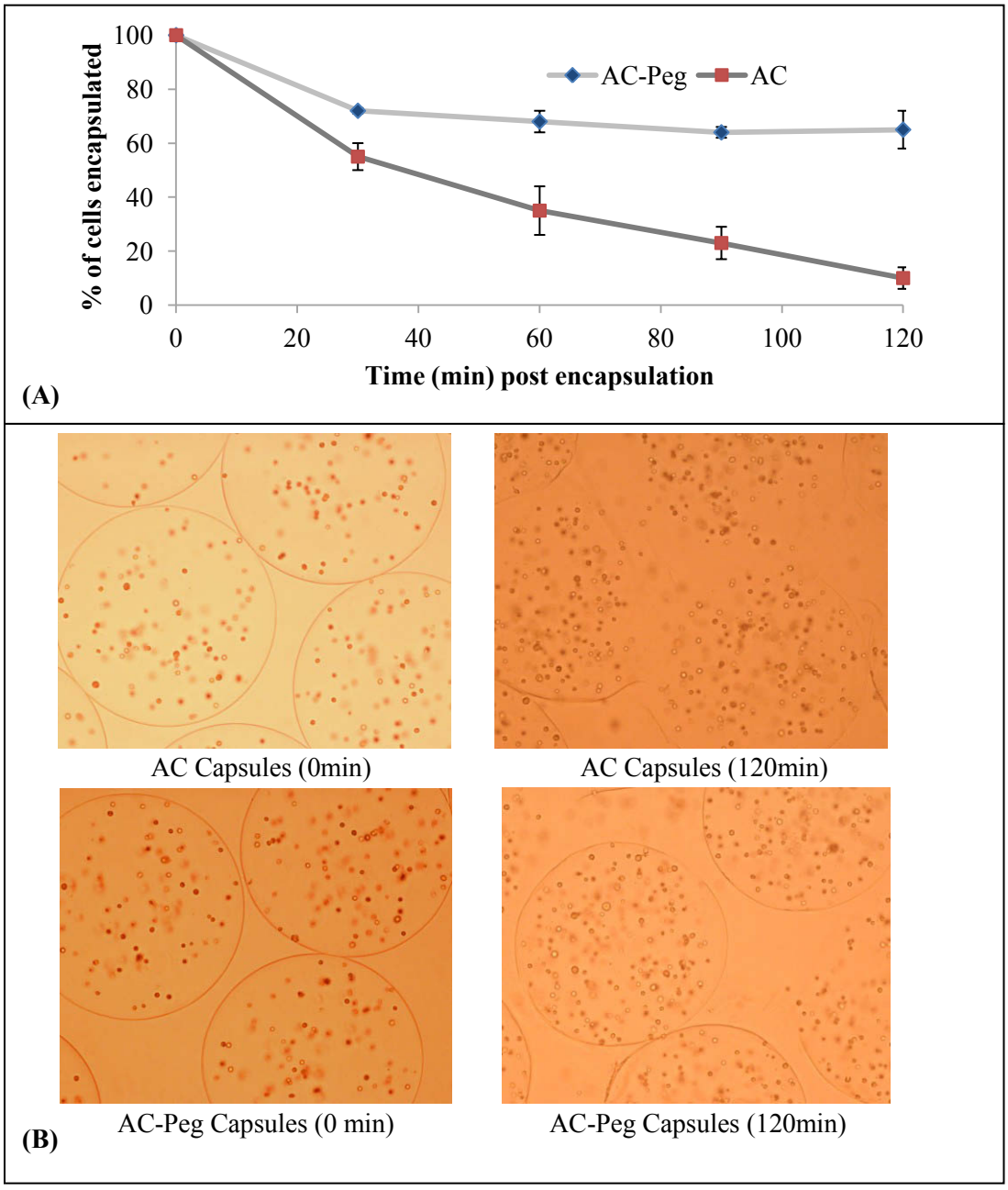

Figure 8.5: Effect of PEG incorporation on mechanical stability of microcapsules. The microcapsules encapsulating cells were subjected to rotational stress by at 150rpm 120min. Samples were collected from time to time number of free cells were counted in hemocytometer to know the percentage of cells still encapsulated inside the intact microcapsules **(A)**. The data represent the mean of three independent experiments ± SD. Representative bright field images of the two types of capsules, encapsulating the cells under 100X magnifications **(B)**.

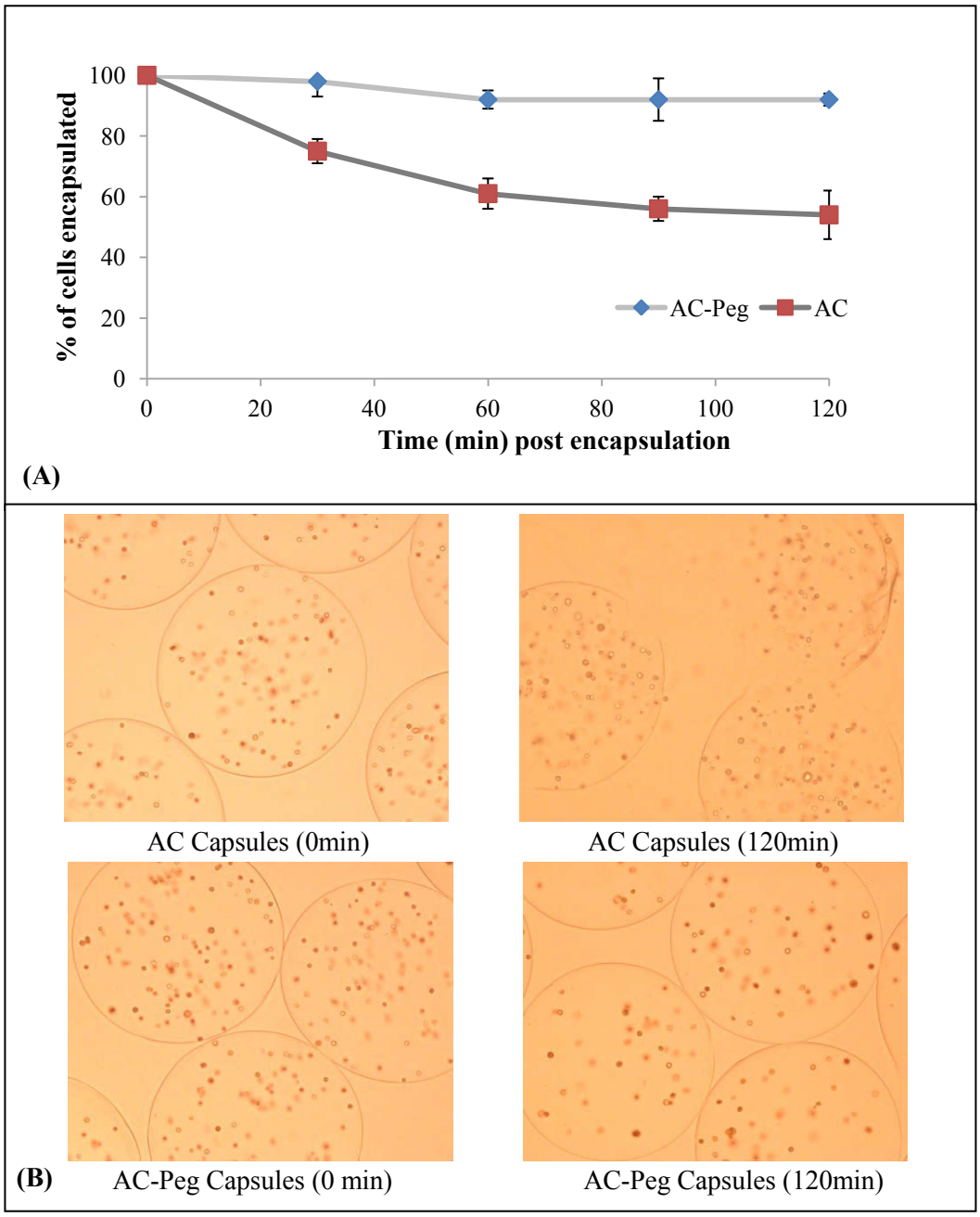

Figure 8.6: Effect of PEG incorporation on osmotic stability of the microcapsules. The test was performed by transferring the microcapsules, previously stored in 0.85% saline solution directly to deionized water. Samples were collected from time to time number of free cells were counted in hemocytometer to know the percentage of cells still encapsulated inside the intact microcapsules **(A).** The data represent the mean of three independent experiments ±SD. Representative bright field images of the two types of capsules, encapsulating the cells under 100X magnifications **(B).**

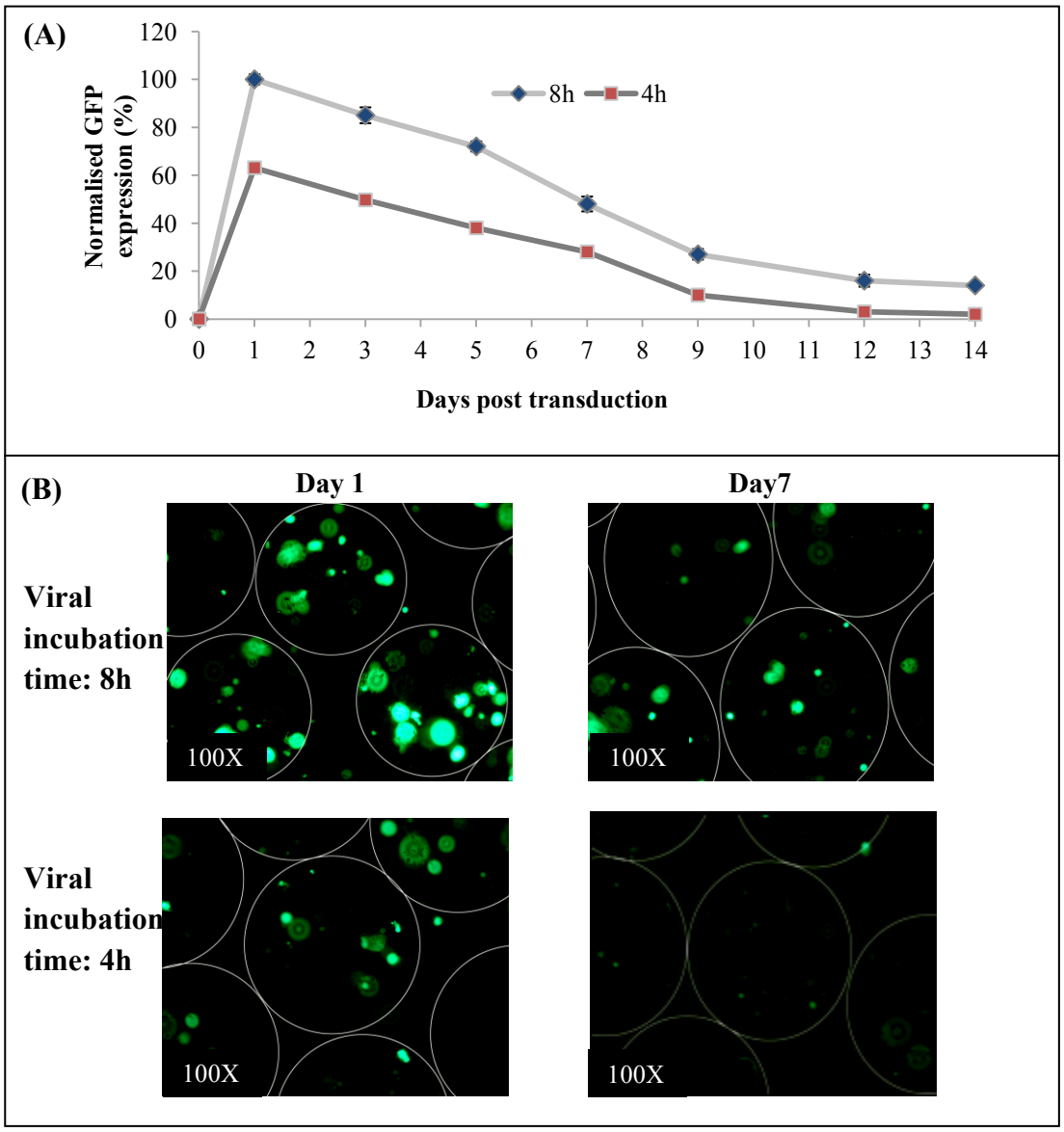

Figure 8.7: Time-course profile of transgene expression of AC-PEG microencapsulated hBMSCs transduced with Bac-MGFP under optimal transduction condition with varied incubation times (4h/8h). The average fluorescein expressed values were normalized to that of cells with 24hpt having 8h of viral incubation (taken as 100%), and are represented as normalized mean expression in percentage value **(A)**. The data represent the mean of three different fields ±SD. Representative photographs of corresponding transduced microencapsulated cells were taken using fluorescence microscope on day 1 and day 7 **(B)**. The white circles show the peripheral surface of the microcapsules.

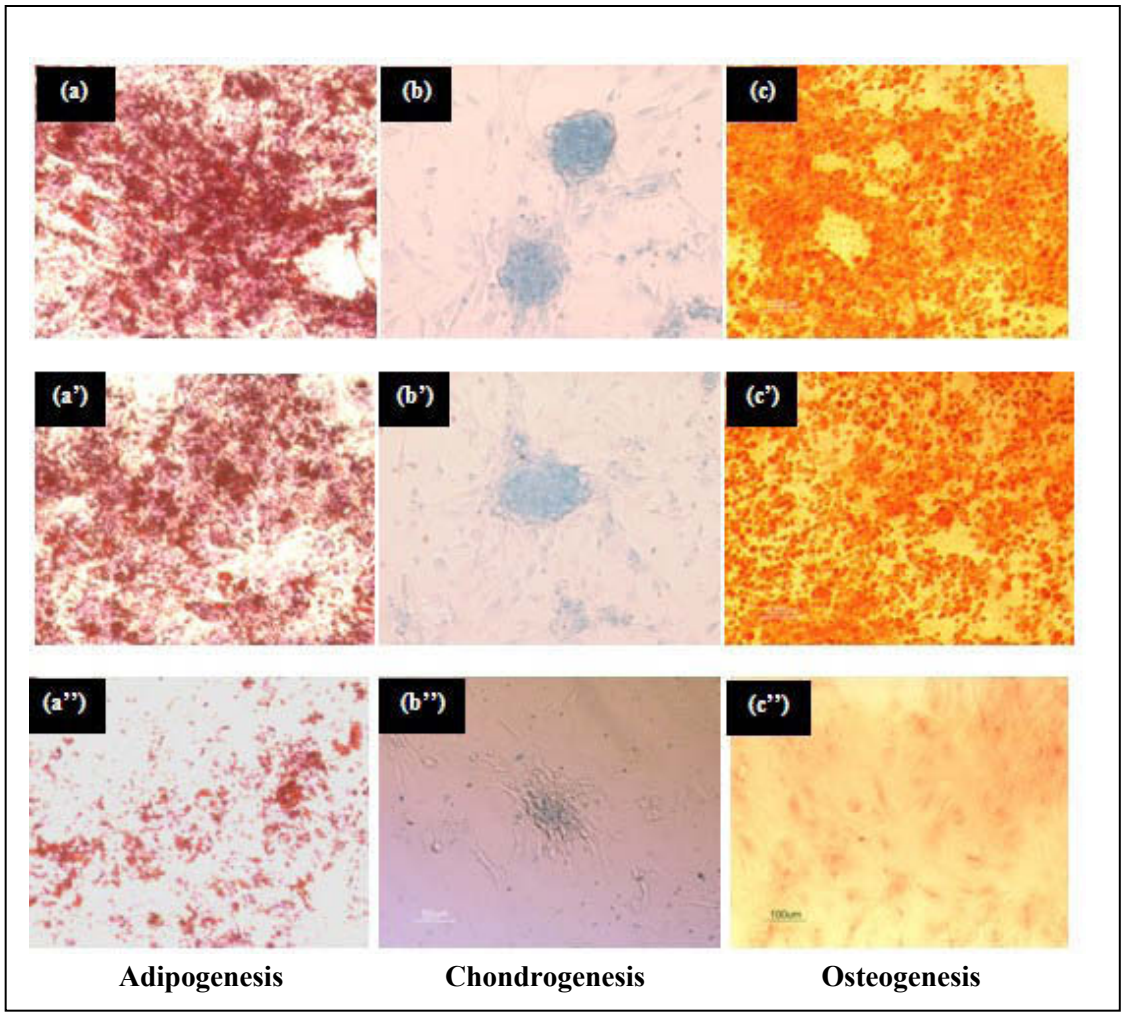

Figure 8.8: Effect of microencapsulation and baculovirus transduction on differentiation potential of hBMSCs. The microencapsulated transduced hBMSCs were isolated from the capsules by depolymerisation. They were seeded for adipogenic (a), chondrogenic (b) and osteogenic (c) differentiation using respective media. Non-encapsulated cells were taken as the postive control for differentiation (a', b' c'), while cells grown in normal cell culture media without any differentiation agents (a'', b'' c''), were taken as the negative control. The cells were stained with oil red O to detect the mature adipocytes. Similarly, after chondrogenic induction, the cells were stained with alcian blue to stain the chondrocytes. After osteogenic induction, the cells were stained with alizarin red to detect the osteogenically differentiated cells.

A nanobiohybrid complex of recombinant baculovirus and Tat/DNA nanoparticles for delivery of Ang-1 transgene in myocardial infarction therapy

Arghya Paul[1], Zyad Binsalamah[2], Afshan Afsar Khan[1], Sana Abbasi[1], Cynthia B. Elias[3], Dominique Shum-Tim[2], Satya Prakash[1*]

[1] Biomedical Technology and Cell Therapy Research Laboratory, Department of Biomedical Engineering, Faculty of Medicine, McGill University, 3775 University Street, Montreal, Quebec H3A 2B4, Canada.

[2] Divisions of Cardiac Surgery and Surgical Research, The Montreal General Hospital, 1650 Cedar Ave, Suite C9-169, Montreal, Quebec H3G 1A4, Canada.

[3] Bulk Manufacturing, Sanofi Pasteur, Connaught Campus, 1755 Steeles Avenue West, Toronto, Ontario, M2R 3T4, Canada.

*Correspondence author; Email: satya.prakash@mcgill.ca
Tel: +1-514-398-3676; Fax: +1-514-398-7461

Preface: Previous chapters have shown the applicability of stem cell based gene therapy using recombinant baculoviruses. As a continuation, this chapter investigates the potential of baculovirus for direct gene therapy. For this, we have developed a novel gene delivery system with baculovirus hybridized to gene carrying nanoparticles for enhanced transduction. *In vitro* and *in vivo* results using angiogenic gene demonstrated the efficacy of this system for therapeutic angiogenesis.

Original article published in ***Biomaterials*** **32(32):8304-18 (2011)**

9.1 Abstract

The study aims to design a new gene delivery method utilizing the complementary strengths of baculovirus, such as relatively high transduction efficiency and easy scale-up, and nonviral nanodelivery systems, such as low immunogenicity. This formulation was developed by generating a self assembled binary complex of negatively charged baculovirus (Bac) and positively charged endosomolytic histidine rich Tat peptide/DNA nanoparticles (NP). The synergistic effect of this hybrid (Bac-NP) system to induce myocardial angiogenesis in acute myocardial infarction (AMI) model has been explored in this study, using Angiopoietin-1 (Ang-1) as the transgene carried by both vector components. Under optimal transduction conditions, Bac-NP_{Ang1} showed 1.75 times higher and sustained Ang-1 expression in cardiomyocytes than Bac_{Ang1}, with significantly high angiogenic potential as confirmed by functional assays. For *in vivo* analysis, we intramyocardially delivered Bac-NP_{Ang1} to AMI rat model. 3 weeks post AMI, data showed increase in capillary density ($p<0.01$) and reduction in infarct sizes ($p<0.05$) in Bac-NP_{Ang1} compared to Bac_{Ang1}, NP_{Ang1} and control groups due to enhanced myocardial Ang-1 expression at peri-infarct regions (1.65 times higher than Bac_{Ang1}). Furthermore, the Bac-NP_{Ang1} group showed significantly higher cardiac performance in echocardiography than Bac_{Ang1} (44.2±4.77% vs 37.46±5.2%, $p<0.01$), NP_{Ang1} and the control group (32.26±2.49% and 31.58±2.26%). Collectively, this data demonstrates hybrid Bac-NP as a new and improved gene delivery system for therapeutic applications.

Keywords: gene therapy, hybrid system, baculovirus, nanoparticle, myocardial angiogenesis

9.2 Introduction

Gene therapy has become an important approach in the treatment of various diseases. However, its success is limited mainly due to the lack of efficient delivery systems to target sites, especially with systemic diseases. Therefore, the outcome of gene therapy *in vivo* depends on the effective delivery of the gene of interest to the target site. Extensive preclinical and clinical trials have been performed with direct vascular endothelial growth factor (VEGF) gene delivery technique to the myocardium using non-viral delivery systems. Although there have been some early encouraging results, but none of these studies were eventually able to induce significant effect on angiogenesis and myocardial viability due to low transfection efficiencies. In order to improve transfection efficiency various compounds have been developed to form complexes with DNA, namely polyethylenimine (PEI), Tat peptide, lipopolymers, poloxamine nanospheres and liposomes [346-350]. Although these vectors improved the gene transfer efficiency, they were sub-optimal to induce desirable therapeutic effects. Thus tmajor limitations such as poor cellular uptake still persisted along with very short transgene expression time period. On the other hand, viral vectors are widely used systems in gene therapy studies to target the heart since they enable highly efficient and extended cardiac gene delivery [351-353]. However, these vectors are limited by only transient gene expression caused by immune response against viral gene products resulting in the clearance of transduced cells. Moreover, there is a risk of immunogenicity, nonspecificity and inherent risks of complications such as interference with the activity of tissue specific promoters [354].

Insect cell culture and baculovirus (Bac) produced in insect cells have been widely used for recombinant protein production on an industrial scale [355]. Research studies have focused on using Bac and insect cells platforms for recombinant adeno-associated virus (rAAV) production- the first rAAV gene therapy product currently in phase III clinical trials [356]. Furthermore, Bac is being considered as a tool for gene delivery to mammalian cells utilizing genetically modified Bac, known as BacMam viruses, carrying therapeutic

transgene under the control of mammalian promoters. Recombinant BacMam viruses are easy to construct and can be generated at high titers simply by infecting insect cells. This advantage, coupled with the easy baculovirus purification process, simplifies the large scale preparation of high titre baculovirus vectors to a great extent. Bac, unlike other commonly used mammalian viruses like retrovirus and adenovirus, are considered non-pathogenic and non-toxic as they cannot replicate in mammalian cells and do not invoke any cytopathic effect [357]. Thus, Bac is a promising tool for gene therapy applications due to a lack of pre-existing memory for immune responses upon initial administration and their comparatively better biosafety profile. On the downside, Bac is comparatively less efficient than mammalian viral vectors, such as adenoviruses, for most mammalian cell transductions.

To increase the transduction efficiency of baculovirus, extensive investigation had been carried to optimize the transduction protocol. This includes regulation of the viral dosage, transduction media and temperature conditions, confluency of mammalian cells, epigenetic factors, and very recently by modulating pH dependant Bac cell entry pathways [358, 359]. Several studies have also used biotechnological tools to modify the Bac viral envelope with different membrane attachment proteins, such as avidin-displaying baculovirus and RGD displaying baculovirus, for improvement in transduction rate towards specific cells [360, 361]. Previous studies have shown significant enhancement in transfection efficiencies of non-viral delivery systems by conjugating them with mammalian viruses [362, 363]. Recent work has also demonstrated galactosylated PEI mediated improved gene delivery to hepatoblastoma and lung carcinoma cells using Bac [364]. We initially attempted to covalently link recombinant baculovirus to various ligands in order to increase vector binding and gene transfer. However, such attempts often reduced gene expression by the viral vector, probably because chemical modification of viral proteins interfered with their functions in effecting gene transfer and expression.

In the work described here, we introduce a new approach by hybridizing recombinant Bac with endosomolytic Tat/plasmid DNA nanoparticles, both

carrying therapeutic genes, and explore its potential to enhance gene delivery efficiency for myocardial therapy. Tat peptide sequence, obtained from the protein transduction domain of HIV-1 viral proteins capable of penetrating cell membrane, has been modified here by incorporating histidine and cysteine residues for enhanced DNA transport, efficient cellular internalization, cell vesicle escape and expression [365].

We reasoned that the efficiency of gene transfer would be improved if we could combine a nonviral vector system, which could mediate cell attachment, with an baculovirus vector system, which could mediate processes in gene transfer subsequent to binding. We thought that such a hybrid system might take advantage of the unique features associated with the two individual vector systems. Molecular cloning, generation of recombinant Bac, *in vitro* protocol optimization and preclinical efficacy of this new nanobiohybrid (Bac-NP) delivery system has been evaluated using Ang-1 angiogenic transgene to induce myocardial angiogenesis in infracted rat heart model. Earlier studies have demonstrated that Ang-1 plays an important role for myocardial angiogenesis and helps in cardiac function improvement in acutely infarcted heart [353, 366, 367]. Interestingly, Ang-1 also enhanced cardiomyocytes and endothelial cell survival against oxidative stress induced apoptosis [368]. It is also known that Ang-1 promotes neovascularization co-operatively with VEGF and their combined action leads to a more mature and functional vasculature [366]. In the present study, we have selected Ang-1 as the therapeutic gene, taking advantage of the fact that AMI induces a high circulating endogenous serum VEGF state [353]. A schematic presentation of the whole procedure from molecular cloning to generation of hybrid Bac-NP is demonstrated in **Figure 9.1**.

9.3 Materials and methods

9.3.1 Cell Culture

H9c2 myogenic cell-line, derived from embryonic rat heart ventricles, was obtained from American Tissue Culture Collection (CRL 1446) and cultured in DMEM supplemented with 10% fetal bovine albumin (FBS). The cells were

routinely maintained as stationary cultures in flasks, incubated at 37^{o}C in a controlled environment with 5% CO_2. Human umbilical vein endothelial cells (HUVECs) (Sciencell, Carlsbad, California, USA) were cultured and expanded on tissue culture flasks according to the supplier's instructions. They were cultured in endothelial cell medium (ECM) (Sciencell, Carlsbad, California, USA) supplemented with 5% FBS and placed in an incubator containing 5% CO_2 at 37°C. Sf9 insect cells (Invitrogen Life Technologies, Carlsbad, CA) were maintained at 27^{o}C in SF900 III serum free medium (Invitrogen). The cells were maintained in exponential growth phase and subcultured twice a week. Larger volumes were prepared in shaker flasks (Erlenmeyer, Corning) which were agitated at 120 rpm in an incubator shaker as described earlier [359].

9.3.2 Generation of recombinant baculoviruses carrying CMV/hAng1

The mammalian expression vector pCI and pVL1392 transfer vector were procured from Promega and BD Biosciences respectively. pCMV-XL4 vector carrying human Angiopoietin1(hAng1) cDNA was bought from Origene Technologies (Rockville, MD). The pVL1392 vector and pCI vector, which harbors the P_{CMV} promoter, were digested with BglII and BamH1 restriction enzymes. The cut out P_{CMV} gene and digested pVL1392 vector were purified and a basic ligation reaction with T4 DNA ligase (Promega, Madison, WI) was performed to insert the P_{CMV} gene into the pVL1392 transfer vector by directional cloning method. The pVL1392-P_{CMV} construct was then linearized by Not1 enzyme digestion. It was then ligated in the similar way to the hAng1 cut out of the Not1 digested P_{CMV}-XL4-hAng1 plasmid to form pVL1392-P_{CMV}-hAng1 as the final transfer vector construct. Similarly, the LacZ gene from pWPTS-nls LacZ plasmid (Didier Trono Lab; Addgene plasmid 12261) was cut out using Xho1 enzyme and ligated to Xho1 linearized pVL1392-P_{CMV} construct to form pVL1392-P_{CMV}-LacZ.

The two recombinant transfer vectors were then transformed into the high efficiency DH5 α competent *E.coli* (Invitrogen Life Technologies, Carlsbad, CA) by heat shock method for amplification. The plasmids were then purified with

QIAprep spin miniprep kit (Qiagen Sciences, MD). The recombinant hAng1 (Bac_{Ang1}) and LacZ (Bac_{LacZ}) baculoviruses were generated by co-transfection of Sf9 insect cells with linearized baculovirus DNA (BD Baculogold) along with their corresponding purified transfer vectors. Cellfectin (Invitrogen Life Technologies, Carlsbad, CA) was used as the transfection reagent and recombinant baculovirus stock was harvested 96 hours post transfection. This was further amplified by using routine procedures previously described elsewhere [165, 359]. For *in vitro* analysis, we also generated baculovirus carrying MGFP reporter gene (Bac_{MGFP}), using procedure mentioned in previous studies [359]. Bac_{null} represents baculovirus with deleted MGFP gene.

9.3.3 Generation of Tat-DNA NPs followed by hybridization of Bac-NP complex

phMGFP vector carrying the Monster Green Fluorescent Protein (MGFP), purchased from Promega (Madison,WI, USA), was used here as a reporter plasmid. The plasmid carrying cDNA for Ang 1 expression was obtained from Origene (Rockville, MD). The plasmids were amplified by transformation into the high efficiency DH5 a competent E. coli (Invitrogen) by heat shock method. The plasmids were then extracted and purified with QIAprep spin miniprep kit (Qiagen Sciences, MD). The highly pure cystein modified, histidine rich Tat peptide (C-5H-Tat-5H-C) was prepared using a conventional solid-phase peptide synthetic method using PTI Symphony peptide synthesizer (Tucson, AZ). The different batches of peptides had indistinguishable transfection properties. The peptide/DNA complexes were prepared using standard method mentioned elsewhere [365]. Briefly, the endosomolytic Tat peptide solution (1 mM) was added dropwise into a 5% glucose solution at pH 7.0 containing plasmid DNA by vortexing with an N/P ratio of 1, 3 and 6. This was followed by air-bubbling for 2h to form the Tat/DNA nanoparticles (NP). NP_{null} represents NP prepared from plasmid with deleted MGFP gene.

In order to form the Bac-NP hybrid complex, desired plaque forming units (pfu) of baculovirus was ultracentrifuged down at 24,000rpm for 30min and resuspended in Phosphate Buffered Saline (PBS). This was added to the NP

suspension with gentle vortexing and incubated for 30 min at room temperature. The mixture was further centrifuged at 20,000rpm for 10min and the pellet, containing the heavier hybrid Bac-NP product, was collected leaving the unreacted NPs and Bac in the supernatant. For every experiment, the hybrid system suspended in PBS was freshly used.

9.3.4 Characterization of Bac-NP hybrid complex using particle sizer, zeta potential and TEM

The particle size and zeta potential of the NP, Bac and Bac-NP hybrid particles were measured by the technique of electrophoretic laser Doppler anemometry using a Zeta Potential Analyzer (Brookhaven Instruments Corporation**,** HotsVille, New York, USA). ZetaPlus Particle Sizer Software Version 4.11 was used to determine the size distribution of the particles and Zeta Potential Analyzer Version 3.57 software was used for the zeta potential analysis. Both the particle size and the zeta potential were measured for three independent preparations and each measurement was obtained after taking the average of the three runs. Transmission Electron Microscopy (TEM) was used to obtain the size characterization. The nanoparticles were suspended in 1X PBS and analyzed on CM200 FEG-TEM (Philips, Markham, Ontario, Canada). As negative control, Bac was pre-coated with PEI (MW 25kDa) to give it a positive charge before mixing with the NP [304].

9.3.5 Transduction of cardiomyocytes

In order to achieve maximum transduction, three important parameters MOI [Multiplicity of Infection defined as pfu per cell] and N/P ratio of Tat/DNA nanocomplex and their combinatorial effects on the hybrid Bac-NP system were optimized. For this, MOI ranging from 150 to 500 and N/P ratio (the ratios of moles of the amine groups of cationic Tat to those of the phosphate ones of DNA) of 1, 3 and 6 were used. Initially, the h9c2 cells were seeded in 6-well plates at $0.5x10^6$ cells/well and incubated overnight at 5% CO_2 and 37^oC. Following this, an appropriate volume of transduction solutions from different experimental groups (Bac_{MGFP}, NP $_{MGFP}$, Bac_{null}-NP_{MGFP}, Bac_{MGFP}-NP_{MGFP}, Bac_{MGFP}-NP_{null}),

suspended in PBS, was added to each well according to varied MOI and N/P ratio, and incubated for 4h at 25^{o}C. The wells were replenished with fresh media and grown 37^{o}C in CO_2 incubator. The relative fluorescence units of each well were measured 24 h post-transduction (hpt) using a plate reader Victor3 Multi Label Plate Counter (Perkin Elmer, USA) as described elsewhere [359]. The experiment was done in triplicates, and the mean was calculated. Representative pictures of the wells were taken using fluorescence microscope (Nikon Eclipse TE2000-U). For experiments, where Ang-1 transgenes were used, conditioned media (CM) was collected at regular intervals for 15 days and stored at -80^{o}C for Ang1 ELISA (R&D Systems) analysis following manufacturer's protocol. For biological assays of released hAng1, CM released after 48h from transduced h9c2 cells was used.

9.3.6 Cell proliferation and cytotoxicity assays

For the cell proliferation assay, 2x10^4 HUVEC cells/well were seeded in triplicate for each sample in 96-well plates. After 8hrs of culturing, the cells were washed twice with PBS and 200µl of conditioned media from h9c2 cells transduced with NP_{Ang1}, Bac_{Ang1}, Bac-NP_{Ang1}, transduced with and without anti-hAng1 antibody supplementation was added to the corresponding set of wells. As control, conditioned media from non-transduced cells was used. After 96hrs, absorbance was measured at 490nm using Cell Titer 96 Aqueous Non-Radioactive Cell Proliferation Assay (Promega) in a plate reader [280]. The same assay was used to detect the cytotoxicity of NP, Bac and Bac-NP particles towards cardiomyocytes [293]. To perform the cytotoxicity assays, NP, Bac and Bac-NP particles were resuspended in complete culture media and incubated for 12 h with h9c2 cells seeded in 96-well plates. This was followed by the cell proliferation assay to quantify the percentage cell viabilities of different experimental groups taking untransduced cells as the control. All the experiments were performed in triplicates.

9.3.7 Cell Migration assay

Ang1 has chemotactic effects on endothelial cells. To assess the biologic effect of released Ang-1 on endothelial cells, chemotaxis cell migration assay (Millipore, MA, USA) was performed using Boyden's modified chambers consisting of 96-well migration chamber and a feeder tray [369]. Each migration chamber contains a microporous polycarbonate membrane with pore size of 8.0µm that just allows the HUVEC to pass through. Both sides of the membrane are uncoated. $5x10^4$ HUVEC are seeded on the top of the insert. In the lower feeder tray, the conditioned media from different experimental groups were added with or without antibodies against Ang-1 (Anti-Ang1). The plate was incubated for 24 h at 37°C. After incubation, the filter was removed, and the upper side of the filter containing the non-migrated cells was wiped and rinsed. Migrated cells that crossed the pore of the membrane into the feeder chamber were detached, and quantified according to manufacturer's protocol.

9.3.8 Wound Healing Assay

In order to check the wound healing potential of released Ang1, HUVEC were seeded into 24-well plates and grown to confluency. After 24 h of serum starvation (1% FBS), lesions were made in the monolayer using cell scraper [369]. Cells were rinsed with PBS, and then incubated with the h9c2 CM from different experimental groups (NP_{Ang1}, Bac_{Ang1} and Bac-NP_{Ang1}) for 24h. CM from untransduced cardiomyocytes was taken as control. To confirm the beneficial effect of Ang-1 in particular, another experimental group was taken, where the CM from Bac-NP_{Ang1} group was pre-incubated with anti-Ang1 neutralizing antibody (R&D Systems; 1 µg/ml) for 30 min, before adding to the wells. Cells were fixed with 4% paraformaldehyde (Sigma-Aldrich, St Louis) after 24h and the number of cells which had moved across the starting scratched lines were measured for all groups. Three fields were analyzed for each well at 200X magnification.

9.3.9 In vivo experiments on myocardially infarcted rat model

Immunocompetent female Lewis rats (200 to 250 gm, Charles River, QC) were used in an *in vivo* myocardial infarction model according to established protocols [258, 370]. All procedures were in compliance with the Guide for the Care and Use of Laboratory Animals (NIH publication No. 85-23) and the Guide to the Care and Use of Experimental Animals of the Canadian Council on Animal Care. Lewis rats were anesthetized using 5% isoflurane in an induction chamber followed by intubation with an 18-gauge catheter and mechanical ventilation (Harvard Ventilator, PQ, Canada) at 80 breaths/min. Anesthesia was maintained with 3% isoflurane. A left thoracotomy was performed through the fourth intercostal space to expose the left ventricle. The left coronary artery was ligated 2 mm from its origin with a 7-0 polypropylene suture (Ethicon, Inc, Somerville, NJ). The ischemic myocardial segment rapidly became identifiable through its pallor. Fifteen minutes after ligation of the artery, the rats were subjected to myocardial injections. In all the experimental groups 300µl of the PBS was used as the delivery vehicle. 3 equal left ventricular direct intramyocardial injections, 100 µl each, were injected at the peri-infarct regions using 27 gauge needle. The NP_{Ang1} group (n=12) received 300 µl of Tat/DNA nanocomplex (N/P ratio 3) suspension containing 10µg hAng1 plasmid. Bac_{Ang1} group (n=12) received $1x10^{10}$ pfu of Bac-Ang1 suspended in 300 µl of PBS. Bac-NP_{Ang1} group (n=12) received the hybrid of $1x10^{10}$ pfu of Bac-Ang1 and Tat/DNA nanocomplex carrying 10µg hAng1 plasmid. As control, Ctrl group received 300 µl of PBS only. 3 days post injection, 4 animals from each group were sacrificed, and heart samples (peri-infarct and non-infarct region) were minced in tissue homogenizer in presence of homogenization buffer (RIPA lysis buffer). Thereafter the homogenized substance was centrifuged for 10 min at 14,000 ×g rpm at 4°C. The supernatants were collected and analyzed by ELISA for hAng1 according to the manufacturer's instructions (Quantikine, R&D system, Minneapolis, MN).

To further confirm the *in vivo* transduction efficiency of the hybrid gene delivery system, another separate set of experiments were performed. For this, LacZ was used as the reporter transgene for the groups NP_{LacZ}, Bac_{LacZ} and Bac-

NP_{LacZ} (n=3 for each group). *In vivo* LacZ expression at the injection sites was detected using X-gal by sacrificing the animals 3 days post administration as previously described [258].

9.3.10 Histological analysis for scar area detection

21 days post-operation, rats were deeply anesthetized and sacrificed by rapid excision of the heart. The excised hearts were immediately soaked in cold saline to remove excess blood from the ventricles and fixed in neutral-buffered 4% formalin. Paraffin embedded samples were sectioned at 5µm, and Masson's trichrome staining (*DBS,* Pleasanton, CA) was performed to delineate scar tissue (blue color) from the total area of myocardium [353]. Masson's trichrome-stained sections were captured as digital images and analyzed by ImageJ-1.41 software. Infarct area, epicardial and endocardial length of infarction and ventricular and septal wall thickness were calculated and expressed as a percentage.

9.3.11 Immunohistochemistry for detecting neovascularization

Neovascularization was evaluated by analyzing the capillary and arteriole density in the peri-infarct area. For this, immunohistochemical staining was performed with antibodies against PECAM (Santa Cruz) for identification of endothelial cells and smooth muscle α-actin (Santa Cruz) for tracing the smooth muscle cells as described elsewhere [353]. Briefly, for measurement of capillary density, five fields in the peri-infarct area were imaged with 200x magnification and average numbers of capillaries with less than 10µm diameter were counted. The capillary density was quantified as the (mean total CD31-positive microvessels)/mm^2 using three tissue sections spanning per-infarct tissue region of each animal. Similarly, arteriole densities were quantified as the (mean total smooth muscle α-actin-positive microvessels)/mm^2.

9.3.12 Echocardiogram analysis

Transthoracic echocardiography was performed in all the rat groups NP_{Ang1} (n=8), Bac_{Ang1} (n=8), Bac-NP_{Ang1} (n=8), and untreated control Crl (n=8) on day 3, day14 and day 21 post infarction. Echocardiograms were obtained with a commercially available system (SonoSite, Titan- Washington, Seattle, WA) equipped with a 15-MHz transducer, as mentioned in earlier studies [258, 370].

9.13 Statistical Analysis

Data are presented as mean ± Standard Deviation (SD) from independent experiments as described in the figure legends. Statistics were performed using two-way and/or one-way ANOVA by Bonferroni's multiple comparison post-hoc test. All statistical analyses were performed with Prism 5 (GraphPad Software).

9.4 Results

9.4.1 Characterization of hybrid Bac-NP complex

The Bac-NP complex was first characterized by measuring the zeta potential of the nanocomplex with laser Doppler electrophoresis (**Figure 9.2A**). At physiological pH 7.4, the free baculoviruses were negatively charged with a zeta potential of -12mv±3.2. On the other hand, prepared Tat/DNA nanoparticles showed highly positive charges, based on the N/P ratios 1 (21±2.2mv), 3 (28±3.4mv) and 6 (31±4.2mv). The positively charged Tat/DNA nanoparticles, upon conjugation with the negatively charged baculoviruses, formed slightly positively charged (~4.2mv) Bac-NP hybrid nanocomplexes with the different N/P ratios.

To reconfirm the successful formation of the Bac-NP complexes, particle sizes of each complex were measured. Free baculoviruses showed an average size of 228±19.5nm, whereas free Tat/DNA NP showed an average size of around 70nm, which varied slightly based on N/P ratio (**Figure 9.2B**). The Bac-NP hybrid complexes showed an average size of 382±27.5nm (N/P=1), 489±28.7nm (N/P=3) and 492±25.1nm (N/P=6). This significant increase in size of the Bac-NP

particles, compared to that of free baculoviruses and nanoparticles, indicates the efficient production of the nanobiohybrid complexes, generated by strong electrostatic interactions of the baculoviruses with the nanoparticles.

In order to look for the morphological evidences for successful conjugation of the budded baculovirus particles with the nanoparticles, TEM was used. Electron micrographs showed the well dispersed NP (**Figure 9.2C**). On coming in contact with Bac (the rod-shaped particles with a length of 200–250 nm), there was an instant virus-nanoparticle complex formation by the negatively charged baculoviruses with the positively charged NP, as indicated in **Figure 9.2D**. **Figure 9.2E** confirms that this nanocomplex is stable for at least 8h, which suggests that the transduction time can be enhanced to at least 8h, if required. The images of Bac-NP complexes also confirm the proper retention of the typical rod-shaped morphological appearance and envelope structure of the baculovirus, suggesting that the baculoviruses were able to sustain their morphological integrity even after hybridization with the NP. The negative control in **Figure 9.2F** shows that PEI pre-coated positively charged Bac does not hybridize with similar charged NP. This confirms that it is primarily because of the electrostatic interaction that the two oppositely charged components hybridize.

9.4.2 Optimization of *in vitro* transduction conditions

To optimize the transduction protocol of the Bac-NP hybrid system with cardiomyocyte cells, MGFP expression of transduced h9c2 cells was measured using different transduction conditions such as MOI and N/P ratio of the Tat/DNA nanoparticles. The transduction efficiency of Bac-NP was first evaluated in relation to the N/P ratio (**Figure 9.3A**) with a constant MOI of 200. N/P ratio of 3 demonstrated markedly increased GFP expressions in most groups with Bac-NP_{MGFP} revealing significantly higher normalized GFP expression compared to all the other groups (NP_{MGFP}, Bac_{MFP}-NP_{null}, Bac_{null}-NP_{MGFP}) irrespective of the N/P ratios. The significantly higher transduction ability of Bac-NP_{MGFP} compared to Bac_{MFP}-NP_{null} suggests that NP_{MGFP} component of the Bac-NP_{MGFP} hybrid complex largely supplemented the baculoviruses for the enhanced transduction,

which was not noticed in Bac_{MFP}-NP_{null}. The data also demonstrated that, keeping N/P ratio constant, Bac_{null}-NP_{MGFP} can transduce h9c2 cells much more efficiently than NP_{MGFP} alone. This explains why baculoviruses, upon conjugation to the NP, enhance the transduction potential of the free NP.

To investigate the effect of baculovirus MOI on transduction efficiency of Bac-NP hybrid system, GFP expression was measured with various MOI (150, 300, and 600) at a constant N/P ratio of 3 as shown in **Figure 9.3B**. The transduction efficiency was MOI-dependent in every group tested, indicating that the virus remained functional even after formation of the nanohybrid system which contains non-viral components. The transduction efficiency achieved with MOI of 300 was significantly higher compared to other MOIs, with Bac-NP_{MGFP} group showing the highest efficiency. In addition, Bac_{MGFP}-NP_{null} showed higher gene delivery efficiency than free Bac_{MGFP} indicating the positively charged Tat containing nanoparticles contribute significantly to the enhanced baculovirus mediated transduction. Bac_{MGFP}-NP_{null} also showed higher transduction compared to Bac_{null}-NP_{MGFP} in both **Figure 9.3A** and **9.3B** illustrating that it is baculovirus which mainly contributes to the gene delivery and NP component mainly helps in enhancing the transduction level complimented with non-viral delivery of its transgene. Representative florescence images of transduced cells in **Figure 9.3C** reconfirm the above findings where Bac-NP_{MGFP} hybrid system showed maximum GFP expression in h9c2 cells, followed by free Bac_{MGFP} and free NP_{MGFP}. None of the experimental groups showed any significant level of cytotoxicity (around 100% viability) when incubated with the cells for 12h as shown in **Figure 9.4.**

9.4.3 Induction of hAng1 expression *in vitro*

To verify the ability of Bac-NP_{Ang1} to express the transgene, hAng1, and to confirm the recognition of the protein by ELISA analysis, h9c2 cardiomyocytes were transduced with NP_{Ang1}, Bac_{Ang1} and Bac-NP_{Ang1} at MOI 300 with N/P ratio 3 using the optimized transduction protocol. The data (**Figure 9.5A**) was in agreement with the above findings where Bac-NP_{Ang1} showed highest Ang1

expression (34.8±3.6ng/10^6 cells) 72h post transduction compared to NP_{Ang1}(3.7±1.1ng/10^6 cells) and Bac_{Ang1}(20.45±3.25ng/10^6 cells). As shown in **Figure 9.5B**, the hAng1 release profile of Bac-NP_{Ang1} transduced cells showed a rapid expression of Ang1 transgene which reaches peak values on day 4 (36.2±3.3ng/10^6 cells), and gradually decrease with time as observed in the 15 day analysis.

9.4.4 Mitotic and chemotactic effect of hAng1 on HUVEC

The bioactivity of the released hAng-1 in media from the transduced cells was evaluated *in vitro* by observing the proliferative capacity of the HUVECs. Cell Proliferation MTS Assay kit was used to assess the proliferation capabilities of the HUVECs treated with CM from different experimental samples. The results were reported as the percent increase in cell proliferation relative to the unstimulated control (taken as 100%). As shown in **Figure 9.6A**, the least cell proliferation occurs with CM from group NP_{Ang1} (104.5±3.22%), moderate proliferation from Bac_{Ang1} (131.6±4.12%), and finally the highest proliferation is observed with CM from Bac-NP_{Ang1} group (144.0±5.4%). As expected, CM from groups treated with antibodies against hAng1 showed no proliferative effects proving that it was because of the active natural bioactivities of released hAng1 that the contributed to the significant HUVEC proliferations. This proliferation rate was directly dependant on the amount of the Ang-1 released. This result illustrates why Bac-NP_{Ang1} hybrid gene delivery system is superior to other gene delivery systems.

Having shown that secreted hAng1 promotes significant mitotic effects on endothelial cells, we tested the ability of Ang1 to trigger HUVEC motility using two different techniques: Boyden chamber assay and wound healing assay. We used Boyden's chamber in which chemoattraction or chemokinesis was assayed by inducing cell migration through CM stimulant. In Boyden's chamber, CM from different treatment groups was added to the lower chamber, whereas the cells were placed on the upper chamber. As a negative control, we used CM from non-transduced cells and the results were presented as the percent cell migrated

relative to the unstimulated control (taken as 100%). When CM from NP_{Ang1} was present in the lower chamber, there was no indication of chemokinesis compared to control (**Figure 9.6B**). Negligible migratory effect was detected in CM from Bac_{Ang1} (106.6±1.12%). However, CM from Bac-NP_{Ang1} group showed significantly higher migration (122.5±5.24%) compared to all the remaining groups. When CM was supplemented with anti-Ang1, HUVEC migrations in all groups were significantly limited. Furthermore, we tested the ability of CM (containing secreted hAng1) to increase HUVEC wound healing in a monolayer. As depicted in **Figure 9.7**, stimulation of wounded HUVEC monolayer with CM from Bac_{Ang1} (27.3±2.1%) and Bac-NP_{Ang1} (58.5±4.5%) induced a significant reduction of wound compared with the unstimulated control (4.4±1.9%), although CM from NP_{Ang1} (8.6±4.2%) did not show any significant scratch recovery. Thus, consistent to the mitotic and chemotactic assay results, Bac-NP_{Ang1} showed highest healing potential indicating that efficient overexpression of Ang-1 is one of the determining factors for inducing substantial biological effects. Pre-incubation of CM with the neutralizing anti-Ang1 antibodies completely inhibited Bac-NP_{Ang1} CM induced wound healing, clearly suggesting that chemotactic signals from hAng1 are essential for this effect.

9.4.5 Myocardial delivery of transgene to *in vivo* model

After confirming efficient *in vitro* transgene delivery and high expression of biologically active proteins by Bac-NP, we evaluated Bac-NP gene expression in infarcted heart. To achieve highly selective transduction of myocardial tissue, Bac-NP vector expressing the β-galactosidase (LacZ) gene, Bac-NP_{LacZ}, were administered via direct intramyocardial injections at the peri-infarct region post infarction and evaluated for gene expression after 3 days. LacZ expression was observed in cardiac muscle around the injected areas in peri-infarct region. As shown in **Figure 9.8A-9.8C**, LacZ expression in NP_{LacZ} was much lower than that in Bac_{LacZ}, while the gene expression was higher in Bac-NP_{LacZ}. An overall analysis of X-gal-stained heart revealed that the gene expression was limited to the viable cardiac muscles surrounding the areas of infarct; while expression was not detected in the remote areas, such as right ventricle and septum.

To confirm and quantify the hAng1 expression *in vivo*, 3 days post transduction the myocardial expression in the peri-infarct area (injection site) and non-infarct area were analyzed. For this, we extracted cardiac proteins and confirmed hAng1 expression by hAng1 ELISA. As shown in **Figure 9.8D**, the Bac-NP_{Ang1} group was able to express significantly higher protein (25.4±5.6 ng/mg protein) compared to Bac_{Ang1} (15.4±4.3ng/mg protein) and NP_{Ang1} (4.5±1.3ng/mg protein) in the peri-infarct region. On the other hand, non-infarct region showed negligible amount of Ang1 expression in all groups. This reconfirmed our earlier findings that the Bac-NP mediated gene delivery occurs locally, mainly specific to the injected sites, and had minimal influence on other parts of the organ.

9.4.6 Attenuation of myocardial scar area

A total of 24 rats were analyzed for the determination of infarct size (no treatment Ctrl, 8; NP_{Ang1}, 8; Bac_{Ang1}, 8; Bac-NP_{Ang1}, 8). The infarct size and wall thickness in the left ventricles at the section of the middle point between ligation and apex were measured. Macroscopic views of Masson's Trichome stained heart sections are shown in **Figure 9.9**. In both the control and the treated groups, positively stained fibrous infarct areas were clearly observed in the heart 21 days post myocardial infarction. Thin infarcts and left ventricular wall with dilated left ventricular cavity were observed in the untreated control heart. Whereas, heart tissue sections in the treatment groups had significantly ($p<0.01$) lesser infarct areas and higher left ventricular wall thickness than the control hearts (Table 1). Moreover, Bac-NP_{Ang1} group showed significantly lower infarct area (19.27 ±1.31% for Bac-NP_{Ang1} vs 23.38±2.21% for Bac_{Ang1}, $p<0.05$) and thicker left ventricular wall (1.82 ±0.06 mm for Bac-NP_{Ang1} vs. 1.67±0.13 mm for control, $p<0.05$).

9.4.7 Induction of myocardial angiogenesis and arteriogenesis

In this section, we tried to comprehend whether it was the angiogenic effect of overexpressed hAng1 that was responsible for the scar area reduction in

treatment groups. We assessed the neovasculature formation in the peri-infarct area by detecting the capillary (**Figure 9.10: A-D**) and artery densities (**Figure 9.10: E-H**). As shown in **Figure 9.10 (I),** we noticed a significant improvement in angiogenesis in the Bac_{Ang1} and Bac-NP_{Ang1} groups compared to the control (151 ± 9.59/mm^2 for Bac-NP_{Ang1}, 125.87 ± 21.39/mm^2 for Bac_{Ang1} vs. 52.37±6.54/mm^2 for control, $p<0.001$). Moreover, Bac-NP_{Ang1} group also showed significantly higher capillary density compared to Bac_{Ang1}. Similar results were obtained with arteriole density in Bac-NP_{Ang1} group (12.12 ± 2.47/mm^2 for Bac-NP_{Ang1}, 10.5 ± 1.92/mm^2 for Bac_{Ang1} vs. 4.87±1.72/mm^2 for control, $p<0.001$) as presented in **Figure 9.10(J).** Unlike capillary density, Bac-NP_{Ang1} group showed no significant enhancement in arteriole density compared to Bac_{Ang1}. Also, NP_{Ang1} alone did not show any significant effect on capillary and arteriole density in infarcted heart compared to untreated control.

9.4.8 Bac-NP_{Ang1} treatment showed significant cardiac functional improvement

To investigate if the reduction of scar area after Bac-NP mediated gene therapy results in improved heart function, the % EF in a rat model of myocardial infarction at different time periods (day 3, 14 and 28) was monitored. EF of the all the groups was around 30% on day 3 post infarction, indicating successful acute myocardial infarction in all groups [258] . As presented in **Figure 9.11,** there were significant improvements in EF% in groups treated with Bac-NP_{Ang1} ($p<0.001$) and Bac_{Ang1} ($p<0.05$) compared to the control group on day 14 and day 28, although there were no significant differences between the groups on day 3 post infarction. In addition, the Bac-NP_{Ang1} treated group showed a significantly greater increase in %EF as compared to Bac_{Ang1} treated groups on day 14 (42.23±6.45% vs 37.46±5.2% vs $p<0.05$) and day 28 (44.2±4.77% vs 37.46±5.2% vs $p<0.01$). Thus, the analysis using echocardiographic %EF data suggests that Bac-NP_{Ang1} can be a better alternative to Bac_{Ang1} to improve cardiac function after acute myocardial damage. Moreover, similar to our previous results, NP_{Ang1} alone did not show any significant effect on heart functionality over the study period.

9.5 Discussion

In the present study, we report the application of a vascular gene carrying baculovirus for myocardial infarction. For this, we developed a recombinant baculovirus carrying Ang-1 and investigated its potential on transducing cardiomyocytes and eventually inducing efficient therapeutic angiogenesis. We further explored its potential to enhance gene transfer efficiency using a hybrid model of Tat/DNA_{Ang1} nanoparticles conjugated to the baculovirus. **Figure 9.2** confirms the successful formation of hybrid nanocomplex using particle sizer, zeta potential and TEM images. Our data revealed that gene transfer efficiency can be significantly enhanced by this new hybrid formulation, where a greater amount of transgene is carried into the cells by the combined effort of Bac and NP (**Figure 9.3**) with no change in cytotoxicity level (Figure 4). *In vitro* analysis showed that Bac-NP transduced cells can express their transgene for at least two weeks (Figure 5) which is even more than other experimental results [293, 371]. This temporal expression of the delivery system is beneficial in many cases, particularly for angiogenesis where the expression ceases once its therapeutic job is done. Following this, we demonstrated the functional (mitotic and chemotatic) activities of the released Ang-1 using HUVEC proliferation, migration and wound healing assays (**Figure 9.6 and 9.7**). Before performing the *in vivo* therapeutic experiments, we compared and confirmed the superior expression potential of the Bac-NP delivery systems using LacZ reporter expression and later by detecting Ang1 expression level at the peri-infarct (site of delivery) and non-infarct sites (**Figure 9.8**). The data illustrates that the gene expression was mostly limited to the local injected sites and was negligible at other regions of the heart.

Despite the recent advances with the different types of gene delivery systems, gene therapy for the treatment of myocardial ischemia and myocardial infarction still constitutes a rather new approach in cardiovascular medicine [350]. However, the immense potential of this approach has already been realized from the available data in the literature. Thus, the idea of treating the non-functional cardiac tissues post myocardial infarction by inducing local angiogenesis in the infarct region was put forward using both viral and non-viral delivery systems.

For non-viral transfection, various compounds have been developed to form complexes with DNA. In a recent study, Ye and co-workers demonstrated that nanoparticle based delivery of hypoxia-regulated VEGF transgene using transfected skeletal myoblasts during AMI in rabbits effectively preserved LV regional blood flow and contractile function of the heart [372]. Interestingly, a combination of erythropoietin (Epo) enhancer and water-soluble lipopolymer (WSLP) was used in one study for myocardial hypoxia-inducible VEGF gene therapy [347] which showed promising results for potential ischemic heart disease treatments. Using a completely new approach, Affleck *et al* developed a gene delivery system by injecting plasmid DNA complexed with stearyl-poly (L-lysine)-low density lipoprotein (TerplexDNA) into the rabbits hearts which showed improved myocardial transfection compared to a naked plasmid DNA system alone [373].

There is an increasing awareness on importance of Ang-1 proteins for cardiovascular regenerative disease research. This is because Ang-1 supports promotion of vessel maturation of newly formed blood vessels in addition to stabilization of existing vasculature. *In vitro* studies using Ang-1 demonstrate the ability of this protein to significantly enhance endothelial cell attachment, migration, tube formation, sprouting and induce anti-apoptotic effect [374]. Researchers have been trying to study the effect of Ang-1 administration to treat ischemic heart diseases through different delivery techniques. The study by Suri *et al*. reported that the therapeutic effect of Ang-1 over expression in transgenic rat model, where larger more branched blood vessels were observed over time [375]. Further *in vivo* studies demonstrated that the application of adenovirus as a vehicle for Ang-1 gene transfer reduced infarct size, promoted arteriogenesis and angiogenesis, maintained the left ventricular wall thickness and significantly improved cardiac function [353, 376]. Through our studies using Bac-NP system we were also able to achieve such positive results which was significantly better than that of Bac or NP alone. Bac-NP mediated Ang-1 therapy clearly inhibited the progression of the impairment in cardiac performance 21 days after myocardial infarction (**Figure 9.11**). This improvement in cardiac function may

be because of the reduction in the infarct size and the increase in viable mass of cardiac muscles in the Ang-1 treated group (**Figure 9.9 and Table 9.1**). In the myocardium that received Bac-NP_{Ang1} vector, a marked increase in blood vessel density was observed, and the vascular density in the peri-infarct was higher than that in other groups (**Figure 9.10**). Sufficient blood flow as a result of this increased blood vessel formation might contribute to the prevention of cardiomyocyte loss, the maintenance of contractility in the border zone area adjacent to infarction, and the suppression of the progression of post-infarction cardiac failure associated with the left ventricular remodeling.

As a first step to explore the potential of this newly developed hybridized Tat/DNA- baculovirus system we characterized the nanocomplex, optimized the *in vitro* and *in vivo* gene delivery protocol and evaluated its therapeutic capability through pre-clinical studies in myocardially infarcted model in this study. Extensive future work needs to be done to develop strategies for making this delivery system target specific. This can be achieved using a cardiac-specific promoter sequence to prevent expression in non-specific sites. An interesting work with similar aim was carried out using cardiac myosin light chain 2v (MLC-2v) promoter and the hypoxia-response element to mediate cardiac-specific and hypoxia-inducible VEGF expression [377]. This resulted in high delivery efficacy and target specificity of VEGF expression with insignificant transgene expression in other organs. Modification of the natural tropism of the hybrid nanosystem may be another promising approach to decrease potential side effects due to extracardiac gene transfer. This can also be achieved by functionalizing the NP surface with targeting ligands or antibodies, and/or genetically manipulating the baculovirus to express cardiac targeting peptides on viral envelope that can enhance their cardiac-specific transduction abilities [350].

Recent reports suggest that combined intramyocardial delivery of Ang-1 and VEGF using Bac-NP complex can further improve the cardiac function and attenuate ventricular infarct area as reported in other studies using mammalian vectors [366, 367]. Thus, a combinatorial approach of delivering multiple genes using the two components of the hybrid complex can further enhance the

therapeutic potential of this nanodelivery system. Stem cells and genetically modified stem cells are also being studied along with different delivery systems as potential angiogenic therapeutic tool for heart diseases [280, 378]. Thus, Bac-NP gene delivery system can also be utilized for cell-based and *ex-vivo* gene therapy applications.

9.6 Conclusion

Although viral vectors are most commonly used for gene delivery, the new Bac-NP nanodelivery system will bring together the advantages of both non-viral (lack of specific immunogenecity, simplicity of use, and ease of large-scale production) and viral gene therapy (efficient transduction, easy scale-up) systems. The data reported here collectively demonstrated the unique potential of hybrid Bac-NP in gene delivery and implicated its use in treating myocardial therapy. Further studies on chemically conjugating a targeting moiety to Bac-NP nanocomplex will be able to facilitate this new gene delivery system for enhanced tissue specific targeting.

9.7 Acknowledgments

We gratefully acknowledge the assistance received from the Canadian Institutes of Health Research (MOP 64308) to S Prakash, and the Natural Sciences and Engineering Research Council of Canada (NSERC) to S Prakash, D Shum-Tim and C Elias. A Paul acknowledges the Alexander Graham Bell Post Graduate Scholarship—Doctoral from NSERC. S Abbasi acknowledges the support of the McGill Faculty of Medicine Internal Scholarship. We are grateful to Dr. Maryam Tabrizian for providing us with facilities in her laboratory at McGill University, Canada. The authors confirm that there are no known conflicts of interest associated with this publication.

Table 9.1: Effect of nanobiohybrid complex of baculovirus and Tat-plasmid nanoparticles on infarcted heart: morphometric analysis of the left ventricle after infarction. Values indicate the mean ± SD (n=8). Rats were sacrificed three weeks after myocardial infarction. All parameters were measured on the mid-line horizontal sections between ligation-point and apex of heart, and calculated according to the following formulae: % infarct size=infarct area/total LV area × 100; % endocardial infarct length= endocardial length of infarction/endocardial circumference of LV × 100; % epicardial infarct length= epicardial length of infarction/epicardial circumference of LV × 100. ANOVA statistical analysis with Bonferroni *post hoc* test was performed to determine the significance of the experiments. Ψ: significant compared to Ctrl, †: significant between Bac-NP_{Ang1} and Bac_{Ang1}.

Group	**Average Infarction area/area at risk**	**Average Left Ventricular wall thickness**	**Epicardial length of infarction/ epicardial circumference**	**Endocardial length of infarction/ endocardial circumference**
	%	mm	%	%
Ctrl	33.05±2.28	0.835±0.1	47.4±1.05	61.5±4.32
NP_{Ang1}	27.28±2.12$^{\Psi}$	1.35±0.08$^{\Psi}$	38.2±3.88$^{\Psi}$	58.1±2.02
Bac_{Ang1}	23.38±2.21$^{\Psi}$	1.67±0.13$^{\Psi}$	32.2±2.42$^{\Psi}$	44.7±4.12$^{\Psi}$
Bac-NP_{Ang1}	19.27±1.31$^{\Psi, \dagger}$	1.824±0.06$^{\Psi, \dagger}$	30.1±4.81$^{\Psi,\dagger}$	43.1±3.72$^{\Psi}$

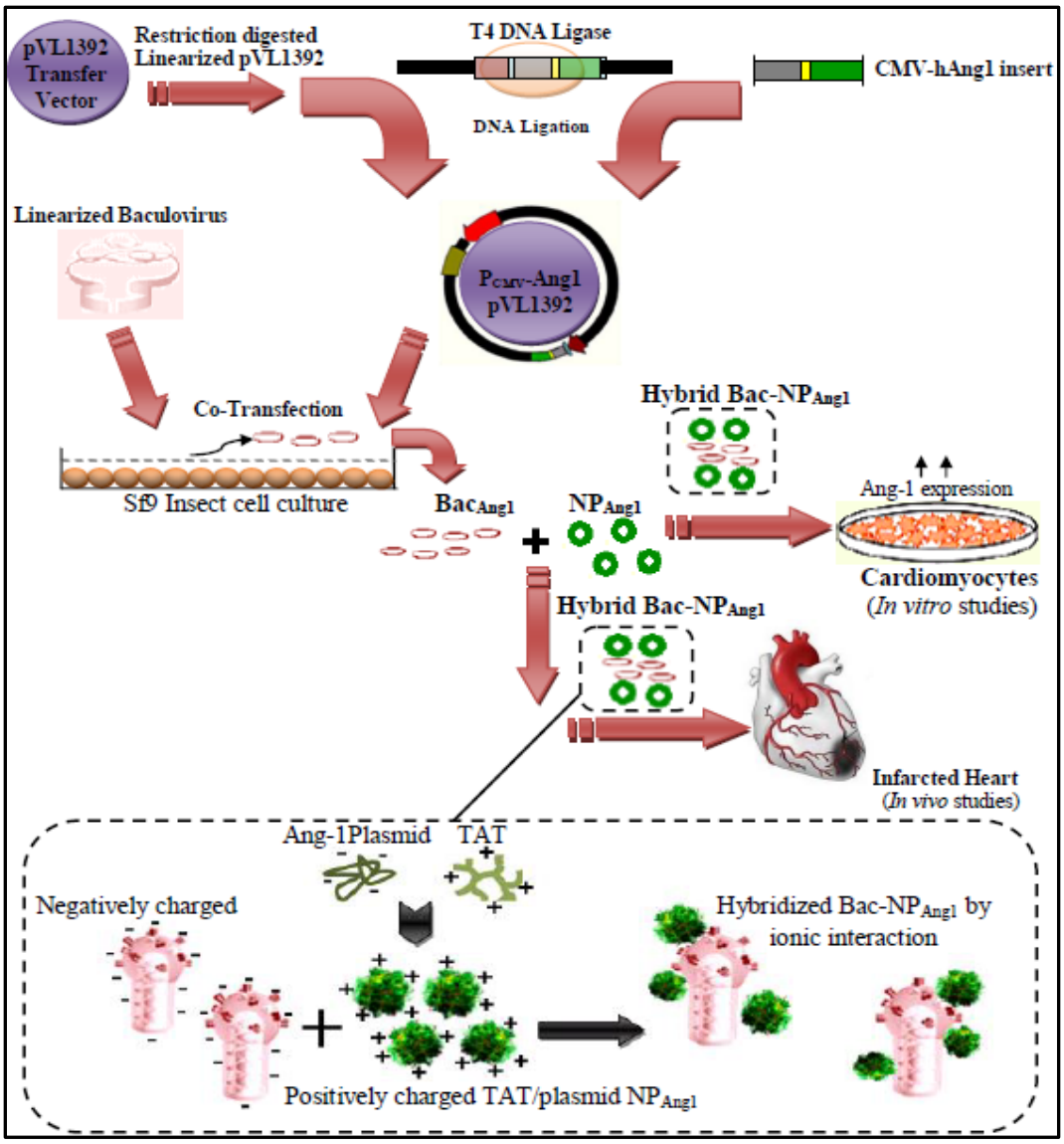

Figure 9.1: Scheme for nanobiohybrid complex preparation and subsequent intramyocardial delivery to the infarcted rat heart. Firstly, recombinant baculovirus carrying hAng1 was generated using molecular biology tools. This was followed by hybridization of the baculovirus with NP by ionic interaction, as illustrated in the dotted rectangle. The prepared nanohybrid gene delivery system was then studied *in vitro* for h9c2 cardiomyocyte transduction optimization, and *in vivo* in myocardially infarcted rat model to induce therapeutic effects through intramyocardial route of administration.

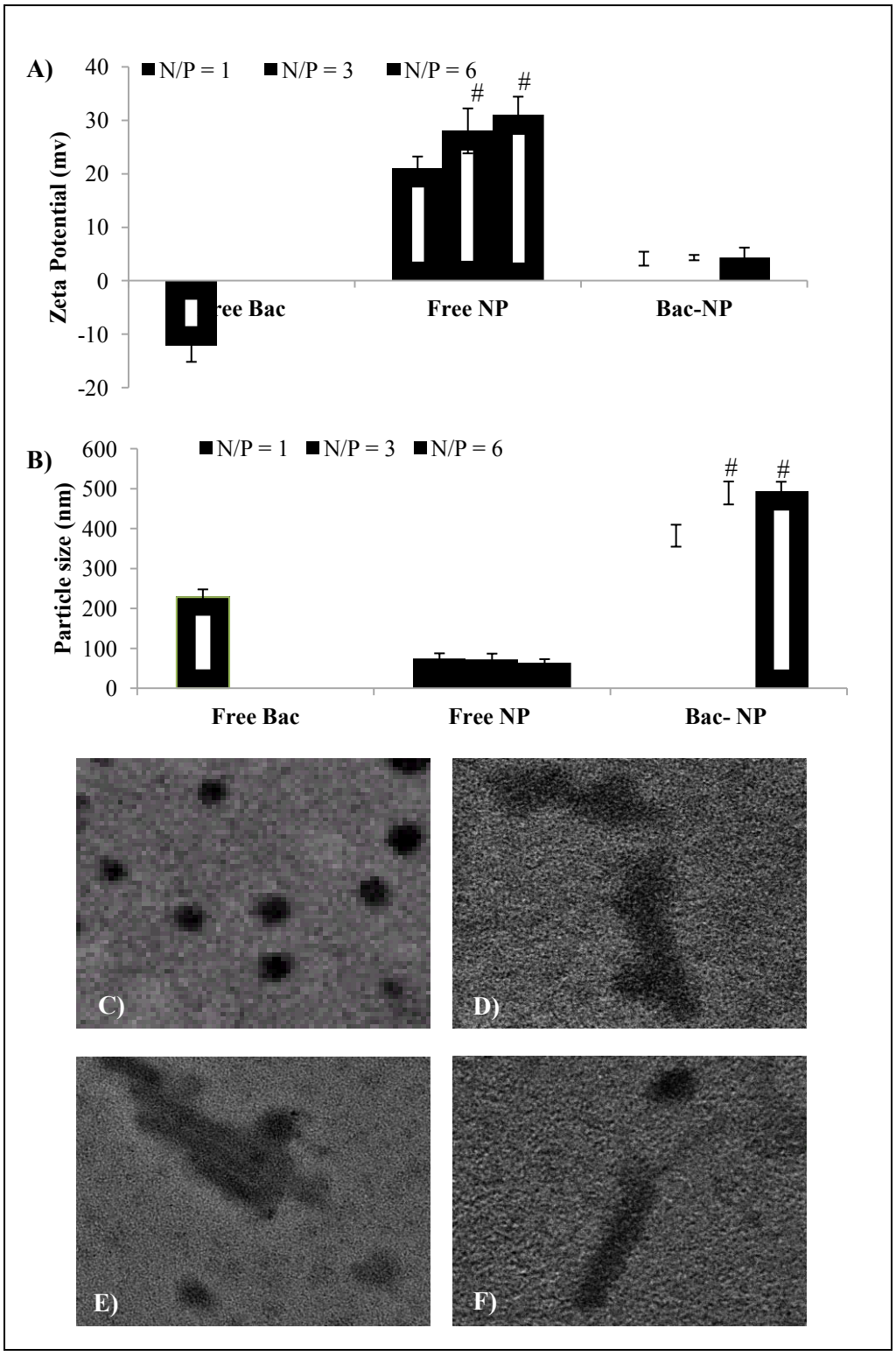

Figure 9.2: Characterization of the Bac-NP hybrid gene delivery nanocomplexes. (A): Zeta potential of free Bac, free NP and hybrid Bac-NP nanocomplexes at pH7.2 with N/P ratio 1, 3 and 6. The complexes were prepared from 1µg DNA

(complexed with TAT) per 10^9 pfu baculovirus. (B): Particle size of the above complexes at various N/P ratios. Three independent experiments were performed and the mean± Standard Deviation (SD) are represented in the graphs. ANOVA analysis: # = $P<0.05$, vs. group-matched N/P ratio 1. TEM images of NP (C) with N/P=3, Bac-NP after 1h (D), Bac-NP after 8h (E) suspended in PBS. Negative control (F) represents the non-hybridized Bac and NP, where the baculovirus particles were pre-coated with positively charged PEI before complexing with positively charged NP. The scale bar indicates 100nm.

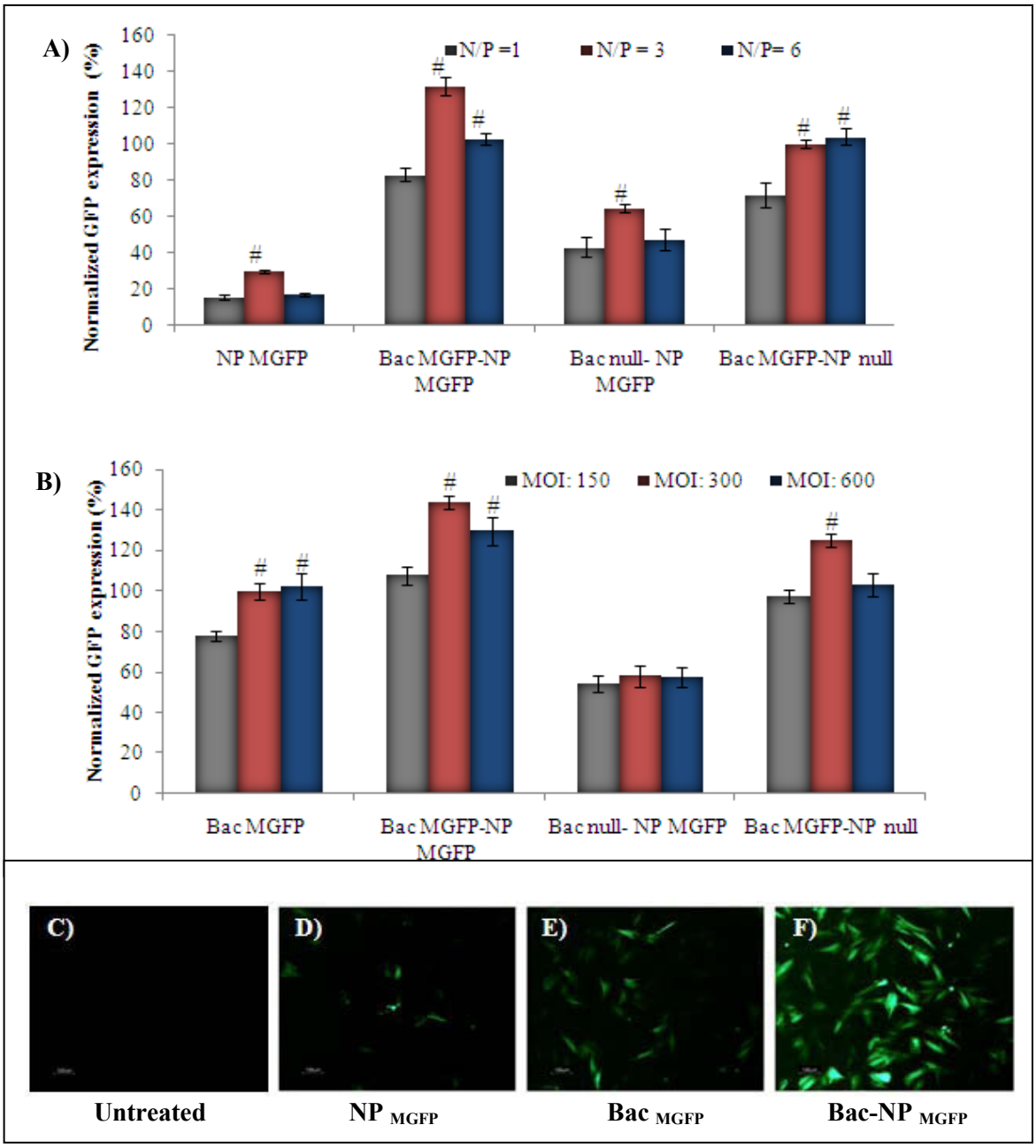

Figure 9.3: Optimization of transduction condition in h9c2 cells with Bac-NP_{MGFP}. $2x10^4$ cells were seeded in each well of 96 well plates and cultured overnight. The nanobiohybrid complexes were prepared from 1µg DNA (complexed with TAT) per 10^9 pfu baculovirus. A) Effect of N/P ratio of the nanoparticles on Bac-NP mediated cell transduction. Cells were transduced with Bac-NP, along with other groups, at constant MOI of 200 and N/P ratio of 1, 3

and 6. After 4h transduction, cells were washed with PBS and replenished with complete media. 24h post transduction, cells of each well was analyzed for MGFP expression (percentage normalized taking Bac_{MGFP}-NP_{null}, N/P=3, expression as 100%) in plate reader. B) Effect of baculovirus MOI on Bac-NP mediated cell transduction. Cells were similarly transduced with the prepared Bac-NP at constant N/P ratio of 3 with MOI of 150, 300 and 500 and analyzed for MGFP expression (percentage normalized taking Bac_{MGFP}, MOI=300, expression as 100%). Three independent experiments were performed and the mean ± SD are represented in the graphs. Representative fluorescence microscopic images (magnification 200X) of transduced cells 24h post transduction: (C) Untreated, (D) NP $_{MGFP}$ (N/P ratio 3), (E) Bac $_{MGFP}$ (MOI 300), and (F) Bac-NP $_{MGFP}$ (MOI 300, N/P ratio 3). ANOVA analysis: # = P<0.05, vs. group-matched N/P 1 (A) and MOI 150(B).

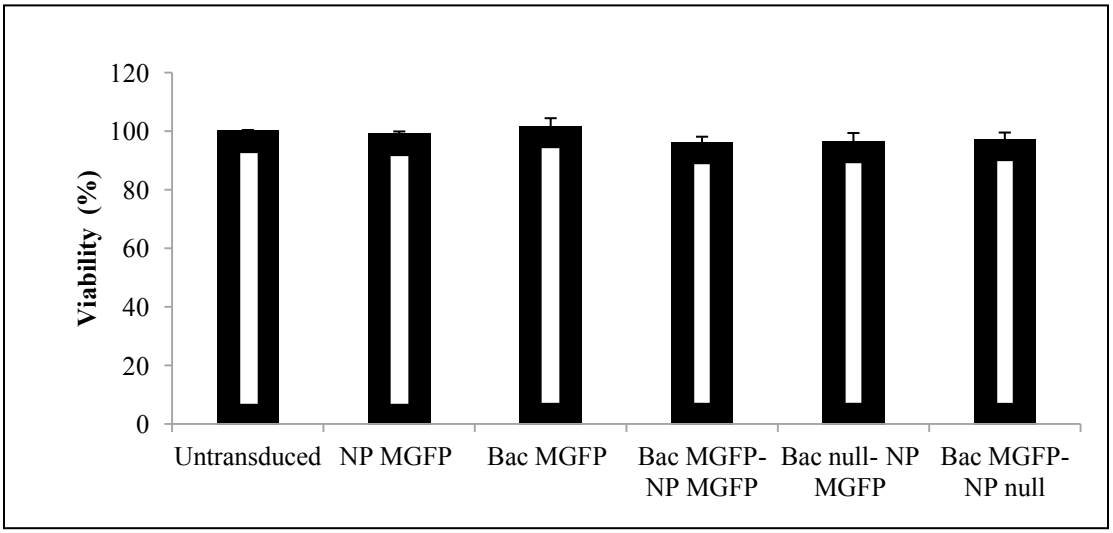

Figure 9.4: Cytotoxic effects of Bac-NP hybrid complexes on cardiomyocytes. $2x10^4$ cells were seeded in each well of 96 well plates and cultured overnight. The cells were incubated with NP (N/P ratio 3) only, Bac (MOI 300) only and Bac-NP (MOI 300 and N/P ratio 3) for 12h followed by cell toxicity analysis. Three independent experiments were performed and the mean ± SD are represented above. One way ANOVA analysis: There were no significant differences in percentage viability between the groups.

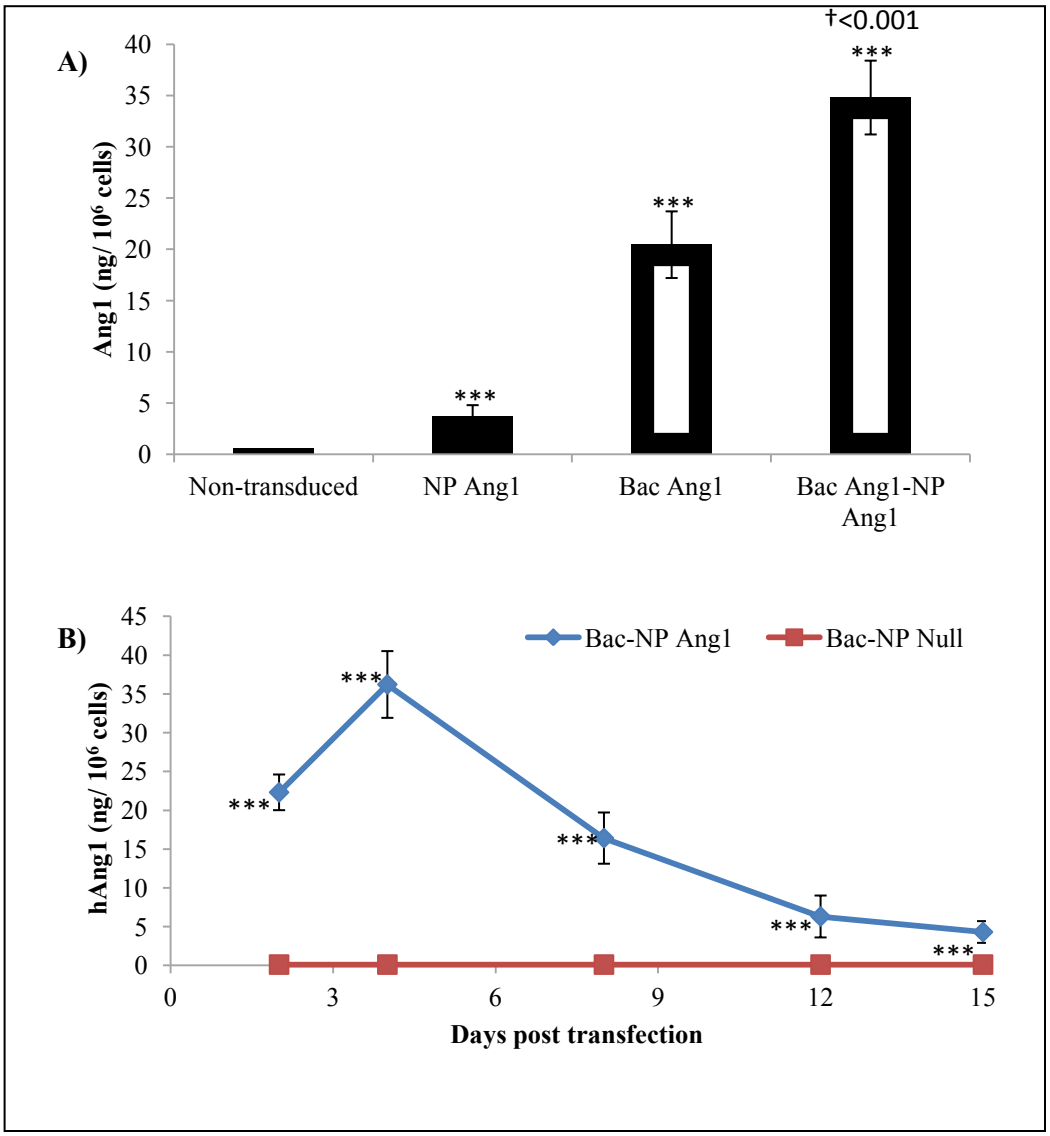

Figure 9.5: Effect of Bac-NP$_{Ang1}$gene delivery system on hAng1 protein expression in h9c2 cells. (A) Ang1 concentrations as measured by ELISA 72 h post transduction. (B) Time course release profile of hAng1 from Bac-NP Ang1 transduced h9c2 cells over 15 days. H9c2 cells (10^6cells/well) were transduced by NP $_{Ang1}$, Bac $_{Ang1}$, and Bac-NP$_{Ang1}$ using standard transduction protocol. The Ang1 expressed by the transduced cells in the conditioned media from time to time were quantified by hAng1 ELISA. The data represent the mean± SD of triplicate experiments. One way ANOVA analysis: Statistically significant differences between groups compared to unstimulated control are indicated as *** = P<0.001. P value on comparing Bac$_{Ang1}$ and Bac-NP$_{Ang1}$ are indicated by †.

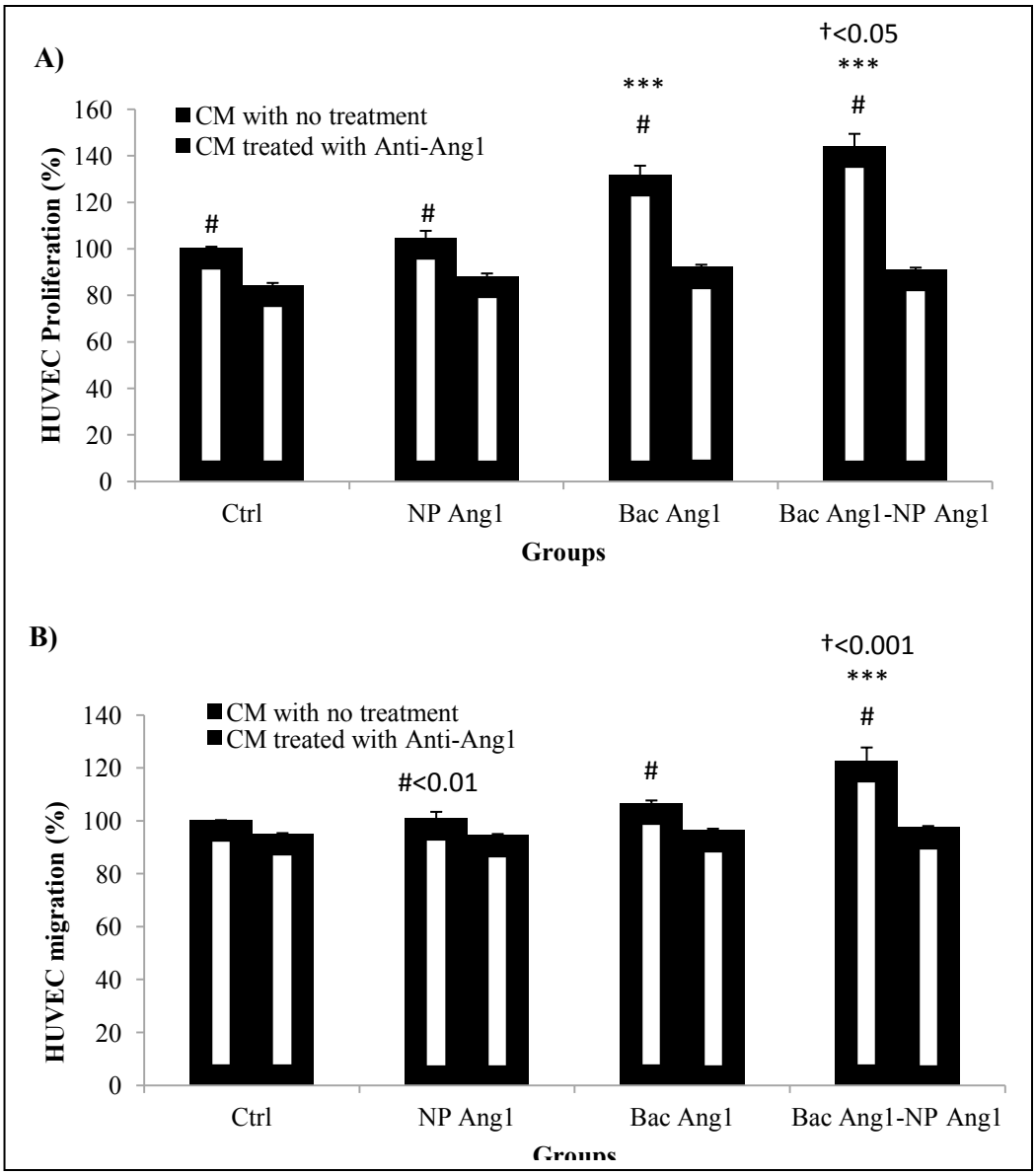

Figure 9.6: A) Proliferation of HUVECs grown in the presence of CM from NP_{Ang1}transfected h9c2, grown in the presence of CM from cells transduced with Bac_{Ang1} or with Bac-NP_{Ang1}. As control group, CM from non-transduced cells (Ctrl) was taken. To perform this experiment, $2x10^4$ cells were taken as the initial cell number per well of 96 well plate. In another set of experiments, CM from individual groups was previously treated with an excess of neutralizing ani-hAng1 antibodies (1µg/ml) before adding to the cells. Proliferation was measured by a colorimetric assay after 3 days of growth and data were normalized to control group and represent three independent experiments. B) Effect of released hAng1

on HUVEC migration was studied using Boyden's Modified Chambers. The chamber was set up as mentioned in Materials and methods. CM, with or without antibody treated, from different groups placed in the lower chamber. To perform this experiment, $5x10^4$ cells were seeded on the upper chamber in each well of 96 well plates. After 24h incubation at 37^oC, the cells that migrated from the upper chamber through the porous membrane to the lower chamber (containing stimulant CM) were quantified. Mean values ± SD from three independent experiments are shown. ANOVA analysis: Statistically significant differences between group-matched no antibody treated sample data compared with that of antibody treated sample are represented by # denoting $P<0.001$, unless otherwise stated. Statistically significant differences between groups (without antibody treatment) compared to control are indicated as *** = $P<0.001$, ** = $P<0.01$, * = $P<0.05$. P values on comparing Bac_{Ang1} and $Bac\text{-}NP_{Ang1}$ are indicated by †.

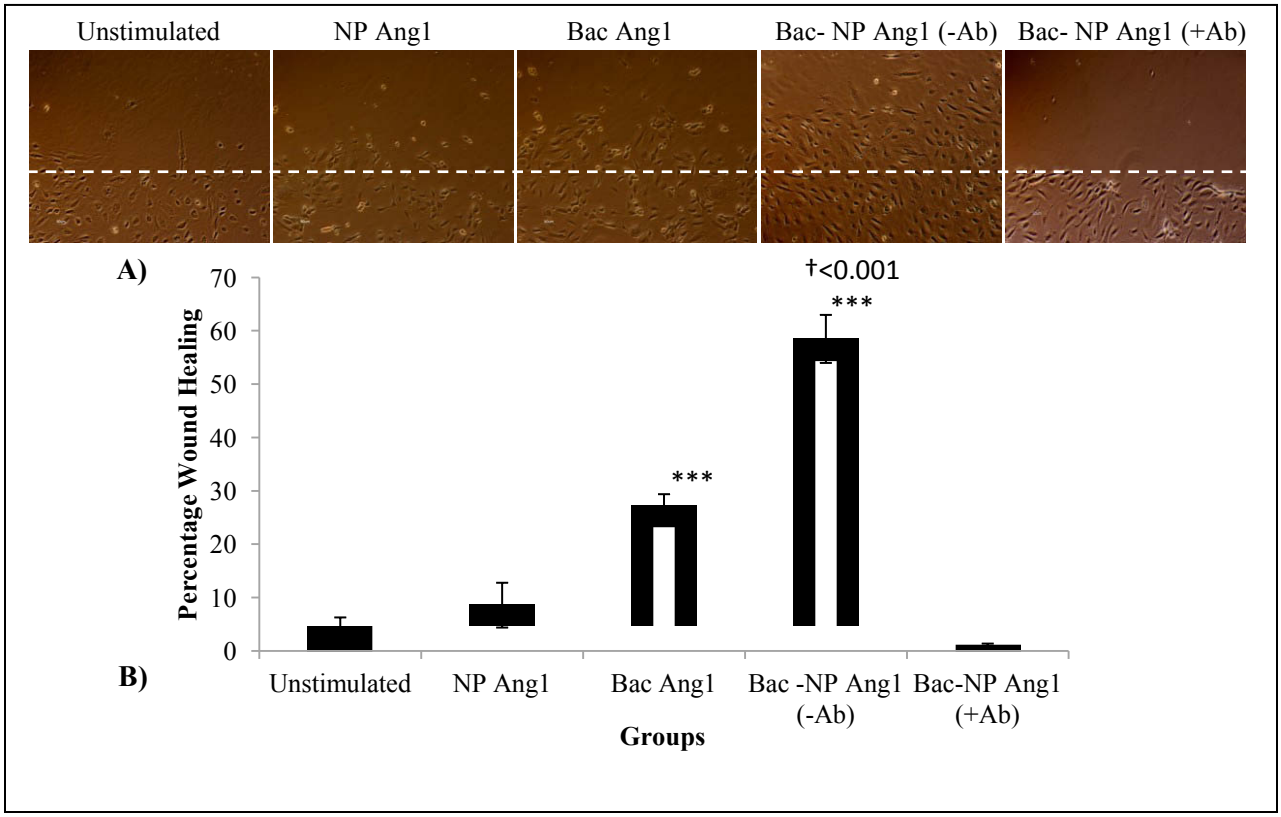

Figure 9.7: hAng1 induces migration of endothelial cells in a wound healing assay. HUVEC cell monolayer was wounded with cell scraper and treated with CM from NP_{Ang1} transfected h9c2 cells, CM from cells transduced with Bac_{Ang1} and with Bac-NP_{Ang1}. As control group, CM from non-transduced cells was used. In another set of experiments, CM from different groups were previously treated with an excess of neutralizing ani-hAng1 antibodies (Ab: 1µg/ml) before performing the wound healing assay. HUVEC were photographed (200X) after 24 h treatment (A) and percentage of scratched area (which was initially free of cells, marked by the white dotted border line) covered by the migrated cells were analyzed using Image J software (B). Mean values ± SD from three independent experiments are shown. One way ANOVA analysis: Statistically significant differences between groups compared to unstimulated control are indicated as *** = P<0.001, ** = P<0.01, * = P<0.05. P values on comparing Bac_{Ang1} and Bac-NP_{Ang1} are indicated by †. Cell migration observed with CM from Bac-NP_{Ang1} was completely inhibited with an excess (1 µg/ml) of neutralizing anti-Ang1 antibody treatment.

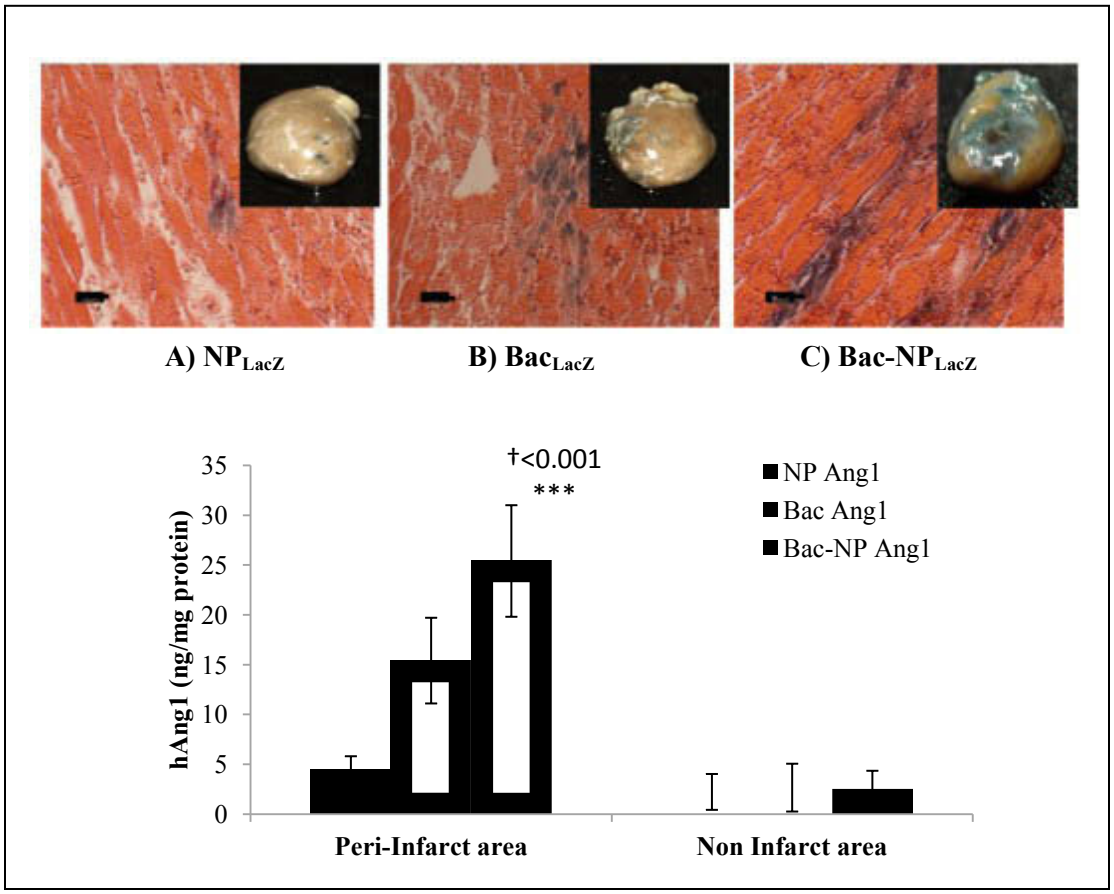

Figure 9.8: Detection of LacZ transgene expression (3 days post injection) in the peri-infarct (site of injection) and non-infarct regions of rat ventricular hearts transduced with NP_{LacZ} (A), Bac_{LacZ} (B) and Bac-NP_{LacZ} (C), as observed in microscopic images of histological tissue sections (insets showing the corresponding whole hearts stained blue with LacZ). The samples were treated with X-gal to detect the LacZ gene expressing stained cells (stained in blue) and counterstained with eosin to stain cell cytoplasm (pink-orange). Scale bar indicated 50µm. D) Quantification of myocardial expression of hAng1 at the peri-infarct (site of intramyocardial injection) and non-infarct ventricular region (n=4) analyzed by hAng1 ELISA assays. Mean values ± SD (n=4) are shown. ELISA analysis 2-way ANOVA: Groups: F= 21.21, p<0.0001; Area: F=90.04, p<0.0001; Interaction: F=19.92, p<0.0001; *** = P<0.001, ** = P<0.01, * = P<0.05 vs. area-matched control. P values comparing area-matched Bac_{Ang1} and Bac-NP_{Ang1} are indicated by †.

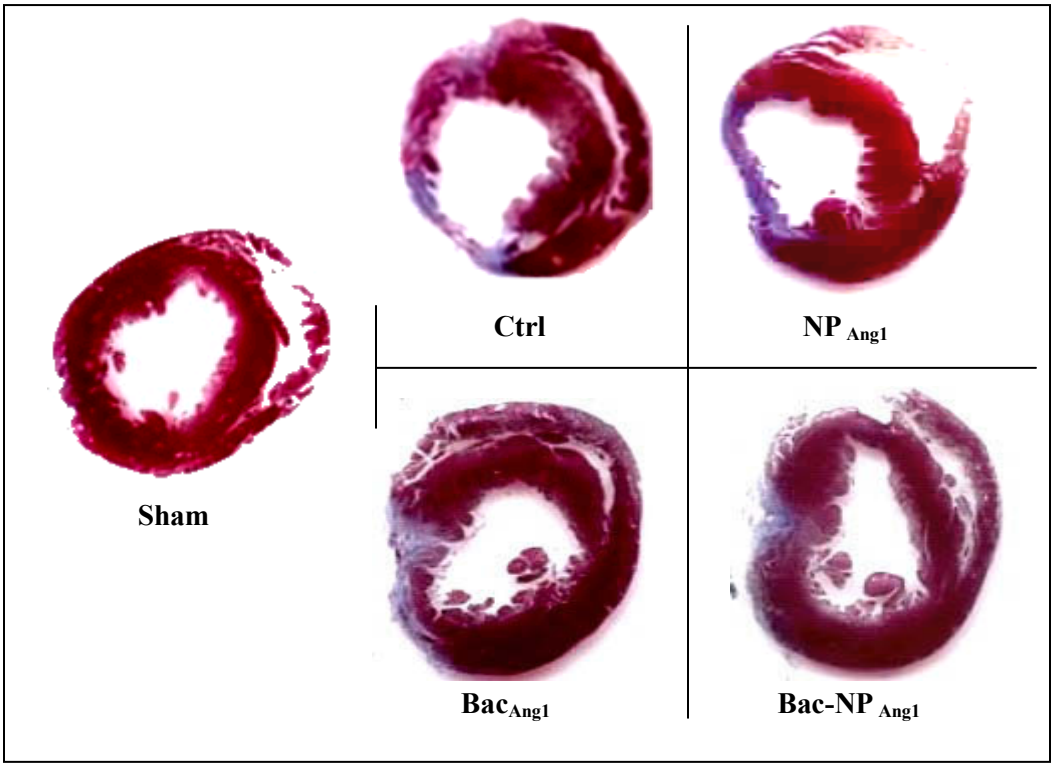

Figure 9.9: Scar area analysis 21 days post infarction. Representative images of LV myocardial sections stained with Masson's Trichome show the cardiac fibrosis region (in blue) after gene delivery of Ang1 through NP $_{Ang1}$, Bac$_{Ang1}$ and Bac-NP $_{Ang1}$. Sham operated and untreated infarcted group are used as controls. The blue area represents extracellular matrix deposition in the scar tissue and the red area represents the myocardium.

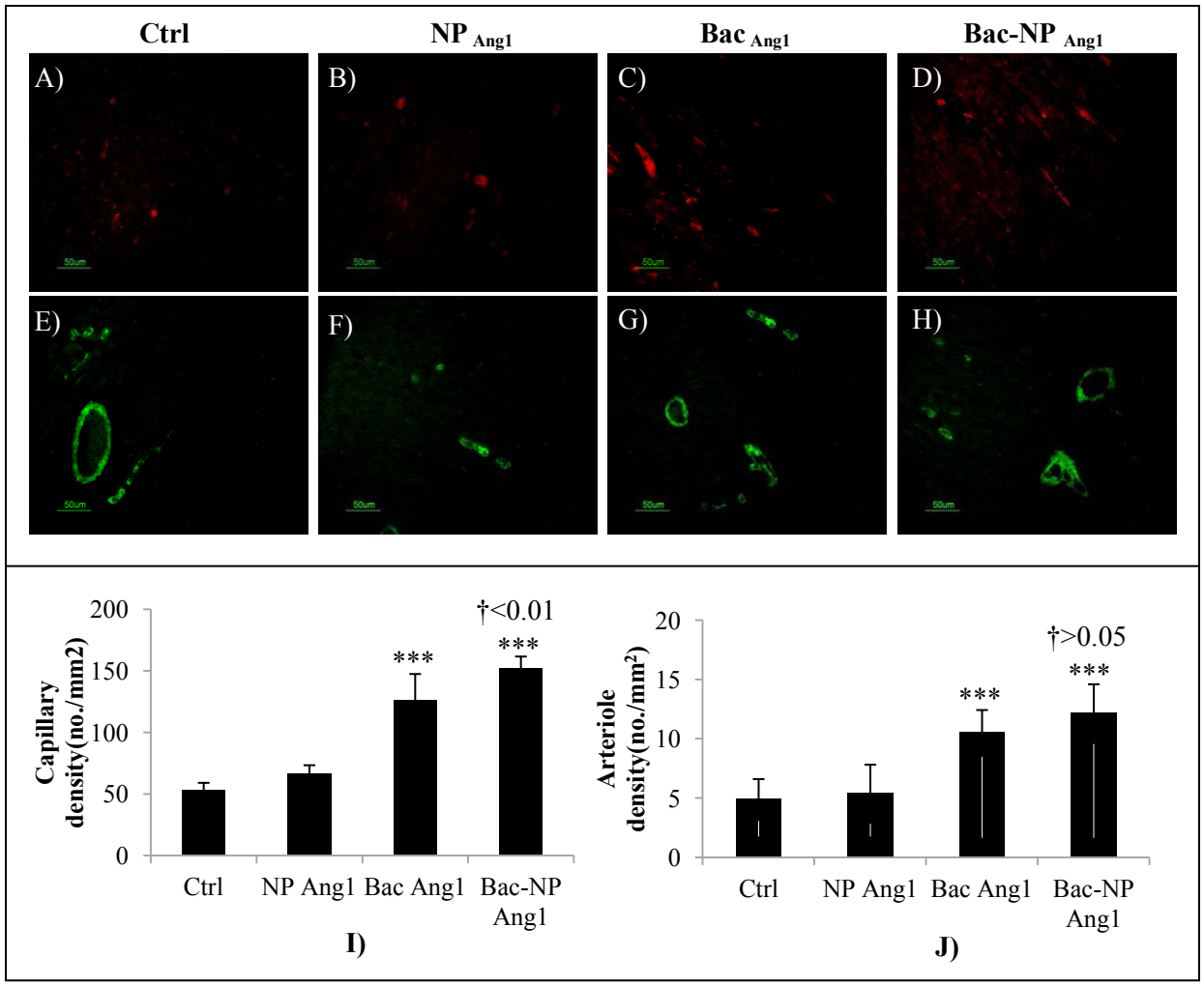

Figure 9.10: Angiogenesis and arteriogenesis in the peri-infarct area. Immunohistological staining of CD31 to detect endothelial cells in (A) Ctrl, (B) NP_{Ang1}, (C) Bac_{Ang1} and (D) Bac-NP_{Ang1} groups. Immunohistological staining of smooth muscle α-actin for smooth muscle cells in (E) ctrl, (F) NP_{Ang1}, (G) Bac_{Ang1} and (H) Bac-NP_{Ang1} groups. Scale bar indicates 50µm. Quantification of (I) capillary and (J) arteriole density. Data are expressed as mean density ±SD. One-way ANOVA analysis: Treatment Groups: $F= 112.2$, $p<0.0001$ (I) and $F= 22.54$, $p<0.0001$ (J). Statistically significant differences between groups compared to control are indicated as *** = $P<0.001$, ** = $P<0.01$, * = $P<0.05$. P values comparing Bac_{Ang1} and Bac-NP_{Ang1} are indicated by †.

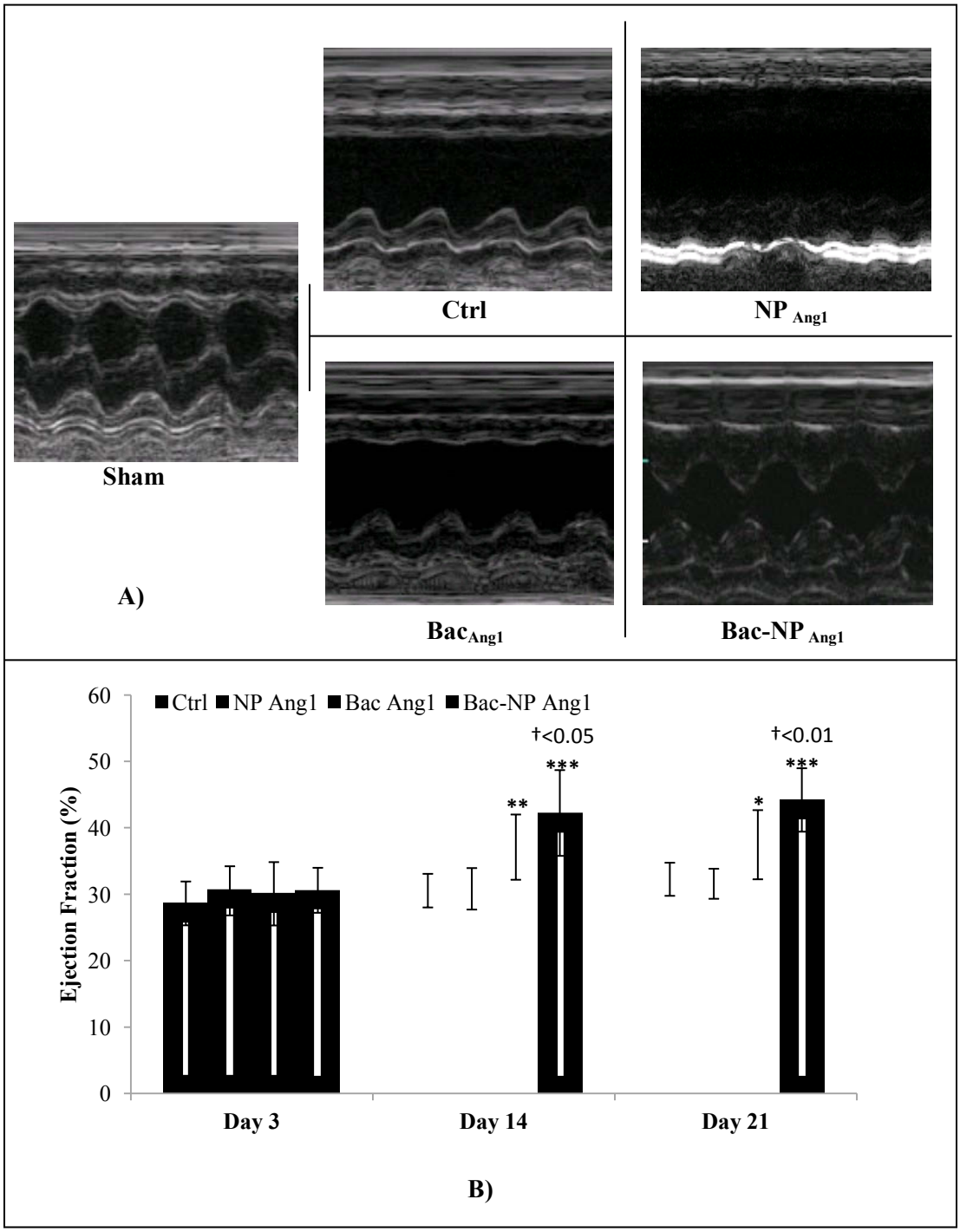

Figure 9.11: Echocardiographic assessment of cardiac function. Effect of Bac-NP mediated Ang1 delivery on cardiac function was analyzed over 21 days post infarction. For this, heart EF% was monitored at day 3, 14 and 21 after transplantation of Ctrl (n=8), NP $_{Ang1}$ (n=8), Bac $_{Ang1}$ (n=8) and Bac-NP $_{Ang1}$ (n=8) in rat myocardial infarction. (A) represents the M-mode echocardiograms of different groups on day 21. As demonstrated in the graph (B**),** the EF% increased

significantly after treatment in the Bac-NP_{Ang1} and Bac_{Ang1} groups over the 21 days post infarction compared to control group, but the NP_{Ang1} group did not show any sign of improvement at any time point. Furthermore, Bac-NP_{Ang1} group showed a significantly better EF% than Bac_{Ang1} group with time. Mean EF% values ± SD are shown in graph. Echocardiogram analysis 2-way ANOVA: Treatment: $F= 10.74$, $p<0.0001$; Time: $F=49.02$, $p<0.0001$; Interaction: $F=9.94$, $p<0.0001$; Subjects (matching): $F= 4.631$, $p<0.0001$; *** = $P<0.001$, ** = $P<0.01$, * = $P<0.05$ vs. time-matched control. P values comparing time-matched Bac_{Ang1} and Bac-NP_{Ang1} are indicated by †.

Angiopoietin-1 expressing adipose stem cells genetically modified with baculovirus nanocomplex: investigation in rat heart with acute infarction

Arghya Paul[1], Madhur Nayan[2], Afshan Afsar Khan[1], Dominique Shum-Tim[2], Satya Prakash[1]*

[1] Biomedical Technology and Cell Therapy Research Laboratory, Department of Biomedical Engineering, Faculty of Medicine, McGill University, 3775 University Street, Montreal, Quebec H3A 2B4, Canada.

[2] Divisions of Cardiac Surgery and Surgical Research, The Montreal General Hospital, 1650 Cedar Ave, Suite C9-169, Montreal, Quebec H3G 1A4, Canada.

*Corresponding author; Email: satya.prakash@mcgill.ca
Tel: +1-514-398-3676; Fax: +1-514-398-7461

Preface: As described in the previous chapter, a new, simple and highly effective gene delivery system has been developed for therapeutic angiogenesis. Another important application of this system can be its use for combined stem cell-gene therapy. The present chapter explores its ability to transduce adipose stem cells without affecting its natural characteristics including differentiation potential. Results confirm its safety and efficacy to genetically modify stem cells and further extend its application to treat myocardial infarction. Data confirms significantly enhanced angiogenesis, attenuated infarct formation and improved cardiac function in the treated group compared to controls. The work demonstrates the potential of hybrid baculovirus gene delivery system for stem cell based gene therapy applications.

Original article accepted (in press) in ***International Journal of Nanomedicine (2012)***

10.1 Abstract

Aim: The objective of this study is to develop Angiopoietin-1 (Ang1) expressing genetically modified human adipose tissue derived stem cells (hASCs) for myocardial therapy. For this we used an efficient gene delivery system using recombinant baculovirus (Bac) complexed with cell penetrating TAT peptide/DNA nanoparticles (NP), through ionic interactions. It is hypothesized that the hybrid Bac-NP_{Ang1} system can efficiently transduce hASCs and induce favorable therapeutic effects when transplanted *in vivo*. **Methods and Results:** To evaluate our hypothesis, we employed a rat model with acute myocardial infarction and intramyocardially transplanted Angiopoietin-1 (Ang-1) expressing hASCs, genetically modified by Bac-NP_{Ang1}. Ang-1 is a crucial pro-angiogenic factor for vascular maturation and neovasculogenesis. The released hAng-1 from hASC-Ang1 demonstrated profound mitotic and anti-apoptotic activities on endothelial cells and cardiomyocytes. The transplanted hASC-Ang1 group showed higher cell retention compared to hASC and control groups. A significant increase in capillary density and reduction in infarct sizes were noted in the infarcted hearts with hASC-Ang1 treatment compared to infarcted hearts treated with hASC or untreated group. Furthermore, the hASC-Ang1 group showed significantly higher cardiac performance in echocardiography (ejection fraction of 46.28±6.3%, $P < 0.001$ vs control, n=8) than the hASC (36.35±5.7%, P<0.01, n=8), 28 days post infarction. **Conclusion:** The study identified Bac-NP complex as an advanced gene delivery vehicle for stem cells and demonstrated its potential to treat ischemic heart disease with high therapeutic index for combined stem cell-gene therapy strategy.

Keywords: combined stem cell-gene therapy, baculovirus, nanoparticle, myocardial therapy, angiogenesis, tissue engineering

10.2 Introduction

A promising therapeutic approach currently under intensive clinical trials is mesenchymal stem cell (MSC) therapy for congestive heart diseases, which depends on several corroborated mechanisms, such as myocyte formation and neovascularization to improve cardiac function and attenuate ventricular remodeling [379, 380]. Despite promising initial results, such clinical application remains limited due to logistic, economic, and timing issues when harvesting autologous stem cells from elderly patients. Moreover, it has been reported that MSCs obtained from elderly donors and patients with diabetes or ischemic heart disease have a significantly reduced capacity for neovascularization, proliferation, and differentiation potential [381].

Delivering pro-angiogenic proteins, such as vascular endothelial growth factor (VEGF) and Ang-1, using MSC based gene therapy approaches are currently being employed in recent studies as an alternative strategy to promote myocardial angiogenesis and regeneration [382-384]. However, the mammalian gene delivery vectors widely used in such studies have various drawbacks and severe safety concerns [385-387]. These vectors are prone to integration into coding regions of transcriptionally active genes, raising concerns about gene silencing and insertional mutagenesis. Unlike the aforementioned vectors, baculovirus is an insect cell originated viral vector that is considered nonpathogenic to humans as they cannot replicate in mammalian cells [358, 387]. The viral genome remains in episomal form within the nucleus and is degraded within the mammalian cells over time eliminating the chance of potential mutagenesis. Then can efficiently transduce a wide range of mammalian cells with minimal cytotoxicity. They can efficiently transduce MSCs, as shown in our earlier studies, and reports confirm the safety of transplanting baculovirus-engineered MSCs into immunocompetent animals for cell-based gene therapy [165, 387].

The present study aims to develop a hybrid nanodelivery system to genetically modify MSCs efficiently, utilizing the complementary strengths of

baculovirus, such as relatively high transduction efficiency and easy scale-up, and TAT/DNA nanoparticles, such as low immunogenicity. TAT peptide sequence, obtained from the protein transduction domain of HIV-1 virus responsible for nuclear import of HIV genome, has been modified here by incorporating histidine and cysteine residues for enhanced DNA transport, efficient cell penetration, cell vesicle escape and transgene expression [365]. We have recently demonstrated the potential of this new system for direct gene therapy with cardiomyocytes [388].

Here, we hypothesized that the MSC transduction efficiency can also be significantly enhanced by this new system where the negatively charged baculovirus (Bac) is coupled with positively charged endosomolytic histidine rich TAT peptide/DNA nanoparticles (NP), both carrying the transgene. For this we used a unique pool of MSCs located within the adipose tissue, called adipose tissue-derived stem cells (ASCs), mainly because of their practical availability, pro-angiogenic, immunomodulatory and other unique properties [280, 389]. Based on the positive efficacy data in disease-relevant animal models, ASCs have recently entered into its first clinical trial [390]. In a recent intriguing study, Metzele *et al* reported that hASCs can fuse to newborn rat heart cells to form new cardiomyocytes with several nuclei, which can beat when maintained in a culture environment [391]. ASCs possess a natural ability to secrete VEGF, which overexpresses under hypoxic conditions in ischemic tissues [162].

It has been reported that VEGF in co-operation with another angiogenic growth factor, Ang-1, promotes significant neovascularization, and their combined action leads to a formation of mature and functional vasculature [376, 392, 393]. Thus we hypothesized that the secretion of Ang1 along with naturally releasing VEGF from the genetically modified ASCs, together with their inherent transdifferentiation abilities to cardiomyocytes, can induce a superior synergistic therapeutic effect for myocardial regeneration therapy. Additionally, acute myocardial infarction also induces a high circulating endogenous serum VEGF state [353]. With these rationales, we generated Ang1 cDNA carrying

recombinant Bac and TAT nanoparticles, prepared a self-assembled binary nanocomplex by hybridizing the two, and determined its efficiency to express functionally active Ang1 using optimized transduction protocol with hASCs. The *in vivo* efficacy of the formulated nanobiohybrid (Bac-NP) system for combined stem cell-gene therapy applications has also been evaluated using hAng1 expressing genetically modified hASCs for myocardial therapy using immunocompetent infracted rat heart model. A schematic presentation of the entire procedure is demonstrated in the **Figure 10.1**.

10.3 Methods and materials

10.3.1 Cell culture and preparation of baculovirus gene delivery complex

Human ASCs (n=1 male donor) were obtained from Invitrogen and cultured in DMEM (Invitrogen) supplemented with 10% fetal bovine albumin (FBS). The cells were routinely maintained as stationary cultures in 75 cm^2 tissue culture flasks and incubated at 37^o C in a controlled environment with an air atmosphere of 5% CO_2. Human umbilical vein endothelial cells (HUVECs) (Sciencell, Carlsbad, California, USA) were cultured and expanded on tissue culture flasks according to the supplier's instructions. They were cultured in endothelial cell medium (ECM) (Sciencell, Carlsbad, California, USA) supplemented with 5% FBS and placed in an incubator containing 5% CO_2 at 37°C. H9c2 myogenic cell-line derived from embryonic rat heart ventricles, was obtained from American Tissue Culture Collection (CRL 1446) and cultured in DMEM supplemented with 10% FBS. The cells were routinely maintained as stationary cultures in flasks, incubated at 37^{o}C in a controlled environment with 5% CO_2. Sf9 insect cells (Invitrogen Life Technologies, Carlsbad, CA) were maintained at 27^{o}C in SF900 III serum free medium (Invitrogen). The cells were maintained in exponential growth phase and subcultured twice per week. Larger volumes were prepared in shaker flasks (Erlenmeyer, Corning) which were agitated at 120 rpm in an incubator shaker as mentioned in earlier studies [165].

Generation of LacZ and Ang1 gene carrying recombinant Bac and their subsequent hybridization with NPs to form Bac-NP_{Ang1} and Bac-NP_{Lacz} were performed using protocol as mentioned in our earlier work [388].

10.3.2 Detection of hAng-1 expressed by the transduced hASCs: Elisa and immunofluorostaining

In order to evaluate the transduction efficiency of Bac-NP on hASCs and compare it with free Bac and NP gene system, NP_{Ang1}, Bac_{Ang1} and Bac-NP_{Ang1} at MOI [Multiplicity of Infection defined as pfu per cell] of 200 were used. hASCs were seeded in 6-well plates at $0.5x10^6$ cells/well and were incubated overnight at 5% CO_2 and 37^oC. Following this, an appropriate volume of the nanocomplexes suspended in PBS was added to each well according and incubated for 4h. Following this, the transduction solution was replaced with fresh media and grown in cell culture incubator. Conditioned media were collected every alternate day for 21 days and stored at -80^oC for Ang1 ELISA (R&D Systems, Minneapolis) analysis using standard procedure provided by the manufacturer [388]. To detect the Ang-1 expressed within the transduced cells, in another set of experiment, hASCs transduced with NP_{Ang1}, Bac_{Ang1} and Bac-NP_{Ang1} or non-treated controls were grown on polylysine coated glass microscope slides for 96 hr. After washing with phosphate-buffered saline (PBS), the cells were fixed with −20°C methanol for 10 minutes followed by immunostaining as mentioned elsewhere[394]. Briefly, after blocking for 1 hour with 10% donkey serum, the cells were incubated over night at 37°C with 1:50 dilution of goat anti-hAng-1 (Santa Cruz Biotechnology Inc., Santa Cruz, California) primary antibodies. On the second day, the cells were thoroughly washed with wash buffer. The cells were incubated with donkey anti-goat IgG-TRITC (Santa Cruz Biotechnology Inc.) with 1:200 dilutions for 1 hour. The proportions and intensities of TRITC-positive hASCs, as seen under fluorescence microscope (Nikon Eclipse TE2000-U), gave a qualitative idea of the relative amount of cellular Ang-1 expressed due to transgene delivery by the different delivery systems.

10.3.3 Cell proliferation and viability assay

For the cell proliferation assay, $2x10^4$ HUVEC cells/well were seeded in triplicate for each sample in 96-well plates. After 8hrs of culturing, the cells were washed twice with PBS and 200µl of conditioned media from non-transduced hASCs, Bac-NP_{LacZ} transduced hASCs, Bac-NP_{Ang1} transduced hASCs and Bac-NP_{Ang1} transduced hASCs supplemented with anti-hAng1 antibodies were added to the corresponding set of wells. After 96hrs absorbance was measured at 490nm using Cell Titer 96 Aqueous Non-Radioactive Cell Proliferation Assay (Promega, Madison, WI) in a plate reader [293]. In a similar way, cardiomyocyte cell viabilities under oxidative stress in groups treated with different conditioned media were measured as described later in the study, using the same assay. The experiment was performed in triplicates.

10.3.4 Wound healing assay with HUVEC

In order to check the wound healing potential of released Ang1, HUVEC were seeded into 24-well plates and grown to confluency. After 24 h of serum starvation (1% FBS), lesions were made in the monolayer using cell scraper [388]. Cells were rinsed with PBS, and then incubated with the hASC CM from different experimental groups (NP_{Ang1}, Bac_{Ang1} and Bac-NP_{Ang1}) for 24h. CM from untransduced cardiomyocytes was taken as control. To confirm the beneficial effect of Ang-1 in particular, another experimental group was taken, where the CM from Bac-NP_{Ang1} group was pre-incubated with anti-Ang1 neutralizing antibody (R&D Systems; 1 µg/ml) for 30 min, before adding to the wells. Cells were fixed with 4% paraformaldehyde (Sigma-Aldrich, St Louis) after 24h and the number of cells which had moved across the starting scratched lines were measured for all groups. Three fields were analyzed for each well at 200X magnification.

10.3.5 Apoptosis assay using cardiomyocytes

H9c2 cells were seeded in 96-well microtiter plates at a density of 2×10^4 cells/well and cultured overnight. The media was replaced with CM from

different treatment groups and oxidative stress was induced by adding 200 μM H_2O_2 to the media as described elsewhere [395]. After 6h, the apoptotic cells were detected by tracking the loss of mitochondrial membrane potential using MitoCapture (BioVision, Moutain View, CA) cell staining cationic dye, according to the manufacturers protocol, that fluorescence differently in healthy *and* apoptotic cells under fluorescence microscope (488-nm and 543-nm excitation filters). The red emission of the dye is due to a potential-dependent aggregation in the mitochondria reflecting normal membrane potential and the green fluorescence detects the monomeric form of MitoCapture, appearing in the cytosol after mitochondrial membrane depolarization [396]. For each experimental group, total cell number was counted and put into relation to the number of cells that displayed fluorescence. In a similar way, after oxidative stress of 6h, the cell viabilities were also checked using MTS assay as mentioned above.

10.3.6 *In vivo* studies in myocardially infarcted rat model

Immunocompetent female Lewis rats (200 to 250 gm, Charles River, QC) were used. All procedures were in compliance with the Guide for the Care and Use of Laboratory Animals (NIH publication No. 85-23) and the Guide to the Care and Use of Experimental Animals of the Canadian Council on Animal Care. Female Lewis rats were anesthetized using 5% isoflurane in an induction chamber. The rats were intubated with an 18-gauge catheter and mechanically ventilated (Harvard Ventilator, PQ, Canada) at 80 breaths/min. Anesthesia was maintained with 3% isoflurane. A left thoracotomy was performed through the fourth intercostal space to expose the left ventricle. The left coronary artery was ligated 2 mm from its origin with a 7-0 polypropylene suture (Ethicon, Inc, Somerville, NJ) using standard protocol [388]. The ischemic myocardial segment rapidly became identifiable through its pallor. Fifteen minutes after ligation of the artery, intramyocardial injections were given. In control group with no hASC (n=8), 300ul of the culture medium was divided into 3 equal peri-infarct left ventricular intramyocardial injections using a 27 gauge needle. In hASC group

(n=8), the same procedure was repeated using culture medium containing $3x10^6$ hASCs, while in the group hASC-Ang1 (n=8) received same number of cells transduced with Bac-NP_{Ang1} (MOI:200) suspended in culture medium.

To detect the transgene expression in transplanted cells 3 animals underwent same experimental procedure as described above, followed by injection of 3 million cells transduced with Bac-NP_{LacZ} at MOI 200. 3 days post transplantation, Lac Z expressions were detected in histological samples using standard staining Lac Z staining procedure [388].

10.3.7 Detection of transplanted male hASCs in female rat hearts: PCR analysis for human Y chromosome

In order to detect the transplanted hASCs from male donor in heart tissue, groups with no hASC (n=6), hASC (n=6) and hASC-Ang1 (n=6) were taken. After 3 and 28 days post injection, 3 animals from each group were sacrificed and heart tissue samples were snap frozen. PCR analysis was done on the extracted DNA samples to confirm the survival of the implanted gender-mismatched cells in the hearts using standard procedure followed in our earlier studies [397]. Briefly, equal amount of DNA were extracted from peri-infarct portions of ventricular heart in each group and PCR analysis was done to confirm the survival of the implanted gender-mismatched cells in the hearts at 3 and 28 days post operation. Genomic DNA was purified using DNeasy (Qiagen, Valencia, CA) according to the manufacturer's instructions, and the presence of living male cells in female hearts was confirmed by targeting a specific microsatellite sequence within the Y chromosome (DYS390). The primer pairs used were forward primer 5' TATATTTTACACATTTTTGGGCC3' and reverse primer 5'TGACAGTAAAATGAACACATTGC3' with product length of 250 bp.

10.3.8 Scar Area Analysis: Myocardial infarct size

Twenty eight days post-operation, rats were deeply anesthetized and sacrificed by rapid excision of the heart. The excised hearts were immediately soaked in cold saline to remove excess blood from the ventricles and fixed in

neutral-buffered 4% formalin. Paraffin embedded samples were sectioned at 5µm, and Masson's trichrome staining (*DBS,* Pleasanton, CA) was performed to delineate scar tissue (blue color) from the total area of myocardium [241]. Masson's trichrome-stained sections were captured as digital images and analyzed by ImageJ-1.41 software. Infarct area, epicardial and endocardial length of infarction and ventricular and septal wall thickness were calculated and expressed as a percentage.

10.3.9 Immunohistochemistry for detecting neovascularization

Neovascularization was evaluated by analyzing the capillary and arteriole density in the peri-infarct area. For this, immunohistochemical staining was performed with anti-PECAM (Santa Cruz) for identification of endothelial cells and anti-smooth muscle α-actin (Santa Cruz) for tracing the smooth muscle cells as described elsewhere [353]. Briefly, for measurement of capillary density, five fields in the peri-infarct area were imaged with 200x magnification and average numbers of capillaries with less than 10µm diameter were counted. The capillary density was quantified as the (mean total PECAM-positive microvessels)/mm^2 using three tissue sections spanning per-infarct tissue region of each animal. Similarly, arteriole densities were quantified as the (mean total smooth muscle α-actin-positive microvessels)/mm^2.

10.3.10 Transthoracic echocardiography

Transthoracic echocardiography was performed on all surviving animals in rat groups treated with hASC (n=8), hASC-Ang1 (n=8) and untreated control (n=8) on day 3, day14 and day 28 post infarction. Echocardiograms were obtained with a commercially available system (SonoSite, Titan- Washington, Seattle, WA) equipped with a 15-MHz transducer. After sedating the animals with 2% isoflurane, echocardiography was performed according to the American Society of Echocardiology leading-edge method [397]. Briefly, parasternal long- and short-axis views were obtained with both M-mode and two-dimensional images.

End diastolic (LVEDD) and end-systolic (LVESD) diameteres were measured with M-mode tracings between the anterior and posterior walls from the short-axis view just below the level of the papillary muscles of the mitral valve. Two images on average were obtained in each view and averaged over three consecutive cardiac cycles. Left ventricular end-diastolic volume (LVEDV) was calculated as 7.0 x $LVEDD^3$/ (2.4+LVEDD), and left ventricular end-systolic volume (LVESV) as 7.0 x $LVESD^3$/ (2.4+LVESD). Ejection fraction (EF) was estimated as (LVEDV-LVESV)/ LVEDV.

10.3.11 Statistical Analysis

Quantitative variables are presented as mean ± Standard Deviation (SD) from independent experiments as described in the figure legends. Statistics were performed using two-way and/or one-way ANOVA by Bonferroni's multiple comparison post-hoc test. All statistical analyses were performed with Prism 5 (GraphPad Software). P value <.05 was considered significant.

10.4 Results

10.4.1 Bac-Ang1 transduced hASCs can be efficiently release hAng1

The released Ang-1 from the transduced hASCs was analyzed at protein level by hAng1 Elisa assay. As shown in **Figure 10.2A-2C**, hAng-1 expression was detected from day 1 post transduction till day 21 with regular intervals with all the groups (NP_{Ang1}, Bac_{Ang1} and Bac-NP_{Ang1}). The highest expression was seen on day 4 with the gene delivery systems. However, with Bac-NP_{Ang1} we achieved highest expression (18.5±1.2 ng/10^6 cells) which stayed persistently higher than other groups all throughout the experimental period. Moreover, the cellular Ang-1 expression demonstrated by the TRITC stained cells, 96h post transduction, was shown to be highest in Bac-NP_{Ang1} treated group as compared to NP_{Ang1} and Bac_{Ang1} (**Figure 10.2D-2G**). The ELISA and immunostaining analysis confirmed that Bac-NP_{Ang1} was a superior gene delivery vehicle than free Bac_{Ang1} and NP_{Ang1} alone which was able to express higher amount of hAng-1 transgene at both extracellular and intracellular level.

10.4.2 Biologic activity of the secreted hAng1 on vascular endothelial cells

To confirm the functionality of the expressed hAng1 we performed HUVEC proliferation assay using the conditioned media from Bac-NP_{Ang1} transduced hASCs and compared it with that of control Bac-NP_{LacZ} transduced hASCs and untransduced hASCs. As reported in **Figure 10.3A,** the samples with high Ang1 concentrations, i.e., from CM of Bac-NP_{Ang1} transduced hASCs, significantly increased the proliferation rate of HUVECs (2.67 $x10^4$ cells compared to 1.85 $x10^4$ cells in Bac-NP_{LacZ} CM, 1.89 $x10^4$ in control non-transduced CM, and 1.59 $x10^4$ cells in CM with antibody, where 2 $x10^4$ cells were taken as the initial density).

Furthermore, we tested the ability of CM (containing secreted hAng1) to increase HUVEC wound healing in a monolayer. As depicted in **Figure 10.3B&3C,** stimulation of wounded HUVEC monolayer with CM from Bac-NP_{Ang1} (33.3±2.0%) induced a significant reduction of wound compared with the unstimulated control (16.8±1.4%), and CM from Bac-NP_{LacZ} (16.1±4.2%). Thus, consistent to the mitotic assay results, Bac-NP_{Ang1} showed highest healing potential indicating that efficient overexpression of Ang-1 is one of the determining factors for inducing substantial biological effects. Pre-incubation of CM with the neutralizing anti-Ang1 antibodies completely inhibited Bac-NP_{Ang1} CM induced wound healing, clearly suggesting that chemotactic signals from hAng1 are essential for this effect.

10.4.3 Biologic activity of the secreted hAng1 on cardiomyocytes

In order to access whether the secreted hAng1 have a protective effect on cardiomyocytes under oxidative stress, the treated h9c2 cells from different groups underwent cell viability studies after 6h oxidative stress using H_2O_2. The data in **Figure 10.4A** shows that CM from Bac-NP_{Ang1} was able to significantly reduce the cell death compared to Bac-NP_{LacZ} and Bac-$NP_{Ang1+antibody}$ (1.82±0.02 vs 1.04±0.04 vs 0.93±0.08), taking a normalized value of cell number in untreated ctrl group as 1.0. As positive control, cells with no oxidative stress were taken which showed a viability amount of 1.82±0.02.

Furthermore, we checked the anti-apoptotic effect of the released hAng1 on cardiomyocytes under oxidative stress and quantified its effect by Mitocapture cell staining (**Figure 10.4B&4C**). Cultivation of h9c2 cardiomyocytes under H_2O_2 induced oxidative stress for 6h provoked a strong apoptotic response with 60.7±3.7% of apoptotic cells in untransduced control CM group. Addition of CM from Bac-NP_{Ang1} hASCs strongly suppressed cardiomyocyte apoptosis (24.1±2.9%) in comparison to other groups which did not show any significant effect.

10.4.4 hASCs can survive and efficiently express their transgene *in vivo*

To analyze whether the xenotransplanted genetically modified hASCs were able to survive and express the transgene in the rat heart, hearts (n=3) were myocardially infarcted and injected with hASCs transduced with Bac-NP_{LacZ} in the left ventricular region as described earlier. 3 days post transplantation, the rat hearts were harvested and ventricular tissue samples were stained with X-gal in order to trace the transplanted LacZ expressing hASCs in the peri-infarct region of the heart. The picture in **Figure 10.5A** confirms that the transplanted cells were able to survive and express the transgene in the heart.

10.4.5 Higher retention of implanted hASC-Ang1 in rat myocardium

After confirming the transplant survival and transgene expression, we wanted to explore the effect of Ang1 expressing hASCs compared to normal hASCs on cardiac cellular transplant retention with time, three groups [no hASC (n=6), group hASC (n=6) and hASC-Ang1 (n=6)] were taken in the similar way as mentioned earlier. 3 and 28 days post injection, 3 animals from each group were sacrificed for PCR analysis.

DNA was extracted from the injected sites of the heart tissues to detect the presence of Y chromosome of transplanted male hASC using standard PCR. The gel electrophoresis of the PCR products shows a clear distinction in band intensities of hASC-Ang1 and normal hASCs (**Figure 10.5B**). The hASC-Ang1 group showed around 1.72 times higher retention of viable transplanted cells in

the heart in comparison to normal hASCs (0.55 times vs 0.32 times, taking initial 3 day band intensity as 1.0; $p<0.05$) as quantified by relative band intensities using Image J software. This semi-quantitative analysis indicates that much higher number of cells were able to survive the transplantation when they were genetically modified to express Ang1 protein.

10.4.6 Bac-Ang1 hASCs can significantly attenuate scar area formation in infarcted heart

Macroscopic views of Masson's Trichome stained heart sections are shown in **Figure 10.6A**. In both the control and the cell treated groups, positively stained fibrous infarct areas were clearly observed in the heart 28 days after myocardial infarction. Thin infarcts and left ventricular wall with dilated left ventricular cavity were observed in the control hearts. On the other hand, the hearts in the cell-treated groups had significantly lesser infarct areas (**Figure 10.6B**: 13.0 ±3.1% for hASC-Ang1, 31.5± 5.0% for hASCs vs. 38.0±3.3 % for control, $p<0.01$) and higher left ventricular wall thickness (**Figure 10.6C:** 2.53 ±0.19 mm for hASC-Ang1, 1.44± 0.24mm for hASCs vs. 0.91±0.07mm for control, $p<0.001$) than the control heart. A total of 24 rats were analyzed for the determination of infarct size (no hASC control, 8; hASCs, 8; hASC-Ang1, 8). The infarct size and wall thickness in the left ventricles at the section of the middle point between ligation and apex were measured as described elsewhere [353]. There was also a significant improvement in the group treated with hASC-Ang1 compared to hASCs group ($p<0.001$) with respect to the percentage LV infract area and LV infarct wall thickness.

10.4.7 Ang-1 expressing hASCs induce angiogenesis and arteriogenesis

Reporting the significant attenuation of scar area with Ang1 expressing hASCs in the last section, here we tried to understand whether it was only the paracrine effect of the hASCs or a combinatorial effect of hASC released Ang1 and paracrine factors which was responsible for the improvement. For this we assessed the neovasculature formation in the peri-infarct area by detecting the

angiogenesis and arteriogenesis densities (**Figure 10.7**). Indeed, we noticed a significant improvement in angiogenesis in the hASC and hASC-Ang1 groups compared to the control (201 ± 25/mm^2 for hASC-Ang1, 174 ± 14/mm^2 for hASCs vs. 141.5±6/mm^2 for control, $p<0.01$). Moreover, hASC-Ang1 group showed significantly higher capillary density compared to hASC. Similar results were obtained with arteriole density in hASC-Ang1 group (12.25 ± 2.4/mm^2 for hASC-Ang1, 9.5 ± 1.8/mm^2 for hASCs vs. 6.5±1.32/mm^2 for control, $p<0.05$), with hASC-Ang1 group showing significantly higher arteriole density compared to hASC.

10.4.8 Significantly improved cardiac function is detected in hASC-Ang1 treated infarcted heart

To investigate if the reduction of scar area after stem cell therapy results in improved heart function, the EF% in a rat model of myocardial infarction at different time periods (day 3, 14 and 28) were monitored. EF of the all the groups was around 30% on day 3 post infarction, indicating successful acute myocardial infarction in all groups [397]. As presented in **Figure 10.8**, there were significant improvements in EF% in groups treated with hASC-Ang1 and hASCs compared to the control group on day 14 and day 28, although there were no significant differences between the groups on day 3 post infarction ($p>0.05$). In addition, the hASC-Ang1 treated group showed a significantly greater increase in EF% as compared to hASC treated groups on day 14 (44.78±6.14% vs 37.1±4.9% vs $p<0.01$) and day 28 (46.28±6.3% vs 36.35±5.77% vs $p<0.01$). Thus, the analysis using echocardiographic EF% data suggests that hASC-Ang1 can be a better alternative to hASCs to improve cardiac function after acute myocardial damage.

10.5 Discussion

Cardiovascular and ischemic heart disease is a major health concern in both developing and industrialized countries. Although different gene therapy approaches are being employed to treat the disease, clinical trials showed limited results suggesting the need for a better gene therapy strategy [398]. It has been

demonstrated in small animals, that ASCs induce wound healing effects in damaged ischemic tissues mainly through pro-angiogenic paracrine mechanism followed by neovascularization, local recruitment of progenitor cells and exhibition of cardiomyocyte like properties [391, 399]. Moreover, ASCs secrete VEGF which has favorable impact on myocardial neovascularization, tissue perfusion and contractile performance. In addition, a larger number of ASCs can be easily harvested using non-invasive standard fat extraction techniques, which is of immense importance under clinical settings because of their ready availability [162, 280]. Most importantly, as allogeneic hASCs can be easily obtained from young healthy donors, they could be of great value in elderly patients with advanced diseases, where their own ASCs could be dysfunctional.

The present study reports for the first time, the angiogenic potential of a newly formulated hybrid nanodelivery system composed of vascular gene carrying recombinant baculovirus armed with non-covalently conjugated TAT/DNA nanoparticles. The initial step involved development of a recombinant baculovirus carrying Ang-1 and assessing its potential to transduce hASCs for efficient therapeutic angiogenesis. We then worked on further improving its potential for gene delivery. Using a hybrid model of Tat/DNA_{Ang1} NPs coupled to the Bac_{Ang1} under optimized conditions **(Figure 10.S1)**, we achieved significantly higher gene transfer efficiency and gene carrying capacity than free Bac_{Ang1} or NP_{Ang1} alone (**Figure 10.2 and Figure 10.S2**). **Figure 10.S2** demonstrates that Bac-NP, with baculovirus MOI of 200 and N/P ratio = 3 of TAT/DNA NP, was optimal so as to achieve the highest transduction efficiency with no cytotoxic effects (**Figure 10.S3**). Our data also confirms that the gene transfer efficiency can be significantly enhanced by this hybrid nano-formulation of Bac and NP, as compared to their individual efficiencies. *In vitro* analysis showed that Bac-NP transduced cells were able to express their transgene for at least three weeks (**Figure 10.2C**) which is comparable to other experimental results [293, 371]. This temporal expression of the delivery system is beneficial in many cases, particularly for angiogenesis where the expression of the therapeutic protein ceases once its job is done. Further studies needs to be done to comprehend the

exact mechanism of such gene delivery system. Rapid attachment of cationic nanoparticles to negatively charged cell surface followed by efficient intracellular gene entry to the nucleus by the baculovirus may be a probable way. Optimizing the pH condition and transduction time may further enhance the gene delivery efficiency of Bac-NP system [358].

Baculovirus surface modification by chemical coupling and electrostatic interactions are recently being exploited in different ways for enhanced gene delivery[303]. It has been demonstrated that galactosylated PEI/DNA hybridized baculovirus improves gene delivery to hepatoblastoma and lung carcinoma cells [364]. Coating of baculovirus using positively charged polymer PEI is also shown to significantly enhance their *in vivo* gene therapy potential compared to uncoated viruses [304]. Recently Chen *et al* demonstrated that genetically modified baculovirus generated by fusing the protein transduction domain of HIV TAT protein with VP39, the major capsid protein, resulted in improved transduction of various mammalian cells [400]. Similarly, our present study demonstrates that surface modifying the baculovirus with TAT/DNA nanoparticles can also improve gene transfer efficiency. But, to achieve significant therapeutic effects, specifically with stem cells, maintenance of their natural functionalities is of immense importance. Our study confirmed this by successfully differentiating the genetically modified hASCs to adipogenic and osteogenic lineages (**Figure 10.S4**). In addition, our data revealed that the Bac-NP mediated hAng-1 expression from hASCs are biologically active as indicated by their enhanced mitotic and chemotatic activities on HUVEC (**Figure 10.3**). The study also confirmed that the released Ang-1 possesses anti-apoptotic and protective effects on cardiomyocytes (**Figure 10.4**). This supports the findings reported by Wang *et al* who reported that Ang1 can protect cardiomyocytes from oxidative stress-induced apoptosis [395].

In addition to efficient transgene expression, retention of viability of transplanted cells at the infarct site is an important parameter that determines the myocardial therapeutic index of the study. This is because higher the retention of

viable cells directly co-relates with enhanced secretion of paracrine factors and better scope for cellular cardiomyoplasty. Our previous works have aimed to address this problem using polymeric microcapsules to reduce the biologic and mechanical loss of implanted cells in the continuously beating heart [45, 165, 280]. In an interesting study, Liu *et al* demonstrated that Ang-1 can protect MSC against serum deprivation and hypoxia-induced apoptosis [401]. Detection of significantly higher amount human Y chromosome–positive hASCs in the recipient female rat hearts treated with hASC-Ang1 compared to hASC, 28 days post implantation, confirmed these findings (**Figure 10.5B**).

Most importantly, the hASC-Ang1 treatment resulted in enhancement of vascular density (**Figure 10.7**), thereby significantly improved the cardiac function (**Figure 10.8**) compared to hASC and control groups, although cadiomyogenic transdifferentiation of grafted cells were not detected in any of the groups [384]. Moreover, histological findings confirmed the reduction of fibrosis in the infarct area (**Figure 10.6**), which is an important indicator for improved heart function since late reperfusion of infarcted vascular beds attenuates left ventricular remodeling including infarct expansion [382]. Measurement of blood flow using cardiac MRI-based techniques can give us a better real time picture on the progress of such myocardial regenerative process post cell transplantation. Although our preclinical findings exemplify the beneficial effects of such combined adipose stem cell-gene therapy treatment, further *in vivo* studies are needed to elucidate the precise mechanism and to investigate its prolonged effects on cardiac function; these will help us understand whether one-time cell delivery is a viable option or whether multiple cell transplantations are required to achieve a long term desirable outcome.

10.6 Conclusion

From clinical standpoint, the study promises major advancements where ASCs could be easily harvested and mass-produced well in advance, genetically modified to express biologically active therapeutic proteins, and stored for

immediate off-the-shelf use on any patient without delay after an acute myocardial infarction.

In summary, we demonstrated our postulation that a hybrid nanodelivery complex of baculovirus and nanoparticles can take advantage of the unique features associated with the two individual vector systems and exhibit enhanced gene transfer efficiency, supported by *in vitro* and *in vivo* experimental demonstrations. We have illustrated that genetically engineered hASCs, using hybrid nanocomplex, enhanced the transplant retention in myocardially infarcted rat model, induced significant favorable impact on tissue perfusion and contractile performance, which have been corroborated with vasculogenesis. Taken together, our current findings confirms the feasibility of a combined stem cell based gene therapy for ischemic heart diseases using a novel, biologically safe nanobiohybrid gene delivery system.

Acknowledgments

We gratefully acknowledge the assistance received from the Canadian Institutes of Health Research (CIHR; MOP # 64308) to S Prakash, and the Natural Sciences and Engineering Research Council of Canada (NSERC) to S Prakash and D Shum-Tim. A Paul acknowledges the Alexander Graham Bell Post Graduate Scholarship—Doctoral from NSERC.

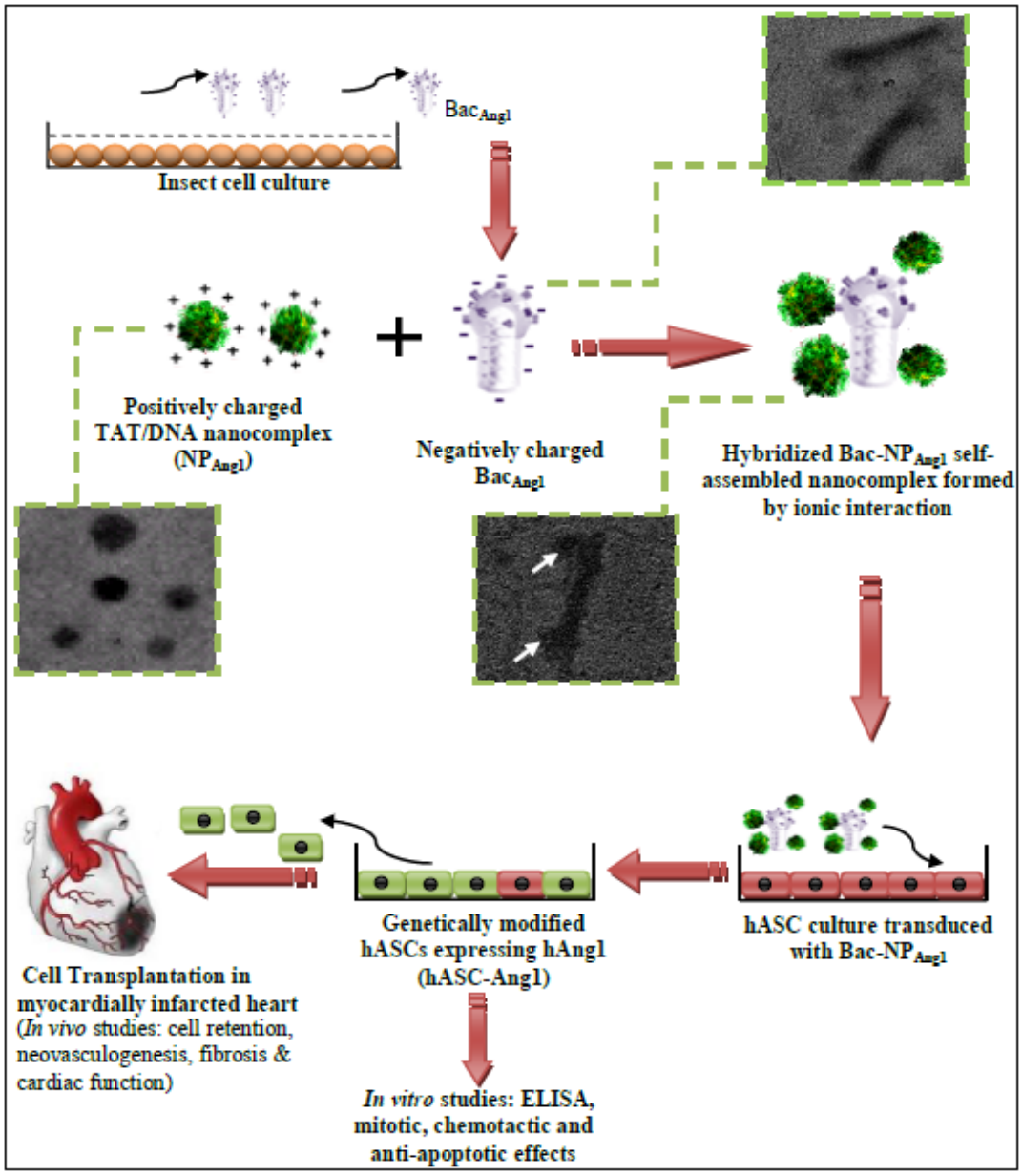

Figure 10.1: Schematic representation of the overall scheme. Generation of recombinant baculovirus (Bac$_{Ang1}$), preparation of hybridized baculovirus with TAT/DNA nanoparticles (Bac-NP), *in vitro* hASC transduction and *in vivo* investigation using direct intramyocardial transplantation of ASC-Ang1 using rat model with acute myocardial infarction. Transmission electronic microscopic pictures of Bac, NP and Bac-NP shown in subsets (with dotted outlines) confirm the formation of the nanocomplex (in white arrows).

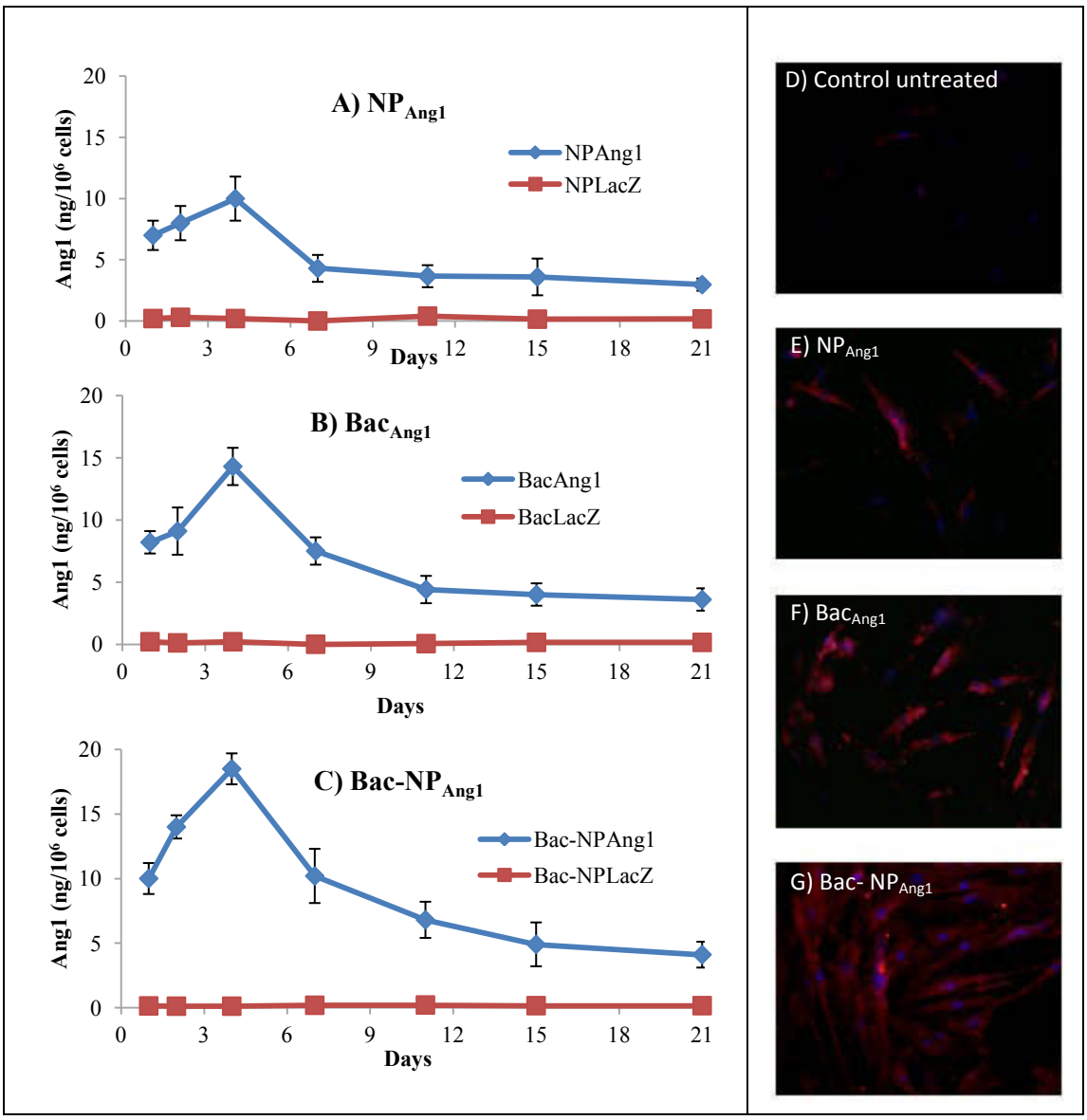

Figure 10.2: Time course profile of hAng1 expression by hASCs transduced with NP_{Ang1} (A), Bac_{Ang1} (B) and Bac-NP_{Ang1}(C). As control groups NP_{LacZ}, Bac_{LacZ} and Bac-NP_{LacZ} were taken for the experiments. Quantification of secretory hAng1 expression in the media by ELISA was done at different time points after hASC transduction in different. Results are mean values ± standard deviation (SD) for three independent experiments. Fluorescent immunostaining of untreated control **(D),** NP_{Ang1} (E), Bac_{Ang1} (F) and Bac-NP_{Ang1} (G) transduced hASCs to detect intracellular hAng-1 expression. hAng1 expression was visualized by tetramethyl rhodamine isothiocyanate (TRITC)-conjugated secondary antibodies (red, TRITC; blue, DAPI).

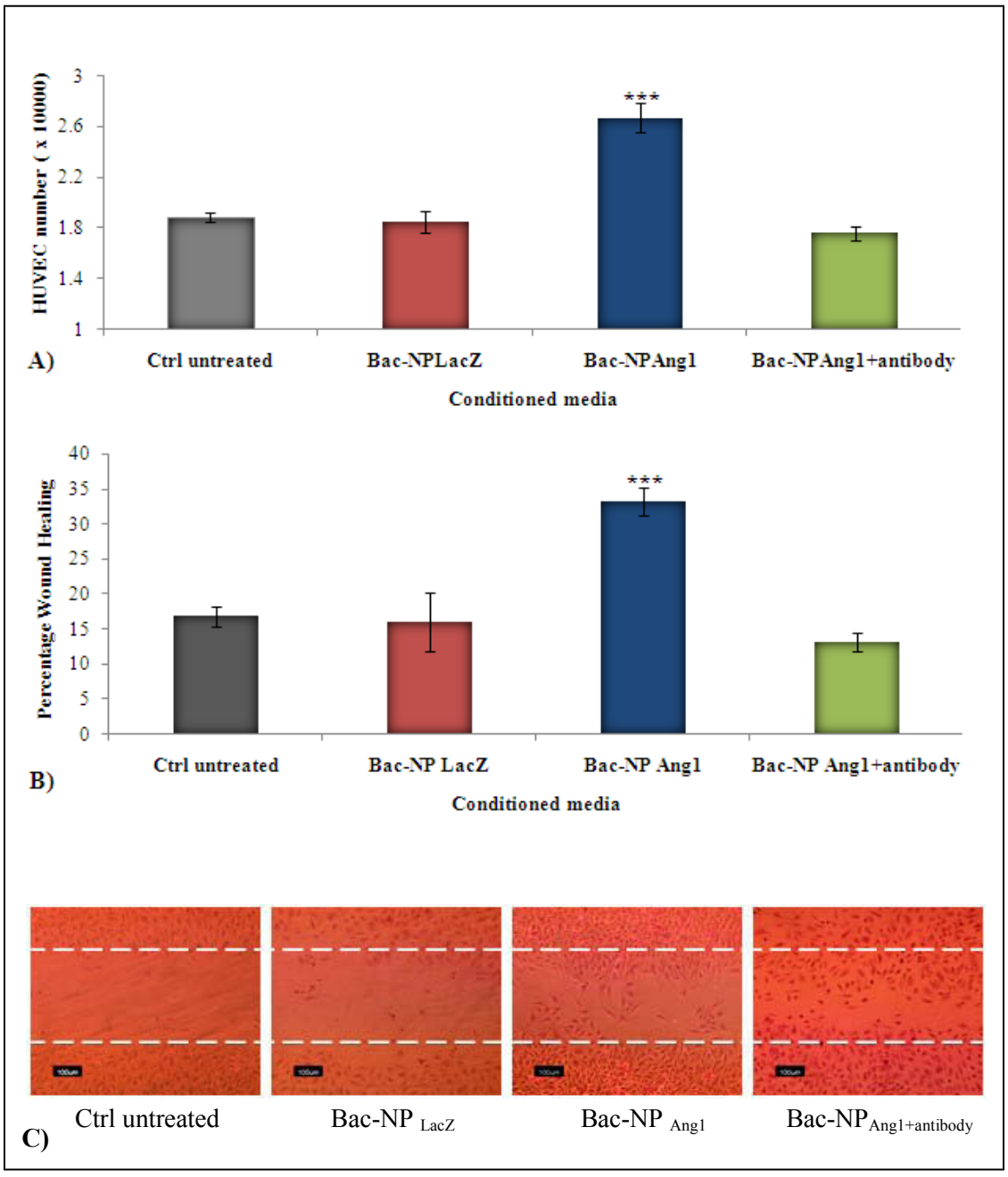

Figure 10.3: (A) Proliferation of HUVECs grown in the presence of CM from Bac-NP_{LacZ}, Bac-NP_{Angl} and non-treated ctrl hASCs. In another group, CM from Bac-NP_{Angl} transduced hASCs was pretreated with antibodies against Ang1 (Ab: 1µg/ml). For this, the initial seeding density was $2x10^4$ cells/ well. Proliferation was measured by a colorimetric assay after 96h of growth. Mean values ± SD from three experiments are shown. **(B)** hAng-1 induces migration of endothelial

cells in a wound healing assay. HUVEC cell monolayer was wounded with cell scraper and treated with CM from Bac-NP_{LacZ} transduced hASCs, CM from cells transduced with Bac-NP_{Ang1}. As another group, CM from Bac-NP_{Ang1} was previously treated with an excess of neutralizing ani-hAng1 antibodies (Ab: 1µg/ml) before performing the wound healing assay. As control group, CM from untreated/non-transduced cells was used. **(C)** HUVEC were photographed (200X) after 24 h treatment and percentage of scratched area (which was initially free of cells, marked by the white dotted border line) covered by the migrated cells were analyzed using Image J software as presented in **B.** Mean values ± SD from three independent experiments are shown. One way ANOVA analysis: statistically significant differences between groups compared to unstimulated control are indicated as *** = P<0.001, ** = P<0.01, * = P<0.05.

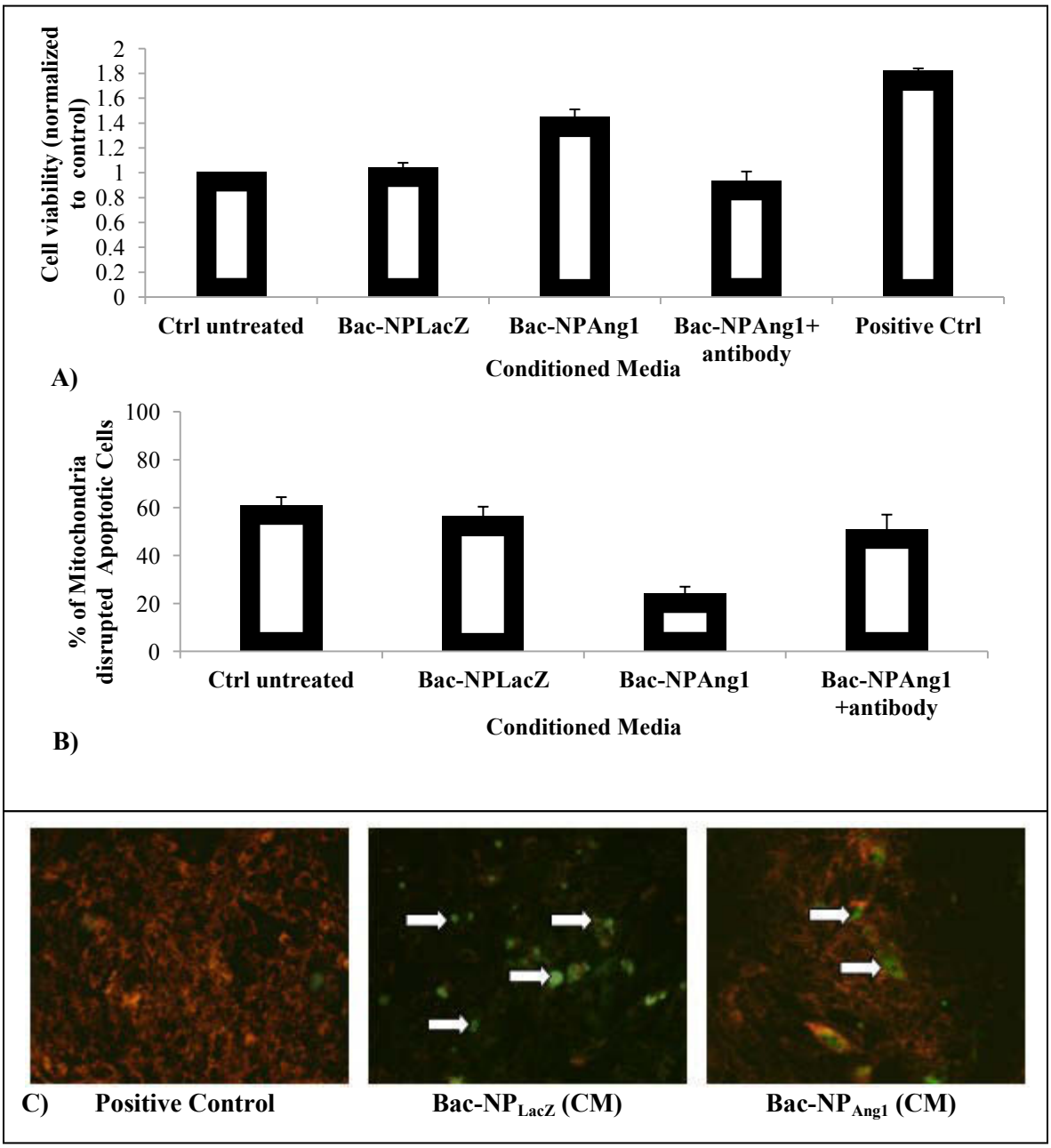

Figure 10.4: A. Quantification of viable h9c2 cells when exposed to oxidative stress. H9c2 cells under different hASC CM (ctrl non-transduced, Bac-NP_{LacZ} and Bac-NP_{Ang1} and Bac-NP_{Ang1} with antibody against Ang1) were exposed to 200 µmol/L H_2O_2 for 6 h. This was followed by cell viability analysis. The viabilities of h9c2 cells in all the groups were normalized to that of control untreated **B.** Under same condition, quantification of H9c2 cardiomyocyte apoptosis was performed Mitocapture probe by detecting the intact and disrupted

mitochondrial membrane potential using. After oxidative insult, Mitocapture staining was performed and the percentage of apoptotic cells was calculated for each group. Cells with mitochondrial damage show diffuse green fluorescence, whereas cells with intact mitochondrial membrane potential exhibit red fluorescence (**C**; Magnification 200X). Cells without oxidative stress were taken as positive control. Arrows indicate the apoptotic cells. The graph in upper panel represents the mean ± SD from three independent experiments. ANOVA analysis: statistically significant differences between groups compared to control untreated (CM) are indicated. *** = $P<0.001$, ** = $P<0.01$, * = $P<0.05$. The data confirms the hAng1 released from Bac-NP_{Ang1} transduced hASCs are functionally active and can significantly inhibit cardiomyocyte cell death and apoptosis induced by hypoxic condition.

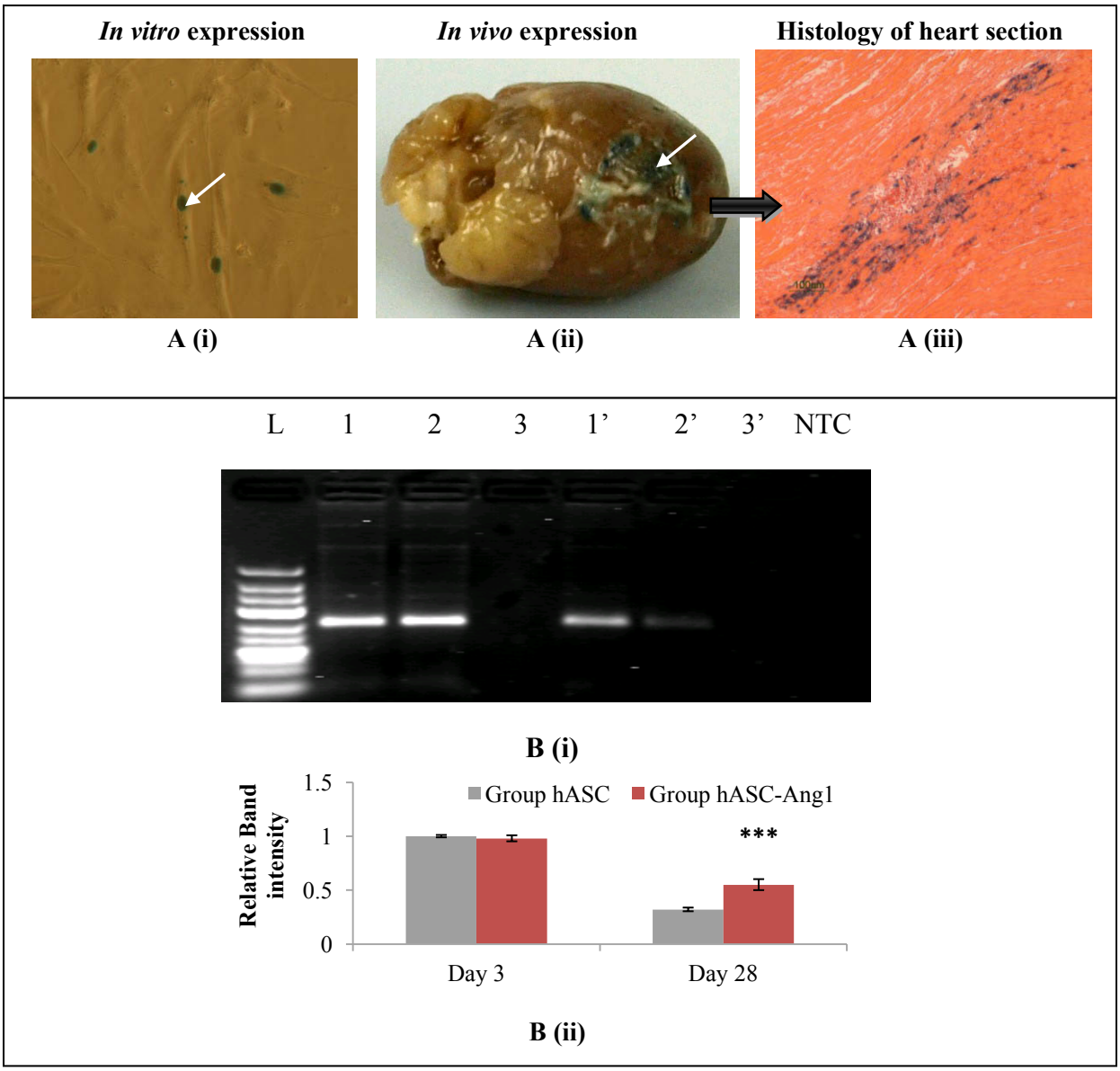

Figure 10.5: (A) Detection of transgene expression (LacZ) in baculovirus transduced hASCs transplanted in the myocardium. 3 million cells were transduced with Bac-NP_{LacZ} at MOI: 200 **(A. i)** and intramyocardially injected in the left ventricular myocardium. 3 days post transplantation, hearts (n=3) were harvested and traced for LacZ expression **(A. ii)**. Histological analysis of ventricular portion (200X: stained with eosin) shows the transplanted cells expressing the LacZ **(A.iii)**. Arrows showing the transplanted stained hASC-LacZ cells in the peri-infarct ventricle region. B. Higher retention of hAng-1 expressing hASCs compared to only hASCs in the left ventricular myocardium 28 days post

transplantation. **(B. i)** PCR products (250bp) specific for the human Y chromosome (DYS390 sequence) as detected in 2% agarose gel. There were clear distinct bands in group hASC-Ang1 (A1 and A1') and group hASC (A2 and A2') in all female rat hearts both on day 3 and day 28, while these bands were absent in no hASC control group (A3 and A3'). Note that these band intensities were much lower in day 28 compared to day 3, with group hASC having the least intensity. Representative PCR products from each group are shown here. **(B. ii)** Image J analysis of the band intensities show the hASC group has a mean of 0.32 times (n=3) and group hASC-Ang1 has a mean of 0.55 times (n=3) band intensities, taking the band intensity of group hASC on day3 as 1.0. NTC represents the no template control for the PCR experiment. 2-way ANOVA: Treatment Groups: $F= 34.86$, $p=0.0004$; Day: $F=974.0$, $p<0.0001$; Interaction: $F=49.41$, $p=0.0001$; *** = $P<0.001$ vs. day-matched control hASC.

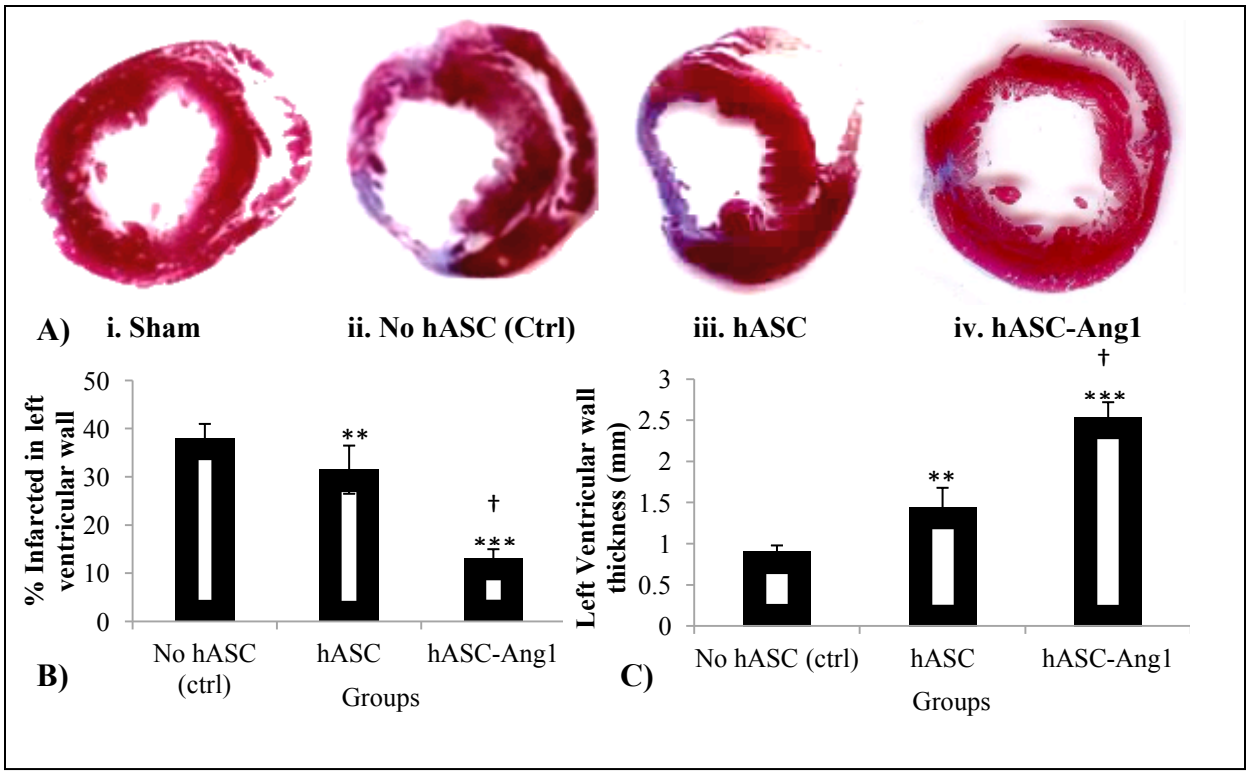

Figure 10.6: (A) Histomorphometric analysis of infarct ventricular scar area. (A. i-iv) Representative images of LV myocardial sections stained with Masson's Trichome show the markedly decreased cardiac fibrosis after hASC and hASC-Ang1 transplantations 28 days post infarction compared to the control. The blue area represents extracellular matrix deposition in the scar tissue and the red area represents the myocardium. (B) Semi-quantitative analysis of the images of the stained collagen fractions in the infarct region, using Image J software, show that hASC and hASC-Ang1 transplantations significantly decreased cardiac fibrosis compared to untreated group (n=8) in terms of percent infarction size in LV wall. (C) Moreover, hASC and hASC-Ang1 groups have significantly thicker LV walls than untreated group. In both analyses, hASC-Ang1 treatment proved to be significantly better than hASC treatment. Data are expressed as mean ±SD. One-way ANOVA analysis: Treatment Groups: $F= 101.3$, $p<0.0001$ (B) and $F= 166.1$, $p<0.0001$ (C). Statistically significant differences between groups compared to control no hASC are indicated as *** = $P<0.001$, ** = $P<0.01$. Significant difference between hASC and hASC-Ang1 is indicated by †= $P<0.001$.

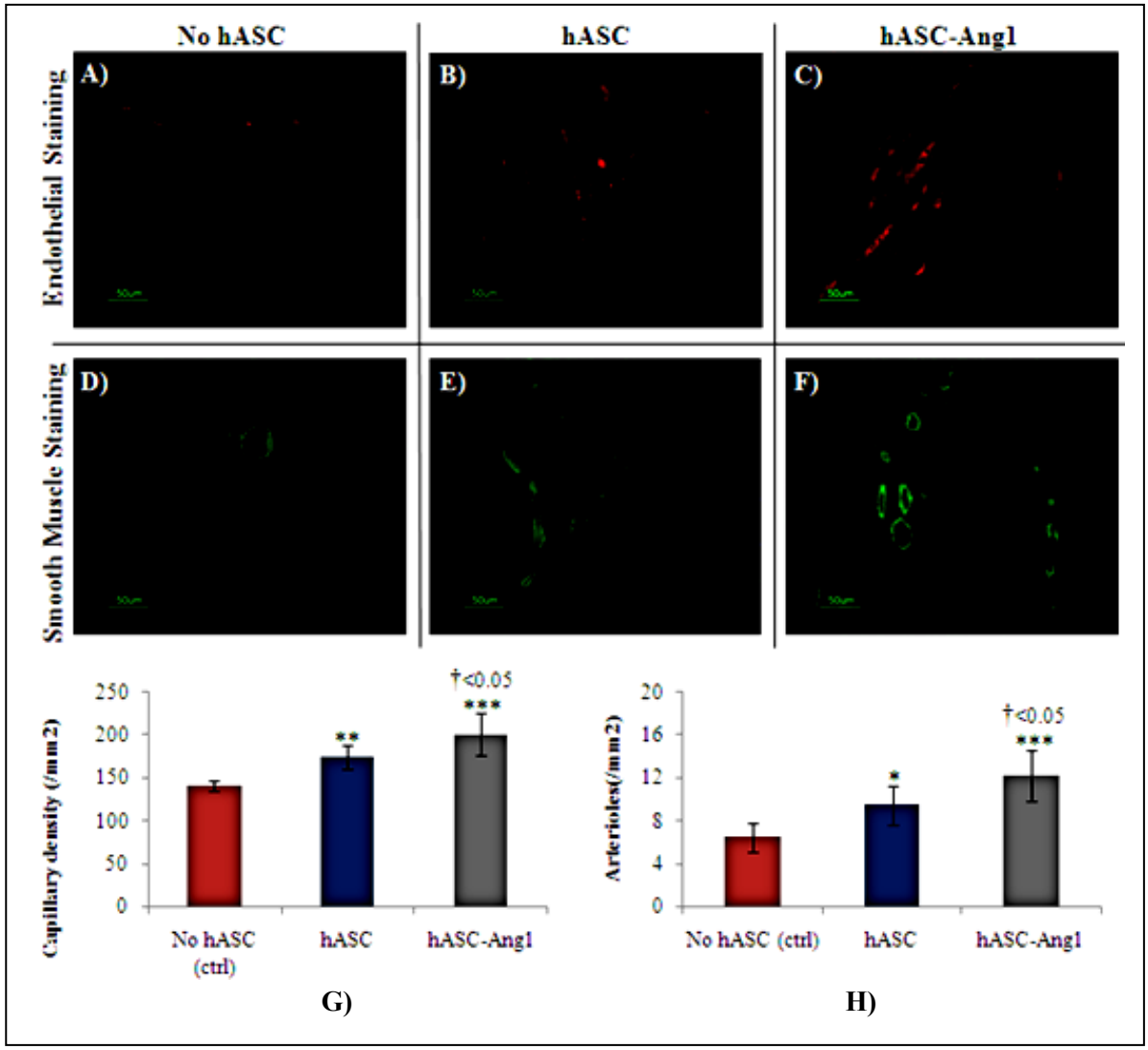

Figure 10.7: Angiogenesis and arteriogenesis in the peri-infarct area. Immunohistological staining of CD31 to detect endothelial cells in (A) no hASC, (B) hASC and (C) hASC-Ang1 groups. Immunohistological staining of smooth muscle α-actin for smooth muscle cells in (D) no hASC, (E) hASC and (F) hASC-Ang1 groups. Quantification of (G) capillary and (H) arteriole density. Data are expressed as mean ±SD. One-way ANOVA analysis: Treatment Groups: $F= 24.86$, $p<0.0001$ (G) and $F= 18.48$, $p<0.0001$ (H). Statistically significant differences between groups compared to control no hASC are indicated as *** = $P<0.001$, ** = $P<0.01$, * = $P<0.05$. Significant difference between hASC and hASC-Ang1 is indicated by †.

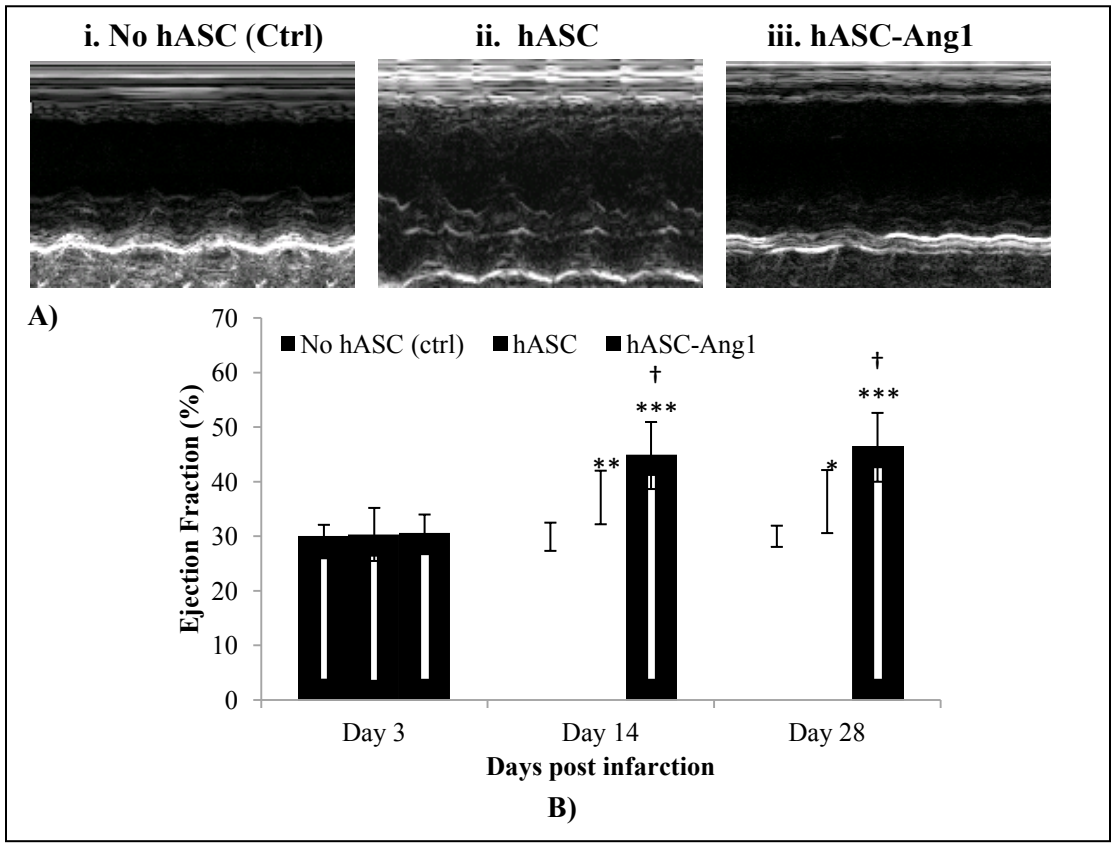

Figure 10.8: Echocardiographic assessment of cardiac function. Effect of Ang1 expressing hASC transplantation on cardiac function was analyzed over 28 days post infarction. For this, heart EF% was monitored at day 3, 14 and 28 after transplantation of medium (n=8), hASCs (n=8) and hASC-Ang1 (n=8) in rat myocardial infarction model using M-mode echocardiograms (**A. i-iii** represents data of day 28**).** As demonstrated in the graph **(B),** the EF% increased significantly after treatment in the hASC-Ang1 and hASC groups over the 28 days post infarction, but the untreated control group did not show any sign of improvement. The EF% was significantly higher in the treated groups compared to the control at day 14 and 28 after treatment. Furthermore, hASC-Ang1 group showed a significantly better EF% than hASC group with time. Mean EF% values ±SD are shown in graph. Echocardiogram analysis 2-way ANOVA: Treatment: F= 13.28, p=0.0002; Time: F=77.95, p<0.0001; Interaction: F=28.47, p<0.0001; Subjects (matching): F= 9.716, p<0.0001; *** = P<0.001, ** = P<0.01, * = P<0.05 vs. time-matched control. † = P<0.01 vs. time-matched hASC.

SUPPLEMENTARY INFORMATION:

Characterization of Bac-NP hybrid complex

The particle size and zeta potential of the NP, Bac and Bac-NP hybrid particles were measured by the technique of electrophoretic laser Doppler anemometry using a Zeta Potential Analyzer (Brookhaven Instruments Corporation**,** HotsVille, New York, USA). ZetaPlus Particle Sizer Software Version 4.11 was used to determine the size distribution of the particles and Zeta Potential Analyzer Version 3.57 software was used for the zeta potential analysis. Both the particle size and the zeta potential were measured for three independent preparations and each measurement was obtained after taking the average of the three runs. Transmission Electron Microscopy (TEM) was used to obtain the size characterization. The nanoparticles were suspended in 1X PBS and analyzed on CM200 FEG-TEM (Philips, Markham, Ontario, Canada). Results are presented in **Figure 10.S1.**

The SEM and AFM photomicrographs in Figure 2A and 2B confirm the formation of NP by TAT and DNA complexation. The formed NPs were further studied by TEM and zeta potential analyzer, as demonstrated in **Figure 10.S1C-F**. The Bac-NP complex was first characterized by measuring the zeta potential of the nanocomplex with laser Doppler electrophoresis (**Figure 10.S1C**). At its natural pH 6.8, the baculoviruses are negatively charged with zeta potential of -6.5±1.4mv. At physiological pH 7.4, the baculoviruses were with a zeta potential of -12.8mv±3.1. On the other hand, prepared Tat/DNA nanoparticles showed high positive charge of 26.5±3.2mv at N/P ratio 3. The positively charged Tat/DNA nanoparticles, upon conjugation with the negatively charged baculoviruses, formed positively charged (5.1±2.7mv) Bac-NP hybrid nanocomplexes.

To reconfirm the successful formation of the Bac-NP complexes, particle sizes of each complex were measured. Free baculoviruses had an average size of 238±10nm, whereas free Tat/DNA NP showed an average size of around 72±4.6nm. The Bac-NP hybrid complexes had an average size of 480±18.2nm. This significant increase in size of the Bac-NP particles, compared to that of free

baculoviruses and nanoparticles, indicates the efficient production of the nanobiohybrid complexes, generated by strong electrostatic interactions of the baculoviruses with the nanoparticles.

In order to look for the morphological evidences for successful conjugation of the budded baculovirus particles with the nanoparticles, TEM was used. Electron micrographs showed the well dispersed NP (**Figure 10.S1D**). On coming in contact with free Bac (**Figure 10.S1E**; the rod-shaped particles with a length of 200–250 nm), there was an instant virus-nanoparticle complex formation by the negatively charged baculoviruses with the positively charged NP, as indicated in **Figure 10.S1F** to form the hybridized Bac-NP complex. The images of Bac-NP complexes also confirm the proper retention of the typical rod-shaped morphological appearance and envelope structure of the baculovirus, suggesting that the baculoviruses were able to sustain their morphological integrity even after hybridization with the NP.

Optimization of viral dose for Bac-NP mediated hASC transduction

In order to achieve maximum transduction, the effect of MOI [Multiplicity of Infection defined as pfu per cell] and their combinatorial effects on the hybrid Bac-NP system were optimized. For this, MOI ranging from 100 to 400 and N/P ratio of 3 were used. Initially, the hASCs were seeded in 6-well plates at $0.5x10^6$ cells/well and incubated overnight at 5% CO_2 and 37^oC. Following this, an appropriate volume of transduction solutions from different experimental groups (Bac_{LacZ}, NP_{LacZ}, Bac_{null}-NP_{LacZ}, Bac_{LacZ}-NP_{LacZ}, Bac_{LacZ}-NP_{null}), suspended in PBS, was added to each well according to varied MOI, and incubated for 4h at 25^oC. Bac_{null} and NP_{null} represents delivery systems carrying DNA with no gene of interest.The wells were replenished with fresh media and grown 37^oC in CO_2 incubator. After 24h, the cells were stained with x-gal to detect the transduced LacZ expressing cells. Results are presented in **Figure 10.S2.**

Bac-NP has no toxic effects on hASCs: cytotoxicity assay

For the cytotoxicity assay, $2x10^4$ hASCs/well were seeded in triplicate for each sample in 96-well plates. After culturing overnight, the cells were washed twice with PBS. 200µl of NP, Bac and Bac-NP particles suspended in culture media were added to the corresponding set of wells. As control, non-transduced cells were used. After 24h, absorbances of each well were measured at 490nm using Cell Titer 96 Aqueous Non-Radioactive Cell Proliferation Assay (Promega) in a plate reader. The percentage of viable cells in different experimental groups was quantified. All the experiments were performed in triplicates. Results are presented in **Figure 10.S3.**

Bac-NP transduced hASCs retain their differentiation potential

Bac-NP transduced hASCs were then seeded in a 24-well plate at a high confluency of 6 x 10^4 cells/well. As control, non-transduced cells were taken. After 24 h, the medium was replaced with either adipogenic or osteogenic differentiation medium (Invitrogen). Osteogenic differentiation was assessed using Alizarin Red staining after a 21-day period of induction towards this lineage. After a 15-day period, adipogenic differentiation was evaluated by LipidTOX Red neutral lipid staining. Results are presented in **Figure 10.S4**.The presence of calcium deposits following osteogenic induction, as well as lipid vacuoles following adipogenic induction, is indicative of the transduced ASCs' ability for multi-lineage differentiation.

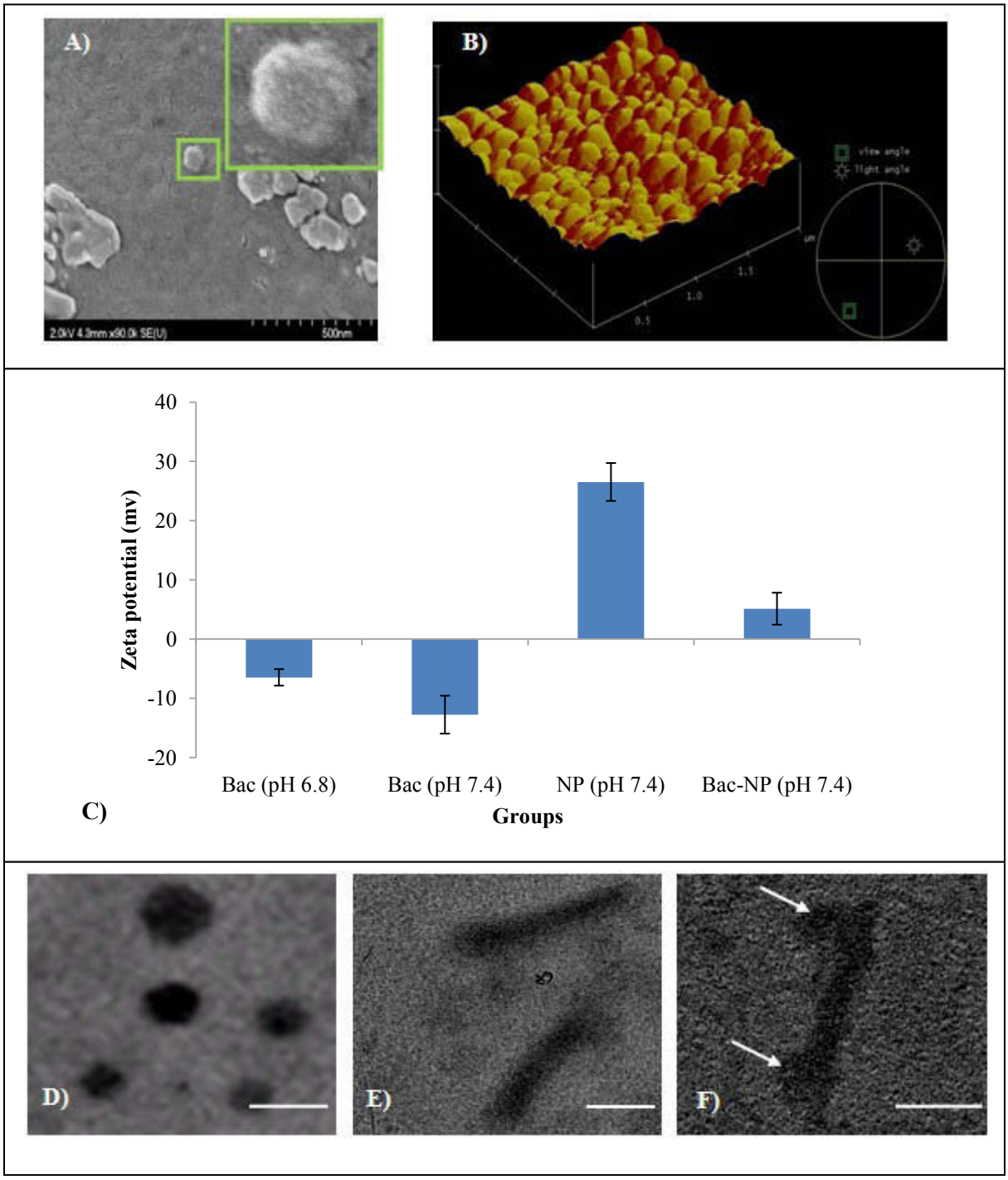

Figure 10.S1: Characterization of the Bac-NP hydrid nanocomplex. (A) SEM photograph of TAT/DNA nanoparticles with subset showing a magnified image. (B) AFM photograph of the nanoparticles demonstrating their surface topography. (C) Zeta potential of free Bac at pH6.8 (pH of insect cells media), free Bac at pH 7.4 (pH of mammalian cell culture), free NP (PBS: pH 7.4) and hybrid Bac-NP

nanocomplexes at pH7.4, with N/P ratio 3. The complexes were prepared from 1µg DNA (complexed with TAT) per 10^9 pfu baculovirus. TEM images of NP (D) with N/P=3, Bac (E), Bac-NP (F) suspended in PBS. Arrows indicate the NPs hybridized on the baculovirus surface. Scale bar: 100nm.

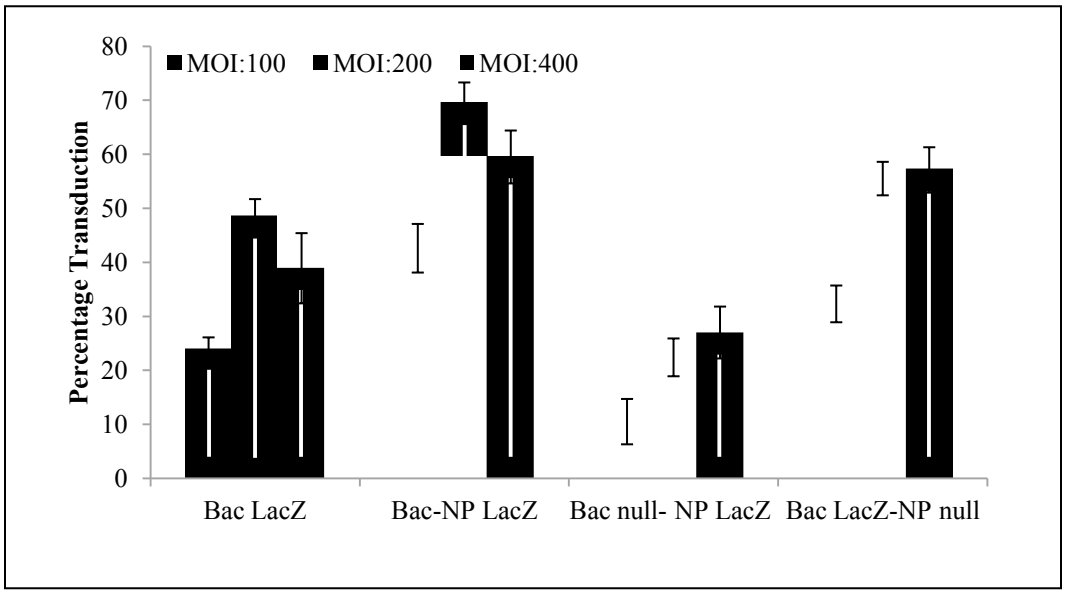

Figure 10.S2: Optimization of transduction condition in hASCs with Bac-NP_{LacZ}. $2x10^4$ cells were seeded in each well of 96 well plates and cultured overnight. The nanobiohybrid complexes were prepared from 1µg DNA (complexed with TAT) per 10^9 pfu baculovirus. Effect of baculovirus MOI on Bac-NP mediated cell transduction. Cells were transduced with the prepared Bac-NP at constant N/P ratio of 3 with MOI of 100, 200 and 400 and stained with X-gal, 24 h post transduction, to determine the percentage cells transduced with LacZ expression. Three independent experiments were performed and the mean ± SD are represented in the graphs. Bac-NP_{LacZ} with MOI of 200 showed highest transduction as compared to other groups.

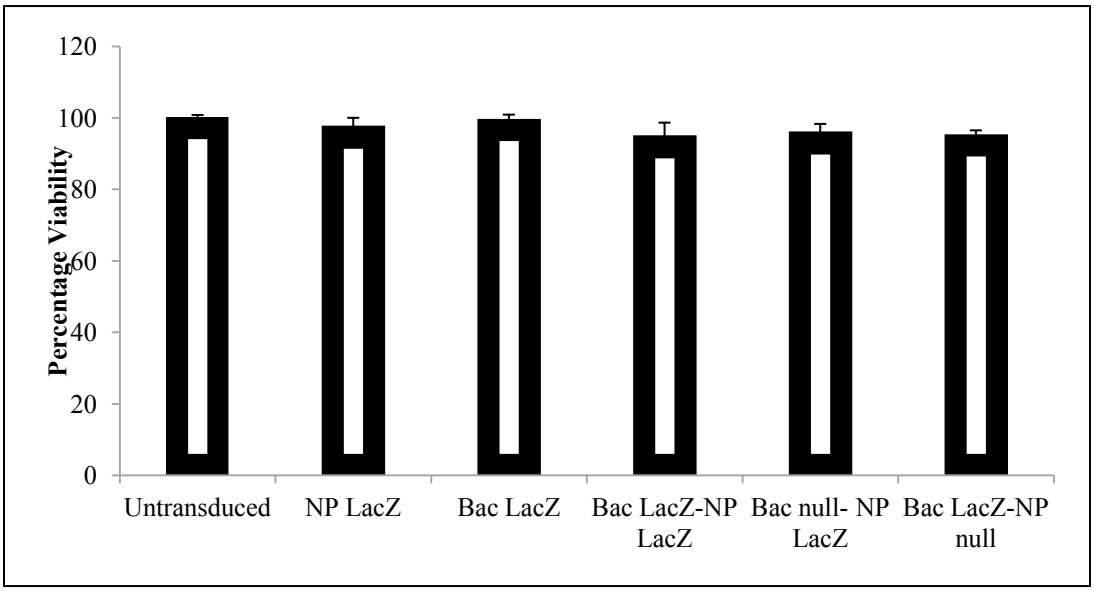

Figure 10.S3: Cytotoxic effects of Bac-NP hybrid complexes on hASCs. $2x10^4$ cells were seeded in each well of 96 well plates and cultured overnight. The cells were incubated with NP (N/P ratio 3) only, Bac (MOI 200) only and Bac-NP (MOI 200 and N/P ratio 3) for 12h followed by cell toxicity analysis. Three independent experiments were performed and the mean ± SD are represented above. There were no significant differences in percentage viability between the groups, confirming that the Bac-NP complex did not have any toxic effect on the hASCs.

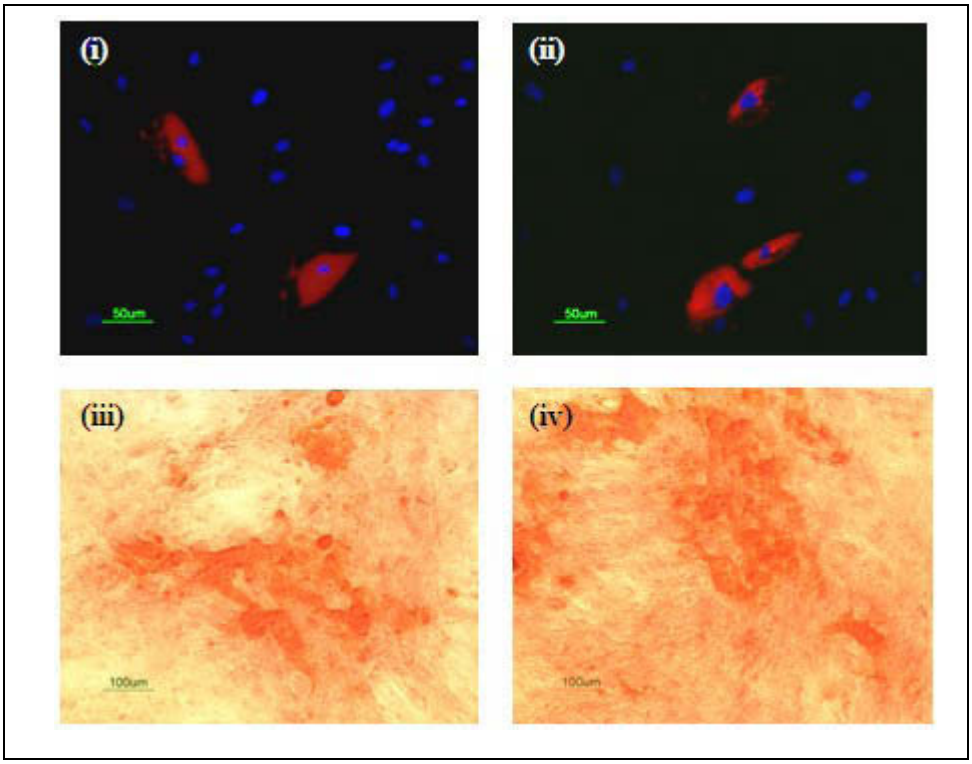

Figure 10.S4: Adipogenic and osteogenic differentiation of Bac-NP transduced hASCs. Transduced ASCs were cultured in either adipogenic or osteogenic differentiation media. Adipogenic differentiation was assessed via LipidTOX Red neutral lipid staining of lipid vacuoles and DAPI staining of nucleus (i. transduced differentiated, ii. non-transduced differentiated), while osteogenic differentiation was determined by Alizarin Red staining of calcium deposits (i. transduced differentiated, ii. non-transduced differentiated). The arrows show the cell differentiated area. The results confirm that hASCs retain their multi-lineage differential potential even after Bac-NP transduction.

Novel gene eluting stent containing Vegf carrying recombinant baculovirus formulated in microspheres: investigation in balloon denuded canine femoral artery

Arghya Paul[1], Dominique Shum-Tim[2], Satya Prakash[1]*

[1] Biomedical Technology and Cell Therapy Research Laboratory, Department of Biomedical Engineering, Faculty of Medicine, McGill University, 3775 University Street, Montreal, Quebec H3A 2B4, Canada.

[2] Cardiothoracic Surgery and Surgical Research, Royal Victoria Hospital, Room # S8.73B 687 Avenue Des Pins Ouest, Montreal, Quebec H3A 1A1, Canada.

*Correspondence author; Email: satya.prakash@mcgill.ca
Tel: +1-514-398-3676; Fax: +1-514-398-7461

Preface: Previous chapters have shown the potential of baculovirus for gene therapy and combined cell based gene therapy for myocardial applications. The present work explores another widely occurring complication related cardiovascular diseases - in stent restenosis. We develop a novel vascular gene-eluting stent using baculovirus formulated in microspheres for controlled local delivery of therapeutics. *In vitro* characterization and histomorphometric & angiogenic analysis from denuded canine arteries shows evidence of high therapeutic efficacy of the developed stent on local vascular biology, significantly attenuating the occurrence of restenosis by promoting endothelial recovery.

Original article filed for ***provisional patent*** **(2012; McGill ROI#12048)**

11.1 Abstract

Stent based gene transfer to enhance the regenerative capacity of endothelial cells offers a promising alternative to widely used antiproliferative drug eluting stent (DES) for the treatment of postangioplasty in-stent restenosis (ISR). The present study, for the first time, explores the potential of insect cell-specific baculovirus as a gene delivery vector for vascular re-endothelialisation and aims to develop a novel baculovirus (Bac) gene-eluting polymer coated stent using microspheres to promote endothelial recovery by local overexpressing vascular endothelial growth factor A-165 (Vegf). We demonstrated that hybridized complex of baculovirus and generation 0 polyamidoamine (PAMAM) dendrimer (Bac-PAMAM) formulated in biodegradable poly(D,L-lactic-co-glycolic acid) (PLGA) microspheres (MS) using water/oil/oil (w/o/o) double emulsion solvent evaporation method significantly enhances gene transfer efficiency for smooth muscle cells (SMCs) and serum stability compared to free Bac. *In vitro* data confirms the efficient gene transfer and expression of biologically active Vegf from the fibrin multilayered stent surface impregnated with Bac_{Vegf}-PAMAM entrapped MS (Coated+ stent group). Site-specific local transgene expression was noticed at proximal, middle and distal stented portions of balloon-denuded canine femoral artery in Coated (+) group at week 2 post implantation, which disappeared when traced at week 16. At week 2, re-endothelialization was eminent and significantly higher in Coated (+) compared to Coated (-) group (Bac_{Null}-PAMAM entrapped MS) (55.36 ± 4.64% vs 37.5± 6.51%, $P < 0.05$; n=3) with further recovery by week 16. There was a significant reduction in neointimal formation (2.23±0.56mm^2 vs 2.78±0.49mm^2 and 3.11±0.23mm^2, p<0.05; n=8) and percent stenosis (61.36±15.15% vs 78.41±13.84 and 87.66 ± 8.54%, $P < 0.05$; n=8) in Coated (+) compared to Control (-) and Uncoated groups as assessed by morphometry and angiographic analysis (54.58±14.1% vs 69.6± 15.51 and 85.4 ± 10.14%, $P < 0.05$; n=8). These data collectively implicate the potential of baculovirus loaded biohybrid stent as a

promising treatment strategy to ameliorate the damaged vascular biology by augmenting endothelial recovery and attenuating intimal hyperplasia.

11.2 Introduction

Percutaneous transvascular coronary angioplasty and stenting is one of the most commonly employed interventional procedures for the treatment of coronary artery disease [402]. A frequent long-term complication of this treatment modality is the phenomenon of ISR which occurs at the site of the atherosclerotic lesion, leading to the obstruction of dialated arteries in 20-30% of patients within 6 months of stenting [403, 404]. The primary contributors of this multifactorial pathological event are incomplete endothelial recovery and vascular SMC proliferation in the inner lining of the artery. Several approaches have been used to improve stent design and durability, such as the use of covered stents to improve biocompatibility of the stent material and intracoronary radiation to inhibit inflammation and proliferation of smooth muscle cells [405-407] . Radiation therapy, although effective, was accompanied by delayed healing and incomplete endothelial recovery; whereas coated stents have not been completely successful in eliminating the problem.

The introduction of DES has been seen as a significant improvement in the existing stent design [408, 409]. The drugs used are mostly antiproliferative which target the smooth muscle cell proliferation and related inflammatory systems. But the direct use of these chemical factors is limited by the problems associated with drug washout, their inadvertent effects on non-target cells, as well as the unselected inhibition of vascular cell division by the drugs leading to incomplete endothelial recovery of stented vessels [410, 411]. Moreover, recent long term meta-analysis of DES studies demonstrating increased risk of late-stent thrombosis has raised questions on the long term safety of DES [412]. As the pathological recurrence of stenosis mainly stem from the endothelial cell lining damage and dysfunction caused by the stent implantation, approaches to promote accelerated re-endothelialization can be of significant importance to reduce the risk of ISR and late in-stent thrombosis [413, 414]. Moreover, this strategy will

evade the harmful consequences of discontinuation of antiplatelet drug therapy which are otherwise needed post DES implantation. Therapeutic induction of vascular cells by transferring proangiogenic vascular genes, such as Vegf, to promote re-endothelization has been proposed as a potent way to attenuate neointima formation and reduce resteonosis [404, 413-418]. Vegf cytokines are a family of endothelial specific mitogenic factors that bind to tyrosine kinase receptors 1 and 2, expressed almost exclusively on the endothelial cells, and widely used for selective proliferation and repair of damaged vascular endothelial structures [404]. Although mammalian viral vectors have been efficiently used for vascular gene therapy, clinical applications are limited due to safety concerns related to risk of inclusion of replication competent viruses and proper optimization of the human tolerization level to these pathogens [419, 420]. Moreover, there are associated problems of immunogenicity due to high viral titre, induction of innate toxicity and inflammatory reactions coupled with the inherent risk of viral integration to the host genome. On the other hand, non-viral gene delivery systems are mainly limited by low *in vivo* gene transfer efficiencies.

The present study extends the findings of previous investigations and introduces a new approach where invertebrate originated insect cell specific recombinant baculovirus has been used to locally deliver Vegf transgene encoding 165-amino acid isoform of human Vegf. Baculovirus offers a unique advantage over other delivery systems because of its ability to efficiently transduce non-dividing cells, inherent inability to replicate in mammalian cells, low cytotoxicity even at high viral dosage, absence of preexisting antibodies against baculovirus in animals and also easy production scale up to high titres [421, 422]. Moreover, as documented in our earlier study, it can be an ideal vector for transient gene therapy applications such as wound healing and endothelial recovery where the expression ceases once its job is done [423]. In order to enhance the gene efficiency we surface functionalized the baculovirus with cationic PAMAM dendrimer synthetic nanoparticles and investigated its effect on transduction efficiency. Furthermore, to protect them from serum inactivation and to achieve a controlled release at the target site, the baculovirus has been encapsulated within

polymeric microspheres and analyzed. A multi layered fibrin-microsphere coated stent platform has been used as the scaffold to deliver the viral vectors. We postulated that this new gene eluting stent formulation can efficiently deliver angiogenic vascular genes to the affected site and induce favorable therapeutic effect in the local vascular biology as illustrated in **Figure 11.1A**. Accordingly, the study assessed the hypothesis by characterizing the device using Vegf carrying recombinant baculovirus followed by evaluating its efficacy to accelerate re-endothelization and attenuate ISR in balloon injured canine femoral artery.

11.3 Materials and methods

11.3.1 Generation of recombinant baculoviruses

The mammalian expression vector pCI and pVL1392 transfer vector were procured from Promega and BD Biosciences respectively. pCMV-XL4 mammalian expression vector carrying human hVEGF cDNA was obtained from Origene Technologies (Rockville, MD). The pVL1392 vector and pCI vector, which harbors the P_{CMV} promoter, were digested with BglII and BamH1 restriction enzymes. The cut out P_{CMV} gene and digested pVL1392 vector were purified and a basic ligation reaction with T4 DNA ligase (Promega) was performed to insert the P_{CMV} gene into the pVL1392 transfer vector by directional cloning method. The pVL1392-P_{CMV} construct was then linearized by Not1 enzyme digestion. It was then ligated in the similar way to the hVEGF cut out of the Not1 digested P_{CMV}-XL4-hVEGF plasmid to form pVL1392-P_{CMV}-hVEGF as the final transfer vector construct. The recombinant transfer vector was then transformed into the high efficiency DH5 α competent *E.coli* (Invitrogen) by heat shock method for amplification. The plasmids were then purified with Qiaprep spin miniprep kit (Qiagen Sciences, MD). The recombinant hVEGF baculoviruses (Bac_{VEGF}) were generated by cotransfection of Sf9 insect cells with linearized baculovirus DNA (BD Baculogold) along with purified recombinant transfer vectors using cellfectin (Invitrogen Life Technologies, Carlsbad, CA) transfection reagent as mentioned in earlier study [423]. The recombinant baculovirus stock (Bac_{VEGF}) was harvested 72 hours post transfection and further amplified using

routine procedures. The viral titre [plaque forming unit(pfu) /mL] of the amplified viral stock was then determined using the Baculovirus Fast Plax Titer Kit (Novagen, Madison, WI) according to the manufacturer's protocol. Similarly, baculoviruses carrying MGFP gene (Bac_{MGFP}) and no transgene (Bac_{Null}) were generated as mentioned in previous work [423].

11.3.2 Preparation methods for virus encapsulation : w/o/o and w/o/w

In order to encapsulate the the viral particles by water-oil-water (w/o/w) double emulsion and solvent evaporation method[270, 424], $5x10^{13}$ pfu was resuspended in 100µl of PBS containing 10% glycerol and 50 mg/ml BSA. This primary w/o emulsion solution was prepared by homogenising the above mixture in 1ml of dichloromethane (DCM) containing 50 or 100 mg of PLGA (poly(D,L-lactic-co-glycolic acid) for 1 min at 10,000rpm using PowerGen Homogenizer 125 (Fisher Scientific). The resulting primary emulsion was added to 3ml of 10% polyvinyl alcohol (PVA) and homogenised for 3 min at 14,000rpm to form the secondary w/o/w emulsion. This solution was further agitated with a magnetic stirring bar in 10ml of of 1% PVA for 4h to evaporate the the dichloromethane. The hardened PLGA microspheres were centirfuged at 9000g for 10 min, washed thrice with PBS and resuspended in fibrinogen solution for further experiments.

In order to encapsulate the the viral particles by w/o/o double emulsion and solvent evaporation method [425], $5x10^{13}$ pfu was prepared as mentioned above. This primary w/o emulsion solution was homogenised in 1ml of DCM containing 50 or 100 mg of PLGA and 1 ml acetonitrile for 1 min at 10,000rpm. The resulting primary emulsion was added to 5ml of corn oil containing 2% span80 and homogenised for 3 min at 14000rpm to form the secondary w/o/o emulsion. This solution was further agitated with a magnetic stirring bar in 10ml of of corn oil containing 2% span80 for 4h to evaporate the the DCM. The hardened PLGA microspheres were centirfuged at 9000g for 10 min, washed thrice with PBS and stored temporarily at $4^{o}C$. The entire mechanism of PLGA microencapsulation of virus particles are demonstrated schematically in **Figure 11.1B**. To visulalize and surface characterize, the microspheres were micrphotographed with scanning

electron microscope (SEM; Hitachi S-4700 FE), as well as with Atomic Force Microscope (AFM) with a Nanoscope III (Digital Instruments, USA) using a silicon cantilever in tapping mode and nanoscope v 5.12r5 image analysis software. To view the inner structure of the virus loaded microspheres, the dried PLGA microspheres were exposed to OsO_4 vapor at room temperature for 24 h in the presence of 1% OsO_4 solution, and then dipped in an epoxy matrix, cured at room temperature for 24 h and microtomed. The ultrathin cross-sections were noticed using Transmission Electron Microscope (TEM; Philips CM200 FEG-TEM).

The encapsulation efficiency of Bac within PLGA microspheres was determined by digesting the PLGA polymer with 1N NaOH for 24h at 4^oC to extract the Bac particles into the aqueous solution [424]. The titre of Bac was then determined by standard Bac titre assay. As an experimental control, another set of experiment was carried out where the free Bac were treated in the similar way with 1N NaOH before determining the viral titre. The encapsulation efficiency was then calculated by dividing the titre of encasulated viral particles by the initial titre of viral particle used. All experiments were carried out in triplicates.

11.3.3 Formulation of Bac-PAMAM nanocomplex

PAMAM dendrimer (generation 0) with ethylenediamine core (MW: 516.68) containing 4 surface primary amino groups was procured from Sigma Chemicals and resuspended in phosphate buffered saline (PBS). The concentration of PAMAM peptide stock solution was initially adjusted to 10 µmol in PBS solution. In order to form the PAMAM-baculovirus nanocomplex, the solutions of the PAMAM and baculoviruses were first brought to room temperature and adjusted to desired concentrations. Then the PAMAM solution and baculovirus solution were mixed according to a desired PAMAM/virus ratio (0, 0.01µmol, 0.1µmol, 0.5 µmol and 1.0 µmol PAMAM molecules per 10^8 baculovirus). The mixture was incubated at room temperature for 30 min to form complexes, with gentle vortexing from time to time. The mixture was further centrifuged at 24,000rpm for 45min, and the pellet containing the heavier Bac-

PAMAM nanocomplex was collected, leaving the unreacted excess dendrimer in the supernatant. The collected Bac-PAMAM was washed twice using PBS using the same centrifugation process. For every experiment, the preparation was freshly made.

11.3.4 Stent coating formulation

Firstly, the baculovirus was coated with PAMAM (0.5 µmol) and formulated in PLGA microspheres by w/o/o method. The prepared PLGA microspheres were resuspended in 5mg/ml of bovine plasma derived fibrinogen, supplemented with aprotinin (20µg/ml) to reduce fibrin degradation, and loaded in a 3ml syringe with a 0.2-mm nozzle. The balloon expandable bare metal stainless steel stents with basic dimensions of 16mm x 3.5mm (Liberte Monorail stent, Boston Scientific, Mississauga, Ontario) was first mounted on a PTFE (polytetrafluoroethylene) mandrel that was driven by a rotator. The loaded aqueous fibrinogen mixture in the syringe was then gradually drip-coated on the surface of the mounted stent layer by layer (0.2 ml of Bac loaded aqueous fibrinogen per layer). In between every layer, 0.05ml of thrombin solution (20U/ml) was added all over the stent surface using a micropipette with 200µl micropipette tip and waited for 15 min to form thin fibrin gel layer. Polymerization of the fibrin occurred around the stent which completely encased the stent (**Figure 11.1**). The stent was subsequently coated with a top layer of fibrinogen (2.5 mg/ml) cross-linked with genipin (0.045 mg/mL final) followed by polymerization with thrombin. The process resulted in a microsphere impregnated fibrin coated stent loaded with $5x10^{12}$ pfu Bac. The device was then crimped onto standard collapsed angioplasty balloon and delivered to the femoral artery. To visualize the PLGA microspheres impregnated on the fibrin coated stent surface (without the topmost fibrin/genipin layer) under fluorescence microscope (Nikon Eclipse TE2000-U), 1 mg Nile red was mixed in the PLGA /dichloromethane solution before preparing the microspheres and fabricating them on the stent. Similarly, the stents were also observed under SEM to envisage the

surface topography. As control for *in vitro* transduction study, free virus containing fibrinogen complex were coated on the stents.

11.3.5 *In vitro* transduction via stent

The stents with different formulations were crimped on the balloon catheter and inflated in scintillation vials containing 5ml of phosphate buffer saline (PBS) solution (pH 7.4) with 9 atm pressure. The expanded stent was incubated at 37^{o}C for 24h, with constant agitation at 100 rpm. The PBS solutions containing the released viruses were collected at 12h, 18h and 24h post incubation.

The 12h incubation buffer was diluted and added at MOI of 250 to 1x10^{6} seeded human aortic artery smooth muscle cells (HASMCs; Sciencell, Carlsbad, California, USA) after removing the standard smooth muscle cell media (SMCM) provided by the supplier. The 18h and 24h incubation buffers were similarly diluted with same dilution factor and added to HASMCs. After incubating the cells with the stent incubation buffer for 8h, the buffers were aspirated and replenished with complete growth medium for 24h. After fixation, microphotographs were taken and the total cell numbers were determined per 200X magnification under bright field. GFP-expressing cells were also visually counted in the same fields, and results reported as the percentage of cells transduced (mean±SD) of at least five fields per culture in triplicate cultures.

To check the inactivation effect of serum on baculovirus present on the stent surface, the virus loaded stent with different formulations were incubated in 50% FBS or PBS for 1h. This was followed by addition of the viruses resuspended in fresh PBS to 2x10^{4} HASMCs per well in 96 well plate with an MOI of 250 for checking the GFP expression as mentioned above. 24h post transduction, the fluorescein expressions per well were quantified using plate reader Victor3 Multi Label Plate Counter (Perkin Elmer, USA) in terms of normalized percentage GFP expression. The experiments were performed with triplicates.

To check the effect of storage conditions on stent bioactivity, the stents were stored in cryovials for 3 months at different temperatures (4^{o}C, -20^{o}C and -

80°C). As control, freshly prepared stent was taken. After thawing, the stents were balloon expanded and incubated for 24h in PBS solution in scintillation vials as mentioned earlier. The PBS solution was collected from the release vials and added to $2x10^4$ HASMCs per well in 96 well plate with an MOI of 250 as mentioned above. The fluorescein expressions after 24h were detected in plate reader and presented as normalized percentage GFP expression.

11.3.6 *In vitro* transduction via Bac_{Vegf}-PAMAM loaded stent

VEGF release kinetics from transduced cells

In order to investigate the Vegf release kinetics from transduced HASMCs, three types of stents (Bac_{Vegf}-PAMAM, Bac_{Vegf} only and ctrl stent with no virus) were expanded in PBS solution using balloon catheter and incubated for 24h as illustrated earlier. The PBS solution containing the released viruses were collected and added to $1x10^6$ HASMCs seeded per well in 6 well plate with an MOI 500. This was followed by 8h incubation at 25°C with subsequent replenishment of the incubated cells with fresh culture media. The conditioned media were collected on day 0, 2, 4, 9, 12 and 15 post-transduction and quantified for Vegf expression using hVegf ELISA kit (R&D Systems).

HUVEC proliferation assay

For the cell proliferation assay, $2x10^4$ Human Umbilical Endothelial Cells (HUVECs) /well were seeded in triplicate for each sample in 96-well plates. After culturing for 8h in standard endothelial cell media (ECM), the cells were washed twice with PBS. 0.1ml of CM from transduced HASMCs (Day 4 CM from Bac_{Vegf}-PAMAM, Bac_{Vegf} only and ctrl stent with no virus groups) with and without hVegf antibodies (Ab) along with 0.1 ml of fresh ECM without cell growth supplements were added to the corresponding set of wells. Similarly, CM from unstimulated control group mixed with fresh ECM was taken as the control group. After 3 days of culture, absorbance was measured at 490nm using Cell Titer 96 Aqueous Non-Radioactive Cell Proliferation Assay (Promega) in a plate reader as mentioned in previous study [423]. This assay was also used to measure the cytototoxic effects of stent-released baculoviruses towards HASMCs.

Wound healing assay

HUVECs were seeded into six well plates and grown to confluency. After 24 hr of serum starvation, the monolayer was carefully mechanically wounded with a 200ul pipette tip. The wells were then washed twice with PBS to remove the cell debris and the seeded cells were replenished with 0.1 ml of the fresh ECM (without cell growth supplements) and 0.1ml of the CM from different groups (CM from day4 Bac_{Vegf}, Bac_{Vegf}-PAMAM and ctrl unstimulated group), in presence or absence of 1µg/mL Vegf antibody. Following HUVEC migration for 12h, the cells were fixed with 4% paraformaldehyde and stained with crystal violet. The wound healing was visualized under inverted bright field microscope and microphotographs with 100X magnification were taken. The number of cells which had moved across the starting line (mean ± SD; n=3) in each group was assessed and analyzed using ImageJ software to measure the wound healing as mentioned earlier[423].

HUVEC Tube formation Assay

In vitro angiogenesis assay was performed using Cell Biolabs Endothelial Tube Formation Assay as mentioned elsewhere [426]. Briefly, 50µl of ECM gel prepared from Engelbreth–Holm–Swarm (EHS) tumor cells were added to the 96well plate and incubated for 1 h at 37^{o}C to allow the gel to solidify. 2x10^{4} cells suspended in CM from different groups (Day 4 CM from Bac_{Vegf}-PAMAM, Bac_{Vegf} only and ctrl stent with no virus groups), in presence or absence of Vegf antibody were seeded per well. After 18h incubation period, media were removed and the cells were then incubated with 50µL of 1X Calcein AM for 30 mins at 37^{o}C. The cells were washed twice with 1X PBS and the endothelial capillary-like tube formation in each well was examined using a fluorescent microscope under 100X magnification and the HUVEC-made capillary network was analyzed by ImageJ software. The results were quantified as the mean relative tubule length/view field ± SD, taking total tubule length/view field from control group as 100.

11.3.7 *In vivo* surgical procedures for arterial injury and stent implantation

All procedures were in compliance with the Canadian Council on Animal Care and McGill University animal use protocol, following all the ethical guidelines for experimental animals. Adult beagle dogs (Marshall Farms, North Rose, NY) weighing 9.5 to 11 kg were used in this study.

One week before the surgery the animals were treated daily with aspirin (325mg/day) along with normal 21% protein dog diet (Harlan, Montreal, Canada) to avoid thrombosis. A total of 28 stents were implanted bilaterally in deep femoral arteries of 14 dogs in a randomized, blinded fashion following denudation of the arterial endothelial wall, with contralateral arteries receiving stents from different groups. The animals were divided into three groups: fibrin coated stent loaded with microencapsulated PAMAM-Bac_{VEGF} virus [Coated (+); n=11 stents per group), fibrin coated stent loaded with microencapsulated PAMAM-Bac_{Null} virus [Coated (-); n=11 stents per group] and bare metal stent (Uncoated; n=8 stents per group). To confirm the transgene delivery and re-endothelization, animals from first two groups were sacrificed (n=3) after 2 weeks and arteries were harvested. The remaining animals were sacrificed after 6 weeks for further analysis.

On the day of the stent implantation, after subcutaneous pre-anesthetic medication with butorphanol (0.2mg/Kg), acepromazine (0.125 mg/Kg) and atropine (0.025mg/Kg), the dogs were subjected to general anesthesia with sodium pentobarbital (20mg/Kg, injected intravenous via catheter along with the lactated Ringer's fluid) and endotracheal intubation for mechanical ventilation and isoflurane (2-3% along with supplemental oxygen) for anesthetic maintenance. Denudation of the femoral arterial endothelial layer and stent implantation was performed according to the procedure performed in earlier studies [427, 428]. Briefly, the dog, placed in supine position under anesthetized condition, was administered intravenously with heparin (30U/Kg) as blood thinner. Under sterile conditions, the superficial femoral arteries on both legs were surgically exposed and held in position by surgical clips. Continuous monitoring of blood pressure (iBP), respiration, temperature, pulse oximeter

oxygen saturation (SpO2), hemodynamic and surface electrocardiograms were performed throughout the experimental procedure using patient monitoring system (Bionet Vet, QST Technologies, Singapore). The artery lumens were flushed with PBS to avoid mixture with arterial blood. On the basis of angiograms, femoral segments with comparable diameters were selected on both legs so that the stent-to-artery diameter ratio remains approximately 1.3. After an arteriotomy, a fogarty arterial embolectomy balloon catheter (Edwards Lifesciences Canada Inc, Ontario) was infused through the saphenous arteries and advanced to the two preselected femoral segments and secured with a tie as mentioned elsewhere [419]. This was followed by severe balloon injury of the inner lumen of the artery with inflated balloon (balloon/artery ratio 1.2:1) to induce endothelial abrasion. Eventually the balloon catheter mounted stents were inflated at the sites of endothelial damage in the femoral arteries with nominal pressure (9 atm) for 1 min and was then slowly withdrawn leaving the stent in place. After stent deployment and closure of the arteriotomy site with 7-0 prolene suture, doppler ultrasound probe was used to check the vessel patency and confirm normal blood flow through of the stented arteries. The experimental animal is then extubated and administered with Buprenorphine (0.02mg/Kg, subcutaneously) analgesic for 1-2 days. 3 animals were euthanized by overdose of sodium pentobarbital (200 mg/Kg, intravenous at week 2, while the remaining at week 16.

11.3.8 Analysis of transgene expression

RT-PCR analysis

At week 2 post stent placement, the stented femoral arteries (n=3 stents/ group) were harvested from Coated (+) and Coated (-) groups and divided laterally into three sections (proximal, mid and distal) after removing the stents. A part of the sections were used to detect hVegf transcript by RT-PCR, while the remaining parts were used for to detect the hVegf protein by immunostaining and reendothelization by staining. Similarly, sections were also collected at week 16. For detection of Vegf gene expression, total RNA was extracted from stented

artery samples (stored in RNAlater, Qiagen) using RNA Extraction kit (Qiagen) according to the manufacturer's instructions. The obtained RNA was quantified and reverse transcribed to Vegf cDNA using the Qiagen's Reverse Transcription (RT) kit following the supplied instructions. PCR amplification was performed on the reverse transcribed product using Taq DNA Polymerase (Invitrogen) and forward primer (5'CTTGCCTTGCTGCTCTACCTCC3') and reverse primer (5'GCTGCGCTGATAGACATCCATG3') for hVegf gene (112-bp product). Amplifications were carried out for 25 cycles at 94 ^{o}C for 35 s (denaturation), 57^{o}C for 35 s (annealing), and 72^{o}C for 25 s (extension).

Immunohistochemical studies

For immunostaining, paraffin embedded 5µm sections were deparaffinised, blocked with donkey serum and incubated over night with 1:50 dilution of rabbit anti-hVegf (Santa Cruz Biotechnology Inc., Santa Cruz, California) primary antibodies. On the second day, the slides were thoroughly washed with wash buffer and incubated with donkey anti-rabbit IgG-FITC (Santa Cruz Biotechnology Inc.) with 1:200 dilutions for 1 hour. The proportions and intensities of FITC-positive regions in the tissue sections, as seen under fluorescence microscope (Nikon Eclipse TE2000-U), gave a qualitative idea of the relative amount of hVegf expressed in the stented vascular tissue regions due to the transgene delivery from stent platform.

11.3.9 Assessment of stent re-endothelization

Evans blue staining

Two weeks after stent deployment animals were anesthetized (n = 3 , Coated +and -) and a portion of the harvested artery was incubated in 1% Evans blue (Sigma-Aldrich, Dublin, Ireland) for 15min, followed by washing ,fixing and examining longitudinally using image software as mentioned elsewhere [429].

Scanning electron microscope

Re-endothelialization was also assessed at 2 week and 16 week post implantation (n = 3 each). Retrieved stents were washed with saline, fixed in 4%

paraformaldehyde and longitudinally incised as above and examined using scanning electron microscopy (SEM).

Histological assessment

Stents were retrieved after twelve weeks and harvested vessels were embedded in methylmethacrylate plastic (Accel Lab Inc, Quebec, Canada and McGill SAIL Lab). After polymerization, the proximal, mid and distal sections of the stents were cut into 5µm sections and stained with hematoxylin and eosin. Re-endothelialization was assessed directly under the microscope by a histologist blinded to treatment. Endothelial coverage was expressed as the percentage of the average lumen circumference covered by the endothelial cells [429].

11.3.10 Assessment of ISR

Angiogram analysis

Initial and follow-up angiograms were performed with fluoroscopic angiography (GE Stenoscop) using Omnipaque Iohexol contrast dye in anterior oblique projection and percent diameter stenosis at follow-up was calculated by (minimal stent diameter at follow-up/ the mean diameter of the stent at full expansion) x 100, using standard procedure as described elsewhere [430]. Sections were also used to evaluate the presence of inflammation and vessel wall injury at the stented sites of all the groups by injury and inflammation score method [431].

Morphometric analysis

Retrieved vessels were embedded in methylmethacrylate plastic, cut into thin sections as mentioned earlier, and stained with elastic Van Gieson stain. All sections were examined by light microscopy and photographed to quantify the neointima formation and stenotic area using methods mentioned elsewhere [431, 432].

11.3.11 Statistical analysis

Quantitative variables are presented as mean ± Standard Deviation (SD) from independent experiments as described in the figure legends. Statistics were

performed using student's t-test or one-way ANOVA by Bonferroni's multiple comparison post-hoc test. All statistical analyses were performed with Prism 5 (GraphPad Software). P value <0.05 was considered significant.

11.4 Results

11.4.1 Encapsulation of baculovirus in PLGA microspheres

In order to encapsulate the baculoviruses, the method of preparation and energy source required for formation of the primary emulsion were studied extensively and optimized in vitro. Bac was added to PLGA dissolved in DCM and the mixture was either sonicated or homogenized in presence or absence of BSA/glycerol. By comparing these preparation methods we tried to figure out the best way to efficiently encapsulate the baculovirus without damaging its bioactivity. We checked the viral titre before and after encapsulation in order to measure the encapsulation efficiency. As the viral titre measures only the amount of active virus, the data represented as the amount of encapsulated virus denotes the actual number of active virus, and not the overall number which will consist of both active and inactive/disrupted viral particles. Our data, as presented in **Table 11.1**, reveals that sonication method did not increase the encapsulation efficiency; in fact, it has a deleterious effect on the viral viability compared to mechanical homogenization technique. This may be because the high energy ultrasound produced by the sonicator disrupts the viral surface while preparing the MS, which leads to reduced viability and encapsulation efficiency of active virus. On the other hand, homogenization technique produces the water oil emulsion in a much simpler mechanical agitation method which resulted in lesser loss of active virus. To further improve the encapsulation method, BSA/glycerol was mixed with the viruses to increase the virus stability, to enhance their steric hindrance against the harsh external shear stress during MS preparation and for better cryopreservation.

We next asked if the second emulsion solvent or the continuous phase can affect the encapsulation efficiency. We used hydrophobic (corn oil) solvent for second emulsion step and compared it with standard hydrophilic (PVA) solvent.

Oil was selected instead of water in order to reduce the viral loss in the second emulsion phase and subsequent solvent evaporation step. A significantly higher amount of encapsulation efficiency was noticed in the w/o/o method which confirms that there was less viral loss using oil compared to water in the continuous phase. The particle diameters were checked for every preparation which varied between 5-10µm. Thus, as evident from **Table 11.1**, we concluded that a w/o/o double emulsion procedure using mechanical homogenizer can efficiently encapsulate the baculoviruses which can be further enhanced by supplementing them with BSA/glycerol to protect the viral activity.

SEM photomicrographs were taken to confirm the formation of spherical shaped virus loaded microparticles (**Figure 11.2A and 2A'**), while the AFM images (**Figure 11.2B. i and 2B. ii**) identifies the regular, uniform and consistent surface topography of the microspheres. TEM images demonstrate empty and baculovirus loaded microspheres, while **Figure 11.2E** reconfirms the successful microencapsulation procedure showing the entrapped baculoviruses in the cut section of a virus loaded PLGA microsphere.

11.4.2 Baculovirus eluting stent: physical characteristics and *in vitro* release profile

The prepared polymer coated stents containing the PLGA microspheres (by w/o/o method), mixed with Red Nile dye as tracer, were air dried and photographed to confirm that the polymeric stent was able to hold the embedded microspheres after stent expansion. **Figure 11.3A and 3B** shows a stent before and after coating with MS embedded fibrin layers, while the pinkish color of the stent in **Figure 11.3C** confirms retention of the loaded MS on the stent surface post stent expansion using balloon catheter. A fluorescence image of the coated stents under fluorescence microscope (Nikon Eclipse TE2000-U) as shown in the **Figure 11.3D** further confirms the above findings, where a uniform coating of the microspheres was seen on the stent surface. SEM images of the stents (**Figure 11.3E-3G**) provided further morphological evidence on the surface characteristics of the coated stents demonstrating the uncoated bare metal stent struts (**Figure**

11.3E), plain surface of the uniformly coated stent struts with fibrin multilayers (**Figure 11.3F**) and evenly distributed PLGA MS embedded on the fibrin multilayered stent strut surfaces.

To determine the release kinetics of the encapsulated baculoviruses from the stent surface and modulate their release behavior, two different PLGA concentrations (50 and 100 mg/ml of DCM) were used using w/o/o emulsion method and compared with standard w/o/w method.

In both the methods the stent group with MS prepared from lower PLGA concentration showed much faster and higher percentage of viral release with time compared to the higher concentration (**Figure 11.3H**). Moreover, w/o/o group showed significantly higher release of active virus at lower PLGA concentration than w/o/w group, 24h post- incubation in PBS. A further decrease in PLGA concentration led to non-uniform MS formations and hence we restricted to 50 mg/ml DCM PLGA MS formulation protocol using w/o/o method for further studies.

11.4.3 Baculovirus surface functionalization with PAMAM dendrimer enhances transduction

To confirm the successful formation of Bac-PAMAM complex, zeta potential of the nanocomplexes were measured as shown in **Figure 11.4A.** At pH 7.4, the zeta potential of the free baculoviruses was negatively charged with a zeta potential of -13.4mV±0.6. The positively charged PAMAM dendrimers, upon conjugation with the negatively charged baculoviruses, formed nanocomplexes which resulted in an increment of surface charge towards positive. Bac-PAMAM (0.01) showed a zeta potential of -10.6±1.8 mv, while Bac-PAMAM (0.1) showed -2.36±2.2mv, Bac-PAMAM (0.05) showed 8.7±2.4mv and Bac-PAMAM (1.0) showed 11.5±4.7mv, where the values within brackets indicate the ratio of PAMAM/virus used in preparing the nanocomplexes. This was further confirmed by measuring the particle size of the formed nanocomplexes (**Figure 11.4B**). Free baculovirus showed an average size of 226±17.6nm, while Bac-PAMAM (0.01) showed a size of 228.5±30.8 nm, Bac-PAMAM (0.1) showed 588±54.1nm, Bac-

PAMAM (0.05) showed 328±29.5nm and Bac-PAMAM (1.0) showed 289±27nm. The significantly increased size of the Bac-PAMAM (0.05) particles compared to the free baculovirus indicates the efficient formation of Bac-PAMAM nanocomplexes, generated by strong electrostatic interactions between baculovirus and PAMAM dendrimers. The excessively bigger size in Bac-PAMAM (0.1) group is probably because of the formation of larger aggregates and clumps of the formed complexes. To reconfirm the complex formation, TEM images the products were taken for morphological evidences. **Figure 11.4C and D** demonstrates the efficient binding of the rod like baculovirus with PAMAM dendrimers (0.05) leading to the formation of stable Bac-PAMAM hybrid complex.

11.4.4 Baculovirus-PAMAM eluting stent: *in vitro* release, transduction and cytotoxicity analysis

To investigate whether the released Bac_{MGFP} were bioactive and can transduce the HASMCs, the incubation buffers from different release time points were collected, diluted in same proportions and added to HASMCs for transduction. After 72h, the GFP expressions were quantified in terms of percentage cells transduced. For the study, four different baculovirus formulations using varied concentrations of PAMAM dendrimers were prepared before encapsulating and loading them on the stent surface. The data in **Figure 11.5A to 11.5E** demonstrate that PAMAM dendrimer functionalization has a positive effect on baculovirus mediated transduction with Bac_{MGFP}-PAMAM (0.5) showing consistently higher transduction efficiency than other groups, including free Bac_{MGFP} (control). Further increasing the PAMAM concentration in Bac_{MGFP}-PAMAM (1.0) however did not show any significant improvement. Moreover, the percentage of transduction was proportional to hour of incubation buffer. This is because of the higher amount of baculovirus released in the incubation buffer with higher incubation time, although there were no significant differences in transduction efficiencies between 18h and 24h in all groups. This indicates that the active viruses were mostly released within 12h to 18h from the stent.

Furthermore, 72h cytotoxicity studies on the effect of these different formulations on HASMCs show that Bac_{MGFP}-PAMAM can be safely used for cell transduction, although Bac_{MGFP}-PAMAM (1.0) group with high PAMAM concentration showed significantly high cytotoxicity compared to the control (**Figure 11.5F**).

11.4.5 Effect of serum and storage condition on bioactivity of the stent

The *in vivo* applications of baculovirus are limited mostly because of their serum inactivation. Thus, to check our formulations we incubated the stents in 50% FBS for 1 h followed by incubation in PBS for 24h. As control, 50% FBS was replaced by PBS solution. The incubation buffer was then used to transduce the HASMCs as mentioned earlier and GFP expression was detected and quantified using plate reader. **Figure 11.6A** shows that compared to control PBS, serum has an inactivation effect in all the groups which was more distinct Bac_{MGFP} stent control group where baculoviruses were loaded directly on the stent surface without microencapsulation. In the Bac_{MGFP} MS stent group, there was much higher GFP expression compared to Bac stent in presence of serum demonstrating that the MSs were able to protect the entrapped baculoviruses against serum inactivation. However, Bac_{MGFP}-PAMAM MS stent group showed highest GFP expression and hence, highest protection against serum. This may be because of the combined effect of the MS encapsulation and PAMAM coating on the viral surface.

To further understand whether the prepared stents can be stored under different storage conditions, they were stored under different temperature conditions for long term storage of 3 months. After thawing and incubation in PBS solution, the incubation buffers were used to transduce the HASMCs as described earlier. **Figure 11.6B** demonstrates that -80^{o}C is ideal for long term storage compared to storage at 4^{o}C and -20^{o}C, although there was significant difference in GFP expression when these groups were compared to freshly prepared one.

11.4.6 Quantification and functional analysis of expressed hVegf from transduced HASMCs

Conditioned media, collected from Bac_{Vegf}-PAMAM (0.5) and Bac_{Vegf} transduced HASMCs at regular intervals, were used to quantify and detect the Vegf release profile using a hVegf ELISA. CM from non-transduced cells was taken as the negative control. The data, as shown in **Figure 11.7A**, demonstrates rapid expressions of hVegf in Bac_{Vegf}-PAMAM and Bac_{Vegf} groups in the first 4 days which gradually decreased over the week. Although Vegf expression decreased considerably in Bac_{Vegf} group after three weeks, Bac_{Vegf}-PAMAM group maintained significantly higher Vegf expression.

The bioactivities of the released hVEGF in media from the Bac_{VEGF}-PAMAM (0.5) transduced HASMCs were evaluated *in vitro* by observing the proliferative capacity of the HUVECs. Cell Proliferation MTS Assay kit was used to assess the proliferation capabilities of the HUVECs treated with CM (containing secreted hVEGF) from experimental samples, collected on day 4 post transduction. As shown in **Figure 11.7B**, groups Bac_{Vegf} and Bac_{Vegf}-PAMAM showed significantly high HUVEC proliferation on day 3 compared to unstimulated control, with Bac_{Vegf}-PAMAM exhibiting the highest proliferation ($3.98\pm0.19x10^4$ cells). As expected, group treated with antibodies against hVEGF showed no proliferative effects proving that it was because of the bioactivity of released hVEGF from genetically modified SMCs that contributed to the drastic HUVEC proliferations. This proliferation rate was directly dependant on the amount of the VEGF released which explains why Bac_{Vegf}-PAMAM demonstrated better results than Bac_{Vegf} and unstimulated control groups.

Similar results were noticed in the wound healing assay where the abilities of CM from different experimental groups, collected on day 4 post transduction, to promote HUVEC migrations were measured. As depicted in **Figure 11.7C**, stimulation of wounded HUVEC monolayer with CM from Bac_{Vegf}-PAMAM exhibited significant healing of wounded area ($89.4\pm7.5\%$) compared to CM from unstimulated control ($12.4\pm2.4\%$) and Bac_{Vegf} ($61.7\pm5.5\%$). Pre-incubation of CM with the neutralizing anti-VEGF antibodies completely hindered Bac_{Vegf}-

PAMAM CM induced wound healing, clearly suggesting that chemotactic signals from hVEGF are required for proper wound healing effect.

In addition, the biologic activities of the CM were also evaluated by HUVEC tube formation assay. As illustrated in **Figure 11.7Di**, cells treated with CM from Bac_{Vegf}-PAMAM induced significantly enhanced effect on HUVEC capillary network formation as compared to the cells treated with CM from Bac_{Vegf} and unstimulated groups. The relative tubule length was significantly enhanced in Bac_{Vegf}-PAMAM and Bac_{Vegf} group compared to control (141.5 ± 7.9 and 100 ± 13.6 vs 47±2.1). Also, to assess the extent of impact of hVegf present in the CM on HUVEC tube formation, anti-VEGF antibody was added to the supernatant with released CM. A significantly reduced tube formation was observed which provides evidence of the strong pro-angiogenic nature of VEGF present in the CM. Similar results were also noticed when total capillary tubule numbers were quantified in Bac_{Vegf}-PAMAM and Bac_{Vegf} group and compared to unstimulated control (15.5 ± 3.4 and 10.1 ± 2.2 vs 4.5±0.7) in **Figure 11.7Dii**.

11.4.7 Detection and localization of Vegf expression *in vivo*

The *in vivo* stent implantation procedure has been demonstrated in **Figure 11.8A**, where the dogs underwent bilateral femoral artery denudation by balloon angioplasty (**Figure 11.8Ai and i**), followed by stent deployment at the injured site (**Figure 11.8Aiii**). Stented femoral arteries transduced with Coated (+) and Coated (-) were harvested 14 days after stent placement. Following qualitatively reverse transcriptase-PCR analysis, hVegf signal expression could be observed in all the proximal, middle and distal sections of the Bac_{Vegf}-PAMAM (Coated+) transduced arteries examined (n = 3 vessels), while nothing was detected in Bac_{Null}-PAMAM (Coated-) transduced arteries (**Figure 11.8B**). Although, the RT-PCR product from 2 weeks Bac_{Vegf} -transduced tissue samples demonstrated the presence of the appropriate-sized band for hVegf in the stented artery sections, no bands were detected from 16 weeks samples proving that the transgene expression is transient and disappears over time. Moreover, artery sections from 1 cm proximal and distal to the stented artery did not show any transgene expression, thus indicating that the gene delivery was localized and restricted to the stented

region where the virus containing polymer coated strut touches the inner wall of the artery.

Stent-based delivery of Bac_{Vegf} to the canine femoral arteries resulted in localized overexpression of Vegf. This transgene expression was localized to the areas around the stent struts in the intimal and medial layers as demonstrated elsewhere with β-galactosidase gene delivery using adenovirus and adeno associated virus-coated stents [433]. The expression detected on day 14 was localized near the stent strut region, mainly on the medial side where the polymer of the stent touches the arterial surface; in contrast, there was no Vegf staining observed in the stented arteries treated with Coated (-) stents.

11.4.8 Endothelial recovery in stented arteries

Endothelial regeneration was determined using three independent methodologies: Evan's blue staining, scanning electron microscopy and histology. Two weeks after balloon injury and stent placement, endothelial regeneration was assessed in the animals treated with Bac_{Vegf}-PAMAM and Bac_{Null}-PAMAM coated stents using Evans blue staining (n = 3 stent). Luminal staining for Evans blue demonstrated that the balloon angioplasty and stenting procedure completely denuded the femoral artery in Control (-) stent while Coated (+) showed marked recovery at week 2 (**Figure 11.9A**). As evident from **Figure 11.9B**, re-endothelialization was significantly greater in the Coated (+) vessels (55.36 ± 4.64%) in comparison with Coated (-) control vessels (37.5± 6.51%, $P < 0.05$).

Furthermore, at 2 weeks and 16 weeks after stent deployment, SEM pictures of the inner surface of the stented arteries were taken. Cells consistent with endothelial morphology were noted on the surface of Bac_{Vegf} -treated stent struts on week 2, which completely covered the stent surface in a uniform way after 16 weeks (**Figure 11.9C**). In contrast, an irregular rough surface, mainly comprising of the exposed stent strut and partially covered neointima tissues, was noticed in the arteries with Bac_{Vegf} -treated stent on both week 2 and week 16.

16 weeks after the stent placement, histological assessment of endothelial regeneration demonstrated a significant difference in endothelial regeneration

between the three groups [Coated +, Coated- and uncoated bare metal stents]. The percentage of endothelial cells observed in the Coated (+) vessels was significantly higher than in the control vessels (93.5 ± 5.2% vs 75.4 ± 9.3% and 72.4±4.1; $P < 0.05$) as shown in **Figure 11.9D.**

11.4.9 Detection of stenotic area in stented artery: morphometric and angiographic analysis

All vessels were angiographically and histologically patent throughout the period of study. Stent malapposition was also not detected in any animal. 16 weeks after site-specific Vegf gene transfer, the stenotic area was significantly reduced in Coated (+) compared to control group stents (54.58±14.1% vs 69.6± 15.51 vs 85.4 ± 10.14%; $P < 0.05$) as analyzed by angiography (**Figure 11.10**). Representative photomicrographs of histologic cross sections from stented arterial segments at 4 month follow up are shown in **Figure 11.10**. The extent of vessel injury at the stent site was similar in all the groups as determined by injury score (Coated+ 1.13±0.14 vs Coated- 1.15±0.27 vs Uncoated 1.21±0.35). Similar results were also obtained with inflammation score (Coated+ 0.66±0.34 vs Coated- 0.7±0.31 and Uncoated 0.81±0.45; p>0.05).

Histomorphometric analysis (**Figure 11.11**) demonstrated a significantly reduced intimal hyperplasia in Coated (+) group compared to other two groups (**Figure 11.11E**, 61.36±15.15% vs 78.41±13.84 and 87.66 ± 8.54%; $P < 0.05$). Similar results were obtained when analyzed in terms of cross-sectional mean neointimal area (**Figure 11.11E**, 2.23±0.56mm^2 vs 2.78±0.49mm^2 and 3.11±0.23mm^2; p<0.05). 1 cm proximal and distal to the stented area showed no signs of intima formation.

11.5 Discussions

ISR caused by intimal hyperplasia post angioplasty and stenting remains a major cause of concern and challenge for clinical investigators and researchers [434]. The rationale for the present study was to develop a therapeutic strategy which would reduce ISR by accelerating local re-endothelization at the stented

site. For this we opted for gene therapy as it offers a promising tool for the treatment of ISR. Efficient gene therapy using suitable nanodelivery systems can induce a therapeutic effect for several days, whereas the half-life of recombinant protein and other pharmaceutics in circulation is much limited and proved to be ineffective in certain human [404, 435]. Although previous preclinical studies have shown promising results and clinical studies have demonstrated the safety and feasibility of vascular gene transfer in patients, none of the randomized controlled phase-II/III gene therapy trials have shown relevant positive effects on inhibiting ISR [420]. The reasons may be inadequate dose response effect due to low gene transfer efficacy, cell-mediated immunity to virus-transduced cells, lack of sophisticated vector delivery method or an amalgamation of several interrelated factors. Taking into account the technical and pharmacological shortcomings of previous studies, here we aimed to develop a clinically relevant gene eluting stent that can successfully ameliorate the vascular biology of the stented site by promoting local endothelial recovery. For this we designed and developed a novel dendrimer coated Bac_{Vegf} eluting stent using a composite polymer containing PLGA microspheres and fibrin biopolymer as the gene delivery platform. The results demonstrated here confirm that Vegf transgene can be effectively delivered to the vessel wall by the microencapsulated baculovirus, as detected *in vivo* in the transcript and protein level on day 10 post stenting. The transgene delivery not only improved early reendothelialization at the stented site but also significantly reduced neointimal proliferation as assessed by angiography and histomorphometric data at 4 months of follow-up. Prior studies have demonstrated that 4 month study period can be considered as an appropriate end point to detect vascular responses post stenting, after which the intimal response stabilizes with little change over the next 2 years [428].

Although substantial advancement has been made in elucidating the biology of baculovirus vectors, but the *in vivo* gene delivery is impeded by their susceptibility to complement-mediated inactivation by serum which drastically reduces the transduction efficiency [436]. Such disproportionate complement activation may also lead to severe systemic inflammatory response and

subsequent tissue damage [304]. Moreover, it has been recently reported that *in vivo* administration of baculovirus provokes cell-mediated immune responses by activating natural killer cells and antigen-specific $CD4^+$ and $CD8^+$ T cells and triggering innate immunity by upregulating certain pro-inflammatory cytokines [421]. These findings from literature raised obvious questions on whether baculovirus can really serve our purpose. Our present work has tried to address this problem by developing a method to efficiently formulate the baculoviruses within polymeric microspheres by mechanical entrapment, at the same time maintaining their biological activity. Somewhat similar strategy using w/o/w microsphere preparation method has been used earlier to protect adenoviruses against neutralizing anti-adenovirus antibodies and potent immune responses against high dose of viruses *in vivo*. In this work, we microencapsulated the baculovirus using a new procedure of w/o/o double emulsion to restrict viral loss to the hydrophilic phase during second emulsion, achieve high encapsulation efficiency and obtain favorable release profile of the active baculoviruses. This method proved much effective in maintaining higher encapsulation efficiency compared to earlier used w/o/w method. Baculovirus formulated in PLGA microspheres was released in two phases, where an initial burst release was noticed within 12h of incubation followed by a slow, continuous release in next 12h where the PLGA microspheres undergo slow degradation by hydrolysis of ester linkages to yield lactic and glycolic acid. We employed both mechanical homegenization and sonication induced emulsification procedures to entrap the viruses within the microspheres. But, sonication process reduced the encapsulation efficiency of active baculoviruses compared to that prepared by homogenization. The vast difference in encapsulation efficiency can be because the sonication procedure is detrimental to baculovirus and induce degradation effect on their membrane, as has been noticed with other viruses. Other methods currently under intense research are genetic manipulation to overexpress complement interfering factors, surface modifications of baculoviruses and administration of complement inhibitors [304, 422, 436].

Recently, we reported for the first time potential of recombinant baculovirus for angiogenic therapy in myocardially infarcted animal model using a nanobiohybrid system [423]. To extend its prospect for further angiogenic therapy applications, we first aimed to improve its transduction efficiency by hybridizing the baculovirus with cationic hyperbranched PAMAM G0 dendrimers before microencapsulating them. We reasoned that the amino terminal groups of dendrimer coated baculovirus facilitate the electrostatic interactions with negatively charged cell surface which augment viral binding to the cell surface and their subsequent entry into the cells. Previous studies have reported that noncovalent complexations of adeno- and retroviral vectors with polymers, such as poly-l-lysine and polybrene, can work as superior gene delivery vectors compared to uncoated viruses [268, 270]. Polyethyleimine has also been used as synthetic cationic molecules for viral complexations [304]. Our present study demonstrates that surface modifying the baculovirus with positively charged PAMAM dendrimers can also improve gene transfer efficiency. Among other widely used polymers, polyamidoamine (PAMAM) dendrimers has been shown to function as highly efficient cationic polymer vectors for gene delivery. PAMAM dendrimers are synthetic nanoparticles with a unique molecular architecture, characterized by their well defined structure, high degree of inter-molecular uniformity, low degree of polydispersity, and multiple terminal amino functional groups [299]. Most importantly, it can be an ideal polymer for conjugation of functional molecules while maintaining low toxicity *in vitro* and *in vivo* [300]. The study presented here has focused only on the generation 0 of PAMAM dendrimers to couple with the baculovirus. Further characterization studies on higher dendrimer generations with baculovirus will provide insight into the pattern on how different generations of dendrimer influence transduction efficiency.

Aside from improved transduction, the present work demonstrates the feasibility of encapsulating dendrimer coated active recombinant baculovirus into microspheres in order to achieve a controlled release from polymeric stent surface with minimum cytotoxicity. Very importantly, the microencapsulated Bac-

PAMAM stent also showed significantly higher protection of bioactive baculoviruses against serum inactivation compared to stents with microencapsulated Bac, and non-encapsulated Bac and Bac-PAMAM stents. Our data confirms that even PAMAM coating can also protect the Bac against serum inactivation to some extent, which is further enhanced by encapsulating them inside PLGA microspheres. The preservation of bioactivity of the stent for at least 3 months, once stored at -80^{o}C, can be of significant logistic advantage under real life clinical settings, where the stored stent can be of immediate off-the-shelf use for any patient undergoing angioplasty and stenting without delay.

As a first step to evaluate the therapeutic potential of this newly formulated gene eluting stent, we loaded the stent with Vegf carrying baculovirus and performed *in vitro* analysis. So far drug-eluting stents has proved to be a useful strategy for the prevention of ISR using antiproliferative drugs like rapamycin, paclitaxel and sirolimus. But recent clinical outcomes indicate that this approach is leading to incomplete endothelization and associated risk for stent thrombosis [437-439]. The underpinning cause for this is that the drugs, apart from restricting the smooth muscle proliferation, impinge the natural endothelial regeneration process [417]. Thus improving the regenerative capacity of the vessel wall endothelial cells, impaired by the antiproliferative agents, is critical to alleviate the risk of stent thrombosis and neointima formation. Earlier studies have shown that site specific arterial Vegf gene transfer lead to collateral vessel formation and increased capillary density in ischemic tissues [440]. As a follow up work, several studies reported that exogenous balloon and stent delivered Vegf gene has the potential to accelerate thrombus recanalization and promote re-endothelization in denuded arteries [403, 404, 413-417, 440-442]. This, in turn, attenuates ISR and inhibits stent thrombosis [417, 441, 443]. Our *in vitro* and *in vivo* findings are in sync with these prior findings and further focuses on advancing the gene delivery technology using optimized stent/polymer/gene combination. Here, we have illustrated that the viruses released from the microsphere embedded stent can efficiently transduce the HASMCs in culture, with Bac_{Vegf}-PAMAM showing significantly higher expression of Vegf compared

to that with Bac_{Vegf}. In addition, i*n vitro* functional assessment by HUVEC proliferation, wound healing and tube formation assays confirm the biological potency of the expressed Vegf protein.

Preclinical studies have confirmed the safety and efficacy of fibrin coated stents post deployment [444, 445]. With that knowledge, here we aimed to develop a biocompatible stent surface by coating the metallic stent with layers of fibrin hydrogel, impregnated with baculovirus loaded biodegradable PLGA microspheres. The topmost genipin/ fibrin layer serves as the barrier to external damages during crimping on the balloon catheter as well as protects the inner layers from premature virus release during its passage through the lumen of the artery at time of implantation at the desired site. The addition of genipin, as a natural cross-linker to fibrin, also works towards reducing the chance of any inflammatory reactions [446]. Through the stent coating method presented here, the inner surface of the stent (i.e., the mandrel contact surface) was not coated with the polymer. Consequently, there was no fibrin coating on the blood contact side of the stent. In this way we tried to reduce the loss of loaded viruses into the blood stream.

As illustrated in this study, the stent acted as an ideal platform for local baculovirus delivery to the stented blood vessel wall with no signs of potential inflammatory responses in the artery. Notably, the recombinant baculovirus showed a rapid expression of transgene within the first 4 days of in *vitro* stent mediated transduction, followed by a gradual decrease in expression level over the next two weeks. Similarly, we have observed localized *in vivo* Vegf transgene expression at the site of stent implantation for at least 2 weeks post deployment as evident by RT-PCR and by immunohistochemical analysis, where the later confirmed gene over-expression around the stent struts. As expected, the expression ceased when analyzed at the transcript level on week 16. This transient nature of baculovirus expression indicates that it can be ideal in treating problems like ISR where the gene expression is no longer needed once endothelial recovery is complete. The present work proves this postulation showing complete recovery of endothelial layer is possible by temporal expression of transgene for

2-3 weeks. This observation supports previous published results, where transgene expression for just 10 days proved sufficient for complete endothelial recovery at the stented site [417]. More importantly, this transient nature of baculovirus expression makes it a prospective gene delivery vehicle for biologically safer clinical applications compared to widely experimented mammalian viral systems. To our best knowledge, this is the first study where recombinant baculoviruses are being efficiently used for gene therapy of post angioplasty ISR. The current report substantiate our finding by demonstrating significantly improved endothelial recovery assessed by Evan's blue staining and scanning electron microscopy, and restricted ISR illustrated by histomorphometric and angiographic analysis in a long-term study of 4 months post implantation. However, the present work does not demonstrate whether this system can inhibit long term in-stent thrombosis. An important area which needs further research is to characterize the *in vivo* dose dependency analysis of the loaded baculoviruses per stent to attenuate ISR in the best possible and safest way without invoking any deleterious consequences by the host inflammatory cytokines and immune system. In the present study we used a high baculovirus dose compared to other viral vectors. This is because, as a first study of its kind with no prior literature data, we aimed to achieve maximum transgene delivery at the stented site to achieve high growth factor expression, which can be a key determinant for the degree of vascular healing. Insufficient Vegf cytokine concentration at the stent site combined with their short half life may lead to suboptimal biological effects to trigger vascular re-endothelization [420]. Moreover, in case of intra-arterial gene delivery there always remains a chance of a percentage of loaded viruses getting inactivated by the blood components while transduction. Further studies on hypercholesterolemic model, where concomitant *hypercholesterolemia* exacerbates the risk of pronounced neointima formation [429], can be an interesting follow up work that will generate more explicatory information regarding the efficacy of the stent.

To conclude, the major findings of the current work capitalize on the development of this novel approach where local delivery of Bac_{Vegf} –PAMAM

vector, entrapped within PLGA microspheres embedded layer by layer on fibrin-coated stent, can significantly enhance endothelial regeneration and thereby block subsequent neointimal proliferation and ISR. Using baculoviruses with surface functionalized targeting ligands, can be the next step to develop a further advanced gene eluting stent where the released viruses can effectively repair the denuded regions in a site-specific way with minimal dosage. This in turn, will reduce the possibility of incurring any adverse inflammatory reactions associated with higher viral dose, thus making the stent much more safe, feasible and effective for future advanced translational research.

6. Acknowledgements

This work is supported by Natural Sciences and Engineering Research Council (NSERC, Canada) strategic grant to Satya Prakash, Dominique Shum-Tim and Cynthia Elias. Arghya Paul acknowledges the financial support from NSERC - Alexander Graham Bell Canada Graduate Scholarship. The authors thank Marie-Eve Robitaille from Montreal General Hospital for animal handling, Dr. Xue-Dong Liu from McGill University Physics Department for electron microscopy imaging, and Accel Lab Inc and McGill SAIL Lab for their technical support in animal tissue processing. We are grateful to Dr. Maryam Tabrizian for providing us with facilities in her laboratory at McGill University, Canada. The authors confirm that there are no known conflicts of interest associated with this publication.

Table 11.1: Effect of PLGA MS preparation procedure on active virus encapsulation efficiency (in terms of percentage of initial loaded viral titre)

Method	Homogenization		Sonication	
	Bac	***Bac+ BSA/glycerol***	***Bac***	***Bac+ BSA/glycerol***
w/o/w (% pfu)	15.5±0.7	35.6±3.1	10.6±1.3	26.4±4.1
Diameter (µm)	7.2±2.3	9.8±3.4	5.2±3.4	5.6±4.2
w/o/o (% pfu)	21.0±1.1	41.4±2.2	17.8±1.0	26.8±3.5
Diameter(µm)	9.2±2.6	8.3±3.2	5.6±1.1	4.9±2.2

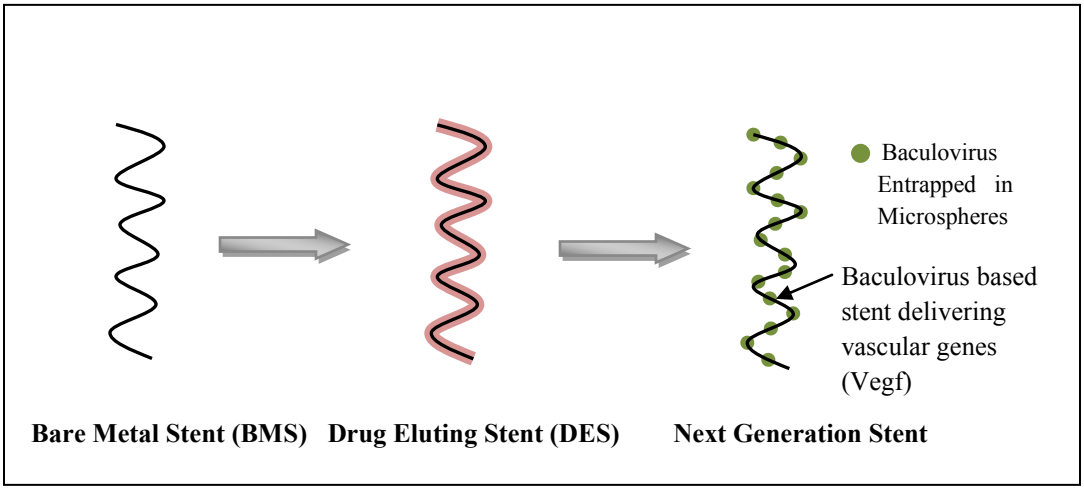

Figure 11.1A: Various stent types and concept of newly designed stent. This new stent loaded with baculovirus will provide therapeutic genes such as VEGF, required healing injured arterial wall by accelerating vascular inner ling re-endothelialization.

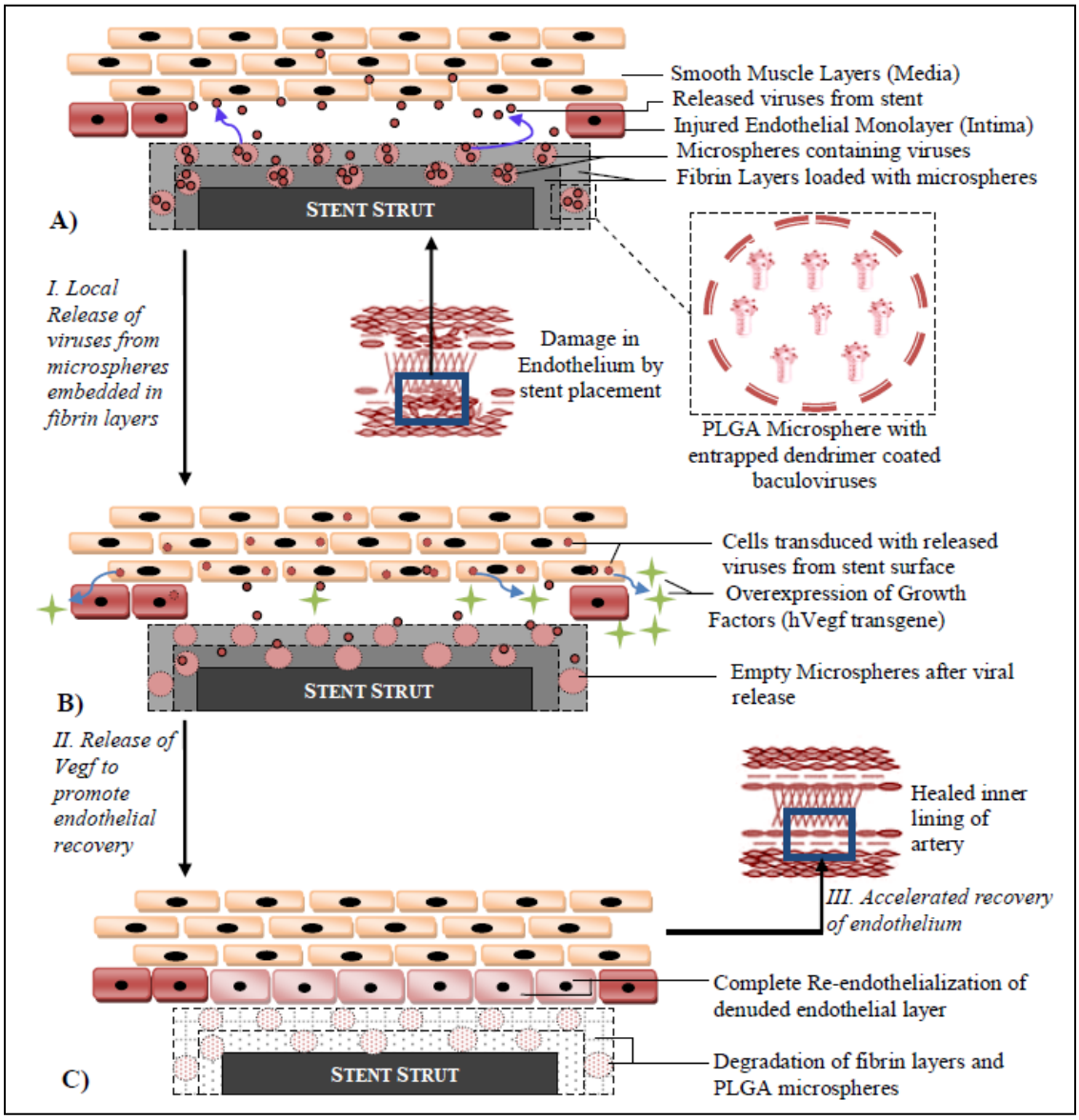

Figure 11.1B: Schematic representation of design, formulation and mode of action of virus loaded bioactive stent to attenuate ISR. **A**. Release of entrapped viruses carrying angiogenic transgene (Vegf) to the adhering vascular wall. **B**. Local overexpression of transgene to enhance endothelial regeneration. **C.** Proper cushioning of intima layer with regenerated endothelial monolayer to reduce risk of restenosis by smooth muscle proliferation and thrombosis by avoiding further exposure to blood. With time, the stent loses its coatings due to the biodegradable nature of the polymers, leaving behind the bare stent struts in the already recovered vascular segment.

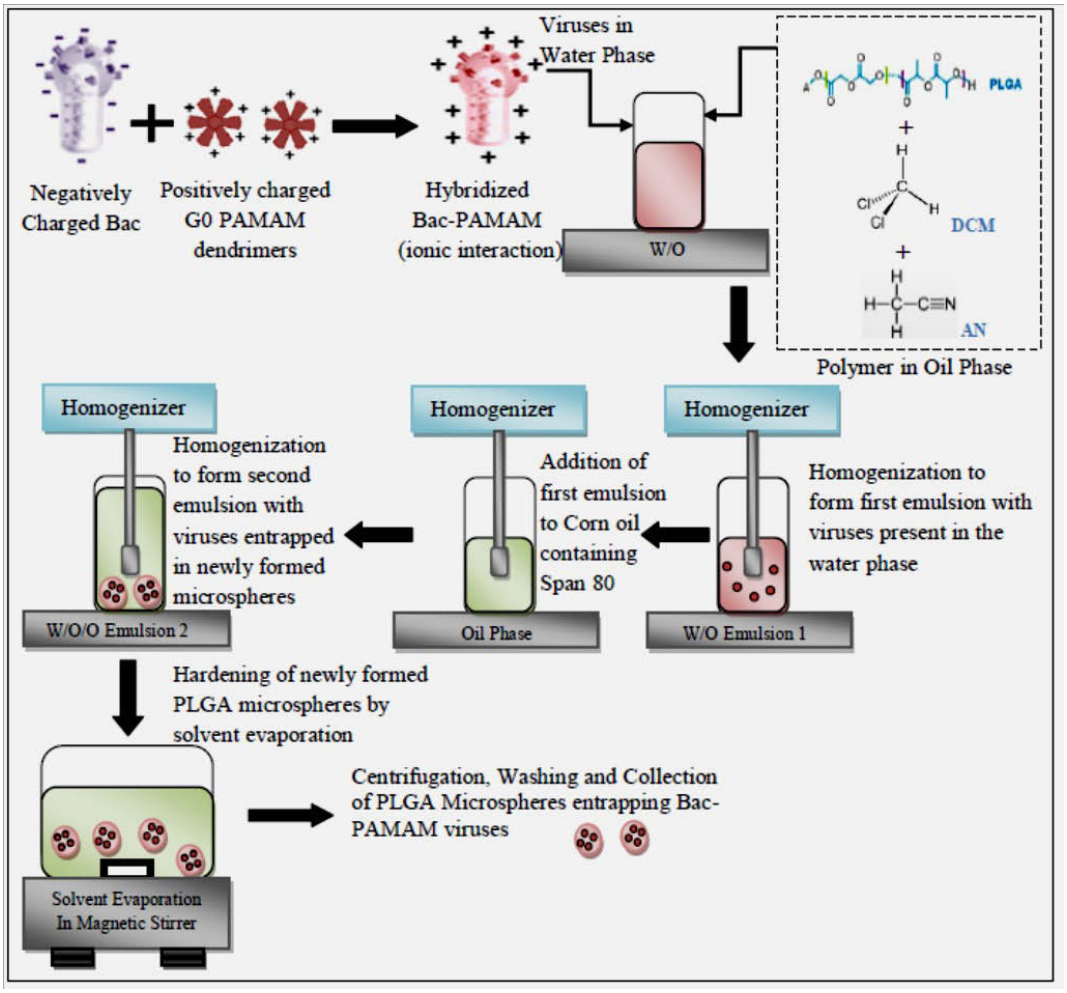

Figure 11.1C: Schematic representation of generation of Bac-PAMAM complex and its subsequent microencapsulation in PLGA microspheres by w/o/o double emulsion solvent evaporation method.

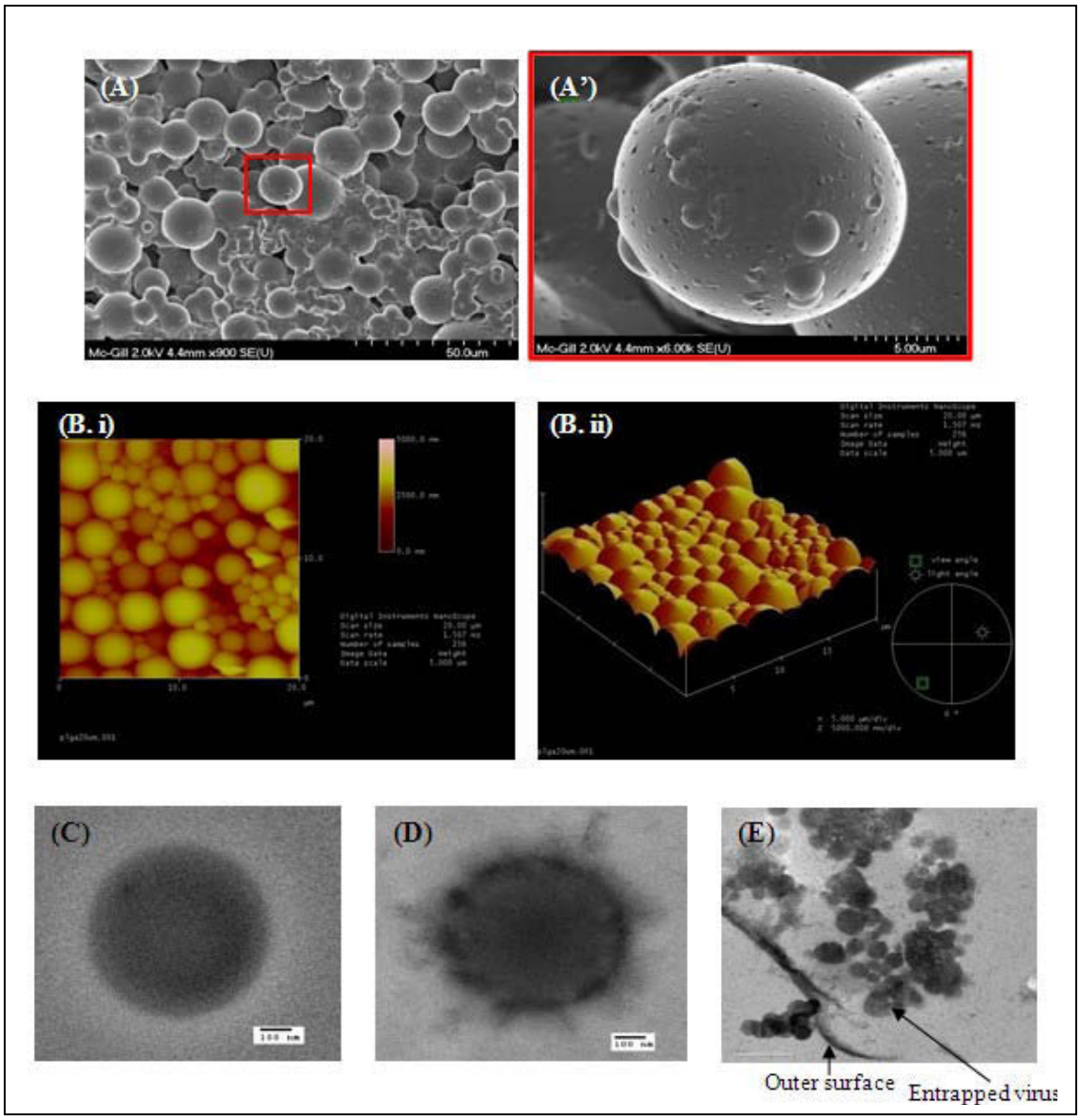

Figure 11.2: SEM (A&A') and AFM (B and B') microphotographs of virus loaded PLGA microspheres demonstrating the surface morphology prepared by w/o/o method. TEM picture of empty microspheres (C) and virus loaded microspheres (D). E represents the ultrathin inner cross-sections of the microspheres loaded with viruses under TEM. Note: The entrapped viruses look circular in the TEM picture because the microphotograph was taken for a single plane on the cut cross-section of the virus loaded microsphere.

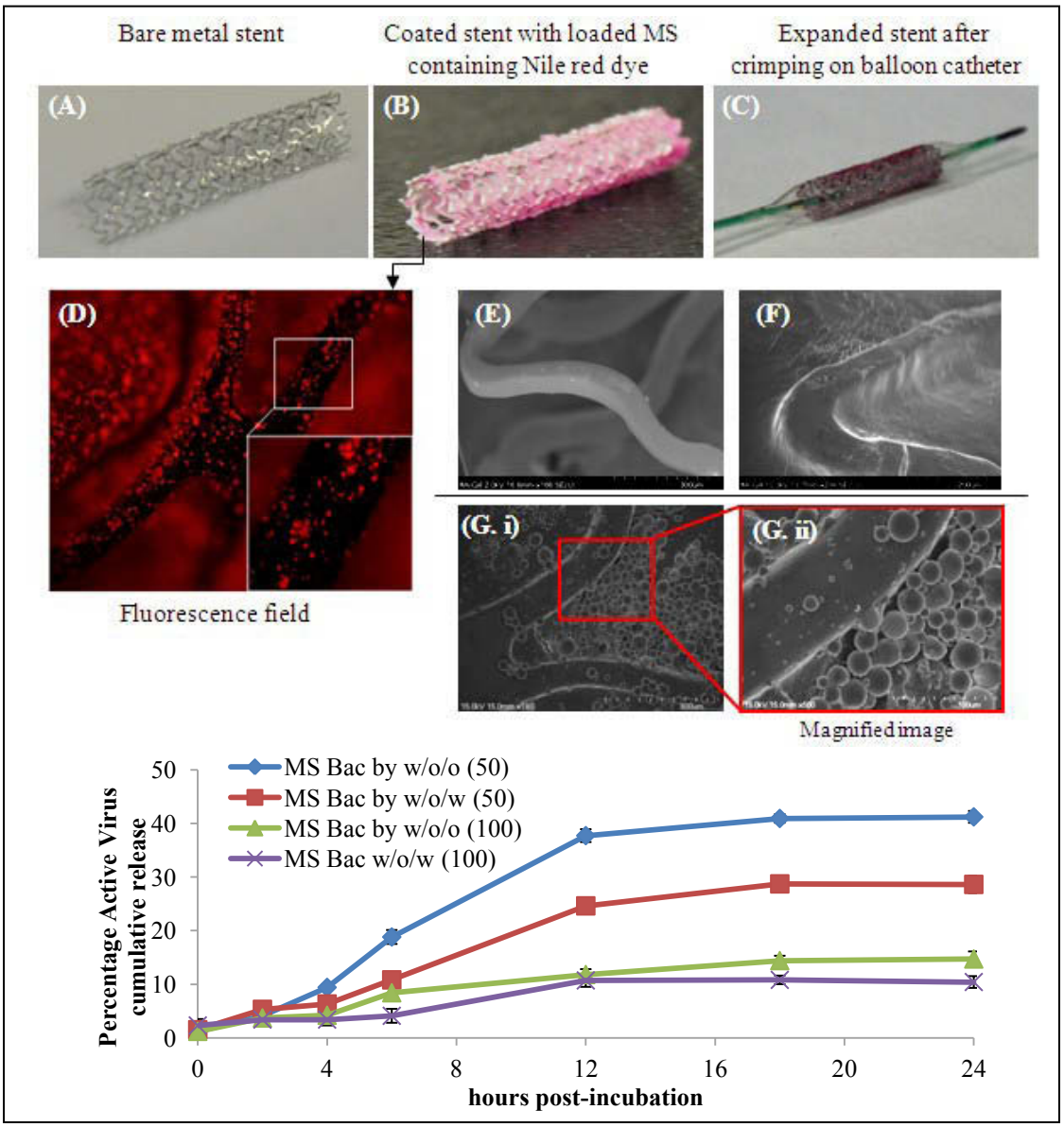

Figure 11.3: Characterization of PLGA MS coated fibrin stent. (A) Uncoated Bare metal, Nile red containing MS loaded stent after coating (B) and balloon expansion(C). Fluorescence image of the stent showing the fluorescent PLGA MS embedded on the fibrin stent surface (D). SEM microphotographs of bare metal (E), fibrin coated (F) and PLGA MS loaded fibrin coated stents (G. i and ii). (H) Cumulative baculovirus release (in terms of % of initial virus loaded) from stents coated with varying concentrations (50 and 100 mg/ ml DCM) of PLGA MS prepared by w/o/w and w/o/o method shows controlled release of virus load over 24 h as a function of the PLGA concentration and MS preparation method.

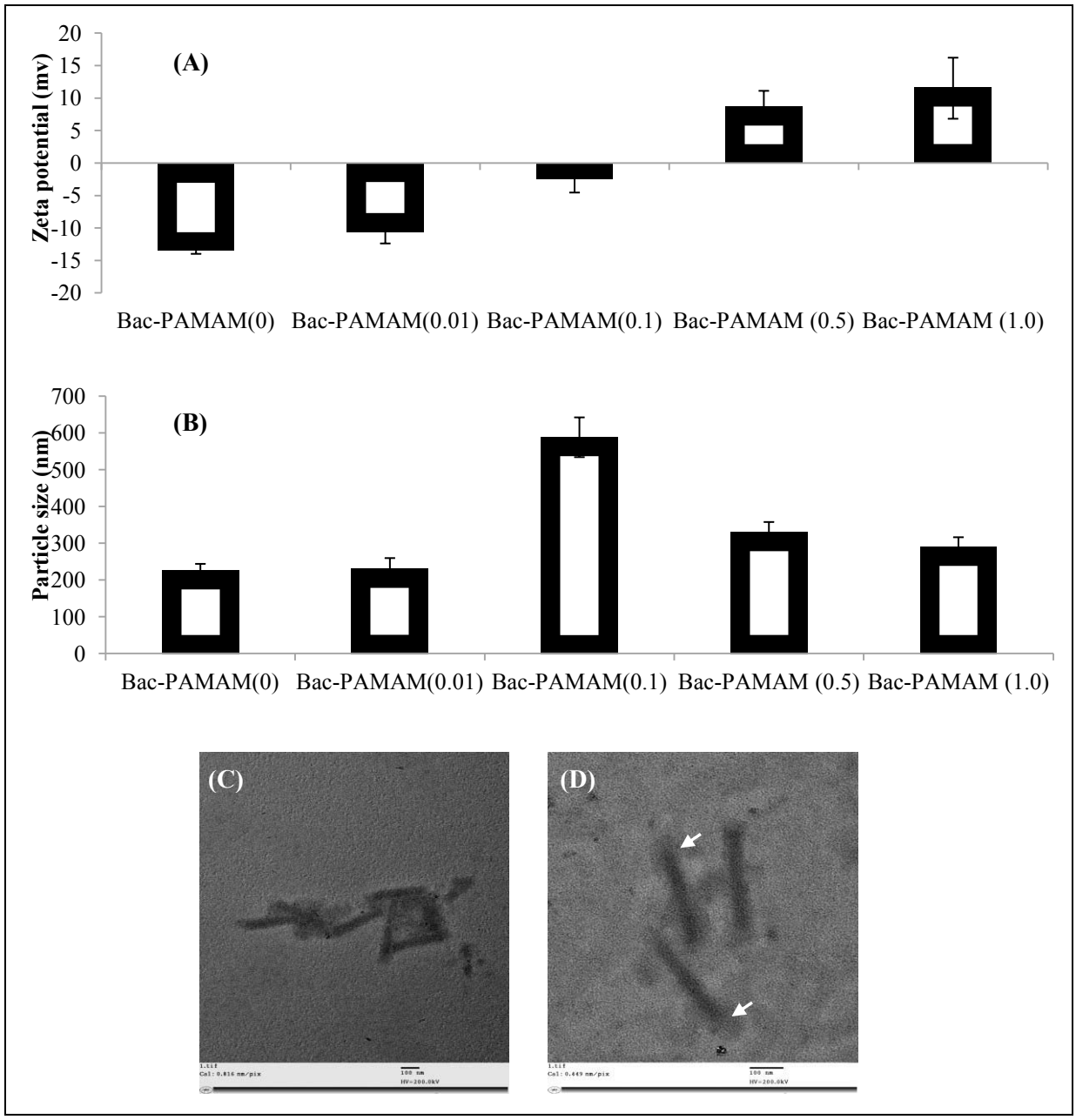

Figure 11.4: Surface modification of baculovirus with PAMAM dendrimer (G0). Zeta potential (A) and particle size (B) of Bac-PAMAM (0) (free Bac), Bac-PAMAM (0.01), Bac-PAMAM (0.1), Bac-PAMAM (0.5), and Bac-PAMAM (1.0), where the values within brackets indicate the ratio of PAMAM molecules in µmol per 10^8 viruses. The data is represented by mean ± standard deviation (SD). TEM images of free Bac (C) and Bac-PAMAM (0.5) (D) suspended in PBS. Arrows indicate the positively charged PAMAM dendrimer coating on the negatively charged baculovirus surfaces to form the hybridized nanostructures. Scale indicates 100nm length.

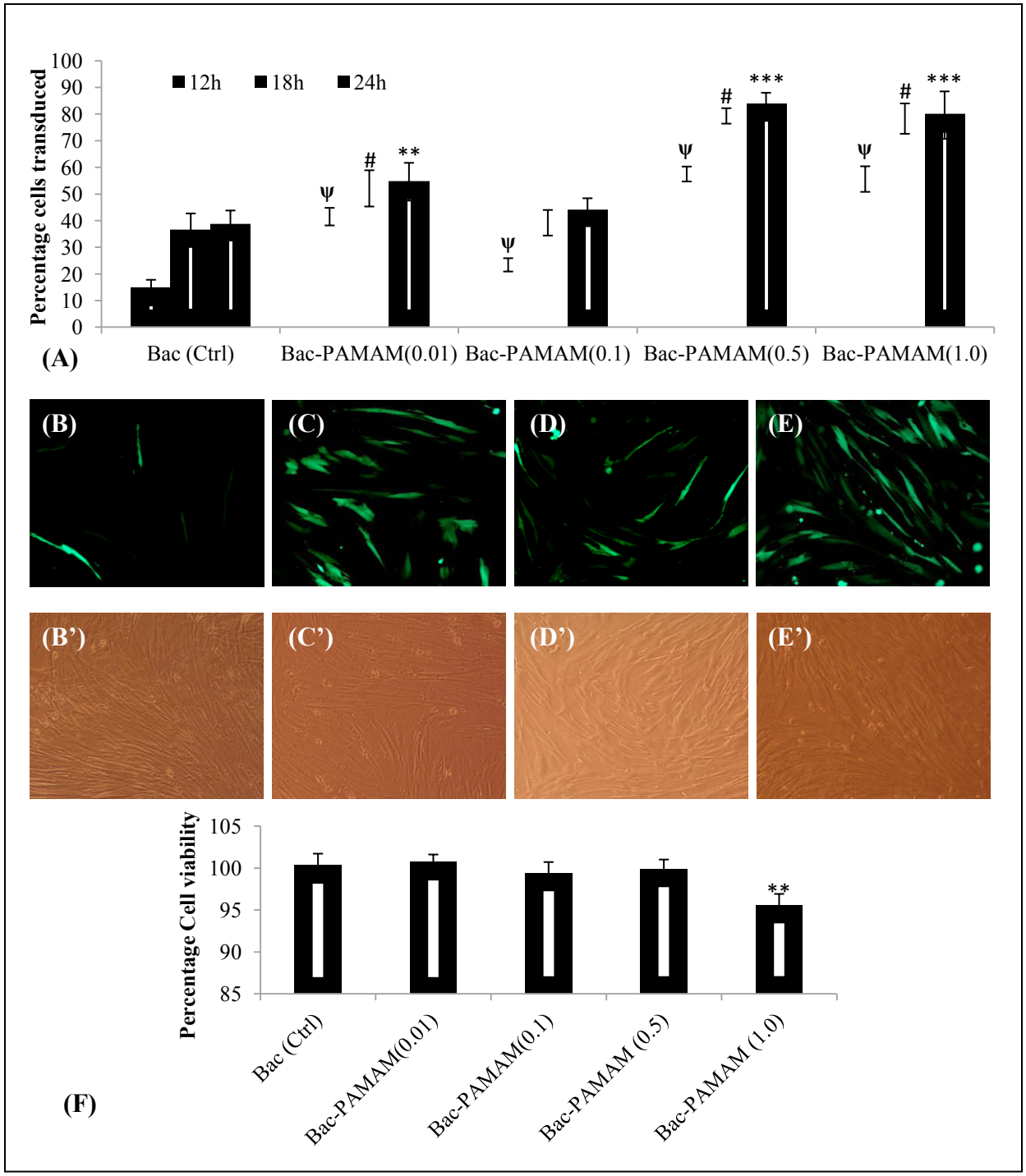

Figure 11.5: A. The kinetics of PLGA-encapsulated Bac_{MGFP} with or without PAMAM coatings. The prepared stents with encapsulated viral preparations containing 0, 0.01, 0.1, 0.5 and 1.0 µmol PAMAM molecules per 10^8 baculovirus were incubated in PBS. At the indicated times PBS was collected and used for transduction of HASMCs using standard procedure mentioned in method section.

B-E represents the transduced cells 24h post transduction under fluorescence field while B'-E' represents the corresponding bright field. Data represent mean ± SD (n=3). ANOVA analysis: *=P<0.05 and **=P<0.01 compared between time (24h)-matched groups. #= P<0.05 compared between time (18h)-matched groups. ψ = P<0.05 compared between time (12h)-matched groups. F. Cytotoxic effect of the above formulations on HASMCs after 12h of incubation was analyzed. Data from different groups were represented in terms of percentage of viable cells. **=P<0.01 compared to control Bac group (n=3).

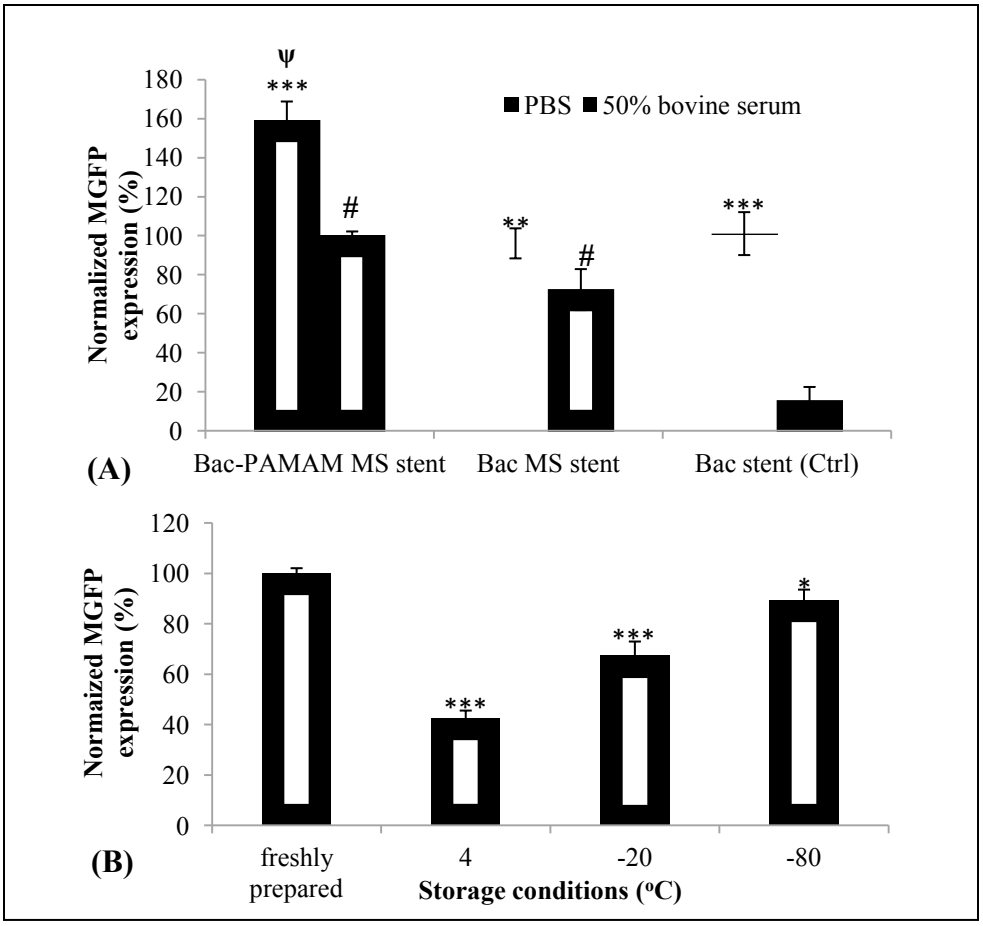

Figure 11.6: Effect of serum and storage temperatures on bioactivity of Bac_{MGFP} loaded stent. The Bac_{MGFP}-PAMAM MS, Bac_{MGFP} MS and Bac_{MGFP} stents, after 1 h incubation in 50% serum or PBS solution, were used to transduce $2x10^4$ HASMCs per well in 96 well plate using standard method as mentioned in method section. Similarly, Bac_{MGFP}-PAMAM MS stents after storage for 3 months at different temperatures (4°C, -20°C, -80°C and control freshly prepared) were used to transduce HASMCs *in vitro*. Data was represented in terms of normalized MGFP expression taking Bac_{MGFP}-PAMAM MS expression as 100% (A) and taking freshly prepared stent expression as 100% (B). Data represent mean ± SD (n=3). Statistically significant differences within groups are denoted by ***=P<0.001 and **=P<0.01, while condition-matched differences between groups are represented by ψ<0.001 (PBS) and #<0.001 (serum).

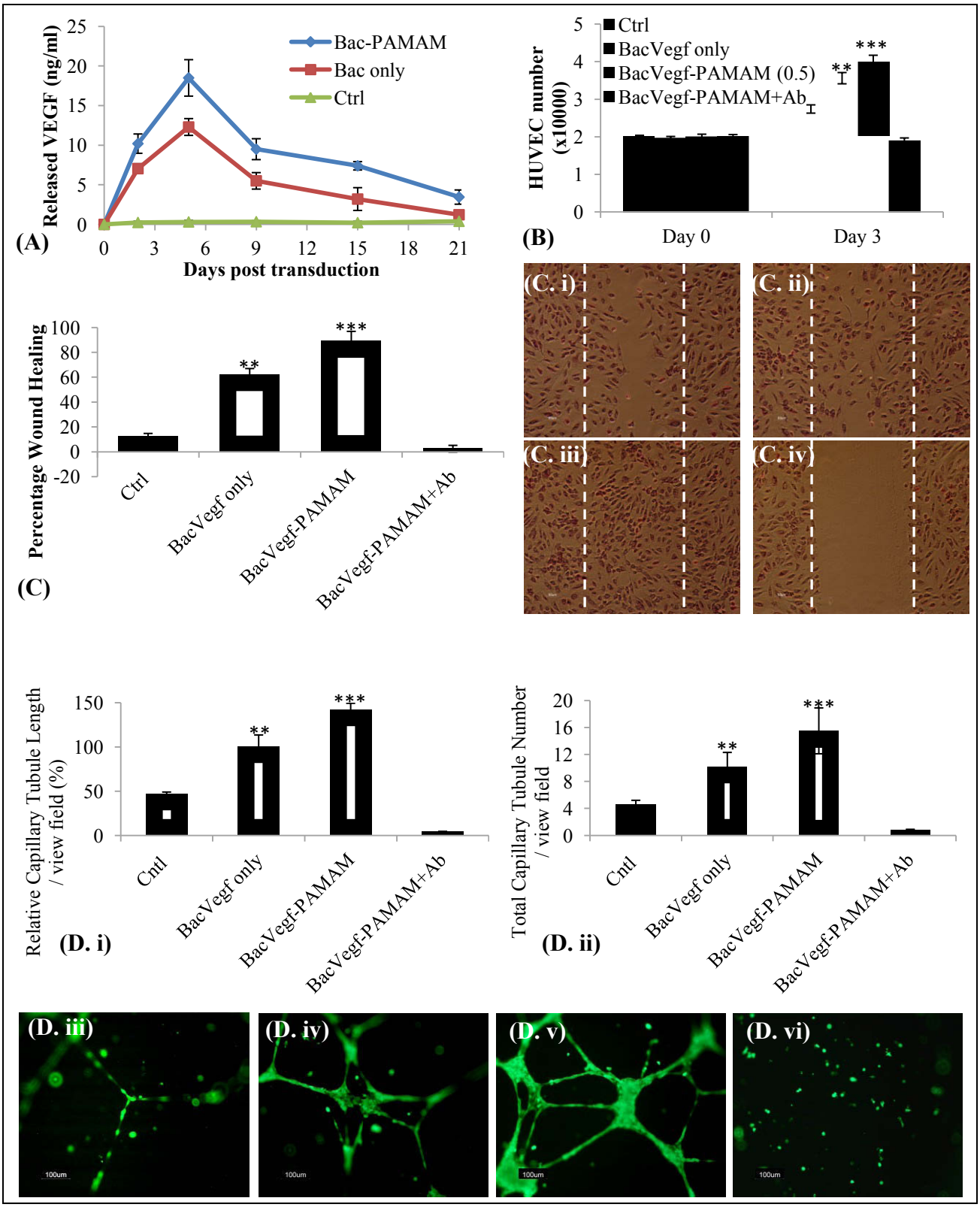

Figure 11.7: A) Quantification of Vegf released by transduced HASMCs over time as detected by ELISA. **B)** Proliferation of HUVECs grown in the presence of CM from

Bac_{Vegf}-PAMAM (with or without Ab) and Bac_{Vegf} transduced HASMCs. As control group, CM from non-transduced cells (Ctrl) was taken. Initial seeding density was $2x10^4$ cells per well in 96 well plate and cell proliferation was detected by a colorimetric assay on day3. **C)** Induction of HUVEC migration in a wound healing assay. HUVEC cell monolayer was wounded with cell scraper and treated with CM from above mentioned groups. HUVEC were photographed (200X) after 24 h treatment **(C)** and percentage of scratched area (marked by the white dotted border line) covered by the migrated cells were analyzed using Image J software (**C. i-iv). D**) Effect of CM from above mentioned groups on tubular formation *in vitro*. After 18 h co-cultivation with HUVECs, tubular formation was evaluated. The graphs represent the relative tubule length in µm taking Bac_{Vegf} as 100% (**D. i**) and counting of capillary tubule number (**D. ii**). The data represent the mean ±SD of three independent experiments. (**D. iii-vi**) Properly formed tubular structure was observed in Bac_{Vegf}-PAMAM and Bac_{Vegf} groups, compared to the unstimulated control and Ab treated group as examined using a fluorescent microscope under 100X magnification. ANOVA: Significantly higher values in groups compared to control are denoted by ***=P<0.001 and **=P<0.01.

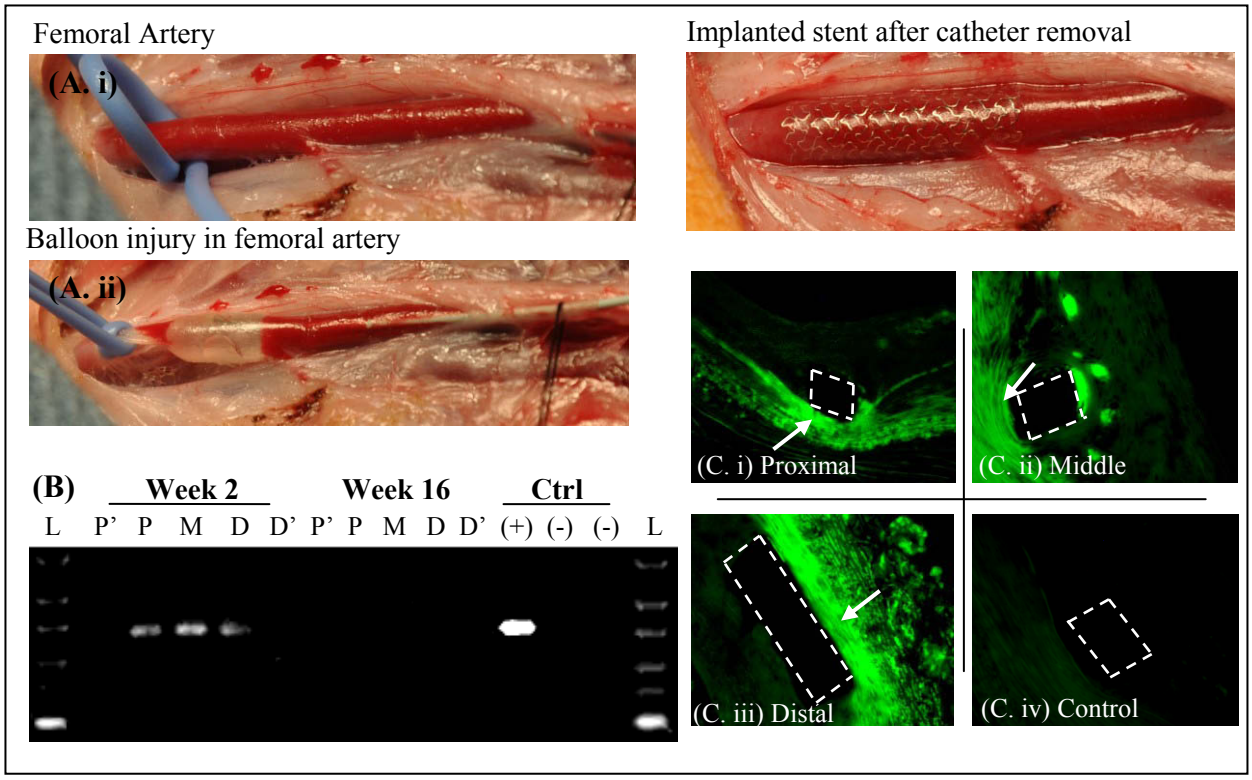

Figure 11.8: A. Experimental procedure for the in vivo experiment in canine model. The femoral artery was first isolated from the normal blood flow using clips (A. i). The selected portion was then flushed with PBS followed by severe bolloon injury using balloon catheter (A. ii). This was followed by the insertion of the crimped polymer coated stent in the damaged artery. The balloon cather carrying the stent was inflated to implant the stent at the site. This was followed by deflation and removal of the ballon catheter (A. iii). B. hVegf transgene delivery delivery and expression in the artery. RT-PCR of tissue retrieved from stented vessel segments was performed to identify the hVegf gene, detecting PCR product. 2 weeks post stent implantation in Coated (+) group, the VEGF transcript was still present in the proximal (P), middle (M) and distal (D) portions of the stented artery. But transcript was undetectable in the artery sections 1 cm proximal (P') and distal (D') to the stented portion as well as in the Coated (-) control group on both week 2 and week 16. Importantly, the transcript also disappeared in Coated (+) group by week16 confirming the transgene nature of expression of the viral system. C. Immunohistochemical localization of Vegf

within stented femoral artery in Coated (+) group at week 2 post stent deployment. Coated (-) was taken as control. The Vegf expression was noticed mainly in the intima and outer medial layer. Note that the expression occurred mainly at the strut area (white dotted) where the stent surface touched the inner lining of the artery, with no significant expression in the neointimal area indicating that the gene transfer from stent surface occurred only at the very early stage of deployment.

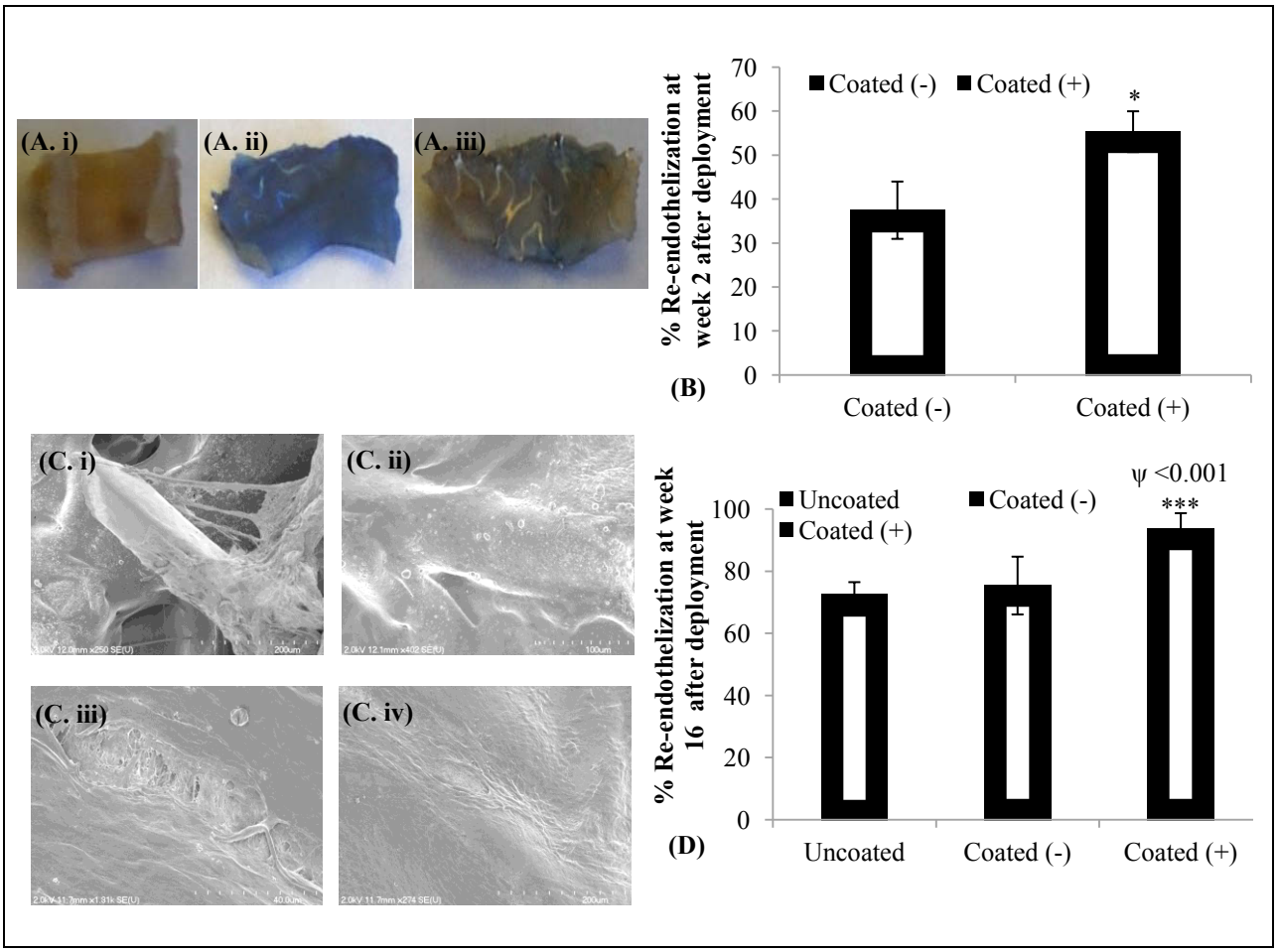

Figure 11.9: Re-endothelialization of vessels following stent implantation. A. Evans blue staining confirms that Coated (+) group was able to recover the injury by endothelialization while in Coated (-) group the wounds was still exposed with high amount of Evans blue uptake. Control artery segment with no injury showed no signs of dye uptake. B. Quantification of percentage re-endothelialization week 2 after staining using imaging software in the Coated (+) and Coated (-) group. The data represent the mean ±SD (n=3). C. SEM pictures of Coated (-) stent on week 2 (C. i) and week 16 (C. ii) and that of Coated (+) stents on week 2 (C. iii) and week 16 (C. iv). Vessels from Coated (-) group lacked endothelial cell morphology between struts, while endothelial cell monolayer completely covered the stent surface with typical fusiform morphology and intact borders in Coated (+) group. D) Histological assessment of re-endothelialization of arterial tissue sections in Uncoated, Coated (-) and Coated (+) at week 16 post stent deployment. The data represent the mean ±SD (n=8). ANOVA: ***=P<0.001 and *=P<0.05, while P value on comparing Coated (+) and Coated (-) in (D) is denoted by ψ.

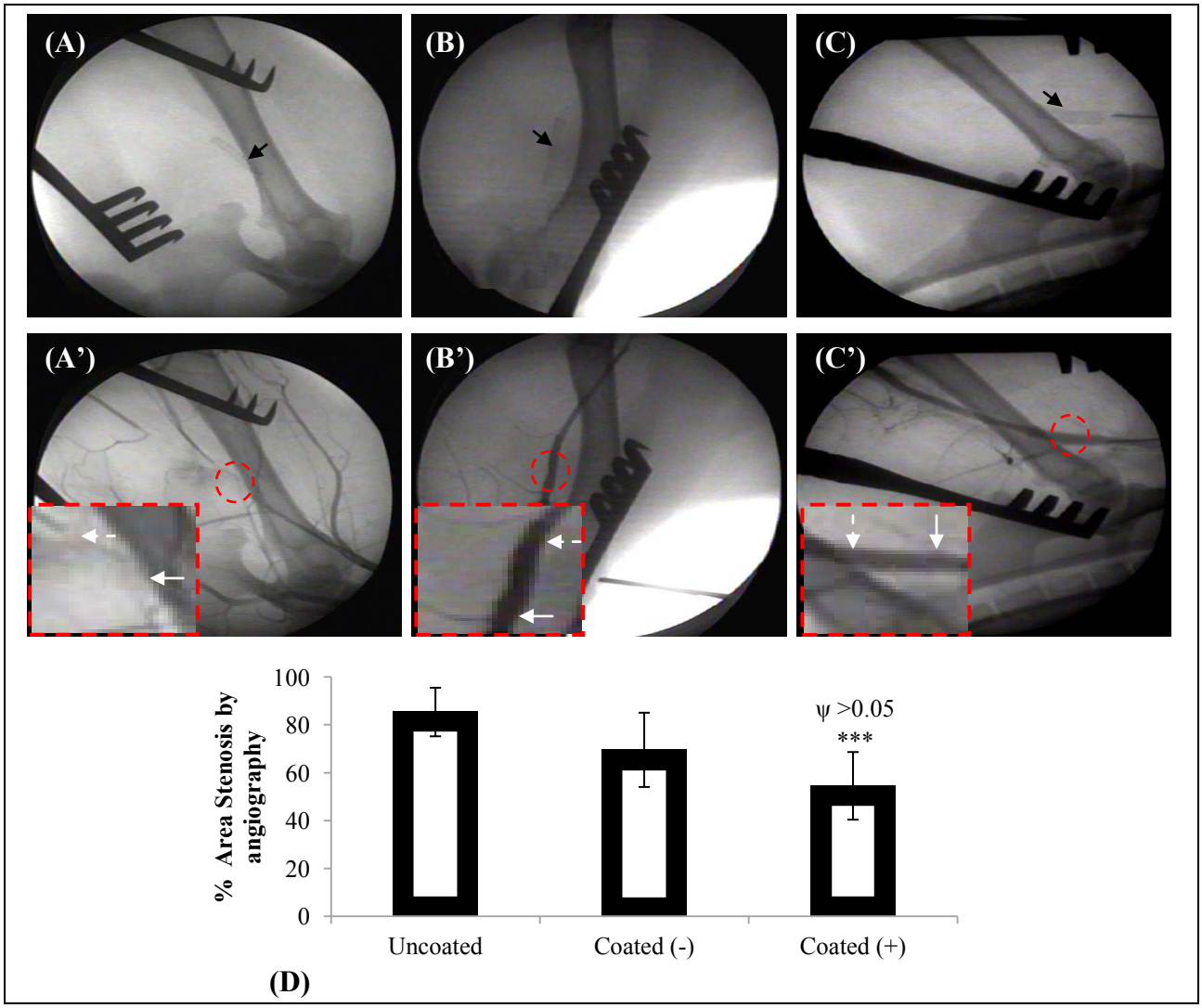

Figure 11.10: The effect of Bac_{Vegf}-PAMAM delivery on ISR assessed by angiography analysis. Comparison of angiography studies at Week 16 after stent deployment in femoral arteries of dogs. Representative angiographic images of femoral arteries with uncoated bare metal stent (A') and stents coated carrying Bac_{Null}-PAMAM (B') and Bac_{Vegf}-PAMAM (C') at week 16 after stent deployment, where A, B and C shows the corresponding stent positions before angiography (black arrows). Image analysis within the proximal (dotted white arrow) and distal (solid white arrow) regions of stented arteries (dotted red line) demonstrated significantly reduced ISR in Coated (+) group compared to Uncoated group, although significance was not achieved when compared to Coated(-) (D). The data represent the mean ±SD (n=8). ANOVA: ***=P<0.001. P value on comparing Coated (+) and Coated (-) is denoted by ψ.

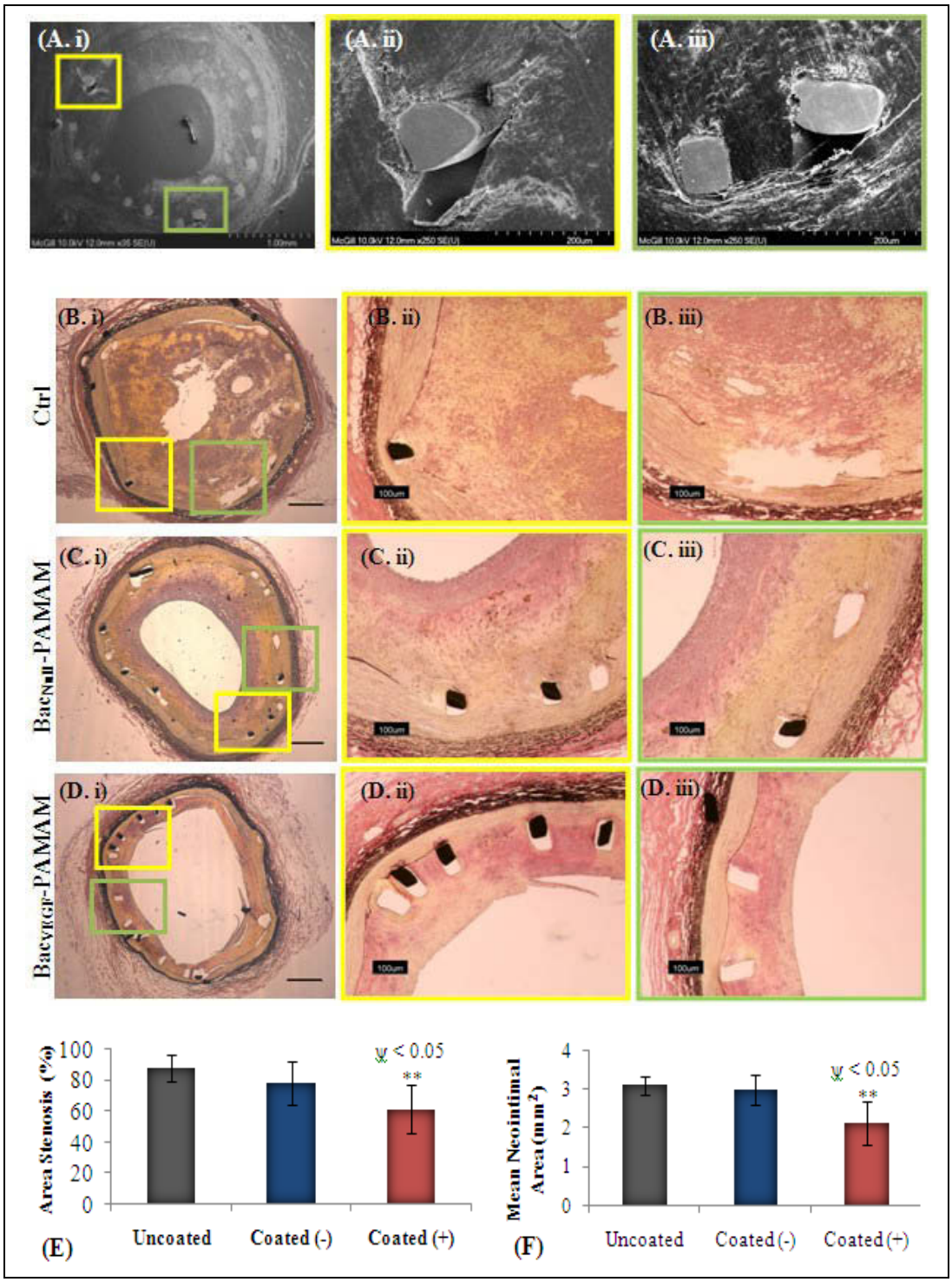

Figure 11.11: (A. i-iii) Cross-sectional view of stented artery through SEM demonstrating the intimal hyperplasia over the protruded stent struts. **B**. The effect of Bac_{Vegf}-PAMAM delivery on ISR assessed by histomorphometric analysis. Comparison of histomorphometric studies at Week 16 after stent deployment in dog femoral arteries. Representative cross-sectional images of

elastic Van Gieson stained femoral arteries with uncoated bare metal stent (**B. i-iii**) and stents coated carrying Bac_{Null}-PAMAM (**C. i-iii**) and Bac_{Vegf}-PAMAM (**D. i-iii**) at week 16 after stent deployment. Percentage stenosis (**E**) and mean neointimal area (**F**) analysis at the stented regions demonstrated significantly reduced ISR in Coated (+) group compared to Uncoated and Coated (-) groups. The data represent the mean ±SD (n=8). ANOVA: **=P<0.01; P value on comparing Coated (+) and Coated (-) is denoted by ψ.

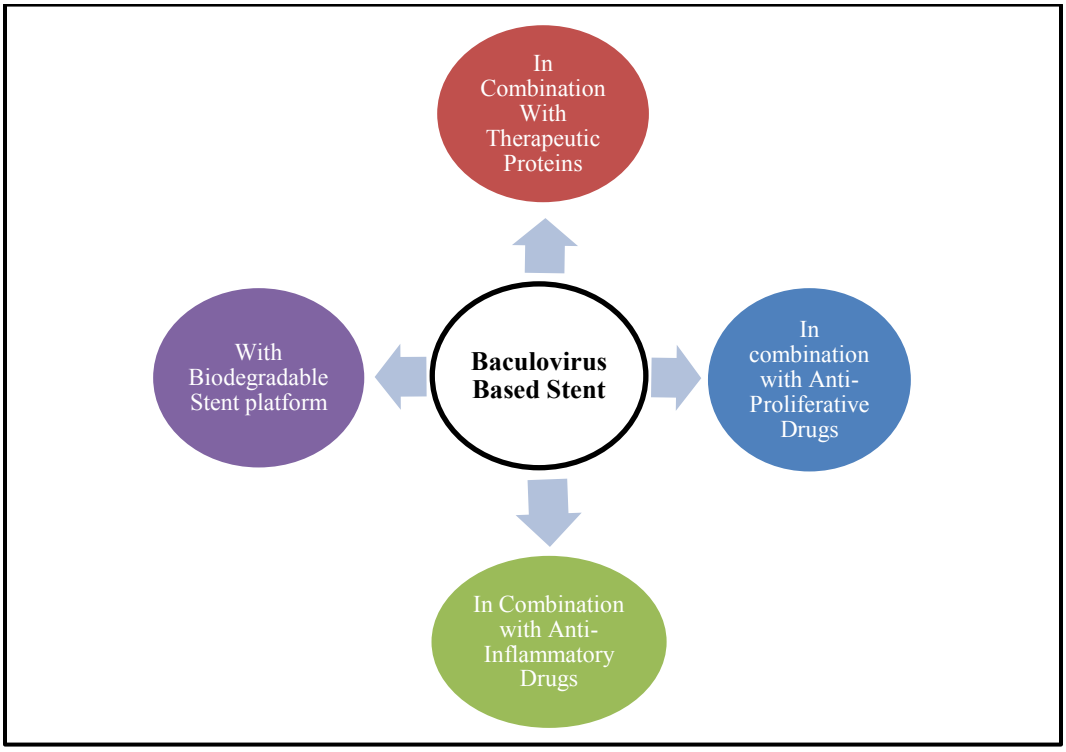

Figure 11.12: Other possible potential configurations of current baculovirus based stent technology.

12.1 STEM CELL BASED HEART THERAPY

Cardiac and vascular diseases originating from atherosclerosis is the primary cause of coronary artery disease, stroke and peripheral vascular disease, and it therefore represents the most common cause of morbidity and mortality worldwide [1]. Patients who develop atherosclerotic plaques in their carotid and coronary arteries, almost completely blocking the blood flow, have a high risk for Major adverse cardiovascular events (MACE) such as stroke and myocardial infarction (MI). Approximately two-thirds of these events arise when the fibrous cap of an unstable atherosclerotic plaque ruptures, leading to release of thrombogenic material and blockage of the artery owing to platelet aggregation. Under such circumstances, aggressive therapeutic interventions are common, which includes coronary artery bypass surgery, percutaneous arterial dilation and stenting. However, despite optimal treatment, the residual risk of another MACE in these patients is estimated to be 70–80%. This is believed to be because post MI, the heart tissue cannot regenerate or repair itself by its native processes, thus leading to a progressive deterioration of heart function. In-stent restenosis of coronary arteries is another frequently occurring disease in cardiovascular patients having stented arteries. Re-occurrence of stenosis at the stented region is the main reason which leads to the re-narrowing of the artery.

The overall goal of this doctoral thesis was to develop potential therapeutic biomedical devices to treat such cardiovascular problems. For this, the study aimed to develop new myocardial transplants to treat post MI damaged heart tissues. In addition, the study also aims to design and develop a novel vascular stent to attenuate the frequent problem of restenosis associated with currently available stents.

Myocardial infarction (MI) is characterized by reduced blood supply to the heart and loss of functioning cardiomyocytes. However, the capacity for self-regeneration of adult heart is limited. Recent studies suggest that stem cells have excellent potential to treat cardiac diseases, particularly MI [259, 380, 382, 383,

390, 391, 401, 447]. Stem cell transplantation is being investigated as a novel means to regenerate heart tissue and enhance cardiac function. The potential of adult stem cells to function as cellular therapy for myocardial regeneration is based on their plasticity, clonogenicity, and self-renewal ability. Recent studies have demonstrated that stem cells have broad differentiation potential and can differentiate into cardiomyocytes. However, available technologies to deliver the cells to the heart muscle are not so efficient [14]. We postulated that a microencapsulated stem cell delivery system armed with the capability to overexpress angiogenic therapeutic proteins can be a suitable myocardial implant for effective myocardial infarction therapy.

As the first step, choosing an ideal stem cell delivery system depending on the target site is the key for the success of any cell based biomedical application. In the last couple of years many different cell sources have been immobilized for delivery, although clearly not all cells are suitable for encapsulation [448-451]. A number of factors should be carefully considered when choosing suitable cell types for immobilization as use of allogeneic versus xenogeneic cells has important immunological repercussions [452]. Further, cells that proliferate following encapsulation could eventually fill the entire capsular space and lead to diminished efficacy of therapeutic diffusion. As a result, the long-term viability of encapsulated cells is often compromised [17]. In contrast, cells that do not proliferate after encapsulation, such as myoblasts fibroblasts, have the potential to deliver therapeutic products for longer periods of time. A key engineering challenge in designing immunoisolating alginate-based microcapsules is that of maintaining unimpeded exchange of nutrients, oxygen and therapeutic factors (released by the encapsulated cells), while simultaneously avoiding swelling and subsequent rupture of the microcapsules. This requires the development of efficient, validated and well-documented technology for cross-linking alginates with divalent cations. Clinical applications also require validated technology for long-term cryopreservation of encapsulated cells to maintaining a product inventory in order to meet end-user demands.

Presently used stem cell population mainly includes embryonic, adult BMSC, pancreatic stem cells, extra pancreatic such as hepatic cells and adipose-derived stem cells. However, the identity of the very small fraction of cells within the widely used bone marrow with the capacity to differentiate into true functional cardiomyocytes is under debate [453]. Furthermore, BMSCs require processing and culturing after bone marrow aspiration, making it difficult to use these cells in an acute clinical setting. Multipotent ASCs derived from adipose tissues are abundant in the human body, and thus are an ideal donor source for autologous transplantation for myocardial therapy [454]. Moreover these cells are better sources than BMSCs for clinical applications, owing to minimal invasive procedures, high proliferation and multi-differentiation potential. ASCs may thus provide an alternative stem cell source, replacing widely used BMSCs for potential stem cell based therapy applications [453, 455]. Considering all these above mentioned parameters we selected two cell types, ASCs and BMSCs, for studies and compared the *in vitro* and *in vivo* potential of these two cell lines for myocardial therapy as the initial step. Upon obtaining superior results with ASCs we developed a new ASC delivery system using biocompatible polymeric microcapsules. Results confirmed that the microencapsulation process did not affect the viability of the stem cells; neither did it alter the natural differentiation potential of the stem cells (both adipose and bone marrow originated) as noticed with BMSCs in other studies [456].

Moreover, myocardial transplantation of microencapsulated ASCs in rat model confirmed the higher retention potential of the microencapsulated cells compared to free cells. Functional analysis also confirmed that this leads to better therapeutic effects in myocardially infarcted heart. Thus, this thesis reports a new class of myocardial implant system using biocompatible membranes to protect and efficiently deliver the entrapped cells at the transplant site using semi-permeable microcapsules. At present, the burgeoning number of cutting edge discoveries is leading to the design of biomimetic and biodegradable microcarriers that can easily combine with stem cells opening new doors in the

protection and transport of the cells to the target injured tissue and even in the control of cell fate.

Recently, genetic engineering has certainly extended the success of cell microencapsulation for biomedical applications [2, 80, 89, 384]. In essence, genes can now be used as templates, cells as reactors to secrete the final therapeutic product and microcapsules as immunoisolation vehicles for *in vivo* delivery of therapeutics. Thus, after confirming the potential of microencapsulated ASCs for myocardial therapy, as a next step, we genetically modified the encapsulated ASCs using recombinant baculovirus to further improve its therapeutic potential by overexpressing angiogenic proteins. Angiogenic proteins, such as VEGF, are critical paracrine mediators in facilitating post-ischemic myocardial recovery and likely play a role in mediating the stem cell therapy [457]. The suitability and significant therapeutic advantages of this system were noticed both with *in vitro* and *in vivo* results in myocardially infarcted immune-competent rat model. As an alternative to stem cell based angiogenic gene therapy, we also proved the effectiveness of recombinant baculovirus for direct myocardial therapy by promoting myocardial angiogenesis and arteriogenesis. Earlier studies have shown the effectiveness of only mammalian viruses for such myocardial gene therapies using VEGF and Ang1 transgenes [353, 376, 392, 393, 458, 459]. Here we developed an advanced gene delivery system using recombinant baculoviruses hybridized to positively charged nanoparticles by simple ionic bonding. The *in vitro* and *in vivo* implications of the developed myocardial implants, presented in this thesis work, have demonstrated encouraging results so far; further studies will investigate its full potential.

12.2 BACULOVIRUS ELUTING STENT FOR ANTI-RESTENOSIS THERAPY

The last part of the thesis aimed to address the recurrent problem of in-stent restenosis (ISR) associated with coronary artery angioplasty and stenting. In general, vascular stents are used to treat coronary heart disease as part of percutaneous coronary intervention and peripheral artery disease [460]. Coronary stents, which are by far the most popular, are commonly used to treat coronary artery disease caused by atherosclerosis. In the last couple of years, since the introduction of stents with polymer-based anti-proliferative drugs, DESs have been extensively used in percutaneous coronary interventions [410, 438, 439]. The introduction of drug eluting stents has been perceived as a significant improvement in the existing stent design. The drugs used are mostly those that target the issues related to the inflammation and subsequent proliferation of smooth muscle cells. Pharmacological stents have significantly reduced the occurrence of restenosis in comparison to commonly used bare metal stent (BMS) and stand alone balloon angioplasty, including in patients with acute ST-segment elevation myocardial infarction [461-465]. Data from randomized clinical trials have confirmed the benefits of DES in terms of decreasing the incidence of in-stent restenosis and the need for repeat revascularization [466-468]. Consequently, there has been a very rapid worldwide shift in the treatment of coronary stenosis from BMS to DES. In order to find out a suitable drug for the stent coating, a vast number of drugs have been studied which includes the paclitaxel and a range of the Limus family related drugs. Sirolimus was the first drug from Limus family to be approved for endovascular prosthesis. Cordis Corp., USA came up with this new Food and Drug Administration approved Cypher sirolimus eluting stent that functions by local delivery of the drug to the damaged inner lining of the arterial walls to inhibit *mammalian target of rapamycin* (mTOR) activity. This was followed up by development of Taxus paclitaxel eluting stent by Boston Scientific Corp, USA which showed significant roles in reducing in-stent restenosis [469-475].

However, the optimal treatment for DES is yet to be achieved [476-484]. A major concern for DES is the need for a very long dual antiplatelet therapy, to

stop late occurring stent thrombosis due to DES implantation. Through the effects of these anti-proliferation agents on vascular smooth muscle cells and inflammatory cells, DES drastically decelerates the rate of target-vessel revascularization. Moreover, the increased risk of late in-stent thrombosis (resulting in acute myocardial infarction and death) associated with use of these stents has become a major concern. These adverse effects are thought to result mainly from the antiproliferative effects of the drugs on the endothelial cells, leading to impaired arterial healing processes and partly from the use of non-biocompatible polymers in stent construction. The probability of acute and sub-acute thrombosis occurring after stent implantation is increased in patient-related factors such as acute myocardial infarction, diabetes mellitus, renal failure, advanced age, and low ejection fraction. Although in DES, the intimal hyperplasia volume can be reduced to less than 15% of stent volume, but stent underexpansion is a consistent finding in DES failures, leading to restenosis and thrombosis [485]. The Cypher stent failed in SIRIUS trials mainly because of stent underexpansion [486]. Another potential limitation of stent performance could be its faulty design that leads to stent foreshortening, which eventually affect stent performance and rate of restenosis [487].

This thesis opted for an alternative strategy. We aimed at repaving the injured artery segment with endothelial cells, instead of inhibiting smooth muscle cell proliferation. Rapid endothelialization has been shown in animal studies as an effective method of minimizing ISR [417]. The ability of certain cytokines which function as mitogens for endothelial cells may be exploited to accelerate the process of re-endothelialization. Direct application of soluble factors to the injured site has not always been successful due to problems associated with delivering and maintaining the relevant concentrations and functionality of the molecules at the site. It may however be possible to use these factors *ex-vivo* for the expansion of potential cells for subsequent use in seeding. The efficacy of such cell therapy depends, to a large extent, on the efficacy of the cell delivery system to the target site and its ability to proliferate and cover the luminal surface

of the injured vessel. Moreover, harvesting autologous cells from individual patients still poses logistic, economic, and timing constraints.

Here we used recombinant baculovirus mediated gene therapy approaches using transgenes to promote endothelial cell growth as an alternative to cell therapy. Plasmid DNA-eluting stents have been an area of interest to target in-stent restenosis via gene therapy [417]. Plasmid vectors gained the interest of researchers primarily due to lesser immunogenicity and pathogenicity than viral vectors. Klugherz *et al.* demonstrated successful transfection of arterial cells by Green fluorescent protein gene (GFP) via stents coated with the copolymer, polylacticpolyglycolic acid (PLGA), over the span of 7 days in porcine coronary arteries. This stent delivery system displayed a controlled release of the plasmid from the coated surface; the localized and sustained presence of DNA was designed to increase transfection efficiency. However, expression of GFP was observed in the lungs, indicating distal plasmid distribution [129]. In the pursuit of increasing the transfection efficiency of the DNA plasmid, this research group used a denatured collagen coating to use the αvβ3-integrin interactions to augment cellular transgene expression within porcine coronary arteries [488]. Among the genes that have been delivered via plasmid vectors is vascular endothelial growth factor (VEGF). Using PC-coated stents, naked plasmids encoding VEGF, an endothelial mitogen, were delivered to accelerate re-endothelialization [489]. Upon deployment of stent in rabbits, results showed an early improvement in endothelial recovery, followed by reduced neointimal growth around the stent after 3 months in hypercholesterolemic animals as compared to animals with only PC-coated stents [489]. Our present study is in sync with earlier works. We find significant beneficial effects of VEGF on local vascular biology.

Although naked plasmids have been used experimentally, but are limited by the poor cellular uptake and low expression level *in vivo*. As mentioned in the literature review section, several viral vectors have been since tried to overcome the problem of poor transfection efficiencies, the most common being the adenovirus vectors for VEGF delivery [404, 413, 414, 416, 419, 442, 443]. Other viral vectors such as recombinant adeno-associated (AAV) and retroviruses have

also been employed. The major disadvantages include cytotoxicity, transfection of non-target cells, and immunological and inflammatory reactions as well as limitations on the size of the transgene that can be expressed. All these vectors are capable of not only expressing genes but also have the potential for replication themselves in mammalian cells, and thus a potential biosafety risk. Clearly, a novel therapeutic stent with fewer associated adverse effects is much needed. Recently, PEI and PEI/PEG polymeric nanoparticles, cationic liposomes are also being used to deliver therapeutic genes like monocyte chemoattractant protein1, VEGF, inducible nitric oxide synthase to inhibit neointima growth by inducing SMC apoptosis or endothelial cell proliferation [490-493]. Apart from developing new biocompatible polymers for stent coating, Hemagglutinating virus of Japan envelope vector based gene delivery is also employed using catheter to inhibit restenosis *in vivo* [494, 495]. Furthermore, targeted delivery using nanoparticles has already been studied [496]. Such targeted nanoparticles can also be deposited onto the stent and eluted locally to the surrounding arterial tissues. Even nanoparticles can be used for efficient drug delivery. These particles have the advantages of biocompatibility, biodegradability, low systemic toxicity with no inflammatory response can be modified to targeted delivery system with provisions to have a controlled release. Polylactic acid nanoparticles were used for site-specific arterial tyrphostin drug delivery in rat carotid artery [497]. The drug release kinetics studies showed that this system has a biphasic drug pharmacokinetic profile with an initial accumulation of nanoparticles on the intima, followed by slower accumulation in the media of the artery. PLA and PLGA nanoparticles are also being used to deliver AG-2034, AG-1295 and U-86 aminochromone drugs for inhibition of vascular smooth muscle proliferation [498, 499]. In a preclinical study by Bhargava *et al* carbon-carbon nanoparticles carrying paclitaxel were coated on cobalt chromium stent and implanted in porcine coronary arteries to evaluate the safety and efficacy of the stent [500]. Clinical investigations on application of nanomedicine in treating in-stent restenosis are already on its way [501-503].

In this thesis, we have developed a nanocomplex of PAMAM dendrimers and biologically safe recombinant baculoviruses for enhanced vascular cell transduction. As a next step, we formulated a novel biocompatible fibrin coated stent carrying the nanocomplexes entrapped in PLGA microspheres to efficiently deliver angiogenic genes locally to the stented site. We characterized the developed stent, determined the *in vitro* kinetics of viral release from microspheres and assessed the functional activities of the released protein from stent-transduced SMCs and evaluated the feasibility of using this innovative platform for effective viral gene delivery *in vivo* in balloon denuded canine femoral arteries. The results obtained show that the stent can release viral particles in a controlled mode and efficiently transduce vascular cells *in vitro* and *in vivo* in a site-specific manner. Results also display the effectiveness of this newly developed stent to induce its therapeutic effect by promoting re-endothelialization of injured arteries and reducing the risk of ISR. Moreover, and in contrast to all other currently marketed drug-eluting stents, Bac_{VEGF} eluting stents result in acceleration of anatomic and functional endothelial recovery.

Prior studies have suggested that acceleration of reendothelialisation by VEGF can consequently attenuate restenosis and inhibit stent thrombosis [404, 417]. Our findings are consistent with these prior data and additionally capitalize on the advent of technology that makes gene delivery a straightforward extension of the standard revascularization procedure. The ability of locally delivered VEGF to accelerate reendothelialisation has been primarily attributed to the ability of VEGF to serve as an endothelial mitogen. Moreover, recent data have revealed direct inhibition of re-endothelialization by paclitaxel and inhibition of endothelial cell proliferation by rapamycin [504]. These findings suggest that endothelial recovery was inhibited by the antiproliferative approach by DESs.

In this context, we have considered the alternative hypothesis that stents that develop intimal thickening may result in part from belated re-endothelialization. Previous studies carried out in a variety of animal species have repeatedly shown that extensive endothelial denudation of the artery wall promotes neointimal thickening [404, 417]. Because it is difficult to achieve

extensive endothelial denudation without injuring the underlying media, it has been difficult to establish with certainty that the loss of endothelial integrity per se constitutes primary basis for neointimal thickening. But the data regarding the relationship between endothelial integrity and neointimal thickening in human arteries, although limited, are consistent with the results of animal experiments. It has been reported that the severity and extent of endothelial defects in coronary varies directly with the severity and extent of intimal disease [505].

So far, the widely used technologies for endovascular stenting procedure are still the bare metal and drug eluting stents. The drugs are mainly anti-proliferative, and while preventing smooth muscle cell overgrowth they lead to incomplete regeneration of the damaged endothelial layer. As an alternate, the newly formulated bioactive stent can enhance the local re-endothelialization mechanism leading to better recovery process and reduced chance of restenosis. Moreover, the bioactivity of stent can be retained once stored in the freezer, which further extends its commercial viability. In addition, the development of effective encapsulation methods to protect the functionality of active baculoviruses also opens up a new area for efficient baculovirus mediated therapies. To summarize, the newly formulated baculovirus based stent has the following unique features and advantages over the existing stent technology:

- *A new delivery system using microencapsulated baculoviruses*

Insect cell originated baculoviruses have long been considered as a biologically safe gene delivery vector for mammalian cells. Although it has been shown to effectively transduce mammalian cells *in vitro*, its full potential for *in vivo* gene therapy is not yet proven. Through this work, we have developed methods to protect it from host immune system as well as enhance its transduction ability which are its main limitations for *in vivo* applications.

Moreover, its transient nature of transgene expression is ideal in such a case where the expression ceases once the job is done. Moreover this also confirms the safety of the system to avoid unnecessary side effects post healing period.

- *Easy scale up procedure for high titre baculovirus production*

The availability of easily grown, suspension-ready host insect cells facilitates the cell growth scale up. As such, it is also easier to obtain high titre of recombinant baculoviruses. This makes the baculovirus expression system logistically beneficial and economically viable for process development and large production capacity. Furthermore, the serum free insect cell culture media reduces the production cost.

- *Targeted local therapy to treat restenosis*

Present invention offers a method for local and site specific delivery of therapeutics using vascular gene-carrying baculovirus eluting stent to reduce restenosis. The baculoviruses, once released from microspheres, locally transduce the tissues adherent to the stent surface; while the other non-stented sites remain untransduced. In contrary, the washed out drugs from DES can have side effects on other parts of the body due to their non-specific nature. Moreover, the locally transduced cells release active biomolecules to heal the stented region effectively in a site-specific way; while DES has relied on the half life of the drugs for their effectiveness.

- *Stent mediated efficient gene delivery to promote re-endothelialization*

Current mode of therapy exploits the therapeutics potential of indigenous growth factors by overexpressing them locally; while DES uses mainly synthetic chemical molecules foreign to the host system to induce the effects. As such, the present system offers a much safer approach using biotherapeutic molecules.

Although DESs are currently being widely used, these stents share the liability of impairing endothelial recovery and increasing the associated risk of stent thrombosis because of its anti-proliferative effect on vascular tissues. Present work has focused on a new anti-restenosis strategy using a gene-eluting stent, which ameliorates, rather than disrupts, the biology of the vessel wall by accelerating endothelial recovery post stent deployment. As an alternative, the proposed gene delivery system can be integrated with existing DES for combined stent therapy to treat restenosis and thrombosis.

- *Simple layer by layer coating method to load the viruses on the stent surface*

The method, developed here, for preparing the bioactive stent is relatively simple compared to commercially used methods where ultrasonic and twin-fluid nozzle technologies are used to spray coat the stent surface with polymers and therapeutics. Biocompatible fibrin hydrogels, containing microencapsulated baculoviruses, are coated on the stent surface by layer by layer manually. The genipin-crosslinked fibrin layer serves as the rigid barrier to external damages as well as protects the inner layers from premature virus release during its passage through the lumen of the artery at time of implantation at the desired site. The stent can also be preserved for at least 3 months in -80^{o}C freezer with intact bioactivity.

Taken together, this thesis evaluates and exemplifies the immense potential of the developed baculovirus based stent and microencapsulated stem cell technologies in the field of biomedical engineering, particularly as cardiovascular therapeutic implants.

13.1 SUMMARY OF OBSERVATIONS

Section I: Stem Cell based Cardiac Therapy

13.1.1 ASCs are suitable alternative to BMSCs for myocardial xenotransplantation

hASCs exhibited better proliferation capability and viability under normoxic and stressed hypoxic conditions respectively compared to hBMSCs. hASCs showed better differential potential towards cardiomyocyte phenotype. Both hASCs and hBMSCs showed significant improvement in myocardial pro/anti inflammatory cytokine levels with no detectable inflammatory reaction in immunocompetent animal model. hASCs also induced significant improvement in cardiac function and reduced infarction compared to hBMSC and untreated control groups.

13.1.2 Preparation of optimized polymeric microcapsule encapsulating stem cells

Three different formulations were prepared to encapsulate stem cells for effective therapeutic purposes. This includes AC microcapsules with outer layer as genipin (GCAC) or PEG (AC-PEG) and branched PEG surface functionalized alginate-poly-lysine microcapsules. Results demonstrate that the GCAC membrane was able to support cell viability, augment cell growth, and showed better results under external rotational and osmotic pressures with about 30% of the ruptured capsules in comparison to widely used 60% ruptured APA capsules. The membrane also provided immune-protection to the entrapped cells as demonstrated by the lymphocyte proliferation assay. The capsule also has potential for long-term storage. Most importantly the capsule maintained the differentiation potential of the entrapped stem cells. These behaviors were consistent with other microcapsule types too.

13.1.3 Angiogenic potential of microencapsulated ASCs

The encapsulated $4x10^6$ ASCs showed steady secretion of approximately 4600 pg VEGF over 15-day time period which is comparable to that of free cells. Under hyoxic condition ASCs can over-expresses VEGF compared to that under normoxic condition. Microencapsulated ASCs also showed similar behavior. Encapsulated ASCs showed 3.8-fold increase in VEGF secretion after 72 h hypoxic conditions in comparison to normoxic conditions. This increased VEGF expression resulted in improved angiogenic potential of the bioactive capsules as analyzed by enhanced endothelial cell proliferation.

13.1.4 Characterization of microencapsulated stem cells genetically modified with baculovirus

Microencapsulated stem cells genetically modified by baculovirus showed rapid expression of transgene within first 3-4days which gradually diminished over the next two weeks. The expression was also dependant on the viral transduction time with 8h viral incubation resulting in highest expression with longer expression time. Moreover, genetic modification and microencapsulation did alter the natural differentiation potential of encapsulated stem cells. Microencapsulated ASCs genetically modified to express VEGF also showed rapid expression of biologically functional secretory VEGF protein. This expression can be further increased by hybridizing them with cationic hyperbranched PAMAM G2 dendrimers.

13.1.5 Higher retention and superior therapeutic effect of microencapsulated ASCs compared to free ASCs after myocardial transplantation

In vivo potential of microencapsulated ASCs compared to free cells were evaluated in immunocompetent rats after induction of myocardial infarction. Results shows significant retention (3.5 times higher) of microencapsulated hASCs compared to free hASCs after 10 weeks of transplantation. Microencapsulated hASCs showed significantly attenuated infarct size compared to free hASCs and empty microcapsule group, enhanced vasculogenesis and

improved cardiac function. Control empty microcapsule group showed no local toxic effects.

13.1.6 Direct Ang1 gene therapy and ASC based Ang1 gene therapy of myocardial tissue using a new nanobiohybrid gene delivery system

A new gene delivery method utilizing the complementary strengths of viral and non-viral gene delivery systems has been developed by self assembly of negatively charged baculovirus and positively charged endosomolytic histidine rich Tat peptide/DNA nanoparticles, both carrying Ang1 cDNA. Under optimal transduction conditions, Bac-NP_{Ang1} showed significantly higher and sustained Ang-1 expression in cardiomyocytes and ASCs than Bac_{Ang1} or NP_{Ang1} alone. The expressed Ang1 has significant angiogenic potential and cardioprotective capacity as confirmed by functional bioassays. *In vivo* analysis with intramyocardially delivered Bac-NP_{Ang1} in MI rat model showed increase in capillary density and reduction in infarct sizes in Bac-NP_{Ang1} compared to Bac_{Ang1}, NP_{Ang1} and control groups due to enhanced myocardial Ang1 expression at peri-infarct regions (1.65 times higher than Bac_{Ang1}). Furthermore, the Bac-NP_{Ang1} group showed significantly higher cardiac performance in echocardiography than other groups. Similar outcomes were also obtained with ASC based Ang1 gene therapy. Thus these studies identified Bac-NP complex as an advanced gene delivery vehicle and demonstrated its potential to treat ischemic heart disease with high therapeutic index for direct gene therapy and combined stem cell-gene therapy strategy.

Section II: Vascular Stent based Anti-Restenosis therapy

13.1.7 Entrapment and protection of baculoviruses within microspheres

Baculovirus formulated in PLGA microspheres by w/o/o double emulsion solvent evaporation method can be efficiently used for controlled viral release, as well as, can be used to protect them against serum-inactivation. Moreover, the transduction efficiency with SMCs and serum-resistant potential can be enhanced

by hybridizing the baculovirus with cationic hyperbranched PAMAM G0 dendrimers before microencapsulating them.

13.1.8 Design and preparation of new baculovirus carrying polymeric vascular stent

The layer by layer coatings of microsphere-embedded fibrin on the stent surface offer a unique way to deliver the entrapped baculoviruses. The viral release from the stent surface can be controlled by altering the microsphere preparation method, fibrin concentration and number of layers depending on the requirements. Surface characterization of the coated stent confirmed even distribution of the microspheres on the stent surface. 24 h *in vitro* release profile study showed that around 41% of loaded viruses are released with a rapid release behavior noticed in the first 12h. The released viruses efficiently transduce the SMCs in culture without any cytotoxic effect. Similar results were obtained with Vegf carrying vectors where the transgene expressions were noticed for at least 21 days with highest expression in the first week. The released Vegf was also biologically active and showed strong mitotic and chemotactic effect on endothelial cells as analyzed by proliferation, wound healing and tube formation assays. The bioactivity of the stent was preserved for at least 3 months, once stored at -80^{o}C, which is an important logistic advantage under real life clinical settings.

13.1.9 Pre-clinical evaluation of stent in denuded canine femoral artery post balloon injury

This is the first study where recombinant baculoviruses are being efficiently used for gene therapy of post angioplasty ISR. Preclinical studies have confirmed the safety and efficacy of fibrin coated stents post deployment. Importantly the transgene expression was highly localized at the stented artery area with no detection of its presence at non-stented area. Moreover, the expression was transient in nature where expression was noticed on week 2, but not on week 16. This is ideal in this case, where the virus does its job locally at

the stent site and then ceases its expression and disappears once its job is done. 4 month study confirmed that the virus eluting stent can significantly accelerate endothelial recovery and attenuate arterial restenosis and neointimal proliferation.

13.2 CLAIMS TO ORIGINAL CONTRIBUTIONS:

Section I: Stem cell based Cardiac Therapy

13.2.1 First study, where vascular gene carrying invertebrate cell-specific recombinant baculoviruses have been generated and used efficiently for angiogenic therapies *in vitro* and *in vivo*.

13.2.2 A novel nano-biohybrid gene delivery system has been developed using recombinant baculoviruses and Tat peptide/DNA nanoparticles for improved mediated gene delivery. Its application has been demonstrated *in vitro* and *in vivo* in myocardial infarction therapy.

13.2.3 The nano-biohybrid complexes efficiently transduce human adipose tissue derived stem cells without any cytotoxic effect; their applications in combined stem cell-gene therapy demonstrate promising results as illustrated in myocardial infarction treatment.

13.2.4 Adipose derived stem cells can be an effective alternative to bone marrow derived stem cells for myocardial therapy and can be used for xenotransplantation.

13.2.5 A new formulation for successful myocardial transplantation of adipose derived stem cell has been developed using polymeric microcapsule cross-linked with naturally occurring genipin.

13.2.6 In addition, a novel microcapsule system has been developed where a branched PEG conjugated polymeric membrane is used to encapsulate adipose derived stem while maintaining its viability and natural potential to differentiate.

13.2.7 Surface functionalizing the baculovirus with cationic PAMAM dendrimers (Generation 2) can enhance the gene transfer efficiency towards ASCs without any cytotoxic effect.

Section II: Stent based therapy for Anti-Restenosis Therapy

13.2.8 A new method to protect baculoviruses from serum inactivation has been developed. The method comprises of (i) coating the surface with PAMAM dendrimers (Generation 0) followed by (ii) encapsulating them within biodegradable polymeric microspheres.

13.2.9 Two different schemes using w/o/o and w/o/w double emulsion solvent evaporation methods have been developed to formulate the bioactive baculoviruses within PLGA microspheres.

13.2.10 A novel gene-eluting vascular stent has been designed and developed using baculoviruses formulated in microsphere embedded hydrogel coated stent.

13.2.11 The stent can locally transfer therapeutic genes to the stented arterial wall and attenuate restenosis as demonstrated in 4 month study in balloon-injured canine femoral arteries.

13.1 Targeted delivery of microcapsules using surface functionalized ligands

Future work to use this ischemic injury marker molecule as the therapeutic target using surface functionalized antibody coated polymeric microcapsules will be interesting approach to target the microcapsules at the infarct region. This will promote efficient delivery of a high number of stem cells to the target site with no significant loss to non-specific sites. This will also allow the microcapsules to be administered in a much convenient intravenous route, compared to invasive intramyocardial injection. Myocardial infarction and perfusion induced ischemic injury has shown over expression of cardiac specific E3 ligase protein, Nrdp-1 in the heart tissue. Thus, surface functionalization of polymeric microcapsules with cardiac-specific Nrp1 antibodies can help in site-specific targeted delivery of stem cells for myocardially infarcted tissues.

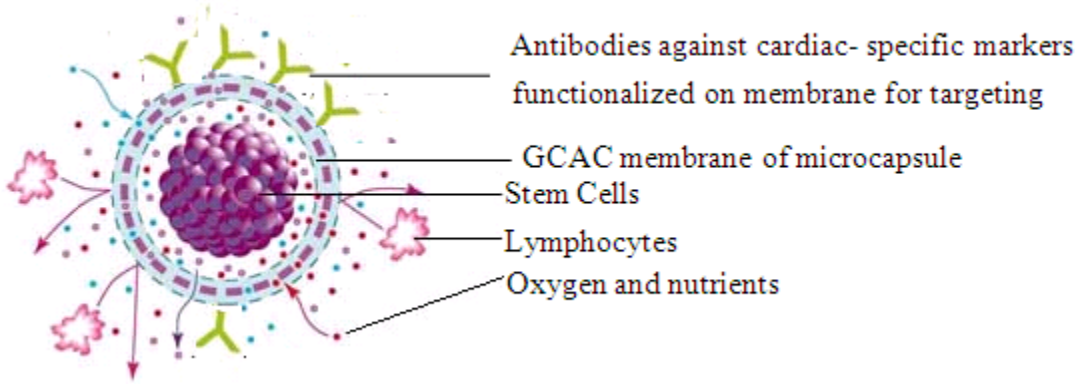

Figure 13.1 Scheme for targeted delivery of microencapsulated cells

13.2 More insight into the safety of microencapsulated cells

Further long term studies are needed to investigate the fate of the transplanted stem cells after degradation of the polymeric microcapsules. Through our studies we have focused on the paracrine effects of the implanted stem cells and proved the maintenance of viability and transgene expression potential *in vivo*. Detailed *in vivo* studies on whether the microencapsulated stem cells can

differentiate to cardiomyocytes or other lineages will be interesting. In case of intravenous administration, size of microcapsules will be an important factor to consider, as a bigger diameter can lead to higher risk of arterial embolism.

13.3 Delivery of microencapsulated ASCs with multiple-protein expressions using nanobiohybrid gene delivery system

As a next step of the present work, delivery of ASCs expressing a combination of therapeutic proteins will be beneficial. A combination of Vegf and Ang1 has been shown to enhance myocardial therapy than the individual proteins. Hybrid (Bac-NP) gene system carrying Vegf and Ang1 genes (one in Bac and other in NP) can be used in such case. This therapy can also be used for bone regeneration. A combined delivery of Vegf and BMP2 genes can enhance the angiogenic and osteogenic potential at the injured site which will be beneficial for the enhancement of bone formation and associated healing by re-establishment of vascularity.

13.4 Understanding the mechanism of stem cell cardiomyoplasty using microcapsules

One of the major problems regarding the current understanding of stem cell cardiomyoplasty is the lack of clear understanding behind the mechanism of stem cell based tissue repair. Over the years, there have been different schools of thoughts advocating the role of cellular transdifferentiation, cell fusion and paracrine secretions for the stem cell-based functional improvement of infarcted myocardial tissues. Although evidence exists to support each mechanism none of them have been very conclusive so far. The main difficulty encountered to understand the stem cell based tissue repairing process *in vivo* is to implicate one mechanism at a time, without any possible influence of other mechanisms. To answer this, application of microencapsulated stem cell technology can be beneficial. Encapsulation of MSCs will allow for exchange of paracrine factors yet prevent cell-cell contact. If indeed cell-cell contact is required for the process of transdifferentiation, then encapsulated MSCs will not adopt the cardiac phenotype. Furthermore, cellular fusion may also be investigated in this matter, as

fusion requires contact between the transplanted and the host myocardium. A seldom mentioned speculation that all the three mechanisms together contribute to the cardiac regeneration, but to different extents, is also an interesting point of view. But earlier investigations supporting the above hypothesis failed to consider all the three parameters in their experiments at the same time. For example, once considering cellular transdifferentiation and fusion, the possible concurrent paracrine effects were compromised. Microencapsulation technology, which isolates paracrine from mechanical effects of cellular therapy, can be utilized in such cases to critically analyze the overall combinatorial as well as individual roles of the three mechanisms for stem cell mediated cellular cardiomyoplasty.

13.5 Application of the nanobiohybrid gene delivery system for stent based therapy

In the present work, we used dendrimer coated baculovirus for stent based gene delivery. Our newly developed nanobiohybrid gene delivery system can further enhance the efficacy of the developed stent by delivering multiple genes (eg. Vegf and Ang1) at a time using the hybrid gene delivery system, as mentioned earlier. Further improvement of gene delivery efficiency can be achieved if the delivery system is surface modified with targeting ligands for tissue specific local delivery.

13.6 Method to reduce the instant viral loss from stent surface upon expansion

An important point while delivering a bioactive stent is to reduce the instant therapeutic loss during stent deployment due to deformation of stent structure. With better delivery technique and limited loss, the therapeutic effect can also be expected to be better. Although the stent developed through the present work showed not much viral loss due to encapsulation, but this can be a vital issue while delivering therapeutics without microspheres. The problem can be addressed by chemically or electrostatically conjugating the vectors (viral,

nanoparticles or non-viral, hybrid systems) to the polymer surface of the coated stent or directly to the stent surface.

13.7 Local delivery of recombinant baculoviruses from a bioresorbable stent platform

The concept of using bioresorbable stent as the platform for gene delivery can be advantageous for catalyzing active healing because bioresorption and elimination of the stent after the healing period will allow better physiologic restoration of the vascular natural environment. It will not only permit proper gene delivery but also will induce positive remodeling of the artery with reduced chance of having late thrombosis. After the healing period, the stent will disappear from the deployed site because of its transient nature. As a consequence, there will be no need to have a prolonged anti platelet therapy as is the case in drug eluting stent.

13.8 Determine optimal viral dosage and long term safety

It is essential to evaluate the effect of the stent over a longer period of time, such as 1 to 2 years. Present study confirmed the safety and effectiveness of the implanted stent over 4 months, but a longer clinical end point will render a bigger picture on biocompatibility of the stent or if there is any associated risk related with it. Experiments towards characterizing the degradation behavior of the composite polymer coated stent with time will also help us delve into this issue. A crucial parameter of this new therapeutic stent is the viral dose-response relationship profile. Characterizing this parameter, together with extensive safety and efficacy studies, will help us bring this innovative technology to the forefront of effective clinical trials.

13.9 Stent based combination therapy and other applications

As an alternative, the proposed gene delivery system can be integrated with existing DESs for stent based combined restenosis and thrombosis. For wider applications, it is also crucial to assess whether the formulated stent can attenuate ISR on other arterial sites too, such as carotid or coronary artery.

Reference List

1. Charo, I. F. and Taub, R. (2011). Anti-inflammatory therapeutics for the treatment of atherosclerosis. *Nature Reviews Drug Discovery*, 10 (5), 365-376.

2. Rissanen, T. T. and Yla-Herttuala, S. (2007). Current status of cardiovascular gene therapy. *Molecular Therapy*, 15 (7), 1233-1247.

3. Yla-Herttuala, S., Rissanen, T. T., Vajanto, I., and Hartikainen, J. (2007). Vascular endothelial growth factors - Biology and current status of clinical applications in cardiovascular medicine. *Journal of the American College of Cardiology*, 49 (10), 1015-1026.

4. Yla-Herttuala, S., Markkanen, J. E., and Rissanen, T. T. (2004). Gene therapy for ischemic cardiovascular disease: Somes lessons learned from the first clinical trials. *Trends in Cardiovascular Medicine*, 14 (8), 295-300.

5. Schachinger, V., Erbs, S., Elsasser, A., Haberbosch, W., Hambrecht, R., Holschermann, H., et al. (2006). Intracoronary bone marrow-derived progenitor cells in acute myocardial infarction. *New England Journal of Medicine*, 355 (12), 1210-1221.

6. Stevenson, W. G. and Stevenson, L. W. (1999). Atrial fibrillation in heart failure. *New England Journal of Medicine*, 341 (12), 910-911.

7. Kostuk, W. J. (2001). Congestive heart failure: What can we offer our patients? *Canadian Medical Association Journal*, 165 (8), 1053-1055.

8. Crespo-Leiro, M. G. and Cuenca-Castillo, J. J. (2006). Surgical treatment of heart failure: heart transplantation and ventricular restoration surgery. *European Heart Journal Supplements*, 8 (E), E39-E42

9. Krishnamani, R., DeNofrio, D., and Konstam, M. A. (2010). Emerging ventricular assist devices for long-term cardiac support. *Nature Reviews Cardiology*, 7 (2), 71-76.

10. Atoui, R., Shum-Tim, D., and Chiu, R. C. J. (2008). Myocardial regenerative therapy: Immunologic basis for the potential "Universal Donor Cells". *Annals of Thoracic Surgery*, 86 (1), 327-334.

11. Saito, T., Kuang, J. G., Lin, C. C. H., and Chiu, R. C. J. (2003). Transcoronary implantation of bone marrow stromal cells ameliorates cardiac function after myocardial infarction. *Journal of Thoracic and Cardiovascular Surgery*, 126 (1), 114-123.

12. Al Kindi, A. H., Asenjo, J. F., Ge, Y., Chen, G. Y., Bhathena, J., Chiu, R. C. J., et al. (2011). Microencapsulation to reduce mechanical loss of microspheres: implications in myocardial cell therapy. *European Journal of Cardio-Thoracic Surgery*, 39 (2), 241-247.

13. Atoui, R., Asenjo, J. F., Duong, M., Chen, G., Chiu, R. C. J., and Shum-Tim, D. (2008). Marrow stromal cells as universal donor cells for myocardial regenerative therapy: Their unique immune tolerance. *Annals of Thoracic Surgery*, 85 (2), 571-580.

14. Teng, C. J., Luo, J., Chiu, R. C. J., and Shum-Tim, D. (2006). Massive mechanical loss of microspheres with direct intramyocardial injection in the beating heart: Implications for cellular cardiomyoplasty. *Journal of Thoracic and Cardiovascular Surgery*, 132 (3), 628-632.

15. Prakash, S. and Chang, T. M. S. (1996). Microencapsulated genetically engineered live E-coli DH5 cells administered orally to maintain normal plasma urea level in uremic rats. *Nature Medicine*, 2 (8), 883-887.

16. Paul, A., Ge, Y., Prakash, S., and Shum-Tim, D. (2009). Microencapsulated stem cells for tissue repairing: implications in cell-based myocardial therapy. *Regenerative Medicine*, 4 (5), 733-745.

17. Zimmermann, H., Zimmermann, D., Reuss, R., Feilen, P. J., Manz, B., Katsen, A., et al. (2005). Towards a medically approved technology for alginate-based microcapsules allowing long-term immunoisolated transplantation. *Journal of Materials Science-Materials in Medicine*, 16 (6), 491-501.

18. Paul, A., Elhayek, E., Shum-Tim, D., and Prakash, S. (2010). Recent Advancements in Pharmacological Stent Therapy Using Polymeric Materials: Opportunities and Challenges. *Curr.Drug Deliv.*,

19. Belli, G., Ellis, S. G., and Topol, E. J. (1997). Stenting for ischemic heart disease. *Progress in Cardiovascular Diseases*, 40 (2), 159-182.

20. Scott, N. A. (2006). Restenosis following implantation of bare metal coronary stents: Pathophysiology and pathways involved in the vascular response to injury. *Advanced Drug Delivery Reviews*, 58 (3), 358-376.

21. Costa, M. A., Gilmore, P., Angiolilo, D. J., Zenni, M. M., Carter, A., Yakubov, S., et al. (2004). One year follow-up of patients with bypass graft versus native coronary disease treated with sirolimus-eluting stent in the SECURE trial. *Circulation*, 110 (17), 648

22. Costa, M. A. and Simon, D. I. (2005). Molecular basis of restenosis and drug-eluting stents. *Circulation*, 111 (17), 2257-2273.

23. Sousa, J. E., Costa, M. A., Abizaid, A., Feres, F., Seixas, A. C., Tanajura, L. F., et al. (2005). Four-year angiographic and intravascular ultrasound follow-up of patients treated with sirolimus-eluting stents. *Circulation*, 111 (18), 2326-2329.

24. van der Hoeven, B. L., Liem, S. S., Jukema, J. W., Oemrawsingh, P. V., Atsma, D. E., Bootsma, M., et al. (2005). Drug elating stents in patients with acute myocardial infarction: Initial results and six months clinical follow-up of the randomized MISSION! Intervention study. *American Journal of Cardiology*, 96 (7A), 56H

25. van der Hoeven, B. L., Pires, N. M. M., Warda, H. M., Oemrawsingh, P. V., van Vlijmen, B. J. M., Quax, P. H. A., et al. (2005). Drug-eluting stents: results, promises and problems. *International Journal of Cardiology*, 99 (1), 9-17.

26. Degertekin, M., Regar, E., Tanabe, K., Smits, P. C., van der Giessen, W. J., Carlier, S. G., et al. (2003). Sirolimus-eluting stent for treatment of complex in-stent restenosis - The first clinical experience. *Journal of the American College of Cardiology*, 41 (2), 184-189.

27. Degertekin, M., Serruys, P., Tanabe, K., Colombo, A., Guagliumi, G., Disco, C., et al. (2003). Serial intravascular ultrasound analysis in TAXUS II: beneficial distal edge effect with paclitaxel-eluting stents. *European Heart Journal*, 24 (421

28. Saia, F., Lemos, P. A., Lee, C. H., Arampatzis, C. A., Hoye, A., Degertekin, M., et al. (2003). Sirolimus-eluting stent implantation in ST-elevation acute myocardial infarction - A clinical and angiographic study. *Circulation*, 108 (16), 1927-1929.

29. Tanabe, K., Serruys, P. W., Grube, E., Smits, P. C., Selbach, G., van der Giessen, W. J., et al. (2003). TAXUS III trial - In-stent restenosis treated with stent-based delivery of paclitaxel incorporated in a slow-release polymer formulation. *Circulation*, 107 (4), 559-564.

30. Camici, G. G., Steffel, J., Akhmedov, A., Schafer, N., Baldinger, J., Schulz, U., et al. (2006). Dimethyl sulfoxide inhibits tissue factor expression, thrombus formation, and vascular smooth muscle cell activation: a potential treatment strategy for drug-eluting stents. *Circulation*, 114 (14), 1512-1521.

31. Camici, G. G., Steffel, J., Amanovic, I., Breitenstein, A., Baldinger, J., Keller, S., et al. (2009). Rapamycin promotes arterial thrombosis in vivo: implications for everolimus and zotarolimus eluting stents. *Eur.Heart J*,

32. Stahli, B. E., Camici, G. G., and Tanner, F. C. (2009). Drug-eluting stent thrombosis. *Ther.Adv.Cardiovasc.Dis.*, 3 (1), 45-52.

33. Wernick, M. H., Jeremias, A., and Carrozza, J. P. (2006). Drug-eluting stents and stent thrombosis: a cause for concern? *Coron.Artery Dis.*, 17 (8), 661-665.

34. Hehrlein, C. (2002). Radioactive stents - Problems and potential solutions. *Herz*, 27 (1), 17-22.

35. Nikas, D. N., Kalef-Ezra, J., Katsouras, C. S., Tsekeris, P., Bozios, G., Pappas, C., et al. (2007). Long-term clinical outcome of patients treated with beta-brachytherapy in routine clinical practice. *International Journal of Cardiology*, 115 (2), 183-189.

36. Schukro, C., Syeda, B., Kirisits, C., Schmid, R., Pichler, P., Pokrajac, B., et al. (2007). Randomized comparison between intracoronary beta-radiation brachytherapy and implantation of paclitaxel-eluting stents for the treatment of diffuse in-stent restenosis. *Radiotherapy and Oncology*, 82 (1), 18-23.

37. Torguson, R., Sabate, M., Deible, R., Smith, K., Chu, W. W., Kent, K. M., et al. (2006). Intravascular brachytherapy versus drug-eluting stents for the treatment of patients with drug-eluting stent restenosis. *American Journal of Cardiology*, 98 (10), 1340-1344.

38. Koizumi, T., Fitzgerald, P. J., Honda, Y., Ellis, S. G., Kent, K., Martin, S. L., et al. (2006). A randomized comparison of paclitaxel-eluting stents vs. intra-coronary brachytherapy in the treatment of in-stent restenosis: Intravascular ultrasound results from the TAXUS-V ISR trial. *Circulation*, 114 (18), 547

39. Paul, A., Abbasi, S., Shum-Tim, D., and Prakash, S. (2010). Nano- and Biotechnological Approaches in Current and Future Generation of Cardiovascular Stents. *Current Nanoscience*, 6 (5), 469-478.

40. Segers, V. F. M. and Lee, R. T. (2008). Stem-cell therapy for cardiac disease. *Nature*, 451 (7181), 937-942.

41. Stone, G. W., Brodie, B. R., Griffin, J. J., Costantini, C., Morice, M. C., Goar, F. G. S., et al. (1999). Clinical and angiographic follow-up after primary stenting in acute myocardial infarction - The primary angioplasty in myocardial infarction (PAMI) stent pilot trial. *Circulation*, 99 (12), 1548-1554.

42. Dangas, G. and Kuepper, F. (2002). Restenosis: Repeat narrowing of a coronary artery - Prevention and treatment. *Circulation*, 105 (22), 2586-2587.

43. Gehi, A. K., Pinney, S. P., and Gass, A. (2005). Recent diagnostic and therapeutic innovations in heart failure management. *Mt.Sinai J.Med.*, 72 (3), 176-184.

44. Kutschka, I., Chen, I. Y., Kofidis, T., Arai, T., von Degenfeld, G., Sheikh, A. Y., et al. (2006). Collagen matrices enhance survival of transplanted cardiomyoblasts and contribute to functional improvement of ischemic rat hearts. *Circulation*, 114 (I167-I173

45. Paul, A., Ge, Y., Prakash, S., and Shum-Tim, D. (2009). Microencapsulated stem cells for tissue repairing: implications in cell-based myocardial therapy. *Regen.Med.*, 4 (5), 733-745.

46. Hua, L., Aoki, T., Jin, Z., Nishino, N., Yasuda, D., Izumida, Y., et al. (2005). Elevation of serum albumin levels in Nagase analbuminemic rats by allogeneic bone marrow cell transplantation. *European Surgical Research*, 37 (2), 111-114.

47. Smits, P. C., van Geuns, R. J. M., Poldermans, D., Bountioukos, M., Onderwater, E. E. M., Lee, C. H., et al. (2003). Catheter-based intramyocardial injection of autologous skeletal myoblasts as a primary treatment of ischemic heart failure - Clinical experience with six-month follow-up. *Journal of the American College of Cardiology*, 42 (12), 2063-2069.

48. Silva, G. V., Perin, E. C., Dohmann, H. F. R., Borojevic, R., Silva, S. A., Sousa, A. L. S., et al. (2004). Catheter-based trans-endocardial delivery of autologous bone-marrow-derived mononuclear cells - in patients listed for heart transplantation. *Texas Heart Institute Journal*, 31 (3), 214-219.

49. Behr, L., Hekmati, M., Fromont, G., Borenstein, N., Noel, L. H., Lelievre-Pegorier, M., et al. (2007). Intra renal arterial injection of autologous mesenchymal stem cells in an ovine model in the postischemic kidney. *Nephron Physiology*, 107 (3), 65-76.

50. Fujii, H., Hirose, T., Oe, S., Yasuchika, K., Azuma, H., Fujikawa, T., et al. (2002). Contribution of bone marrow cells to liver regeneration after partial hepatectomy in mice. *Journal of Hepatology*, 36 (5), 653-659.

51. Liu, Z. C. and Chang, T. M. S. (2006). Transdifferentiation of bioencapsulated bone marrow cells into hepatocyte-like cells in the 90% hepatectomized rat model. *Liver Transplantation*, 12 (4), 566-572.

52. Dib, N., Michler, R. E., Pagani, F. D., Wright, S., Kereiakes, D. J., Lengerich, R., et al. (2005). Safety and feasibility of autologous myoblast transplantation in patients with ischemic cardiomyopathy - Four-year follow-up. *Circulation*, 112 (12), 1748-1755.

53. Schaefer, A., Zwadlo, C., Fuchs, M., Meyer, G. P., Lippolt, P., Wollert, K. C., et al. (2010). Long-term effects of intracoronary bone marrow cell transfer on diastolic function in patients after acute myocardial infarction: 5-year results from the randomized-controlled BOOST trial-an echocardiographic study. *European Journal of Echocardiography*, 11 (2), 165-171.

54. Thompson, C. A., Nasseri, B. A., Makower, J., Houser, S., McGarry, M., Lamson, T., et al. (2003). Percutaneous transvenous cellular cardiomyoplasty - A novel nonsurgical approach for myocardial cell transplantation. *Journal of the American College of Cardiology*, 41 (11), 1964-1971.

55. Laflamme, M. A. and Murry, C. E. (2005). Regenerating the heart. *Nature Biotechnology*, 23 (7), 845-856.

56. McDevitt, T. C., Woodhouse, K. A., Hauschka, S. D., Murry, C. E., and Stayton, P. S. (2003). Spatially organized layers of cardiomyocytes on biodegradable polyurethane films for myocardial repair. *Journal of Biomedical Materials Research Part A*, 66A (3), 586-595.

57. Ishii, O., Shin, M., Sueda, T., and Vacanti, J. P. (2005). In vitro tissue engineering of a cardiac graft using a degradable scaffold with an extracellular matrix-like topography. *Journal of Thoracic and Cardiovascular Surgery*, 130 (5), 1358-1363.

58. Zong, X. H., Bien, H., Chung, C. Y., Yin, L. H., Fang, D. F., Hsiao, B. S., et al. (2005). Electrospun fine-textured scaffolds for heart tissue constructs. *Biomaterials*, 26 (26), 5330-5338.

59. Dar, A., Shachar, M., Leor, J., and Cohen, S. (2002). Cardiac tissue engineering - Optimization of cardiac cell seeding and distribution in 3D porous alginate scaffolds. *Biotechnology and Bioengineering*, 80 (3), 305-312.

60. Yost, M. J., Baicu, C. F., Stonerock, C. E., Goodwin, R. L., Price, R. L., Davis, J. M., et al. (2004). A novel tubular scaffold for cardiovascular tissue engineering. *Tissue Engineering*, 10 (1-2), 273-284.

61. Birla, R. K., Borschel, G. H., Dennis, R. G., and Brown, D. L. (2005). Myocardial engineering in vivo: Formation and characterization of contractile, vascularized three-dimensional cardiac tissue. *Tissue Engineering*, 11 (5-6), 803-813.

62. Radisic, M., Euloth, M., Yang, L. M., Langer, R., Freed, L. E., and Vunjak-Novakovic, G. (2003). High-density seeding of myocyte cells for cardiac tissue engineering. *Biotechnology and Bioengineering*, 82 (4), 403-414.

63. Radisic, M., Deen, W., Langer, R., and Vunjak-Novakovic, G. (2005). Mathematical model of oxygen distribution in engineered cardiac tissue with parallel channel array perfused with culture medium containing oxygen carriers. *American Journal of Physiology-Heart and Circulatory Physiology*, 288 (3), H1278-H1289

64. Sekiya, S., Shimizu, T., Yamato, M., Kikuchi, A., and Okano, T. (2006). Bioengineered cardiac cell sheet grafts have intrinsic angiogenic potential. *Biochemical and Biophysical Research Communications*, 341 (2), 573-582.

65. Pham, Q. P., Sharma, U., and Mikos, A. G. (2006). Electrospinning of polymeric nanofibers for tissue engineering applications: A review. *Tissue Engineering*, 12 (5), 1197-1211.

66. Dimmeler, S., Zeiher, A. M., and Schneider, M. D. (2005). Unchain my heart: the scientific foundations of cardiac repair. *Journal of Clinical Investigation*, 115 (3), 572-583.

67. Suzuki, K., Murtuza, B., Beauchamp, J. R., Brand, N. J., Barton, P. J. R., Varela-Carver, A., et al. (2004). Role of interleukin-1 beta in acute inflammation and graft death after cell transplantation to the heart. *Circulation*, 110 (11), II219-II224

68. Teng, C. J., Luo, J., Chiu, R. C. J., and Shum-Tim, D. (2006). Massive mechanical loss of microspheres with direct intramyocardial injection in the beating heart: Implications for cellular cardiomyoplasty. *Journal of Thoracic and Cardiovascular Surgery*, 132 (3), 628-632.

69. Sun, Z. J., Lv, G. J., Li, S. Y., Yu, W. T., Wang, W., Xie, Y. B., et al. (2007). Differential role of microenvironment in microencapsulation for improved cell tolerance to stress. *Applied Microbiology and Biotechnology*, 75 (6), 1419-1427.

70. Orive, G., Hernandez, R. M., Gascon, A. R., Igartua, M., and Pedraz, J. L. (2003). Survival of different cell lines in alginate-agarose microcapsules. *European Journal of Pharmaceutical Sciences*, 18 (1), 23-30.

71. Chang, T. M. S. (1964). Semipermeable Microcapsules. *Science*, 146 (364), 524-&

72. Chang, T. M. S. and Prakash, S. (2001). Procedures for microencapsulation of enzymes, cells and genetically engineered microorganisms. *Molecular Biotechnology*, 17 (3), 249-260.

73. Cai, X. X., Lin, Y. F., Ou, G. M., Luo, E., Man, Y., Yuan, Q. A., et al. (2007). Ectopic osteogenesis and chondrogenesis of bone marrow stromal stem cells in alginate system. *Cell Biology International*, 31 (8), 776-783.

74. Murua, A., Portero, A., Orive, G., Hernandez, R. M., de Castro, M., and Pedraz, J. L. (2008). Cell microencapsulation technology: Towards clinical application. *Journal of Controlled Release*, 132 (2), 76-83.

75. Stolzing, A. and Scutt, A. (2006). Age-related impairment of mesenchymal progenitor cell function. *Aging Cell*, 5 (3), 213-224.

76. Zhang, H., Zhu, S. J., Wang, W., Wei, Y. J., and Hu, S. S. (2008). Transplantation of microencapsulated genetically modified xenogeneic cells augments angiogenesis and improves heart function. *Gene Therapy*, 15 (1), 40-48.

77. Maguire, T., Novik, E., Schloss, R., and Yarmush, M. (2006). Alginate-PLL microencapsulation: Effect on the differentiation of embryonic stem cells into hepatocytes. *Biotechnology and Bioengineering*, 93 (3), 581-591.

78. Liu, Z. C. and Chang, T. M. S. (2003). Coencapsulation of hepatocytes and bone marrow stem cells: In vitro conversion of ammonia and in vivo lowering of bilirubin in hyperbilirubemia Gunn rats. *International Journal of Artificial Organs*, 26 (6), 491-497.

79. Steinert, A., Weber, M., Dimmler, A., Julius, C., Schutze, N., Noth, U., et al. (2003). Chondrogenic differentiation of mesenchymal progenitor cells encapsulated in ultrahigh-viscosity alginate. *Journal of Orthopaedic Research*, 21 (6), 1090-1097.

80. Zilberman, Y., Turgeman, G., Pelled, G., Xu, N., Moutsatsos, I. K., Hortelano, G., et al. (2002). Polymer-encapsulated engineered adult mesenchymal stem cells secrete exogenously regulated rhBMP-2, and induce osteogenic and angiogenic tissue formation. *Polymers for Advanced Technologies*, 13 (10-12), 863-870.

81. Orlic, D., Hill, J. M., and Arai, A. E. (2002). Stem cells for myocardial regeneration. *Circulation Research*, 91 (12), 1092-1102.

82. Smits, A. M., van Vliet, P., Metz, C. H., Korfage, T., Sluijter, J. P. G., Doevendans, P. A., et al. (2009). Human cardiomyocyte progenitor cells differentiate into functional mature cardiomyocytes: an in vitro model for studying human cardiac physiology and pathophysiology. *Nature Protocols*, 4 (2), 232-243.

83. Arbab, A. S., Jordan, E. K., Wilson, L. B., Yocum, G. T., Lewis, B. K., and Frank, J. A. (2004). In vivo trafficking and targeted delivery of magnetically labeled stem cells. *Human Gene Therapy*, 15 (4), 351-360.

84. Hendrikx, M., Hensen, K., Clijsters, C., Jongen, H., Koninckx, R., Bijnens, E., et al. (2006). Recovery of regional but not global contractile

function by the direct intramyocardial autologous bone marrow transplantation - Results from a randomized controlled clinical trial. *Circulation*, 114 (I101-I107

85. Moelker, A. D., Baks, T., Wever, K. M. A. M., Spitskovsky, D., Wielopolski, P. A., van Beusekom, H. M. M., et al. (2007). Intracoronary delivery of umbilical cord blood derived unrestricted somatic stem cells is not suitable to improve LV function after myocardial infarction in swine. *Journal of Molecular and Cellular Cardiology*, 42 (4), 735-745.

86. Ishida, M., Tomita, S., Nakatani, T., Kagawa, K., Yamaguchi, T., Suga, M., et al. (2004). Acute effects of direct cell implantation into the heart: A pressure-volume study to analyze cardiac function. *Journal of Heart and Lung Transplantation*, 23 (7), 881-888.

87. Takahashi, K., Ito, Y., Morikawa, M., Kobune, M., Huang, J. H., Tsukamoto, M., et al. (2003). Adenoviral-delivered angiopoietin-1 reduces the infarction and attenuates the progression of cardiac dysfunction in the rat model of acute myocardial infarction. *Molecular Therapy*, 8 (4), 584-592.

88. Shah, P. B. and Losordo, D. W. (2005). Non-Viral Vectors for Gene Therapy: Clinical Trials in Cardiovascular Disease. *Non-Viral Vectors for Gene Therapy, Second Edition: Part 2*, 54 (339-361.

89. Pons, J., Huang, Y., Takagawa, J., Arakawa-Hoyt, J., Ye, J. Q., Grossman, W., et al. (2009). Combining angiogenic gene and stem cell therapies for myocardial infarction. *Journal of Gene Medicine*, 11 (9), 743-753.

90. Haider, H. K., Elmadbouh, I., Jean-Baptiste, M., and Ashraf, M. (2008). Nonviral vector gene modification of stem cells for myocardial repair. *Molecular Medicine*, 14 (1-2), 79-86.

91. Fuster, V. and Sanz, J. (2007). Gene therapy and stem cell therapy for cardiovascular diseases today: a model for translational research. *Nat.Clin.Pract.Cardiovasc.Med.*, 4 Suppl 1 (S1-S8

92. Baker, A. H. (2004). Designing gene delivery vectors for cardiovascular gene therapy. *Progress in Biophysics & Molecular Biology*, 84 (2-3), 279-299.

93. Tjia, S. T., Altenschildesche, G. M. Z., and Doerfler, W. (1983). Autographa Californica Nuclear Polyhedrosis-Virus (Acnpv) Dna Does Not Persist in Mass-Cultures of Mammalian-Cells. *Virology*, 125 (1), 107-117.

94. Paul, A., Jardin, B. A., Kulamarva, A., Malhotra, M., Elias, C. B., and Prakash, S. (2010). Recombinant Baculovirus as a Highly Potent Vector

for Gene Therapy of Human Colorectal Carcinoma: Molecular Cloning, Expression, and In Vitro Characterization. *Molecular Biotechnology*, 45 (2), 129-139.

95. Paul, A., Khan, A. A., Shum-Tim, D., and Prakash, S. (2010). BacMam Virus Transduced Cardiomyoblasts Can Be Used for Myocardial Transplantation Using AP-PEG-A Microcapsules: Molecular Cloning, Preparation, and In Vitro Analysis. *Journal of Biomedicine and Biotechnology*,

96. Jardin, B. A., Zhao, Y., Selvaraj, M., Montes, J., Tran, R., Prakash, S., et al. (2008). Expression of SEAP (secreted alkaline phosphatase) by baculovirus mediated transduction of HEK 293 cells in a hollow fiber bioreactor system. *Journal of Biotechnology*, 135 (3), 272-280.

97. Senior, K. (2000). Gene therapy: a rocky start to the new millennium. *Molecular Medicine Today*, 6 (3), 93

98. van Loo, N. D., Fortunati, E., Ehlert, E., Rabelink, M., Grosveld, F., and Scholte, B. J. (2001). Baculovirus infection of nondividing mammalian cells: Mechanisms of entry and nuclear transport of capsids. *Journal of Virology*, 75 (2), 961-970.

99. Matilainen, H., Rinne, J., Gilbert, L., Marjomaki, V., Reunanen, H., and Oker-Blom, C. (2005). Baculovirus entry into human hepatoma cells. *Journal of Virology*, 79 (24), 15452-15459.

100. Long, G., Pan, X. Y., Kormelink, R., and Vlak, J. M. (2006). Functional entry of baculovirus into insect and mammalian cells is dependent on clathrin-mediated endocytosis. *Journal of Virology*, 80 (17), 8830-8833.

101. Bilello, J. P., Delaney, W. E., Boyce, F. M., and Isom, H. C. (2001). Transient disruption of intercellular junctions enables baculovirus entry into nondividing hepatocytes. *Journal of Virology*, 75 (20), 9857-9871.

102. Matilainen, H., Makela, A. R., Riikonen, R., Saloniemi, T., Korhonen, E., Hyypia, T., et al. (2006). RGD motifs on the surface of baculovirus enhance transduction of human lung carcinoma cells. *Journal of Biotechnology*, 125 (1), 114-126.

103. Raty, J. K., Airenne, K. J., Marttila, A. T., Marjomaki, V., Hytonen, V. P., Lehtolainen, P., et al. (2004). Enhanced gene delivery by avidin-displaying baculovirus. *Molecular Therapy*, 9 (2), 282-291.

104. Dong, S. C., Wang, M. L., Qiu, Z. J., Deng, F., Vlak, J. M., Hu, Z. H., et al. (2010). Autographa californica Multicapsid Nucleopolyhedrovirus Efficiently Infects Sf9 Cells and Transduces Mammalian Cells via Direct

Fusion with the Plasma Membrane at Low pH. *Journal of Virology*, 84 (10), 5351-5359.

105. Paul, A. and Prakash, S. (2010). Baculovirus reveals a new pH-dependent direct cell-fusion pathway for cell entry and transgene delivery. *Future Virology*, 5 (5), 533-537.

106. Kost, T. A. and Condreay, J. P. (2002). Recombinant baculoviruses as mammalian cell gene-delivery vectors. *Trends in Biotechnology*, 20 (4), 173-180.

107. Wang, C. Y., Li, F., Yang, Y., Guo, H. Y., Wu, C. M., and Wang, S. (2006). Recombinant baculovirus containing the Diphtheria toxin A gene for malignant glioma therapy. *Cancer Research*, 66 (11), 5798-5806.

108. Nicholson, L. J., Philippe, M., Paine, A. J., Mann, D. A., and Dolphin, C. T. (2005). RNA interference mediated in human primary cells via recombinant baculoviral vectors. *Molecular Therapy*, 11 (4), 638-644.

109. Napoli, C., Maione, C., Schiano, C., Fiorito, C., and Ignarro, L. J. (2007). Bone marrow cell-mediated cardiovascular repair: potential of combined therapies. *Trends in Molecular Medicine*, 13 (7), 278-286.

110. Tang, T., Hu, J. G., Yang, J. F., Zhou, X. M., Yang, Y. F., Yin, B. L., et al. (2004). [Effect of mesenchymal stem cells transplantation on the apoptosis after rat myocardial infarction]. *Zhong.Nan.Da.Xue.Xue.Bao.Yi.Xue.Ban.*, 29 (3), 274-278.

111. Yang, J. F., Zhou, W. W., Zheng, W., Ma, Y. L., Lin, L., Tang, T., et al. (2007). Effects of myocardial transplantation of marrow mesenchymal stem cells transfected with vascular endothelial growth factor for the improvement of heart function and angiogenesis after myocardial infarction. *Cardiology*, 107 (1), 17-29.

112. Lim, Issel Anne L. Biocompatibility of Stent Materials. MIT Undergraduate ResearchJournal. 11, 33-37. 2004. (GENERIC)
Ref Type: Journal (Full)

113. Jimenez-Valero, S., Moreno, R., Sanchez-Recalde, A., Galeote, G., Calvo, L., Viana, A., et al. (2008). Avoiding restenosis: is there a role for glucocorticoids in the drug-eluting stent era? *Ther.Adv.Cardiovasc.Dis.*, 2 (3), 137-146.

114. Barlis, P. and Di Mario, C. (2007). Still a future for the bare metal stent? *International Journal of Cardiology*, 121 (1), 1-3.

115. Koutouzis, M., Nikolidakis, S., Arealis, G., and Kyriakides, Z. S. (2007). Very Late In-Stent Restenosis in a Bare Metal Stent. *Cardiology*, 107 (4), 360-361.

116. Ramos, A. R., Morice, M. C., and Lefevre, T. (2007). Late or very late stent thrombosis can also occur with bare metal stents. *Catheter.Cardiovasc.Interv.*, 70 (2), 229-232.

117. Saia, F., Marzocchi, A., and Branzi, A. (2008). The safety of drug-eluting stents. *Ther.Adv.Cardiovasc.Dis.*, 2 (1), 43-52.

118. Popma, J. J. and Tulli, M. (2006). Drug-eluting stents. *Cardiology Clinics*, 24 (2), 217-+

119. Sollott, S. J., Cheng, L., Pauly, R. R., Jenkins, G. M., Monticone, R. E., Kuzuya, M., et al. (1995). Taxol inhibits neointimal smooth muscle cell accumulation after angioplasty in the rat. *J Clin.Invest*, 95 (4), 1869-1876.

120. Meredith, I. T., Ormiston, J., Whitbourn, R., Kay, I. P., Muller, D., Bonan, R., et al. (2005). First-in-human study of the Endeavor ABT-578-eluting phosphorylcholine-encapsulated stent system in de novo native coronary artery lesions: Endeavor I Trial. *EuroIntervention.*, 1 (2), 157-164.

121. Meredith, I. T., Ormiston, J., Whitbourn, R., Kay, I. P., Muller, D., Popma, J. J., et al. (2007). Four-year clinical follow-up after implantation of the endeavor zotarolimus-eluting stent: ENDEAVOR I, the first-in-human study. *Am.J Cardiol.*, 100 (8B), 56M-61M.

122. Miu, R., Serruys, P. W., and Stone, G. W. (2009). Performance of Everolimus-Eluting Stents: Pooled Analysis from the SPIRIT Trials. *Journal of Interventional Cardiology*, 22 (S41-S47

123. Grube, E., Abizaid, A., and Hauptmann, K. E. (2005). High risk subgroups in patients treated with the BioMatrix (TM) Biolimus A9 (TM)-eluting coronary stent: Results from the STEALTH (Stent Eluting A9 Biolimus (TM) Trial in Humans) trial. *American Journal of Cardiology*, 96 (7A), 208H

124. Missell, E., Abizaid, A., Grube, E., Mattos, L. A., Feres, F., Staico, R. F., et al. (2005). Late intravascular ultrasound volumetric analysis after implantation of sirolimus versus Biolimus A9 eluting stents in human coronary arteries. *American Journal of Cardiology*, 96 (7A), 211H

125. Morice, M. C., Bestehorn, H. P., Carrie, D., Macaya, C., Aengevaeren, W., Wijns, W., et al. (2006). Direct stenting of de novo coronary stenoses with tacrolimus-eluting versus carbon-coated carbostents. The randomized JUPITER II trial. *EuroIntervention.*, 2 (1), 45-52.

126. Garg, U. C. and Hassid, A. (1989). Nitric oxide-generating vasodilators and 8-bromo-cyclic guanosine monophosphate inhibit mitogenesis and proliferation of cultured rat vascular smooth muscle cells. *J Clin Invest*, 83 (5), 1774-1777.

127. Sharif, S., Hynes, S. O., Cooney, R., Howard, L., McMahon, J., Daly, K., et al. (2008). Gene-eluting Stents: Adenovirus-mediated Delivery of eNOS to the Blood Vessel Wall Accelerates Re-endothelialization and Inhibits Restenosis. *Molecular Therapy*, 10 (1674), 1680

128. Johnson, T. W., Wu, Y. X., Herdeg, C., Baumbach, A., Newby, A. C., Karsch, K. R., et al. (2005). Stent-Based Delivery of Tissue Inhibitor of Metalloproteinase-3 Adenovirus Inhibits Neointimal Formation in Porcine Coronary Arteries. *Arterioscler Thromb Vasc Biol*, 25 (4), 754-759.

129. Klugherz, B. D., Jones, P. L., Cui, X., Chen, W., Meneveau, N. F., DeFelice, S., et al. (2000). Gene delivery from a DNA controlled-release stent in porcine coronary arteries. *Nat Biotech*, 18 (11), 1181-1184.

130. Sharif, F., Hynes, S. O., McMahon, J., Cooney, R., Conroy, S., Dockery, P., et al. (2006). Gene-Eluting Stents: Comparison of Adenoviral and Adeno- Associated Viral Gene Delivery to the Blood Vessel Wall In Vivo. *Human gene therapy*, 17 (7),

131. Ye, Y.-W., Landau, C., Willard, J. E., and Rajasubramanian, G. (1998). Bioresorbable Microporous Stents Deliver Recombinant Adenovirus Gene Transfer Vectors to the Arterial Wall. *Annals of Biomedical Engineering*, 26 (3), 398-408.

132. Klugherz, B. D., Song, C., DeFelice, S., Cui, X., Lu, Z., Connolly, J., et al. (2004). Gene Delivery to Pig Coronary Arteries from Stents Carrying Antibody-Tethered Adenovirus. *Human gene therapy*, 13 (3), 443-454.

133. Sharif, F., Hynes, S. O., McCullagh, K., Ganly, S., Greiser, U., Crowley, J., et al. (2009). Abstract 4403: Stent-based Liposomal Gene Delivery: Characterization of Target Cell Population, Pattern of Expression and Therapeutic Potential of Lipostents. *Circulation*, 120 (18_MeetingAbstracts), S952-S95a

134. Stephan, D. J., Yang, Z. Y., San, H., Simari, R. D., Wheeler, C. J., Felgner, P. L., et al. (2008). A New Cationic Liposome DNA Complex Enhances the Efficiency of Arterial Gene Transfer In Vivo. *Human gene therapy*, 7 (15), 1803-1812.

135. Nam, S. H., Nam, H. Y., H, and J (2007). Curcumin-loaded PLGA nanoparticles coating onto metal stent by electrophoretic deposition techniques. *Bulletin of the Korean Chemical Society*, 28 (3), 397-402.

136. Florence, A. T. (2008). Issues in Oral Nanoparticle Drug Carrier Uptake and Targeting. *Journal of Drug Targeting*, 12 (2), 65-70.

137. Kim, T. G., Lee, Y., and Park, T. G. (2010). Controlled gene-eluting metal stent fabricated by bio-inspired surface modification with hyaluronic acid and deposition of DNA/PEI polyplexes. *International Journal of Pharmaceutics*, 384 (1-2), 181-188.

138. Steinhauser, I., Langer, K., Strebhardt, K., and Sp+ñnkuch, B. (2009). Uptake of plasmid-loaded nanoparticles in breast cancer cells and effect on Plk1 expression. *Journal of Drug Targeting*, 17 (8), 627-637.

139. Lloyd, J. (2010). Heart Disease and Stroke Statistics-2009 Update: A Report From the American Heart Association Statistics Committee and Stroke Statistics Subcommittee (vol 119, pg e21, 2009). *Circulation*, 122 (1), E11

140. Knowlton, K. U. and Chien, K. R. (1999). Inflammatory pathways and cardiac repair: the affliction of infarction. *Nature Medicine*, 5 (10), 1122-1123.

141. Opie, L. H., Commerford, P. J., Gersh, B. J., and Pfeffer, M. A. (2006). Controversies in Cardiology 4 - Controversies in ventricular remodelling. *Lancet*, 367 (9507), 356-367.

142. Antonitsis, P., Loannidou-Papagiannaki, E., Kaidogou, A., Charokopos, N., Kalogeridis, A., Kouzi-Koliakou, K., et al. (2008). Cardiomyogenic potential of human adult bone marrow mesenchymal stem cells in vitro. *Thoracic and Cardiovascular Surgeon*, 56 (2), 77-82.

143. Rota, M., Kajstura, J., Hosoda, T., Bearzi, C., Vitale, S., Esposito, G., et al. (2007). Bone marrow cells adopt the cardiomyogenic fate in vivo. *Proceedings of the National Academy of Sciences of the United States of America*, 104 (45), 17783-17788.

144. Dengler, T. J. and Katus, H. A. (2002). Stem cell therapy for the infarcted heart ("cellular cardiomyoplasty"). *Herz*, 27 (7), 598-610.

145. Wojakowski, W. and Tendera, M. (2010). New Concepts in Cardiac Stem Cell Therapy. *Hellenic Journal of Cardiology*, 51 (1), 10-14.

146. Wang, J. S., Shum-Tim, D., Galipeau, J., Chedrawy, E., Eliopoulos, N., and Chiu, R. C. J. (2000). Marrow stromal cells for cellular cardiomyoplasty: Feasibility and potential clinical advantages. *Journal of Thoracic and Cardiovascular Surgery*, 120 (5), 999-1006.

147. Orlic, D., Kajstura, J., Chimenti, S., Bodine, D. M., Leri, A., and Anversa, P. (2001). Transplanted adult bone marrow cells repair myocardial infarcts

in mice. *Hematopoietic Stem Cells 2000 Basic and Clinical Sciences*, 938 (221-230.

148. Janssens, S., Dubois, C., Bogaert, J., Theunissen, K., Deroose, C., Desmet, W., et al. (2006). Autologous bone marrow-derived stem-cell transfer in patients with ST-segment elevation myocardial infarction: double-blind, randomised controlled trial. *Lancet*, 367 (9505), 113-121.

149. Zhang, C. Y., Sun, A. J., Zhang, S. N., Yao, K., Wu, C. N., Fu, M. Q., et al. (2010). Efficacy and Safety of Intracoronary Autologous Bone Marrow-Derived Cell Transplantation in Patients With Acute Myocardial Infarction: Insights From Randomized Controlled Trials With 12 or More Months Follow-Up. *Clinical Cardiology*, 33 (6), 353-360.

150. Wollert, K. C., Meyer, G. P., Lotz, J., Ringes-Lichtenberg, S., Lippolt, P., Breidenbach, C., et al. (2004). Intracoronary autologous bone-marrow cell transfer after myocardial infarction: the BOOST randomised controlled clinical trial. *Lancet*, 364 (9429), 141-148.

151. Stamm, C., Liebold, A., Steinhoff, G., and Strunk, D. (2006). Stem cell therapy for ischemic heart disease: Beginning or end of the road? *Cell Transplantation*, 15 (S47-S56

152. George, J. C. (2010). Stem cell therapy in acute myocardial infarction: a review of clinical trials. *Translational Research*, 155 (1), 10-19.

153. Atoui, R., Shum-Tim, D., and Chiu, R. C. J. (2008). Myocardial regenerative therapy: Immunologic basis for the potential "Universal Donor Cells". *Annals of Thoracic Surgery*, 86 (1), 327-334.

154. Atoui, R., Asenjo, J. F., Duong, M., Chen, G., Chiu, R. C. J., and Shum-Tim, D. (2008). Marrow stromal cells as universal donor cells for myocardial regenerative therapy: Their unique immune tolerance. *Annals of Thoracic Surgery*, 85 (2), 571-580.

155. Chen, G. Y., Nayan, M., Duong, M., Asenjo, J. F., Ge, Y., Chiu, R. C. J., et al. (2010). Marrow Stromal Cells for Cell-Based Therapy: The Role of Antiinflammatory Cytokines in Cellular Cardiomyoplasty. *Annals of Thoracic Surgery*, 90 (1), 190-198.

156. MacDonald, D. J., Luo, J., Saito, T., Duong, M., Bernier, P. L., Chiu, R. C. J., et al. (2005). Persistence of marrow stromal cells implanted into acutely infarcted myocardium: Observations in a xenotransplant model. *Journal of Thoracic and Cardiovascular Surgery*, 130 (4), 1114-1121.

157. Saito, T., Kuang, J. Q., Bittira, B., Al-Khaldi, A., and Chiu, R. C. J. (2002). Xenotransplant cardiac chimera: Immune tolerance of adult stem cells. *Annals of Thoracic Surgery*, 74 (1), 19-24.

158. Toma, C., Pittenger, M. F., Cahill, K. S., Byrne, B. J., and Kessler, P. D. (2002). Human mesenchymal stem cells differentiate to a cardiomyocyte phenotype in the adult murine heart. *Circulation*, 105 (1), 93-98.

159. Min, J. Y., Sullivan, M. F., Yang, Y., Zhang, J. P., Converso, K. L., Morgan, J. P., et al. (2002). Significant improvement of heart function by cotransplantation of human mesenchymal stem cells and fetal cardiomyocytes in postinfarcted pigs. *Annals of Thoracic Surgery*, 74 (5), 1568-1575.

160. De Ugarte, D. A., Morizono, K., Elbarbary, A., Alfonso, Z., Zuk, P. A., Zhu, M., et al. (2003). Comparison of multi-lineage cells from human adipose tissue and bone marrow. *Cells Tissues Organs*, 174 (3), 101-109.

161. Zuk, P. A., Zhu, M., Ashjian, P., De Ugarte, D. A., Huang, J. I., Mizuno, H., et al. (2002). Human adipose tissue is a source of multipotent stem cells. *Molecular Biology of the Cell*, 13 (12), 4279-4295.

162. Rehman, J., Traktuev, D., Li, J. L., Merfeld-Clauss, S., Temm-Grove, C. J., Bovenkerk, J. E., et al. (2004). Secretion of angiogenic and antiapoptotic factors by human adipose stromal cells. *Circulation*, 109 (10), 1292-1298.

163. Yu, L. H., Kim, M. H., Park, T. H., Cha, K. S., Kim, Y. D., Quan, M. L., et al. (2010). Improvement of cardiac function and remodeling by transplanting adipose tissue-derived stromal cells into a mouse model of acute myocardial infarction. *International Journal of Cardiology*, 139 (2), 166-172.

164. Cai, L. Y., Johnstone, B. H., Cook, T. G., Tan, J., Fishbein, M. C., Chen, P. S., et al. (2009). IFATS Collection: Human Adipose Tissue-Derived Stem Cells Induce Angiogenesis and Nerve Sprouting Following Myocardial Infarction, in Conjunction with Potent Preservation of Cardiac Function. *Stem Cells*, 27 (1), 230-237.

165. Paul, A., Shum-Tim, D., and Prakash, S. (2010). Investigation on PEG Integrated Alginate-Chitosan Microcapsules for Myocardial Therapy Using Marrow Stem Cells Genetically Modified by Recombinant Baculovirus. *Cardiovascular Engineering and Technology*, 1 (2), 154-164.

166. Rangappa, S., Fen, C., Lee, E. H., Bongso, A., and Wei, E. S. K. (2003). Transformation of adult mesenchymal stem cells isolated from the fatty tissue into cardiomyocytes. *Annals of Thoracic Surgery*, 75 (3), 775-779.

167. Guan, K., Nayernia, K., Maier, L. S., Wagner, S., Dressel, R., Lee, J. H., et al. (2006). Pluripotency of spermatogonial stem cells from adult mouse testis. *Nature*, 440 (7088), 1199-1203.

168. Paul, A., Ge, Y., Prakash, S., and Shum-Tim, D. (2009). Microencapsulated stem cells for tissue repairing: implications in cell-based myocardial therapy. *Regen.Med.*, 4 (5), 733-745.

169. Davani, S., Marandin, A., Mersin, N., Royer, B., Kantelip, B., Herve, P., et al. (2003). Mesenchymal progenitor cells differentiate into an endothelial phenotype, enhance vascular density, and improve heart function in a rat cellular cardiomyoplasty model. *Circulation*, 108 (10), 253-258.

170. Stumpf, C., Seybold, K., Petzi, S., Wasmeier, G., Raaz, D., Yilmaz, A., et al. (2008). Interleukin-10 improves left ventricular function in rats with heart failure subsequent to myocardial infarction. *European Journal of Heart Failure*, 10 (8), 733-739.

171. Lee, R. H., Kim, B., Choi, I., Kim, H., Choi, H. S., Suh, K., et al. (2004). Characterization and expression analysis of mesenchymal stem cells from human bone marrow and adipose tissue. *Cellular Physiology and Biochemistry*, 14 (4-6), 311-324.

172. Choi, Y. S., Dusting, G. J., Stubbs, S., Arunothayaraj, S., Han, X. L., Collas, P., et al. (2010). Differentiation of human adipose-derived stem cells into beating cardiomyocytes. *Journal of Cellular and Molecular Medicine*, 14 (4), 878-889.

173. Lee, W. C. C., Sepulveda, J. L., Rubin, J. P., and Marra, K. G. (2009). Cardiomyogenic differentiation potential of human adipose precursor cells. *International Journal of Cardiology*, 133 (3), 399-401.

174. Compton, S. J., Cairns, J. A., Holgate, S. T., and Walls, A. F. (1998). The role of mast cell tryptase in regulating endothelial cell proliferation, cytokine release, and adhesion molecule expression: Tryptase induces expression of mRNA for IL-1 beta and IL-8 and stimulates the selective release of IL-8 from human umbilical vein endothelial cells. *Journal of Immunology*, 161 (4), 1939-1946.

175. Lacraz, S., Nicod, L. P., Chicheportiche, R., Welgus, H. G., and Dayer, J. M. (1995). Il-10 Inhibits Metalloproteinase and Stimulates Timp-1 Production in Human Mononuclear Phagocytes. *Journal of Clinical Investigation*, 96 (5), 2304-2310.

176. Schenke-Layland, K., Strem, B. M., Jordan, M. C., DeEmedio, M. T., Hedrick, M. H., Roos, K. P., et al. (2009). Adipose Tissue-Derived Cells Improve Cardiac Function Following Myocardial Infarction. *Journal of Surgical Research*, 153 (2), 217-223.

177. Bai, X. W., Yan, Y. S., Song, Y. H., Droll, L. H., Vykoukal, D., and Alt, E. (2009). Intramyocardial Injection of Human Adipose Tissue-Derived

Stem Cells Improve Cardiac Function Following Acute Myocardial Infarction. *Journal of the American College of Cardiology*, 53 (10), A313

178. van der Bogt, K. E. A., Schrepfer, S., Yu, J., Sheikh, A. Y., Hoyt, G., Govaert, J. A., et al. (2009). Comparison of Transplantation of Adipose Tissue- and Bone Marrow-Derived Mesenchymal Stem Cells in the Infarcted Heart. *Transplantation*, 87 (5), 642-652.

179. Strem, B. M., Hicok, K. C., Zhu, M., Wulur, I., Alfonso, Z., Schreiber, R. E., et al. (2005). Multipotential differentiation of adipose tissue-derived stem cells. *Keio J.Med.*, 54 (3), 132-141.

180. Sanz-Ruiz, R., Fernandez-Santos, E., Dominguez-Munoa, M., Parma, R., Villa, A., Fernandez, L., et al. (2009). Early Translation of Adipose-Derived Cell Therapy for Cardiovascular Disease. *Cell Transplantation*, 18 (3), 245-254.

181. Zuk, P. A., Zhu, M., Ashjian, P., De Ugarte, D. A., Huang, J. I., Mizuno, H., et al. (2002). Human adipose tissue is a source of multipotent stem cells. *Mol.Biol.Cell*, 13 (12), 4279-4295.

182. De Ugarte, D. A., Morizono, K., Elbarbary, A., Alfonso, Z., Zuk, P. A., Zhu, M., et al. (2003). Comparison of multi-lineage cells from human adipose tissue and bone marrow. *Cells Tissues.Organs*, 174 (3), 101-109.

183. Mizuno, H. (2009). Adipose-derived stem cells for tissue repair and regeneration: ten years of research and a literature review. *J.Nippon Med.Sch*, 76 (2), 56-66.

184. Nakagami, H., Morishita, R., Maeda, K., Kikuchi, Y., Ogihara, T., and Kaneda, Y. (2006). Adipose tissue-derived stromal cells as a novel option for regenerative cell therapy. *J.Atheroscler.Thromb.*, 13 (2), 77-81.

185. Nie, C., Yang, D., and Morris, S. F. (2009). Local delivery of adipose-derived stem cells via acellular dermal matrix as a scaffold: a new promising strategy to accelerate wound healing. *Med.Hypotheses*, 72 (6), 679-682.

186. Miranville, A., Heeschen, C., Sengenes, C., Curat, C. A., Busse, R., and Bouloumie, A. (2004). Improvement of postnatal neovascularization by human adipose tissue-derived stem cells. *Circulation*, 110 (3), 349-355.

187. Yu, L. H., Kim, M. H., Park, T. H., Cha, K. S., Kim, Y. D., Quan, M. L., et al. (2010). Improvement of cardiac function and remodeling by transplanting adipose tissue-derived stromal cells into a mouse model of acute myocardial infarction. *International Journal of Cardiology*, 139 (2), 166-172.

188. Cao, Y., Sun, Z., Liao, L. M., Meng, Y., Han, Q., and Zhao, R. C. H. (2005). Human adipose tissue-derived stem cells differentiate into endothelial cells in vitro and improve postnatal neovascularization in vivo. *Biochemical and Biophysical Research Communications*, 332 (2), 370-379.

189. Guan, L. D., Li, S. Q., Wang, Y. F., Yue, H. M., Liu, D. Q., He, L. J., et al. (2006). In vitro differentiation of human adipose-derived mesenchymal stem cells into endothelial-like cells. *Chinese Science Bulletin*, 51 (15), 1863-1868.

190. Madonna, R. and De Caterina, R. (2010). Adipose tissue: a new source for cardiovascular repair. *Journal of Cardiovascular Medicine*, 11 (2), 71-80.

191. Itoi, Y., Takatori, M., Hyakusoku, H., and Mizuno, H. (2009). Comparison of readily available scaffolds for adipose tissue engineering using adipose-derived stem cells. *J.Plast.Reconstr.Aesthet.Surg.*,

192. Mehlhorn, A. T., Zwingmann, J., Finkenzeller, G., Niemeyer, P., Dauner, M., Stark, B., et al. (2009). Chondrogenesis of adipose-derived adult stem cells in a poly-lactide-co-glycolide scaffold. *Tissue Eng Part A*, 15 (5), 1159-1167.

193. Wei, Y., Hu, Y., Hao, W., Han, Y., Meng, G., Zhang, D., et al. (2008). A novel injectable scaffold for cartilage tissue engineering using adipose-derived adult stem cells. *J.Orthop.Res.*, 26 (1), 27-33.

194. Orive, G., Gascon, A. R., Hernandez, R. M., Igartua, M., and Luis, P. J. (2003). Cell microencapsulation technology for biomedical purposes: novel insights and challenges. *Trends Pharmacol.Sci.*, 24 (5), 207-210.

195. Zhang, H., Zhu, S. J., Wang, W., Wei, Y. J., and Hu, S. S. (2008). Transplantation of microencapsulated genetically modified xenogeneic cells augments angiogenesis and improves heart function. *Gene Ther.*, 15 (1), 40-48.

196. Chen, H., Ouyang, W., Jones, M., Metz, T., Martoni, C., Haque, T., et al. (2007). Preparation and characterization of novel polymeric microcapsules for live cell encapsulation and therapy. *Cell Biochem.Biophys.*, 47 (1), 159-168.

197. Orive, G., Tam, S. K., Pedraz, J. L., and Halle, J. P. (2006). Biocompatibility of alginate-poly-L-lysine microcapsules for cell therapy. *Biomaterials*, 27 (20), 3691-3700.

198. Orive, G., Hernandez, R. M., Rodriguez, G. A., Calafiore, R., Chang, T. M., de, V. P., et al. (2004). History, challenges and perspectives of cell microencapsulation. *Trends Biotechnol.*, 22 (2), 87-92.

199. Haque, T., Chen, H., Ouyang, W., Martoni, C., Lawuyi, B., Urbanska, A. M., et al. (2005). Superior cell delivery features of poly(ethylene glycol) incorporated alginate, chitosan, and poly-L-lysine microcapsules. *Mol.Pharm.*, 2 (1), 29-36.

200. Chen, H., Ouyang, W., Lawuyi, B., and Prakash, S. (2006). Genipin cross-linked alginate-chitosan microcapsules: membrane characterization and optimization of cross-linking reaction. *Biomacromolecules.*, 7 (7), 2091-2098.

201. Mwale, F., Iordanova, M., Demers, C. N., Steffen, T., Roughley, P., and Antoniou, J. (2005). Biological evaluation of chitosan salts cross-linked to genipin as a cell scaffold for disk tissue engineering. *Tissue Engineering*, 11 (1-2), 130-140.

202. Chen, H., Ouyang, W., Lawuyi, B., Lim, T., and Prakash, S. (2006). A new method for microcapsule characterization: use of fluorogenic genipin to characterize polymeric microcapsule membranes. *Appl.Biochem.Biotechnol.*, 134 (3), 207-222.

203. Rehman, J., Traktuev, D., Li, J., Merfeld-Clauss, S., Temm-Grove, C. J., Bovenkerk, J. E., et al. (2004). Secretion of angiogenic and antiapoptotic factors by human adipose stromal cells. *Circulation*, 109 (10), 1292-1298.

204. Maguire, T., Novik, E., Schloss, R., and Yarmush, M. (2006). Alginate-PLL microencapsulation: Effect on the differentiation of embryonic stem cells into hepatocytes. *Biotechnology and Bioengineering*, 93 (3), 581-591.

205. Ding, H. F., Liu, R., Li, B. G., Lou, J. R., Dai, K. R., and Tang, T. T. (2007). Biologic effect and immunoisolating behavior of BMP-2 gene-transfected bone marrow-derived mesenchymal stem cells in APA microcapsules. *Biochemical and Biophysical Research Communications*, 362 (4), 923-927.

206. Xu, W. B., Xu, L. H., Lu, H. S., Ou-Yang, D. Y., Shi, H. J., Di, J. F., et al. (2009). The immunosuppressive effect of gossypol in mice is mediated by inhibition of lymphocyte proliferation and by induction of cell apoptosis. *Acta Pharmacologica Sinica*, 30 (5), 597-604.

207. Bassaneze, V., Barauna, V. G., Lavini-Ramos, C., Kalil, J., Schettert, I. T., Miyakawa, A. A., et al. (2010). Shear Stress Induces Nitric Oxide-Mediated Vascular Endothelial Growth Factor Production in Human Adipose Tissue Mesenchymal Stem Cells. *Stem Cells and Development*, 19 (3), 371-378.

208. Nilsson, B., Korsgren, O., Lambris, J. D., and Ekdahl, K. N. (2010). Can cells and biomaterials in therapeutic medicine be shielded from innate immune recognition? *Trends in Immunology*, 31 (1), 32-38.

209. Wang, J. A., Chen, T. L., Jiang, J., Shi, H., Gui, C., Luo, R. H., et al. (2008). Hypoxic preconditioning attenuates hypoxia/reoxygenation-induced apoptosis in mesenchymal stem cells. *Acta Pharmacologica Sinica*, 29 (1), 74-82.

210. Rosova, I., Dao, M., Capoccia, B., Link, D., and Nolta, J. A. (2008). Hypoxic preconditioning results in increased motility and improved therapeutic potential of human mesenchymal stem cells. *Stem Cells*, 26 (8), 2173-2182.

211. Oh, J. S., Ha, Y., An, S. S., Khan, M., Pennant, W. A., Kim, H. J., et al. (2010). Hypoxia-preconditioned adipose tissue-derived mesenchymal stem cell increase the survival and gene expression of engineered neural stem cells in a spinal cord injury model. *Neuroscience Letters*, 472 (3), 215-219.

212. Leroux, L., Descamps, B., Tojais, N. F., Seguy, B., Oses, P., Moreau, C., et al. (2010). Hypoxia Preconditioned Mesenchymal Stem Cells Improve Vascular and Skeletal Muscle Fiber Regeneration After Ischemia Through a Wnt4-dependent Pathway. *Molecular Therapy*, 18 (8), 1545-1552.

213. Hu, X. Y., Yu, S. P., Fraser, J. L., Lu, Z. Y., Ogle, M. E., Wang, J. A., et al. (2008). Transplantation of hypoxia-preconditioned mesenchymal stem cells improves infarcted heart function via enhanced survival of implanted cells and angiogenesis. *Journal of Thoracic and Cardiovascular Surgery*, 135 (4), 799-808.

214. Al Kindi, A. H., Asenjo, J. F., Ge, Y., Chen, G. Y., Bhathena, J., Chiu, R. C., et al. (2010). Microencapsulation to reduce mechanical loss of microspheres: implications in myocardial cell therapy. *Eur.J.Cardiothorac.Surg.*,

215. Goldberg, R. J., Spencer, F. A., Gore, J. M., Lessard, D., and Yarzebski, J. (2009). Thirty-Year Trends (1975 to 2005) in the Magnitude of, Management of, and Hospital Death Rates Associated With Cardiogenic Shock in Patients With Acute Myocardial Infarction A Population-Based Perspective. *Circulation*, 119 (9), 1211-1219.

216. Knowlton, K. U. and Chien, K. R. (1999). Inflammatory pathways and cardiac repair: the affliction of infarction. *Nature Medicine*, 5 (10), 1122-1123.

217. Wei, Y. Y., Hu, H. Y., Wang, H. Q., Wu, Y. S., Deng, L. F., and Qi, J. (2009). Cartilage Regeneration of Adipose-Derived Stem Cells in a

Hybrid Scaffold From Fibrin-Modified PLGA. *Cell Transplantation*, 18 (2), 159-170.

218. Sanz-Ruiz, R., Fernandez-Santos, E., Dominguez-Munoa, M., Parma, R., Villa, A., Fernandez, L., et al. (2009). Early Translation of Adipose-Derived Cell Therapy for Cardiovascular Disease. *Cell Transplantation*, 18 (3), 245-254.

219. Song, S. Y., Chung, H. M., and Sung, J. H. (2010). The pivotal role of VEGF in adipose-derived-stem-cell-mediated regeneration. *Expert Opinion on Biological Therapy*, 10 (11), 1529-1537.

220. Sterodimas, A., de Faria, J., Nicaretta, B., and Pitanguy, I. (2010). Tissue engineering with adipose-derived stem cells (ADSCs): Current and future applications. *Journal of Plastic Reconstructive and Aesthetic Surgery*, 63 (11), 1886-1892.

221. de Villiers, J. A., Houreld, N., and Abrahamse, H. (2009). Adipose Derived Stem Cells and Smooth Muscle Cells: Implications for Regenerative Medicine. *Stem Cell Reviews and Reports*, 5 (3), 256-265.

222. Gimble, J. M. and Guilak, F. (2003). Adipose-derived adult stem cells: isolation, characterization, and differentiation potential. *Cytotherapy*, 5 (5), 362-369.

223. Madonna, R., Geng, Y. J., and De Caterina, R. (2009). Adipose Tissue-Derived Stem Cells Characterization and Potential for Cardiovascular Repair. *Arteriosclerosis Thrombosis and Vascular Biology*, 29 (11), 1723-1729.

224. Parker, A. M. and Katz, A. J. (2006). Adipose-derived stem cells for the regeneration of damaged tissues. *Expert Opinion on Biological Therapy*, 6 (6), 567-578.

225. Teng, C. J., Luo, J., Chiu, R. C. J., and Shum-Tim, D. (2006). Massive mechanical loss of microspheres with direct intramyocardial injection in the beating heart: Implications for cellular cardiomyoplasty. *Journal of Thoracic and Cardiovascular Surgery*, 132 (3), 628-632.

226. Retuerto, M. A., Schalch, P., Patejunas, G., Carbray, J., Liu, N. X., Esser, K., et al. (2004). Angiogenic pretreatment improves the efficacy of cellular cardiomyoplasty performed with fetal cardiomyocyte implantation. *Journal of Thoracic and Cardiovascular Surgery*, 127 (4), 1041-1050.

227. Muller-Ehmsen, J., Whittaker, P., Kloner, R. A., Dow, J. S., Sakoda, T., Long, T. I., et al. (2002). Survival and development of neonatal rat

cardiomyocytes transplanted into adult myocardium. *Journal of Molecular and Cellular Cardiology*, 34 (2), 107-116.

228. Al Kindi, A., Ge, Y., Shum-Tim, D., and Chiu, R. C. J. (2008). Cellular cardiomyoplasty: routes of cell delivery and retention. *Frontiers in Bioscience*, 13 (2421-2434.

229. Nguyen, H., Qian, J. J., Bhatnagar, R. S., and Li, S. (2003). Enhanced cell attachment and osteoblastic activity by P-15 peptide-coated matrix in hydrogels. *Biochemical and Biophysical Research Communications*, 311 (1), 179-186.

230. Yang, F., Xie, Y. T., Li, H. W., Tang, T. T., Zhang, X. L., Gan, Y. K., et al. (2010). Human bone marrow-derived stromal cells cultured with a plasma sprayed CaO-ZrO2-SiO2 coating. *Journal of Biomedical Materials Research Part B-Applied Biomaterials*, 95B (1), 192-201.

231. Wolff, K. D., Swaid, S., Nolte, D., Bockmann, R. A., Holzle, F., and Muller-Mai, C. (2004). Degradable injectable bone cement in maxillofacial surgery: indications and clinical experience in 27 patients. *Journal of Cranio-Maxillofacial Surgery*, 32 (2), 71-79.

232. Chen, H. M., Ouyang, W., Lawuyi, B., and Prakash, S. (2006). Genipin cross-linked alginate-chitosan microcapsules: Membrane characterization and optimization of cross-linking reaction. *Biomacromolecules*, 7 (7), 2091-2098.

233. Chen, H. M., Wei, O. Y., Jones, M., Metz, T., Martoni, C., Haque, T., et al. (2007). Preparation and characterization of novel polymeric microcapsules for live cell encapsulation and therapy. *Cell Biochemistry and Biophysics*, 47 (1), 159-167.

234. Haque, T., Chen, H., Ouyang, W., Martoni, C., Lawuyi, B., Urbanska, A. M., et al. (2005). Superior cell delivery features of poly(ethylene glycol) incorporated alginate, chitosan, and poly-L-lysine microcapsules. *Molecular Pharmaceutics*, 2 (1), 29-36.

235. Zhang, H., Zhu, S. J., Wang, W., Wei, Y. J., and Hu, S. S. (2008). Transplantation of microencapsulated genetically modified xenogeneic cells augments angiogenesis and improves heart function. *Gene Therapy*, 15 (1), 40-48.

236. Prakash, S. and Chang, T. M. S. (1996). Microencapsulated genetically engineered live E-coli DH5 cells administered orally to maintain normal plasma urea level in uremic rats. *Nature Medicine*, 2 (8), 883-887.

237. Al Kindi, A. H., Chen, G., Ge, Y., Bhathena, J., Chiu, R., Prakash, S., et al. (2007). Microencapsulation to reduce mechanical loss of microspheres:

Implications in myocardial cell therapy. *Canadian Journal of Cardiology*, 23 (77C

238. Chen, G. Y., Nayan, M., Duong, M., Asenjo, J. F., Ge, Y., Chiu, R. C. J., et al. (2010). Marrow Stromal Cells for Cell-Based Therapy: The Role of Antiinflammatory Cytokines in Cellular Cardiomyoplasty. *Annals of Thoracic Surgery*, 90 (1), 190-198.

239. Atoui, R., Asenjo, J. F., Duong, M., Chen, G., Chiu, R. C. J., and Shum-Tim, D. (2008). Marrow stromal cells as universal donor cells for myocardial regenerative therapy: Their unique immune tolerance. *Annals of Thoracic Surgery*, 85 (2), 571-580.

240. Kayser, M., Caglia, A., Corach, D., Fretwell, N., Gehrig, C., Graziosi, G., et al. (1997). Evaluation of Y-chromosomal STRs: A multicenter study. *International Journal of Legal Medicine*, 110 (3), 125-+

241. Takahashi, K., Ito, Y., Morikawa, M., Kobune, M., Huang, J. H., Tsukamoto, M., et al. (2003). Adenoviral-delivered angiopoietin-1 reduces the infarction and attenuates the progression of cardiac dysfunction in the rat model of acute myocardial infarction. *Molecular Therapy*, 8 (4), 584-592.

242. Yamada, Y., Wang, X. D., Yokoyama, S. I., Fukuda, N., and Takakura, N. (2006). Cardiac progenitor cells in brown adipose tissue repaired damaged myocardium. *Biochemical and Biophysical Research Communications*, 342 (2), 662-670.

243. Westrich, J., Yaeger, P., He, C., Stewart, J., Chen, R., Seleznik, G., et al. (2010). Factors Affecting Residence Time of Mesenchymal Stromal Cells (MSC) Injected Into the Myocardium. *Cell Transplant*, 19 (8), 937-948.

244. Hansson, E. M., Lindsay, M. E., and Chien, K. R. (2009). Regeneration Next: Toward Heart Stem Cell Therapeutics. *Cell Stem Cell*, 5 (4), 364-377.

245. Hare, J. M., Traverse, J. H., Henry, T. D., Dib, N., Strumpf, R. K., Schulman, S. P., et al. (2009). A Randomized, Double-Blind, Placebo-Controlled, Dose-Escalation Study of Intravenous Adult Human Mesenchymal Stem Cells (Prochymal) After Acute Myocardial Infarction. *Journal of the American College of Cardiology*, 54 (24), 2277-2286.

246. Hatzistergos, K. E., Quevedo, H., Oskouei, B. N., Hu, Q. H., Feigenbaum, G. S., Margitich, I. S., et al. (2010). Bone Marrow Mesenchymal Stem Cells Stimulate Cardiac Stem Cell Proliferation and Differentiation. *Circulation Research*, 107 (7), 913-+

247. Atoui, R., Shum-Tim, D., and Chiu, R. C. J. (2008). Myocardial regenerative therapy: Immunologic basis for the potential "Universal Donor Cells". *Annals of Thoracic Surgery*, 86 (1), 327-334.

248. Prakash, S., Khan, A., and Paul, A. (2010). Nanoscaffold based stem cell regeneration therapy: recent advancement and future potential. *Expert Opin.Biol.Ther.*, 10 (12), 1649-1661.

249. Wei, H. J., Chen, C. H., Lee, W. Y., Chiu, I., Hwang, S. M., Lin, W. W., et al. (2008). Bioengineered cardiac patch constructed from multilayered mesenchymal stem cells for myocardial repair. *Biomaterials*, 29 (26), 3547-3556.

250. Itoi, Y., Takatori, M., Hyakusoku, H., and Mizuno, H. (2010). Comparison of readily available scaffolds for adipose tissue engineering using adipose-derived stem cells. *Journal of Plastic Reconstructive and Aesthetic Surgery*, 63 (5), 858-864.

251. Goren, A., Dahan, N., Goren, E., Baruch, L., and Machluf, M. (2010). Encapsulated human mesenchymal stem cells: a unique hypoimmunogenic platform for long-term cellular therapy. *Faseb Journal*, 24 (1), 22-31.

252. Rokstad, A. M., Holtan, S., Strand, B., Steinkjer, B., Ryan, L., Kulseng, B., et al. (2002). Microencapsulation of cells producing therapeutic proteins: Optimizing cell growth and secretion. *Cell Transplantation*, 11 (4), 313-324.

253. Haque, T., Chen, H., Ouyang, W., Martoni, C., Lawuyi, B., Urbanska, A. M., et al. (2005). In vitro study of alginate-chitosan microcapsules: an alternative to liver cell transplants for the treatment of liver failure. *Biotechnology Letters*, 27 (5), 317-322.

254. Vieira, N. M., Brandalise, V., Zucconi, E., Secco, M., Strauss, B. E., and Zatz, M. (2010). Isolation, Characterization, and Differentiation Potential of Canine Adipose-Derived Stem Cells. *Cell Transplantation*, 19 (3), 279-289.

255. Zhou, L., Ma, W., Yang, Z., Zhang, F., Lu, L., Ding, Z., et al. (2005). VEGF165 and angiopoietin-1 decreased myocardium infarct size through phosphatidylinositol-3 kinase and Bcl-2 pathways (vol 12, pg 196, 2005). *Gene Therapy*, 12 (6), 552

256. Chen, H. K., Hung, H. F., Shyu, K. G., Wang, B. W., Sheu, J. R., Liang, Y. J., et al. (2005). Combined cord blood stem cells and gene therapy enhances angiogenesis and improves cardiac performance in mouse after acute myocardial infarction. *European Journal of Clinical Investigation*, 35 (11), 677-686.

257. Yu, J. S., Du, K. T., Fang, Q. Z., Gu, Y. P., Mihardja, S. S., Sievers, R. E., et al. (2010). The use of human mesenchymal stem cells encapsulated in RGD modified alginate microspheres in the repair of myocardial infarction in the rat. *Biomaterials*, 31 (27), 7012-7020.

258. Atoui, R., Asenjo, J. F., Duong, M., Chen, G., Chiu, R. C., and Shum-Tim, D. (2008). Marrow stromal cells as universal donor cells for myocardial regenerative therapy: their unique immune tolerance. *Ann.Thorac.Surg.*, 85 (2), 571-579.

259. Flynn, A. and O'Brien, T. (2011). Stem cell therapy for cardiac disease. *Expert Opinion on Biological Therapy*, 11 (2), 177-187.

260. Zhukova, N. S. and Staroverov, I. I. (2011). Stem cells in the treatment of patients with coronary heart disease. Part I. *Cardiovascular Therapy and Prevention*, 10 (2), 122-128.

261. Bunnell, B. A., Flaat, M., Gagliardi, C., Patel, B., and Ripoll, C. (2008). Adipose-derived stem cells: Isolation, expansion and differentiation. *Methods*, 45 (2), 115-120.

262. Lu, Z., Roohani-Esfahani, S. I., Wang, G., and Zreiqat, H. (2011). Bone biomimetic microenvironment induces osteogenic differentiation of adipose tissue-derived mesenchymal stem cells. *Nanomedicine*,

263. Bai, X. W., Yan, Y. S., Song, Y. H., Seidensticker, M., Rabinovich, B., Metzele, R., et al. (2010). Both cultured and freshly isolated adipose tissue-derived stem cells enhance cardiac function after acute myocardial infarction. *European Heart Journal*, 31 (4), 489-501.

264. Rehman, J., Traktuev, D., Li, J. L., Merfeld-Clauss, S., Temm-Grove, C. J., Bovenkerk, J. E., et al. (2004). Secretion of angiogenic and antiapoptotic factors by human adipose stromal cells. *Circulation*, 109 (10), 1292-1298.

265. Chuang, C. K., Wong, T. H., Hwang, S. M., Chang, Y. H., Chen, G. Y., Chiu, Y. C., et al. (2009). Baculovirus Transduction of Mesenchymal Stem Cells: In Vitro Responses and In Vivo Immune Responses After Cell Transplantation. *Molecular Therapy*, 17 (5), 889-896.

266. Lin, C. Y., Lin, K. J., Kao, C. Y., Chen, M. C., Lo, W. H., Yen, T. C., et al. (2011). The role of adipose-derived stem cells engineered with the persistently expressing hybrid baculovirus in the healing of massive bone defects. *Biomaterials*, 32 (27), 6505-6514.

267. Duisit, G., Saleun, S., Douthe, S., Barsoum, J., Chadeuf, G., and Moullier, P. (1999). Baculovirus vector requires electrostatic interactions including

heparan sulfate for efficient gene transfer in mammalian cells. *Journal of Gene Medicine*, 1 (2), 93-102.

268. Fasbender, A., Zabner, J., Chillon, M., Moninger, T. O., Puga, A. P., Davidson, B. L., et al. (1997). Complexes of adenovirus with polycationic polymers and cationic lipids increase the efficiency of gene transfer in vitro and in vivo. *Journal of Biological Chemistry*, 272 (10), 6479-6489.

269. Landazuri, N., Krishna, D., Gupta, M., and Le Doux, J. M. (2007). Retrovirus-polymer complexes: Study of the factors affecting the dose response of transduction. *Biotechnology Progress*, 23 (2), 480-487.

270. Matthews, C. B., Jenkins, G., Hilfinger, J. M., and Davidson, B. L. (1999). Poly-L-lysine improves gene transfer with adenovirus formulated in PLGA microspheres. *Gene Therapy*, 6 (9), 1558-1564.

271. Yang, Y., Lo, S. L., Yang, J. Y., Yang, J., Goh, S. S. L., Wu, C. X., et al. (2009). Polyethylenimine coating to produce serum-resistant baculoviral vectors for in vivo gene delivery. *Biomaterials*, 30 (29), 5767-5774.

272. Kim, Y. K., Kwon, J. T., Choi, J. Y., Jiang, H. L., Arote, R., Jere, D., et al. (2010). Suppression of tumor growth in xenograft model mice by programmed cell death 4 gene delivery using folate-PEG-baculovirus. *Cancer Gene Therapy*, 17 (11), 751-760.

273. Morales-Sanfrutos, J., Megia-Fernandez, A., Hernandez-Mateo, F., Giron-Gonzalez, M. D., Salto-Gonzalez, R., and Santoyo-Gonzalez, F. (2011). Alkyl sulfonyl derivatized PAMAM-G2 dendrimers as nonviral gene delivery vectors with improved transfection efficiencies. *Organic & Biomolecular Chemistry*, 9 (3), 851-864.

274. Santos, J. L., Pandita, D., Rodrigues, J., Pego, A. P., Granja, P. L., Balian, G., et al. (2010). Receptor-Mediated Gene Delivery Using PAMAM Dendrimers Conjugated with Peptides Recognized by Mesenchymal Stem Cells. *Molecular Pharmaceutics*, 7 (3), 763-774.

275. Nam, H. Y., Hahn, H. J., Nam, K., Choi, W. H., Jeong, Y., Kim, D. E., et al. (2008). Evaluation of generations 2, 3 and 4 arginine modified PAMAM dendrimers for gene delivery. *International Journal of Pharmaceutics*, 363 (1-2), 199-205.

276. Harris, J. M., Dust, J. M., Mcgill, R. A., Harris, P. A., Edgell, M. J., Sedaghatherati, R. M., et al. (1991). New Polyethylene Glycols for Biomedical Applications. *Acs Symposium Series*, 467 (418-429.

277. Heuberger, R., Sukhorukov, G., Voros, J., Textor, M., and Mohwald, H. (2005). Biofunctional polyelectrolyte multilayers and microcapsules:

Control of non-specific and bio-specific protein adsorption. *Advanced Functional Materials*, 15 (3), 357-366.

278. Paul, A., Ge, Y., Prakash, S., and Shum-Tim, D. (2009). Microencapsulated stem cells for tissue repairing: implications in cell-based myocardial therapy. *Regen.Med.*, 4 (5), 733-745.

279. Al Kindi, A. H., Asenjo, J. F., Ge, Y., Chen, G. Y., Bhathena, J., Chiu, R. C. J., et al. (2011). Microencapsulation to reduce mechanical loss of microspheres: implications in myocardial cell therapy. *European Journal of Cardio-Thoracic Surgery*, 39 (2), 241-247.

280. Paul, A., Cantor, A., Shum-Tim, D., and Prakash, S. (2010). Superior Cell Delivery Features of Genipin Crosslinked Polymeric Microcapsules: Preparation, In Vitro Characterization and Pro-Angiogenic Applications Using Human Adipose Stem Cells. *Mol.Biotechnol.*,

281. Paul, A., Binsalamah, Z. M., Khan, A. A., Abbasia, S., Elias, C. B., Shum-Tim, D., et al. (2011). A nanobiohybrid complex of recombinant baculovirus and Tat/DNA nanoparticles for delivery of Ang-1 transgene in myocardial infarction therapy. *Biomaterials*, 32 (32), 8304-8318.

282. Haque, T., Chen, H., Ouyang, W., Martoni, C., Lawuyi, B., Urbanska, A. M., et al. (2005). Superior cell delivery features of poly(ethylene glycol) incorporated alginate, chitosan, and poly-L-lysine microcapsules. *Molecular Pharmaceutics*, 2 (1), 29-36.

283. Herve, M. A., Buteau-Lozano, H., Mourah, S., Calvo, F., and Perrot-Applanat, M. (2005). VEGF189 stimulates endothelial cells proliferation and migration in vitro and up-regulates the expression of Flk-1/KDR mRNA. *Experimental Cell Research*, 309 (1), 24-31.

284. Huang, N. F., Lam, A., Fang, Q. Z., Sievers, R. E., Li, S., and Lee, R. J. (2009). Bone marrow-derived mesenchymal stem cells in fibrin augment angiogenesis in the chronically infarcted myocardium. *Regenerative Medicine*, 4 (4), 527-538.

285. Paul, A., Khan, A. A., Shum-Tim, D., and Prakash, S. (2010). BacMam Virus Transduced Cardiomyoblasts Can Be Used for Myocardial Transplantation Using AP-PEG-A Microcapsules: Molecular Cloning, Preparation, and In Vitro Analysis. *J.Biomed.Biotechnol.*, 2010 (858094

286. Ranjan, A. and Webster, T. J. (2007). Stem cell differentiation on nano patterned hydrogels for functional cardiac tissue regeneration. *Nanomedicine-Nanotechnology Biology and Medicine*, 3 (4), 347

287. Segers, V. F. M. and Lee, R. T. (2008). Stem-cell therapy for cardiac disease. *Nature*, 451 (7181), 937-942.

288. Han, S. W., Nakamura, C., Kotobuki, N., Obataya, I., Ohgushi, H., Nagamune, T., et al. (2008). High-efficiency DNA injection into a single human mesenchymal stem cell using a nanoneedle and atomic force microscopy. *Nanomedicine-Nanotechnology Biology and Medicine*, 4 (3), 215-225.

289. Christman, K. L. and Lee, R. J. (2006). Biomaterials for the Treatment of Myocardial Infarction. *Journal of the American College of Cardiology*, 48 (5), 907-913.

290. Zhao, H., Yang, K., Martinez, A., Basu, A., Chintala, R., Liu, H. C., et al. (2006). Linear and branched bicin linkers for releasable PEGylation of macromolecules: Controlled release in vivo and in vitro from mono- and multi-PEGylated proteins. *Bioconjugate Chemistry*, 17 (2), 341-351.

291. Talpaz, M., Rakhit, A., Rittweger, K., O'Brien, S., Cortes, J., Fettner, S., et al. (2005). Phase I evaluation of a 40-kDa branched-chain long-acting pegylated IFN-alpha-2a with and without cytarabine in patients with chronic myelogenous leukemia. *Clinical Cancer Research*, 11 (17), 6247-6255.

292. Zalipsky, S. (1995). Chemistry of Polyethylene-Glycol Conjugates with Biologically-Active Molecules. *Advanced Drug Delivery Reviews*, 16 (2-3), 157-182.

293. Paul, A., Khan, A. A., Shum-Tim, D., and Prakash, S. (2010). BacMam Virus Transduced Cardiomyoblasts Can Be Used for Myocardial Transplantation Using AP-PEG-A Microcapsules: Molecular Cloning, Preparation, and In Vitro Analysis. *Journal of Biomedicine and Biotechnology*,

294. Song, S. Y., Chung, H. M., and Sung, J. H. (2010). The pivotal role of VEGF in adipose-derived-stem-cell-mediated regeneration. *Expert Opinion on Biological Therapy*, 10 (11), 1529-1537.

295. Zuk, P. A. (2011). Viral transduction of adipose-derived stem cells. *Methods Mol.Biol.*, 702 (345-357.

296. Morizono, K., De Ugarte, D. A., Zhu, M., Zuk, P., Elbarbary, A., Ashjian, P., et al. (2003). Multilineage cells from adipose tissue as gene delivery vehicles. *Human Gene Therapy*, 14 (1), 59-66.

297. Yukawa, H., Noguchi, H., Oishi, K., Miyazaki, T., Kitagawa, Y., Inoue, M., et al. (2008). Recombinant Sendai virus-mediated gene transfer to adipose tissue-derived stem cells (ASCs). *Cell Transplantation*, 17 (1-2), 43-50.

298. Bielinska, A., KukowskaLatallo, J. F., Johnson, J., Tomalia, D. A., and Baker, J. R. (1996). Regulation of in vitro gene expression using antisense oligonucleotides or antisense expression plasmids transfected using starburst PAMAM dendrimers. *Nucleic Acids Research*, 24 (11), 2176-2182.

299. Goodwin, A. P., Lam, S. S., and Frechet, J. M. J. (2007). Rapid, efficient synthesis of heterobifunctional biodegradable dendrimers. *Journal of the American Chemical Society*, 129 (22), 6994-+

300. Bielinska, A. U., Yen, A., Wu, H. L., Zahos, K. M., Sun, R., Weiner, N. D., et al. (2000). Application of membrane-based dendrimer/DNA complexes for solid phase transfection in vitro and in vivo. *Biomaterials*, 21 (9), 877-887.

301. Wang, Y. O., Boros, P., Liu, J. H., Qin, L. H., Bai, Y. L., Bielinska, A. U., et al. (2000). DNA/dendrimer complexes mediate gene transfer into murine cardiac transplants ex vivo. *Molecular Therapy*, 2 (6), 602-608.

302. Johnson, T. A., Stasko, N. A., Matthews, J. L., Cascio, W. E., Holmuhamedov, E. L., Johnson, C. B., et al. (2010). Reduced ischemia/reperfusion injury via glutathione-initiated nitric oxide-releasing dendrimers. *Nitric Oxide-Biology and Chemistry*, 22 (1), 30-36.

303. Chen, C. Y., Lin, C. Y., Chen, G. Y., and Hu, Y. C. (2011). Baculovirus as a gene delivery vector: Recent understandings of molecular alterations in transduced cells and latest applications. *Biotechnol.Adv.*,

304. Yang, Y., Lo, S. L., Yang, J. Y., Yang, J., Goh, S. S. L., Wu, C. X., et al. (2009). Polyethylenimine coating to produce serum-resistant baculoviral vectors for in vivo gene delivery. *Biomaterials*, 30 (29), 5767-5774.

305. Roger, V. L., Weston, S. A., Redfield, M. M., Hellermann-Homan, J. P., Killian, J., Yawn, B. P., et al. (2004). Trends in heart failure incidence and survival in a community-based population. *JAMA*, 292 (3), 344-350.

306. Tang, J. M., Xie, Q. Y., Pan, G. D., Wang, J. N., and Wang, M. J. (2006). Mesenchymal stem cells participate in angiogenesis and improve heart function in rat model of myocardial ischemia with reperfusion. *European Journal of Cardio-Thoracic Surgery*, 30 (2), 353-361.

307. Wakitani, S., Saito, T., and Caplan, A. I. (1995). Myogenic cells derived from rat bone marrow mesenchymal stem cells exposed to 5-azacytidine. *Muscle Nerve*, 18 (12), 1417-1426.

308. Saito, T., Kuang, J. Q., Lin, C. C., and Chiu, R. C. (2003). Transcoronary implantation of bone marrow stromal cells ameliorates cardiac function after myocardial infarction. *J.Thorac.Cardiovasc.Surg.*, 126 (1), 114-123.

309. Bartunek, J., Vanderheyden, M., Vandekerckhove, B., Mansour, S., De, B. B., De, B. P., et al. (2005). Intracoronary injection of CD133-positive enriched bone marrow progenitor cells promotes cardiac recovery after recent myocardial infarction: feasibility and safety. *Circulation*, 112 (9 Suppl), I178-I183

310. Wang, Y. G., Haider, H. K., Ahmad, N., Zhang, D. S., and Ashraf, M. (2006). Evidence for ischemia induced host-derived bone marrow cell mobilization into cardiac allografts. *Journal of Molecular and Cellular Cardiology*, 41 (3), 478-487.

311. Chang, T. M. S. (1964). Semipermeable Microcapsules.

312. Prakash, S. (1996). Microencapsulated genetically engineered live E-coli DH5 cells administered orally to maintain normal plasma urea level in uremic rats.

313. Prakash, S. (1999). Artificial cell microcapsules containing genetically engineered E-coli DH5 cells for in-vitro lowering of plasma potassium, phosphate, magnesium, sodium, chloride, uric acid, cholesterol, and creatinine: A preliminary report.

314. Prakash, S. (2005). Live bacterial cells as orally delivered therapeutics.

315. Prakash, S. (1999). Growth kinetics of genetically engineered E-coli DH 5 cells in artificial cell APA membrane microcapsules: Preliminary report.

316. Prakash, S. (2000). In vitro and in vivo uric acid lowering by artificial cells containing microencapsulated genetically engineered E-coli DH5 cells.

317. Haque, T. (2005). In vitro study of alginate-chitosan microcapsules: an alternative to liver cell transplants for the treatment of liver failure.

318. Haque, T., Chen, H., Ouyang, W., Martoni, C., Lawuyi, B., Urbanska, A., et al. (2005). Investigation of a new microcapsule membrane combining alginate, chitosan, polyethylene glycol and poly-L-lysine for cell transplantation applications. *International Journal of Artificial Organs*, 28 (6), 631-637.

319. Ding, H. F., Liu, R., Li, B. G., Lou, J. R., Dai, K. R., and Tang, T. T. (2007). Biologic effect and immunoisolating behavior of BMP-2 gene-transfected bone marrow-derived mesenchymal stem cells in APA microcapsules. *Biochemical and Biophysical Research Communications*, 362 (4), 923-927.

320. O'Reilly,D.R., Miller,L.K., and Lucknow,V.A. (1992): Baculovirus Expression Vector: A Laboratory Manual. In: AnonymousW.H.Freeman and Company,New York,

321. Zimmermann, J., Bittner, K., Stark, B., and Mulhaupt, R. (2002). Novel hydrogels as supports for in vitro cell growth: poly(ethylene glycol)- and gelatine-based (meth)acrylamidopeptide macromonomers. *Biomaterials*, 23 (10), 2127-2134.

322. Jardin, B. A., Zhao, Y., Selvaraj, M., Montes, J., Tran, R., Prakash, S., et al. (2008). Expression of SEAP (secreted alkaline phosphatase) by baculovirus mediated transduction of HEK 293 cells in a hollow fiber bioreactor system. *J.Biotechnol.*, 135 (3), 272-280.

323. Haque, T., Chen, H., Ouyang, W., Martoni, C., Lawuyi, B., Urbanska, A. M., et al. (2005). In vitro study of alginate-chitosan microcapsules: an alternative to liver cell transplants for the treatment of liver failure. *Biotechnology Letters*, 27 (5), 317-322.

324. Haque, T., Chen, H., Ouyang, W., Martoni, C., Lawuyi, B., Urbanska, A. M., et al. (2005). Superior cell delivery features of poly(ethylene glycol) incorporated alginate, chitosan, and poly-L-lysine microcapsules. *Molecular Pharmaceutics*, 2 (1), 29-36.

325. Maguire, T., Novik, E., Schloss, R., and Yarmush, M. (2006). Alginate-PLL microencapsulation: Effect on the differentiation of embryonic stem cells into hepatocytes. *Biotechnology and Bioengineering*, 93 (3), 581-591.

326. Kitts, P. A. and Green, G. (1999). An immunological assay for determination of baculovirus titers in 48 hours. *Anal.Biochem.*, 268 (2), 173-178.

327. Ho, Y. C., Chung, Y. C., Hwang, S. M., Wang, K. C., and Hu, Y. C. (2005). Transgene expression and differentiation of baculovirus-transduced human mesenchymal stem cells. *Journal of Gene Medicine*, 7 (7), 860-868.

328. Chuang, C. K., Wong, T. H., Hwang, S. M., Chang, Y. H., Chen, G. Y., Chiu, Y. C., et al. (2009). Baculovirus Transduction of Mesenchymal Stem Cells: In Vitro Responses and In Vivo Immune Responses After Cell Transplantation. *Molecular Therapy*, 17 (5), 889-896.

329. Paul, D., Samuel, S. M., and Maulik, N. (2009). Mesenchymal Stem Cell: Present Challenges and Prospective Cellular Cardiomyoplasty Approaches for Myocardial Regeneration. *Antioxidants & Redox Signaling*, 11 (8), 1841-1855.

330. Georgopoulos, L. J., Elgue, G., Sanchez, J., Dussupt, V., Magotti, P., Lambris, J. D., et al. (2009). Preclinical evaluation of innate immunity to baculovirus gene therapy vectors in whole human blood. *Molecular Immunology*, 46 (15), 2911-2917.

331. Condreay, J. P., Witherspoon, S. M., Clay, W. C., and Kost, T. A. (1999). Transient and stable gene expression in mammalian cells transduced with a recombinant baculovirus vector. *Proc.Natl.Acad.Sci.U.S.A*, 96 (1), 127-132.

332. Kost, T. A. and Condreay, J. P. (1999). Recombinant baculoviruses as expression vectors for insect and mammalian cells. *Curr.Opin.Biotechnol.*, 10 (5), 428-433.

333. Kost, T. A., Condreay, J. P., Ames, R. S., Rees, S., and Romanos, M. A. (2007). Implementation of BacMam virus gene delivery technology in a drug discovery setting. *Drug Discov.Today*, 12 (9-10), 396-403.

334. Cheshenko, N., Krougliak, N., Eisensmith, R. C., and Krougliak, V. A. (2001). A novel system for the production of fully deleted adenovirus vectors that does not require helper adenovirus. *Gene Ther.*, 8 (11), 846-854.

335. Jardin, B. A., Zhao, Y., Selvaraj, M., Montes, J., Tran, R., Prakash, S., et al. (2008). Expression of SEAP (secreted alkaline phosphatase) by baculovirus mediated transduction of HEK 293 cells in a hollow fiber bioreactor system. *Journal of Biotechnology*, 135 (3), 272-280.

336. Paul, A., Jardin, B. A., Kulamarva, A., Malhotra, M., Elias, C. B., and Prakash, S. (2010). Recombinant Baculovirus as a Highly Potent Vector for Gene Therapy of Human Colorectal Carcinoma: Molecular Cloning, Expression, and In Vitro Characterization. *Molecular Biotechnology*, 45 (2), 129-139.

337. Giraud, M. N., Armbruster, C., Carrel, T., and Tevaearai, H. T. (2007). Current state of the art in myocardial tissue engineering. *Tissue Engineering*, 13 (8), 1825-1836.

338. Fukuhara, S., Tomita, S., Nakatani, T., Fujisato, T., Ohtsu, Y., Ishida, M., et al. (2005). Bone marrow cell-seeded biodegradable polymeric scaffold enhances angiogenesis and improves function of the infarcted heart. *Circulation Journal*, 69 (7), 850-857.

339. Ke, Q., Yang, Y., Rana, J. S., Chen, Y., Morgan, J. P., and Xiao, Y. F. (2005). Embryonic stem cells cultured in biodegradable scaffold repair infarcted myocardium in mice. *Sheng Li Xue.Bao.*, 57 (6), 673-681.

340. Fujita, M., Kinoshita, Y., Sato, E., Maeda, H., Ozono, S., Negishi, H., et al. (2005). Proliferation and differentiation of rat bone marrow stromal cells on poly(glycolic acid)-collagen sponge. *Tissue Engineering*, 11 (9-10), 1346-1355.

341. Krupnick, A. S., Kreisel, D., Engels, F. H., Szeto, W. Y., Plappert, T., Popma, S. H., et al. (2002). A novel small animal model of left ventricular tissue engineering. *Journal of Heart and Lung Transplantation*, 21 (2), 233-243.

342. Al Kindi, A., Ge, Y., Shum-Tim, D., and Chiu, R. C. J. (2008). Cellular cardiomyoplasty: routes of cell delivery and retention. *Frontiers in Bioscience*, 13 (2421-2434.

343. Paul, A., Ge, Y., Prakash, S., and Shum-Tim, D. (2009). Microencapsulated stem cells for tissue repairing: implications in cell-based myocardial therapy. *Regenerative Medicine*, 4 (5), 733-745.

344. Seifert, D. B. and Phillips, J. A. (1997). Porous alginate-poly(ethylene glycol) entrapment system for the cultivation of mammalian cells. *Biotechnology Progress*, 13 (5), 569-576.

345. Orive, G., Hernandez, R. M., Gascon, A. R., Calafiore, R., Chang, T. M. S., de Vos, P., et al. (2004). History, challenges and perspectives of cell microencapsulation. *Trends in Biotechnology*, 22 (2), 87-92.

346. Choi, D. (2007). Polymer based cardiovascular gene therapy. *Biotechnology and Bioprocess Engineering*, 12 (1), 39-42.

347. Lee, M., Rentz, J., Bikram, M., Han, S., Bull, D. A., and Kim, S. W. (2003). Hypoxia-inducible VEGF gene delivery to ischemic myocardium using water-soluble lipopolymer. *Gene Therapy*, 10 (18), 1535-1542.

348. Yockman, J. W., Kastenmeier, A., Erickson, H. M., Brumbach, J. G., Whitten, M. G., Albanil, A., et al. (2008). Novel polymer carriers and gene constructs for treatment of myocardial ischemia and infarction. *Journal of Controlled Release*, 132 (3), 260-266.

349. Roques, C., Salmon, A., Fiszman, M. Y., Fattal, E., and Fromes, Y. (2007). Intrapericardial administration of novel DNA formulations based on thermosensitive Poloxamer 407 gel. *International Journal of Pharmaceutics*, 331 (2), 220-223.

350. Ko, Y. T., Hartner, W. C., Kale, A., and Torchilin, V. P. (2009). Gene delivery into ischemic myocardium by double-targeted lipoplexes with anti-myosin antibody and TAT peptide. *Gene Therapy*, 16 (1), 52-59.

351. Miao, W. F., Luo, Z. Y., Kitsis, R. N., and Walsh, K. (2000). Intracoronary, adenovirus-mediated Akt gene transfer in heart limits infarct size following ischemia-reperfusion injury in vivo. *Journal of Molecular and Cellular Cardiology*, 32 (12), 2397-2402.

352. Li, Y. W., Takemura, G., Kosai, K., Yuge, K., Nagano, S., Esaki, M., et al. (2003). Postinfarction treatment with an adenoviral vector expressing hepatocyte growth factor relieves chronic left ventricular remodeling and dysfunction in mice. *Circulation*, 107 (19), 2499-2506.

353. Takahashi, K., Ito, Y., Morikawa, M., Kobune, M., Huang, J. H., Tsukamoto, M., et al. (2003). Adenoviral-delivered angiopoietin-1 reduces the infarction and attenuates the progression of cardiac dysfunction in the rat model of acute myocardial infarction. *Molecular Therapy*, 8 (4), 584-592.

354. Gomez-Navarro, J. and Curiel, D. T. (2000). Conditionally replicative adenoviral vectors for cancer gene therapy. *Lancet Oncol.*, 1 (148-158.

355. Mirzaei, M., Xu, Y., Elias, C. B., and Prakash, S. (2009). Nonviral Production of Human Interleukin-7 in Spodoptera Frugiperda Insect Cells as a Soluble Recombinant Protein. *Journal of Biomedicine and Biotechnology*,

356. Cecchini, S., Virag, T., and Kotin, R. M. (2011). Reproducible high yields of recombinant adeno-associated virus produced using invertebrate cells in 0.02 to 200 liter cultures. *Hum.Gene Ther.*,

357. Kost, T. A. and Condreay, J. P. (2002). Recombinant baculoviruses as mammalian cell gene-delivery vectors. *Trends in Biotechnology*, 20 (4), 173-180.

358. Paul, A. and Prakash, S. (2010). Baculovirus reveals a new pH-dependent direct cell-fusion pathway for cell entry and transgene delivery. *Future Virology*, 5 (5), 533-537.

359. Paul, A., Jardin, B. A., Kulamarva, A., Malhotra, M., Elias, C. B., and Prakash, S. (2010). Recombinant Baculovirus as a Highly Potent Vector for Gene Therapy of Human Colorectal Carcinoma: Molecular Cloning, Expression, and In Vitro Characterization. *Molecular Biotechnology*, 45 (2), 129-139.

360. Raty, J. K., Airenne, K. J., Marttila, A. T., Marjomaki, V., Hytonen, V. P., Lehtolainen, P., et al. (2004). Enhanced gene delivery by avidin-displaying baculovirus. *Molecular Therapy*, 9 (2), 282-291.

361. Ernst, W., Schinko, T., Spenger, A., Oker-Blom, C., and Grabherr, R. (2006). Improving baculovirus transduction of mammalian cells by

surface display of a RGD-motif. *Journal of Biotechnology*, 126 (2), 237-240.

362. Honda, M., Hu, P. C., Huang, C. H., Matsui, H., and Lemon, S. M. (1996). A replication-deficient adenovirus enhances liposome-mediated nucleic acid transfer into a stable cell line expressing T7 RNA polymerase. *Journal of Virological Methods*, 58 (1-2), 41-51.

363. Wagner, E., Zatloukal, K., Cotten, M., Kirlappos, H., Mechtler, K., Curiel, D. T., et al. (1992). Coupling of Adenovirus to Transferrin Polylysine Dna Complexes Greatly Enhances Receptor-Mediated Gene Delivery and Expression of Transfected Genes. *Proceedings of the National Academy of Sciences of the United States of America*, 89 (13), 6099-6103.

364. Kim, Y. K., Choi, J. Y., Jiang, H. L., Arote, R., Jere, D., Cho, M. H., et al. (2009). Hybrid of baculovirus and galactosylated PEI for efficient gene carrier. *Virology*, 387 (1), 89-97.

365. Lo, S. L. and Wang, S. (2008). An endosomolytic Tat peptide produced by incorporation of histidine and cysteine residues as a nonviral vector for DNA transfection. *Biomaterials*, 29 (15), 2408-2414.

366. Tao, Z. X., Chen, B., Tan, X. A., Zhao, Y. M., Wang, L. S., Zhu, T. B., et al. (2011). Coexpression of VEGF and angiopoietin-1 promotes angiogenesis and cardiomyocyte proliferation reduces apoptosis in porcine myocardial infarction (MI) heart. *Proceedings of the National Academy of Sciences of the United States of America*, 108 (5), 2064-2069.

367. Zhou, L., Ma, W., Yang, Z., Zhang, F., Lu, L., Ding, Z., et al. (2005). VEGF165 and angiopoietin-1 decreased myocardium infarct size through phosphatidylinositol-3 kinase and Bcl-2 pathways (vol 12, pg 196, 2005). *Gene Therapy*, 12 (6), 552

368. Dallabrida, S. M., Ismail, N., Oberle, J. R., Himes, B. E., and Rupnick, M. A. (2005). Angiopoietin-1 promotes cardiac and skeletal myocyte survival through integrins. *Circulation Research*, 96 (4),

369. Abdel-Malak, N. A., Mofarrahi, M., Mayaki, D., Khachigian, L. M., and Hussain, S. N. A. (2009). Early Growth Response-1 Regulates Angiopoietin-1-Induced Endothelial Cell Proliferation, Migration, and Differentiation. *Arteriosclerosis Thrombosis and Vascular Biology*, 29 (2), 209-216.

370. Al Kindi, A. H., Asenjo, J. F., Ge, Y., Chen, G. Y., Bhathena, J., Chiu, R. C. J., et al. (2011). Microencapsulation to reduce mechanical loss of microspheres: implications in myocardial cell therapy. *European Journal of Cardio-Thoracic Surgery*, 39 (2), 241-247.

371. Jardin, B. A., Zhao, Y., Selvaraj, M., Montes, J., Tran, R., Prakash, S., et al. (2008). Expression of SEAP (secreted alkaline phosphatase) by baculovirus mediated transduction of HEK 293 cells in a hollow fiber bioreactor system. *Journal of Biotechnology*, 135 (3), 272-280.

372. Ye, L., Zhang, W., Su, L. P., Haider, H. K., Poh, K. K., Galupo, M. J., et al. (2011). Nanoparticle based delivery of hypoxia-regulated VEGF transgene system combined with myoblast engraftment for myocardial repair. *Biomaterials*, 32 (9), 2424-2431.

373. Affleck, D. G., Yu, L., Bull, D. A., Bailey, S. H., and Kim, S. W. (2001). Augmentation of myocardial transfection using TerplexDNA: a novel gene delivery system. *Gene Therapy*, 8 (5), 349-353.

374. Papapetropoulos, A., Garcia-Cardena, G., Dengler, T. J., Maisonpierre, P. C., Yancopoulos, G. D., and Sessa, W. C. (1999). Direct actions of angiopoietin-1 on human endothelium: Evidence for network stabilization, cell survival, and interaction with other angiogenic growth factors. *Laboratory Investigation*, 79 (2), 213-223.

375. Suri, C., McClain, J., Thurston, G., McDonald, D. M., Zhou, H., Oldmixon, E. H., et al. (1998). Increased vascularization in mice overexpressing angiopoietin-1. *Science*, 282 (5388), 468-471.

376. Samuel, S. M., Akita, Y., Paul, D., Thiranavukkarasu, M., Zhan, L. J., Sudhakaran, P. R., et al. (2010). Coadministration of Adenoviral Vascular Endothelial Growth Factor and Angiopoietin-1 Enhances Vascularization and Reduces Ventricular Remodeling in the Infarcted Myocardium of Type 1 Diabetic Rats. *Diabetes*, 59 (1), 51-60.

377. Su, H., Joho, S., Huang, Y., Barcena, A., Arakawa-Hoyt, J., Grossman, W., et al. (2004). Adeno-associated viral vector delivers card iac-specific and hypoxia-inducible VEGF expression in ischemic mouse hearts. *Proceedings of the National Academy of Sciences of the United States of America*, 101 (46), 16280-16285.

378. Chen, S. L., Zhu, C. C., Liu, Y. Q., Tang, L. J., Yi, L., Yu, B. J., et al. (2009). Mesenchymal Stem Cells Genetically Modified with the Angiopoietin-1 Gene Enhanced Arteriogenesis in a Porcine Model of Chronic Myocardial Ischaemia. *Journal of International Medical Research*, 37 (1), 68-78.

379. Zhang, C. Y., Sun, A. J., Zhang, S. N., Yao, K., Wu, C. N., Fu, M. Q., et al. (2010). Efficacy and Safety of Intracoronary Autologous Bone Marrow-Derived Cell Transplantation in Patients With Acute Myocardial Infarction: Insights From Randomized Controlled Trials With 12 or More Months Follow-Up. *Clinical Cardiology*, 33 (6), 353-360.

380. Surder, D., Schwitter, J., Moccetti, T., Astori, G., Rufibach, K., Plein, S., et al. (2010). Cell-based therapy for myocardial repair in patients with acute myocardial infarction: Rationale and study design of the SWiss multicenter Intracoronary Stem cells Study in Acute Myocardial Infarction (SWISS-AMI). *American Heart Journal*, 160 (1), 58-64.

381. Atoui, R., Shum-Tim, D., and Chiu, R. C. J. (2008). Myocardial regenerative therapy: Immunologic basis for the potential "Universal Donor Cells". *Annals of Thoracic Surgery*, 86 (1), 327-334.

382. Das, H., George, J. C., Joseph, M., Das, M., Abdulhameed, N., Blitz, A., et al. (2009). Stem Cell Therapy with Overexpressed VEGF and PDGF Genes Improves Cardiac Function in a Rat Infarct Model. *Plos One*, 4 (10),

383. Kim, S. H., Moon, H. H., Kim, H. A., Hwang, K. C., Lee, M., and Choi, D. (2011). Hypoxia-inducible Vascular Endothelial Growth Factor-engineered Mesenchymal Stem Cells Prevent Myocardial Ischemic Injury. *Molecular Therapy*, 19 (4), 741-750.

384. Chen, S. L., Zhu, C. C., Liu, Y. Q., Tang, L. J., Yi, L., Yu, B. J., et al. (2009). Mesenchymal Stem Cells Genetically Modified with the Angiopoietin-1 Gene Enhanced Arteriogenesis in a Porcine Model of Chronic Myocardial Ischaemia. *Journal of International Medical Research*, 37 (1), 68-78.

385. Phillips, J. E., Gersbach, C. A., and Garcia, A. J. (2007). Virus-based gene therapy strategies for bone regeneration. *Biomaterials*, 28 (2), 211-229.

386. Donsante, A., Miller, D. G., Li, Y., Vogler, C., Brunt, E. M., Russell, D. W., et al. (2007). AAV vector integration sites in mouse hepatocellular carcinoma. *Science*, 317 (5837), 477

387. Chuang, C. K., Wong, T. H., Hwang, S. M., Chang, Y. H., Chen, G. Y., Chiu, Y. C., et al. (2009). Baculovirus Transduction of Mesenchymal Stem Cells: In Vitro Responses and In Vivo Immune Responses After Cell Transplantation. *Molecular Therapy*, 17 (5), 889-896.

388. Paul, A., Binsalamah, Z. M., Khan, A. A., Abbasia, S., Elias, C. B., Shum-Tim, D., et al. (2011). A nanobiohybrid complex of recombinant baculovirus and Tat/DNA nanoparticles for delivery of Ang-1 transgene in myocardial infarction therapy. *Biomaterials*, 32 (32), 8304-8318.

389. Cho, K. S., Park, H. K., Park, H. Y., Jung, J. S., Jeon, S. G., Kim, Y. K., et al. (2009). IFATS Collection: Immunomodulatory Effects of Adipose Tissue-Derived Stem Cells in an Allergic Rhinitis Mouse Model. *Stem Cells*, 27 (1), 259-265.

390. Houtgraaf, H. J., Duckers, H. J., Den Dekker, W., Swager, S., Van Geuns, R. J., Fernandez-Aviles, F., et al. (2010). First-in-man experience of adipose tissue-derived regenerative cell transplantation in the treatment of patients with an acute ST-elevation myocardial infarction (APOLLO trial). *European Heart Journal*, 31 (494

391. Metzele, R., Alt, C., Bai, X. W., Yan, Y. S., Zhang, Z., Pan, Z. Z., et al. (2011). Human adipose tissue-derived stem cells exhibit proliferation potential and spontaneous rhythmic contraction after fusion with neonatal rat cardiomyocytes. *Faseb Journal*, 25 (3), 830-839.

392. Tao, Z. X., Chen, B., Tan, X. A., Zhao, Y. M., Wang, L. S., Zhu, T. B., et al. (2011). Coexpression of VEGF and angiopoietin-1 promotes angiogenesis and cardiomyocyte proliferation reduces apoptosis in porcine myocardial infarction (MI) heart. *Proceedings of the National Academy of Sciences of the United States of America*, 108 (5), 2064-2069.

393. Zhou, L., Ma, W., Yang, Z., Zhang, F., Lu, L., Ding, Z., et al. (2005). VEGF165 and angiopoietin-1 decreased myocardium infarct size through phosphatidylinositol-3 kinase and Bcl-2 pathways (vol 12, pg 196, 2005). *Gene Therapy*, 12 (6), 552

394. Ye, L., Haider, H. K., Jiang, S. J., Ge, R. W., Law, P. K., and Sim, E. K. W. (2005). In vitro functional assessment of human skeletal myoblasts after transduction with adenoviral bicistronic vector carrying human VEGF(165) and angiopoietin-1. *Journal of Heart and Lung Transplantation*, 24 (9), 1393-1402.

395. Wang, Z. Y., Cui, M., Sun, L. J., Jia, Z. Q., Bai, Y., Ma, K. T., et al. (2007). Angiopoietin-1 protects H9c2 cells from H2O2-induced apoptosis through AKT signaling. *Biochemical and Biophysical Research Communications*, 359 (3), 685-690.

396. Li, J. X., Niu, X. L., and Madamanchi, N. R. (2008). Leukocyte Antigen-related Protein Tyrosine Phosphatase Negatively Regulates Hydrogen Peroxide-induced Vascular Smooth Muscle Cell Apoptosis. *Journal of Biological Chemistry*, 283 (49), 34260-34272.

397. Atoui, R., Asenjo, J. F., Duong, M., Chen, G., Chiu, R. C., and Shum-Tim, D. (2008). Marrow stromal cells as universal donor cells for myocardial regenerative therapy: their unique immune tolerance. *Ann.Thorac.Surg.*, 85 (2), 571-579.

398. Stewart, D. J., Kutryk, M. J. B., Fitchett, D., Freeman, M., Camack, N., Su, Y. H., et al. (2009). VEGF Gene Therapy Fails to Improve Perfusion of Ischemic Myocardium in Patients With Advanced Coronary Disease: Results of the NORTHERN Trial. *Molecular Therapy*, 17 (6), 1109-1115.

399. Cai, L. Y., Johnstone, B. H., Cook, T. G., Tan, J., Fishbein, M. C., Chen, P. S., et al. (2009). IFATS Collection: Human Adipose Tissue-Derived Stem Cells Induce Angiogenesis and Nerve Sprouting Following Myocardial Infarction, in Conjunction with Potent Preservation of Cardiac Function. *Stem Cells*, 27 (1), 230-237.

400. Chen, H. Z., Wu, C. P., Chao, Y. C., and Liu, C. Y. Y. (2011). Membrane penetrating peptides greatly enhance baculovirus transduction efficiency into mammalian cells. *Biochemical and Biophysical Research Communications*, 405 (2), 297-302.

401. Liu, X. B., Jiang, J., Gui, C., Hu, X. Y., Xiang, M. X., and Wang, J. A. (2008). Angiopoietin-1 protects mesenchymal stem cells against serum deprivation and hypoxia-induced apoptosis through the PI3K/Akt pathway. *Acta Pharmacologica Sinica*, 29 (7), 815-822.

402. Michaels, A. D. and Chatterjee, K. (2002). Angioplasty versus bypass surgery for coronary artery disease. *Circulation*, 106 (23), E187-E190

403. Bauters, C. and Isner, J. M. (1997). The biology of restenosis. *Progress in Cardiovascular Diseases*, 40 (2), 107-116.

404. Hiltunen, M. O., Laitinen, M., Turunen, M. P., Jeltsch, M., Hartikainen, J., Rissanen, T. T., et al. (2000). Intravascular adenovirus-mediated VEGF-C gene transfer reduces neointima formation in balloon-denuded rabbit aorta. *Circulation*, 102 (18), 2262-2268.

405. Fischell, T. A. (1996). Polymer coatings for stents - Can we judge a stent by its cover? *Circulation*, 94 (7), 1494-1495.

406. Pendyala, L., Jabara, R., Robinson, K., and Chronos, N. (2009). Passive and Active Polymer Coatings for Intracoronary Stents: Novel Devices to Promote Arterial Healing. *Journal of Interventional Cardiology*, 22 (1), 37-48.

407. Hehrlein, C. (2002). Radioactive stents - Problems and potential solutions. *Herz*, 27 (1), 17-22.

408. Abbott, J. D., Voss, M. R., Nakamura, M., Cohen, H. A., Selzer, F., Kip, K. E., et al. (2007). Unrestricted use of drug-eluting stents compared with bare-metal Stents in routine clinical practice - Findings from the national heart, lung, and blood institute dynamic registry. *Journal of the American College of Cardiology*, 50 (21), 2029-2036.

409. Mahmoudi, M., Delhaye, C., Wakabayashi, K., Ben-Dor, I., Gonzalez, M. A., Maluenda, G., et al. (2011). Outcomes After Unrestricted Use of Everolimus-Eluting Stent Compared to Paclitaxel- and Sirolimus-Eluting Stents. *American Journal of Cardiology*, 107 (12), 1757-1762.

410. Shuchman, M. (2007). Debating the risks of drug-eluting stents. *New England Journal of Medicine*, 356 (4), 325-328.

411. Iakovou, I., Schmidt, T., Bonizzoni, E., Ge, L., Sangiorgi, G. M., Stankovic, G., et al. (2005). Incidence, predictors, and outcome of thrombosis after successful implantation of drug-eluting stents. *Jama-Journal of the American Medical Association*, 293 (17), 2126-2130.

412. Holmes, D. R. (2007). Incidence of late stent thrombosis with bare-metal, sirolimus, and paclitaxel stents. *Reviews in Cardiovascular Medicine*, 8 (S11-S18

413. Deiner, C., Schwimmbeck, P. L., Koehler, I. S., Loddenkemper, C., Noutsias, M., Nikol, S., et al. (2006). Adventitial VEGF165 gene transfer prevents lumen loss through induction of positive arterial remodeling after PTCA in porcine coronary arteries. *Atherosclerosis*, 189 (1), 123-132.

414. VanBelle, E., Tio, F. O., Chen, D. H., Maillard, L., Chen, D. F., Kearney, M., et al. (1997). Passivation of metallic stents after arterial gene transfer of phVEGF(165) inhibits thrombus formation and intimal thickening. *Journal of the American College of Cardiology*, 29 (6), 1371-1379.

415. Lahtinen, M., Blomberg, P., Baliulis, G., Carlsson, F., Khamis, H., and Zemgulis, V. (2007). In vivo h-VEGF165 gene transfer improves early endothelialisation and patency in synthetic vascular grafts. *Eur.J.Cardiothorac.Surg.*, 31 (3), 383-390.

416. Pels, K., Denier, C., Coupland, S. E., Noutsias, M., Sutter, A. P., Schultheiss, H. P., et al. (2003). Effect of adventitial VEGF(165) gene transfer on vascular thickening after coronary artery balloon injury. *Cardiovascular Research*, 60 (3), 664-672.

417. Walter, D. H., Cejna, M., Diaz-Sandoval, L., Willis, S., Kirkwood, L., Stratford, P. W., et al. (2004). Local gene transfer of phVEGF-2 plasmid by gene-eluting stents - An alternative strategy for inhibition of restenosis. *Circulation*, 110 (1), 36-45.

418. Gao, F. B., Qiu, B. S., Kar, S., Zhan, X. C., Hofmann, L. V., and Yang, X. M. (2006). Intravascular magnetic resonance/radiofrequency may enhance gene therapy for prevention of in-stent neointimal hyperplasial. *Academic Radiology*, 13 (4), 524-528.

419. Newman, K. D., Dunn, P. F., Owens, J. W., Schulick, A. H., Virmani, R., Sukhova, G., et al. (1995). Adenovirus-mediated gene transfer into normal rabbit arteries results in prolonged vascular cell activation, inflammation, and neointimal hyperplasia. *Journal of Clinical Investigation*, 96 (6), 2955-2965.

420. Hedman, M., Hartikainen, J., and Yla-Herttuala, S. (2011). Progress and prospects: hurdles to cardiovascular gene therapy clinical trials. *Gene Therapy*, 18 (8), 743-749.

421. Chuang, C. K., Wong, T. H., Hwang, S. M., Chang, Y. H., Chen, G. Y., Chiu, Y. C., et al. (2009). Baculovirus Transduction of Mesenchymal Stem Cells: In Vitro Responses and In Vivo Immune Responses After Cell Transplantation. *Molecular Therapy*, 17 (5), 889-896.

422. Kaikkonen, M. U., Maatta, A. I., Yla-Herttuala, S., and Airenne, K. J. (2010). Screening of Complement Inhibitors: Shielded Baculoviruses Increase the Safety and Efficacy of Gene Delivery. *Molecular Therapy*, 18 (5), 987-992.

423. Paul, A., Binsalamah, Z. M., Khan, A. A., Abbasia, S., Elias, C. B., Shum-Tim, D., et al. (2011). A nanobiohybrid complex of recombinant baculovirus and Tat/DNA nanoparticles for delivery of Ang-1 transgene in myocardial infarction therapy. *Biomaterials*, 32 (32), 8304-8318.

424. Mok, H., Park, J. W., and Park, T. G. (2007). Microencapsulation of PEGylated adenovirus within PLGA microspheres for enhanced stability and gene transfection efficiency. *Pharmaceutical Research*, 24 (12), 2263-2269.

425. Lee, J. H., Park, T. G., and Choi, H. K. (2000). Effect of formulation and processing variables on the characteristics of microspheres for water-soluble drugs prepared by w/o/o double emulsion solvent diffusion method. *International Journal of Pharmaceutics*, 196 (1), 75-83.

426. Jiang, J., Liu, W., Guo, X., Zhang, R., Zhi, Q., Ji, J., et al. (2011). IRX1 influences peritoneal spreading and metastasis via inhibiting BDKRB2-dependent neovascularization on gastric cancer. *Oncogene*,

427. Welt, F. G., Edelman, E. R., Simon, D. I., and Rogers, C. (2000). Neutrophil, not macrophage, infiltration precedes neointimal thickening in balloon-injured arteries. *Arterioscler.Thromb.Vasc.Biol.*, 20 (12), 2553-2558.

428. Worsey, M. J., Laborde, A. L., Miller, B. V., Bower, T. R., Landas, S., Kresowik, T. K., et al. (1993). Endovascular Canine Anastomotic Stenting. *Journal of Surgical Research*, 54 (1), 29-33.

429. Sharif, F., Hynes, S. O., Cooney, R., Howard, L., McMahon, J., Daly, K., et al. (2008). Gene-eluting stents: Adenovirus-mediated delivery of eNOS to the blood vessel wall accelerates re-endothelialization and inhibits restenosis. *Molecular Therapy*, 16 (10), 1674-1680.

430. Kornowski, R., Hong, M. K., Tio, F. O., Bramwell, O., Wu, H. S., and Leon, M. B. (1998). In-stent restenosis: Contributions of inflammatory responses and arterial injury to neointimal hyperplasia. *Journal of the American College of Cardiology*, 31 (1), 224-230.

431. Schwartz, R. S., Huber, K. C., Murphy, J. G., Edwards, W. D., Camrud, A. R., Vlietstra, R. E., et al. (1992). Restenosis and the Proportional Neointimal Response to Coronary-Artery Injury - Results in A Porcine Model. *Journal of the American College of Cardiology*, 19 (2), 267-274.

432. Schwartz, R. S., Murphy, J. G., Edwards, W. D., Camrud, A. R., Vlietstra, R. E., and Holmes, D. R. (1990). Restenosis After Balloon Angioplasty - A Practical Proliferative Model in Porcine Coronary-Arteries. *Circulation*, 82 (6), 2190-2200.

433. Sharif, F., Hynes, S. O., McMahon, J., Cooney, R., Conroy, S., Dockery, P., et al. (2006). Gene-eluting stents: Comparison of adenoviral and adeno-associated viral gene delivery to the blood vessel wall in vivo. *Human Gene Therapy*, 17 (7), 741-750.

434. Gershlick, A. H. (2001). Coronary disease - Role of stenting in coronary revascularisation. *Heart*, 86 (1), 104-112.

435. Brito, L. and Amiji, M. (2007). Nanoparticulate carriers for the treatment of coronary restenosis. *International Journal of Nanomedicine*, 2 (2), 143-161.

436. Hofmann, C. and Strauss, M. (1998). Baculovirus-mediated gene transfer in the presence of human serum or blood facilitated by inhibition of the complement system. *Gene Therapy*, 5 (4), 531-536.

437. Finn, A. V., Joner, M., Nakazawa, G., Kolodgie, F., Newell, J., John, M. C., et al. (2007). Pathological correlates of late drug-eluting stent thrombosis - Strut coverage as a marker of endothelialization. *Circulation*, 115 (18), 2435-2441.

438. Spurgeon, D. (2009). Drug eluting stents remain a "major concern" in the longer term, finds study. *British Medical Journal*, 338 (

439. Venkitachalam, L., Lei, Y., Stolker, J. M., Mahoney, E. M., Amin, A. P., Lindsey, J. B., et al. (2011). Clinical and Economic Outcomes of Liberal Versus Selective Drug-Eluting Stent Use: Insights From Temporal Analysis of the Multicenter Evaluation of Drug Eluting Stents and Ischemic Events (EVENT) Registry. *Circulation*,

440. Isner, J. M., Pieczek, A., Schainfeld, R., Blair, R., Haley, L., Asahara, T., et al. (1996). Clinical evidence of angiogenesis after arterial gene transfer

of phVEGF(165) in patient with ischaemic limb. *Lancet*, 348 (9024), 370-374.

441. Asahara, T., Chen, D. H., Tsurumi, Y., Kearney, M., Rossow, S., Passeri, J., et al. (1996). Accelerated restitution of endothelial integrity and endothelium-dependent function after phVEGF(165) gene transfer. *Circulation*, 94 (12), 3291-3302.

442. Modarai, B., Humphries, J., Burnand, K. G., Gossage, J. A., Waltham, M., Wadoodi, A., et al. (2008). Adenovirus-mediated VEGF gene therapy enhances venous thrombus recanalization and resolution. *Arterioscler.Thromb.Vasc.Biol.*, 28 (10), 1753-1759.

443. Makinen, K., Manninen, H., Hedman, M., Matsi, P., Mussalo, H., Alhava, E., et al. (2002). Increased vascularity detected by digital subtraction angiography after VEGF gene transfer to human lower limb artery: A randomized, placebo-controlled, double-blinded phase II study. *Molecular Therapy*, 6 (1), 127-133.

444. Holmes, D. R., Camrud, A. R., Jorgenson, M. A., Edwards, W. D., and Schwartz, R. S. (1994). Polymeric Stenting in the Porcine Coronary-Artery Model - Differential Outcome of Exogenous Fibrin Sleeves Versus Polyurethane-Coated Stents. *Journal of the American College of Cardiology*, 24 (2), 525-531.

445. McKenna, C. J., Camrud, A. R., Sangiorgi, G., Kwon, H. M., Edwards, W. D., Holmes, D. R., et al. (1998). Fibrin-film stenting in a porcine coronary injury model: Efficacy and safety compared with uncoated stents. *Journal of the American College of Cardiology*, 31 (6), 1434-1438.

446. Dare, E. V., Griffith, M., Poitras, P., Kaupp, J. A., Waldman, S. D., Carlsson, D. J., et al. (2009). Genipin Cross-Linked Fibrin Hydrogels for in vitro Human Articular Cartilage Tissue-Engineered Regeneration. *Cells Tissues Organs*, 190 (6), 313-325.

447. Haider, H. K., Elmadbouh, I., Jean-Baptiste, M., and Ashraf, M. (2008). Nonviral vector gene modification of stem cells for myocardial repair. *Molecular Medicine*, 14 (1-2), 79-86.

448. Wang, X. L., Wang, W., Ma, J., Guo, X., Yu, X. J., and Ma, X. J. (2006). Proliferation and differentiation of mouse embryonic stem cells in APA microcapsule: A model for studying the interaction between stem cells and their niche. *Biotechnology Progress*, 22 (3), 791-800.

449. Serra, M., Correia, C., Malpique, R., Brito, C., Jensen, J., Bjorquist, P., et al. (2011). Microencapsulation Technology: A Powerful Tool for Integrating Expansion and Cryopreservation of Human Embryonic Stem Cells. *Plos One*, 6 (8),

450. Zussman, E. (2011). Encapsulation of cells within electrospun fibers. *Polymers for Advanced Technologies*, 22 (3), 366-371.

451. Fu, Y. L., Kedziorek, D., Crisostomo, V., Gilson, W., Azene, N., Arepally, A., et al. (2008). Perfluorocarbon Microcapsules for X-ray Visualization of Mesenchymal Stem Cell Delivery and Engraftment. *Circulation*, 118 (18), S519

452. Atoui, R., Shum-Tim, D., and Chiu, R. C. J. (2008). Myocardial regenerative therapy: Immunologic basis for the potential "Universal Donor Cells". *Annals of Thoracic Surgery*, 86 (1), 327-334.

453. Bai, X. W., Yan, Y. S., Song, Y. H., Seidensticker, M., Rabinovich, B., Metzele, R., et al. (2010). Both cultured and freshly isolated adipose tissue-derived stem cells enhance cardiac function after acute myocardial infarction. *European Heart Journal*, 31 (4), 489-501.

454. Palpant, N. J. and Metzger, J. M. (2010). Aesthetic cardiology: adipose-derived stem cells for myocardial repair. *Curr.Stem Cell Res.Ther.*, 5 (2), 145-152.

455. Bai, X. W. and Alt, E. (2010). Myocardial regeneration potential of adipose tissue-derived stem cells. *Biochemical and Biophysical Research Communications*, 401 (3), 321-326.

456. Goren, A., Dahan, N., Baruch, L., Goren, E., and Machluf, M. (2009). Encapsulated Human Mesenchymal Stem Cells: A Unique Hypo-Immunogenic Platform for Cellular-Based Tumor Therapy. *Human Gene Therapy*, 20 (5), 545

457. Markel, T. A., Wang, Y., Herrmann, J. L., Crisostomo, P. R., Wang, M. J., Novotny, N. M., et al. (2008). VEGF is critical for stem cell-mediated cardioprotection and a crucial paracrine factor for defining the age threshold in adult and neonatal stem cell function. *American Journal of Physiology-Heart and Circulatory Physiology*, 295 (6), H2308-H2314

458. Ferrarini, M., Arsic, N., Recchia, F. A., Zentilin, L., Zacchigna, S., Xu, X. B., et al. (2006). Adeno-associated virus-mediated transduction of VEGF165 improves cardiac tissue viability and functional recovery after permanent coronary occlusion in conscious dogs. *Circulation Research*, 98 (7), 954-961.

459. Kim, I., Kim, H. G., So, J. N., Kim, J. H., Kwak, H. J., and Koh, G. Y. (2000). Angiopoietin-1 regulates endothelial cell survival through the phosphatidylinositol 3'-kinase/Akt signal transduction pathway. *Circulation Research*, 86 (1), 24-29.

460. Kraitzer, A., Kloog, Y., and Zilberman, M. (2008). Approaches for prevention of restenosis. *Journal of Biomedical Materials Research Part B-Applied Biomaterials*, 85B (2), 583-603.

461. Zakliczynski, M., Lekston, A., Osuch, M., Swierad, M., Nadziakiewicz, P., Przybylski, R., et al. (2007). Comparison of long-term results of drug-eluting Stent and bare metal Stent implantation in heart transplant recipients with coronary artery disease. *Transplantation Proceedings*, 39 (9), 2859-2861.

462. Ueda, Y., Oyabu, J., Okada, K., Ogasawara, N., Hrayama, A., and Kodama, K. (2006). Angioscopic evaluation of neointima coverage: Sirolimus drug-eluting stent vs, bare metal stent. *Circulation*, 114 (18), 453

463. Cutlip, D. E., Windecker, S., Mehran, R., Boam, A., Cohen, D. J., van Es, G. A., et al. (2007). Clinical end points in coronary stent trials - A case for standardized definitions. *Circulation*, 115 (17), 2344-2351.

464. Abbott, J. D., Voss, M. R., Nakamura, M., Cohen, H. A., Selzer, F., Kip, K. E., et al. (2007). Unrestricted use of drug-eluting stents compared with bare-metal Stents in routine clinical practice - Findings from the national heart, lung, and blood institute dynamic registry. *Journal of the American College of Cardiology*, 50 (21), 2029-2036.

465. Mauri, L., Silbaugh, T. S., Wolf, R. E., Zelevinsky, K., Lovett, A., Zhou, Z., et al. (2008). Long-Term Clinical Outcomes After Drug-Eluting and Bare-Metal Stenting in Massachusetts. *Circulation*, 118 (18), 1817-1U64.

466. Stone, G. W., Ellis, S. G., Cox, D. A., Hermiller, J., O'Shaughnessy, C., Mann, J. T., et al. (2004). A polymer-based, paclitaxel-eluting stent in patients with coronary artery disease. *New England Journal of Medicine*, 350 (3), 221-231.

467. Stone, G. W., Ellis, S. G., Cannon, L., Mann, J. T., Greenberg, J. D., Spriggs, D., et al. (2005). Comparison of a polymer-based paclitaxel-eluting stent with a bare metal stent in patients with complex coronary artery disease - A randomized controlled trial. *Jama-Journal of the American Medical Association*, 294 (10), 1215-1223.

468. Chieffo, A. and Colombo, A. (2004). Polymer-based paclitaxel-eluting coronary stents - Clinical results in de novo lesions. *Herz*, 29 (2), 147-151.

469. Stone, G. W., Ellis, S. G., Cox, D. A., Hermiller, J., O'Shaughnessy, C., Mann, J. T., et al. (2004). A polymer-based, paclitaxel-eluting stent in patients with coronary artery disease. *New England Journal of Medicine*, 350 (3), 221-231.

470. Doven, O., Ozcan, T. I., Cicek, D., Camsari, A., Akkus, N., Aytacoglu, B. N., et al. (2006). Angiographic and clinical outcome following paclitaxel-eluting stent (Taxus) implantation - A single center experience. *International Heart Journal*, 47 (1), 1-12.

471. Silber, S., Hamburger, J., Grubel, E., Pfisterer, M., Belardi, J., Webb, J., et al. (2004). Direct stenting with TAXUS stents seems to be as safe and effective as with predilatation - A post hoc analysis of TAXUS II. *Herz*, 29 (2), 171-180.

472. Silber, S., Colombo, A., Banning, A. P., Hauptmann, K., Drzewiecki, J., Grube, E., et al. (2009). Final 5-Year Results of the TAXUS II Trial A Randomized Study to Assess the Effectiveness of Slow- and Moderate-Release Polymer-Based Paclitaxel-Eluting Stents for De Novo Coronary Artery Lesions. *Circulation*, 120 (15), 1498-1504.

473. Moses, J. W., Mehran, R., Nikolsky, E., Lasala, J. M., Corey, W., Albin, G., et al. (2005). Outcomes with the paclitaxel-eluting stent in patients with acute coronary syndromes - Analysis from the TAXUS-IV trial. *Journal of the American College of Cardiology*, 45 (8), 1165-1171.

474. Stone, G. W., Ellis, S. G., O'Shaughnessy, C. D., Martin, S. L., Satler, L., McGarry, T., et al. (2006). Paclitaxel-eluting stents vs vascular brachytherapy for in-stent restenosis within bare-metal stents - The TAXUS VISR randomized trial. *Jama-Journal of the American Medical Association*, 295 (11), 1253-1263.

475. Abizaid, A., Chan, C., Lim, Y. T., Kaul, U., Sinha, N., Patel, T., et al. (2006). Twelve-month outcomes with a Paclitaxel-eluting stent transitioning from controlled trials to clinical practice (the WISDOM registry). *American Journal of Cardiology*, 98 (8), 1028-1032.

476. Holmes, D. R. (2007). Incidence of late stent thrombosis with bare-metal, sirolimus, and paclitaxel stents. *Reviews in Cardiovascular Medicine*, 8 (S11-S18

477. Qian, J. Y., Zhang, F., Fan, B., Ge, L., Wang, Q. B., and Ge, J. B. (2008). A more than 2-year follow-up of incomplete apposition after drug-eluting stent implantation. *Chinese Medical Journal*, 121 (6), 498-502.

478. Hong, M. K., Mintz, G. S., Lee, C. W., Park, D. W., Lee, S. W., Kim, Y. H., et al. (2007). Impact of late drug-eluting stent malapposition on 3-year clinical events. *Journal of the American College of Cardiology*, 50 (15), 1515-1516.

479. Qian, J. Y., Zhang, F., Wu, H. Y., Fan, B., Ge, L., and Ge, J. B. (2007). Late stent malapposition after drug eluting stent implantation is, related to

high incidence of very late stent thrombosis. *American Journal of Cardiology*, 100 (8A), 192L

480. Petronio, A. S., De Carlo, M., Branchitta, G., Papini, B., Ciabatti, N., Gistri, R., et al. (2007). Randomized comparison of sirolimus and paclitaxel drug-eluting stents for long lesions in the left anterior descending artery - An intravascular ultrasound study. *Journal of the American College of Cardiology*, 49 (5), 539-546.

481. Van der Hoeven, B. L., Liem, S. S., Jukema, J. W., Suraphakdee, N., Putter, H., Dijkstra, J., et al. (2008). Sirolimus-eluting stents versus bare-metal stents in patients with ST-segment elevation myocardial infarction: 9-month angiographic and intravascular ultrasound results and 12-month clinical outcome - Results from the MISSION! Intervention study. *Journal of the American College of Cardiology*, 51 (6), 618-626.

482. Finn, A. V., Nakazawa, G., Joner, M., Kolodgie, F. D., Mont, E. K., Gold, H. K., et al. (2007). Vascular responses to drug eluting stents - Importance of delayed healing. *Arteriosclerosis Thrombosis and Vascular Biology*, 27 (7), 1500-1510.

483. Zhang, F., Qian, J. Y., and Ge, J. B. (2007). Very late stent thrombosis in-late stent malapposition after sirohmus-eluting stent implantation. *International Heart Journal*, 48 (5), 591-596.

484. Park, D. W., Park, S. W., Park, K. H., Lee, B. K., Kim, Y. H., Lee, C. W., et al. (2006). Frequency of and risk factors for stent thrombosis after drug-eluting stent implantation during long-term follow-up. *American Journal of Cardiology*, 98 (3), 352-356.

485. Mintz, G. S. and Weissman, N. J. (2006). Intravascular ultrasound in the drug-eluting stent era. *Journal of the American College of Cardiology*, 48 (3), 421-429.

486. Sonoda, S., Morino, Y., Ako, J., Terashima, M., Hassan, A. H. M., Bonneau, H. N., et al. (2004). Impact of final Stent dimensions on long-term results following sirolimus-eluting stent implantation - Serial intravascular ultrasound analysis from the SIRIUS trial. *Journal of the American College of Cardiology*, 43 (11), 1959-1963.

487. LaDisa, J. F., Jr., Olson, L. E., Hettrick, D. A., Warltier, D. C., Kersten, J. R., and Pagel, P. S. (2005). Axial stent strut angle influences wall shear stress after stent implantation: analysis using 3D computational fluid dynamics models of stent foreshortening. *Biomed.Eng Online*, 4 (59

488. Perlstein, I., Connolly, J. M., Cui, X., Song, C., Li, Q., Jones, P. L., et al. (2003). DNA delivery from an intravascular stent with a denatured

collagen-polylactic-polyglycolic acid-controlled release coating: mechanisms of enhanced transfection. *Gene Ther*, 10 (17), 1420-1428.

489. Walter, D. H., Cejna, M., Diaz-Sandoval, L., Willis, S., Kirkwood, L., Stratford, P. W., et al. (2004). Local Gene Transfer of phVEGF-2 Plasmid by Gene-Eluting Stents: An Alternative Strategy for Inhibition of Restenosis. *Circulation*, 110 (1), 36-45.

490. Hedman, M., Hartikainen, J., Syvanne, M., Stjernvall, J., Hedman, A., Kivela, A., et al. (2003). Safety and feasibility of catheter-based local intracoronary vascular endothelial growth factor gene transfer in the prevention of postangioplasty and in-stent restenosis and in the treatment of chronic myocardial ischemia: phase II results of the Kuopio Angiogenesis Trial (KAT). *Circulation*, 107 (21), 2677-2683.

491. Pelisek, J., Fuchs, A. T., Kuehnl, A., Tian, W., Kuhlmann, M. T., Rolland, P. H., et al. (2006). C-type natriuretic peptide for reduction of restenosis: gene transfer is superior over single peptide administration. *J.Gene Med.*, 8 (7), 835-844.

492. Pfeiffer, T., Wallich, M., Sandmann, W., Schrader, J., and Godecke, A. (2006). Lipoplex gene transfer of inducible nitric oxide synthase inhibits the reactive intimal hyperplasia after expanded polytetrafluoroethylene bypass grafting. *J.Vasc.Surg.*, 43 (5), 1021-1027.

493. Lenter, M. C., Garidel, P., Pelisek, J., Wagner, E., and Ogris, M. (2004). Stabilized nonviral formulations for the delivery of MCP-1 gene into cells of the vasculoendothelial system. *Pharm.Res.*, 21 (4), 683-691.

494. Kawauchi, M., Suzuki, J., Morishita, R., Wada, Y., Izawa, A., Tomita, N., et al. (2000). Gene therapy for attenuating cardiac allograft arteriopathy using ex vivo E2F decoy transfection by HVJ-AVE-liposome method in mice and nonhuman primates. *Circulation Research*, 87 (11), 1063-1068.

495. Yin, M., Yuan, Y., Liu, C. S., and Wang, J. (2009). Development of mussel adhesive polypeptide mimics coating for in-situ inducing re-endothelialization of intravascular stent devices. *Biomaterials*, 30 (14), 2764-2773.

496. Wartlick, H., Michaelis, K., Balthasar, S., Strebhardt, K., Kreuter, J. +., and Langer, K. (2004). Highly Specific HER2-mediated Cellular Uptake of Antibody-modified Nanoparticles in Tumour Cells. *Journal of Drug Targeting*, 12 (7), 461-471.

497. Fishbein, I., Chorny, M., Banai, S., Levitzki, A., Danenberg, H. D., Gao, J. C., et al. (2001). Formulation and delivery mode affect disposition and activity of tyrphostin-loaded nanoparticles in the rat carotid model. *Arteriosclerosis Thrombosis and Vascular Biology*, 21 (9), 1434-1439.

498. Banai, S., Chorny, M., Gertz, S. D., Fishbein, I., Gao, J. C., Perez, L., et al. (2005). Locally delivered nanoencapsulated tyrphostin (AGL-2043) reduces neointima formation in balloon-injured rat carotid and stented porcine coronary arteries. *Biomaterials*, 26 (4), 451-461.

499. Xu, X. H., Lu, P., Guo, M. Q., and Fang, M. Z. (2010). Cross-linked gelatin/nanoparticles composite coating on micro-arc oxidation film for corrosion and drug release. *Applied Surface Science*, 256 (8), 2367-2371.

500. Bhargava, B., Reddy, N. K., Karthikeyan, G., Raju, R., Mishra, S., Singh, S., et al. (2006). A novel paclitaxel-eluting porous carbon-carbon nanoparticle coated, nonpolymeric cobalt-chromium stent: Evaluation in a porcine model. *Catheterization and Cardiovascular Interventions*, 67 (5), 698-702.

501. McDonald, J. E., Klinke, W. P., Margolis, J., Hilton, J. D., Heuser, R., Waksman, R., et al. (2005). Systemic Nanoparticle Albumin-bound Paclitaxel (ABI-007) for prevention of In-stent ReSTenosis (SNAPIST-I): A first in man safety and dose finding study. *European Heart Journal*, 26 (696

502. McDonald, J. E., Klinke, P., Fung, A., Ricci, D., Suciu, C., Ortan, F., et al. (2006). Systemic nanoparticle albumin-bound paclitaxel (nab-paclitaxel) for the prevention of in-stent restenosis (SNAPIST-II): A randomized comparison of single dose and single dose plus repeat dose at 2 months. *American Journal of Cardiology*, 98 (8A), 224M

503. Margolis, J., McDonald, J., Heuser, R., Klinke, P., Waksman, R., Virmani, R., et al. (2007). Systemic nanoparticle paclitaxel (nab-paclitaxel) for in-stent Restenosis I (SNAPIST-1): A first-in-human safety and dose-finding study. *Clinical Cardiology*, 30 (4), 165-170.

504. Guba, M., von Breitenbuch, P., Steinbauer, M., Koehl, G., Flegel, S., Hornung, M., et al. (2002). Rapamycin inhibits primary and metastatic tumor growth by antiangiogenesis: involvement of vascular endothelial growth factor. *Nature Medicine*, 8 (2), 128-135.

505. Davies, M. J., Woolf, N., Rowles, P. M., and Pepper, J. (1988). Morphology of the Endothelium Over Atherosclerotic Plaques in Human Coronary-Arteries. *British Heart Journal*, 60 (6), 459-464.